103rd Scientific Assembly and Annual Meeting

November 26 to December 1 McCormick Place, Chicago



Wednesday

Complete RSNA 2017 Meeting Program available at **Meeting.RSNA.org**







103rd Scientific Assembly and Annual Meeting November 26 to December 1 McCormick Place, Chicago



SPDL40

Game of Bones: Radiology in the Seven Kingdoms (Case-based Competition)

Wednesday, Nov. 29 7:15AM - 8:15AM Room: E451B



AMA PRA Category 1 Credit ™: 1.00 ARRT Category A+ Credit: 1.00

Participants

Eric B. England, MD, Cincinnati, OH (*Presenter*) Nothing to Disclose Carl C. Flink, MD, Cincinnati, OH (*Presenter*) Nothing to Disclose

For information about this presentation, contact:

eric.england@uc.edu

LEARNING OBJECTIVES

1) Review the presentation, imaging features and complications of a variety of common and uncommon injuries. 2) Understand the mechanisms of certain injuries and associated imaging findings. 3) Identify congenital, infectious, and metabolic musculoskeletal imaging pathology; some of which would be more prevalent in a pre-industrial society. *This interactive session will use RSNA Diagnosis Live*TM. *Please bring your charged mobile wireless device (phone, tablet or laptop) to participate*.





103rd Scientific Assembly and Annual Meeting November 26 to December 1 McCormick Place, Chicago



SPSC40

Controversy Session: Imaging of the Pelvis: When is Ultrasound Enough?

Wednesday, Nov. 29 7:15AM - 8:15AM Room: E350



AMA PRA Category 1 Credit ™: 1.00 ARRT Category A+ Credit: 1.00

Participants

Carol B. Benson, MD, Boston, MA (Moderator) Nothing to Disclose

LEARNING OBJECTIVES

1) Utilize ultrasound as the primary imaging modality for diagnosing of a variety of gynecologic abnormalities. 2) Understand which gynecologic findings on ultrasound are adequate to make a specific diagnosis and do not require further imaging. 3) Recognize which sonographic findings in the pelvis require further investigation with other imaging modalities and which do not.

Sub-Events

SPSC40A Imaging of the Pelvis: Ultrasound is Enough

Participants Beryl R. Benacerraf, MD, Boston, MA (*Presenter*) Nothing to Disclose

LEARNING OBJECTIVES

View learning objectives under main course title.

SPSC40B Imaging of the Pelvis: Ultrasound is Not Always Enough

Participants

Deborah Levine, MD, Boston, MA (Presenter) Editor with royalties, UpToDate, Inc; Editor with royalties, Reed Elsevier;

For information about this presentation, contact:

dlevine@bidmc.harvard.edu

LEARNING OBJECTIVES

1) Illustrate adenxal masses where MR adds additional information that can alter decision to perform surgery. 2) Discuss how MR can be utilized in pre-procedure planning for women with fibroids. 3) Discuss use of MR in pregnancy when additional information is needed regarding complex uterine pathology.

ABSTRACT

Ultrasound is first line imaging for the female pelvis. However, there are instances where additional imaging is needed for further assessment. MRI can frequently add additional information that can alter patient care. Examples include: the indeterminate adnexal mass, where findings could alter the decision to perform surgery; precise delineation of size and location of fibroids when this information is needed prior to surgery or other intervention; and assessment of complex uterine pathology during pregnancy.





103rd Scientific Assembly and Annual Meeting November 26 to December 1 McCormick Place, Chicago



SPSH40

Hot Topic Session: Deep Learning for Mammography

Wednesday, Nov. 29 7:15AM - 8:15AM Room: E450A



AMA PRA Category 1 Credit ™: 1.00 ARRT Category A+ Credit: 1.00

FDA Discussions may include off-label uses.

Participants

Joseph Lo, PhD, Durham, NC (Moderator) Nothing to Disclose

For information about this presentation, contact:

Joseph.Lo@Duke.edu

ABSTRACT

This session will discuss the hot topic of deep learning in mammography from three different perspectives: (1) We will learn about the recent computational challenge involving a massive amount of image data. (2) We will dive deeper into the state of the art machine learning research in breast imaging. (3) We will discuss the opportunities and challenges for the practice of breast imaging in particular and radiology in general.

Sub-Events

SPSH40A The Deep Learning DREAM - Can a Computer Teach Itself to Screen?

Participants

Joseph Lo, PhD, Durham, NC (Presenter) Nothing to Disclose

For information about this presentation, contact:

Joseph.Lo@Duke.edu

LEARNING OBJECTIVES

1) Understand the motivation and goals behind the Digital Mammography (DM) DREAM Challenge.2) Appreciate the scientific achievements accomplished during the challenge.3) Learn about the implications to radiology of machine learning empowered with large data sets.

ABSTRACT

In fall 2016, the Digital Mammography (DM) DREAM Challenge was launched. This computational challenge boasted an unprecedented data set of over 640,000 de-identified digital mammograms, and was organized by a large consortium of private and public entities including Sage Bionetworks, IBM, Group Health Cooperative, Apple, FDA, NCI, and Icahn School of Medicine at Mount Sinai. The goal of the challenge was to create machine learning models that may reduce the recall rate of breast cancer screening. Researchers from all over the world eagerly submitted thousands of models over multiple rounds of competition. The challenge is transitioning to the community phase, where the former competitors will come together and collaborate to improve their models even further and hopefully create viable approaches for clinical translation. Although most teams entered the challenge with little or no experience in medical imaging or mammography, after just a few short months, the top teams' performance already rival that of decades of CAD research and commercial development. Pending analyses of final results, the current models may even approach the performance of radiologists, with potentially more improvements to come during the collaboration phase. This stunning success of imaging data.

SPSH40B Development of Deep Learning Systems for Improving Breast Cancer Screening

Participants

Nico Karssemeijer, PhD, Nijmegen, Netherlands (*Presenter*) Director and Shareholder, ScreenPoint Medical BV; Shareholder, Volpara Health Technologies Limited; Consultant, QView Medical, Inc; Shareholder, QView Medical, Inc;

LEARNING OBJECTIVES

1) Assess the state of art of deep learning systems for mammography screening. 2) Understand the potential of Artificial Intelligence to improve workflow and reduce workload in breast screening. 3) Understand differences between new deep learning applications and existing CAD systems.

ABSTRACT

Recent developents in machine learning offer unprecedented opportunities for researchers to develop fully automated systems for the reading of mammograms and breast tomosynthesis. The scope of these systems will be much wider than that of existing CAD systems for mammography. They will provide decision support to improve recall decisions and pre-screening of exams by computers will become a reality. This will lead to more efficient screening procedures where human readers rely on automation to select normal exams that they don't need to read. This will allow them to focus on making optimal decisions for women with potentially abnormal exams in which cancer is most likely. In the presentation experimental results will be highlighted in which radiologists are compared to deep learning systems.

URL

http://www.diagnijmegen.nl

SPSH40C Will Computers Replace Radiologists for Mammography Interpretation?

Participants

Christoph I. Lee, MD, Seattle, WA (Presenter) Nothing to Disclose

LEARNING OBJECTIVES

1) Describe what machine learning is and how it is applicable to breast imaging. 2) Identify potential avenues where machine learning can improve breast cancer screening and diagnosis. 3) Describe current research endeavors in machine learning related to breast cancer screening.

ABSTRACT

Machine and deep learning, applied to medical imaging, has the ability to assess diagnostic and prognostic likelihoods based on previously unimagined configurations of vast amounts of raw data. Recently, digital screening mammography has been one area where machine learners have attempted to improve accuracy. This presentation will review the rationale for using machine and deep learning in breast cancer screening, and provide an overview of ongoing national and international research activities that aim to develop more robust algorithms using supercomputing to better predict malignancy based on mammography image features.





103rd Scientific Assembly and Annual Meeting November 26 to December 1 McCormick Place, Chicago



MSRT41

ASRT@RSNA 2017: Recent Advances in Neuroimaging

Wednesday, Nov. 29 8:00AM - 9:00AM Room: N230B

NR

AMA PRA Category 1 Credit ™: 1.00 ARRT Category A+ Credit: 1.00

Participants

Max Wintermark, MD, Lausanne, Switzerland (Presenter) Advisory Board, General Electric Company;

LEARNING OBJECTIVES

1) Understand the different facets of the latest anatomical and functional neuroimaging techniques. 2) Understand their potential as clinical tools for evaluating the breadth of diseases affecting the brain.

ABSTRACT

During the past decade, we have seen an explosion of innovation in structural and functional neuroimaging techniques, providing exciting insights into new aspects of the human brain that transcend simple visualization of anatomy. New scanners that are faster with better image quality and higher magnetic field strength — as well as higher spatial and temporal resolution — allow fully quantitative assessment of the brain, including macroscopic structure, microstructural organization, functional connectivity, perfusion and metabolism. The resultant exponential increase in highly granular neuroimaging data that can be rapidly acquired creates challenges — but also opportunities — for better characterization of neurological, neurosurgical and psychiatric disorders that arise from complex central nervous system dysfunction. Indeed, neuroimaging is now appropriately recognized as a big data technique, sharing similar needs with other data-rich methods for further innovation in analysis and meaningful information extraction, as well as for integration with the other big data disciplines such as genomics and proteomics. There is a continued need for this technology to be translated from basic "bench top" science into clinical practice, so that these remarkable advances in the ability to characterize the brain can benefit patients. Critical to meaningful clinical translation is comparative effectiveness and outcome research to gain widespread acceptance in the modern, economically constrained healthcare system.





103rd Scientific Assembly and Annual Meeting November 26 to December 1 McCormick Place, Chicago



RCB41

Prostate MRI (Hands-on) Course will be repeated Monday, Tuesday, Wednesday and Thursday from 8am-10am

Wednesday, Nov. 29 8:00AM - 10:00AM Room: S401CD



AMA PRA Category 1 Credits ™: 2.00 ARRT Category A+ Credits: 2.25

Participants

Jelle O. Barentsz, MD, PhD, Nijmegen, Netherlands (*Presenter*) Advisor, SPL Medical BV Jurgen J. Futterer, MD, PhD, Nijmegen, Netherlands (*Presenter*) Research Grant, Siemens AG Roel D. Mus, MD, Nijmegen, Netherlands (*Presenter*) Nothing to Disclose Geert M. Villeirs, MD, PhD, Ghent, Belgium (*Presenter*) Nothing to Disclose Marloes van der Leest, MD, Nijmegen, Netherlands (*Presenter*) Nothing to Disclose Renske L. van Delft, Nijmegen, Netherlands (*Presenter*) Nothing to Disclose Rianne R. Engels, Cuijk, Netherlands (*Presenter*) Nothing to Disclose Leonardo K. Bittencourt, MD, PhD, Rio De Janeiro, Brazil (*Presenter*) Investor, Healfies LLC Joseph J. Busch, MD, Chattanooga, TN (*Presenter*) Nothing to Disclose Baris Turkbey, MD, Bethesda, MD (*Presenter*) Nothing to Disclose Daniel J. Margolis, MD, Los Angeles, CA (*Presenter*) Nothing to Disclose Antonio C. Westphalen, MD, Mill Valley, CA (*Presenter*) Scientific Advisory Board, 3DBiopsy LLC ; Research Grant, Verily Life Sciences LLC

Philippe A. Puech, MD, Lyon, France (Presenter) Nothing to Disclose

For information about this presentation, contact:

Geert.Villeirs@UGent.be

jelle.barentsz@radboudumc.nl

jurgen.futterer@radboudumc.nl

Rianne.Engels@radboudumc.nl

Renske.vandelft@Radboudumc.nl

Lkayat@gmail.com

LEARNING OBJECTIVES

1) Understand the Pi-RADS v2 Category assessment to detect and localize significant cancer for both peripheral zone and transitional zone lesions. 2) Recognize benign pathology like inflammation and BPH and to differentiate these from significant prostate cancers.

ABSTRACT

In this Hands-on Workshop, the participants will able to review up to 30 multi-parametric MRI cases with various prostatic pathology using a dedicated workstation. Focus will be on the overall assessment of PI-RADS v2 category, which enables them to score the probability of the presence of a significant cancer in patients with elevated PSA and/or clinical suspicion. All cases are from daily non-academic practice, and have various levels of difficulty. The cases include: easy and difficult significant peripheral-transition- and central zone cancers, inflammation, BPH, and the most common pitfalls. Internationally renowned teachers will guide the participants during their PI-RADS v2 scoring. <u>PLEASE NOTICE:</u> Based on last year's experience we expect this course to be very popular. We only have 50 computes, and two spots per computer. Only the first 100 people will be accepted in the room. The front rows are reserved for beginners. In case you have experience with prostate MR: Please take a seat at the computers in the back of the room. We will not have space for any additional listeners this year. The coursebook can be found as handout to this course. Please take it with you to the course on your tablet or other device.

Active Handout:Renske Lian van Delft

http://abstract.rsna.org/uploads/2017/16002005/Active RCB.pdf







MSCP41

Case-based Review of Pediatric Radiology (An Interactive Session)

Wednesday, Nov. 29 8:30AM - 10:00AM Room: S406A

PD

AMA PRA Category 1 Credits ™: 1.50 ARRT Category A+ Credit: 1.75

FDA Discussions may include off-label uses.

Participants

Ricardo Restrepo, MD, Miami, FL (Director) Nothing to Disclose

Sub-Events

MSCP41A Fetal Thoracoabdominal Disorders

Participants Pedro Daltro, MD, Rio De Janeiro, Brazil (*Presenter*) Nothing to Disclose

For information about this presentation, contact:

daltro.pedro@gmail.com

LEARNING OBJECTIVES

1) Discuss commonly encounteed thoracoadominal disorders on fetal imaging. 2) Learn current imaging techniques for evaluating fetal thoracoabdominal disorders. 3) Review characteristic fetal imaging findings of thoracoabdominal disorders.

ABSTRACT

This will be an interactive session with case presentations of fetal thoracoabdominal disorders. The cases will be presented as unknows with audience response. Examples of commonly encountered fetal thoracoabdominal disorders in daily clinical practice will be included

MSCP41B Pediatric Thoracic Disorders

Participants

Jaishree Naidoo, MD, Johannesburg, South Africa (Presenter) Nothing to Disclose

LEARNING OBJECTIVES

1) Have a systematic approach to common pediatric thoracic disorders. 2) Discuss the role of imaging in the management of pediatric respiratory disorders and the advantages and limitations of each imaging technique. 3) Have an imaging approach to patients with recurrent infections.

ABSTRACT

Pediatric respiratory disorders are a common cause of morbidity and mortality in children.Both medical and surgical diseases affect the respiratory system.Imaging has an important role to play in the evaluation of pediatric respiratory disorders, especially in patients who present with recurrent infections. Through the demonstration and discussion of pediatric thoracic cases one would be able to have an approach to imaging of the common paediatric thoracic disorders, identify important imaging features and the most appropiate imaging modality to make the diagnosis.

MSCP41C Pediatric Vascular Disorders

Participants Govind B. Chavhan, MD, Toronto, ON (*Presenter*) Nothing to Disclose

For information about this presentation, contact:

govind.chavhan@sickkids.ca

LEARNING OBJECTIVES

1) List the types of vascular lesions seen in children. 2) Discuss the role of imaging in the evaluation of these lesions. 3) Discuss proper imaging techniques including ultrasound, MR imaging and angiography to image these lesions in children.

ABSTRACT

Vascular abnormalities seen in children include renal artery stenosis from various causes, vasculitis, syndromic vasculopathy and vascular malformations among others. Imaging plays important role in their assessment. Commonly seen pediatric vascular disorders will be illustrated with discussion of salient features, appropriate choice of imaging modality and technique. Advantages and disadvantages if imaging techniques will also be discussed.

For information about this presentation, contact:

nfmahmoo@texaschidlrens.org

LEARNING OBJECTIVES

1) Examine common and rare pediatric musculoskeletal disorders. 2) Learn the characteristic imaging features and optimal imaging techniques. 3) Discuss differential diagnoses and pitfalls of which to be wary.

ABSTRACT

This will be an interactive session that is case based and will discuss common and uncommon pediatric musculoskeletal disorders. Cases will be accompanied by a discussion of common clinical features, diagnostic modality of choice along with appropriate imaging techniques. Common pitfalls to avoid when interpreting pediatric musculoskeletal cases will also be examined.







MSES41

Essentials of Cardiac Imaging

Wednesday, Nov. 29 8:30AM - 10:00AM Room: S100AB



AMA PRA Category 1 Credits ™: 1.50 ARRT Category A+ Credit: 1.75

Sub-Events

MSES41A Cardiac MRI: From Basics to Practice

Participants

Isabel B. Oliva, MD, New Haven, CT (Presenter) Author, Reed Elsevier; Editor, Reed Elsevier

LEARNING OBJECTIVES

1) Understand the basics of cardiac MRI acquisition. 2) Recognize normal anatomy. 3) Learn the MR findings of common cardiomyopathies.

ABSTRACT

This course will review the basics of cardiac MRI acquisition including imaging planes and sequences. We will review normal cardiac anatomy and discuss the findings of the most common cardiomyopathies.

Active Handout: Isabel Borges Oliva

http://abstract.rsna.org/uploads/2017/17000033/Active MSES41A.pdf

MSES41B Spectral CT

Participants

Suhny Abbara, MD, Dallas, TX (*Presenter*) Author, Reed Elsevier; Editor, Reed Elsevier; Institutional research agreement, Koninklijke Philips NV; Institutional research agreement, Siemens AG

Honored Educators

Presenters or authors on this event have been recognized as RSNA Honored Educators for participating in multiple qualifying educational activities. Honored Educators are invested in furthering the profession of radiology by delivering high-quality educational content in their field of study. Learn how you can become an honored educator by visiting the website at: https://www.rsna.org/Honored-Educator-Award/ Suhny Abbara, MD - 2014 Honored EducatorSuhny Abbara, MD - 2017 Honored Educator

MSES41C Cardiac MR of Acute MI: Imaging Patterns and Prognostic Implications

Participants Marco Francone, MD, Rome, Italy (*Presenter*) Speakers Bureau, Bracco Group

For information about this presentation, contact:

marco.francone@uniroma1.it

LEARNING OBJECTIVES

1) To review basic pathophysiology of the ischemic cascade preceding acute myocardial infarction, integrating pathological models with CMR imaging findings. 2) To illustrate spectrum of findings and relative significance of different patterns of tissue necrosis depicted with CMR. 3) To understand added value of MR in the setting as a prognostic indicator of adverse remodeling and major events following myocardial infarction.

ABSTRACT

Current therapeutic strategies in ST-elevation acute myocardial infarction (STEMI) aim to recanalize culprit vessel within the shortest temporal window in order to restore myocardial blood flow within the ischemic territory and save the highest amount of myocardial tissue according to the so-called "open-artery" theory.As a matter of fact, a large spectrum of tissue changes may occur following acute necrosis, ranging between the occurrence of the so-called "aborted infarction" which is characterized by a predominantly edematous injury with minimal necrotic component up to the presence of extensive microvascular damage with no-reflow within the area-at-risk.Cardiac MR represent imaging technique of choice for the in-vivo depiction of STEMI allowing to comprehensively evaluate functional impairment and tissue changes characterizing the processs consisting with direct visualization and quantification of necrotic region and corresponding edematous area representing the area-at-risk.Relevant prognostic implications derive from CMR imaging of myocardial infarction affecting functional recovery and patient's prognosis.Present lecture will review different aspect of CMR imaging in STEMI, from pathophysiology to STEMI imaging patterns with corresponding impact on patient's prognosis.

MSES41D CT Calcium Scoring

Participants

For information about this presentation, contact:

r.vliegenthart@umcg.nl

LEARNING OBJECTIVES

1) To discuss latest results on the diagnostic and prognostic value of the coronary calcium score. 2) To learn about the impact of CT calcium scoring on cardiovascular risk stratification. 3) To understand the role of CT calcium scoring in asymptomatic individuals and symptomatic patients.

ABSTRACT

Accurate identification of asymptomatic individuals who will later suffer a coronary event is challenging. Risk-factor based algorithms to estimate cardiovascular risk in the general population are neither very sensitive nor specific. Evaluation of the extent of coronary atherosclerotic plaque by CT calcium scoring can improve risk prediction and risk stratification. Multiple large-scale prospective studies have shown the strong predictive value of the calcium score for coronary heart disease. The calcium score improves cardiovascular risk stratification beyond cardiovascular risk factors in asymptomatic individuals, in particular in those at intermediate risk, and reduces over- and undertreatment. Whether management based on the calcium score reduces the incidence of coronary events is being studied in the Dutch ROBINSCA trial. In symptomatic patients, in particular those with atypical symptoms of chest pain, there is increasing interest in the zero calcium score to exclude relevant coronary artery disease. In this presentation, the latest results and status of CT calcium scoring will be discussed.





103rd Scientific Assembly and Annual Meeting November 26 to December 1 McCormick Place, Chicago



MSRO41

BOOST: Pediatric-Oncology Anatomy (An Interactive Session)

Wednesday, Nov. 29 8:30AM - 10:00AM Room: S103CD



AMA PRA Category 1 Credits ™: 1.50 ARRT Category A+ Credit: 1.75

Participants

Stephanie A. Terezakis, MD, Baltimore, MD (*Presenter*) Research Grant, Elekta AB Thierry Huisman, MD, Baltimore, MD (*Presenter*) Nothing to Disclose

LEARNING OBJECTIVES

1) Learn how to define normal structures relevant to the most common pediatric brain tumors for contouring purposes. 2) Assess patterns of spread of the most common pediatric tumors, including brain tumors, and the relevant implications for contouring. 3) Review contouring principles for common pediatric tumors, including brain tumors, with specific discussion on optimum ways to incorporate MRI imaging to guide target delineation.

ABSTRACT

Pediatric tumors present with particular contouring challenges for the radiation oncologist given the variety of disease presentations and the critical need to define normal tissues accurately given the concern for RT-related late toxicities in children. In this session, we will review basic normal tissue anatomy with particular emphasis on the brain and skull base. We will also discuss patterns of disease spread in the most common pediatric tumors, including a special emphasis on brain tumors, and implications for target volume delineation.





MSSR41

RSNA/ESR Hybrid Imaging Symposium: The ABCs of Hybrid Imaging (An Interactive Session)

Wednesday, Nov. 29 8:30AM - 10:00AM Room: S402AB



AMA PRA Category 1 Credits ™: 1.50 ARRT Category A+ Credit: 1.75

FDA Discussions may include off-label uses.

Participants

Alexander Drzezga, MD, Cologne, Germany (*Moderator*) Consultant, Siemens AG; Consultant, Bayer AG; Consultant, General Electric Company; Consultant, Eli Lilly and Company; Consultant, The Piramal Group; Speakers Bureau, Siemens AG; Speakers Bureau, Bayer AG; Speakers Bureau, General Electric Company; Speakers Bureau, Eli Lilly and Company; Speakers Bureau, The Piramal Group Katrine Riklund, MD, PhD, Umea, Sweden (*Moderator*) Nothing to Disclose

For information about this presentation, contact:

katrine.riklund@umu.se

LEARNING OBJECTIVES

1) What you need to know about PET-physics. 2) How MR physics influence image quality in hybrid imaging.

Sub-Events

MSSR41A What You Need to Know about PET-Physics

Participants

Jan Axelsson, Umea, Sweden (Presenter) Founder, Dicom Port AB

LEARNING OBJECTIVES

1) To understand the basics of physics in PET imaging. 2) To learn about the different approaches of PET attenuation correction. 3) To learn about potential artefacts in hybrid imaging.

ABSTRACT

This lecture gives a basis to understand the underlying mechanism to why PETCT image quantitation sometimes fails. Examples and false PET uptakes, explanation on the underlying mechanism, and rules of thumb how you may reveal if an uptake is physiological will be given.

MSSR41B How MR Physics Influence Image Quality in Hybrid Imaging

Participants

Ciprian Catana, MD, PhD, Charlestown, MA (Presenter) Nothing to Disclose

LEARNING OBJECTIVES

1) Learn about MR artefacts influencing PET image quality. 2) Understand the complexity of physics in MR-PET. 3) Learn about MR for attenuation and motion correction.

MSSR41C Interactive Case Discussion

Participants Jan Axelsson, Umea, Sweden (*Presenter*) Founder, Dicom Port AB Ciprian Catana, MD, PhD, Charlestown, MA (*Presenter*) Nothing to Disclose

LEARNING OBJECTIVES

1) Learn how to identify common MR artefacts. 2) Learn how to identify common PET artefacts. 3) Learn how to identify common CT artefacts.





103rd Scientific Assembly and Annual Meeting November 26 to December 1 McCormick Place, Chicago



RC501

High Resolution CT of Diffuse Lung Disease: Read Cases with the Experts (An Interactive Game)

Wednesday, Nov. 29 8:30AM - 10:00AM Room: E450A



AMA PRA Category 1 Credits ™: 1.50 ARRT Category A+ Credit: 1.75

Participants

Georgeann McGuinness, MD, New York, NY (*Moderator*) Nothing to Disclose Brett M. Elicker, MD, San Francisco, CA (*Presenter*) Nothing to Disclose Daria Manos, MD, FRCPC, Halifax, NS (*Presenter*) Nothing to Disclose Sharyn L. MacDonald, MBChB, Christchurch, New Zealand (*Presenter*) Nothing to Disclose Georgeann McGuinness, MD, New York, NY (*Presenter*) Nothing to Disclose

For information about this presentation, contact:

daria.manos@nshealth.ca

brett.elicker@ucsf.edu

jerasmus@mdanderson.org

LEARNING OBJECTIVES

1) Understand the applications and limitations of HRCT in detecting and characterizing diffuse lung disease through the review and discussion of cases. 2) Apply correct usage of the HRCT lexicon to specific findings, to better elucidate pathophysiology and to refine differential considerations. 3) Develop diagnosis and management algorithms by working through problematic cases with the expert discussants.

ABSTRACT

This interactive session will use RSNA Diagnosis Live[™]. Please bring your charged mobile wireless device (phone, tablet or laptop) to participate.

SAM

New in 2017: PLEASE NOTE - All courses designated for SAM credit at RSNA 2017 will require attendees bring a personal device e.g. phone, iPad, laptop to complete the required test questions during the live session.







RC502

Research Development/Mentoring Trainees and Junior Faculty

Wednesday, Nov. 29 8:30AM - 10:00AM Room: E353B



AMA PRA Category 1 Credits ™: 1.50 ARRT Category A+ Credit: 1.75

Participants

Pina C. Sanelli, MD, Manhasset, NY (Moderator) Nothing to Disclose

LEARNING OBJECTIVES

1) Provide an overview of the departmental and institutional infrastructure needed to promote research in Radiology. 2) Understand how to develop a research curriculum for young investigators. 3) Describe metrics for tracking a successful research program.

SAM

New in 2017: PLEASE NOTE - All courses designated for SAM credit at RSNA 2017 will require attendees bring a personal device e.g. phone, iPad, laptop to complete the required test questions during the live session.

Sub-Events

RC502A Departmental Research Infrastructure and Support

Participants Pina C. Sanelli, MD, Manhasset, NY (*Presenter*) Nothing to Disclose

LEARNING OBJECTIVES

1) Provide an overview of the departmental and institutional infrastructure needed to promote research in Radiology. 2) Understand how to develop a research curriculum for young investigators. 3) Describe metrics for tracking a successful research program.

RC502B Developing a Research Curriculum and Mentoring

Participants Paul P. Cronin, MD, MS, Ann Arbor, MI (*Presenter*) Nothing to Disclose

LEARNING OBJECTIVES

View Learning Objectives under main course title

Active Handout: Paul P. Cronin

http://abstract.rsna.org/uploads/2017/17000160/Active RC502B.pdf

RC502C Research Organization at the Institutional Level

Participants Carolyn C. Meltzer, MD, Atlanta, GA (*Presenter*) Nothing to Disclose

For information about this presentation, contact:

cmeltze@emory.edu

LEARNING OBJECTIVES

View Learning Objectives under main course title

RC502D Strategic Planning for Obtaining Research Funding

Participants Ruth C. Carlos, MD, MS, Ann Arbor, MI (*Presenter*) Nothing to Disclose

For information about this presentation, contact:

rcarlos@umich.edu

LEARNING OBJECTIVES

View Learning Objectives under main course title

Honored Educators

Presenters or authors on this event have been recognized as RSNA Honored Educators for participating in multiple qualifying educational activities. Honored Educators are invested in furthering the profession of radiology by delivering high-quality educational content in their field of study. Learn how you can become an honored educator by visiting the website at:

https://www.rsna.org/Honored-Educator-Award/ Ruth C. Carlos, MD, MS - 2015 Honored Educator

RC502E Measuring and Tracking a Successful Research Program

Participants Jeffrey C. Weinreb, MD, New Haven, CT (*Presenter*) Consultant, Bracco Group;

For information about this presentation, contact:

jeffrey.weinreb@yale.edu

LEARNING OBJECTIVES

1) Understand metrics that may be used to quantitatively and qualitatively evaluate an academic research program. 2) Learn how to implement various principle and tools to build a successful academic research program.







RC503

Adult Congenital Heart Disease

Wednesday, Nov. 29 8:30AM - 10:00AM Room: S404CD



AMA PRA Category 1 Credits ™: 1.50 ARRT Category A+ Credit: 1.75

Participants

Dianna M. Bardo, MD, Phoenix, AZ (*Moderator*) Speaker, Koninklijke Philips NV; Consultant, Koninklijke Philips NV; Author, Thieme Medical Publishers, Inc

For information about this presentation, contact:

dbardo@phoenixchildrens.com

LEARNING OBJECTIVES

1) Recognize the most common congenital heart disease (CHD) findings in adults with unsuspected CHD. 2) Recognize findings of CHD in patients with know CHD and the findings which may trigger surgical intervention. 3) Know the commonly performed surgical procedures for palliation of CHD. 4) Understand why CT is an important imaging modality and is complementary to echo and MR for adult patients with CHD.

SAM

New in 2017: PLEASE NOTE - All courses designated for SAM credit at RSNA 2017 will require attendees bring a personal device e.g. phone, iPad, laptop to complete the required test questions during the live session.

Sub-Events

RC503A Coronary Artery Fistulas and Other Abnormal Connections

Participants

Jonathan D. Dodd, MD, Dublin 4, Ireland (Presenter) Nothing to Disclose

LEARNING OBJECTIVES

To recognize, analyze and report the important findings for coronary artery fistulas. To recognize, analyze and report the important findings of unroofed coronary sinus To recognise, analyse and report the important findings of partial anomalous pulmonary venous return

ABSTRACT

Coronary artery fistulas are important coronary anomalies that may present in adult life and are essential to recognize on cardiac CT, MRI and even on routine chest CT. The clinical presentations, diagnosis and treatment options for coronary artery fistulas will be described. Several additional abnormal vascular connections that can be identified on CT and MRI will also be presented, ranging from normal variants to hemodynamically insignificant connections to major shunts. A spectrum of the most common abnormal vascular connections will be covered with a focus on unroofed coronary sinus and partial anomalous pulmonary venous return and recognition of these important entities as well as potential treatment options.

RC503B CT of Complex Congenital Cardiac Anomalies

Participants Linda B. Haramati, MD, MS, Bronx, NY (*Presenter*) Spouse, Board Member, Kryon Systems Ltd

For information about this presentation, contact:

lharamati@gmail.com

LEARNING OBJECTIVES

1) To recognize complex congenital heart disease on chest CT scans performed for other indications. 2) To tailor cardiac CT protocols and reconstructions to answer specific clinical questions for patients with treated congenital heart. 3) disease-specifically congenitally corrected transposition of the great arteries, Ebstein anomaly and tetralogy of Fallot. 4) To provide information that guides therapy related to longstanding complications of congenital heart disease and its treatment.

ABSTRACT

Advances in treatment of congenital heart disease has resulted in prolonged survival of patients with congenital heart disease. These patients present for imaging to radiologists with general chest complaints and for dedicated cardiac imaging to resolve specific clinical questions. This lecture will focus on three complex congenital heart disease diagnoses; congenitally corrected transposition of the great arteries, Ebstein anomaly and tetralogy of Fallot. The chest CT findings of complex congenital heart disease should be recognized by radiologists in practice. Adults with milder spectrum complex congenital heart disease may initially be diagnosed during adulthood. Those who have had successful childhood treatment often fall through the gaps in care during the transition from pediatric to adulthood. Proper recognition of these diagnoses is of great importance and radiologists who are not subspecialized in cardiac imaging have the opportunity to greatly contribute to the care of these patients. Additionally, cardiac CT is a good alternative to MRI in answering crucial questions that arise during clinical care and on echocardiography. Emphasis will be placed on indications for CT, technical tips to achieve diagnostic images and on demonstrating complications that require intervention.

RC503C Role of MRI in Adult CHD Management

Participants

Mini V. Pakkal, FRCR, MBBS, Toronto, ON (Presenter) Nothing to Disclose

LEARNING OBJECTIVES

View Learning Objectives under main course title

RC503D Multimodality Approach to Congenital Heart Disease Diagnosis

Participants

Matthias Gutberlet, MD, PhD, Leipzig, Germany (*Presenter*) Speaker, Siemens AG; Speaker, Koninklijke Philips NV; Speaker, Bayer AG; Speaker, Bracco Group; Author, Thieme Medical Publishers, Inc

For information about this presentation, contact:

matthias_gutberlet@hotmail.com

LEARNING OBJECTIVES

1) To understand the non-ivasive assessment of surgically corrected Congenital Heart Disease (CHD) with different imaging modalities (x-ray, echocardiography, MDCT and MRI). 2) To understand the use of different non-invasive imaging modalities for the assessment of pathologic/postsurgical anatomy, ventricular function, flow quantification and tissue characterization using typical clinical examples. 3) To be able to choose the right imaging strategy for different CHD.

ABSTRACT

Transthoracic echocardiography remains the working-horse in children and adults with CHD. However, cross-sectional imaging modalities are getting more and more important, especially in adults with CHD. The number of patients with a lack of an adequate acoustic window for transthoracic echocardiography is increasing with age. The need for regular follow-up examinations is high in patients with CHD. Therefore, especially Cardiac Magnetic Resonance Imaging (CMR) with all its different options without the burden of radiation exposure is very benefitial and a good alternative to echocardiography and sometimes even better than echo. However, if mainly the correct depiction of the pathologic anatomy, especially after surgically corrected CHD, has to be evaluated or the patient is in a critical condition MDCT is the imaging modality of choice also in CHD. Of course, in these very young patients it is of utmost importance to use all methods to reduce radiation exposure. In a case based manner the pros an cons of the different imaging modalities and techniques available will be described during the refresher course.CHD after surgical correction like Tetralogy of Fallot and D-Transposition of the Great Arteries (TGA) will be covered as well as often accidentally discoverd CHD like partially anomalous pulmonary venous return.



103rd Scientific Assembly and Annual Meeting November 26 to December 1 McCormick Place, Chicago



RC504

Musculoskeletal Series: MRI of Small Joints

Wednesday, Nov. 29 8:30AM - 12:00PM Room: S406B



ARRT Category A+ Credits: 4.00 AMA PRA Category 1 Credits [™]: 3.25

FDA Discussions may include off-label uses.

Participants

David A. Rubin, MD, Saint Louis, MO (*Moderator*) Nothing to Disclose Hilary R. Umans, MD, Ardsley, NY (*Moderator*) Nothing to Disclose Stacy E. Smith, MD, Weston, MA (*Moderator*) Nothing to Disclose Connie Y. Chang, MD, Boston, MA (*Moderator*) Nothing to Disclose Ogonna K. Nwawka, MD, New York, NY (*Moderator*) Research Grant, General Electric Company

For information about this presentation, contact:

rubinda@wustl.edu

LEARNING OBJECTIVES

1) Learn some of the unique technical challenges associated with MR imaging of smaller joints in the body, and will be exposed to typical and atypical appearances of disorders in the hand, wrist, fingers, thumb, foot, and ankle.

Sub-Events

RC504-01 Small Joint Technique

Wednesday, Nov. 29 8:30AM - 8:55AM Room: S406B

Participants David A. Rubin, MD, Saint Louis, MO (*Presenter*) Nothing to Disclose

For information about this presentation, contact:

rubinda@wustl.edu

LEARNING OBJECTIVES

1) To better understand the proper use of RF coils and patient positioning to maximize image quality and minimize imaging artifacts when performing MR of small joints in the body.

RC504-02 Ankle

Wednesday, Nov. 29 8:55AM - 9:20AM Room: S406B

Participants Stacy E. Smith, MD, Weston, MA (*Presenter*) Nothing to Disclose

LEARNING OBJECTIVES

View Learning Objectives under main course title

RC504-03 Efficient High-Resolution MRI of Ankle Injuries: Comparison of a Novel 10-min 3D TSE Protocol against a 20-min 2D TSE Standard of Reference

Wednesday, Nov. 29 9:20AM - 9:30AM Room: S406B

Participants

Benjamin Fritz, MD, Zurich, Switzerland (*Presenter*) Nothing to Disclose Susanne Bensler, Zurich, Switzerland (*Abstract Co-Author*) Nothing to Disclose Gaurav K. Thawait, MD, Baltimore, MD (*Abstract Co-Author*) Nothing to Disclose Steven E. Stern, Brisbane, Australia (*Abstract Co-Author*) Nothing to Disclose Jan Fritz, MD, Baltimore, MD (*Abstract Co-Author*) Nothing to Disclose Jan Fritz, MD, Baltimore, MD (*Abstract Co-Author*) Research Grant, Siemens AG; Scientific Advisor, Siemens AG; Scientific Advisor, Alexion Pharmaceuticals, Inc; Speaker, Siemens AG

For information about this presentation, contact:

jfritz9@jhmi.edu

PURPOSE

To test the hypothesis that MRI of the ankle with a 4-fold accelerated 10-min 3D CAIPIRINHA SPACE prototype protocol is noninferior to a 2-fold accelerated 2D TSE standard for the diagnosis of internal derangement.

METHOD AND MATERIALS

Following institutional review board approval and informed consent, 70 symptomatic patients underwent ankle MRI using a 3T MRI system and boot-shaped surface coil. Six axial, sagittal and coronal IW and T2FS 2D TSE (20 min) and two sagittal isotropic IW and T2FS 3D TSE (10 min) pulse sequences were acquired. The novel 2x2-acclerated 3D SPACE TSE sequences used bi-directional parallel imaging and a CAIPIRINHA sampling pattern. The 70 2D/3D TSE data sets were separated into 140 anonymized and randomized individual studies. In each of the 140 studies, two musculoskeletal radiologists independently evaluated 6 joints, 12 ligaments, 9 tendons, and 9 bones for integrity and diagnostic confidence. Descriptive statistics, inter-rater reliability, intermodality concordance, and diagnostic confidence test were applied. A p-value of <0.05 was considered significant.

RESULTS

The overall inter-rater reliability was high with > 80% of matching ratings. The rater agreement was significantly higher for 3D TSE (p<0.05). The degree of diagnostic concordance between 2D and 3D TSE was high with a Kendall's coefficient W for cartilage of 0.784, ligaments of 0.732, tendons of 0.810, and bone of 0.847. Raters diagnosed a total of 116 cartilage defects on 2D and 109 on 3D images, 35 ligament tears on 2D and 65 on 3D, 18 tendon tears on 2D and 20 on 3D, and 137 bone abnormalities on 2D and 149 on 3D. The disagreements between 2D and 3D diagnoses for cartilage, ligaments, tendons, and bones were 15.7%, 4.5%, 1.4%, and 5.5%, respectively. The readers' diagnostic confidence was significantly higher for 3D TSE (p<0.05).

CONCLUSION

A novel 10-min 3D CAIPIRINHA SPACE MRI protocol is at least equivalent for the diagnosis of internal derangement of the ankle when compared to a 20-min 2D TSE standard of reference. Rater concordance and confidence were significantly higher for 3D TSE studies, indicating a higher rater definitiveness and possibly increased accuracy.

CLINICAL RELEVANCE/APPLICATION

Rapid 3D CAIPIRINHA SPACE TSE MRI is at least equivalent to a 2D TSE MRI reference standard for the diagnosis of internal ankle derangement and holds promise to substantially improve the efficiency of ankle MRI exams.

RC504-04 MRI Evaluation of Midtarsal (Chopart) Joint Sprain in the Setting of Acute Ankle Injury

Wednesday, Nov. 29 9:30AM - 9:40AM Room: S406B

Awards

Student Travel Stipend Award

Participants William Walter, MD, New York, NY (*Presenter*) Nothing to Disclose Zehava S. Rosenberg, MD, New York, NY (*Abstract Co-Author*) Nothing to Disclose Anna Hirschmann, MD, Basel, Switzerland (*Abstract Co-Author*) Nothing to Disclose Erin F. Alaia, MD, New York, NY (*Abstract Co-Author*) Nothing to Disclose Elisabeth R. Garwood, MD, New York, NY (*Abstract Co-Author*) Nothing to Disclose

For information about this presentation, contact:

william.walter@nyumc.org

PURPOSE

Midtarsal sprain is commonly misdiagnosed and may cause joint instability and chronic pain. Our study describes the normal MRI appearance of Chopart joint, determines patterns and frequency of osseous and ligamentous injuries, and evaluates prospective diagnosis and interobserver agreement for diagnosing midtarsal sprains in patients with acute ankle injuries.

METHOD AND MATERIALS

Two patient cohorts were created based on retrospective PACS searches (2/2014-8/2016): atraumatic controls and patients who obtained MRIs <8 weeks from ankle injury. MRIs were retrospectively reviewed in consensus for rmidtarsal sprains. Two radiologists independently reviewed the cases for midtarsal ligament and bony injuries, with attention to the dorsal calcaneocuboid, bifurcate, short and long plantar, and dorsal talonavicular ligaments. Interobserver agreement (kappa) was calculated. Prospective radiology reports and interobserver agreement were reviewed.

RESULTS

MRIs were reviewed from 47 patients with acute ankle injury (26 female, 21 male; mean age = 35 years, range 19-80). MRIs of 16 controls were also reviewed. Normal dorsal calcaneocuboid and calcaneocuboid component of the bifurcate ligaments were variably seen. The remaining normal ligaments were always seen. 11 patients (23%) had midtarsal sprain (8 acute/subacute, 1 probable, and 2 old). Six (67%) of the 9 recent sprains had concomitant lateral collateral ligament injury. 89% of osseous injuries were reported prospectively but 83% of ligament injuries were missed. Substantial interobserver agreement (kappas = 0.62-0.81) was achieved for diagnosis of midtarsal sprain.

CONCLUSION

Midtarsal sprains are commonly associated with acute ankle and lateral collateral ligament injuries. Presently, the entity is often unrecognized by musculoskeletal radiologists. Greater familiarity with the MRI spectrum of ligamentous and osseous injury at Chopart joint is important for accurate diagnosis and appropriate clinical management.

CLINICAL RELEVANCE/APPLICATION

Midtarsal sprains are often clinically misdiagnosed and overlooked on imaging. Radiologists should consider the diagnosis, especially in patients who have failed conservative management for presumed lateral ankle sprain and it should be sought in all lateral ankle sprains. Although conservative management is most common, surgical repair has been reported in the literature and shows promise to address chronic instability following midtarsal sprain.

Honored Educators

Presenters or authors on this event have been recognized as RSNA Honored Educators for participating in multiple qualifying

educational activities. Honored Educators are invested in furthering the profession of radiology by delivering high-quality educational content in their field of study. Learn how you can become an honored educator by visiting the website at: https://www.rsna.org/Honored-Educator-Award/ Zehava S. Rosenberg, MD - 2014 Honored Educator

RC504-05 Regional Variations of Ankle and Hindfoot Cartilage T2 Mapping Normative Values in Asymptomatic Subjects at 3.0 T MRI

Wednesday, Nov. 29 9:40AM - 9:50AM Room: S406B

Participants

Angela Chang, BS, Vail, CO (*Abstract Co-Author*) Nothing to Disclose Carly Lockard, MS, Vail, CO (*Presenter*) Nothing to Disclose Richard C. Shin, MD, Pasadena, CA (*Abstract Co-Author*) Nothing to Disclose Thomas Clanton, MD, Vail, CO (*Abstract Co-Author*) Research funded, Siemens AG; Research funded, Smith & Nephew plc; Research funded, Arthrex, Inc; Research funded, Ossur HF Charles P. Ho, MD, PhD, Vail, CO (*Abstract Co-Author*) Research funded, Siemens AG Research funded, Smith & Nephew plc Research funded, Arthrex, Inc Research funded, Ossur HF Scientific Advisory Board, Rotation Medical, Inc

For information about this presentation, contact:

clockard@sprivail.org

PURPOSE

To establish joint-specific methodology and baseline T2 values for ankle/hindfoot joint cartilage in asymptomatic subjects for clinical application in detecting ankle/hindfoot cartilage degeneration.

METHOD AND MATERIALS

Unilateral ankle scans with sagittal plane T2 mapping (TR: 1810 ms, TE: 10.7,21.4,32.1,42.8,53.5 ms; voxel size: 0.47×0.47×2.0 mm) were acquired at 3.0 T in 30 asymptomatic subjects, aged 23 - 64 years, with the ankle in neutral. All subjects provided informed consent and completed a subjective ankle symptom and function questionnaire and clinical exam. Images were manually segmented by two raters (a 3rd year medical student and a musculoskeletal radiologist) to separate the cartilage surfaces (tibiotalar, middle and posterior talocalcaneal, talonavicular, calcaneocuboid; proximal and distal articular surfaces). Regional median T2 was calculated for each subject and then the means and standard deviations of all subject medians were found. A 2-sample t-test was used to test for significant differences in mean T2* between regions. The anterior talocalcaneal joints were not analyzed due to small segmented volume and inconsistent visualization.

RESULTS

The tibial-side tibiotalar cartilage had the lowest mean T2 (39 ± 3 ms) and was significantly different than the tibiotalar talar-side, posterior talocalcaneal, middle talocalcaneal calcaneal-side, and calcaneocuboid calcaneal-side regions. The middle talocalcaneal calcaneal-side ms) and was significantly different than the talonavicular and tibial-side tibiotalar cartilage. Significant differences were also found between the tibiotalar talar-side cartilage and the talonavicular navicular-side cartilage.

CONCLUSION

Baseline T2 values for ankle/hindfoot joint cartilage regions were established. Mean T2 differed significantly for several ankle/hindfoot joint cartilage regions. These differences in normative ankle/hindfoot cartilage mean T2 should be considered when using T2 mapping to evaluate for ankle/hindfoot cartilage degeneration.

CLINICAL RELEVANCE/APPLICATION

T2 mapping may enable early cartilage degeneration detection. Regional differences in asymptomatic ankles/hindfeet should be considered when using T2 mapping to evaluate patients.

RC504-06 Ligament Evaluation of the Hind and Midfoot: Better Depiction by using Dixon Method in Ankle MRI

Wednesday, Nov. 29 9:50AM - 10:00AM Room: S406B

Participants

Esther Koh, Chonju, Chonbuk, Korea, Republic Of (*Presenter*) Nothing to Disclose Eun Hae Park, Jeon Ju, Korea, Republic Of (*Abstract Co-Author*) Nothing to Disclose Eunha Jeong, JEON-JU, Korea, Republic Of (*Abstract Co-Author*) Nothing to Disclose Weon Jang, Jeonju, Korea, Republic Of (*Abstract Co-Author*) Nothing to Disclose Ji Soo Song, MD, Jeonju, Korea, Republic Of (*Abstract Co-Author*) Nothing to Disclose Sol ki Kim, Chonju, Korea, Republic Of (*Abstract Co-Author*) Nothing to Disclose

For information about this presentation, contact:

kohesther@naver.com

PURPOSE

To determine if ankle magnetic resonance (MR) imaging using Dixon technique helps to depict hind and midfoot ligaments compared with those achieved without using Dixon technique.

METHOD AND MATERIALS

From July to December 2015 ankle MRI using Dixon technique of 48 ankles was obtained from 25 asymptomatic healthy volunteers. Twenty-three ligaments from hind and midfoot were chosen for evaluation. Two experienced reviewers separately rated the depiction of 23 ligaments from 7 sequences; axial T1-weighted image, axial, coronal, and sagittal T2-weighted Dixon in-phase image (represented as conventional T2-weighted image) and water phase image (represented as conventional fat-suppressed T2weighted image). The images were divided in to two sets. Set 1 was MRI using Dixon technique which composed of all 7 sequences. Set 2 represented conventional MRI composed of subsets with 4 different sequences including 2 nonfat-suppressed and 2 fatsuppressed plane. Ligaments were divided in to two groups. Major ligament included ATFL, CFL, PTFL, Lisfranc ligament, deltoid ligament, spring ligament. Other ligaments were categorized as minor ligament. The depiction rate was calculated using generalized estimating equations.

RESULTS

The depiction rate was significantly higher on set 1 compared with set 2; 91.3% versus 73.2 %, respectively. This was consistently observed for major ligament; 96.4% versus 76.1% (p<0.005). In set 2, the depiction rate was higher for subset with nonfat-suppressed axial and sagittal plane compared with those with axial and sagittal plane and coronal and saggital plane (82.7%, 77.6%, 70.7%, respectively).

CONCLUSION

For better depiction of hind and midfoot ligaments, all three axial, coronal and sagittal plane with non-fat suppressed sequences are required. The Ankle MRI using Dixon technique yielded better depiction rate of hind and midfoot ligaments by supplying both nonfat-suppressed and fat-suppressed sequences in single scan.

CLINICAL RELEVANCE/APPLICATION

Imaging of hind and midfoot ligament has few important points. Since ligaments of ankle and foot vary in their direction the optimization of plane of imaging is important. In addition, choosing right sequences are essential. By applying Dixon technique we can obtain multidirection multisequences in given time compared with conventional MR and this enables better delineation of ligaments of hind and midfoot.

RC504-07 Foot

Wednesday, Nov. 29 10:00AM - 10:20AM Room: S406B

Participants Hilary R. Umans, MD, Ardsley, NY (*Presenter*) Nothing to Disclose

Active Handout: Hilary Ruth Umans

http://abstract.rsna.org/uploads/2017/17000351/Active RC504-07.pdf

LEARNING OBJECTIVES

1) To review optimal MRI technique in imaging the distal forefoot. 2) To review normal anatomy and MRI appearance of the Hallucal-Sesamoid Complex and Metatarsophalangeal joints. 3) To review the etiology, clinical symptoms, physical exam findings and MRI correlates of Lesser Metatarsophalangeal joint Plantar Plate tear and Turf Toe. 4) To review the spectrum of painful soft tissue masses that may occur around the metatarsophalangeal joints and toes and their MRI appearance. 5) To review the spectrum of other painful conditions that affect the metatarsophalangeal joint region and hallucal sesamoids and their MRI imaging findings. 6) To review the relevant role of radiographs, ultrasound and computed tomography in diagnosis of distal forefoot pathology.

RC504-08 Wrist

Wednesday, Nov. 29 10:30AM - 10:50AM Room: S406B

Participants

Laura W. Bancroft, MD, Orlando, FL (Presenter) Author with royalties, Wolters Kluwer nv

For information about this presentation, contact:

laura.bancroft.md@flhosp.org

LEARNING OBJECTIVES

1) Review normal anatomy of the triangular fibrocartilage complex, intrinsic and extrinsic ligaments, and tendons on the wrist. 2) Evaluate pathology of the bones, TFCC, ligaments and tendons.

RC504-09 Magnetic Resonance Arthrography of the Wrist: Does Injection of the Distal Radioulnar Joint Alter Management?

Wednesday, Nov. 29 10:50AM - 11:00AM Room: S406B

Awards

Student Travel Stipend Award

Participants

Nathaniel B. Meyer, MD, Ann Arbor, MI (*Presenter*) Nothing to Disclose Corrie M. Yablon, MD, Ann Arbor, MI (*Abstract Co-Author*) Nothing to Disclose Yoav Morag, MD, Ann Arbor, MI (*Abstract Co-Author*) Nothing to Disclose Jon A. Jacobson, MD, Ann Arbor, MI (*Abstract Co-Author*) Nothing to Disclose Steven Haase, MD, Ann Arbor, MI (*Abstract Co-Author*) Nothing to Disclose

For information about this presentation, contact:

nbmeyer@med.umich.edu

PURPOSE

Magnetic resonance arthrography (MRA) of the wrist is commonly performed with a single radiocarpal joint (RCJ) injection dilute gadolinium (Gd) contrast. At our institution, if no contrast extends from the RCJ into the distal radioulnar joint (DRUJ) through the triangular fibrocartilage (TFC), then an additional injection of the DRUJ using iodinated contrast is performed to assess for a partial non-communicating, or one-way valve full thickness tear of the TFC. Although the literature has shown DRUJ injections improve the detection of such tears, it is unknown whether this alters surgical management. The aim of this retrospective study was to see if a clinical benefit is derived from the inclusion of a DRUJ injection in wrist MRA.

METHOD AND MATERIALS

The radiology database was searched for all wrist MRA's performed from January 2011 - May 2016. Fluoroscopic arthrogram reports were reviewed for findings of contrast extension through the TFC from the radiocarpal injection. MRA reports were reviewed on patients who subsequently underwent wrist arthroscopy or open surgical exploration. The presence of all types of TFCC tears was noted, including non-communicating peripheral tears extending from the DRUJ into the TFCC. Findings were correlated with surgical reports and interventions were noted.

RESULTS

A total of 282 patients underwent wrist MRA. Thirty-five of 282 patients underwent wrist arthroscopy or open exploration. Twentyone of 35 surgical patients had DRUJ injections in addition to a RCJ injection. Of these, 5 patients had suspected noncommunicating peripheral TFCC tears with possible extension to the DRUJ on MRA. Two of these 5 patients went on to surgical repair of the peripheral tear; however, both of these patients' tears were identified on arthroscopy using a radiocarpal portal. In no cases was the DRUJ inspected arthroscopically.

CONCLUSION

Our preliminary data suggests that DRUJ injection during wrist MRA does not alter surgical management. All surgical findings via open repair or radiocarpal arthroscopy were identified on single compartment RCJ injection.

CLINICAL RELEVANCE/APPLICATION

Distal radioulnar joint injection does not alter surgical management in patients with suspected TFCC injury and can be omitted during MRA of the wrist.

RC504-10 Primary Dorsal Ulnotriquetral Ligament Injury: An Uncommon yet Distinct Cause of Ulnar-Sided Wrist Pain

Wednesday, Nov. 29 11:00AM - 11:10AM Room: S406B

Participants

Mathieu Boily, MD, Montreal, QC (*Presenter*) Nothing to Disclose Rehana Jaffer, MD, Montreal, QC (*Abstract Co-Author*) Nothing to Disclose Emilie Sandman, Montreal, QC (*Abstract Co-Author*) Nothing to Disclose Alison C. Simioni, PhD, Westmount, QC (*Abstract Co-Author*) Nothing to Disclose Paul Martineau, MD, Montreal, QC (*Abstract Co-Author*) Nothing to Disclose

For information about this presentation, contact:

mathieu.boily@mcgill.ca

PURPOSE

Ulnar-sided wrist pain is a common presenting complaint. Determining the specific cause of ulnar-sided wrist pain is a challenge, largely due to the intricacy of the wrist's anatomy. One possible cause of ulnar-sided wrist pain is primary damage to the dorsal ulnotriquetral (DUT) ligament. Here, we tested this hypothesis. First, we identified a subgroup of patients with DUT ligament injury (confirmed at surgery) to devise specific MRI criteria for primary DUT ligament injury. Then, we retrospectively examined wrist arthrogram studies, using the aforementioned MRI criteria to detect the existence of primary DUT ligament pathology.

METHOD AND MATERIALS

Seventy-four MRI wrist arthrogram studies (46 male) were examined. Two fellowship trained musculoskeletal radiologists evaluated the arthrograms independently, without knowledge of previous clinical notes, MRI or surgical reports. Each study was examined for the following criteria: 1) DUT ligament abnormality (i.e. thickening, increased signal), 2) localized ulnar-sided wrist synovitis, 3) focal triguetral bone marrow edema, and 4) adjacent triguetral bone erosion. Other ulnar-sided wrist abnormalities were noted.

RESULTS

Abnormal DUT ligament was detected in 36.5% (27/74) of the wrist arthrogram studies. Of the 27 abnormal DUT ligament arthrograms, 7% (2/27) showed combined findings of localized ulnar-sided synovitis, adjacent triquetral bone marrow edema and erosion, suggesting primary DUT ligament pathology. In contrast, 93% (25/27) showed other ulnar-sided pathology (e.g. triangular fibrocartilage (13/25), extensor carpi ulnaris (5/25) pathology or a combination of both (7/25)) and were free of synovitis, triquetral bone marrow edema and erosion, suggestive of secondary or reactive DUT ligament pathology. MRI's were normal in 15/74 cases. Interobserver agreement was very good (K=0.89)

CONCLUSION

These findings argue that primary isolated injury to the DUT ligament is an uncommon, yet distinct source of ulnar-sided wrist pain. Secondary DUT ligament abnormalities are more common and associated with triangular fibrocartilage and extensor carpi ulnaris pathology.

CLINICAL RELEVANCE/APPLICATION

Primary and secondary DUT abnormalities can be identified on MR arthrograms. Primary DUT injury has specific clinical and MRI findings and should be included in the differential diagnosis of ulnar sided wrist pain. Its diagnosis is important as surgical intervention may be indicated in some cases.

RC504-11 Fingers

Wednesday, Nov. 29 11:10AM - 11:35AM Room: S406B

Participants Rosemary J. Klecker, MD, Columbus, OH (*Presenter*) Nothing to Disclose

For information about this presentation, contact:

LEARNING OBJECTIVES

1) To review the normal anatomy of the fingers including the pulley and capsule ligaments and the tendons. 2) To review MR Imaging technique of fingers. 3) To review etiology, clinical symptoms and physical findings with MR Imaging correlation of ligament, tendon and bone pathology. 4) To review the spectrum of painful conditionditions that affect the fingers. 5) To review the relevent and complimentary role of radiographs, ultrasound, and computed tomography in the diagnosis of pathological conditions of the finger.

RC504-12 Thumb

Wednesday, Nov. 29 11:35AM - 12:00PM Room: S406B

Participants

Linda Probyn, MD, Toronto, ON (Presenter) Nothing to Disclose

LEARNING OBJECTIVES

1) To describe relevant normal anatomy of the thumb including tendons, ligaments and pulleys. 2) To review MR Imaging technique of the thumb. 3) To improve knowledge of common pathologies affecting the thumb including trauma (tendon and ligaments - Stener's lesion), arthropathies, inflammatory conditions and tumors. 4) To describe how other imaging modalities (ultrasound, plain films, CT) can be complimentary to assist in diagnosing pathology of the thumb.



103rd Scientific Assembly and Annual Meeting November 26 to December 1 McCormick Place, Chicago



RC505

Neuroradiology Series: Brain Tumors

Wednesday, Nov. 29 8:30AM - 12:00PM Room: E451B



ARRT Category A+ Credits: 4.00 AMA PRA Category 1 Credits ™: 3.25

FDA Discussions may include off-label uses.

Participants

Rajan Jain, MD, Hartsdale, NY (*Moderator*) Consultant, Cancer Panels; Royalties, Thieme Medical Publishers, Inc James M. Provenzale, MD, Durham, NC (*Moderator*) Consultant, ArmaGen; Research Grant, Bayer AG; Consultant, Bayer AG; Consultant, Biomedical Systems; Consultant, Laboratory Corporation of America Holdings; Consultant, CurAccel, LLC; Research Grant, General Electric Company; Consultant, sanofi-aventis Group; Consultant, Guerbet SA; Consultant, Takeda Pharmaceutical Company Limited; Consultant, F. Hoffmann-La Roche Ltd

For information about this presentation, contact:

rajan.jain@nyumc.org

LEARNING OBJECTIVES

1) To review latest advances in brain tumor imaging diagnosis and assessment of therapy.

Sub-Events

RC505-01 Treatment of Glioblastoma in 2017: Where Do We Stand?

Wednesday, Nov. 29 8:30AM - 9:00AM Room: E451B

Participants

Roger Stupp, MD, Chicago, IL (*Presenter*) Spouse, Employee, Celgene Corporation; Research Consultant, Celgene Corporation; Research Consultant, Merck & Co, Inc; Research Consultant, Novartis AG; Research Consultant, NovoCure Ltd; Research Consultant, F. Hoffmann-La Roche Ltd

RC505-02 Compactness of Peritumoral Edema on Routine MRI Appears to Distinguish Tumor Recurrence from Pseudo-Progression in Primary Brain Tumors: Preliminary Findings

Wednesday, Nov. 29 9:00AM - 9:10AM Room: E451B

Participants

Marwa Ismail, PhD, Cleveland, OH (*Abstract Co-Author*) Nothing to Disclose Prateek Prasanna, Cleveland, OH (*Abstract Co-Author*) Nothing to Disclose Raymond Y. Huang, MD, PhD, Boston, MA (*Abstract Co-Author*) Nothing to Disclose Gagandeep Singh, MD, Cleveland, OH (*Abstract Co-Author*) Nothing to Disclose Rajat Thawani, Cleveland, OH (*Abstract Co-Author*) Nothing to Disclose Anant Madabhushi, PhD, Piscataway, NJ (*Abstract Co-Author*) Nothing to Disclose Pallavi Tiwari, PhD, Cleveland, OH (*Presenter*) Nothing to Disclose

For information about this presentation, contact:

pxt130@case.edu

PURPOSE

Following aggressive chemo-radiation, a significant challenge in brain tumors is distinguishing pseudo-progression (PsP), a temporary radiation-induced treatment effect, from tumor recurrence (TR). On conventional MRI, PsP closely mimics the appearance of TR, making their visual identification challenging. It is suggested that PsP causes a pronounced local inflammatory tissue response due to inherent and radiotherapy-induced capillary permeability, leading to more pronounced edema. Unfortunately, guidelines set by RANO/Macdonald's criteria are based solely on 2-dimensional (2D) measurements of the enhancing tumor alone, and do not capture subtle morphometric differences in the edema component across PsP and TR. In this work, we hypothesized that quantitative 3D shape features (e.g. roundness, spherical radius, flatness, compactness) obtained from the edema component contribute to morphometric differences across PsP and TR, and may help distinguish them on routine MRI.

METHOD AND MATERIALS

33 MRI studies (Gd-T1w, T2w, FLAIR) were acquired from an IRB approved study (11 PsP, 22 TR cases). Co-registration, bias correction, and intensity standardization were first performed. Expert delineation of enhancing lesion was performed on T1w, and of peritumoral edema on T2w and FLAIR. 14 shape features, including volume, major and minor axis lengths, eccentricity, elongation, orientation, perimeter, roundness, spherical radius, flatness, compactness, were then computed from enhancing tumor and edema regions for all subjects. Finally, Wilcoxon Rank-Sum Test was employed to identify the statistically significant features between PsP and TR.

Compactness in edema component showed significant differences between the two groups (p=0.05). Mean and standard deviation of the edema compactness were found to be 2.9 +/- 0.63 and 2.4 +/- 0.48 for TR and PsP groups respectively.

CONCLUSION

Differences in compactness of the edema region were reported between PsP and TR in this preliminary study. These morphometric differences may be attributed to pronounced edema in PsP due to increased inflammation, leading to less compact lesion characteristics.

CLINICAL RELEVANCE/APPLICATION

Reliable distinction of PsP from TR would allow for early identification of patients with TR who are subject to "wait-and-watch" as their tumor continues to grow, while avoiding overtreatment in PsP.

RC505-03 The Role of Apparent Diffusion Coefficient in Patients with Choroid Plexus Tumors

Wednesday, Nov. 29 9:10AM - 9:20AM Room: E451B

Participants

Tomoaki Sasaki, MD, Iowa City, IA (*Presenter*) Nothing to Disclose Toshio Moritani, MD, PhD, Iowa City, IA (*Abstract Co-Author*) Nothing to Disclose Aristides A. Capizzano, MD, Iowa City, IA (*Abstract Co-Author*) Nothing to Disclose Yutaka Sato, MD, Iowa City, IA (*Abstract Co-Author*) Nothing to Disclose Patricia A. Kirby, Iowa City, IA (*Abstract Co-Author*) Nothing to Disclose Shunta Ishitoya, Asahikawa, Japan (*Abstract Co-Author*) Nothing to Disclose Akiko Oya, Asahikawa, Japan (*Abstract Co-Author*) Nothing to Disclose Masahiro Toda, Asahikawa, Japan (*Abstract Co-Author*) Nothing to Disclose Koji Takahashi, MD, Asahikawa, Japan (*Abstract Co-Author*) Nothing to Disclose

For information about this presentation, contact:

tomoaki-sasaki@uiowa.edu

PURPOSE

The aim of this study is to explore the role of apparent diffusion coefficient (ADC) as a predictor of outcome for choroid plexus tumors.

METHOD AND MATERIALS

We retrospectively analyzed ADC maps in 14 patients histologically proven with 8 choroid plexus papillomas (CPP, WHO grade 1), 3 atypical choroid plexus papillomas (aCPP, grade 2), and 3 choroid plexus carcinomas (CPC, grade 3). Mean ADC and tumor volume were assessed with the WHO grades using Spearman rank test, Kruskal-Wallis test, ROC analysis, and multiple linear regression analysis. Moreover, we performed Log-rank test to determine survival.

RESULTS

The median mean ADCs were $1.82 \times 10-3 \text{ mm2/s}$ in the CPP, $1.26 \times 10-3 \text{ mm2/s}$ in the aCPP, and $0.983 \times 10-3 \text{ mm2/s}$ in the CPC, respectively (Spearman rank coefficient r = -0.741, P = 0.002; Kruskal-Wallis test, P = 0.028). The median tumor volumes were $1.22 \times 104 \text{ mm3}$ in the CPP, $1.30 \times 104 \text{ mm3}$ in the aCPP, and $8.37 \times 104 \text{ mm3}$ in the CPC, respectively (Spearman rank coefficient r = 0.650, P = 0.012; Kruskal-Wallis test, P = 0.033). The post-hoc tests revealed the significant differences between the CPP and CPC (P = 0.040 in the mean ADC, p = 0.028 in the tumor volume, respectively). The ROC analyses demonstrated the cutoff ADC value, $1.38 \times 10-3 \text{ mm2/s}$, showed sensitivity 0.833 and specificity 1.00 for aCPP, sensitivity 1.00 and specificity 0.818 for CPC, respectively. In the tumor volume, the ROC showed the cutoff value, $4.39 \times 104 \text{ mm3}$, to diagnose CPC with sensitivity 1.00 and specificity 1.00. The multiple linear regression analysis demonstrated both the mean ADC ($\beta = -0.582$, P = 0.002) and tumor volume ($\beta = 0.499$, P = 0.005) significantly contributed to the WHO grades (Adjusted R2 0.769, P = 0.005). The mean follow-up period was 52 months. Three patients (1 aCPP and 2 CPC) died of their diseases during the follow-up period. The Log-rank test revealed the cutoff ADC value, $1.38 \times 10-3 \text{ mm2/s}$, or lower presented significantly worse prognosis (P = 0.007).

CONCLUSION

The mean ADC negatively and tumor volume positively correlated with WHO grade in the choroid plexus tumors. Both ADC and tumor volume contributed to the WHO grade. The lower ADC could be an adverse prognostic factor.

CLINICAL RELEVANCE/APPLICATION

A combination of ADC and tumor volume could distinguish the WHO grades in choroid plexus tumors. In addition to the WHO grades, lower ADC value could be an adverse prognostic factor.

RC505-04 Comparison of Dynamic Contrast Enhanced (DCE) and Dynamic Susceptibility Contrast (DSC) in Differentiating Tumor Recurrence and Radiation Necrosis in High Grade Gliomas

Wednesday, Nov. 29 9:20AM - 9:30AM Room: E451B

Participants

Nader Z. Zakhari, MBBCh, Ottawa, ON (*Presenter*) Nothing to Disclose Michael Taccone, Ottawa, ON (*Abstract Co-Author*) Nothing to Disclose Carlos H. Torres, MD,FRCPC, Ottawa, ON (*Abstract Co-Author*) Nothing to Disclose Santanu Chakraborty, FRCR, FRCPC, Ottawa, ON (*Abstract Co-Author*) Grant, Bayer AG Grant, General Electric Company John Sinclair, MD, Ottawa, ON (*Abstract Co-Author*) Nothing to Disclose Thanh Nguyen, MD, Ottawa, ON (*Abstract Co-Author*) Research Grant, GE; Gerard Jansen, MD, Ottawa, ON (*Abstract Co-Author*) Nothing to Disclose John Woulfe, MD, Ottawa, ON (*Abstract Co-Author*) Nothing to Disclose Gregory O. Cron, Ottawa, ON (*Abstract Co-Author*) Nothing to Disclose Rebecca Thornhill, PhD, Ottawa, ON (*Abstract Co-Author*) Nothing to Disclose

PURPOSE

The appearance of a new enhancing lesion after surgery and chemoradiation for high grade glioma (HGG) presents a common diagnostic dilemma. We compare the diagnostic accuracy of DCE and DSC in differentiating tumor recurrence (TR) from radiation necrosis (RN) in this clinical scenario.

METHOD AND MATERIALS

We prospectively enrolled 98 consecutive HGG patients with a new enhancing lesion on post-treatment MRI. Each patient underwent a 3T MR examination including DCE, DSC sequences . The lesions were classified as TR and RN based on histopathology or clinical/imaging follow-up. A neuropathologist identified the percentage of TR and RN in each surgical lesion. We performed hot spot and histogram quantitative analysis of CBV, corrected CBV, Ktrans, AUC, Vp and ADC maps using a commercial software (Olea Sphere 1, Olea Medical). Ratio (lesion/white matter) was also obtained. Differences between the two patient groups were assessed via Mann-Whitney U test. ROC curve analysis was also performed. Correlation coefficient was used to express the correlation between TR percentage and perfusion parameters.

RESULTS

Thirty-two patients were excluded due to inadequate follow up or technical limitation. Total of 68 lesions (37 TR, 28 RN, 3 equal proportions of TR and RN), 43 lesions were surgically resected. TR had significantly higher CBV (p=0.01), corrected CBV (p=0.03), CBV ratio (p=0.02), corrected CBV ratio (p=0.02), AUC ratio (p=0.02) and Vp ratio (p=0.02) than RN on hot spot analysis with ROC area under the curve 0.69 (p=0.0049), 0.67 (p=0.02), 0.67 (p=0.02), 0.68 (p=0.01), 0.67 (p=0.02) and 0.67 (p=0.01) respectively. On histogram analysis, TR had significantly higher CBV and corrected CBV maximal value (p=0.02, p=0.01) compared with RN. There is correlation between the TR % and corrected CBV (r=0.31, p=0.049), CBV (r=0.35, p=0.02) and AUC ratio (r=0.52, p=0.0005). No significant difference or correlation seen for the rest of the maps.

CONCLUSION

MR perfusion parameters assessing the blood volume (CBV, corr CBV, Vp) are more useful than leakage measurement in differentiating TR and RN. Permeability MR derived Ktrans did not show significant difference between the two groups nor significant correlation with TR percentage.

CLINICAL RELEVANCE/APPLICATION

The results of this study suggest that blood volume measurements from DSC or DCE are more useful than DCE derived permeability measurements (Ktrans) in differentiating TR and RN.

Honored Educators

Presenters or authors on this event have been recognized as RSNA Honored Educators for participating in multiple qualifying educational activities. Honored Educators are invested in furthering the profession of radiology by delivering high-quality educational content in their field of study. Learn how you can become an honored educator by visiting the website at: https://www.rsna.org/Honored-Educator-Award/ Carlos H. Torres, MD,FRCPC - 2017 Honored Educator

RC505-05 High Resolution Two and Three Dimensional Fast Magnetic Resonance Spectroscopic Imaging of Brain Tumors at 7 T

Wednesday, Nov. 29 9:30AM - 9:40AM Room: E451B

Participants

Stephan Gruber, MD, Vienna, Austria (*Presenter*) Nothing to Disclose Gilbert Hangel, Vienna, Austria (*Abstract Co-Author*) Nothing to Disclose Eva Heckova, Vienna, Austria (*Abstract Co-Author*) Nothing to Disclose Bernhard Strasser, Vienna, Austria (*Abstract Co-Author*) Nothing to Disclose Michal Povazan, Vienna, Austria (*Abstract Co-Author*) Nothing to Disclose Siegfried Trattnig, MD, Vienna, Austria (*Abstract Co-Author*) Nothing to Disclose Wolfgang Bogner, MSc, Vienna, Austria (*Abstract Co-Author*) Nothing to Disclose

For information about this presentation, contact:

stephan@nmr.at

PURPOSE

Magnetic resonance spectroscopic imaging (MRSI) of the brain allows to map several metabolites and provide complementary metabolic information to the conventional MR imaging methods. High field systems (7 T) offer increased SNR and spectral resolution which can be transformed to increased spatial resolution, better characterization of overlapping metabolites and/or acceleration of the measurement. With accelerated 2D/3D-FID-MRSI at 7 T metabolic maps of eight different metabolites can be obtained in clinical feasible measurement times. In this study, we applied accelerated MRSI with ultrashort acquisition delays (TE*) of 1.5ms in 9 patients with brain tumors.

METHOD AND MATERIALS

9 patients with glioma (6m/3f, age:42±5) were measured with 2D/3D-FID-MRSI (8/1 patients) at 7T (7T Magnetom, Siemens, Germany) using a 32-channel head coil. A 5-fold accelerated 2D-FID-MRSI sequence with 64×64 phase encoding steps, FOV=220×220mm2, TR=600ms, TE*=1.5ms, in plane voxel size 3.4×3.4 mm2, and a slice thickness of 10 mm was used (scan time 6min). One patient was measured with accelerated 3D-FID-MRSI (Hadamard encoded; 4 slices 0.8 cm thick, TE*s= 1.3, 2.3, 3.3, 4.3 ms; scan time 13.3 min). Metabolic maps were created based on results from LCModel.

RESULTS

Good data quality was achieved from all patients measured at 7T. Compared to techniques using pre-localization techniques (e.g. STEAM, PRESS) FID-CSI allows to acquire whole slices. The high matrix size and hamming filtering prevented fat contamination from the sculp. With the high in-plane resolution of 3.4×3.4 mm2 metabolic maps showing anatomical details could be created. In all patients, tNAA was reduced in glioma. tCho was increased in all patients, except in the patient with diffuse astrocytoma. In addition, we found alternations in several (j-coupled) resonances such as myo-Inositol, glutamate, glutamine and glycine.

CONCLUSION

Accelerated MRSI at 7 T allows to measure an extended neurochemical profile in only $\sim 6 \text{min}/\sim 13 \text{min}$ (2D-/3D-MRSI). This allows the quantification of potentially therapy-relevant metabolites such as myo-Inositol, glutamate, glutamine and glycine with low CRLBs and highlights the potential of fast clinical FID-MRSI at 7T in tumor patients.

CLINICAL RELEVANCE/APPLICATION

Accelerated, full-slice, high-resolution FID-MRSI with ultrashort TE* at 7T unveils the potential of clinical MRSI in tumor patients and neurologic studies in general.

RC505-06 WHO Decided to Reclassify Brain Tumors?

Wednesday, Nov. 29 9:40AM - 10:10AM Room: E451B

Participants

Soonmee Cha, MD, San Francisco, CA (Presenter) Nothing to Disclose

LEARNING OBJECTIVES

1) Succinctly review the main highlights of 2016 WHO CNS Tumor Classification focusing on new or restructured CNS tumors. 2) Become familiar with several key molecular markers that define specific CNS tumor entities. 3) Discuss imaging relevance of the new or restructured CNS tumors. 4) Present importance of integrated diagnosis of CNS tumors and the role of imaging in the molecular era of tumor diagnosis and classification.

RC505-07 How Should Radiogenomics Influence Image Interpretation?

Wednesday, Nov. 29 10:20AM - 10:50AM Room: E451B

Participants

Rivka R. Colen, MD, Houston, TX (Presenter) Research Grant, General Electric Company;

LEARNING OBJECTIVES

1) Understand and review the literature on radiogenomics focusing on the predictions of key genomic markers such as MGMT, EGFR, IDH1, etc. 2) Obtain basic knowledge on the potential clinical radiogenomic biomarkers. 3) Understand the use of 2HG MRS for evaluation of IDH1 mutation. 4) Interpreting imaging in the era of genomics and radiogenomics.

ABSTRACT

Radiogenomics is the linkage of imaging characteristics with the genomic profile of the tumor or tissue. Currently, imaging is typically reviewed in isolation of the genomic profile of the patient. However, with the use of genomics for stratification into molecular-targeted clinical trials, use for prognosis, and evaluation of likely response, imaging reads and analysis in the context specific important genomic markers is important.

RC505-08 Assessment of Tissue Heterogeneity Using MR Textural Analysis for Grading Gliomas

Wednesday, Nov. 29 10:50AM - 11:00AM Room: E451B

Awards

Student Travel Stipend Award

Participants

Austin Ditmer, Cincinnati, OH (*Presenter*) Nothing to Disclose Bin Zhang, PhD, Cincinnati, OH (*Abstract Co-Author*) Nothing to Disclose Taimur Shujaat, MD, Cincinnati, OH (*Abstract Co-Author*) Nothing to Disclose Andrew A. Pavlina, MD, Cincinnati, OH (*Abstract Co-Author*) Nothing to Disclose Nicholas Luibrand, MD, Cincinnati, OH (*Abstract Co-Author*) Nothing to Disclose Mary F. Gaskill-Shipley, MD, Cincinnati, OH (*Abstract Co-Author*) Nothing to Disclose Achala S. Vagal, MD, Cincinnati, OH (*Abstract Co-Author*) Research Grant, F. Hoffmann-La Roche Ltd

For information about this presentation, contact:

ditmerad@mail.uc.edu

PURPOSE

Textural analysis can quantify variations in surface intensity or patterns, including some that are imperceptible to the human visual system. Our objective was to determine the diagnostic accuracy of textural analysis (TA) in differentiating high from low-grade gliomas by assessing tumor heterogeneity.

METHOD AND MATERIALS

Patients with a histopathological diagnosis of glioma and preoperative 3T MRI imaging were included in this retrospective study. A region of interest enclosing the largest cross-sectional area of the tumor was manually delineated on post contrast T1 images. TA was assessed with a commercially available research software (TexRAD Ltd, Cambridge, UK) using a filtration-histogram technique. The histogram parameters including mean pixel intensity, standard deviation of the pixel histogram (SD), entropy, mean of the positive pixels (MPP), skewness (asymmetry), and kurtosis (peakness) were analyzed at various spatial scaling factors (SSF) ranging from 0-6 mm. The parameters were correlated with WHO glioma grade using Spearman correlation. Areas under the curve (AUC) were calculated using ROC curve analysis to distinguish tumor grades.

RESULTS

Of a total of 94 patients, 14 had WHO low-grade gliomas (LGG) (Gr I = 2, Gr II =12) and 80 had WHO high-grade gliomas (HGG) (Gr III = 17, Gr IV = 63). TA parameters including mean, SD, MPP, entropy and kurtosis showed significant differences between glioma grades for different filters, most prominently at SSF 2 mm with lower values in LGG vs. HGG (p<0.001). The correlation between the glioma grades and HGG vs. LGG for all parameters except skewness for SSF 2 mm was significant (p<0.001) (Image). Diagnostic

ability for TA to differentiate between the different sub-groups (grade II-IV) at SSF 2 mm was also significant. LGG and HGG were best-discriminated using mean of 2 mm fine texture scale, with a sensitivity and specificity of 93% and 86 % (AUC of 0.90).

CONCLUSION

Quantitative measurement of heterogeneity using textural analysis can discriminate high versus low-grade gliomas.

CLINICAL RELEVANCE/APPLICATION

Textural analysis can be a complimentary tool for lesion characterization, particularly where conventional MR features may not be sufficient.

RC505-09 A CAD System to Track Brain Metastases on MRI Over Time

Wednesday, Nov. 29 11:00AM - 11:10AM Room: E451B

Participants

Michel Bilello, MD, PhD, Philadelphia, PA (Presenter) Nothing to Disclose

PURPOSE

Interpreting serial brain MRI studies can be a tedious and error-prone task for the neuroradiologist, in both qualitative and quantitative assessment of change in metastatic disease load. This is particularly relevant as gamma knife radiotherapy is becoming widely used to treat metastases, and it is therefore critical to report response to treatment and possibly new metastases accurately. These limitations and opportunities highlight the need for the development of a computer-aided detection (CAD) system to detect and quantify changes in brain metastatic disease over time.

METHOD AND MATERIALS

Brain MRI images were acquired from 15 patients with known metastatic disease who had undergone gamma knife therapy, for a total of 17 cases with current and prior studies. The system applies a pre-processing pipeline to the T2/FLAIR and postgadolinium T1 sequences of both prior and current studies, including coregistration, skull-stripping, and intensity normalization. The program then generates forward and backward difference maps on each modality, highlighting interval increase or decrease in lesion load on T1 postgad, and interval change in abnormal signal (representing vasogenic edema or treatment-related changes) on T2/FLAIR respectively. Detected changes are color-coded and displayed on subtraction maps. The program takes 2 to 3 minutes to run on a desktop Linux workstation. Performance, including sensitivity and rate of false positive detection, was assessed by comparison with a human expert.

RESULTS

Results demonstrate a sensitivity around 95% for new/progressed enhancing lesions on postgadolinium T1 images, 95% for new/progressed areas of abnormal T2 signal on T2/FLAIR, 82% for resolved/improved enhancing lesions on postgadolinium T1, and 86% for resolved/improved areas of abnormal T2 signal on T2/FLAIR. False positives occured mainly in the extracranial structures such as skull base and orbits, and were easily discarded.

CONCLUSION

This preliminary work demonstrates the feasibility of a CAD system to monitor changes in both abnormal T2 signal and enhancing lesions associated with metastatic disease in the brain.

CLINICAL RELEVANCE/APPLICATION

A CAD system that helps monitor temporal changes in brain metastases on MRI would improve clinical care through increased reproducibility and accuracy, and shorter turn-around time over human-only interpretation.

RC505-11 Application of Machine Learning Algorithm and ADC Histogram Profile for Differentiation of Posterior Cranial Fossa Brain Tumors

Wednesday, Nov. 29 11:20AM - 11:30AM Room: E451B

Awards

Student Travel Stipend Award

Participants Seyedmehdi Payabvash, MD, San Francisco, CA (*Presenter*) Nothing to Disclose Tarik Tihan, San Francisco, CA (*Abstract Co-Author*) Nothing to Disclose Soonmee Cha, MD, San Francisco, CA (*Abstract Co-Author*) Nothing to Disclose

For information about this presentation, contact:

spayab@gmail.com

PURPOSE

To apply machine learning algorithm for differentiation of posterior cranial fossa brain tumors using ADC histogram variables and structural MR imaging characteristics.

METHOD AND MATERIALS

All patients with intra-axial/intra-ventricular posterior cranial fossa tumors, and surgical pathology diagnosis (2004-2015), were included. The ADC percentile values of solid tumor component were calculated. For machine learning analysis, decision tree algorithm was applied to identify specific ADC and imaging variables to identify each specific tumor.

RESULTS

A total of 256 patients were included with histologic tumor subtypes listed in Table 1. Medulloblastomas had the lowest, and Pilocytic astrocytomas had the highest ADC values (Figure 1). Separate decision tree analyses identified different ADC histogram variables, age cut offs, enhancement patterns, and tumor textures that could differentiate specific tumor types. A 5th percentile

ADC value<700×10-6mm2/s identified all *medulloblastomas* (p<0.001); and a minimum ADC value<550×10-6mm2/s identified all *atypical teratoid/rhabdoid tumors* (ATRTs) (p=0.021). The majority (31/43) of patients with *pilocytic astrocytomas* were <25 years old (YO), and all were <47 YO (p<0.001). But all patients with *metastasis* were >30 YO, and the majority (53/65) were >47 YO (p<0.001). Also, 7/8 patients with *lymphoma* were >55 YO (p=0.003). A homogenous enhancement pattern (p<0.001), and cystic texture (p=0.025) could identify *hemangioblastomas*. All lower grade *gliomas and astrocytomas* had T2 hyperintense solid component (p<0.001). A 4th ventricular location (25/27) was predictor of *ependymomas* (p<0.001), but not of *medulloblastomas*. Five of 6 *subependymomas* (p<0.001) and all *choroid plexus papillomas* (n=4, p<0.001) were localized to the 4th ventricle floor or obex. However, all 7 *anaplastic astrocytomas*, and 6 *glioblastomas* originate from brainstem or cerebellar hemispheres (p=0.001).

CONCLUSION

Machine learning decision tree algorithms can help differentiate brain tumors based on ADC histogram variables and imaging characteristics. Specifically, quantitative assessment of the highly cellular component in posterior cranial fossa brain tumors represented by lower percentile ADC values can identify medulloblastomas and ATRT.

CLINICAL RELEVANCE/APPLICATION

Radiologists can use decision tree algorithms to determine main imaging characteristics for identification of tumor type and formulating the differential diagnoses.

RC505-12 Deep Learning and Traditional Machine Learning for Radiogenomics

Wednesday, Nov. 29 11:30AM - 12:00PM Room: E451B

Participants

Bradley J. Erickson, MD, PhD, Rochester, MN (*Presenter*) Stockholder, OneMedNet Corporation; Stockholder, VoiceIt Technologies, LLC; Stockholder, FlowSigma; Researcher, nVIDIA Corporation

For information about this presentation, contact:

bje@mayo.edu

LEARNING OBJECTIVES

1) Become familiar with the state of the art of deep learning applied to medical imaging. 2) Learn the distinciton between traditiona lmachine learning methods and deep learning. 3) Learn the capabilities of deep learning to identify genomic and repsonse properties of tumors.





103rd Scientific Assembly and Annual Meeting November 26 to December 1 McCormick Place, Chicago



RC506

Head & Neck College Bowl: A Game Show (Case-Based Competition)

Wednesday, Nov. 29 8:30AM - 10:00AM Room: E450B



AMA PRA Category 1 Credits ™: 1.50 ARRT Category A+ Credit: 1.75

Participants

C. Douglas Phillips, MD, New York, NY (*Presenter*) Stockholder, MedSolutions, Inc Consultant, Guerbet SA Richard H. Wiggins III, MD, Salt Lake City, UT (*Presenter*) Nothing to Disclose Tabassum A. Kennedy, MD, Madison, WI (*Presenter*) Nothing to Disclose

LEARNING OBJECTIVES

1) Review the normal imaging anatomy of the head and neck. 2) Identify imaging pathologies of the head and neck. 3) Describe the important imaging differentials of pathologies of the head and neck.

ABSTRACT

This interactive session will use RSNA Diagnosis Live[™]. Please bring your charged mobile wireless device (phone, tablet or laptop) to participate. Head & Neck College Bowl: A Diagnosis Live Game Show 1) Review the normal imaging anatomy of the head and neck. 2) Identify imaging pathologies of the head and neck. 3) Describe the important imaging differentials of pathologies of the head and neck. The head and neck region has some of the most intricate anatomy of the human body. This refresher course will review the complex anatomy of the head and neck, such as the cervical soft tissues, orbit, skull base, temporal bone, and cranial nerves, as well as the imaging techniques to best evaluate this region. The anatomy and normal imaging appearances will be described and reviewed. You will laugh, you will cry, you will like it more than Cats.

Honored Educators

Presenters or authors on this event have been recognized as RSNA Honored Educators for participating in multiple qualifying educational activities. Honored Educators are invested in furthering the profession of radiology by delivering high-quality educational content in their field of study. Learn how you can become an honored educator by visiting the website at: https://www.rsna.org/Honored-Educator-Award/ Richard H. Wiggins III, MD - 2012 Honored Educator



KSNA° 2017

103rd Scientific Assembly and Annual Meeting November 26 to December 1 McCormick Place, Chicago



RC507

A Case-based Audience Participation Session (Genitourinary) (An Interactive Session)

Wednesday, Nov. 29 8:30AM - 10:00AM Room: N226

GU

AMA PRA Category 1 Credits ™: 1.50 ARRT Category A+ Credit: <u>1.75</u>

FDA Discussions may include off-label uses.

Participants

William W. Mayo-Smith, MD, Boston, MA (*Coordinator*) Author with royalties, Reed Elsevier; William W. Mayo-Smith, MD, Boston, MA (*Moderator*) Author with royalties, Reed Elsevier; Andrea G. Rockall, MRCP, FRCR, London, United Kingdom (*Presenter*) Nothing to Disclose Christine O. Menias, MD, Chicago, IL (*Presenter*) Nothing to Disclose

For information about this presentation, contact:

menias.christine@mayo.edu

LEARNING OBJECTIVES

1) The participant will be introduced to a series of Genitourinary case studies via an interactive team game approach designed to encourage 'active' consumption of educational content. 2) The participant will be able to use their mobile wireless device (tablet, phone, laptop) to electronically respond to various Genitourinary case challenges; participants will be able to monitor their individual and team performance in real time. 3) The attendee will receive a personalized self-assessment report via email that will review the case material presented during the session along with individual and team performance.

ABSTRACT

The extremely popular audience participation educational experience is back! GU Diagnosis Live is an expert-moderated session featuring a series of interactive Genitourinary case studies that will challenge radiologists' diagnostic skills and knowledge. Building on last year's successful Diagnosis Live premiere, GU Diagnosis Live is a lively, fast-paced game format: participants will be automatically assigned to teams who will then use their personal mobile devices to test their knowledge of GU radiology in a fast-paced session that will be both educational and entertaining. After the session, attendees will receive a personalized self-assessment report via email that will revview the case material presented durinig the session, along with individual and team performance. This interactive session will use RSNA Diagnosis LiveTM. Please bring your charged mobile wireless device (phone, tablet or laptop) to participate.

Honored Educators

Presenters or authors on this event have been recognized as RSNA Honored Educators for participating in multiple qualifying educational activities. Honored Educators are invested in furthering the profession of radiology by delivering high-quality educational content in their field of study. Learn how you can become an honored educator by visiting the website at: https://www.rsna.org/Honored-Educator-Award/ Andrea G. Rockall, MRCP, FRCR - 2017 Honored EducatorChristine O. Menias, MD - 2013 Honored EducatorChristine O. Menias, MD - 2014 Honored EducatorChristine O. Menias, MD - 2015 Honored EducatorChristine O. Menias, MD - 2017 Honored Educator





103rd Scientific Assembly and Annual Meeting November 26 to December 1 McCormick Place, Chicago



RC508

Emergency Radiology Series: Current Imaging of the Acute Abdomen

Wednesday, Nov. 29 8:30AM - 12:00PM Room: S405AB



ARRT Category A+ Credits: 4.00 AMA PRA Category 1 Credits ™: 3.25

Participants

Michael N. Patlas, MD, FRCPC, Hamilton, ON (*Moderator*) Nothing to Disclose John J. Hines JR, MD, New Hyde Park, NY (*Moderator*) Nothing to Disclose Douglas S. Katz, MD, Mineola, NY (*Moderator*) Nothing to Disclose Mariano Scaglione, MD, Castel Volturno, Italy (*Moderator*) Nothing to Disclose Ferco H. Berger, MD, Toronto, ON (*Moderator*) Nothing to Disclose

For information about this presentation, contact:

patlas@hhsc.ca

jhines@northwell.edu

dkatz@winthrop.org

Sub-Events

RC508-01 Imaging of Acute Pancreatitis

Wednesday, Nov. 29 8:30AM - 9:00AM Room: S405AB

Participants Jorge A. Soto, MD, Boston, MA (*Presenter*) Royalties, Reed Elsevier

For information about this presentation, contact:

jorge.soto@bmc.org

LEARNING OBJECTIVES

1) Review the appropriate terminology that should be implemented when describing glandular and peri-glandular findings in acute pancreatitis, following the revision of the Atlanta classification. 2) Identify the importance of glandular necrosis in defining the prognosis of acute pancreatitis. 3) Illustrate specific situations where MR can be a valuable tool in the evaluation of acute pancreatitis.

Honored Educators

Presenters or authors on this event have been recognized as RSNA Honored Educators for participating in multiple qualifying educational activities. Honored Educators are invested in furthering the profession of radiology by delivering high-quality educational content in their field of study. Learn how you can become an honored educator by visiting the website at: https://www.rsna.org/Honored-Educator-Award/ Jorge A. Soto, MD - 2013 Honored EducatorJorge A. Soto, MD - 2014 Honored EducatorJorge A. Soto, MD - 2015 Honored EducatorJorge A. Soto, MD - 2017 Honored Educator

RC508-02 Abdominal Tomogram: Ultra-Low Dose CT of the Abdomen Has Replaced Abdominal Plain Films in the Emergency Department

Wednesday, Nov. 29 9:00AM - 9:10AM Room: S405AB

Participants

Patrik Rogalla, MD, Toronto, ON (*Presenter*) Institutional Research Grant, Toshiba Medical Systems Corporation Tanya Spiegelberg, Toronto, ON (*Abstract Co-Author*) Nothing to Disclose James Hong, RT, Toronto, ON (*Abstract Co-Author*) Nothing to Disclose Sam Sabbah, Toronto, ON (*Abstract Co-Author*) Nothing to Disclose Silvio G. Bruni, MD, Toronto, ON (*Abstract Co-Author*) Nothing to Disclose Janet Pereira-Ross, Toronto, ON (*Abstract Co-Author*) Nothing to Disclose Joanna Talotta, Toronto, ON (*Abstract Co-Author*) Nothing to Disclose Corwin Burton, Toronto, ON (*Abstract Co-Author*) Nothing to Disclose Jerry Plastino, Toronto, ON (*Abstract Co-Author*) Nothing to Disclose Christin Farrell, Toronto, ON (*Abstract Co-Author*) Nothing to Disclose Christin Farrell, Toronto, ON (*Abstract Co-Author*) Employee, Toshiba Medical Systems Corporation Bernice E. Hoppel, PhD, Vernon Hills, IL (*Abstract Co-Author*) Nothing to Disclose

For information about this presentation, contact:

patrik.rogalla@uhn.ca

To analyse the impact of replacing abdominal plain films (APF) in the Emergency Department (ED) with ultra-low dose CT (Abdominal Tomogram) on workflow, turn-around times (TAT), radiation dose and recall rate.

METHOD AND MATERIALS

Over a period of 50 days, all APFs (Group I; Carestream DRX Evolution, GE Optima/Definium) ordered by the ED for the four most common non-trauma indications (abdominal pain NYD, rule out free air, bowel obstruction, or constipation) were analysed in respect to wait time (time from ordering to exam execution), report TAT (time from exam completion to verified report, TAT) during day and night time, radiation dose per patient and recall rate (subsequent standard dose CT for the same indications within 48 hours). Over the following period of 50 days, all requests for APFs for the same four indications were converted to Abdominal Tomograms (Group II; Toshiba Aquilion One, 135 kV, 20-40 mAs weight based, AIDR-3D, 3 mm axials and MPRs, 10 cm coronals), analysed by using the same metrics and compared to Group I. The dose-area-product on APFs was converted to mSv by applying a factor of 0.21 mSv/Gycm2, the dose-lengths-product in CT was converted to mSv with a conversion factor of 0.016 mSv/mGycm.

RESULTS

There was no difference in demographics between the groups (Group I: 243 patients, 127/116 w/m, 64±19y), Group II: 235 patients, 124/111 w/m, 64±20y). 1 to 6 views (mean, 2.6±0.9) were required to complete the X-ray exam. Mean wait times and TAT for Group I/II during the day were $222\pm379/39\pm49$ and $267\pm317/107\pm78$ min, and at night $235\pm269/38\pm58$ and $549\pm345/328\pm197$ min (all p<.0001); radiation doses were $2.85\pm9.1/1.5\pm0.6$ mSv (p<.0001), and the recall rates were 29/11% (p<.0001), respectively. In one patient, the AT was repeated due to insufficient dose.

CONCLUSION

The conversion of APFs to Abdominal Tomograms for non-trauma ED patients has improved wait times and report TAT, decreased radiation dose and lowered the recall rate.

CLINICAL RELEVANCE/APPLICATION

Replacing abdominal X-rays by ultra-low-dose CTs for non-trauma indications may help improve the workflow and decision making in the Emergency Department.

RC508-03 CT and MR Imaging of Appendicitis

Wednesday, Nov. 29 9:10AM - 9:40AM Room: S405AB

Participants

Perry J. Pickhardt, MD, Madison, WI (*Presenter*) Co-founder, VirtuoCTC, LLC; Stockholder, Cellectar Biosciences, Inc; Stockholder, SHINE Medical Technologies, Inc; Stockholder, Elucent Medical; Advisor, Check-Cap Ltd; Research Grant, Koninklijke Philips NV

LEARNING OBJECTIVES

1) Assess the relative advantages and disadvantages for CT and MR imaging in the setting of suspected appendicitis. 2) Compare the diagnostic performance of CT and MR for both appendicitis and alternative conditions. 3) Describe the increasing use of MR for abdominal imaging in the ED setting.

Honored Educators

Presenters or authors on this event have been recognized as RSNA Honored Educators for participating in multiple qualifying educational activities. Honored Educators are invested in furthering the profession of radiology by delivering high-quality educational content in their field of study. Learn how you can become an honored educator by visiting the website at: https://www.rsna.org/Honored-Educator-Award/ Perry J. Pickhardt, MD - 2014 Honored Educator

RC508-04 Imaging of Gangrenous Appendicitis: Do Dual Energy Virtual Monoenergetic Images Add Clinical Value?

Wednesday, Nov. 29 9:40AM - 9:50AM Room: S405AB

Participants

Mohammed F. Mohammed, MBBS, Vancouver, BC (Abstract Co-Author) Speaker, Siemens AG; Employee, X-Ray Teleradiology Services

Khaled Y. Elbanna, MBChB, FRCR, Vancouver, BC (*Presenter*) Nothing to Disclose Tejbir S. Chahal, BSc, Vancouver, BC (*Abstract Co-Author*) Nothing to Disclose Rawan Abu Mughli, Vancouver, BC (*Abstract Co-Author*) Nothing to Disclose Savvas Nicolaou, MD, Vancouver, BC (*Abstract Co-Author*) Institutional research agreement, Siemens AG Faisal Khosa, Vancouver, BC (*Abstract Co-Author*) Nothing to Disclose

For information about this presentation, contact:

mohammed.f.mohammed@gmail.com

PURPOSE

Appendicitis remains the most common acute surgical condition of the abdomen. One unique form of this disease is gangrenous appendicitis. This form carries a very high perforation risk which leads to an increase in morbidity and mortality. There have been numerous publications on the role of CT in the diagnosis of acute appendicitis, however the accuracy of CT in diagnosing gangrenous appendicitis is less established. In our study, we propose that the use of Dual Energy (DE) and spectral imaging techniques can improve diagnostic accuracy of acute gangrenous appendicitis.

METHOD AND MATERIALS

For this retrospective, IRB-approved study, the hospital RIS was queried for all abdominopelvic CT scans performed in the emergency department between January 1, 2013 to December 31, 2016 that were positive for appendicitis on histopathology. Non DECT studies and those with frank perforation, phlegmon or peri-appendicular abscess formation were excluded. A total of 236 cases were included in our study. 40 keV VMI and 120 kVp simulated images were reviewed by two abdominal radiologists in a randomized fashion who were blinded to the results of the histopathology for presence of gangrene. Sensitivity, specificity, positive

and negative likelihood ratios and interobserver agreement were calculated for each set of images. Confidence was rated on a 5 point Likert scale with 1 being completely uncertain and 5 being absolutely confident.

RESULTS

59.7 % (141) of patients were male. The mean age of patients was 43.5 ± 1.2 years. 51 patients (21.6 %) were positive for gangrenous appendicitis on histopathology. The sensitivity, specificity, positive and negative likelihood ratios, confidence and interobserver agreement for 40 keV VMI were 100 %, 80.5 %, 5.1, 0, 5 and 0.99 respectively (p < 0.0001), compared to 21.6 %, 95.1 %, 4.4, 0.82, 3.75 and 0.98 respectively (p < 0.0001) for 120 kVp simulated images.

CONCLUSION

Review of 40 keV VMI reconstructions adds significant clinical value to the DECT of the abdomen and pelvis for assessment of acute appendicitis as well as the presence of gangrene within the appendix.

CLINICAL RELEVANCE/APPLICATION

40 keV VMI reconstructions should be reviewed along side the simulated 120 kVp in cases of suspected appendicitis to diagnose or exclude presence of gangrenous appendicitis.

RC508-05 Risk Stratification of Non-Diagnostic Ultrasounds to Guide Management and CT Utilization in Pediatric ED Patients Suspected of Acute Appendicitis

Wednesday, Nov. 29 9:50AM - 10:00AM Room: S405AB

Awards

Student Travel Stipend Award

Participants

Gary X. Wang, MD, PhD, Boston, MA (*Presenter*) Nothing to Disclose Pallavi Sagar, MBBS, Boston, MA (*Abstract Co-Author*) Nothing to Disclose Randheer Shailam, MD, Boston, MA (*Abstract Co-Author*) Nothing to Disclose Ari Cohen, MD, Boston, MA (*Abstract Co-Author*) Nothing to Disclose Michael S. Gee, MD, PhD, Jamaica Plain, MA (*Abstract Co-Author*) Nothing to Disclose

For information about this presentation, contact:

gxwang@partners.org

PURPOSE

Though ultrasound (US) is the initial imaging test of choice for pediatric ED patients suspected of acute appendicitis, its ability to guide management is limited by its inability to visualize the appendix in some patients. Here, we study the feasibility of risk-stratifying patients with non-diagnostic US to guide CT use and ED management.

METHOD AND MATERIALS

This study was performed in a tertiary care academic hospital with a pediatric ED. Structured reporting is used for pediatric appendicitis US. Non-visualized appendix is designated "low probability" or "concerning" for appendicitis based on absence or presence of concerning secondary findings: right lower quadrant fat stranding, enlarged lymph nodes, free fluid, and/or tenderness. Designation of "concerning" is at the interpreting radiologist's discretion. Technically limited exams can be called "indeterminate". An IRB approved retrospective electronic medical record review identified ED patients < 19 y.o. who received appendicitis US from December, 2016 to March, 2017. Age, gender, imaging results, clinical outcomes, and operative and pathology reports were analyzed.

RESULTS

305 patients underwent US (avg. age 11 ± 4 y.o., 56% female). 69 (22%) were ultimately diagnosed with appendicitis. US diagnosed 23% (n = 54) of normal appendix and 64% (n = 44) of appendicitis PPV = 0.92, NPV = 0.98). 202 (66%) exams were non-diagnostic: 72 (36%) "low probability", 18 (9%) "concerning", and 41 (20%) "indeterminate"; 71 (35%) were not given a category ("no comment"). Appendicitis was less likely with "low probability" vs "concerning" (5/72, 7% vs. 7/18, 39%; p < 0.01, Fisher's exact test) but not significantly different vs. "indeterminate" (5/41, 12%; p = 0.49) or "no comment" (7/71, 10%; p = 0.56). CT was used after US in 13/18 (72%) of "concerning" vs. 13/72 (18%) of "low probability" patients, was positive for appendicitis in 6/13 (46%) vs. 2/13 (15%), and suggested an alternate diagnosis in 4 (22%) vs 0.

CONCLUSION

In pediatric ED patients, non-diagnostic appendicitis US can be stratified as low and high risk for acute appendicitis based on secondary findings. CT obtained in patients after low-risk US very rarely showed appendicitis and did not offer an alternate diagnosis of symptoms.

CLINICAL RELEVANCE/APPLICATION

For pediatric ED patients suspected with acute appendicitis, risk-stratification of non-diagnostic ultrasound exams is feasible and can be used to guide further management and CT utilization.

RC508-06 How Reliably Can We Identify the Appendix on Unenhanced Ultra-Low-Dose CT in the Era of Iterative Reconstruction? Factors Influencing Residents' Accuracy in the Identification of the Normal Appendix

Wednesday, Nov. 29 10:00AM - 10:10AM Room: S405AB

Participants

Arif Deniz Ordu, MD, Augsburg, Germany (*Presenter*) Nothing to Disclose Ludovica-Paola Rollandi, MD, Augsburg, Germany (*Abstract Co-Author*) Nothing to Disclose Andreas Adam, MD, Augsburg, Germany (*Abstract Co-Author*) Nothing to Disclose Christian Scheurig-Muenkler, Berlin, Germany (*Abstract Co-Author*) Nothing to Disclose Thomas J. Kroencke, MD, Berlin, Germany (*Abstract Co-Author*) Nothing to Disclose Florian Schwarz, MD, Augsburg, Germany (*Abstract Co-Author*) Nothing to Disclose Katharina Rippel, Augsburg, Germany (*Abstract Co-Author*) Nothing to Disclose

For information about this presentation, contact:

Florian.Schwarz@klinikum-augsburg.de

PURPOSE

To determine factors influencing the accuracy in the identification of the normal appendix on ultra-low-dose CT by residents with on-call experience.

METHOD AND MATERIALS

We included 163 consecutive patients presenting to the ED over a 5 month period who were referred for an unenhanced ultra-lowdose CT of the abdomen for urolithiasis (2nd-gen. Dual-Source CT, auto-kV- and auto-mAs-selection). A model-based iterative algorithm was used for image reconstruction. As reference standard, two faculty radiologists in consensus evaluated all CT datasets and all information from the electronic health records to determine if patients had had prior appendectomy and digitally marked the appendix if identified. Two residents blinded towards this reference standard and all clinical information independently analyzed all datasets using multiplanar reformations for the presence of the appendix and marked it if identified. Residents' markings were compared with the reference standard and classified as correct or incorrect. Receiver-Operating-Characteristic analyses were used to quantify the predictive value of BMI, CTDI and Image Noise for the correct identification of the appendix.

RESULTS

35 patients were excluded due to uncertain AE-status. Of the remaining 128 patients (80 men, median age 47, median DLP 46mGy*cm), 56 had had prior appendectomy. Interobserver agreement was high (88% of cases, κ =0.75). Readers had a sensitivity, specificity and accuracy of 91%, 88%, 90% and 92%, 91%, 91%, respectively. The subgroup of patients with incorrect identification of the appendix had lower BMI (23.5±4 vs. 28±7kg/m², p=0.02) and tendencies towards lower CTDI (0.91±0.3 vs. 1.21±0.6mGy,p=0.1) and lower DLP (43±13 vs. 53±25mGy*cm,p=0.16) but there was no difference in image noise (15.9±3.8 vs. 15.9±3.6HU,p=1.0). BMI had high predictive value for an incorrect identification of the appendix (AUC=0.73,p< 0.01), while image noise lacked any measurable effect (AUC=0.52,p=0.84).

CONCLUSION

The normal appendix or its absence can be correctly identified on unenhanced ultra-low-dose CT scans(<1 mSv) in the vast majority of cases by residents with on-call experience. Low BMI was a strong predictor for misclassification, while image noise lacked any measurable effect in the observed ranges.

CLINICAL RELEVANCE/APPLICATION

Unenhanced ultra-low-dose CT appears promising for the initial CT workup of patients with right lower quadrant pain particularly in patients with higher BMIs.

RC508-07 Imaging of Colonic Emergencies

Wednesday, Nov. 29 10:20AM - 10:50AM Room: S405AB

Participants

Vincent M. Mellnick, MD, Saint Louis, MO (Presenter) Nothing to Disclose

For information about this presentation, contact:

mellnickv@wustl.edu

LEARNING OBJECTIVES

1) Identify acute colonic conditions that may cause a patient to present to the emergency department. 2) Utilize CT to characterize colonic emergencies and to correlate these findings with plain film and fluoroscopy. 3) Compare the underlying causes and imaging findings of colonic emergencies, broadly: inflammation, infection, ischemia, obstruction, perforation, and hemorrhage. 4) Assist referring clinicians in guiding treatment, particularly when stratifying patients into operative or non-operative management.

Honored Educators

Presenters or authors on this event have been recognized as RSNA Honored Educators for participating in multiple qualifying educational activities. Honored Educators are invested in furthering the profession of radiology by delivering high-quality educational content in their field of study. Learn how you can become an honored educator by visiting the website at: https://www.rsna.org/Honored-Educator-Award/ Vincent M. Mellnick, MD - 2016 Honored Educator

RC508-08 Ultrasound for the Diagnosis of Acute Appendicitis in the Emergency Department: Imaging Trends and Utility Over 6+ Years

Wednesday, Nov. 29 10:50AM - 11:00AM Room: S405AB

Participants

Stella Lam, MD, Boston, MA (*Presenter*) Nothing to Disclose Robin B. Levenson, MD, Boston, MA (*Abstract Co-Author*) Nothing to Disclose Andrew T. Colucci, MD, Boston, MA (*Abstract Co-Author*) Nothing to Disclose Karen S. Lee, MD, Boston, MA (*Abstract Co-Author*) Nothing to Disclose

PURPOSE

Assess the imaging utilization and diagnostic accuracy of ultrasound (US) in the diagnosis of appendicitis in adults in an urban, tertiary care Emergency Department (ED) over a 6+-year period.

METHOD AND MATERIALS

Retrospective analysis was performed on consecutive patients, age 17 years and older, who underwent US to assess for

appendicitis from January 2010 to October 2016, in the ED. Data recorded include patient demographics, imaging findings, additional imaging performed within 24 hrs of initial US, surgeon experience, surgical pathology, and final discharge diagnosis. US findings were categorized as normal appendix, appendix not visualized(NV), and acute appendicitis. Sensitivity, specificity, positive and negative predictive values(PPV and NPV, respectively) for US in the diagnosis of appendicitis were calculated. Pearson's Chi-squared test was also used.

RESULTS

736 patients were included (mean age 28 years, range 17-72 years), 637 females and 99 males. The appendix was seen on US in 106 (14.4%) cases. When the appendix was seen and abnormal, the rate of appendicitis was significantly greater than when the appendix was not seen (94.8% vs 7.3 %, p<0.001). Appendix was seen more frequently in patients with appendicitis than in patients without (61.7% vs 5.2%, p<0.001). Appendix visualization rate was lower in females than in males (10.7% vs 38.4%, p<0.001). There was no significant difference(p=0.07) in rate of follow-up CT between male and non-pregnant females. Sensitivity, specificity, PPV, and NPV of US for appendicitis were 98.6%, 87.5%, 94.8%, and 96.5%, respectively, when the appendix was seen. When cases with NV appendices were considered negative for appendicitis (n=630), sensitivity, specificity, PPV, and NPV of US for appendicities for appendicities (n=630), sensitivity, specificity, PPV, and NPV of US for appendicities of appendicities (n=630), sensitivity, specificity, PPV, and NPV of US for appendicities of appendicities (n=630), sensitivity, specificity, PPV, and NPV of US for appendicities of appendicities (n=630), sensitivity, specificity, PPV, and NPV of US for appendicities were 60.8%, 99.4%, 94.8%, and 92.9%, respectively. Follow-up CT to further assess for appendicitis was performed in 53% after US showed normal or NV appendix and in 63% after an US positive for appendicitis.

CONCLUSION

In the ED, US is more commonly used to assess for appendicitis in females than in males. In our experience, the appendix is seen infrequently on US, but when seen, most are positive for appendicitis.

CLINICAL RELEVANCE/APPLICATION

US should be considered as an initial imaging tool in ED patients suspected of having acute appendicitis. When the appendix is seen on US, the diagnostic accuracy of US for appendicitis is high, and subsequent CT imaging may not be necessary.

RC508-09 MRI as the First Line Imaging Study for Suspected Appendicitis in Pregnancy

Wednesday, Nov. 29 11:00AM - 11:10AM Room: S405AB

Participants

Brandon Andrew, MD, Pittsburgh, PA (*Abstract Co-Author*) Nothing to Disclose Christiane M. Hakim, MD, Pittsburgh, PA (*Abstract Co-Author*) Nothing to Disclose Bestoun Ahmed, MD, Pittsburgh, PA (*Abstract Co-Author*) Nothing to Disclose Jason Chang, MD, Pittsburgh, PA (*Abstract Co-Author*) Nothing to Disclose William Gourash, RN, Pittsburgh, PA (*Abstract Co-Author*) Research funded, Medtronic plc; Research funded, Johnson & Johnson Balasubramanya Rangaswamy, MD, Pittsburgh, PA (*Presenter*) Nothing to Disclose

For information about this presentation, contact:

rangaswamyb@upmc.edu

PURPOSE

To compare the accuracy of ultrasound (US) and MRI in pregnant patients with clinical suspicion of acute appendicitis, with the goal of determining whether MRI can be used as first line imaging modality.

METHOD AND MATERIALS

We performed an IRB approved retrospective study of 210 consecutive pregnant patients with clinical suspicion of acute appendicitis at a single center over a four year period. Patients underwent US as first line imaging as per ACR recommendations using graded compression technique. MRI was performed when diagnostic uncertainity remained. MRI was chosen as first line imaging in just one patient. Non contrast MRI was performed on GE Excite HDx 1.5T magnet with dedicated body Phase Array coil. Central re-review of the imaging was done. Final diagnosis was based on operative records, pathology reports, discharge summaries and follow up visits. Sensitivity and specificity for US and MRI were calculated.

RESULTS

Eight patients out of 210 (3.8%) were found to have acute appendicitis. 209 patients underwent US and 65 patients underwent MRI. The appendix visualization rates for US and MRI respectively were 1.4% (3 out of 209) and 84.6% (55 out of 65) respectively. Sensitivity and specificity for the diagnosis of appendicitis by US were 37.5% and 100% and by MRI were 100% and 100%. All appendixes visualized on US had appendicitis. No patient with a normal appendix on MRI or with nonvisualization of appendix on MRI had appendicitis.

CONCLUSION

Timely diagnosis of acute appendicitis in pregnant patients is vital to avoid serious complications. This large retrospective study showed lower US sensitivity in visualization and diagnosis of appendicitis when compared to MRI.

CLINICAL RELEVANCE/APPLICATION

MRI could be considered as a first line imaging modality for the assessment of pregnant patients with high clinical suspicion of acute appendicitis in institutions where MRI is readily available. We acknowledge the cost and duration of MRI.

RC508-10 Imaging of Right Upper Quadrant Pain

Wednesday, Nov. 29 11:10AM - 11:40AM Room: S405AB

Participants

Jennifer W. Uyeda, MD, Boston, MA (Presenter) Nothing to Disclose

LEARNING OBJECTIVES

1) Review common causes of right upper quadrant pain with reasonable differential diagnoses and their imaging apperances. 2) Improve basic knowledge and skills relevant to clinical practice in evaluating right upper quadrant pain. 3) Describe common

diagnoses and important secondary findings on various imaging modalities that are helpful for the evaluation of acute or emergent right upper quadrant pain.

RC508-11 Utility of Ultrasound Examination Following Computed Tomography in the Setting of Acute Non-Traumatic Abdominal Pain

Wednesday, Nov. 29 11:40AM - 11:50AM Room: S405AB

Awards

Student Travel Stipend Award

Participants David Li, MD, Hamilton, ON (*Presenter*) Nothing to Disclose Kristopher W. McLean, MD, MSc, Milton, ON (*Abstract Co-Author*) Nothing to Disclose Michael N. Patlas, MD, FRCPC, Hamilton, ON (*Abstract Co-Author*) Nothing to Disclose

For information about this presentation, contact:

david.li@medportal.ca

PURPOSE

To assess the utility of abdominal and/or pelvic ultrasound (US) examination following abdominal/pelvic computed tomography (CT) in providing new clinical information or changing the management for adult patients in the emergency department (ED) presenting with acute non-traumatic abdominal pain.

METHOD AND MATERIALS

Among all adult patients who presented to the ED at an academic medical center over a three-year time period, those who underwent a contrast-enhanced CT examination of the abdomen/pelvis followed by an US study of the abdomen and/or pelvis within 72 hours were selected for the IRB-approved retrospective review. Patients presenting in the setting of trauma and those who underwent surgical or radiologic intervention in the intervening time period were excluded. The proportions of US exams that were either concordant or discordant with the initial CT were determined, with note made of any relevant added clinical information in concordant cases. Useful added information included changes in treatment or management, or narrowing or clarification of the differential diagnosis. The Chi-square test was used to compare the utility of US examinations suggested by the radiologist with those independently requested by the nonradiologist.

RESULTS

319 cases between July 1, 2013 and June 30, 2016 satisfied the study criteria. 312 cases (97.8%) included US examinations that were concordant with the initial CT. From these 312 concordant cases, 100 (32.1%) provided relevant additional clinical information and 212 (67.9%) provided no additional information. Out of the 319 total cases, the radiologist suggested the follow-up US examination in 90 instances (28.2%) compared to 229 independently ordered by the nonradiologist (71.8%). US examinations suggested by the radiologist had a much higher proportion of added utility compared to those ordered by the nonradiologist (70.0% vs 19.2%, p < 0.001).

CONCLUSION

A high rate of concordance exists between CT and US examinations in the setting of acute non-traumatic abdominal pain, with a low rate of relevant additional clinical information. US examinations suggested by the radiologist were more likely to provide more utility than those independently ordered by the nonradiologist.

CLINICAL RELEVANCE/APPLICATION

Selective use of US exams following CT in ED patients with acute non-traumatic abdominal pain may help reduce strain on healthcare resources, given the high rate of agreement between studies.

RC508-12 Accuracy of MRI for Diagnosis of Internal Hernia in Pregnant Women with Prior Roux-En-Y Gastric Bypass

Wednesday, Nov. 29 11:50AM - 12:00PM Room: S405AB

Participants

Satheesh Krishna, MD, Ottawa, ON (*Presenter*) Nothing to Disclose Matthew D. McInnes, MD, FRCPC, Ottawa, ON (*Abstract Co-Author*) Nothing to Disclose Nicola Schieda, MD, Ottawa, ON (*Abstract Co-Author*) Nothing to Disclose Sabarish Narayanasamy, MBBS, MD, Ottawa, ON (*Abstract Co-Author*) Nothing to Disclose Adnan M. Sheikh, MD, Ottawa, ON (*Abstract Co-Author*) Nothing to Disclose Ania Z. Kielar, MD, Ottawa, ON (*Abstract Co-Author*) Research Grant, General Electric Company

For information about this presentation, contact:

dr.satheeshkrishna@gmail.com

PURPOSE

Internal hernia (IH) is a life-threatening complication following Roux-en-Y gastric bypass surgery (RGB). With 80% of bariatric surgeries performed in women, IH can occur during pregnancy since the enlarging uterus can predispose to bowel herniation through mesenteric defects. Although CT is the standard of care for diagnosis of IH, MR is preferred in pregnant women. The purpose is to evaluate the accuracy of MRI for diagnosis of IH in pregnant women with prior RGB.

METHOD AND MATERIALS

With IRB approval, 15 consecutive pregnant women (n=8 with surgery proven IH; n=7 without IH) with prior RGB who were referred for MRI to rule out IH between December 2009 and July 2016 were identified. Two blinded fellowship-trained abdominal radiologists (R1/R2) retrospectively identified on MRI, presence or absence of 15 established features of IH which have been previously described on CT. Final diagnosis of IH was evaluated both subjectively and using two models previously validated on CT

(M1=mesenteric swirl and small bowel obstruction (SBO); M2= "beaking" of superior mesenteric vein (SMV) and SBO). Diagnostic accuracy and interobserver agreement were calculated for each feature as well as for subjective and model based diagnosis of IH, and Chi-square analysis was used for comparison between them.

RESULTS

There were no differences in the patient age, gestational age or time since RGB (p=0.68, 0.35, 0.55) between the two groups. The signs with best accuracy and interobserver agreement were beaking of SMV (accuracy=86.7%/ 86.7% (R1/R2); kappa=1.00), mesenteric swirl (accuracy=80.0%/86.7%(R1/R2); kappa=0.86) and engorgement of mesenteric vessels (accuracy=80.0%/73.3% (R1/R2); kappa=0.84). The rest of the signs had either low accuracy, poor interobserver agreement or both. Overall accuracy with subjective assessment, M1 and M2 was 80.0%/ 86.7% for each of the 3 methods for R1/R2. (Sens/spec for R1/R2 in Table 1). There was no difference in accuracy between the three methods (p=0.92).

CONCLUSION

MR for diagnosis of IH in preganancy using subjective assessment and 2 models previously validated for CT demonstrates comparable diagnostic accuracy to that reported with CT.

CLINICAL RELEVANCE/APPLICATION

In our small cohort, MRI for diagnosis of IH in pregnancy demonstrates comparable accuracy to CT in non-pregnant patients. We propose that MR is a suitable alternative in pregnant patients.

Honored Educators

Presenters or authors on this event have been recognized as RSNA Honored Educators for participating in multiple qualifying educational activities. Honored Educators are invested in furthering the profession of radiology by delivering high-quality educational content in their field of study. Learn how you can become an honored educator by visiting the website at: https://www.rsna.org/Honored-Educator-Award/ Ania Z. Kielar, MD - 2017 Honored Educator





103rd Scientific Assembly and Annual Meeting November 26 to December 1 McCormick Place, Chicago



RC509

MR Advances in Oncologic Imaging

Wednesday, Nov. 29 8:30AM - 10:00AM Room: E353A

MR OI

AMA PRA Category 1 Credits ™: 1.50 ARRT Category A+ Credit: 1.75

FDA Discussions may include off-label uses.

SAM

New in 2017: PLEASE NOTE - All courses designated for SAM credit at RSNA 2017 will require attendees bring a personal device e.g. phone, iPad, laptop to complete the required test questions during the live session.

Sub-Events

RC509A Diffusion-Weighted MR Imaging

Participants

Ihab R. Kamel, MD, PhD, Baltimore, MD (Presenter) Research Grant, Siemens AG

LEARNING OBJECTIVES

1) Discuss conventional response criteria and their limitations after loco-regional therapy. 2) Illustrate the basic concept of DWI and ADC. 3) Highlight the advantages of volumetric assessment compared to linear measurements. 4) Discuss novel DWI volumetric criteria in quantifying response and predicting patient survival.

Honored Educators

Presenters or authors on this event have been recognized as RSNA Honored Educators for participating in multiple qualifying educational activities. Honored Educators are invested in furthering the profession of radiology by delivering high-quality educational content in their field of study. Learn how you can become an honored educator by visiting the website at: https://www.rsna.org/Honored-Educator-Award/ Ihab R. Kamel, MD, PhD - 2015 Honored Educator

RC509B MR Elastography

Participants

Sudhakar K. Venkatesh, MD, FRCR, Rochester, MN (Presenter) Nothing to Disclose

For information about this presentation, contact:

venkatesh.sudhakar@mayo.edu

LEARNING OBJECTIVES

1) Learn basic concept of tissue stiffness. 2) Tumor stiffness and why its different from normal tissues. 2) Technique of MR elastography. 3) Application of MR elastography for detection and characterization of tumors.

Honored Educators

Presenters or authors on this event have been recognized as RSNA Honored Educators for participating in multiple qualifying educational activities. Honored Educators are invested in furthering the profession of radiology by delivering high-quality educational content in their field of study. Learn how you can become an honored educator by visiting the website at: https://www.rsna.org/Honored-Educator-Award/ Sudhakar K. Venkatesh, MD, FRCR - 2017 Honored Educator

RC509C PET/MR

Participants Alexander R. Guimaraes, MD, PhD, Portland, OR (*Presenter*) Consultant, Agfa-Gevaert Group

LEARNING OBJECTIVES

1) Discuss why MRI & PET are complementary in Cancer Imaging. 2) Discuss the pitfalls and solutions in clinical FDG PET MRI including: a. Billing b. Workflow c. Interpretation d. Motion compensation. 3) Advanced Techniques and tracers.

ABSTRACT

This course is designed to update the attendee on novel PET/ MRI technology and the benefits of PET/MRI in oncology. Multiparametric MRI offers the unique ability to monitor the tumor microenvironment. Increasingly, multiparametric MRI is used for diagnosis and grading of malignancy in various organ systems (e.g. prostate cancer). Novel PET tracers allow for interrogation of various targets associated with malignant processes at the cellular level.

RC509D New MR Contrast Agents

Participants

Rajan T. Gupta, MD, Durham, NC (Presenter) Consultant, Bayer AG; Speakers Bureau, Bayer AG; Consultant, Invivo Corp.;

Consultant, Halyard Health, Inc; Consultant, Siemens AG

For information about this presentation, contact:

rajan.gupta@duke.edu

LEARNING OBJECTIVES

1) Learn about some of the new MR contrast agents as well as their potential uses in the oncologic and non-oncologic setting.





103rd Scientific Assembly and Annual Meeting November 26 to December 1 McCormick Place, Chicago



RC510

Gynecologic Ultrasound Including 3D

Wednesday, Nov. 29 8:30AM - 10:00AM Room: E350



AMA PRA Category 1 Credits ™: 1.50 ARRT Category A+ Credit: 1.75

LEARNING OBJECTIVES

1) Review findings of the 'First International Consensus Report on Adnexal Masses: Management Recommendations which is to be published in 2017. 2) Assess the potential of risk prediction models to improve practice patterns. 3) Improve knowledge of the malignant potential of various sonographic biomarkers. 4) Integrate these findings into daily practice with goal of reducing excess surgery for benign masses while improving triage to gynecology-oncology in women with suspicious adnexal masses. 5) Recognize the varied appearance of the uterus and endometrium throughout a woman's life. 6) Improve sonographic visualization of the endometrium utilizing some technical tips and tricks. 7) Recite a basic differential diagnosis for uterine/cervical masses and endometrial thickening. 8) Apply appropriate terminology when describing abnormal bleeding, location of myomas and mullerian duct anomalies. 9) Understand the controversies, cutoffs and considerations in the context of the role of US in postmenopausal bleeding. 10) Define clinical and epidemiological aspects of endometriosis. 11) Define the importance of imaging mapping for deeply infiltrative endometriosis before clinical counseling. 12) Apply the most appropriate technique to investigate endometriosis. 4) Define the bowel preparation required for the transvaginal ultrasound to investigate endometriosis. 13) Apply the imaging algorithm to map deeply infiltrative endometriosis. 14) Assess the ultrasonographic findings of deeply infiltrative endometriosis in the most common sites such as bladder, vesicouterine pouch, retrocervical space, vagina, ureters, appendix and rectosigmoid colon. 15) To discuss the multiplanar reconstruction technique in scanning the pelvis, including the usefulness of looking at the coronal view of the uterus to evaluate the endometrium and uterine shape. 16) To discuss the use of 3D ultrasound to look for causes of pelvic pain. 17) To discuss the use of 3D ultrasound when evaluating a potential hydrosalpinx.

SAM

New in 2017: PLEASE NOTE - All courses designated for SAM credit at RSNA 2017 will require attendees bring a personal device e.g. phone, iPad, laptop to complete the required test questions during the live session.

Sub-Events

RC510A Ovarian Cysts & Masses - Evidence Based Guidelines 2017

Participants

Phyllis Glanc, MD, Toronto, ON (Presenter) Nothing to Disclose

LEARNING OBJECTIVES

1) Review findings of the 'First International Consensus Report on Adnexal Masses: Management Recommendations which is to be published in 2017. 2) Assess the potential of risk prediction models to improve practice patterns. 3) Improve knowledge of the malignant potential of various sonographic biomarkers. 4) Integrate these findings into daily practice with goal of reducing excess surgery for benign masses while improving triage to gynecology-oncology in women with suspicious adnexal masses.

ABSTRACT

The goal of this session is to review strategies which may aid in the reduction of excess surgery for benign masses while improving triage to gynecology-oncology in women with suspicious adnexal masses. The recently published 'First International Consensus Report on Adnexal Masses: Management Recommendations ' has focused on these two goals and we will review the analysis and recommendations from this report.

RC510B Uterus and Endometrium: A Primer with Pearls to Perfect Your US Performance

Participants

Loretta M. Strachowski, MD, San Francisco, CA (Presenter) Nothing to Disclose

LEARNING OBJECTIVES

1) Recognize the varied appearance of the uterus and endometrium throughout a woman's life. 2) Improve sonographic visualization of the endometrium utilizing some technical tips and tricks. 3) Recite a basic differential diagnosis for uterine/cervical masses and endometrial thickening. 4) Apply appropriate terminology when describing abnormal bleeding, location of myomas and mullerian duct anomalies. 5) Understand the controversies, cutoffs and considerations in the context of the role of US in postmenopausal bleeding.

Active Handout:Loretta M. Strachowski

http://abstract.rsna.org/uploads/2017/17000102/Active RC510B.pdf

RC510C Ultrasound for Deeply Infiltrative Endometriosis

Participants Luciana P. Chamie, MD, PhD, Sao Paulo, Brazil (*Presenter*) Nothing to Disclose

For information about this presentation, contact:

LEARNING OBJECTIVES

1) Define clinical and epidemiological aspects of endometriosis. 2) Define the importance of imaging mapping for deeply infiltrative endometriosis before clinical counseling. 3) Apply the most appropriate technique to investigate endometriosis. 4) Define the bowel preparation required for the transvaginal ultrasound to investigate endometriosis. 5) Apply the imaging algorithm to map deeply infiltrative endometriosis. 6) Assess the ultrasonographic findings of deeply infiltrative endometriosis in the most common sites such as bladder, vesicouterine pouch, retrocervical space, vagina, ureters, appendix and rectosigmoid colon.

ABSTRACT

Endometriosis is a very common gynecological disease affecting millions of women in their reproductive life, often causing pelvic pain and infertility. Clinical history and physical examination may suggest endometriosis, but imaging mapping is necessary to identify the disease and mandatory for clinical couseling and surgical planning. Transvaginal ultrasound after bowel preparation is the best imaging modality as the first-line technique to evaluate patients suspected of endometriosis. The bowel preparation is relatively simple and includes the day before and the day of the examination. This method is highly accurate to identify intestinal endometriosis and to determine which layers of the bowel wall are affected. In addition, it provides better assessment of small peritoneal lesions of the retrocervical space, vagina and bladder. Pelvic adhesions can also be evaluated during the exam.

URL

http://chamie.com.br/download

RC510D 3D Ultrasound in Gynecology

Participants

Beryl R. Benacerraf, MD, Boston, MA (Presenter) Nothing to Disclose

LEARNING OBJECTIVES

1) To discuss the multiplanar reconstruction technique in scanning the pelvis, including the usefulness of looking at the coronal view of the uterus to evaluate the endometrium and uterine shape. 2) To discuss the use of 3D ultrasound to look for causes of pelvic pain. 3) To discuss the use of 3D ultrasound when evaluating a potential hydrosalpinx.

ABSTRACT

NA







Pediatric Malignancies

Wednesday, Nov. 29 8:30AM - 10:00AM Room: S504CD



AMA PRA Category 1 Credits ™: 1.50 ARRT Category A+ Credit: 1.75

Sub-Events

RC511A The New International Neuroblastoma Response Criteria (INRC): The Key Role of The Radiologist

Participants

Susan L. Cohn, MD, Chicago, IL (Presenter) Nothing to Disclose

For information about this presentation, contact:

scohn@peds.bsd.uchicago.edu

LEARNING OBJECTIVES

1) To comprehend the imaging modalities required to assess response of primary tumor, metastatic soft tissue disease, and metastatic bone/marrow disease in the new International Neuroblastoma Response Criteria (INRC) system. 2) To apply the new INRC to assess overall neuroblastoma response.

ABSTRACT

The National Cancer Institute sponsored a Clinical Trials Planning Meeting (CTPM) in 2012 to update and refine the International Neuroblastoma Response Criteria (INRC). In the revised INRC, response to treatment of the primary tumor, soft tissue and bone metastases, and bone marrow will be assessed. Primary and metastatic soft tissue site response will be evaluated using RECIST and 123I-metaiodobenzylguanidine (123I-MIBG) or 18F-fluorodeoxyglucose (FDG)-Positron emission tomography (PET) scans if the tumor is MIBG non-avid. Bone marrow will be assessed by histology/immunohistochemistry and cytology/immunocytology. Overall response will taken into account the responses of all the anatomic sites and be defined as complete response, partial response, minor response, stable disease and progressive disease. These revised criteria will provide a uniform assessment of disease response, improve the interpretability of clinical trial results, and facilitate collaborative trial designs.

RC511B Neuroblastoma

Participants Marguerite T. Parisi, MD, Seattle, WA (*Presenter*) Nothing to Disclose

RC511C Lymphoma

Participants Stephan D. Voss, MD, PhD, Boston, MA (*Presenter*) Nothing to Disclose

For information about this presentation, contact:

stephan.voss@childrens.harvard.edu

LEARNING OBJECTIVES

1) To review staging and response criteria used in Pediatric Hodgkin Lymphoma and non-Hodgkin Lymphoma patients. 2) To review of anatomic imaging (CT, MRI) and functional imaging (PET/CT and PET/MRI) in response assessment. 3) Introduce dose reduction strategies in PET/CT, including integration of diagnostic CT and PET exams. 4) To introduce the audience to efforts aimed at reducing surveillance imaging in pediatric Hodgkin Lymphoma.

RC511D Optimized Pediatric Imaging Protocols for PET/CT and SPECT/CT

Participants

Susan E. Sharp, MD, Cincinnati, OH (Presenter) Nothing to Disclose

LEARNING OBJECTIVES

1) Discuss the North American and EANM guidelines for radiopharmaceutical administered doses in children. 2) Describe PET/CT and SPECT/CT protocol options for optimizing image quality and radiation dose in children.







Vascular Series: MR Angiography: New Techniques and Their Application

Wednesday, Nov. 29 8:30AM - 12:00PM Room: N227B



ARRT Category A+ Credits: 4.00 AMA PRA Category <u>1 Credits ™: 3.25</u>

FDA Discussions may include off-label uses.

Participants

Vincent B. Ho, MD, MBA, Bethesda, MD (Moderator) Institution, In-kind support, General Electric Company

Tim Leiner, MD, PhD, Utrecht, Netherlands (*Moderator*) Speakers Bureau, Koninklijke Philips NV; Research Grant, Bayer AG; Thomas K. Foo, PhD, Niskayuna, NY (*Moderator*) Employee, General Electric Company

Martin R. Prince, MD, PhD, New York, NY (*Moderator*) Patent agreement, General Electric Company; Patent agreement, Hitachi, Ltd; Patent agreement, Siemens AG; Patent agreement, Toshiba Medical Systems Corporation; Patent agreement, Koninklijke Philips NV; Patent agreement, Nemoto Kyorindo Co, Ltd; Patent agreement, Bayer AG; Patent agreement, Lantheus Medical Imaging, Inc; Patent agreement, Bracco Group; Patent agreement, Mallinckrodt plc; Patent agreement, Guerbet SA; Patent agreement, Topspins, Inc; Stockholder, Topspins, Inc

For information about this presentation, contact:

thomas.foo@ge.com

map2008@med.cornell.edu

t.leiner@umcutrecht.nl

LEARNING OBJECTIVES

1) To review the latest MR techniques for vascular imaging. 2) Learn how to optimize MR Angiography pulse sequences. 3) Review a spectrum of Vascular Disease on MRI/MRA.

Sub-Events

RC51201 Non-Contrast MRA

Wednesday, Nov. 29 8:30AM - 9:05AM Room: N227B

Participants

Martin R. Prince, MD, PhD, New York, NY (*Presenter*) Patent agreement, General Electric Company; Patent agreement, Hitachi, Ltd; Patent agreement, Siemens AG; Patent agreement, Toshiba Medical Systems Corporation; Patent agreement, Koninklijke Philips NV; Patent agreement, Nemoto Kyorindo Co, Ltd; Patent agreement, Bayer AG; Patent agreement, Lantheus Medical Imaging, Inc; Patent agreement, Bracco Group; Patent agreement, Mallinckrodt plc; Patent agreement, Guerbet SA; Patent agreement, Topspins, Inc; Stockholder, Topspins, Inc

RC512-02 The Influence of Obesity on the Image Quality and Accuracy of Noncontrast Quiescent-Interval Single-Shot Lower Extremity MRA in Patients with Peripheral Artery Disease: A Comparison with CTA and Digital Subtraction Angiography

Wednesday, Nov. 29 9:05AM - 9:15AM Room: N227B

Participants

Akos Varga-Szemes, MD, PhD, Charleston, SC (*Presenter*) Research Grant, Siemens AG Domenico Mastrodicasa, MD, Charleston, SC (*Abstract Co-Author*) Nothing to Disclose Carlo N. De Cecco, MD, PhD, Charleston, SC (*Abstract Co-Author*) Research Grant, Siemens AG Moritz H. Albrecht, MD, Charleston, SC (*Abstract Co-Author*) Nothing to Disclose Taylor M. Duguay, Charleston, SC (*Abstract Co-Author*) Nothing to Disclose U. Joseph Schoepf, MD, Charleston, SC (*Abstract Co-Author*) Research Grant, Astellas Group; Research Grant, Bayer AG; Research Grant, General Electric Company; Research Grant, Siemens AG; Research support, Bayer AG; Consultant, Guerbet SA; ; ; Pal Suranyi, MD, PhD, Charleston, SC (*Abstract Co-Author*) Nothing to Disclose Domenico De Santis, MD, Charleston, SC (*Abstract Co-Author*) Nothing to Disclose Marwen Eid, MD, Charleston, SC (*Abstract Co-Author*) Nothing to Disclose Georg Apfaltrer, MD, Thal, Austria (*Abstract Co-Author*) Nothing to Disclose Philipp L. von Knebel Doeberitz, Charleston, SC (*Abstract Co-Author*) Nothing to Disclose Shivraman Giri, PhD, Chicago, IL (*Abstract Co-Author*) Employee, Siemens AG Thomas M. Todoran, MD, Charleston, SC (*Abstract Co-Author*) Nothing to Disclose

For information about this presentation, contact:

schoepf@musc.edu

PURPOSE

Body habitus may significantly affect CT angiography (CTA) image quality. This study aimed to evaluate the influence of obesity on

the image quality and accuracy of non-contrast quiescent interval single-shot (QISS) MR angiography (MRA) in patients with peripheral artery disease (PAD) compared to CTA and digital subtraction angiography (DSA).

METHOD AND MATERIALS

Forty-six patients (64±12 years, 25 male) with PAD underwent lower extremity CTA with a third-generation dual-source dualenergy CT and 1.5T MRA using a prototype QISS sequence (FOV 400x260mm2, TR/TE 3.5/1.4ms, flip angle 90°, acquisition length 144mm). DSA was performed within 50 days. Eighteen arterial segments per patient were analyzed. Patients were grouped (Gr) based on body mass index (BMI; kg/m2): Gr1: <30 (normal and overweight); and Gr2 >30 (obese). Subjective image quality (5point Likert scale) and degree of stenosis (<= or >50%) were evaluated by two readers and compared by Mann-Whitney U-testing. Sensitivity and specificity of MRA and CTA to detect >50% stenosis were calculated using the McNemar-test.

RESULTS

The average BMI in Gr1 (n=25) and Gr2 (n=21) were 23.4 \pm 3.4 and 34.9 \pm 3.5kg/m2 (P<0.0001). Of 828 arterial segments, 37 (4.4%; 20 in Gr1 and 17 in Gr2, P=0.1087) and 71 (8.5%; 26 in Gr1 and 45 in Gr2, P=0.0191) were excluded from MRA and CTA evaluation, respectively (P<0.0001). Subjective image quality in MRA was rated similar in Gr1 and Gr2 (4.2 [3.8-4.6] vs 4.0 [3.7-4.3], P=0.0764), while a significant difference was observed between groups with CTA images (Gr1 4.5 [4.3-4.7], Gr2 3.9 [3.7-4.1], P=0.0247). The sensitivity and specificity of MRA for >50% stenosis were similar between the groups (Gr1 85.4% and 97.0%, vs 84.2% and 96.1%, respectively). However, higher sensitivity (88.1% vs 85.9%) and specificity (96.2% vs 90.8%) were measured with CTA in Gr1 compared to Gr2.

CONCLUSION

Body habitus significantly affects image quality and consequently reduces diagnostic accuracy of CTA for the detection of >50% arterial stenosis. Obesity, however, has no influence on QISS MRA, establishing it as a potential advantageous alternative for the visualization of lower extremity arterial anatomy in obese patients.

CLINICAL RELEVANCE/APPLICATION

QISS MRA is a potential alternative for the non-contrast evaluation of the lower extremity arteries with comparable diagnostic accuracy to CTA, especially in patients with larger body habitus.

RC512-03 Simultaneous Acquisition of MR Angiography and Diagnostic Images on Contrast-Enhanced View-Sharing Multi-Arterial Phases

Wednesday, Nov. 29 9:15AM - 9:25AM Room: N227B

Participants

Yoshifumi Noda, MD, PhD, Gifu, Japan (*Presenter*) Nothing to Disclose Satoshi Goshima, MD, PhD, Gifu, Japan (*Abstract Co-Author*) Nothing to Disclose Kimihiro Kajita, Gifu, Japan (*Abstract Co-Author*) Nothing to Disclose Hiroshi Kawada, MD, Gifu, Japan (*Abstract Co-Author*) Nothing to Disclose Nobuyuki Kawai, MD, Gifu, Japan (*Abstract Co-Author*) Nothing to Disclose Yukichi Tanahashi, MD, Tokyo, Japan (*Abstract Co-Author*) Nothing to Disclose Masayuki Matsuo, Gifu, Japan (*Abstract Co-Author*) Nothing to Disclose Tomohiro Namimoto, MD, Kumamoto, Japan (*Abstract Co-Author*) Nothing to Disclose Norihiro Shinkawa, MD, Miyazaki, Japan (*Abstract Co-Author*) Nothing to Disclose Masataka Nakagawa, Kumamoto, Japan (*Abstract Co-Author*) Nothing to Disclose Toshinori Hirai, MD, PhD, Miyazaki, Japan (*Abstract Co-Author*) Nothing to Disclose Yasuyuki Yamashita, MD, Kumamoto, Japan (*Abstract Co-Author*) Nothing to Disclose

PURPOSE

To prospectively evaluate the feasibility of magnetic resonance angiography (MRA) during abdominal dynamic contrast-enhanced MR imaging and to compare the contrast effect and conspicuity of aortic branches in MRA between gadobutrol and gadoterate meglumine.

METHOD AND MATERIALS

Institutional review board approval was obtained for this prospective multi-center HIPAA-compliant study and written informed consent was obtained from all patients. At three institutions, a total of 88 patients (46 men and 42 women; age range, 36-84 years; mean 64.4 ± 11.0 years) with known and suspected upper abdominal disease performed view-sharing dynamic contrastenhanced MR imaging with five arterial phases. The axial, maximum intensity projection (MIP), and volume-rendered images (VR) angiography was generated by the first or second arterial phase images. The artery-to-muscle signal intensity ratio (SIR) and conspicuity of aortic branches were evaluated. Conspicuity of focal pancreatic lesions were evaluated on fourth or fifth arterial phase images and compared between gadobutrol and gadoterate meglumine.

RESULTS

View-sharing multi-arterial phase imaging was successfully performed in all patients. The SIRs of common hepatic artery (P = 0.0051) and left renal artery (RA) (P = 0.045), vascular conspicuities of right and left hepatic arteries (P = 0.010 and 0.030) and right and left RAs on axial (P = 0.0065 and 0.036), and that of gastroduodenal artery on MIP (P = 0.039) in gadobutrol were significantly higher than those in gadoterate meglumine. No significant differences were observed in the depiction of all aortic branches on VR images (P = 0.12-0.98) and the conspicuity of focal pancreatic lesions (P = 0.73) between gadobutrol and gadoterate meglumine.

CONCLUSION

Simultaneous acquisition of MRA and diagnostic images was feasible in contrast-enhanced upper abdominal MR imaging, and aortic branches were clearly visualized on MRA.

CLINICAL RELEVANCE/APPLICATION

Simultaneous acquisition of MRA and diagnostic images was feasible in contrast-enhanced upper abdominal MR imaging without significant differences in contrast effect and conspicuity regardless of contrast material with different r1 value.

RC512-04 Coronary CT Angiography and Carotid MRI Improve Phenotyping of Disease Extent Compared to AHA Risk Score Alone

Wednesday, Nov. 29 9:25AM - 9:35AM Room: N227B

Awards

Student Travel Stipend Award

Participants

Ashley Chorath, BS, Philadelphia, PA (Presenter) Nothing to Disclose Younhee Choi, BS, Bethesda, MD (Abstract Co-Author) Nothing to Disclose Evrim B. Turkbey, MD, Bethesda, MD (Abstract Co-Author) Nothing to Disclose Mark A. Ahlman, MD, Bethesda, MD (Abstract Co-Author) Nothing to Disclose Christopher Sibley, Bethesda, MD (Abstract Co-Author) Employed by Merck Songtao Liu, MD, Bethesda, MD (Abstract Co-Author) Nothing to Disclose Anna E. Zavodni, MD, MPH, Hamilton, ON (Abstract Co-Author) Nothing to Disclose Veit Sandfort, MD, Bethesda, MD (Abstract Co-Author) Nothing to Disclose David A. Bluemke, MD, PhD, Bethesda, MD (Abstract Co-Author) Research agreement, Siemens AG; Research support, Siemens AG; Research agreement, Carestream Health, Inc; Research support, Carestream Health, Inc

For information about this presentation, contact:

ashley.chorath@jefferson.edu

PURPOSE

Novel anti-atherosclerotic therapies promise marked reduction of LDL levels, but therapy costs are high, suggesting the need for precise identification of at-risk patients. The purpose of this study was to determine the relationship between cardiovascular risk (2013 ACC/AHA risk) and actual plaque phenotype assessed directly using CT and MR imaging in the coronary and carotid arteries.

METHOD AND MATERIALS

In an interventional study asymptomatic subjects eligible for statin therapy underwent coronary calcium scoring (CAC), coronary CT angiography (CTA) and MRI of the carotid artery. Quartiles were calculated for non-calcified plaque (NCP), CAC, carotid wall volume and were compared to AHA risk quartiles. Characteristics of patients with an AHA risk score misclassification of two or more quartiles were compared. Models were fitted to predict carotid plaque based on AHA risk and coronary imaging tests. C-statistics and net reclassification improvement (NRI) were calculated.

RESULTS

206 subjects were enrolled (60% men, mean age 65). There was fair correlation between average carotid wall plaque (Kendall's tau=0.30), NCP (tau=0.23), and CAC (tau=0.34, all p<0.001). However, AHA risk alone misclassified plaque extent in comparison to direct measurement by carotid wall volume, CAC, and NCP in 25.7%, 23.8% and 29.1% of subjects, respectively. On average 11.75% of the subjects were under-classified and 12.25% over-classified. 31 subjects (15.04%) were under-classified in two or more imaging methods. Subjects who were under-classified in all methods were younger and over-classified patients were older (p<0.001). Correlation between carotid wall volume and CAC was low (tau=0.17, p=0.004). When predicting carotid plaque based on AHA risk, there was no significant improvement when adding CAC to the model, while the addition of NCP led to significant improvement (AUC of 0.75 and 0.79, respectively, NRI 0.52, p=0.001).

CONCLUSION

Approximately 25% of patients have large discrepancies between ACC/AHA risk and the actual plaque burden measured with noninvasive imaging. These results suggest that treatment based on risk score models alone may result in substantial over- and under-treatment of at-risk individuals.

CLINICAL RELEVANCE/APPLICATION

Imaging shows that the risk score substantially over- or underestimates plaque in some asymptomatic patients. This may be relevant to novel anti-atherosclerotic therapies with high treatment costs.

RC51205 MR Biomarkers for Vascular Disease

Wednesday, Nov. 29 9:35AM - 10:10AM Room: N227B

Participants

Albert De Roos, MD, Leiden, Netherlands (Presenter) Nothing to Disclose

For information about this presentation, contact:

a.de_roos@lumc.nl

LEARNING OBJECTIVES

1) Learning MRI techniques for assessing vascular biomarkers. 2) Focus on aortic distensibility and vascular stiffness. 3) Clinical implications of vascular function related to end-organs. 4) Focus on aortic stiffness and brain disease.

ABSTRACT

Vascular biomarkers assessed by MRI techniques may contribute to better risk stratification and understanding the pathophysiological interaction between the vasculature and end-organs. MRI is well suited to assess vascular morphology and function in territories that may be difficult to explore with other imaging techniques (e.g. proximal aorta). Stiffening and distensibility of the proximal aorta can be directly assessed using standard MRI techniques.Stiffening of the aorta is one of the earliest manifestations of disease and plays a central role in causing increased pulsatility to the brain and other end-organs. Aortic function also interacts with heart function and perfusion and may be a contributory factor in causing heart failure. The focus of this presentation will be on the role of vascular biomarkers in causing end-organ disease in the heart and brain.

Participants

Tim Leiner, MD, PhD, Utrecht, Netherlands (Presenter) Speakers Bureau, Koninklijke Philips NV; Research Grant, Bayer AG;

For information about this presentation, contact:

t.leiner@umcutrecht.nl

LEARNING OBJECTIVES

1) To understand the role of MRA in the clinical workup of patients with peripheral vascular disease. 2) To learn about MRI techniques such as flow and perfusion that provide functional information about the peripheral circulation in addition to anatomical assessment. 3) To learn how to interpret information obtained with these adjunctive MRA techniques. 4) To learn how these MRI techniques can be incorporated into a clinical scanning protocol.

RC512-07 Automated Detection and Labeling of the Intracranial Arterial Tree in Routine MR Angiography: A Machine Learning Approach Enhanced with Structural Saliency

Wednesday, Nov. 29 10:55AM - 11:05AM Room: N227B

Participants

Li Chen, BS, Seattle, WA (Presenter) Nothing to Disclose Jie Sun, Seattle, WA (Abstract Co-Author) Nothing to Disclose Niranjan Balu, PhD, Seattle, WA (Abstract Co-Author) Nothing to Disclose Thomas S. Hatsukami, MD, Seattle, WA (Abstract Co-Author) Research Grant, Koninklijke Philips NV Mahmud Mossa-Basha, MD, Seattle, WA (Abstract Co-Author) Nothing to Disclose Kristi D. Pimentel, Seattle, WA (Abstract Co-Author) Nothing to Disclose Jenq-Neng Hwang, Seattle, WA (Abstract Co-Author) Nothing to Disclose Chun Yuan, PhD, Seattle, WA (Abstract Co-Author) Research Grant, Koninklijke Philips NV; Consultant, BGI; ;

For information about this presentation, contact:

cyuan@uw.edu

PURPOSE

Intracranial arteries constitute a complex network with considerable anatomical variations. Automated detection and labeling of the various segments of the intracranial arterial tree allow time-efficient characterization of regional differences in distal distributing arteries in routine MR angiography, which are overlooked in clinical review but may afford novel information on vascular health.

METHOD AND MATERIALS

Algorithm Vessels on time-of-flight (TOF) MRA were enhanced by Frangi filter and traced by open-curve snake to acquire topology of arteries. Bifurcations of interest (BoI) were classified so that arteries could be labeled indirectly. Besides positional and directional features, we introduced structural saliency, a weighted index calculated from regional graph structure and vessel likelihood to improve detection performance of BoI. A model graph calculated with multivariate Gaussian distribution from previously labeled cases was used to match unlabeled cases by calculating Gaussian probability density from each feature. Maximum a posteriori estimation was used to label BoI to the type with highest possibility. Arteries are then labeled according to BoI types in both ends . Validation Performance of the algorithm was tested on 48 clinical cases with vascular disease (59±13 years, 32 males). Arteries were also labeled manually by experienced reader as ground truth. Using leave-one-out validation, we calculated accuracy of BoI labeling with and without structural saliency.

RESULTS

The proposed algorithm could identify and classify major arteries of brain MRA. The percent of BoI labels agreed with ground truth was 96.1%, but the percent dropped to 93.8 % without using structural saliency as one of the features.

CONCLUSION

An automatic algorithm for detecting and labeling intracranial arteries was developed, which can generate regional measures of cerebrovascular structure from routine MR angiography for additional insights into cerebral arteries and it is also a promising framework to develop additional neuroradiology tools that use vascular structural information.

CLINICAL RELEVANCE/APPLICATION

Automatically labeling intracranial arteries is beneficial for description of vascular structures and provide valuable information for the identification of geometric risk factors of vascular disease.

RC512-08 Time-resolved Magnetic Resonance Angiography at 3 Tesla in Active Dorsi-and Plantarflexion of Suspected Popliteal Artery Entrapment Syndrome

Wednesday, Nov. 29 11:05AM - 11:15AM Room: N227B

Participants

Yoo Jin Lee, MD, Charlottesville, VA (Presenter) Nothing to Disclose Patrick T. Norton, MD, Charlottesville, VA (Abstract Co-Author) Nothing to Disclose Jessie Jahjah, MD, Charlottesville, VA (Abstract Co-Author) Nothing to Disclose Klaus D. Hagspiel, MD, Charlottesville, VA (Abstract Co-Author) Research Grant, Siemens AG

For information about this presentation, contact:

Yoojinleerad@gmail.com

PURPOSE

Popliteal artery entrapment syndrome (PAES) is an important diagnostic consideration in younger patients with exertional calf pain. PAES is diagnosed when popliteal artery deviation or stenosis is present on angiography during active dorsi or plantar flexion. Cross-sectional imaging can demonstrate the anatomical cause and type of PAES. At our institution, positional stress time resolved contrast-enhanced MRA in active plantar and dorsiflexion (STR-MRA) along with axial MRI is routinely performed for the evaluation of suspected PAES. We aim to analyze the utility of stress TR-MRA for the diagnosis of PAES.

METHOD AND MATERIALS

Between 5/2010 and 9/2015, 51 patients underwent coronal STR-MRA on a 3T scanner (TWIST; Trio or Skyra, Siemens Medical Solutions, Germany): spatial resolution 1.3 x 1.3 x 2mm, temporal resolution 2.1 sec. MIP images were used for analysis. Axial anatomical sequences of the popliteal fossa included a pre and post contrast T1 fat suppressed 3D radio-frequency-spoiled 3D GRE sequence (VIBE) as well as a T1 TSE and STIR sequences. Presence, degree, and length of popliteal arterial or venous deviation and stenosis as well as anatomical causes were documented and the type of PAES was recorded according to the classification of Whelan and Rich. Initial presentation, management, and clinical / surgical outcomes were also documented using electronic medical records.

RESULTS

STR-MRA for 102 limbs were obtained, all technically successful without motion artifact. 25/102 (25%) limbs in 15/51 (29%) patients showed deviation or stenosis of the popliteal artery during stress. 9 patients had bilateral findings. The degree of stenosis ranged from 10% to 100% (mean 45%), and the length from 15mm to 85mm (mean 38mm). The type of PAES in the 25 affected limbs were: type 4 (n=1, 4%), type 5 (n=7, 28%), type 6 (n=15, 60%), deviation without stenosis (n=2, 8%). DSA was performed in 8 patients and correlated with STR-MRA in 100%. Entrapment release surgery was performed in 9 limbs in 7 patients, all of which had positive STR-MRA findings. Six patients responded to surgery with significant clinical improvement.

CONCLUSION

Evaluation of patients with suspected PAES with STR-MRA and MRI allows reliable non-invasive identification of vascular abnormalities and classification of PAES.

CLINICAL RELEVANCE/APPLICATION

Time-resolved stress MRA in conjunction with MRI allows comprehensive assessment of patients with suspected PAES.

RC512-09 Impact of Field Strength on Feasibility of Decreased Temporal Resolution in Intracranial 4D Flow MRI

Wednesday, Nov. 29 11:15AM - 11:25AM Room: N227B

Participants

Maria Aristova, BEng, Chicago, IL (Presenter) Nothing to Disclose Sebastian Schmitter, Braunschweig, Germany (Abstract Co-Author) Nothing to Disclose Can Wu, Chicago, IL (Abstract Co-Author) Nothing to Disclose Pierre-Francois Van de Moortele, Minneapolis, MN (Abstract Co-Author) Nothing to Disclose James C. Carr, MD, Chicago, IL (Abstract Co-Author) Research Grant, Astellas Group; Research support, Siemens AG; Speaker, Siemens AG; Advisory Board, Guerbet SA Kamil Ugurbil, Minneapolis, MN (Abstract Co-Author) Nothing to Disclose Michael Markl, PhD, Chicago, IL (Abstract Co-Author) Institutional research support, Siemens AG; Consultant, Circle Cardiovascular Imaging Inc; Susanne Schnell, Chicago, IL (Abstract Co-Author) Nothing to Disclose

For information about this presentation, contact:

maria.aristova@northwestern.edu

PURPOSE

Dual-venc 4D flow MRI provides comprehensive cerebrovascular blood flow assessment with high velocity dynamic range. However, long scan times limit this approach particularly for large target regions. By comparing flow values from single-timepoint to standard multi-timepoint dual-venc 4D flow MRI at 3T and 7T, we characterize the tradeoff between temporal resolution, coverage and scan time to identify clinically acceptable parameters.

METHOD AND MATERIALS

ECG-gated dual-venc 4D flow MRI was acquired at 3T in 15 healthy volunteers covering Circle of Willis at two temporal resolutions: 7 cardiac phases (MTP: 103.6ms) and 1 cardiac phase (1TP: 725.2ms). 5 subjects were also scanned at 7T. All images were corrected for concomitant gradient terms, eddy currents and background noise. Phase-contrast angiograms were extracted from each data set to generate a 3D segmentation of main intracranial vessels and streamlines to visualize blood flow. For each scan, net flow and peak velocity were calculated with analysis planes at main intracranial vessels. Net flow ratios between inlet and outlet at vessel branch points characterize flow conservation. Streamline continuity was assessed qualitatively. Noise was determined using velocity standard deviation in static tissue.

RESULTS

1TP scan time was comparable to MTP with 3-fold increased volumetric coverage and no significant difference in streamline continuity (p=0.14 at 3T, 0.48 at 7T) or image noise (p=0.11 at 3T, 0.08 at 7T) at 3T or 7T. Noise was 53% lower in 7T scans. Bland-Altman analysis shows mean difference (offset) between MTP and 1TP peak velocity measurements differs significantly from 0 (p<10-4 at 3T and 7T) and difference varies with mean value (nonzero slope, p<10-6 at 3T and 7T). However, net flow offset and slope are significant (p<0.05) at 3T but not 7T (p>0.1). Net flow ratio had no significant offset at any vessel branch point at 3T or 7T.

CONCLUSION

MTP and 1TP data have better net flow agreement and internal consistency at 7T than 3T, with no significant continuity or noise difference between MTP and 1TP data at either field. At 7T, decreasing temporal resolution while recovering consistent net flow values would suffice for many applications.

CLINICAL RELEVANCE/APPLICATION

High-field, low temporal resolution intracranial 4D flow MRI could provide accurate flow distribution assessment in arteriovenous malformation or aneurysm, especially in post-surgical monitoring.

RC51210 MRA at 3T or Higher Field Strength

Wednesday, Nov. 29 11:25AM - 12:00PM Room: N227B

Participants

Winfried A. Willinek, MD, Trier, Germany (Presenter) Speakers Bureau, Bayer AG; Speakers Bureau, Bracco Group; Speakers Bureau, General Electric Company; Speakers Bureau, Koninklijke Philips NV; Speakers Bureau, Sirtex Medical Ltd

LEARNING OBJECTIVES

1) Identify advantages and disadvantages of MRA at 3T and higher field strength. 2) Practice solutions and new techniques to overcome limitations. 3) Acces the results of new research related to high field MRA. 4) Apply technical innovations to clinical practice.





Pediatric Series: Pediatric Radiology

Wednesday, Nov. 29 8:30AM - 12:00PM Room: E352



AMA PRA Category 1 Credits ™: 3.25 ARRT Category A+ Credits: 3.75

FDA Discussions may include off-label uses.

Participants

Teresa Chapman, MD, MA, Seattle, WA (*Moderator*) Nothing to Disclose M. Beth McCarville, MD, Memphis, TN (*Moderator*) Consultant, General Electric Company Harriet J. Paltiel, MD, Boston, MA (*Moderator*) Nothing to Disclose Sara M. O'Hara, MD, Cincinnati, OH (*Moderator*) Author, Reed Elsevier; Speakers Bureau, Toshiba Medical Systems Corporation; Medical Advisory Board, Toshiba Medical Systems Corporation

For information about this presentation, contact:

teresa.chapman@seattlechildrens.org

Sub-Events

RC513-01 Pediatric Liver Doppler

Wednesday, Nov. 29 8:30AM - 8:50AM Room: E352

Participants

Sara M. O'Hara, MD, Cincinnati, OH (*Presenter*) Author, Reed Elsevier; Speakers Bureau, Toshiba Medical Systems Corporation; Medical Advisory Board, Toshiba Medical Systems Corporation

For information about this presentation, contact:

s.ohara@cchmc.org

LEARNING OBJECTIVES

1. Learn tips for optimizing liver Doppler exams in pediatric patients. 2. Improve understanding and application of newest ultrasound technologies to liver Doppler. 3. Recognize common and uncommon pediatric disease states diagnosed with liver Doppler.

LEARNING OBJECTIVES

1) Learn tips for optimizing liver Doppler exam in pediatric patients. 2) Improve understanding and application of newest ultrasound technologies to liver Doppler. 3) Recognize common and uncommon pediatric disease states diagnosed with liver Doppler.

RC513-02 Monitoring Pediatric Liver Transplantation: Comparison of B-Flow Sonography with Color Doppler Sonography to Assess Detectability of the Hepatic Artery

Wednesday, Nov. 29 8:50AM - 9:00AM Room: E352

Participants

Leonhard A. Steinmeister, Hamburg, Germany (*Presenter*) Nothing to Disclose Michael Groth, Hamburg, Germany (*Abstract Co-Author*) Nothing to Disclose Lutz Fischer, Hamburg, Germany (*Abstract Co-Author*) Nothing to Disclose Gerhard B. Adam, MD, Hamburg, Germany (*Abstract Co-Author*) Nothing to Disclose Jochen Herrmann, MD, Hamburg, Germany (*Abstract Co-Author*) Nothing to Disclose

PURPOSE

Ultrasound plays a decisive role in the postoperative monitoring of pediatric liver transplantation. Detectability of the hepatic artery (HA) and portal vein (PV) is important to rule out early vascular complications. We evaluated whether B-Flow Sonography (BFS) is superior to Color Doppler Sonography (CDS) for the detectability of the hepatic artery.

METHOD AND MATERIALS

Standardized postoperative ultrasound examinations of 37 consecutive children (mean age 6.5 years, range 1 month - 22 years) who underwent liver transplantation between November 2015 and November 2016 were retrospectively evaluated. Freehand horizontal BFS and CDS cine sweeps produced with a curved array (GE Logiq 9 ultrasound system, GE Medical Systems, Milwaukee, WI, USA) were visually rated. The degree of detectability of the HA was assessed at an extrahepatic, neohilar and segmental location: (0) HA not detectable; (1) HA discontinuously detectable, not separable from the PV; (2) HA discontinuously detectable, separable from the PV; (3) HA continuously detectable and completely separable from the PV. Wilcoxon paired sample rank-sum test was performed to compare both methods.

RESULTS

Assessment of cine sweeps demonstrated a significantly higher degree of detectability of the HA using BFS compared with CDS

technique at the neohilum (2.2 ± 0.97 vs. 1.1 ± 0.83 ; p < 0.0001) and at the segmental location (2.8 ± 0.63 vs. 0.6 ± 0.77 ; p < 0.0001). No difference was noted at the extrahepatic level (1.3 ± 1.2 vs. 1.2 ± 0.94). The portal vein was similarly detectable by both methods.

CONCLUSION

Substantially improved delineation of the hepatic artery in pediatric liver transplants can be achieved with BFS compared with CDS technique. By documenting cine sweeps, vascular integrity can be reassessed offline and thus allowing for improved transplant monitoring.

CLINICAL RELEVANCE/APPLICATION

With BFS substantially better vessel delineation can be achieved in pediatric liver transplants thus increasing the degree of certainty to rule out vascular complications.

RC513-03 Availation of Intima-Media Thickness of the Carotid and Brachial Artery Intraluminal Diameter as Cardiovascular Risks in Children and Adolescents

Wednesday, Nov. 29 9:00AM - 9:10AM Room: E352

Participants

Alessandra C. Ribeiro, MD, Sao Paulo, Brazil (*Presenter*) Nothing to Disclose Eduardo F. Fleury, PhD, Sao Paulo, Brazil (*Abstract Co-Author*) Nothing to Disclose Cristiane Kochi, Sao Paulo, Brazil (*Abstract Co-Author*) Nothing to Disclose

PURPOSE

Correlate anthropometric, laboratory and ultrasonographic intima-media thickness of the carotid and brachial intraluminal diameter data in obese adolescents with cardiovascular risk predictors.

METHOD AND MATERIALS

Retrospective study of 77 pubertal overweight patient, with the mean (SD) chronological age of 12.9 (2.5) years. Weight, height (to calculate BMI), waist circumference (WC), percentage of abdominal fat by bioelectrical impedance (BIA), serum total cholesterol (TC) and fractions, triglycerides (TG) and glucose oral tolerance test with glucose and insulin dosages were evaluated as cardiovascular risk predictors. BMI was expressed in SDS score (BMI SDS-WHO) and the ratios WC/Height, TG/HDL-C, HOMA-IR and sum of insulin values were made. The image data were obtained through the ultrasound to obtain the intima-media thickness (IMT) of the carotid artery and in the longitudinal axis of the brachial artery. We also evaluated the arterial blood velocity of the brachial artery in the first 15 seconds of reactive hyperemia after inflating the cuff on the patient's arm up to 30 mmHg above their systolic BP for 5 minutes.

RESULTS

The mean BMI SDS was +2.5 (0.7), the WC/height 0.6 (0.05) and the percentage of fat (BIA) of 38% (6.6). We found 36.4% of inadequacy values of TC, 72,7% of HDL, 36,4% of LDL and 53,2% of TG. The mean (SD) fasting insulin was 20 (10.9) and carotid IMT = 0.5 (0.08). None of the patients have diabetes mellitus type 2 and four were intolerant to glucose. There was a positive correlation between the TG/HDL-C ratio with the sum of insulin (r = 240, p <0.036) and the zIMC with carotid IMT (r = 0.226, p <0.049). There was an inverse correlation between the arterial blood velocity rate and the sum of insulin (r = - .297, p <0.009).

CONCLUSION

Our results demonstrate that the average carotid IMT was above the threshold value, and the higher the BMI, the greater the IMT, suggesting that this population may be at cardiovascular risk.

CLINICAL RELEVANCE/APPLICATION

The relation between TG/HDL-c and the sum of insulin values suggests that it can be used as a marker of insulin resistance. The negative correlation between brachial artery blood velocity rate with the sum of insulin shows the change of the response of the endothelium to vasoconstriction (mediated by nitric oxide) in patients with insulin resistance.

RC513-04 A New and Simple Method to Estimate Weight and Gestational Age in Critically III Newborns: The Return Journey of Chest X-Ray

Wednesday, Nov. 29 9:10AM - 9:20AM Room: E352

Participants

Joan Albert Prat-Matifoll, MD, Barcelona, Spain (*Presenter*) Nothing to Disclose Joaquim Piqueras, PhD, Barcelona, Spain (*Abstract Co-Author*) Nothing to Disclose Albert Prats-Uribe, Barcelona, Spain (*Abstract Co-Author*) Nothing to Disclose Carmen Parra-Farinas, MD, Barcelona, Spain (*Abstract Co-Author*) Nothing to Disclose Shelagh C. Dyer, MD, Barcelona, Spain (*Abstract Co-Author*) Nothing to Disclose Cesar Augusto A. Ortiz Andrade SR, MD, Barcelona, Spain (*Abstract Co-Author*) Nothing to Disclose Joan Carles Carreno, MD, Barcelona, Spain (*Abstract Co-Author*) Nothing to Disclose

For information about this presentation, contact:

joanalbertpratrx@gmail.com

PURPOSE

The purpose is to describe a reliable method to estimate the weight and gestational age by measurements taken in A-P chest x-ray exams of newborns admitted to a neonatal intensive care unit (NICU)

METHOD AND MATERIALS

This is a cross-sectional study of 376 plain chest films of 284 newborns. <u>Patient characteristics</u>: This study includes full-term, critically ill and premature newborns admitted to NICU between September 2014 and September 2015. This scientific exhibit divides

newborns into 3 main groups: pre-term, term and post-term. The preterm group was subdivided in extremely, very and moderate/late preterm. <u>Chest x-ray assessment:</u> One chest x-ray was assessed in 216 (76%) newborns; two chest x-rays were assessed in 48 (17%) newborns during the first two consecutive days of life and three in 16 newborns during the first three consecutive days. Three simple measures were taken from chest A-P exams: -Dorsal spine length: A straight line from the superior rim of D1 to the lower rim of D12 -Right pulmonary length: From the right pulmonary apex to the center of the right diaphragmatic dome -Transversal chest width: Between the outer margins of the ribs at the maximum transverse diameter (9th rib) <u>Other relevant variables:</u> Weight, assessed prematurity, small for gestational age, multiple pregnancy, persistent ductus arteriosus, congenital malformations, metabolopathies, and maternal complications.

RESULTS

Multiple threshold measures were obtained in order to establish an optimal value to classify newborns. The threshold values obtained were: <u>One key measure to differentiate preterm from term and postterm newborns</u> -Dorsal Spine length:90mm <u>Three key measures</u> to differentiate between extremely and very preterm from late preterm and term newborns -Dorsal Spine length:80mm -Right pulmonary length:47mm -Transversal chest width:93mm <u>The triple combination of 3 measures</u>, helps to improve the PPV for differentiating extremely/very preterm from late/term newborns: PPV: 93.1% / NPV: 82.1%

CONCLUSION

Dorsal Spine, Right Pulmonary, and Chest width measurements, and their combinations, are quick and reliable estimates of weight and gestational age in preterm and full-term newborns

CLINICAL RELEVANCE/APPLICATION

Pediatric radiologists often report initial chest x-ray of critically ill newborns without clinical information. Fast estimation of gestational age and weight may contribute to more accurate diagnoses

RC513-05 Marginal Diagnostic Yield from Double Reading Initial Skeletal Surveys versus Follow-Up Skeletal Surveys for Suspected Non-Accidental Trauma

Wednesday, Nov. 29 9:20AM - 9:30AM Room: E352

Participants

Sarah M. Bahouth, MD, Houston, TX (*Presenter*) Nothing to Disclose Robert Orth, MD, PhD, Houston, TX (*Abstract Co-Author*) Nothing to Disclose James E. Crowe, MD, Kansas City, MO (*Abstract Co-Author*) Nothing to Disclose

For information about this presentation, contact:

rcorth@texaschildrens.org

PURPOSE

We hypothesize that double reading initial SSs decreases the number of new fractures identified on follow-up SSs. The purpose of this study is to compare the marginal diagnostic yield of double reading initial SSs performed for suspected non-accidental trauma to the marginal diagnostic yield of follow-up SSs following single reading of initial exams.

METHOD AND MATERIALS

All SSs (initial and follow-up) performed between February 2, 2013, and March 23, 2015 for suspected non-accidental trauma at a large children's hospital were double-read by a non-blinded pediatric radiologist within 72 hours of primary interpretation. Fractures detected on the primary and secondary (double reading) interpretations of initial SSs and primary interpretations of follow-up SSs were recorded. The number of additional fractures identified by double-reading initial SSs to the number of additional fractures identified on follow-up SSs was compared via McNemar's test.

RESULTS

During the study period, 1056 initial SSs were performed (M:F=616:440; 13.2 months +/-13.9 months; age range 0.1-108 months), of which 293/1056 (28%) had follow-up SSs. Of cases with follow-up exams, primary and secondary interpretations of initial exams were concordant in 263/293 (90%) with follow-up SSs showing additional fractures in 32/263 (12%) and no additional fractures in 231/263 (88%). In 30/293 (10%) initial SSs, fractures were identified on the secondary (double-reading) interpretations that were not identified on primary interpretations with follow-up SSs showing additional fractures in 5/30 (17%) not identified on either the primary or secondary interpretations and no additional fractures in 25/30 (83%). The difference between the marginal diagnostic yield of secondary interpretations (10%) and follow-up SSs for initial exams not double-read (13%) was not statistically significant (0.43)

CONCLUSION

Both double reading initial SSs and follow-up increased diagnostic yield, but the comparative diagnostic yield was not statistically different. These results show the benefit of double-reading initial skeletal surveys and indicate the need for further studies to determine if double reading initial SSs can obviate the need for follow-up exams in select cases.

CLINICAL RELEVANCE/APPLICATION

The increased diagnostic yield from double reading skeletal surveys may decrease the need for follow-up exams and strengthen the confidence in the diagnosis of nonaccidental trauma.

RC513-06 Centile Charts for Cranial Sutures Under One Year of Life Based on Ultrasound Measurements

Wednesday, Nov. 29 9:30AM - 9:40AM Room: E352

Participants

Katya Rozovsky, MD, Winnipeg, MB (*Presenter*) Nothing to Disclose Nick Barrowman, Ottawa, ON (*Abstract Co-Author*) Nothing to Disclose Elka Miller, MD, Ottawa, ON (*Abstract Co-Author*) Nothing to Disclose

PURPOSE

To provide reference for normal ultrasound measurements of cranial sutures during the first year of life.

METHOD AND MATERIALS

All children 0 to 12 months referred from March 2011 to September 2013 for radiographic evaluation of the cranial sutures were approached for a prospective cranial ultrasound (CUS). CUS was performed with a 12-MHz linear transducer in supine or semi-sitting position. Sagittal, coronal, lambdoid, and metopic sutures were evaluated. Two radiologists independently measured cranial sutures by locating the PACS measurement tool between the hyperechoic bone edges. Values of sutural width were obtained in 3 points of the sagittal suture (anterior, middle and posterior), and the middle point for the metopic, each coronal and lambdoid sutures. The readers were blinded to clinical indications and previous reports.

RESULTS

150 children met the study inclusion criteria. 21 parents did not consent to the CUS study. 129 children underwent CUS, 3 patients were excluded due to poor cooperation, and 11 due to closed cranial sutures (craniosynostosis). 115 children (75 females, 40 males; mean age 5.6 month (standard deviation 2.7)) became the study group with normal cranial sutures. Each suture demonstrated significant decrease in size with age (p<0.001). During the first year of life the metopic suture decreased rapidly, while the lambdoid sutures demonstrated a slowest closure. There were no statistically significant differences in age related suture size in male and female patients.

CONCLUSION

Centile charts of normal ultrasound measurements of cranial sutures during the first year of life are presented. Defining normal size of the sutures and the changes over the first year of life is necessary to determine abnormality, particularly synostosis or diastatic sutures. This normative ultrasound data will help the radiologist recognizing normal and abnormal sutures.

CLINICAL RELEVANCE/APPLICATION

1. Cranial ultrasound is a radiation free technique that can be used as a first line imaging modality for evaluation of the cranial sutures in children under 1 year of life (Rozovsky et al, Pediatrics 2016) 2. Potential indications for cranial sutures ultrasound measurments include conditions associated with premature closure of cranial sutures (craniosynostosis) as well as widening or delayed closure of main cranial sutures. The provided normal measurements can be used by radiologists as a reference tool in clinical practice.

RC513-07 Abdominal Complications in Pediatric Oncology

Wednesday, Nov. 29 9:40AM - 10:00AM Room: E352

Participants

M. Beth McCarville, MD, Memphis, TN (Presenter) Consultant, General Electric Company

For information about this presentation, contact:

beth.mccarville@stjude.org

LEARNING OBJECTIVES

1) To review the common abdominal complications associated with the treatment of childhood cancers. 2) To discuss the imaging features of a variety of abdominal complications resulting from the treatment of pediatric malignancies. 2) To discuss the most appropriate imaging modalities to diagnose and monitor abdominal comlications of childhood cancer therapy.

LEARNING OBJECTIVES

1) Learn the most common abdominal complications of cancer therapy in children and conditions that predispose patients to their development. 2) Understand the indications for and role of imaging in the diagnosis and management of these patients. 3) Recognize the imaging features that suggest the diagnosis of abdominal complications.

RC513-08 Sonography of Vascular Anomalies

Wednesday, Nov. 29 10:20AM - 10:40AM Room: E352

Participants

Harriet J. Paltiel, MD, Boston, MA (Presenter) Nothing to Disclose

LEARNING OBJECTIVES

1) Be able to discuss the ISSVA classification of vascular anomalies. 2) List the most important lesions presenting in the prenatal and neonatal periods. 3) Identify the differential diagnostic features of these entities.

RC513-09 Differentiation of Benign and Malignant Lymph Nodes in Pediatric Patients on Ferumoxytol-Enhanced PET/MR

Wednesday, Nov. 29 10:40AM - 10:50AM Room: E352

Participants

Anne M. Muehe, MD, Stanford, CA (*Presenter*) Nothing to Disclose Ashok Joseph Theruvath, MD, Mainz, CA (*Abstract Co-Author*) Nothing to Disclose Samantha Holdsworth, PhD, Palo Alto, CA (*Abstract Co-Author*) Nothing to Disclose Jarrett Rosenberg, PhD, Stanford, CA (*Abstract Co-Author*) Nothing to Disclose Sandra Luna-Fineman, MD, Palo Alto, CA (*Abstract Co-Author*) Nothing to Disclose Heike E. Daldrup-Link, MD, Palo Alto, CA (*Abstract Co-Author*) Nothing to Disclose Accurate detection of malignant lymph nodes is important for cancer staging of pediatric patients. Previous studies reported distinct iron oxide nanoparticle enhancement patters of benign and malignant lymph nodes in adult patients. The purpose of our study was to compare imaging characteristics of benign and malignant lymph nodes in pediatric patients on ferumoxytol-enhanced PET/MR.

METHOD AND MATERIALS

12 children (11-18 years) with malignant tumors underwent PET/MR imaging at 4 hours or at 24 hours after intravenous injection of the iron oxide nanoparticle compound ferumoxytol. MR sequences included T1-weighted LAVA, T2-weighted FSE, DWI, and T2*-weighted multi-echo IDEAL sequences. Follow up imaging for at least 6 months and/or histopathology served as the standard of reference. Different morphologies of 154 benign and 87 malignant lymph nodes on T2-FSE sequences were compared with the gold standard using McNemar's test. In addition, ADC-values, SUVmax and T2*-relaxation times of benign and malignant lymph nodes were compared with t-tests.

RESULTS

On T2-FSE images, benign lymph nodes showed a T2-hypointense hilum, surrounded by a T2-hyperintense parenchyma, while malignant lymph nodes showed loss of the hilum signal. This difference in morphologies was significant (p = 0.02). Benign lymph nodes showed mean diameters of 11.3 mm. There was no significant difference in quantitative data within experimental groups at 4 and 24 hours post ferumoxytol. Benign and malignant lymph nodes with diameters > 1 cm showed mean T2* relaxation times of 5.4 ms and 10.4 ms, mean SUVmax values of 3.6 and 9.2 and mean ADC values of 894 x 10-6 mm2/s and 1852 x 10-6 mm2/s, respectively. These differences were significant with p values of 0.014, < 0.001 and 0.027. Benign and malignant lymph nodes with diameters < 1 cm showed mean T2* relaxation times of 1351 x 10-6 mm2/s and 1991 x 10-6 mm2/s, resulting in significant differences with p values of <0.001 respectively..

CONCLUSION

Benign and malignant lymph nodes in pediatric patients show specific imaging characteristics on ferumoxytol-enhanced PET/MR.

CLINICAL RELEVANCE/APPLICATION

Lymph nodes of pediatric patients can show different imaging patterns on ferumoxytol-enhanced PET/MR compared to lymph nodes of adult patients.

RC513-10 Evaluation of a New Computer Aided Diagnosis (CAD) System for Automated Bone Age Assessment in Children compared with the Greulich Pyle Atlas Method: A Multireader Study

Wednesday, Nov. 29 10:50AM - 11:00AM Room: E352

Awards

Student Travel Stipend Award

Participants

Christian Booz, MD, Frankfurt am Main, Germany (*Presenter*) Nothing to Disclose Julian L. Wichmann, MD, Frankfurt, Germany (*Abstract Co-Author*) Speaker, General Electric Company; Speaker, Siemens AG Sabine Boettger, Frankfurt Am Main, Germany (*Abstract Co-Author*) Nothing to Disclose Ahmed Al Kamali, Frankfurt, Germany (*Abstract Co-Author*) Nothing to Disclose Simon S. Martin, MD, Frankfurt, Germany (*Abstract Co-Author*) Nothing to Disclose Boris Bodelle, MD, Frankfurt Am Main, Germany (*Abstract Co-Author*) Nothing to Disclose Doris Leithner, MD, Frankfurt Am Main, Germany (*Abstract Co-Author*) Nothing to Disclose Lukas Lenga, Frankfurt, Germany (*Abstract Co-Author*) Nothing to Disclose Moritz H. Albrecht, MD, Charleston, SC (*Abstract Co-Author*) Nothing to Disclose Jan-Erik Scholtz, MD, Boston, MA (*Abstract Co-Author*) Nothing to Disclose Thomas J. Vogl, MD, PhD, Frankfurt, Germany (*Abstract Co-Author*) Nothing to Disclose

For information about this presentation, contact:

boozchristian@gmail.com

PURPOSE

To investigate a new computer aided diagnosis (CAD) system (BoneXpert) for bone age assessment in children compared with the Greulich Pyle (GP) atlas method.

METHOD AND MATERIALS

This study was approved by the institutional review board, and the requirement to obtain informed consent was waived. Data from clinically indicated hand and wrist radiographs of 305 pediatric patients were included. Total bone age, the bone age of left distal radius and the bone age of carpal bones were analyzed by three different radiologists with varying levels of experience independently using the GP atlas method. In comparison, total bone age and the bone age of the left distal radius of each patient were analyzed using the CAD system. Pearson product-moment correlation coefficient, Bland-Altman plot and further regression analyses were evaluated for correlation analysis. Inter-reader correlation was assessed with weighted κ .

RESULTS

A total of 305 radiographs of left hands were analyzed in all 305 patients (mean age, 10.2 years; range, 1-18 years), further divided into 172 male (mean age, 10.6 years; range, 1-18 years) and 133 female patients (mean age, 9.6 years; range, 1-18 years). Mean total bone age was 9.76 years determined by CAD and 9.81 years determined by the GP atlas method. There was very high correlation between both approaches (r=0.985). Mean bone age of the left distal radius was 9.5 years determined by CAD and 9.82 determined by the GP atlas method (r=0.963). Mean bone age of carpal bones assessed by three radiologists was 9.94 years. The correlation analysis demonstrated significantly higher correlation between total bone age values and bone age values of the left distal radius (r=0.969) than between total bone age values and bone age values of carpal bones (r=0.923).

CONCLUSION

The evaluated CAD system (bonexpert) is reasible for automated bone age assessment and shows very high correlation with the GP atlas method. A method assessing bone age of the left distal radius may be more accurate than methods analyzing the carpal bones for bone age assessment.

CLINICAL RELEVANCE/APPLICATION

A new CAD system (BoneXpert) is feasible for automated bone age assessment and shows very high correlation with the Greulich Pyle atlas method.

RC513-11 AI Increases Accuracy and Decreases Variance of Bone Age Assessment by Radiologists

Wednesday, Nov. 29 11:00AM - 11:10AM Room: E352

Awards

Trainee Research Prize - Resident

Participants

Shahein H. Tajmir, MD, Boston, MA (*Presenter*) Nothing to Disclose
Hyunkwang Lee, Boston, MA (*Abstract Co-Author*) Nothing to Disclose
Randheer Shailam, MD, Boston, MA (*Abstract Co-Author*) Nothing to Disclose
Heather I. Gale, MD, Boston, MA (*Abstract Co-Author*) Nothing to Disclose
Jie C. Nguyen, MD,MS, Philadelphia, PA (*Abstract Co-Author*) Nothing to Disclose
Sjirk J. Westra, MD, Boston, MA (*Abstract Co-Author*) Nothing to Disclose
Ruth Lim, MD, Boston, MA (*Abstract Co-Author*) Nothing to Disclose
Ruth Lim, MD, Boston, MA (*Abstract Co-Author*) Consultant, Alexion Pharmaceuticals, Inc; Officer, New England PET Imaging
System
Michael S. Gee, MD, PhD, Jamaica Plain, MA (*Abstract Co-Author*) Nothing to Disclose
Synho Do, PhD, Boston, MA (*Abstract Co-Author*) Nothing to Disclose

For information about this presentation, contact:

shahein@stajmir.com

PURPOSE

Radiographic bone age assessment (BAA) is commonly used in the evaluation of pediatric endocrine and metabolic disorders. We previously developed a fully automated deep learning pipeline to perform BAA using convolutional neural networks. In this experiment, we compared the performance of a cohort of pediatric radiologists at performing BAA with and without AI assistance.

METHOD AND MATERIALS

6 board certified, subspecialty trained pediatric radiologists interpreted 280 age and gender matched bone age radiographs ranging from 5 to 18 years, viewed the automated BAA results, and gave their final interpretation of the bone age. Bone age accuracy, Root mean squared error (RMSE), and variance were used as measures of comparison. Mean cohort rating in years was considered the reference standard.

RESULTS

AI BAA accuracy was 63.6% overall and 97.1% within 1 year, and the 6 reader cohort accuracy was 61.1% and 97.9% when compared to the original clinical reports. Mean AI interpretation time was 0.54 seconds. When compared to mean cohort rating, AI RMSE was 0.649 years and single-reader RMSE averaged 0.656 years, (0.524-0.802). For the radiologists who utilized AI, pooled RMSE decreased from 0.645 to 0.548 years, all individually decreasing (0.524 to 0.504, p = 0.290; 0.802 to 0.595, p < e-5; 0.576 to 0.541, p = 0.041). Mean variance also decreased from 0.270 to 0.155, all individually decreasing (0.193 to 0.139, p < e-3; 0.366 to 0.170, p < e-10; 0.250 to 0.155, p < e-8). Combined AI + radiologist interpretation resulted in lower RMSE and variance than AI alone or the 6 reader cohort mean.

CONCLUSION

AI improves radiologist's interpretation by decreasing the variance and RMSE while decreasing interpretation time. The utilization of AI by radiologists improves performance compared to AI alone, a radiologist alone, or a pooled cohort of experts. This suggests that AI may optimally be utilized as an adjunct to radiologist interpretation of imaging studies.

CLINICAL RELEVANCE/APPLICATION

AI is likely to decrease variability and speed interpretation time for BAA. This suggests a model for how AI can be used in imaging settings.

RC513-12 Dose Reduction Impact in Pediatric Plain Radiography: The Importance of an Optimization Program

Wednesday, Nov. 29 11:10AM - 11:20AM Room: E352

Participants Graciano N. Paulo, PhD, PhD, Coimbra, Portugal (*Presenter*) Nothing to Disclose Joana Santos, PhD, Coimbra, Portugal (*Abstract Co-Author*) Nothing to Disclose

For information about this presentation, contact:

graciano@estescoimbra.pt

PURPOSE

Radiation doses to paediatric patients from plain radiography are relatively low, but because of the high frequency of these procedures, their optimisation is important for the radiology practice. The main objective of optimisation of radiological procedures is to adjust imaging parameters and implement measures in such a way that the required image is obtained with the lowest possible radiation dose and maximised benefit.

METHOD AND MATERIALS

To analyse the relationship between exposure factors, the use of technical features and dose, experimental tests were made using

two anthropomorphic phantoms. The new exposure criteria for each age group were defined according to the results obtained from the anthropomorphic phantoms tests and by reviewing the exposure criteria published in the literature and the outcome of several group meetings held with radiographers and radiologists working at the radiology department.

RESULTS

Using the post optimisation exposure criteria led to a significant reduction in exposure time, ESAK and KAP values, indicating a lower patient dose exposure. Using the post optimisation exposure criteria for chest plain radiography reduced the KAPP75 values by 22 to 60%. The KAPP75 reduction was highest in age group 5 - 10. The ESAKP75 values were reduced by 7 to 31%, with the highest reduction in age group <1 .Using the post optimisation exposure criteria for abdomen plain radiography reduced the KAPP75 values by 35 to 87%. The KAPP75 reduction was highest in age group 10 - 16. The ESAKP75 values were reduced by 17 to 87%, with the highest reduction in age group 10 - 16. Using the post optimisation exposure criteria for plain radiography reduced the KAPP75 values by 35 to 87%. The KAPP75 reduction was highest in age group 10 - 216. The ESAKP75 values were reduced by 17 to 87%, with the highest reduction in age group 10 - 216. Using the post optimisation exposure criteria for plain radiography reduced the KAPP75 values by 7 to 89%. The KAPP75 reduction was highest in age group 16 - 218. The ESAKP75 values were reduced by 12 to 86%, with the highest reduction in age group 16 - 218.

CONCLUSION

Considering the post optimisation data analysis one can conclude that the two major benefits that were expected: a) a harmonisation of practice; b) a significant reduction of ExT, KAP and ESAK values with the post optimization results for chest, abdomen and pelvis were achieved.

CLINICAL RELEVANCE/APPLICATION

This work allowed proposing new and harmonised exposure parameters for chest, abdomen and pelvis plain radiography, facilitating dose reduction by up to 94%.

RC513-13 Ultrasound Assessment of Corpus Callosum in Normal Neonates

Wednesday, Nov. 29 11:20AM - 11:30AM Room: E352

Awards

Student Travel Stipend Award

Participants

Chetankumar M. Mehta, MBBS, MD, Vadodara, India (*Presenter*) Nothing to Disclose Chandni D. Wadhwani, MD, Vadodara, India (*Abstract Co-Author*) Nothing to Disclose Deepa R. John, MBBS, MD, Vadodara, India (*Abstract Co-Author*) Nothing to Disclose Shubhangi T. Girbide II, MBBS, Vadodara, India (*Abstract Co-Author*) Nothing to Disclose Ayaz J. Dabivala, MBBS, Vadodara, India (*Abstract Co-Author*) Nothing to Disclose Bhumika P. Suthar, MD, MBBS, Baroda, India (*Abstract Co-Author*) Nothing to Disclose Niyati Parmar, MD, Vadodara, India (*Abstract Co-Author*) Nothing to Disclose

For information about this presentation, contact:

drchetan_mehta@yahoo.com

PURPOSE

To measure the parameters of corpus callosum in sagital and coronal section of neonatal brain. To correlate the corpus callosum dimensions with gestational age(Preterm vs term), weight(Low birth weight vs normal) and gender (female and male).

METHOD AND MATERIALS

The measurements were taken with a Philips IU22 ultrasound system using C8-5 neonatal brain probe The AP diameter of genu was taken in coronal plane and length, thickness of genu, body and splenium in sagital plane through the anterior fontanelle .Statistical analysis was carried out by calculating the mean and standard deviation for the corpus callosum dimensions and applying unpaired t tests for two groups using MEDCALC software and calculating p values. A value of p < 0.05 was considered statistically significant.

RESULTS

Measurements of 300 neonates included the anteroposterior diameter of the genu(coronal) (2.65 ± 0.43 mm) and in mid-sagittal plane length(49.62 ± 6.3 mm), thickness of the genu (3.98 ± 1.48 mm), body (2.9 ± 0.54 mm)and splenium (3.68 ± 0.9 mm). 300 neonates were divided into 2 different birth-weight groups: low birth weight< 2500 g (n =219) and normal >= 2 500 g (n = 81). A statistical significant difference at 95% and 99% confidence interval is noticed in the corpus callosum AP diameter and thickness of genu between the two groups with values of p=0.017 and p=0.001 respectively. There was no significant difference in the dimensions of corpus callosum body, splenium and length among them. An increase in the values of corpus callosum in term neonates >=37 weeks(n =187) was observed as compared to the pre-term neonates< 37weeks (n=113), however the difference was not statistically significant. Effect of gender :154 male and 146 female.No significant difference in the mean birth weight (P = 0.42) or mean gestational age (P = 0.49) between the two groups . This analysis revealed that there was no significant difference in all corpus callosum dimensions between male and female neonates (P > 0.05)

CONCLUSION

The increase in coronal and sagital genu between low and normal birth weight is statistically significant (p<0.05) at 95 and 99% confidence interval respectively. There is no significant difference in the dimensions of corpus callosum with change in gestational age and gender of neonate.

CLINICAL RELEVANCE/APPLICATION

Ultrasound is a modality of choice for evaluation of corpus callosum in neonates.

RC513-14 What Does the Single Axial Rotation with 16cm Wide-Detector Bring in Imaging Infant Head? The Comparison of 256-Row CT with 64-Row CT

Wednesday, Nov. 29 11:30AM - 11:40AM Room: E352

Zhian Pi, Ankang, China (*Presenter*) Nothing to Disclose Yanan Zhu, Ankang, China (*Abstract Co-Author*) Nothing to Disclose Xianfeng Qu, Ankang, China (*Abstract Co-Author*) Nothing to Disclose Faqing Lei, Ankang, China (*Abstract Co-Author*) Nothing to Disclose Zhengjun Li, Ankang, China (*Abstract Co-Author*) Nothing to Disclose Heping Zhou, MD, Ankang, China (*Abstract Co-Author*) Nothing to Disclose Jianying Li, Beijing, China (*Abstract Co-Author*) Employee, General Electric Company

For information about this presentation, contact:

840252419@qq.com

PURPOSE

To explore the innovation of using a single axial rotation with 16cm wide-detector CT in imaging infant head.

METHOD AND MATERIALS

Prospectively enrolled 20 infants (Group 1) for non-enhanced head CT without sedation using a single axial rotation of 0.5s on a 16cm wide-detector Revolution CT scanner. Patients were scanned with tube current 120mAs and tube voltages of 100kVp. The preparation time, scanning time, radiation dose and image quality were compared with those of 18 infants in Group 2 who underwent a conventional axial scan with sedation using a 64-row VCT with 180mAs tube current and 120 kVp tube voltage. CT number and its standard deviation (SD) of the cerebellum and centrum ovale (used as background) were measured to calculate signal to noise ratio and artifact index (AI): AI = sqrt [SD2(cerebellum) - SD2(centrum ovale)]. The subjective image quality was evaluated by 2 board-certificated radiologists using a 3-point scoring system with equal or greater than 2 being acceptable. Radiation dose was recorded.

RESULTS

There was no statistical difference in preparation time, the artifact index as well as the measured occipital thickness between the two groups. The mean noise(in HU), AI, SNR and CNR of the cerebellum and overall subjective image quality score between the two groups were also similar. However, compared with the conventional group (Group 2), Group 1 significantly reduced the scanning time by 92.2% ($0.5 \text{ vs. } 6.39\pm0.55$), and effective radiation dose by 53% ($0.96\pm0.26 \text{ vs. } 2.03\pm0.56 \text{ mSv}$) (P<0.05). Moreover, sedation was not used in Group 1 while most of the patients in Group 2 used a sedative.

CONCLUSION

The use of axial CT mode in a single rotation on a 16cm wide-detector for imaging infant head without sedation, provides same image quality as the conventional CT with sedation while effectively reduces the radiation dose and scanning time, avoids the complications and the potential risks of sedation, and optimizes scanning procedures.

CLINICAL RELEVANCE/APPLICATION

The use of single rotation, axial CT mode on a 16cm wide-detector for imaging infant head can avoid sedation, shorten scan time, provide good image quality and reduce dose.

RC513-15 Imaging of Pediatric Breast Masses

Wednesday, Nov. 29 11:40AM - 12:00PM Room: E352

Participants

Teresa Chapman, MD, MA, Seattle, WA (Presenter) Nothing to Disclose

For information about this presentation, contact:

Teresa.chapman@seattlechildrens.org

LEARNING OBJECTIVES

Recognize normal glandular tissue of the pediatric patient. Apply appropriate management recommendations to breast ultrasound findings of a girl with a palpable abnormality. Provide an appropriate differential diagnosis for a solid tissue finding in the pediatric breast.

Active Handout:Teresa Chapman

http://abstract.rsna.org/uploads/2017/17000786/Active RC513-15.pdf







Interventional Series: Peripheral and Visceral Occlusive Disease

Wednesday, Nov. 29 8:30AM - 12:00PM Room: S102CD



AMA PRA Category 1 Credits ™: 3.25 ARRT Category A+ Credits: 3.75

FDA Discussions may include off-label uses.

Participants

Parag J. Patel, MD, Milwaukee, WI (*Moderator*) Consultant, Abbott Laboratories; Consultant, C. R. Bard, Inc; Consultant, Penumbra, Inc; Consultant, Boston Scientific Corporation;

Jonathan M. Lorenz, MD, Chicago, IL (Moderator) Nothing to Disclose

For information about this presentation, contact:

papatel@mcw.edu

LEARNING OBJECTIVES

1) Describe pros and cons of intervention for median arcuate ligament compression on the celiac axis. 2) Review clinical presentationand endovascular treatment options for acute and subacute portal vein thrombus. 3) Outline three recommendations for endovascular treatment of peripheral vascular disease. 4) Describe how and when to intervene in patients with mesenteric ischemia. 5) Describe two vascular compression syndromes.

Sub-Events

RC514-01 Compressive Arterial Syndromes

Wednesday, Nov. 29 8:30AM - 8:45AM Room: S102CD

Participants

Minhaj S. Khaja, MD, MBA, Ann Arbor, MI (Presenter) Nothing to Disclose

LEARNING OBJECTIVES

1) Review the role of cross-sectional imaging and IR in the diagnosis and potential treatment of compressive arterial syndromes. 2) Illustrate case based examples of compressive arterial syndromes.

RC514-02 Acute Portal Venous Thrombosis

Wednesday, Nov. 29 8:45AM - 9:00AM Room: S102CD

Participants

Jonathan M. Lorenz, MD, Chicago, IL (Presenter) Nothing to Disclose

LEARNING OBJECTIVES

1) Review the clinical manifestations of patients with acute to subacute portal vein thrombosis. 2) Review the implications of etiology, rapiditiy of onset, surgical history, and extension into the splenic and superior mesenteric veins on prognosis and treatment strategy. 3) Review conservative and endovascular treatment options such as thrombolysis, mechanical thrombectomy, angioplasty and stent placement.

RC514-03 Feasibility of Endovascular Thrombolysis and Angioplasty of Hepatic Artery Thrombosis in the First Postoperative Day after Living Donor Liver Transplantation: A Multi-Center Experience

Wednesday, Nov. 29 9:00AM - 9:10AM Room: S102CD

Participants Omar Abd El Aziz, Cairo, Egypt (*Presenter*) Nothing to Disclose Mohamed S. Mostafa JR, ARRT, Cairo, Egypt (*Abstract Co-Author*) Nothing to Disclose

For information about this presentation, contact:

ohamada@yahoo.com

PURPOSE

Hepatic artery thrombosis (HAT) is a devastating complication after living donor liver transplantation (LDLT). Endovascular management represents a less invasive alternative to open surgery. our aim was to investigate the feasibility and potential complications of endovascular intervention for the management of arterial thrombosis in the first post-operative day after transplantation

METHOD AND MATERIALS

A retrochactive review of 668 recipients, who underwant LDIT between August 2001 and December 2016 in three translant

centers. Endovascular interventions were performed using standard catheter techniques. Thrombolysis was performed using tPA or streptokinase, whereas angioplasty and stent placement were performed if there was an underlying stricture.

CONCLUSION

Endovascular intervention for the management of HAT in the first postoperative day after LDLT carries a considerable risk of potential complications related to the technique and thrombolytic therapy. However, it is feasible and can be attempted for graft salvage if surgery is considered futile.

CLINICAL RELEVANCE/APPLICATION

Endovascular intervention is feasible technique for the management of HAT in the first postoperative day after LDLT.

RC514-04 Median Arcuate Ligament Syndrome

Wednesday, Nov. 29 9:10AM - 9:25AM Room: S102CD

Participants

Jonathan M. Lorenz, MD, Chicago, IL (Presenter) Nothing to Disclose

LEARNING OBJECTIVES

1) To review the current understanding of the pathophysiology of median arcuate ligament syndrome and the latest options and algorithms for diagnosis and treatment. 2) To review the roles of interventional radiology in the diagnosis and management of this disorder.

RC514-05 CT Angiography Predicts the Outcome of Guidewire Crossing through Chronic Total Occlusions of PAD

Wednesday, Nov. 29 9:25AM - 9:35AM Room: S102CD

Participants

Ningning Ding, Xian, China (*Presenter*) Nothing to Disclose Niu Gang, MD, Xi'an, China (*Abstract Co-Author*) Nothing to Disclose Tingting Qu, Xian, China (*Abstract Co-Author*) Nothing to Disclose Yitong Bian, Xian, China (*Abstract Co-Author*) Nothing to Disclose Chao Jin I, PhD,PhD, Xian, China (*Abstract Co-Author*) Nothing to Disclose Jian Yang, MD, PhD, Xian, China (*Abstract Co-Author*) Nothing to Disclose

For information about this presentation, contact:

dingningning1985@126.com

PURPOSE

The aim of this study was to define predictive factors of the outcome of guidewire crossing through chronic total occlusions of PAD by CT angiography.

METHOD AND MATERIALS

Patients with peripheral artery CTO were examined with CTA before undergoing endovascular therapy. Two Radiologist assessed the transluminal calcification of CTO lesions, occlusion length, CT value of the proximal occlusion and vascular wall circular ringenhancement sign on CT images. According the outcome of guidewire crossing through CTO, patency success group and patency failure group were divided. The significance of CTA variables in association with patency were analyzed binary logistic regression mode.

RESULTS

89 PAD patients with 92 CTO lesions, 73 lesions were successfully traversed, 19 were failed of crossing the CTO lesions with guidewires. The difference of the length of CTO and Transluminal calcification between patency success group and patency failure group is statistically significant(P<0.05). Transluminal calcification >=50% as assessed on CTA was strongly associated with failed Patency (odds ratio [OR] of Patency success =0.14, 95% confidence interval [CI]: 0.04-0.46. There was no difference of vascular wall circular ring-enhancement sign and CT value of the proximal occlusion between two groups(P>0.05).

CONCLUSION

Transluminal calcification>=50% as assessed with CTA is an independent predictor of failed Patency of peripheral artery CTO. CTA may have a role in the work-up of peripheral artery CTO patients prior to endovascular therapy

CLINICAL RELEVANCE/APPLICATION

Further evaluation of peripheral artery CTO lesion with CT angiography may help to better select patients that would benefit from percutaneous revascularization and avoid blind puncture.

RC514-06 Advanced Arterial Revascularization

Wednesday, Nov. 29 9:35AM - 9:50AM Room: S102CD

Participants Aseem Bhandari, MD, Savannah, GA (*Presenter*) Nothing to Disclose

For information about this presentation, contact:

ABhandari@SavannahVascular.com

RC514-07 The 5 Most Important PAD Papers, 2015-2017

Participants

Sanjay Misra, MD, Rochester, MN (Presenter) Cordis/Flexstent; NIH funding

RC514-08 Recent Trends in Percutaneous and Surgical Treatment of Peripheral Arterial Disease (PAD) in the Medicare Population

Wednesday, Nov. 29 10:20AM - 10:30AM Room: S102CD

Participants

David R. Hansberry, MD,PhD, Philadelphia, PA (*Presenter*) Nothing to Disclose David Guez, MD, Philadelphia, PA (*Abstract Co-Author*) Nothing to Disclose Laurence Parker, PhD, Philadelphia, PA (*Abstract Co-Author*) Nothing to Disclose David J. Eschelman, MD, Bryn Mawr, PA (*Abstract Co-Author*) Nothing to Disclose Carin F. Gonsalves, MD, Philadelphia, PA (*Abstract Co-Author*) Nothing to Disclose David C. Levin, MD, Philadelphia, PA (*Abstract Co-Author*) Nothing to Disclose

For information about this presentation, contact:

david.hansberry@jefferson.edu

PURPOSE

Although radiologists developed percutaneous treatment of PAD in the 1980s, vascular surgeons and cardiologists have become increasingly involved and the issue has been contentious. Our purpose was to study utilization trends in percutaneous (PERC) and surgical (SURG) treatment of PAD in recent years.

METHOD AND MATERIALS

The nationwide Medicare Part B fee-for-service databases for 2011 through 2015 were used. 2011 was chosen as the first year because an entire new set of revamped PERC codes was introduced that year. 10 PERC codes (primary procedure only, no add-on codes) and 43 SURG codes were selected, describing the approaches to treating the various peripheral vascular territories. Procedure volumes were tabulated during the 5 study years. Medicare specialty codes were used to group physician providers as radiologists, vascular surgeons, cardiologists, and all other physicians as a group.

RESULTS

Total Medicare fee-for-service PERC volume (all providers) increased steadily from 182,213 in 2011 to 217,810 in 2015 (+20%). Total SURG volume decreased from 67,137 in 2011 to 55,606 in 2015 (-17%). Between 2011 and 2015, PERC volume by vascular surgeons increased from 61,719 to 82,803 (+34%). PERC volume by cardiologists increased from 66,117 to 79,101 (+20%). Radiologists' PERC volume increased from 23,473 to 26,570 (+12%). PERC volume by all others decreased from 30,904 to 29,336 (-5%). Market shares in 2015 were: vascular surgeons 38%, cardiologists 36%, radiologists 12%, all others 13%. There had been relatively little change in share since 2011.

CONCLUSION

In recent years, SURG treatment for PAD has decreased considerably, while PERC has increased considerably. By 2015, Medicare patients requiring revascularization for PAD were almost 4 times more likely to undergo PERC than SURG. Vascular surgeons and cardiologists have aggressively been increasing their volumes and have largely supplanted radiologists. However, radiologists have maintained a small but consequential role and their procedure volume increased by 13% from 2011 to 2015.

CLINICAL RELEVANCE/APPLICATION

Percutaneous treatment of PAD is used much more commonly than surgical treatment and its use has increased rapidly in recent years.

RC514-09 Below-the-Knee Interventions

Wednesday, Nov. 29 10:30AM - 10:45AM Room: S102CD

Participants

Parag J. Patel, MD, Milwaukee, WI (*Presenter*) Consultant, Abbott Laboratories; Consultant, C. R. Bard, Inc; Consultant, Penumbra, Inc; Consultant, Boston Scientific Corporation;

LEARNING OBJECTIVES

1) Descibe clinically oriented goals when treating below-the-knee arterial occlusive disease. 2) Review endovascular treatment options for below-the-knee arterial disease.

RC514-10 Predictors for Outcome of Angioplasty in Patients with Critical Limb Ischemia: A Single-Institution Experience in 1936 Patients

Wednesday, Nov. 29 10:45AM - 10:55AM Room: S102CD

Participants

Wenwen Ni, Singapore, Singapore (*Presenter*) Nothing to Disclose
Farah G. Irani, MD, FRCR, Singapore, Singapore (*Abstract Co-Author*) Nothing to Disclose
Karthikeyan Damodharan, MRCP, FRCR, Liverpool, United Kingdom (*Abstract Co-Author*) Nothing to Disclose
Ankur Patel, BMedSc, MBChB, Singapore, Singapore (*Abstract Co-Author*) Nothing to Disclose
Shaun Xavier Ju Min Chan, MBBS, FRCR, Singapore, Singapore (*Abstract Co-Author*) Nothing to Disclose
Thijs A. Urlings, MSc, Den Haag, Netherlands (*Abstract Co-Author*) Nothing to Disclose
Bien Soo Tan, Singapore, Singapore (*Abstract Co-Author*) Institutional research collaboration, Koninklijke Philips NV; Institutional research collaboration, Siemens AG; Institutional research collaboration, Toshiba Medical Systems Corporation
Kiang Hiong Tay, MBBS, FRCR, Singapore (*Abstract Co-Author*) Nothing to Disclose
Richard H. Lo, MBBS, Singapore, Singapore (*Abstract Co-Author*) Nothing to Disclose

Sivanathan Chandramohan, Singapore, Singapore (*Abstract Co-Author*) Nothing to Disclose Chow Wei Too, Singapore, Singapore (*Abstract Co-Author*) Nothing to Disclose Leong Sum, Singapore, Singapore (*Abstract Co-Author*) Nothing to Disclose Ravi Muli Kumar, Singapore, Singapore (*Abstract Co-Author*) Nothing to Disclose Kun Da Zhuang, MBBS, Singapore, Singapore (*Abstract Co-Author*) Nothing to Disclose Nanda Kumar Karaddi, Singapore, Singapore (*Abstract Co-Author*) Nothing to Disclose Tze Tec Chong, Singapore, Singapore (*Abstract Co-Author*) Nothing to Disclose Seck Guan Tan, MRCS, MBBS, Singapore, Singapore (*Abstract Co-Author*) Nothing to Disclose Siew Ping Chng, Singapore, Singapore (*Abstract Co-Author*) Nothing to Disclose Johne Wang, Singapore, Singapore (*Abstract Co-Author*) Nothing to Disclose Edward Choke, Singapore, Singapore (*Abstract Co-Author*) Nothing to Disclose Jack Kian Ch'ng, Singapore, Singapore (*Abstract Co-Author*) Nothing to Disclose

For information about this presentation, contact:

ni.wenwen@u.duke.nus.edu

PURPOSE

To identify predictors of the outcome of patients with critical limb ischemia (CLI) who underwent percutaneous transluminal angioplasty (PTA) as first line treatment.

METHOD AND MATERIALS

A retrospective study, analyzing a total of 1936 patients who underwent 3271 PTA procedures in 2378 limbs for CLI in a single institution between 2005 and 2015, was performed. The mean age of the patients were 68+/-11 years old and 1036 (54%) patients were male. Diabetes mellitus was present in 1709 patients (88%) and end stage renal failure (ESRF) in 567 patients (29%). The majority of the patients (2950 patients, 90%) had tissue loss (Rutherford V-VI).

RESULTS

During the follow-up period, the limb salvage rate at 1,3,5,10 years were 73,71,69,60% while the survival rate were 81,66,58,37% respectively. After univariable analysis, presence of diabetes mellitus (hazard ratio: 3.07, p<0.001), ESRF (1.493, p<0.001), Rutherfold VI (1.581, p<0.001) and high C-reactive protein (1.006, p<0.001) were associated with lower limb salvage rate. Stent use (0.646, p=0.004) and presence of one straight flow to the foot (0.437, p<0.001) were identified as predictors of better limb salvage outcome. Female (1.235, p=0.006), presence of hypertension (1.272, p=0.018), ischemic heart disease (1.407, p<0.001), ESRF (2.231, p<0.001) and Rutherfold VI (1.203, p=0.018) were associated with lower survival rate. Ambulatory status (0.492, p=0.001), high albumin (0.932, p<0.001) and hemaglobin (0.835, p<0.001) were identified as predictors of better survival outcome.

CONCLUSION

CLI carries higher mortality and lower limb salvage rate among periphery vascular disease. Further studies are needed to confirm these predictors, to identify potentially modifiable factors, and to guide the patient selection for PTA.

CLINICAL RELEVANCE/APPLICATION

Awareness of the predictors will help facilitate patient selection for percutaneous transluminal angioplasty to achieve optimal outcome.

RC514-11 Mesenteric Ischemia

Wednesday, Nov. 29 10:55AM - 11:10AM Room: S102CD

Participants Laura K. Findeiss, MD, Knoxville, TN (*Presenter*) Speakers Bureau, Bayer AG

RC514-12 Biology of Vascular Disease

Wednesday, Nov. 29 11:10AM - 11:25AM Room: S102CD

Participants

Sanjay Misra, MD, Rochester, MN (Presenter) Cordis/Flexstent; NIH funding

LEARNING OBJECTIVES

1) Become familiar with different vascular biology pathways causing vascular injury. 2) Describe translational therapies that can be used to decrease vascular injury. 3) Identify new novel therapies that can be used for vascular disease.

RC514-13 Hyperlipidemia Accelerates Neointimal Formation in the Apoe Null Mouse Model

Wednesday, Nov. 29 11:25AM - 11:35AM Room: S102CD

Participants

Zhihui Chang, BMedSc, MMed, Shenyang, China (*Abstract Co-Author*) Nothing to Disclose Weibin Shi, MD, PHD, Charlottesville, VA (*Presenter*) Nothing to Disclose

PURPOSE

Restenosis remains the most significant challenge limiting the success of angioplasty and/or stenting. Hyperlipidemia is a major risk factor for atherosclerotic vascular disease. Apoe-deficient (Apoe-/-) mice develop moderate hyperlipidemia on a chow diet and severe hyperlipidemia on a high fat diet. The objective of this study was to investigate the influence of hyperlipidemia on neointimal formation in the Apoe-/- mouse model.

METHOD AND MATERIALS

The left common carotid artery of Apoe-/- mice was ligated with a suture at the distal end. One group of mice were started on a Western diet one week before ligation and maintained on the diet throughout the entire observation period, and one group was fed

RESULTS

One week after ligation, no noticeable neointimal lesions were observed in the artery of either group. Two weeks after ligation, mice fed the Western diet developed significantly larger neointimal lesions in the ligated artery than those fed the chow diet ($40446\pm9422 \mu$ m2 vs. $13353\pm4226\mu$ m2; p<0.05). Neointimal lesions contained numerous macrophage foam cells and smooth muscle cells in high fat fed mice but few in chow diet fed mice. CD8-positive lymphocytes were only observed in chow diet fed mice. By 4 weeks after ligation, both groups of mice formed pronounced neointimal lesions that comprised of primarily smooth muscle cells.

CONCLUSION

These results indicate that hyperlipidemia accelerates neointimal growth by promoting foam cell formation in hyperlipidemic mice.

CLINICAL RELEVANCE/APPLICATION

Inflammatory reactions play an important role in restenosis. For patients with hyperlipidemia, inhibition of macrophage exudation and the formation of foam cells may become a potential intervention therapy for restenosis.

RC514-14 Patterns of Blood Pressure Response after Renal Artery Stenting Placement of Atherosclerotic Renal Artery Stenosis (ARAS)

Wednesday, Nov. 29 11:35AM - 11:45AM Room: S102CD

Participants

Qian Li, MD, PhD, Boston, MA (*Presenter*) Nothing to Disclose Xueying Lin, MD, Fuzhou, China (*Abstract Co-Author*) Nothing to Disclose Yuhong Shao, Beijing, China (*Abstract Co-Author*) Nothing to Disclose Xi Zhang, Shanghai, China (*Abstract Co-Author*) Nothing to Disclose Anthony E. Samir, MD, Boston, MA (*Abstract Co-Author*) Consultant, Pfizer Inc; Consultant, General Electric Company; Consultant, PAREXEL International Corporation; Research Grant, Koninklijke Philips NV; Research Grant, Siemens AG; Research Grant, Toshiba Medical Systems Corporation; Research Grant, General Electric Company; Research Grant, Samsung Electronics Co, Ltd; Research Grant, Analogic Corporation; Research support, SuperSonic Imagine; Research support, Hitachi, Ltd

PURPOSE

To explore the patterns of BP response after renal artery stenting, and their potential value for RAS treatment decision-making.

METHOD AND MATERIALS

Retrospectively collected ARAS patients who underwent PTRAS and pre-stenting renal artery (RA) ultrasonography (US) exams in 5 years at a single institution. Patients with accessory RA and contralateral RA occultation were excluded. Baseline characteristics, including age, gender, eGFR, BP, anti-hypertension medication, and US parameters (kidney length, PSV, RAR, and RI) of the stenting involved RA were recorded no more than 2 weeks before stenting, and BP and anti-hypertension medication were followed up at 1, 3, 6, 12 and 18 months after stenting. The BP response was classified into benefit (cure/improvement) or failure at each follow-up time point based on the guideline (2003). The patterns of BP change over time, and patients' characters in each pattern group was compared.

RESULTS

Totally 74 patients were identified, including 51 of unilateral RA stenting and 23 of bilateral RA stenting. As shown in Figure 1, 5 patterns of BP response after RA stenting were found in unilateral group, including (1) normal presenting BP with consistent BP benefit throughout the follow-up (10/51, 19.6%), (2) pre-stenting hypertension with no BP response (7/51, 13.7%), (3) pre-stenting hypertension with consistent BP benefit throughout the follow up (14/51, 27.5%), (4) fluctuant BP response within 6 months followed by late BP benefit (9/51, 17.6%), (5) fluctuant BP response within 6 months followed by late BP deterioration (3/51, 5.9%). Pre-stenting eGFR was found significantly different among the patterns (p<0.05). Patterns of BP response in bilateral stenting group showed more variation between benefit and failure.

CONCLUSION

This study demonstrated four patterns of BP response after unilateral RA stenting of ARAS. Recognition of these patterns and characters of their population may be helpful for indication confirmation, and follow-up strategy decision making.

CLINICAL RELEVANCE/APPLICATION

The patterns of blood pressure (BP) response to percutaneous transluminal renal angioplasty with stent placement (PTRAS) of atherosclerotic renal artery stenosis (ARAS) has not been well documented.

RC514-15 Renovascular Occlusive Disease-Current Paradigm

Wednesday, Nov. 29 11:45AM - 12:00PM Room: S102CD

Participants

Bulent Arslan, MD, Chicago, IL (*Presenter*) Advisory Board, Nordion, Inc Advisory Board, Angiotech Pharmaceuticals, Inc Speakers Bureau, Nordion, Inc Speakers Bureau, W. L. Gore & Associates, Inc Consultant, Bayer AG





103rd Scientific Assembly and Annual Meeting November 26 to December 1 McCormick Place, Chicago



RC515

Digital Breast Tomosynthesis

Wednesday, Nov. 29 8:30AM - 10:00AM Room: E353C

BR

AMA PRA Category 1 Credits ™: 1.50 ARRT Category A+ Credit: 1.75

Participants

Cherie M. Kuzmiak, DO, Chapel Hill, NC (Moderator) Nothing to Disclose

LEARNING OBJECTIVES

1) To describe financial considerations during the transition to digital breast tomosynthesis (DBT) in clinical practice. 2) To describe the personnel training requirements to perform DBT in the United States. 3) To describe process for maintaining accreditation with FDA during clinical transition to DBT. 4) To describe workflow considerations during transition to DBT in clinical practice. 5) Describe the latest data that support use of digital breast tomosynthesis (DBT). 6) Identify the changes that will occur with the audit after multiple rounds of screening with DBT. 3) Recognize pitfalls when using DBT. 7). Know the areas needed for future research. 8.) Apply principles of digital breast tomosynthesis to clinical case interpretation. 9) Improve problem solving skils and decision making in breast imaging with the use of tomosynthesis. 10) Access the results of published studies and their application to challenging digital breast tomosynthesis cases. 11) Improve understanding of the strengths andlimitations of digital breast tomosynthesis.

SAM

New in 2017: PLEASE NOTE - All courses designated for SAM credit at RSNA 2017 will require attendees bring a personal device e.g. phone, iPad, laptop to complete the required test questions during the live session.

Sub-Events

RC515A Nuts & Bolts

Participants Jay R. Parikh, MD, Houston, TX (*Presenter*) Nothing to Disclose

LEARNING OBJECTIVES

1) To describe financial considerations during the transition to digital breast tomosynthesis (DBT) in clinical practice. 2) To describe the personnel training requirements to perform DBT in the United States. 3) To describe process for maintaining accreditation with FDA during clinical transition to DBT. 4) To describe workflow considerations during transition to DBT in clinical practice.

Active Handout:Jay R. Parikh

http://abstract.rsna.org/uploads/2017/17000179/Active RC515A.pdf

RC515B Clinical Implications

Participants

Sarah M. Friedewald, MD, Chicago, IL (Presenter) Consultant, Hologic, Inc; Research Grant, Hologic, Inc;

For information about this presentation, contact:

sarah.friedewald@nm.org

LEARNING OBJECTIVES

1) Describe the latest data that support use of digital breast tomosynthesis (DBT). 2) Identify the changes that will occur with the audit after multiple rounds of screening with DBT. 3) Recognize pitfalls when using DBT. 4. Know the areas needed for future research.

RC515C Challenging Cases

Participants

Kathleen R. Brandt, MD, Rochester, MN (Presenter) Nothing to Disclose

LEARNING OBJECTIVES

1) Apply principles of digital breast tomosynthesis to clinical case interpretation. 2) Improve problem solving skils and decision making in breast imaging with the use of tomosynthesis. 3) Access the results of published studies and their application to challenging digital breast tomosynthesis cases. 4) Improve understanding of the strengths and limitations of digital breast tomosynthesis.







Unconscious Bias in Recruiting Radiologists (In Conjunction with the American Association for Women Radiologists)

Wednesday, Nov. 29 8:30AM - 10:00AM Room: S104A

LM

AMA PRA Category 1 Credits ™: 1.50 ARRT Category A+ Credit: 1.75

Participants

Margaret M. Szabunio, MD, Lexington, KY (Moderator) Nothing to Disclose

For information about this presentation, contact:

margaret.szabunio@uky.edu

LEARNING OBJECTIVES

1) Define Unconscious Bias. 2) Understand relationship of Unconscious Bias to diversity and inclusion. 3) Develop strategies to mitigate inherent individual and organizational biases that affect faculty search process. 4) Apply strategies to recruit best faculty into Department of Radiology. 5). Identify steps to mitigate the effects of unconscious bias in the resident and fellow selection process. 6). Discuss reasons why women medical students do not choose radiology and review strategies to increase recruitment.

Sub-Events

RC516A Unconscious Bias in Recruiting Radiology Faculty

Participants

M. Elizabeth Oates, MD, Lexington, KY (Presenter) Nothing to Disclose

For information about this presentation, contact:

meoate2@email.uky.edu

LEARNING OBJECTIVES

1) Define Unconscious Bias. 2) Understand relationship of Unconscious Bias to diversity and inclusion. 3) Develop strategies to mitigate inherent individual and organizational biases that affect faculty search process. 4) Apply strategies to recruit best faculty into Department of Radiology.

RC516B Unconscious Bias in Recruiting Radiology Residents & Fellows

Participants Madelene C. Lewis, MD, Charleston, SC (*Presenter*) Nothing to Disclose

For information about this presentation, contact:

lewism@musc.edu

LEARNING OBJECTIVES

1) Define unconscious bias and how it relates to resident and fellow recruitment. 2) Apply tools to increase awareness of your biases. 3) Identify steps to mitigate the effects of unconscious bias in the resident and fellow selection process.

RC516C Encouraging Women Medical Students for Radiology

Participants

Katarzyna J. Macura, MD, PhD, Baltimore, MD (*Presenter*) Author with royalties, Reed Elsevier; Research Grant, Profound Medical Inc

For information about this presentation, contact:

kmacura@jhmi.edu

LEARNING OBJECTIVES

1) Discuss reasons for why women medical students do not choose radiology. 2) Review strategies for engagement of female medical students to spur recruitment at institutions across the country. 3) Discuss examples of successful pipeline initiatives involving minority medical students.

Honored Educators

Presenters or authors on this event have been recognized as RSNA Honored Educators for participating in multiple qualifying educational activities. Honored Educators are invested in furthering the profession of radiology by delivering high-quality educational content in their field of study. Learn how you can become an honored educator by visiting the website at: https://www.rsna.org/Honored-Educator-Award/ Katarzyna J. Macura, MD, PhD - 2012 Honored EducatorKatarzyna J. Macura, MD, PhD - 2014 Honored Educator







Emerging Technology: Elastography - Opportunities and Challenges

Wednesday, Nov. 29 8:30AM - 10:00AM Room: S505AB



AMA PRA Category 1 Credits ™: 1.50 ARRT Category A+ Credit: 1<u>.75</u>

FDA Discussions may include off-label uses.

Participants

Juergen K. Willmann, MD, Stanford, CA (*Moderator*) Research Consultant, Bracco Group Research Grant, Siemens AG Research Grant, Bracco Group Research Grant, Koninklijke Philips NV Research Grant, General Electric Company Advisory Board, Lantheus Medical Imaging, Inc Advisory Board, Bracco Group

For information about this presentation, contact:

Willmann@stanford.edu

LEARNING OBJECTIVES

1) To understand how elastography measurements are integrated into the management of patients with chronic liver disease. 2) To learn imaging techniques and protocols of ultrasound and MR elastography. 3) To compare US and MR elastography in assessing liver fibrosis. 4) To review emerging clinical indications of US and MR elastography. 5) To understand limitations of current elastography techniques.

Sub-Events

RC517A Elastography of the Liver: What the Clinician Wants to Know

Participants

Mindie Nguyen, MD, Stanford, CA (*Presenter*) Consultant, Intercept Pharmaceuticals, Inc; Consultant, Johnson & Johnson; Consultant, Gilead Sciences, Inc; Consultant, Alynam Pharmaceuticals, Inc; Consultant, Dynavax Technologies Corporation; Research Grant, Johnson & Johnson; Research Grant, Gilead Sciences, Inc; Research Grant, Bristol-Myers Squibb Company

LEARNING OBJECTIVES

View learning objectives under the main course title.

RC517B Ultrasound Elastography: How and When?

Participants

Juergen K. Willmann, MD, Stanford, CA (*Presenter*) Research Consultant, Bracco Group Research Grant, Siemens AG Research Grant, Bracco Group Research Grant, Koninklijke Philips NV Research Grant, General Electric Company Advisory Board, Lantheus Medical Imaging, Inc Advisory Board, Bracco Group

For information about this presentation, contact:

Willmann@stanford.edu

LEARNING OBJECTIVES

1) Understand the clinical indications of ultrasound elastography (USE). 2) Learn about the various techniques and imaging protocols of USE. 3) Review the diagnostic accuracy of USE in the assessment of elasticity in liver fibrosis and other clincal applications in the body. 4) Compare USE with MR elastography. 5) Understand current limitations of USE.

ABSTRACT

Ultrasound elastography (USE) is a general term for various techniques available for objectively and quantitatively assessing tissue stiffness using ultrasonic techniques, creating noninvasive images of mechanical characteristics of tissues. Elastography is based on the fact that the elasticity of a tissue is changed by pathological or physiological processes. For example, cancer or fibrosis associated with various disease processes including chronic liver disease or chronic pancreatitis result in increased tissue stiffness. Recently, various USE techniques have been cleared by the FDA and all major ultrasound companies offer different approaches of measuring tissue stiffness on their ultrasound machines. The objective of this talk is to familiarize the audience with the clinical indications, imaging techniques and protocols, interpretation, diagnostic accuracy, and limitations of the various USE technique for assessment of tissue stiffness, with special focus on assessment of fibrosis in chronic liver disease.

RC517C MR Elastography: How and When?

Participants

Richard L. Ehman, MD, Rochester, MN (Presenter) CEO, Resoundant, Inc; Stockholder, Resoundant, Inc;

LEARNING OBJECTIVES

1) To be able to understand the basic physical principles of MR Elastography (MRE). 2) To be able to describe the clinical indications for MRE in liver disease. 3) To be able to describe published evidence on the diagnostic performance of MRE in assessing

liver fibrosis. 4) To be able to compare ultrasound based elastography to MRE. 5) To be able to describe the current limitations of MRE.

Honored Educators

Presenters or authors on this event have been recognized as RSNA Honored Educators for participating in multiple qualifying educational activities. Honored Educators are invested in furthering the profession of radiology by delivering high-quality educational content in their field of study. Learn how you can become an honored educator by visiting the website at: https://www.rsna.org/Honored-Educator-Award/ Richard L. Ehman, MD - 2016 Honored Educator







Deconstructing Tumors with Imaging

Wednesday, Nov. 29 8:30AM - 10:00AM Room: S104B



AMA PRA Category 1 Credits ™: 1.50 ARRT Category A+ Credit: 1.75

FDA Discussions may include off-label uses.

Participants

Richard Kinh Gian Do, MD, PhD, New York, NY (Moderator) Consultant, Guerbet SA

For information about this presentation, contact:

dok@mskcc.org

Sub-Events

RC518A Imaging of Angiogenesis: What Do Vessels Tell Us about Tumors?

Participants

Roberto Garcia Figueiras, MD, PhD, Santiago de Compostela, Spain (Presenter) Nothing to Disclose

LEARNING OBJECTIVES

1) Improve basic knowledge and skills relevant to the evaluation of angiogenesis in clinical practice. 2) Get an overview of the most relevant functional imaging modalities that are available. 3) Apply the most appropriate imaging technique for evaluating tumor angiogenic phenotype and tumor response. 4) Understand imaging limitations and technical requirements.

ABSTRACT

Tumor angiogenesis is the process whereby new blood vessels are formed in order to supply nutrients and oxygen to support the growth of tumors. Angiogenesis is a key cancer hallmark and an important target for cancer therapy. This lecture reviews the biological basis behind imaging features and the different imaging modalities used to assess the status of tumor neovasculature in vivo and tumor vascular changes secondary to different therapies.

Active Handout: Roberto Garcia Figueiras

http://abstract.rsna.org/uploads/2017/16000386/Active RC518A.pdf

RC518B Multiparametric Imaging of Bone Marrow Metastatic Disease

Participants

Anwar R. Padhani, MD, FRCR, Northwood, United Kingdom (*Presenter*) Advisory Board, Siemens AG Speakers Bureau, Siemens AG Researcher, Siemens AG Speakers Bureau, Johnson & Johnson

LEARNING OBJECTIVES

1) To become familiar with the normal appearances of bone marrow on PET/MRI/CT scans and how these reflect underlying biologic properties. 2) To understand the biologic mechanisms responsible for osteoblastic and osteolytic lesions in malignancy settings. 3) To explain how imaging appearances of normal and pathologic bone marrow reflect therapy effects. 4) To ennumerate the professional challenges for implementing multiparametric imaging in bone therapy monitoring.

Honored Educators

Presenters or authors on this event have been recognized as RSNA Honored Educators for participating in multiple qualifying educational activities. Honored Educators are invested in furthering the profession of radiology by delivering high-quality educational content in their field of study. Learn how you can become an honored educator by visiting the website at: https://www.rsna.org/Honored-Educator-Award/ Anwar R. Padhani, MD, FRCR - 2012 Honored Educator

RC518C Imaging Tumor Metabolism with Hyperpolarized MRI

Participants

Kayvan Keshari, PhD, New York, NY (Presenter) Nothing to Disclose

For information about this presentation, contact:

rahimikk@mskcc.org

LEARNING OBJECTIVES

1) Comprehend the basic principles of hyperpolarized MRS. 2) Assess the potential of using hyperpolarized probes to study cancer metabolism. 3) Assess the changes in cancer metabolism across multiple tumor types.

ABSTRACT

 Oncogenic transformation has been shown to have a dramatic impact on the metabolic state of the cell. Recent work has shown that hyperpolarization of endogenous substrates can be used to trace metabolism in the setting of cancer, non-invasively in vivo. In this this educational lecture, we will discuss the use of hyperpolarized 13C molecules in the setting of cancer imaging, spanning a number of molecules, which have been used preclinically as well as hyperpolarized pyruvate which has recently been used in the clinic.







Challenges in Non-Hodgkin Lymphoma (NHL) Management and Imaging Response Assessment

Wednesday, Nov. 29 8:30AM - 10:00AM Room: S503AB



AMA PRA Category 1 Credits ™: 1.50 ARRT Category A+ Credit: 1.75

Participants

Chelsea C. Pinnix, MD, PhD, Houston, TX (*Presenter*) Research Grant, Merck & Co, Inc Steve Cho, MD, Madison, WI (*Presenter*) Nothing to Disclose Satish P. Shanbhag, MBBS, MPH, Baltimore, MD (*Presenter*) Nothing to Disclose

For information about this presentation, contact:

scho@uwhealth.org

shanbhag@jhmi.edu

LEARNING OBJECTIVES

1) Understand current criteria and emerging methods for NHL imaging response assessment. 2) Understand the role of imaging in NHL patient management.







Advances in CT: Technologies, Applications, Operations-Special Purpose CT

Wednesday, Nov. 29 8:30AM - 10:00AM Room: N229



AMA PRA Category 1 Credits ™: 1.50 ARRT Category A+ Credit: 1.75

Participants

Ehsan Samei, PhD, Durham, NC (*Coordinator*) Research Grant, General Electric Company; ; Research Grant, Siemens AG; ; Advisory Board, medInt Holdings, LLC

Norbert J. Pelc, DSc, Stanford, CA (*Coordinator*) Research support, Koninklijke Philips NV; Research support, General Electric Company; Research support, Siemens AG; Consultant, Varian Medical Systems, Inc; Consultant, NanoX; Scientific Advisory Board, RefleXion Medical Inc; Scientific Advisory Board, Prismatic Sensors AB; Scientific Advisory Board, Theranos, Inc; Medical Advisory Board, OurCrowd, LP

For information about this presentation, contact:

samei@duke.edu

Sub-Events

RC521A Breast

Participants John M. Boone, PhD, Sacramento, CA (*Presenter*) Patent agreement, Isotropic Imaging Corporation; Consultant, RadSite;

LEARNING OBJECTIVES

1) Demonstrate the technology associated with cone-beam CT of the breast. 2) Show performance metrics of the cone-beam CT system. 3) Demonstrate the potential of breast CT for breast cancer screening and diagnosis.

RC521B MSK

Participants

Wojciech Zbijewski, PhD, Baltimore, MD (Presenter) Research Grant, Carestream Health, Inc; Research Grant, Siemens AG

For information about this presentation, contact:

wzbijewski@jhu.edu

LEARNING OBJECTIVES

1) Describe the special prupose CT systems for musculoskeletal (MSK) imaging. 2) Compare the capabilities of special purpose MSK CT systems to conventional modalities. 3) Identify diagnostic applications enabled by special purpose MSK CT.

RC521C Interventional

Participants

Charles M. Strother, MD, Madison, WI (*Presenter*) Research Consultant, Siemens AG; Research support, Siemens AG; License agreement, Siemens AG







MRI: Imaging for Radiation Treatment Guidance and Verification

Wednesday, Nov. 29 8:30AM - 10:00AM Room: S105AB



AMA PRA Category 1 Credits ™: 1.50 ARRT Category A+ Credit: 0

Participants

John E. Bayouth, PhD, Madison, WI (Moderator) Nothing to Disclose

LEARNING OBJECTIVES

1) Understand the main concepts of MRI-guided radiation therapy. 2) Understand the advantages and limitations of MRI-guided radiotherapy systems currently in use or under development. 3) Understand the use of in-room MRI guidance for management of intr- and inter-fraction variations in anatomy.

SAM

New in 2017: PLEASE NOTE - All courses designated for SAM credit at RSNA 2017 will require attendees bring a personal device e.g. phone, iPad, laptop to complete the required test questions during the live session.

Sub-Events

RC522A In-Room MRI for Treatment Guidance

Participants

John E. Bayouth, PhD, Madison, WI (Presenter) Nothing to Disclose

RC522B Integrating MRI: The Clinician Perspective

Participants

Caroline Chung, MD, FRCPC, Houston, TX (Presenter) Nothing to Disclose

LEARNING OBJECTIVES

1) Understand how MRI can be integrated into the clinical workflow of radiation treatment delivery. 2) Learn about the potential benefits of integrating MRI at each step of radiotherapy: treatment planning, radiation delivery and response assessment. 3) Appreciate the challenges of using MRI for radiation treatment guidance and ongoing research to overcome these challenges.







RC523

Clinical Applications of Molecular Imaging: Neuro MRS and PET

Wednesday, Nov. 29 8:30AM - 10:00AM Room: S502AB

NR MI OI PH

AMA PRA Category 1 Credits ™: 1.50 ARRT Category A+ Credit: 1.75

Sub-Events

RC523A Oncology Applications

Participants

Hyunsuk Shim, PhD, Atlanta, GA (Presenter) Nothing to Disclose

LEARNING OBJECTIVES

1) To learn the capability/potential of MR spectroscopy in brain tumor patient management. 2) To learn the limitation of the current standard MRIs that guide surgery and radiation therapy. 3) To learn about the potential of combining an advanced spectroscopic MR imaging with standard MR images to reduce the recurrence rate in glioblatomas.

ABSTRACT

Radiation therapy (RT) is as good as the images that guide RT planning. RT based on conventional MRIs may not fully target tumor extent in glioblastomas (GBM), which may, in part, account for high recurrence rates (60-70 percent at 6 months). Magnetic resonance spectroscopy, a molecular imaging modality that quantifies endogenous metabolite levels without relying on perfusion, leakage and diffusion of injected material, may better define extent of actively proliferating tumor. In addition, advances in this technology now permit acquisition of whole-brain high-resolution 3D spectroscopic MRI (sMRI) in 12-14 minutes. We correlated state-of-the-art sMRI metabolite maps and their ratio maps with tissue histopathology to validate further its use for identifying non-enhancing and infiltrating tumors that may not be fully imaged by conventional MRI sequences and provide support for its adjunctive use in tumor contouring for RT planning. Integration of histologically-verified, whole brain 3D sMRI into RT planning is feasible and may considerably modify target volumes. Thus, RT planning for GBMs may be augmented by sMRI potentially leading to reduced or delayed recurrence rates.

RC523B Functional Applications

Participants

Satoshi Minoshima, MD, PhD, Salt Lake City, UT (*Presenter*) Research Consultant, Hamamatsu Photonics KK; Research Grant, Hitachi, Ltd; Research Grant, Nihon Medi-Physics Co, Ltd;



KSNA° 201' Explore. Invent. Transform

103rd Scientific Assemblu and Annual Meeting November 26 to December 1 McCormick Place, Chicago



RC524

Publishing in Radiology: Understanding and Using the STARD and PRISMA Guidelines

Wednesday, Nov. 29 8:30AM - 10:00AM Room: S403B



AMA PRA Category 1 Credits ™: 1.50 ARRT Category A+ Credit: 1.75

Participants

Herbert Y. Kressel, MD, Boston, MA (Moderator) Stockholder, Pfizer Inc; Stockholder, UnitedHealth Group;

LEARNING OBJECTIVES

1) To familiarize attendees with reasons why quality improvement initiatives are important for the dissemination of published research. 2) To discuss the components of the STARD criteria and why these are important for studies of diagnostic accuracy. 3) To describe the PRISMA statement and why these make up key components of high quality systematic reviews. 4) To enable authors to improve completeness of reporting in their submitted manuscripts, to demonstrate study quality and thus enhance the liklihood that their manuscripts will be favorably reviewed when submitted to journals such as Radiology for publication.

ABSTRACT

The purpose of this session is to describe STARD and PRISMA, two documents that aim to improve scientific study quality by improving reporting. The Editor-in-Chief of Radiology, Dr. Herbert Kressel, Professor Radiology at Harvard Medical School, will introduce the importance of quality metrics in scientific research. Dr. Patrick Bossuyt, Professor of Clinical Epidemiology at University of Amsterdam, and one of the original authors of the STARD manuscript, who recently worked to revise STARD, will discuss the components of the STARD criteria and why these are important for studies of diagnostic accuracy. Dr. Matthew McInnes, Associate Professor of Radiology at University of Ottawa, and our 2014 Eyler Editorial fellow will describe the PRISMA statement and the important key components of high quality systematic reviews. Dr. Deborah Levine, Professor of Radology at Harvard Medical School and the Senior Deputy Editor of Radiology will describe how to put all of this information together into your final study plan and written manuscript. Our goal is to enable authors to improve completeness of reporting in their submitted manuscripts, to demonstrate study quality and thus enhance the liklihood that theirmanuscripts will befavorably reviewed when submitted for publication to Radiology as well as to other biomedical journals. Please see our publication information for authors at : http://pubs.rsna.org/page/radiology/pia as well as information about checklists at:

http://pubs.rsna.org/page/radiology/pia/checklists

URL

http://pubs.rsna.org/page/radiology/pia

Sub-Events

RC524A Introduction: Why Reporting Guidelines are Useful

Participants

Herbert Y. Kressel, MD, Boston, MA (Presenter) Stockholder, Pfizer Inc; Stockholder, UnitedHealth Group;

LEARNING OBJECTIVES

View learning objectives under the main course title.

RC524B STARD (Standards for Reporting Diagnostic Accuracy)

Participants Patrick M. Bossuyt, PhD, Amsterdam, Netherlands (Presenter) Nothing to Disclose

For information about this presentation, contact:

p.m.bossuvt@amc.nl

LEARNING OBJECTIVES

View learning objectives under the main course title.

RC524C PRISMA (Preferred Reporting Items for Systematic Reviews and Meta-Analyses)

Participants

Matthew D. McInnes, MD, FRCPC, Ottawa, ON (Presenter) Nothing to Disclose

For information about this presentation, contact:

mmcinnes@toh.ca

RC524D Putting It All Together

Participants

Deborah Levine, MD, Boston, MA (Presenter) Editor with royalties, UpToDate, Inc; Editor with royalties, Reed Elsevier;

dlevine@rsna.org

LEARNING OBJECTIVES

1) Describe reporting guidelines and why they are important for improving the quality of published research. 2) Illustrate the STARD reporting guidelines for Diagnostic Accuracy studies and how these can help authors and readers understand bias in research studies. 3) Discuss PRISMA guidelines for meta-analyses and systematic reviews.







RC525

Quantitative Imaging Mini-Course: Promise and Challenges

Wednesday, Nov. 29 8:30AM - 10:00AM Room: S504AB



AMA PRA Category 1 Credits ™: 1.50 ARRT Category A+ Credit: 1.75

Participants

Michael F. McNitt-Gray, PhD, Los Angeles, CA (Coordinator) Institutional research agreement, Siemens AG; ; ; ; ;

Sub-Events

RC525A The Perspective of the RSNA Quantitative Imaging Biomarkers Alliance (QIBA)

Participants

Edward F. Jackson, PhD, Madison, WI (Presenter) Nothing to Disclose

For information about this presentation, contact:

efjackson@wisc.edu

LEARNING OBJECTIVES

1) Describe the need for and benefits of implementing quantitative image analyses in clinical trials and clinical practice. 2) Describe the key challenges of extracting uniform, standardized quantitative measures from clinical imaging scans. 3) Provide examples of approaches to resolving of these challenges. 4) Understand the activities that RSNA supports to help move the profession of radiology from a primarily qualitative interpretation paradigm to a more quantitative-based interpretation model.

ABSTRACT

The added value of quantification in both research and clinical environments is likely to increase as health care initiatives place increased pressure on radiologists to provide decision support for evidence-based care. There remain substantial barriers to the widespread use of quantitative measures in clinical radiology, including an inherently large number of variables that impede validation of specific metrics, diversity of proprietary industry platforms, and lack of acceptance by radiologists. A critical barrier to the implementation of quantitative imaging in radiology is the lack of standardization among vendor platforms. Collaboration in the pre-competitive space is challenging yet crucial to address standardization, and integrating quantitative measurement into workflow will be necessary for wide adoption. The Quantitative Imaging Biomarkers Alliance (QIBA, www.rsna.org/qiba) was launched in 2007 as a means to unite researchers, healthcare professionals, and industry stakeholders in the advancement of quantitative imaging. QIBA's mission is to improve the value and practicality of quantitative imaging biomarkers (QIBs) by reducing variability across devices, imaging centers, patients, and time. The four QIBA modality-driven Coordinating Committees (CT, MR, Nuclear Medicine, Ultrasound) currently oversee 12 Biomarker Committees and 16 Task Forces. Selected QIBs that are considered to be transformational, translational, feasible, practical, and collaborative are addressed by Profiles, which are technical standards that include one or more clinical context-specific claims and inform users what quantitative results can be achieved by following the Profile. Sources of bias and variance, and methods to minimize each, are considered in Profile development. This presentation will summarize the goals and objectives of QIBA, including international efforts. The QIBA perspective on opportunities for QIB applications in the practice of precision medicine, challenges to be overcome, and approaches to addressing such challenges will be presented.

RC525B NCI's Quantitative Imaging Network (QIN) Perspective

Participants Robert J. Nordstrom, PhD, Rockville, MD (*Presenter*) Nothing to Disclose

For information about this presentation, contact:

nordstrr@mail.nih.gov

LEARNING OBJECTIVES

1) The current status of the Quantitative Imaging Network and the nature and purpose of the most recent program announcement for research efforts in this area will be discussed.

ABSTRACT

The Quantitative Imaging Netwo9rk, created in 2008 by NCI, is now entering its ninth year. Its purpose ciontinues to be tto develop, optimize and validate quantitative imaging tools for measurement or prediction of therapy response in clinical trials. To date a large numer of tools and methods have been developed and are under test and validation in clinical trials across the country. To streamline this process from development to validation, the NCI is using a phased mechanism to support research in this area. The first phase (called teh UG3 phase) will focus on development and optimization, while the second phase (the UH3 phase) will emphasize clinical validation in single-site or multisite clinical trials. Th purpose of teh phased approach is to separate the development efforts from validation efforts. This will be discussed in this presentation.

RC525C Clinical Trials Perspective

Participants Michael V. Knopp, MD, PhD, Columbus, OH (*Presenter*) Nothing to Disclose







RC527

Radiologist Peer-Review and Peer Learning-Options, Best Practices, and Future Directions

Wednesday, Nov. 29 8:30AM - 10:00AM Room: S404AB



AMA PRA Category 1 Credits ™: 1.50 ARRT Category A+ Credit: 1.75

Participants

Jay K. Pahade, MD, New Haven, CT (*Moderator*) Consultant, Precision Imaging Metrics, LLC David B. Larson, MD, MBA, Stanford, CA (*Presenter*) Grant, Siemens AG; Grant, Koninklijke Philips NV Danny C. Kim, MD, White Plains, NY (*Presenter*) Nothing to Disclose

For information about this presentation, contact:

Danny.Kim@nyumc.org

LEARNING OBJECTIVES

1) To provide a brief review on radiologist peer review history, practices and discuss implementation of a department wide peer review conference. 2) To review methods of peer review and peer learning through IT improvements, institutional consensus criteria development, and creation of Rad-Path modules. 3) To discuss new methods addressing peer review with an emphasis on peer learning principles and quality improvement. 4) To allow open discussion with audience members on the pro's and con's of current peer review practices and changes to expect in the future.

Honored Educators

Presenters or authors on this event have been recognized as RSNA Honored Educators for participating in multiple qualifying educational activities. Honored Educators are invested in furthering the profession of radiology by delivering high-quality educational content in their field of study. Learn how you can become an honored educator by visiting the website at: https://www.rsna.org/Honored-Educator-Award/ David B. Larson, MD, MBA - 2014 Honored Educator







MR Imaging of Rectal Cancer Before and After Therapy and Recent Advances in Imaging (An Interactive Session)

Wednesday, Nov. 29 8:30AM - 10:00AM Room: E451A

BQ GI MR

AMA PRA Category 1 Credits ™: 1.50 ARRT Category A+ Credit: 1.75

Participants

Hero K. Hussain, MD, Ann Arbor, MI (Moderator) Nothing to Disclose

Sub-Events

RC529A Pre-operative MRI Staging of Rectal Cancer: What Every Report Should Address

Participants Kartik S. Jhaveri, MD, Toronto, ON (*Presenter*) Nothing to Disclose

LEARNING OBJECTIVES

1) Highlight Key Relevant Clinical Backgroud of Imaging in rectal cancer. 2) Review Structured Reporting Template for Rectal Cancer Evaluation with MRI. 3) Demonstrate Key Points for Reporting of MRI of rectal cancer staging.

RC529B Response to Chemoradiotherapy: How Do We Assess?

Participants

Marc J. Gollub, MD, New York, NY (Presenter) Nothing to Disclose

LEARNING OBJECTIVES

1) Review the available methods ro evaluate response to chemoradiotherapy including T2 signal, DWI, volumetry and quantitative functional MRI. 2) Introduce the concept of complete response and its assessment at MRI. 3) Illustrate pitfalls in tumor and node assessment after therapy.

RC529C MRI as a Prognostic Biomarker and Guide to New Therapies

Participants Regina G. Beets-Tan, MD, PhD, Amsterdam, Netherlands (*Presenter*) Nothing to Disclose

For information about this presentation, contact:

r.beetstan@nki.nl







Common Spinal Injection Procedures for Diagnosis and Treatment of Back Pain (Hands-on)

Wednesday, Nov. 29 8:30AM - 10:00AM Room: E263



AMA PRA Category 1 Credits ™: 1.50 ARRT Category A+ Credit: 1.75

Participants

A. Orlando Ortiz, MD, MBA, Mineola, NY (*Presenter*) Nothing to Disclose Bassem A. Georgy, MD, MSc, San Diego, CA (*Presenter*) Consultant, Johnson & Johnson; Consultant, Merit Medical Systems, Inc; Stockholder, Merit Medical Systems, Inc ; Stockholder, Spine Solutions, Inc; ; Todd S. Miller, MD, Bronx, NY (*Presenter*) Nothing to Disclose Stanley Golovac, MD, Coral Gables, FL (*Presenter*) Nothing to Disclose Allan L. Brook, MD, Bronx, NY (*Presenter*) Nothing to Disclose Michele H. Johnson, MD, New Haven, CT (*Presenter*) Nothing to Disclose Afshin Gangi, MD, PhD, Strasbourg, France (*Presenter*) Proctor, Galil Medical Ltd

For information about this presentation, contact:

oortiz@winthrop.org

Sgolovac@mac.com

afshin.gangi@chru-strasbourg.fr

tmiller@montefiore.org

LEARNING OBJECTIVES

1) To introduce common spinal injection procedures that are used for the diagnosis and treatment of neck and back pain disorders. 2) To learn the indications and contraindications for these procedures. 3) To understand how imaging guidance is used to perform these procedures. 4) To introduce some of the equipment and techniques that are helpful in performing spine injection procedures in a hands on format with an opportunity for attendees to address their specific questions and concerns with the course faculty.

ABSTRACT

Image guided spine interventions can be used for the diagnosis and/or treatment of painful conditions of the spinal access. Diagnostic procedures often include specific nerve blocks that can be performed with anesthetic agents. Facet joint and sacroiliac joint pain syndromes can likewise be managed with spine interventional techniques. Epidural steroid injections can be performed using interlaminar, caudal or transforaminal techniques in the management of focal back or neck pain with an associated radicular pain component. More advanced longer lasting treatments inclued radiofrequency neuolysis which can also be used to manage facet or sacroiliac joint related pain that temporarily responds to diagnostic median branch blocks or specific joint injections. Spinal cord stimulator placement is another advanced technique that can be used to manage chronic pain syndromes. The workshop emphasizes patient selection, imaging evaluation, procedure indication and contraindications in order to optimize treatment outcome.

Active Handout:Todd Stuart Miller

http://abstract.rsna.org/uploads/2017/3010360/Active RC531.pdf







Value-Added Initiatives for a Healthcare System

Wednesday, Nov. 29 8:30AM - 10:00AM Room: N228



AMA PRA Category 1 Credits ™: 1.50 ARRT Category A+ Credit: 1.75

Sub-Events

RC532A Quality, Value and Outcome Metrics in Diagnostic Radiology: A New Frontier

Participants

Steven E. Seltzer, MD, Boston, MA (Presenter) Travel support, General Electric Company; Travel support, Siemens AG

LEARNING OBJECTIVES

1) To understand the options for Radiologists to add value to the current health care system by a: Leading population health management efforts, particularly in image-based cancer screening programs, b: Leading care redesign initiatives to improve the efficiency of care, c) Leading payment redesign initiatives to encourage providers to share responsibility for managing costs and resource utilization.

RC532B Imaging Informatics

Participants

Keith J. Dreyer, DO, PhD, Boston, MA (Presenter) Nothing to Disclose

LEARNING OBJECTIVES

1) Understand the essentials of imaging informatics and its importance in the role of patient care in today's healthcare climate. 2) Appreciate how accessibility to images from other institutions increases patient care and safety by reducing the need for repetitive scans. 3) Learn how the use of technology can improve providers' ability to interpret, diagnose and treat while improving efficiency, quality, and reducing cost.

RC532C Leveraging IT to Optimize Quality in Radiology

Participants

Paul J. Chang, MD, Chicago, IL (*Presenter*) Co-founder, Stentor/Koninklijke Philips NV; Researcher, Koninklijke Philips NV; Advisory Board, Bayer AG; Advisory Board, Aidoc Ltd; Advisory Board, McCoy

For information about this presentation, contact:

pchang@radiology.bsd.uchicago.edu

LEARNING OBJECTIVES

1) Discuss how modern radiology quality expectations require a greater degree of "meaningful innovation" in imaging IT and informatics. 2) Be introduced to examples of next generation IT tools and models that can help achieve both improved efficiency and quality. 3) Describe how and why radiology must redefine and re-engineer itself in order to fully take advantage of these next generation electronic based practice tools. The impact these changes in practice management can have on quality, workflow efficiency, and productivity will be discussed.

ABSTRACT

Radiology practices have benefited from the adoption of electronic-based information technology, especially with respect to practice efficiency. However, there is great opportunity to further leverage information technology to significantly improve quality within the radiology practice. However, electronic tools, such as PACs, RIS, and speech recognition (along with their associated workflow), are still relatively immature and arguably support only "commodity-level" capability. There is a critical need for a new generation of "meaningful innovation" in radiology IT that will allow radiology to maximize value to patients and other stakeholders by significantly improving both efficiency and quality. Radiologists must be "value innovators" who maximally leverage information technology to ensure their relevance and value to patient care through measureable improvements in quality, efficiency, and safety.







RC550

Techniques of Musculoskeletal Interventional Ultrasound (Hands-on)

Wednesday, Nov. 29 8:30AM - 10:00AM Room: E260



AMA PRA Category 1 Credits ™: 1.50 ARRT Category A+ Credit: 1.75

Participants

Patrick Warren, MD, Columbus, OH (*Presenter*) Nothing to Disclose Veronica J. Rooks, MD, Tripler AMC, HI (*Presenter*) Nothing to Disclose James W. Murakami, MD, Columbus, OH (*Presenter*) Nothing to Disclose Carmen Gallego, MD, Madrid, Spain (*Presenter*) Nothing to Disclose Stephen C. O'Connor, MD, Boston, MA (*Presenter*) Nothing to Disclose Mabel Garcia-Hidalgo Alonso, MD, Majadahonda, Spain (*Presenter*) Nothing to Disclose Michael A. Mahlon, DO, Tacoma, WA (*Presenter*) Nothing to Disclose Paolo Minafra, MD, Pavia, Italy (*Presenter*) Nothing to Disclose Paula B. Gordon, MD, Vancouver, BC (*Presenter*) Stockholder, OncoGenex Pharmaceuticals, Inc ; Scientific Advisory Board, Real Imaging Ltd; ; Horacio M. Padua JR, MD, Boston, MA (*Presenter*) Nothing to Disclose Ebonee Carter, MD, Honolulu, HI (*Presenter*) Nothing to Disclose Ulises Barajas, MD, Juarez, Mexico (*Presenter*) Nothing to Disclose Peter L. Cooperberg, MD, Vancouver, BC (*Presenter*) Nothing to Disclose Kathleen M. Boyer, DO, Honolulu, HI (*Presenter*) Nothing to Disclose

For information about this presentation, contact:

Stephen.o'connor@bhs.org

Tarsomsn@hotmail.com

paolominafra@gmail.com

cgallego@salud.madrid.org

LEARNING OBJECTIVES

1) Identify basic skills, techniques, and pitfalls of freehand invasive sonography. 2) Define and discuss technical aspects, rationale, and pitfalls involved in musculoskeletal interventional sonographic care procedures. 3) Successfully perform basic portions of handson US-guided MSK procedures in a tissue simulation learning module, including core biopsy, small abscess drainage, cyst aspiration, soft tissue foreign body removal, and intraarticular steriod injection. 4) Incorporate these component skill sets into further life-long learning for expansion of competency and prepartaion for more advanced interventional sonographic learning opportunities.







RC552

Carotid and Abdominal Doppler (Hands-on)

Wednesday, Nov. 29 8:30AM - 10:00AM Room: E264



AMA PRA Category 1 Credits ™: 1.50 ARRT Category A+ Credit: 1.75

Participants

Gowthaman Gunabushanam, MD, New Haven, CT (*Presenter*) Nothing to Disclose Shweta Bhatt, MD, MBBS, Rochester, NY (*Presenter*) Nothing to Disclose Wui K. Chong, MD, Houston, TX (*Presenter*) Advisory Board, Bracco Group; Corinne Deurdulian, MD, Los Angeles, CA (*Presenter*) Nothing to Disclose Vikram S. Dogra, MD, Rochester, NY (*Presenter*) Editor, Wolters Kluwer nv; Ulrike M. Hamper, MD, MBA, Baltimore, MD (*Presenter*) Nothing to Disclose Davida Jones-Manns, Hampstead, MD (*Presenter*) Nothing to Disclose Mark E. Lockhart, MD, Birmingham, AL (*Presenter*) Author, Oxford University Press; Author, JayPee Brothers Publishers; Deputy Editor, John Wiley & Sons, Inc Margarita V. Revzin, MD, New Haven, CT (*Presenter*) Nothing to Disclose Michelle L. Robbin, MD, Birmingham, AL (*Presenter*) Consultant, Koninklijke Philips NV; Leslie M. Scoutt, MD, New Haven, CT (*Presenter*) Nothing to Disclose Sadhna Verma, MD, Cincinnati, OH (*Presenter*) Nothing to Disclose Sadhna Verma, MD, Cincinnati, OH (*Presenter*) Nothing to Disclose William D. Middleton, MD, St. Louis, MO (*Presenter*) Nothing to Disclose

For information about this presentation, contact:

drsadhnaverma@gmail.com

margarita.revzin@yale.edu

mrobbin@uabmc.edu

wkchong@mdanderson.org

leslie.scoutt@yale.edu

LEARNING OBJECTIVES

1) Describe the technique and optimally perform carotid Doppler ultrasound. 2) Describe the technique and optimally perform abdominal Doppler ultrasound. 3) Review qualitative and quantitative criteria for diagnosing abnormalities in carotid and abdominal ultrasound Doppler examinations.

ABSTRACT

This hands-on course will provide participants with a combination of didactic lectures and an extended 'live' scanning opportunity on normal human volunteers, as follows: Didactic lectures (30 minutes): Carotid Doppler ultrasound: scanning technique, diagnostic criteria and interesting teaching cases. Abdominal Doppler ultrasound: scanning technique, diagnostic criteria and interesting teaching cases. Mentored scanning (60 minutes): Following the didactic lectures, the participants will proceed to a scanning area with normal human volunteers and ultrasound machines from different manufacturers. Participants will be able to perform live scanning with direct assistance, as needed, by faculty. Faculty will be able to offer feedback, help participants improve their scanning technique as well as answer any questions. Time permitting, faculty will also be available to answer general questions relating to all aspects of vascular ultrasound, not just limited to carotid and abdominal Doppler studies.

Honored Educators

Presenters or authors on this event have been recognized as RSNA Honored Educators for participating in multiple qualifying educational activities. Honored Educators are invested in furthering the profession of radiology by delivering high-quality educational content in their field of study. Learn how you can become an honored educator by visiting the website at: https://www.rsna.org/Honored-Educator-Award/ Margarita V. Revzin, MD - 2017 Honored EducatorLeslie M. Scoutt, MD - 2014 Honored EducatorSadhna Verma, MD - 2013 Honored Educator







Growing Your Business with Social Media: Tips and Tricks for Department and Practice Managers

Wednesday, Nov. 29 8:30AM - 10:00AM Room: E351



AMA PRA Category 1 Credits ™: 1.50 ARRT Category A+ Credit: 0

Participants

Alex Towbin, MD, Cincinnati, OH (*Moderator*) Author, Reed Elsevier; Grant, Guerbet SA; Grant, Siemens AG; Consultant, Reed Elsevier; Advisory Board, IBM Corporation; Saad Ranginwala, MD, Cincinnati, OH (*Presenter*) Nothing to Disclose

For information about this presentation, contact:

alexander.towbin@cchmc.org

sranginwala@gmail.com

LEARNING OBJECTIVES

1) Describe how social media can be used to promotoe a radiology practice. 2) Name three social media platforms, their benefits, and their contraints.







Want to Learn More About Imaging Informatics? Education, Resources and Certifications

Wednesday, Nov. 29 8:30AM - 10:00AM Room: S403A



AMA PRA Category 1 Credits ™: 1.50 ARRT Category A+ Credit: 1.75

Participants

Christopher J. Roth, MD, Durham, NC (Moderator) Nothing to Disclose

LEARNING OBJECTIVES

1) Summarize the forces driving physician adoption and leadership in local and national informatics initiatives. 2) Outline freely available educational resources to expand imaging informatics understanding. 3) Describe available imaging informatics courses and fellowships. 4) Detail common certifications available to imaging and non-imaging informatics leaders to demonstrate their knowledge. 5) Know the current imaging informatics 'hot topics.'

Sub-Events

RC554A Landscape of Online Resources for Informatics Self-Study

Participants

Marc D. Kohli, MD, San Francisco, CA (Presenter) Nothing to Disclose

LEARNING OBJECTIVES

1) Identify online sources of content for didactic informatics self-study. 2) Identify online resources for hands-on study of database and programming concepts.

RC554B Formal Opportunities and Resources for Imaging Informatics Training

Participants

Tessa S. Cook, MD, PhD, Philadelphia, PA (Presenter) Nothing to Disclose

For information about this presentation, contact:

tessa.cook@uphs.upenn.edu

RC554C Imaging and Non-imaging Informatics Society Certifications: What is Out There and is it Valuable?

Participants

Christopher J. Roth, MD, Durham, NC (Presenter) Nothing to Disclose

LEARNING OBJECTIVES

1) Describe the value of obtaining certifications as an informatics leader. 2) Compare available opportunities for pursuing three common informatics certifications relevant to RSNA members and attendees: American Board of Imaging Informatics Certified Imaging Informatics Professional (ABII CIIP) certification, the American Board of Preventative Medicine Clinical Informatics (ABPM CI) ABMS board certification, and Healthcare Information and Management Systems Society Certified Professional in Health Information & Management System (HIMSS CPHIMS).







RCA41

3D Printing Hands-on with Open Source Software: Advanced Techniques (Hands-on)

Wednesday, Nov. 29 8:30AM - 10:00AM Room: S401AB

IN

AMA PRA Category 1 Credits ™: 1.50 ARRT Category A+ Credit: 1.75

Participants

Anish Ghodadra, MD, New Haven, CT (*Presenter*) Consultant, PECA Labs; Advisory Board, axial3D Limited Michael W. Itagaki, MD, MBA, Lynnwood, WA (*Presenter*) Owner, Embodi3D, LLC Beth A. Ripley, MD, PhD, Seattle, WA (*Presenter*) Nothing to Disclose Tatiana Kelil, MD, San Francisco, CA (*Presenter*) Nothing to Disclose Carissa M. White, MD, Los Angeles, CA (*Presenter*) Nothing to Disclose Dmitry Levin, Seattle, WA (*Presenter*) Nothing to Disclose Steve D. Pieper, PhD, Cambridge, MA (*Presenter*) CEO, Isomics, Inc; Employee, Isomics, Inc; Owner, Isomics, Inc; Research collaboration, Siemens AG; Research collaboration, Novartis AG; Consultant, Harmonus; Research collaboration, gigmade

For information about this presentation, contact:

carissamwhite@gmail.com

aghodadramd@gmail.com

LEARNING OBJECTIVES

1) To learn advanced techniques for converting a medical imaging scan into a digital 3D printable model with free and open-source software. 2) To perform advanced customizations to the digital 3D printable model with free software prior to physical creation with a 3D printer.

ABSTRACT

'3D printing' refers to fabrication of a physical object from a digital file with layer-by-layer deposition instead of conventional machining, and allows for creation of complex geometries, including anatomical objects derived from medical scans. 3D printing is increasingly used in medicine for surgical planning, education, and device testing. This advanced hands-on course builds upon the introductory course given by the same faculty. It will teach the learner advanced segmentation techniques used to convert a standard Digital Imaging and Communications in Medicine (DICOM) data set from a medical scan into a 3D printable model. Advanced manipulation of the digital model in preparation for 3D printing will then be discussed. All software used will be free. Methods described will work with Windows, Macintosh, and Linux computers. The learner will be given access to comprehensive resources for self-study before and after the meeting, including an extensive training manual and online video tutorials.

Honored Educators

Presenters or authors on this event have been recognized as RSNA Honored Educators for participating in multiple qualifying educational activities. Honored Educators are invested in furthering the profession of radiology by delivering high-quality educational content in their field of study. Learn how you can become an honored educator by visiting the website at: https://www.rsna.org/Honored-Educator-Award/ Tatiana Kelil, MD - 2017 Honored Educator







RCC41

Research Opportunities Using the NIH The Cancer Imaging Archive (TCIA) That Links Cancer Imaging to Clinical Data, Genomics, Proteomics, Quantitative Imaging and Deep Learning

Wednesday, Nov. 29 8:30AM - 10:00AM Room: S501ABC



AMA PRA Category 1 Credits ™: 1.50 ARRT Category A+ Credit: 0

Participants

John B. Freymann, BS, Bethesda, MD (Presenter) Nothing to Disclose

Evis Sala, MD, PhD, New York, NY (Presenter) Nothing to Disclose

Sandy Napel, PhD, Stanford, CA (*Presenter*) Medical Advisory Board, Fovia, Inc; Consultant, Carestream Health, Inc; Scientific Advisor, EchoPixel, Inc; Scientific Advisor, RADLogics, Inc

Maryellen L. Giger, PhD, Chicago, IL (*Presenter*) Stockholder, Hologic, Inc; Stockholder, Quantitative Insights, Inc; Shareholder, QView Medical, Inc; Co-founder, Quantitative Insights, Inc; Royalties, Hologic, Inc; Royalties, General Electric Company; Royalties, MEDIAN Technologies; Royalties, Riverain Technologies, LLC; Royalties, Mitsubishi Corporation; Royalties, Toshiba Medical Systems Corporation

Brian M. Rodgers, MD, New Orleans, LA (*Presenter*) Nothing to Disclose Keyvan Farahani, PhD, Bethesda, MD (*Presenter*) Nothing to Disclose Luis E. Selva, PhD, Boston, MA (*Presenter*) Nothing to Disclose Lin Chen, PhD, Chicago, IL (*Presenter*) Nothing to Disclose

For information about this presentation, contact:

john.freymann@nih.gov

salae@mskcc.org

luis.selva@va.gov

LEARNING OBJECTIVES

1) Learn how advanced imaging research teams combine image data with linked meta-data (clinical, genomic, proteomic, etc) using the publicly available image data from the NIH The Cancer Imaging Archive (TCIA). 2) Learn how major projects are depositing their data in TCIA for community use (eg Moonshot, Quantitative Imaging Network, image analysis/processing competitions). 3) Learn how authors have gained by publishing their data along with research articles to reach a wider audience and increase their impact.

ABSTRACT

Diagnostic images, analyzed by expert radiologists with computational analytic tools assistance can offer reliable, reproducible data that connect tumor tissue genetics, proteomics and pathology images. This didactic session will highlight major projects utilizing TCIA with presentations from leading researchers using projects such as the Moonshot/APOLLO, proteomics (CPTAC Phase III), The Cancer Genome Atlas (TCGA), Immunotherapy, Challenges, Precision Medicine, NCI Quantitative Imaging Network.

Honored Educators

Presenters or authors on this event have been recognized as RSNA Honored Educators for participating in multiple qualifying educational activities. Honored Educators are invested in furthering the profession of radiology by delivering high-quality educational content in their field of study. Learn how you can become an honored educator by visiting the website at: https://www.rsna.org/Honored-Educator-Award/ Evis Sala, MD, PhD - 2013 Honored EducatorEvis Sala, MD, PhD - 2017 Honored Educator







MSRT42

ASRT@RSNA 2017: Where Does the Radiation Hurt in Low Dose, High Dose and Multiple Dose Radiology?

Wednesday, Nov. 29 9:20AM - 10:20AM Room: N230B

sq

AMA PRA Category 1 Credit ™: 1.00 ARRT Category A+ Credit: 1.00

Participants

Subhendra N. Sarkar, PhD, Brookline, NY (Presenter) Nothing to Disclose

For information about this presentation, contact:

ssarkar@citytech.cuny.edu

LEARNING OBJECTIVES

1) To understand small, added risks of long term low dose radiation, particularly how diagnostic radiology plays a role toward increased radiation risk for follow up patients and hospital workers. 2) To appreciate why experts disagree over the exact definition and effects of "low dose" and other risk factors that make radiation effect calculation challenging. 3) To appreciate that medical Ionizing radiation has sufficient energy to cause chemical changes in cells and damage them. 4) To assist physicians for deciding on non-ionizing or low-dose modalities as multiple ionizing follow-ups for the same patients accumulate non-negligible cancer risk. 5) To compare the significant variation in radiation dose among various scanners, among vendors and among radiological departments such that dose assumptions could be wrong. 6) To model technologists practice as one leading to chronic low-level exposure that may manifest after the expected delay to an observed health effect. 7) To draw similarity between multi-country nuclear industry worker data who got chronic low-dose exposures and Japan atomic bomb survivors and appreciate chronic accumulated risk of low-dose ionizing radiation and slight increase in death frequency caused by leukemia. 8) To critically look at the leukemia risk that seems to be higher for radiologic technologists who have worked for more than 30 years compared to those who had worked for less than 10 years. 9) To appreciate that although the effect of ionizing radiation on cells and tissue is dependent on the radiation dose and KeV or MeV, there is not enough clarity on how the tumor cells respond to low and high doses of radiation present in medical diagnostic and treatment modalities. 10) To qualitatively compare after-effects of radiation therapy in radiosensitive organs as the number of cancer survivors grow, for example, the adverse cardiovascular effects of radiation treatment on such populations.

Active Handout:Subhendra Nath Sarkar

http://abstract.rsna.org/uploads/2017/17001468/Active MSRT42.pdf







MSCP42

Case-based Review of Pediatric Radiology (An Interactive Session)

Wednesday, Nov. 29 10:30AM - 12:00PM Room: S406A

PD

AMA PRA Category 1 Credits ™: 1.50 ARRT Category A+ Credit: 1.75

Participants

Ricardo Restrepo, MD, Miami, FL (Director) Nothing to Disclose

Sub-Events

MSCP42A Pediatric Pancreatic Disorders

Participants

Donald P. Frush, MD, Durham, NC (Presenter) Nothing to Disclose

For information about this presentation, contact:

donald.frush@duke.edu

LEARNING OBJECTIVES

1) Learn the often unique features of the normal pancreas in children. 2) Understand embryological role in congential pancreatic disorders. 3) Be able to discuss the spectrum of acquired pancreatic disorders in children.

MSCP42B Pediatric Intestinal Disorders

Participants

Khalid Khashoggi, MD, MBBCh, Vancouver, BC (Presenter) Nothing to Disclose

LEARNING OBJECTIVES

1. This presentation is an educational review of pediatric gastric mass lesions. 2. Clinical presentation is varied with upper GI bleeding, feeding intolerance, pain, weight loss and fatigue manifesting. 3. The imaging work-up might initially have been endoscopy or ultrasound. Cross section imaging (CT MR) can be invaluable. 4. The role and impact of FDG PET on the management, staging and follow up of the oncologic pathology will be emphasized.

ABSTRACT

During this session , multiple common pediatric gastrointestinal disorders will be presented. The presentation will emphasize the characteristic imaging findings and the differential diagnosis.

MSCP42C Pediatric Genitourinary Disorders

Participants Sarah S. Milla, MD, Atlanta, GA (*Presenter*) Nothing to Disclose

For information about this presentation, contact:

sarah.milla@emory.edu

LEARNING OBJECTIVES

1) Identify imaging characteristics of several common pediatric genitourinary disorders. 2) Understand imaging features characteristic of classic pediatric genitourinary syndromes. 3) Recognize fetal imaging of genitourinary disorders.

ABSTRACT

During this interactive session, learners will participate in diagnosing several pediatric genitourinary disorders which may present before birth, in neonatal life, or during childhood/adolescence. Emphasis on important imaging findings necessary for accurate diagnosis and appropriate differential diagnoses will be made. Discussion of additional findings or clinical features in syndromes and associations will allow learners to briefly review embryology, development, and neoplasia.

MSCP42D Pediatric Interventional Cases

Participants

Ricardo Restrepo, MD, Miami, FL (Presenter) Nothing to Disclose

LEARNING OBJECTIVES

1) Discuss the indications and technique of image guided tissue sampling and treatment in pediatric musculoskeletal neoplasms. 2) Discuss the classification, treatment and complications of complex vascular anomalies in children. 3) Discuss some pitfalls of vascular malformations in children.

In this interactive session several cases will be presented as vignettes allowing the participant to recognize imaging findings of certain pediatric diseases, narrow the differential diagnosis, become familiar with the indications and choose the appropriate image guided procedures. Cases discussed will include complex vascular anomalies, osteoid osteoma, bone and soft tissue sarcomas as well as pitfalls of vascular malformations.

LEARNING OBJECTIVES

1) Learn the differential diagnosis of some vascular anomalies in children and their treatment. 2) Recognize some arterial and venous pathologies in children and their treatment. 3) Recognize benign and malignant features of thyroid nodules in children and be familiar with the guidelines for thyroid nodule biopsy in pediatric patients. 4) Be familiar with complications associated with acute pancreatitis in pediatric patients including the proper terminology and indications for treatment.







MSES42

Essentials of Genitourinary Imaging

Wednesday, Nov. 29 10:30AM - 12:00PM Room: S100AB

GU

AMA PRA Category 1 Credits ™: 1.50 ARRT Category A+ Credit: 1.75

Sub-Events

MSES42A Endometriosis: The Great Imitator

Participants

Paula J. Woodward, MD, Salt Lake City, UT (Presenter) Editor, Reed Elsevier

For information about this presentation, contact:

paula.woodward@hsc.utah.edu

LEARNING OBJECTIVES

1) Identify which imaging features (both ultrasound and MRI) are more specific for endometriosis and help to distinguish it from other adnexal masses. 2) Recognize and diagnose more unusual manifestations and complications of this disorder.

ABSTRACT

Endometriosis is an important gynecologic disorder primarily affecting women during their reproductive years. Pathologically, it is the result of functional endometrium located outside the uterus. It may vary from microscopic endometriotic implants to large cysts (endometriomas). The physical manifestations are protean, with some patients being asymptomatic and others having disabling pelvic pain, infertility, or adnexal masses. Ultrasonographic features are variable and can mimic those of other benign and malignant ovarian lesions. Low-level internal echoes and echogenic wall foci are more specific US features for endometriomas. MRI improves diagnostic accuracy, with endometriotic cysts typically appearing with high signal intensity on T1-weighted images and demonstrating "shading" on T2-weighted images. The ovaries are the most common sites affected, but endometriosis can also involve the gastrointestinal tract, urinary tract, chest, and soft tissues.

MSES42B Differential Diagnosis of Focal Renal Masses

Participants

Harriet C. Thoeny, MD, Bern, Switzerland (Presenter) Advisory Board, Guerbet SA

LEARNING OBJECTIVES

1) To become familiar with surgical and nonsurgical cystic renal lesions. 2) To know the typical imaging findings of the most frequent benign renal masses. 3) To know the typical imaging findings of renal cell carcinomas including subtype classification.

ABSTRACT

Focal renal masses are frequently detected incidentally on cross-sectional imaging. These lesions are cystic or solid. Cystic renal lesions are stratified according to the Bosniak classification. Bosniak I and II cysts are non-surgical lesions, Bosniak III and IV cysts are surgical lesions and Bosniak IIF need to be followed up. Solid lesions are often smaller than 4 cm in diameter (small renal masses=SMR) when incidentally detected and mainly correspond to renal cell carcinomas (RCCs). RCCs are divided in clear cell, chromophob and papillary with typical imaging features on CT and MRI. Clear cell RCC is the most frequent and most aggressive subtype and typically shows strong enhancement on CT or MRI, necrotic areas and a high ADC on DWI. Papillary RCCs are typically homogenous, show little enahncment, have a low ADC on DWI and are hypointense on T2w MRI. The imaging features of chromophob RCCs are in between. The most frequent benign solid renal masses are angiomyolipomas (AML) and oncocytomas. AML contains fat, whereas lipid poor AMLs are hypointense on T2w and show strong enhancement. Oncocytomas are typically homogneous solid lesions and show strong enehancment with a high ADC value, however its differentiation from clear cell RCC often remains a challenge.

MSES42C Prostate MRI: Revolution, Now Evolution

Participants

Tristan Barrett, MBBS, Cambridge, United Kingdom (Presenter) Nothing to Disclose

For information about this presentation, contact:

tristan.barrett@addenbrookes.nhs.uk

LEARNING OBJECTIVES

1) To understand the evolving role of multiparametric MRI in the work-up of prostate cancer. 2) To appreciate the evolution in MRI protocols and their interpretation. 3) To recognise the advantages and limitations of each technique. 4) To understand the clinical relevance of MRI for treatment decision-making and management triage.

ABSTRACT

Multiparametric MRI of the prostate is changing the paradigm of prostate diagnostic pathways, leading to an exponential increase in

demand form clinicians. Increasingly MRI is being performed in patients without a cancer diagnosis in order to subsequently guide prostatic biopsy. This has shifted the emphasis of radiological interpretation from one of basic staging to lesion detection and characterisation. In order to accurately assess the differential diagnosis there needs to be an appreciation of the sequences performed, their limitations in terms of sensitivity and specificity, and the expected normal anatomical appearances. Further knowledge of how MRI results affect clinical outcomes can enable the radiologist to optimise patient management as part of a multidisciplinary team.

Active Handout:Tristan Barrett

http://abstract.rsna.org/uploads/2017/17000073/Active MSES42C.pdf

MSES42D A Simple Guide to Adrenal Gland Imaging

Participants

Antonio C. Westphalen, MD, Mill Valley, CA (*Presenter*) Scientific Advisory Board, 3DBiopsy LLC ; Research Grant, Verily Life Sciences LLC

For information about this presentation, contact:

antonio.westphalen@ucsf.edu

LEARNING OBJECTIVES

1) Understand the role of imaging for the characterization of an incidentaloma of the adrenal gland and for the assessment of symptomatic patients. 2) Be able to list the most prevalent causes of adrenal nodules and apply imaging to make a few specific diagnoses. 3) Be able to correctly recommend further evaluation with imaging or tissue sampling, as appropriate.

ABSTRACT

The increase in use of cross-sectional imaging in the last decade or two has led to a parallel growth in the detection of incidental adrenal lesions, or 'incidentalomas'. This has become a common diagnostic dilemma for radiologists, as these must at least be characterized as benign, malignant or indeterminate. While most incidental nodules are benign, usually an adenoma, the possibility of malignant involvement requires accurate imaging assessment to inform management decisions. In this presentation, I review a systematic approach to the evaluation of adrenal nodules with imaging, with emphasis on computed tomography and magnetic resonance imaging.

Honored Educators

Presenters or authors on this event have been recognized as RSNA Honored Educators for participating in multiple qualifying educational activities. Honored Educators are invested in furthering the profession of radiology by delivering high-quality educational content in their field of study. Learn how you can become an honored educator by visiting the website at: https://www.rsna.org/Honored-Educator-Award/ Antonio C. Westphalen, MD - 2017 Honored Educator







MSRO42

BOOST: Lymphoma-Oncology Anatomy (An Interactive Session)

Wednesday, Nov. 29 10:30AM - 12:00PM Room: S103CD



AMA PRA Category 1 Credits ™: 1.50 ARRT Category A+ Credit: 1.75

Participants

Chelsea C. Pinnix, MD, PhD, Houston, TX (*Presenter*) Research Grant, Merck & Co, Inc Bradford Hoppe, MD, Jacksonville, FL (*Presenter*) Nothing to Disclose Steve Cho, MD, Madison, WI (*Presenter*) Nothing to Disclose Sarah A. Johnson, MD, Toronto, ON (*Presenter*) Nothing to Disclose

For information about this presentation, contact:

scho@uwhealth.org

LEARNING OBJECTIVES

1) Improve their understanding of the anatomical distribution of Hodgkin lymphoma using PET/CT imaging. 2) Improve their understanding of the anatomical distribution of Non-Hodgkin lymphoma. 3) Understand the Deauville response scale for lymphoma using PET/CT scan.



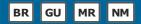




MSSR42

RSNA/ESR Hybrid Imaging Symposium: Hybrid Imaging in the Female (An Interactive Session)

Wednesday, Nov. 29 10:30AM - 12:00PM Room: S402AB



AMA PRA Category 1 Credits ™: 1.50 ARRT Category A+ Credit: 1.75

Participants

Alexander Drzezga, MD, Cologne, Germany (*Moderator*) Consultant, Siemens AG; Consultant, Bayer AG; Consultant, General Electric Company; Consultant, Eli Lilly and Company; Consultant, The Piramal Group; Speakers Bureau, Siemens AG; Speakers Bureau, Bayer AG; Speakers Bureau, General Electric Company; Speakers Bureau, Eli Lilly and Company; Speakers Bureau, The Piramal Group Katrine Riklund, MD, PhD, Umea, Sweden (*Moderator*) Nothing to Disclose

For information about this presentation, contact:

katrine.riklund@umu.se

Sub-Events

MSSR42A Pelvic Tumors

Participants Farrokh Dehdashti, MD, Saint Louis, MO (*Presenter*) Nothing to Disclose

LEARNING OBJECTIVES

1) Learn about different tracers. 2) Understand how to interpret hybrid imaging examinations of the pelvis. 3) Learn about the role of hybrid imaging in staging, treatment evaluation and follow-up.

ABSTRACT

This presentation summarizes the literature in PET/CT and PET/MRI in the evaluation of the three most common gynecologic malignancies: cervical, endometrial and ovarian cancers. The advantages and challenges of each hybrid modality will be briefly discussed. In addition to clinically used 2-[18F]fluoro-2-deoxy-D-glucose (FDG), novel tracers that are currently used for research purposes in these malignancies will be briefly discussed.

MSSR42B Breast Cancer

Participants

Osman Ratib, MD, PhD, Geneva, Switzerland (Presenter) Nothing to Disclose

LEARNING OBJECTIVES

1) Learn about pathophysiology and relation to different tracers. 2) Understand how to interpret hybrid imaging examinations of the breast. 3) Learn about the role of hybrid imaging in staging, treatment evaluation and follow-up.

MSSR42C Interactive Case Discussion

Participants Farrokh Dehdashti, MD, Saint Louis, MO (*Presenter*) Nothing to Disclose Osman Ratib, MD, PhD, Geneva, Switzerland (*Presenter*) Nothing to Disclose

LEARNING OBJECTIVES

1) Understand how to interpret hybrid imaging in female pelvic tumours. 2) Understand how to interpret hybrid imaging in breast cancer. 3) Learn how to avoid common pitfalls.

ABSTRACT

Imaging is critical for staging, determining prognosis and treatment strategy, and in predicting prognosis in gynecological malignancies. In this case presentation session, common clinical applications of PET/CT and PET/MRI in the evaluation of the most common gynecologic malignancies will be presented. In addition, the advantages and disadvantages of each hybrid modality will be illustrated and discussed.







RCA42

3D Printing (Mimics) (Hands-on)

Wednesday, Nov. 29 10:30AM - 12:00PM Room: S401AB

IN

AMA PRA Category 1 Credits ™: 1.50 ARRT Category A+ Credit: 1.75

Participants

Adnan M. Sheikh, MD, Ottawa, ON (Moderator) Nothing to Disclose Adnan M. Sheikh, MD, Ottawa, ON (Presenter) Nothing to Disclose Frank J. Rybicki III, MD, PhD, Ottawa, ON (Presenter) Nothing to Disclose Dimitris Mitsouras, PhD, Boston, MA (Presenter) Research Grant, Toshiba Medical Systems Corporation; Leonid Chepelev, MD, PhD, Ottawa, ON (Presenter) Nothing to Disclose Taryn Hodgdon, MD, Ottawa, ON (Presenter) Nothing to Disclose Carolina A. Souza, MD, Ottawa, ON (Presenter) Consultant, Pfizer Inc; Consultant, Boehringer Ingelheim GmbH; Consultant, F. Hoffmann-La Roche Ltd; Speaker, Pfizer Inc; Speaker, Boehringer Ingelheim GmbH; Speaker, F. Hoffmann-La Roche Ltd Waleed M. Althobaity, MD, Ottawa, ON (Presenter) Nothing to Disclose Nicole Wake, MS, New York, NY (Presenter) In-kind support, Stratasys, Ltd Peter C. Liacouras, PhD, Bethesda, MD (Presenter) Nothing to Disclose Jonathan M. Morris, MD, Rochester, MN (Presenter) Nothing to Disclose Jane S. Matsumoto, MD, Rochester, MN (Presenter) Nothing to Disclose Elizabeth George, MD, Boston, MA (Presenter) Nothing to Disclose Satheesh Krishna, MD, Ottawa, ON (Presenter) Nothing to Disclose Carlos H. Torres, MD, FRCPC, Ottawa, ON (Presenter) Nothing to Disclose Olivier Miguel, BEng, Ottawa, ON (Presenter) Nothing to Disclose Shannon T. Lee, BEng, Ottawa, ON (Presenter) Nothing to Disclose Ekin P. Akyuz, BSc, Ottawa, ON (Presenter) Nothing to Disclose Andy Christensen, BS, Littleton, CO (Presenter) Consultant, 3D Systems, Inc; Consultant, Integrum AB; Board Member, Integrum AB Amy E. Alexander, BEng, Rochester, MN (Presenter) Nothing to Disclose Anji Tang, Boston, MA (Presenter) Nothing to Disclose

For information about this presentation, contact:

egeorge6@partners.org

catorres@toh.ca

nicole.wake@med.nyu.edu

csouza@toh.on.ca

LEARNING OBJECTIVES

1) To become familiar with the computational processing of cross-sectional images required to enable 3D printing using practical examples from diverse organ systems and pathologies. 2) To learn to use software to identify and extract anatomical parts from cross-sectional images using manual and semi-automated segmentation tools, including thresholding, region growing, and manual sculpting. 3) To gain exposure to techniques involving model manipulation, refinement, and addition of new elements to facilitate creation of customized models. 4) To learn the application of tools and techniques, including 'wrapping' and 'smoothing' to enable the accurate printing of the desired anatomy, pathology, and model customizations using Computer Aided Design (CAD) software. 5) To become exposed to Standard Tessellation Language (STL) file format and interfacing with a 3D printer.

ABSTRACT

3D printing is gaining traction and momentum in the clinical setting, with constantly evolving advances in printing and software technologies. Recently, the RSNA 3D Printing Special Interest Group has adopted a position statement reflecting the FDA recommendation for FDA-approved software to be used where 3D printed models used for clinical applications are created. This course covers the use of industry-standard FDA-cleared software for the design and fabrication of 3D printed models for a diverse range of pathologies. Musculoskeletal, body, neurological, and vascular systems and related pathologies will be segmented as part of this course and practically usable models will be created as part of this course to reflect the expanding applications of 3D printing. The purpose of this hands-on course is to convert a set of DICOM files into a 3D printed model through a series of simple steps. Some of the initial post-processing steps may be familiar to the radiologist, as they share common features with 3D visualization tools that are used for image post-processing tasks such as 3D volume rendering. However, some are relatively or completely new to radiologists, including the manipulation of files in Standard Tessellation Language (STL). It is the STL format that is read by the 3D printer and used to reproduce a part of the patient's anatomy by depositing material in a layer-by-layer fashion. This 90 minute session will begin with a DICOM file and review the commonest tools and techniques required to create a customized printable STL model. An extensive training manual will be provided before the meeting. It is highly recommended that participants review the training manual to optimize the experience at the workstation.

Honored Educators

Presenters or authors on this event have been recognized as RSNA Honored Educators for participating in multiple qualifying educational activities. Honored Educators are invested in furthering the profession of radiology by delivering high-quality educational content in their field of study. Learn how you can become an honored educator by visiting the website at:

https://www.rsna.org/Honored-Educator-Award/ Frank J. Rybicki III, MD, PhD - 2016 Honored EducatorCarlos H. Torres, MD, FRCPC - 2017 Honored Educator







RCB42

Getting Stuff Done: A Hands-on Technology Workshop to Enhance Personal Productivity (Hands-on)

Wednesday, Nov. 29 10:30AM - 12:00PM Room: S401CD

IN

AMA PRA Category 1 Credits ™: 1.50 ARRT Category A+ Credit: 1.75

Participants

Matthew B. Morgan, MD, Sandy, UT (*Presenter*) Consultant, Reed Elsevier Puneet Bhargava, MD, Seattle, WA (*Presenter*) Editor, Reed Elsevier Dushyant V. Sahani, MD, Boston, MA (*Presenter*) Research support, General Electric Company; Medical Advisory Board, Allena Pharmaceuticals, Inc

For information about this presentation, contact:

bhargp@uw.edu

dsahani@mgh.harvard.edu

mattmorganmd@gmail.com

LEARNING OBJECTIVES

Introduce the concept of "Getting Things Done". 2) Learn the concepts of Inbox Zero and other email management techniques.
 Using tools such as note-taking applications, citation and password managers.

Honored Educators

Presenters or authors on this event have been recognized as RSNA Honored Educators for participating in multiple qualifying educational activities. Honored Educators are invested in furthering the profession of radiology by delivering high-quality educational content in their field of study. Learn how you can become an honored educator by visiting the website at: https://www.rsna.org/Honored-Educator-Award/ Puneet Bhargava, MD - 2015 Honored EducatorDushyant V. Sahani, MD - 2012 Honored EducatorDushyant V. Sahani, MD - 2015 Honored EducatorDushyant V. Sahani, MD - 2017 Honored Educator







RCC42

Platforms and Infrastructures for Accelerated Discoveries in Machine Learning and Radiomics

Wednesday, Nov. 29 10:30AM - 12:00PM Room: S501ABC

IN

AMA PRA Category 1 Credits ™: 1.50 ARRT Category A+ Credit: 1.75

Participants

Luciano M. Prevedello, MD, MPH, Columbus, OH (Moderator) Nothing to Disclose

LEARNING OBJECTIVES

1) Understand the challenges involved in creating machine learning and radiomics experiments with standard clinical systems. 2) Review some of the tools that can bridge the gap between existing clinical systems and translational research in medical imaging. 3) Provide use case examples using open source tools.

ABSTRACT

Machine Learning and Radiomics promise to revolutionize the field of Radiology by allowing more quantification of medical images exposing previously "hidden" information within the imaging data. More recently, the combination machine learning techniques such as deep learning with radiomics, open new opportunities for researchers in this space. However, standard clinical systems are not suited for machine learning and radiomics experiments posing a significant challange for individuals together started. The pupose of this session is to review existing and custom developed infrastructures and platforms to bridge this gap.

Sub-Events

RCC42A Introduction

Participants

Luciano M. Prevedello, MD, MPH, Columbus, OH (Presenter) Nothing to Disclose

LEARNING OBJECTIVES

1) Understand some of the challenges and potential solutions to create machine learning and radiomics experiments using existing clinical systems.

RCC42B Integrating Deep Learning into Enterprise Medical Imaging

Participants

Barbaros S. Erdal, PhD, Columbus, OH (Presenter) Nothing to Disclose

LEARNING OBJECTIVES

1) Understand clinical data integration standards available to enable translational research in machine learning. 2) Gain introductory knowledge on enterprise data warehouses and understand how they can be used to augment machine learning systems. 3) Understand complexities associated with handling sensitive patient data.

RCC42C Open Source Tools for Rapidly Indexing, Searching, and Processing Image Data from the PACS

Participants

Joshy Cyriac, Basel, Switzerland (Presenter) Nothing to Disclose

LEARNING OBJECTIVES

1) Learn about existing open source tools for indexing and searching. 2) Learn how to build a pipeline of getting the image data from a PACS and reports from a RIS. 3) Learn how to use web tools to make the data easily accessible to the physicians and researchers.

RCC42D Machine Learning and Radiomics in Practice: Tools and Case Example

Participants Daniel L. Rubin, MD, MS, Stanford, CA (*Presenter*) Nothing to Disclose

For information about this presentation, contact:

daniel.l.rubin@stanford.edu

LEARNING OBJECTIVES

1) To understand the role of image annotations in capturing essential information about images in radiomics. 2) To learn about tools, platforms, infrastructures, standards, and machine learning methods that can leverage medical images to better understand disease and enable decision support. 3) To see example use cases of radiomics and machine learning methods for accelerating research and improving clinical practice.

Presenters or authors on this event have been recognized as RSNA Honored Educators for participating in multiple qualifying educational activities. Honored Educators are invested in furthering the profession of radiology by delivering high-quality educational content in their field of study. Learn how you can become an honored educator by visiting the website at: https://www.rsna.org/Honored-Educator-Award/ Daniel L. Rubin, MD, MS - 2012 Honored EducatorDaniel L. Rubin, MD, MS - 2013 Honored Educator



KSNA° 2017

103rd Scientific Assembly and Annual Meeting November 26 to December 1 McCormick Place, Chicago



SSK01

Breast Imaging (Intervention Path Correlation)

Wednesday, Nov. 29 10:30AM - 12:00PM Room: E450A

BR

AMA PRA Category 1 Credits ™: 1.50 ARRT Category A+ Credit: 1.75

FDA Discussions may include off-label uses.

Participants

Michael A. Cohen, MD, Atlanta, GA (Moderator) Nothing to Disclose

Jennifer A. Harvey, MD, Charlottesville, VA (*Moderator*) Research Grant, Hologic, Inc Stockholder, Hologic, Inc Research Grant, Volpara Health Technologies Limited Stockholder, Volpara Health Technologies Limited

Sub-Events

SSK01-01 Reflector-guided Breast Tumor Localization versus Wire Localization for Lumpectomies: A Comparison of Surgical Outcomes

Awards

Student Travel Stipend Award

Participants

Sejal N. Patel, MD, New York, NY (*Presenter*) Nothing to Disclose Victoria Mango, MD, New York, NY (*Abstract Co-Author*) Nothing to Disclose Priya Jadeja, MD, New York, NY (*Abstract Co-Author*) Nothing to Disclose Lauren C. Friedlander, MD, White Plains, NY (*Abstract Co-Author*) Nothing to Disclose Elise Desperito, MD, New York, NY (*Abstract Co-Author*) Nothing to Disclose Everick Ayala-Bustamante, MD, FRCPC, New York, NY (*Abstract Co-Author*) Nothing to Disclose Ralph T. Wynn, MD, New York, NY (*Abstract Co-Author*) Nothing to Disclose Sheldon Feldman, New York, NY (*Abstract Co-Author*) Nothing to Disclose Richard S. Ha, MD, New York, NY (*Abstract Co-Author*) Nothing to Disclose

For information about this presentation, contact:

rh2616@cumc.columbia.edu

PURPOSE

To compare surgical outcomes of SAVI SCOUT reflector localization (SSL) versus wire localization (WL).

METHOD AND MATERIALS

An IRB approved retrospective study was conducted. Inclusion criteria were single SSL or single WL with subsequent surgery performed by a single-surgeon (SF) to eliminate inter-operator variability. Exclusion criteria were bracketed lesions, multicentric disease and patients with neo-adjuvant chemotherapy. Tumors measuring greater than 2 cm were also excluded due to variability in neoadjuvant utilization and bracketing. Among 97 patients that underwent SSL and excised by SF from 7/2015 to 1/2017, 42 patients met the criteria. For the WL group, 42 consecutive patients were selected matched for age, size of the tumor and single WL performed from 1/2015 to 6/2015. Final surgical pathology was recorded including tumor size, histologic type, ER/PR/HER2/Ki67 status, margin status and re-excision rates. Positive and close margins were defined as tumor on ink and tumor <=1 mm from ink, respectively. Statistical analysis was performed (SPSS, v24).

RESULTS

100% (42/42) of SSL was performed prior to the day of the surgery (range 1-10 days, mean 2.8 days and median 2 days) and all were successfully excised. All patients (42/42) with WL underwent same day wire placement with successful excision. There was no significant difference in clinical-pathologic features between the SSL and WL groups (p>0.05). The mean distance [0.4 cm (range 0-1.9 cm)] between the target and SSL reflector on post localization mammogram was not statistically different than the mean distance [0.3 cm (range 0-1.3 cm)] between the target and the re-enforcement segment of the wire (p=0.45). No significant differences were present in surgical outcomes (p>0.05) including rates of re-excision (SSL, 7.1% vs. WL, 9.5%), margin positivity (SSL, 9.5% vs. WL, 7.1%), close margins (SSL 7.1% vs. WL, 11.9%) and specimen volume (SSL, 15.2 cm3 vs. WL, 16.3 cm3).

CONCLUSION

SSL is an acceptable alternative to WL with no significant differences in surgical outcomes with previously described advantages of SSL in scheduling efficiency and less patient discomfort.

CLINICAL RELEVANCE/APPLICATION

Reflector guided breast tumor localization can be done prior to the day of surgery and overcomes many of the limitations of wire localization with comparable surgical outcomes.

SSK01-02 Ultrasound Guided High Intensity Focused Ultrasound Ablation of Breast Fibroadenoma: A Pilot Study

Participants

Carrie M. Rochman, MD, Charlottesville, VA (*Presenter*) Research Consultant, Theraclion George Stukenborg, PhD, Charlottesville, VA (*Abstract Co-Author*) Nothing to Disclose Brandi T. Nicholson, MD, Charlottesville, VA (*Abstract Co-Author*) Nothing to Disclose Jonathan Nguyen, MD, Charlottesville, VA (*Abstract Co-Author*) Nothing to Disclose Jennifer A. Harvey, MD, Charlottesville, VA (*Abstract Co-Author*) Research Grant, Hologic, Inc Stockholder, Hologic, Inc Research Grant, Volpara Health Technologies Limited Stockholder, Volpara Health Technologies Limited David Brenin, MD, Charlottesville, VA (*Abstract Co-Author*) Research funded, Theraclion

For information about this presentation, contact:

cs3yd@virginia.edu

PURPOSE

Fibroadenoma is a common benign breast mass that can cause pain or an undesirable palpable lump. Current management includes observation, core needle biopsy, and/or surgical excision. This study evaluates the safety, feasibility, and efficacy of Ultrasound guided High Intensity Focused Ultrasound (USgHIFU) ablation for treatment of fibroadenomas. USgHIFU provides noninvasive thermal ablation of the fibroadenoma with real-time US guidance during treatment.

METHOD AND MATERIALS

Twenty women with a palpable breast fibroadenoma were enrolled in a single arm IRB and FDA approved clinical trial (IDE #G130252). Histologic confirmation of fibroadenoma on core needle biopsy was required. Patients underwent treatment utilizing the Echopulse device (Theraclion, France). All tumors had a minimum diameter >= 1 cm with volume between 0.3 cc and 10 cc. Volume calculation formula = length (mm) x width (mm) x height (mm) x π / (6 x 1000) in cc. During treatment, multiple sonications were delivered within the mass to achieve coagulative necrosis. Optimal energy delivered per sonication was established by determining the minimal setting found to produce a hyperechoic mark observed on real-time B-mode image. Energy settings were also influenced by patient tolerance. Change in tumor size, toxicity, cosmesis, and patient experience were obtained immediately after treatment and at 3, 6, and 12 months.

RESULTS

Twenty patients successfully completed therapy. Mean patient age was 35.2. Mean power/sonication = 38.3 watts. Mean number of sonications = 34.3. Pre-treatment mean tumor volume was 1.8 cc (SD 1.23, Range 0.57 - 5.7). Mean reduction in volume of the fibroadenoma at 12 months was -1.12 cc (65%), SD -0.61 cc (22%), Range -2.22 to -0.31 cc (98 to 25%), p-value < 0.0001. All adverse events (AE) were grade 1 or 2. Mild pain was the most common AE. No skin burns, damage to adjacent structures, or other major toxicities were observed. On clinical exam, mass was no longer palpable in 80% of patients at 12 months. Patient satisfaction was 4.4 on a scale of 1-5 (5 = most satisfied).

CONCLUSION

USgHIFU ablation is a safe, feasible and efficacious treatment option for breast fibroadenoma. Our results are limited by the small size of our study.

CLINICAL RELEVANCE/APPLICATION

Based on the results of this pilot study, there is evidence to support a larger multi-center clinical trial.

SSK01-03 Incidence of Anaplastic Large Cell Lymphoma in Women with Silicone Breast Implants at MR Imaging

Wednesday, Nov. 29 10:50AM - 11:00AM Room: E450A

Participants

Elizabeth J. Sutton, MD, New York, NY (*Presenter*) Nothing to Disclose Brittany Z. Dashevsky, MD,DPhil, Chicago, IL (*Abstract Co-Author*) Nothing to Disclose Elizabeth J. Watson, MD, MPH, Springfield, MA (*Abstract Co-Author*) Nothing to Disclose Blanca Bernard-Davila, MPH,MS, New York, NY (*Abstract Co-Author*) Nothing to Disclose Danny F. Martinez, BSC,MSc, New York, NY (*Abstract Co-Author*) Nothing to Disclose Elizabeth A. Morris, MD, New York, NY (*Abstract Co-Author*) Nothing to Disclose

PURPOSE

To assess the incidence of benign and malignant peri-implant fluid collections and/or masses at magnetic resonance (MR) imaging among women with a history of silicone implant reconstruction.

METHOD AND MATERIALS

The institutional review board approved this HIPAA-compliant retrospective study and waived informed consent. Women were identified who (a) underwent silicone implant oncoplastic and/or cosmetic surgery and (b) underwent postoperative implant-protocol MR imaging to evaluate for rupture between 2000 and 2014. Peri-implant fluid and/or masses were measured volumetrically. A benign peri-implant fluid collection was pathologically proven or defined as showing 1 year of imaging stability and/or no clinical evidence of disease. A malignant peri-implant fluid collection was pathologically proven. Incidence of peri-implant fluid collections and/or masses and positive predictive value (PPV) were calculated on a per-patient level by using proportions and exact 95% confidence intervals (CIs).

RESULTS

In total, 1070 women with silicone implants were included (median age, 56 years; range, 26-95 years). The median time between reconstructive surgery and first MR imaging examination was 48.96 months (range, 24-53months). Of the 1070 women, 263 had more then one imaging study. Of the 1070 women, 18 (1.7%) had a peri-implant fluid and/or mass; 16 (88.9%) had adequate follow-up; only 1 of the 16 peri-implant fluid collections was malignant implant associate anaplastic large cell lymphoma, with a PPV of 6.25% (95% CI: 0.003-0.0005). The median peri-implant fluid collection was 89 cc (range, 18-450 cc).

CONCLUSION

Peri-implant fluid collections and/or masses identified at silicon implant-protocol breast MR imaging are rarely seen 24 months after reconstructive surgery. Image guided fine-needle aspiration with flow cytometry may be warranted to evaluate for implant-associated lymphoma.

CLINICAL RELEVANCE/APPLICATION

Peri-implant fluid collections and/or masses on implant-protocol breast MRI are rarely seen 24 months after surgery and the diagnostic radiologist should consider recommending ultrasound guided fine needle aspiration.

SSK01-04 Feasibility and Accuracy of Digital Breast Tomosynthesis-Guided Vacuum Assisted Breast Biopsy (DBT-VAB) for Non-Calcified Targets

Wednesday, Nov. 29 11:00AM - 11:10AM Room: E450A

Participants

Gunjan M. Senapati, MD, Boston, MA (*Presenter*) Nothing to Disclose Sona A. Chikarmane, MD, Boston, MA (*Abstract Co-Author*) Nothing to Disclose Christine M. Denison, MD, Boston, MA (*Abstract Co-Author*) Nothing to Disclose Catherine S. Giess, MD, Wellesley, MA (*Abstract Co-Author*) Nothing to Disclose

For information about this presentation, contact:

gsenapati@bwh.harvard.edu

PURPOSE

To (1) determine feasibility and accuracy of DBT-VAB for non-calcified breast lesions without a sonographic correlate and (2) assess concordance of imaging and pathology findings.

METHOD AND MATERIALS

A HIPAA-compliant IRB waived retrospective review of our mammographic database between 12/11/15-8/31/16, identified 72 women with 73 non-calcified lesions on DBT who underwent attempted DBT-VAB with imaging available for review. Mammography and biopsy imaging were reviewed in consensus by three breast radiologists; imaging features and biopsy parameters were collected. Medical records were reviewed for imaging follow-up, patient characteristics, and histopathology.

RESULTS

The target lesion was sampled by DBT-VAB in 72 of 73 lesions. One biopsy was canceled because the target could not be identified at biopsy. Mean time to complete DBT-VAB was 17.3 minutes +/- 5. No major complications were reported. Findings included: 3 focal asymmetries (FA) (4%), 7 asymmetries (A) (10%), 21 masses (M) (29%) and 41 architectural distortions (AD) (57%). DBT-VAB histopathology showed invasive malignancy in 15 (21%) of 72 lesions: 1/3 FA (33%), 7/41 AD (17%), 7/21 M (33%). ADH was found in 2 (3%) of 72 lesions (both masses). 7/7 A, 2/3 FA, and 11/21 M showed benign core pathology concordant with imaging. 1/21 M had benign discordant core pathology and was malignant on excision. 34/41 (83%) AD were benign on core pathology, of which 14 (41%) were complex sclerosing lesions (CSL); 6 were excised with no upgrades. Ten of 34 (29%) AD were benign and considered concordant with imaging. The remaining 10 of 34 (29%) were benign discordant pathology at core biopsy and surgically excised; 4/10 (40%) showed CSL on final pathology. Therefore, a total of 11/72 (15%) cases were considered discordant on VAB with 1/11 (9%) malignancies on final pathology.

CONCLUSION

DBT-VAB is a quick and feasible biopsy method for targeting non-calcified mammographic lesions without a sonographic correlate. The 21% malignancy rate reaffirms biopsy is necessary for suspicious mammographic lesions occult on ultrasound. Meticulous radiology-pathology correlation is required in interpretation of DBT-VAB results, with surgical excision of discordant cases.

CLINICAL RELEVANCE/APPLICATION

DBT-VAB is a feasible biopsy method for non-calcified lesions, however, careful radiology-pathology correlation is necessary, with a low threshold to surgically excise any potentially discordant cases.

SSK01-05 Optical Coherence Tomography (OCT): A Novel Imaging Method for Ex-Vivo Breast Specimens-A Reader Feasibility Study

Wednesday, Nov. 29 11:10AM - 11:20AM Room: E450A

Participants

Victoria Mango, MD, New York, NY (*Presenter*) Nothing to Disclose Lauren C. Friedlander, MD, White Plains, NY (*Abstract Co-Author*) Nothing to Disclose Hanina Hibshoosh, MD, New York, NY (*Abstract Co-Author*) Nothing to Disclose Soojin Ahn, New York, NY (*Abstract Co-Author*) Nothing to Disclose Margaret Akens, Toronto, ON (*Abstract Co-Author*) Nothing to Disclose Hank Schmidt, MD, New York, NY (*Abstract Co-Author*) Nothing to Disclose Sheldon Feldman, New York, NY (*Abstract Co-Author*) Nothing to Disclose Maryann Fitzmaurice, MD, Toronto, ON (*Abstract Co-Author*) Nothing to Disclose Christine Hendon, New York, NY (*Abstract Co-Author*) Nothing to Disclose Brian C. Wilson, Toronto, ON (*Abstract Co-Author*) Nothing to Disclose Richard S. Ha, MD, New York, NY (*Abstract Co-Author*) Nothing to Disclose

For information about this presentation, contact:

mangov@mskcc.org

PURPOSE

To assess subspecialty reader sensitivity, specificity and overall accuracy to distinguish non-suspicious versus suspicious areas of

ex-vivo breast tissue using OCT images (a near-infrared based imaging technique) with histology correlation.

METHOD AND MATERIALS

This IRB exempt, HIPAA compliant study was performed on 63 surgically excised breast specimens from 35 female patients. OCT images of the specimens were performed providing micrometer resolution with tissue visualization 1-2 mm subsurface. 40 volumetric image data sets were created from the specimens for reader interpretation (16 malignant cases (8 invasive ductal carcinoma, 4 DCIS, 4 mixed IDC/DCIS) and 24 benign). 3 breast imaging fellowship trained radiologists, 2 pathologists, 2 breast surgeons and 1 non-clinical reader were first trained to interpret OCT images and then read 40 OCT data sets blinded to clinical data and corresponding histology slides. Readers were asked to distinguish non-suspicious from suspicious findings.

RESULTS

Sensitivity, specificity, PPV, NPV, and the AUC for each reader was calculated as well as averages by subspecialty. Histology was the reference standard. The overall average reader sensitivity, specificity and accuracy for all 8 readers was 80%, 87% and 0.87, respectively, Radiologists demonstrated the highest average among the disciplines, 85%, 93% and 0.94, followed by Pathologists, 79%, 90%, and 0.84, and Surgeons, 76%, 84%, and 0.82 respectively.

CONCLUSION

Multidisciplinary readers are able to distinguish suspicious from non-suspicious OCT imaging findings in ex-vivo breast tissue as confirmed by histology. These results support the potential of OCT as a real time intra-operative tool for imaging ex-vivo breast tissue. Future studies are needed to evaluate the technology in an intraoperative setting.

CLINICAL RELEVANCE/APPLICATION

Real time OCT images of ex-vivo breast tissue could be viewed intraoperatively by the surgeon to assess for suspicious tissue at the edge/margin of a specimen. Images could be exported for radiologist consultation.

SSK01-06 Use of Artificial Intelligence to Reduce Breast Biopsies

Wednesday, Nov. 29 11:20AM - 11:30AM Room: E450A

Participants

Alyssa T. Watanabe, MD, Manhattan Beach, CA (*Presenter*) Consultant, CureMetrix, Inc Rebecca Rakow-Penner, MD, PhD, San Diego, CA (*Abstract Co-Author*) Nothing to Disclose Hoanh X. Vu, PhD, San Diego, CA (*Abstract Co-Author*) Employee, CureMetrix, Inc William Daughton, PhD, La Jolla, CA (*Abstract Co-Author*) Employee, CureMetrix, Inc Eric Weise, San Diego, CA (*Abstract Co-Author*) Researcher, CureMetrix, Inc William G. Bradley JR, MD, PhD, La Jolla, CA (*Abstract Co-Author*) Officer, CureMetrix, nc

PURPOSE

Almost 2% of screening mammograms result in biopsy, and approximately 70% of these biopsies are benign. Decreasing the number of unnecessary biopsies would be cost effective and decrease patient anxiety about breast cancer screening. We evaluated a quantitative CAD algorithm that differentiates benign and malignant calcifications and compared these results to those of experienced radiologists in selecting cases for biopsy. The algorithm is based on a combined use of artificial intelligence (deep learning) and physics based mathematical classifiers that makes predictions of suspiciousness through quantitative scoring.

METHOD AND MATERIALS

In this IRB approved study, we performed a comparative analysis on patients' screening and diagnostic 2D mammograms where tissue was sent to biopsy based on suspicious calcifications detected by MQSA certified breast radiologists. 10,500 consecutive cases from 3 different institutions were reviewed. These images were evaluated with a quantitative CAD (qCAD) that employs deep learning (DL), a form of artificial intelligence (AI) to make predictions of suspiciousness of mammographic findings. These predictions were compared to the expert radiologists' reads. The DL embedded in the algorithm is an analytical function determined by the training datasets that mathematically define both malignant and benign calcifications.

RESULTS

Of the 391 cases sent to biopsy, 302 cases were benign and 89 malignant (including DCIS). The algorithm detected 100% of confirmed cancer cases. If biopsy recommendations had been based on the algorithm up to 56% of biopsies could have been avoided.

CONCLUSION

This CAD algorithm trained with AI can potentially reduce the number of unnecessary biopsies based on suspicious calcifications by up to 56%. The qCAD was more accurate than the radiologists at classifying breast calcifications on mammography.

CLINICAL RELEVANCE/APPLICATION

The use of artificial intelligence in mammography may be useful in reducing false positive breast biopsies and to enhance more accurate detection of breast malignancies. This is likely to lead to health savings costs as well as eliminate pain and distress for many patients.

SSK01-07 Flat Epithelial Atypia Upgrade Rate

Wednesday, Nov. 29 11:30AM - 11:40AM Room: E450A

Participants

Selina Suleman, MPH,BSC, Vancouver, BC (*Abstract Co-Author*) Nothing to Disclose Marie Josee Cloutier, MD,FRCR, Vancouver, BC (*Presenter*) Nothing to Disclose Paula B. Gordon, MD, Vancouver, BC (*Abstract Co-Author*) Stockholder, OncoGenex Pharmaceuticals, Inc ; Scientific Advisory Board, Real Imaging Ltd; ;

PURPOSE

Flat epithelial atypia (FEA) is a controversial breast lesion whose optimal management with surgical excision versus imaging followup is unknown. Widespread implementation of screening mammography programs has resulted in an increased detection of FEA. This study aims to determine the likelihood of upgrade to ductal carcinoma in situ (DCIS) or invasive carcinoma in individuals diagnosed with FEA at stereotactic needle biopsy. In addition, the relationship between family history of breast cancer and likelihood of upgrade is explored.

METHOD AND MATERIALS

Stereotactic biopsies were performed primarily for the assessment of microcalcifications seen on mammography. Initially these were done with 12G core needles, but vacuum devices (10 and 9G) are now the standard. FEA diagnoses were correlated with subsequent excisional biopsy pathology results or imaging follow-up. Patients were included only if there was no concomitant diagnosis of other high-risk lesion, papillary lesion, in-situ or invasive carcinoma. Surgical pathology or follow-up imaging was obtained for 623 patients. Upgraded cases were defined as diagnosis of DCIS or invasive carcinoma at surgery. Additionally, medical charts of women diagnosed with FEA were reviewed for family history of breast cancer.

RESULTS

An upgrade rate of 1.8% (11 lesions in 623 patients; 95% CI, 1.0%-3.2%) is reported. The remaining samples (612/623) had a surgical diagnosis of FEA or ADH, lobular carcinoma in situ, a benign finding with no atypia, or stable follow-up imaging. There is no significant association between family history of breast cancer and upgrade in preliminary results (OR 1.7; 95% CI, 0.39-6.61).

CONCLUSION

The upgrade rate of FEA diagnosed at CNB or VAB at our institution was 1.8%, which is at the low end of the range reported in the literature. Each facility should audit their upgrade rate before implementing a change in practice pattern.

CLINICAL RELEVANCE/APPLICATION

These results indicate that it is reasonable at our institution to avoid surgery in favor of short-term imaging follow-up for the majority, especially when there is no family history of breast cancer.

SSK01-08 Management of Lobular Neoplasia (Atypical Lobular Hyperplasia and Lobular Carcinoma in Situ) on Core Needle Biopsy Performed for Calcifications Using Precise Radiologic-Pathologic Correlation

Wednesday, Nov. 29 11:40AM - 11:50AM Room: E450A

Participants

Jean M. Kunjummen, DO, Atlanta, GA (Presenter) Nothing to Disclose

Karina Rodriguez, MD, Atlanta, GA (Abstract Co-Author) Nothing to Disclose

Mary S. Newell, MD, Atlanta, GA (*Abstract Co-Author*) Stockholder, Kimberly-Clark Corporation ; Stockholder, E. I. du Pont de Nemours & Company ; Stockholder, Bristol-Myers Squibb Company; Stockholder, Merck & Co, Inc; Stockholder, Johnson & Johnson ; Stockholder, Eli Lilly and Company

Michael A. Cohen, MD, Atlanta, GA (Abstract Co-Author) Nothing to Disclose

For information about this presentation, contact:

jean.kunjummen@emory.edu

PURPOSE

To determine if there is a difference in upgrade rate of calcified vs incidental lobular neoplasia (LN) found on core biopsy performed for evaluation of suspicious calcifications.

METHOD AND MATERIALS

The study (approved by our institutional review board) included consecutive patients who underwent core needle biopsy from December, 2009 through December, 2016 directed at suspicious calcifications with results showing LN as the highest-risk lesion. Patients with concurrent atypical ductal hyperplasia, flat epithelial atypia, radial scar, papillary lesion, phyllodes tumor, ductal carcinoma in situ (DCIS), invasive ductal carcinoma (IDC), or invasive lobular carcinoma (ILC) on core were excluded. An upgrade was defined as surgical excisional pathology showing DCIS, IDC or ILC.

RESULTS

Three hundred fifty patients underwent successful core needle breast biopsy showing LN during the study period. Of these, 80 patients had LN as the highest-risk lesion. In sixty-two patients (78%), LN was an incidental histologic finding, and the targeted calcifications were associated with variety of benign concordant entities. In 17 patients (21%), calcifications were an intrinsic part of the LN lesion. Fifteen of those 17 patients (88%) underwent surgical excision, with an upgrade rate of 27% (4/15). Of the 62 patients who had incidental, non-calcified LN, 36 underwent surgical excision, with an upgrade rate of 2.7% (1/36). One patient with incidental LN was felt to have discordant rad-path results; excision showed invasive cancer. Of those with long term follow-up rather than excision, none have developed cancer (avg. length of follow-up =28 months).

CONCLUSION

Careful radiologic-pathologic correlation is needed to determine the appropriate management of lobular neoplasia. Women with core needle biopsy for calcifications that show incidental, non-calcified LN have small rate of upgrade and may not require excisional biopsy. However, surgical excision should be offered to women who have LN associated with calcifications.

CLINICAL RELEVANCE/APPLICATION

Management of LN remains controversial with recommendations ranging from imaging follow-up to mandatory surgical excision in all cases. Our data supports close radiologic-pathologic correlation and suggests that the calcified LN in core biopsy specimens has a greater likelihood of upgrade to cancer than incidental, non-calcified LN.

SSK01-09 Utility of Ultrasonography (US) and US-guided Fine-Needle Aspiration Biopsy for Axillary Staging in Early Breast Cancer: Is the US Diagnosis for Metastatic Lymph Nodes Useful?

Participants Hye Shin Ahn, MD, Seoul, Korea, Republic Of (*Presenter*) Nothing to Disclose Sun Mi Kim, MD, PhD, Seongnam-Si, Korea, Republic Of (*Abstract Co-Author*) Nothing to Disclose Mijung Jang, Seongnam, Korea, Republic Of (*Abstract Co-Author*) Nothing to Disclose Bo La Yun, MD, Seongnam, Korea, Republic Of (*Abstract Co-Author*) Nothing to Disclose

PURPOSE

To evaluate the accuracy of ultrasonography (US) and US-guided fine-needle aspiration biopsy (FNAB) for diagnosing metastatic invasion of the axilla in early breast carcinoma patients and to determine the usefulness of the US diagnosis for axillary staging.

METHOD AND MATERIALS

We retrospectively reviewed data on 2731 patients who were diagnosed as early breast cancer less than T2 stage from January 2006 to December 2015. All included patients underwent preoperative axillary US for axillary staging and US-guided FNAB was performed if lymph nodes showed any suspicious findings as follows: even or uneven cortical thickening, compressed fatty hilum, hypoechoic mass with loss of hilum. US and FNAB findings were compared using sentinel lymph node biopsy (SLNB) and axillary lymph node dissection (ALND) data.

RESULTS

Of 2731 patients, 446 (16.3%) showed suspicious nodes on US and underwent US-guided FNAB. Of these 446 patients, 202 (45.3%) showed positive findings, 244 (54.7%) showed negative findings on FNAB. The sensitivity, specificity, positive predictive value, and negative predictive value of US for pathologic proven metastatic lymph node were 30.4%, 88.2%, 45.3%, and 79.7%, respectively. The sensitivity, specificity, positive predictive value, and negative predictive value of US-guided FNAB were 62.4%, 93%, 88.1%, and 74.9%, respectively.

CONCLUSION

Axillary US and US-guided FNAB in early breast cancer showed relatively low rate of sensitivity. If axillary lymph nodes with suspicious US feature has been found in early breast cancer patients, axillary metastases will not be likely compared with the breast cancer patients with high tumor stage.

CLINICAL RELEVANCE/APPLICATION

In early breast cancer patients, the usefulness of axillary US for axillary staging could be lower than advanced breast cancer patients.







SSK02

Science Session with Keynote: Breast Imaging (Deep Learning, Quantitative Imaging and Big Data)

Wednesday, Nov. 29 10:30AM - 12:00PM Room: E451A



AMA PRA Category 1 Credits ™: 1.50 ARRT Category A+ Credit: 1.75

FDA Discussions may include off-label uses.

Participants

Maryellen L. Giger, PhD, Chicago, IL (*Moderator*) Stockholder, Hologic, Inc; Stockholder, Quantitative Insights, Inc; Shareholder, QView Medical, Inc; Co-founder, Quantitative Insights, Inc; Royalties, Hologic, Inc; Royalties, General Electric Company; Royalties, MEDIAN Technologies; Royalties, Riverain Technologies, LLC; Royalties, Mitsubishi Corporation; Royalties, Toshiba Medical Systems Corporation

Despina Kontos, PhD, Philadelphia, PA (Moderator) Nothing to Disclose

Sub-Events

SSK02-01 Breast Keynote Speaker: Overview of Deep Learning and Breast Imaging

Participants

Maryellen L. Giger, PhD, Chicago, IL (*Presenter*) Stockholder, Hologic, Inc; Stockholder, Quantitative Insights, Inc; Shareholder, QView Medical, Inc; Co-founder, Quantitative Insights, Inc; Royalties, Hologic, Inc; Royalties, General Electric Company; Royalties, MEDIAN Technologies; Royalties, Riverain Technologies, LLC; Royalties, Mitsubishi Corporation; Royalties, Toshiba Medical Systems Corporation

SSK02-02 Detecting Breast Cancer in Mammography: How Close Are Computers to Radiologists?

Wednesday, Nov. 29 10:40AM - 10:50AM Room: E451A

Participants

Alejandro Rodriguez-Ruiz, Nijmegen, Netherlands (Presenter) Nothing to Disclose

Albert Gubern-Merida, PhD, Nijmegen, Netherlands (*Abstract Co-Author*) Nothing to Disclose

Mechli W. Imhof-Tas, MD, PhD, Doorn, Netherlands (Abstract Co-Author) Nothing to Disclose

Susanne Lardenoije, Nijmegen, Netherlands (*Abstract Co-Author*) Nothing to Disclose

Alexander Wanders, MMedSc, Voorhout, Netherlands (Abstract Co-Author) Nothing to Disclose

Ingvar T. Andersson, MD, PhD, Malmo, Sweden (Abstract Co-Author) Nothing to Disclose

Sophia Zackrisson, Malmo, Sweden (*Abstract Co-Author*) Speakers fees and travel support from Astra Zeneca and Siemens Healthineers

Kristina Lang, MD,PhD, Malmo, Sweden (*Abstract Co-Author*) Travel support, Siemens AG; Speaker, Siemens AG Magnus Dustler, Malmo, Sweden (*Abstract Co-Author*) Nothing to Disclose

Nico Karssemeijer, PhD, Nijmegen, Netherlands (Abstract Co-Author) Director and Shareholder, ScreenPoint Medical BV;

Shareholder, Volpara Health Technologies Limited; Consultant, QView Medical, Inc; Shareholder, QView Medical, Inc; Ritse M. Mann, MD, PhD, Nijmegen, Netherlands (*Abstract Co-Author*) Research agreement, Siemens AG; Research agreement, Seno Medical Instruments, Inc; Research agreement, Identification Solutions Inc; Research agreement, Micrima Limited; Scientific Advisor, ScreenPoint Medical BV

Ioannis Sechopoulos, PhD, Atlanta, GA (*Abstract Co-Author*) Research Grant, Siemens AG; Research Grant, Toshiba Medical Systems Corporation; Speakers Bureau, Siemens AG; Scientific Advisory Board, Fischer Medical

For information about this presentation, contact:

alejandro.rodriguezruiz@radboudumc.nl

PURPOSE

To compare the performance of a commercial deep learning computer detection system to radiologists' performance in detecting breast cancer on digital mammography (DM) images.

METHOD AND MATERIALS

Six radiologists (22 years median experience with DM, range 3-44) retrospectively reviewed 155 unilateral two-view DM exams (73 malignant and 82 negatives, of which 42 were biopsy-proven benign lesions, and 40 normal cases defined as BIRADS 1 or 2 with one year follow-up). DM exams were scored on mammography displays using standard reading conditions. For all lesions, a level of suspiciousness score was given (0 - no lesion, 1 definitely benign - 10 definitely malignant). The highest score was used as the overall exam score. A commercially available computer system based on deep learning technology (Transpara 1.2.0, ScreenPoint Medical, Nijmegen, the Netherlands) was applied to the same dataset. This multi-vendor system automatically identifies soft-tissue and calcification lesions and combines the findings of all available views into a single cancer suspiciousness score (same scale as the readers, 0-10). Analysis was performed using Dorfman-Berbaum-Metz Multiple-Reader Multiple-Case mixed model analysis of variance, both including and excluding benign lesions in the negative class. Receiver operating characteristics area under the curve (AUC) and its 95% confidence intervals were used for comparison.

RESULTS

Averaged across radiologists ALIC was 0.83 (CI+ 0.76-0.90) when evaluating the whole dataset, while for the deep learning system

the AUC was 0.79 (CI: 0.72-0.86) (p=0.378). The system did not perform statistically different than any of the readers (reader AUC range: 0.77-0.87, p>0.064). When benign lesions were excluded from the analysis, AUC was 0.90 (CI: 0.85-0.96) and 0.88 (CI: 0.84-0.94) for the radiologists and the computer system (p=0.576), respectively.

CONCLUSION

For the task of detecting breast cancer in DM, the performance of a deep learning computer system is not statistically different from the average performance of 6 radiologists, even though the AUC for radiologists was still slightly higher.

CLINICAL RELEVANCE/APPLICATION

Computer systems with similar clinical performance as radiologists could be used, for instance, as double reading, to automatically discriminate normal cases, or to shorten reading time.

SSK02-03 Differentiating Between Malignant and Benign Masses at Breast US: Improving Radiologists' Diagnostic Performances Using Computer-Aided Diagnosis System Based on Deep Learning Algorithm

Wednesday, Nov. 29 10:50AM - 11:00AM Room: E451A

Participants

Ji Soo Choi, MD, PhD, Seoul, Korea, Republic Of (*Abstract Co-Author*) Nothing to Disclose Boo-Kyung Han, MD, PhD, Seoul, Korea, Republic Of (*Abstract Co-Author*) Nothing to Disclose Eun Sook Ko, MD, Seoul, Korea, Republic Of (*Abstract Co-Author*) Nothing to Disclose Eun Young Ko, MD, PhD, Seoul, Korea, Republic Of (*Abstract Co-Author*) Nothing to Disclose Sohee Song, Seoul, Korea, Republic Of (*Abstract Co-Author*) Nothing to Disclose Mi-Ri Kwon, Seoul, Korea, Republic Of (*Abstract Co-Author*) Nothing to Disclose Jooyeon Cho, Seoul, Korea, Republic Of (*Presenter*) Nothing to Disclose

PURPOSE

To compare performances of computer-aided diagnosis (CAD) system based on deep learning algorithm and radiologists in differentiating between malignant and benign masses at breast ultrasound (US) and to determine whether CAD system could improve the radiologists' performances

METHOD AND MATERIALS

This prospective study was conducted with institutional review board approval. B-mode US images were obtained for 253 breast masses (173 benign, 80 malignant) in 226 concesutive women. US findings of the breast masses were retrospectively analyzed by CAD system (S-DetectTM) and four radiologists. In predicting malignancy, CAD system results were dichotomized (possibly benign vs. possibly malignant). The radiologists independently assessed the Breast Imaging Reporting and Data System (BI-RADS) final assessments for two data sets: US alone, and US with CAD system results. Final assessments of the radiologists were categorized into positive (category 4a or higher) and negative (category 3 or lower) for each data set. Diagnostic performances of CAD system and the radiologists for two data sets were compared.

RESULTS

CAD system showed significantly higher values in accuracy, specificity, and positive predictive value (PPV) (P<0.01), and similar sensitivity (P>0.05) compared to those of the three radiologists, but the differences in the corresponding values between CAD system and the one radiologist were not significant. When CAD result was added to US, the three radiologists showed significant improvement in accuracy, specificity, and PPV, without significant change in sensitivity and negative predictive value, but the one radiologist showed no significant change in diagnostic values.

CONCLUSION

Diagnostic performance of CAD system was higher than or comparable to those of raiologists in differentiating between malignant and benign masses at breast US. Using CAD system may improve the accuracy, specificity, and PPV of the raiologists without loss in sensitivity.

CLINICAL RELEVANCE/APPLICATION

CAD system based on deep learning algorithm can improve the radiologists' diagnostic performances in differentiating between malignant and benign masses at breast US.

SSK02-04 Advanced Data-Driven Imaging Biomarker for Breast Cancer Screening in Mammography

Wednesday, Nov. 29 11:00AM - 11:10AM Room: E451A

Participants

Eun-Kyung Kim, Seoul, Korea, Republic Of (*Presenter*) Nothing to Disclose Hyo-Eun Kim, Seoul, Korea, Republic Of (*Abstract Co-Author*) Employee, Lunit Inc Hak Hee Kim, MD, Seoul, Korea, Republic Of (*Abstract Co-Author*) Nothing to Disclose Boo-Kyung Han, MD, PhD, Seoul, Korea, Republic Of (*Abstract Co-Author*) Nothing to Disclose Vivian Y. Park, MD, Seoul, Korea, Republic Of (*Abstract Co-Author*) Nothing to Disclose Hee Jung Shin, MD, Seoul, Korea, Republic Of (*Abstract Co-Author*) Nothing to Disclose Ji Soo Choi, MD, PhD, Seoul, Korea, Republic Of (*Abstract Co-Author*) Nothing to Disclose Woo Hyun Shim, Seoul, Korea, Republic Of (*Abstract Co-Author*) Nothing to Disclose Beomseok Suh, Seoul, Korea, Republic Of (*Abstract Co-Author*) Nothing to Disclose

For information about this presentation, contact:

ekkim@yuhs.ac

PURPOSE

Previously, we demonstrated data-driven imaging biomarker in mammography (DIB-MG; an imaging biomarker derived from largescale mammography data by using deep learning technology) for classification of cancer and normal. Now, we assess the feasibility of DIB-MG including cancer, normal, and benign exams and evaluate its potential for detection of malignant lesion.

METHOD AND MATERIALS

We collected 37,185 (set-A) and 7,101 (set-B) exams of 4 view digital mammograms from two institutions. For cross-institution validation, we used set-A for training DIB-MG and set-B for evaluating the trained model. Set-A consists of 1,019 cancer, 17,346 normal, and 18,820 benign exams, and set-B consists of 1,987 cancer, 2,982 normal, and 2,132 benign exams. DIB-MG is trained based on deep convolutional neural networks (CNNs). Entire training process is divided into two stages; multi-scale patch-based pre-training followed by image-based fine-tuning with semi-supervised segmentation. Total 128,960 malignant, 252,395 benign, and 200,000 normal patches were densely extracted from four scales of original images. Malignant and benign lesions were finely annotated by radiologists for patch extraction. In the image-based fine-tuning, parameters of initial convolutional layers were fixed and the rest convolutional layers were tuned based on all of 37,185 exams. During training, cancer probability of each exam is compared with the ground-truth diagnosis result, and the error between the prediction and the ground-truth label is propagated backward to optimize parameters in all layers except for the fixed one. Trained DIB-MG predicts the cancer probability of the input exam as well as a DIB map which includes the most probable locations of abnormalities.

RESULTS

AUC was 0.814. Sensitivity (specificity) according to different thresholds for the test set is: 0.764 (0.692), 0.621 (0.924), 0.549 (0.957) with respect to the thresholds 0.1, 0.3, 0.5. An exemplary DIB map is described in Fig.1.

CONCLUSION

This research showed the potential of DIB-MG as a screening tool for breast cancer through the cross-institution evaluation. Further clinical study of DIB-MG is needed for using it as a reliable screening tool for breast cancer.

CLINICAL RELEVANCE/APPLICATION

With further clinical studies, DIB-MG can be practically used as a second-reader in order to help radiologists diagnosing breast cancer and detecting malignant lesions.

SSK02-05 A Predictive Deep Learning Model to Determine the Presence of Breast Cancer on Screening and Diagnostic Mammograms

Wednesday, Nov. 29 11:10AM - 11:20AM Room: E451A

Awards

Student Travel Stipend Award

Participants

Hari Trivedi, MD, San Francisco, CA (*Presenter*) Nothing to Disclose Dmytro Lituiev, San Francisco, CA (*Abstract Co-Author*) Nothing to Disclose April Liang, San Francisco, CA (*Abstract Co-Author*) Nothing to Disclose Michael Kawczynski, San Francisco, CA (*Abstract Co-Author*) Nothing to Disclose Roy Harnish, San Francisco, CA (*Abstract Co-Author*) Nothing to Disclose Yunn-Yi Chen, MD, San Francisco, CA (*Abstract Co-Author*) Nothing to Disclose Karla Kerlikowske, MD, San Francisco, CA (*Abstract Co-Author*) Nothing to Disclose John A. Shepherd, PhD, San Francisco, CA (*Abstract Co-Author*) Nothing to Disclose Bonnie N. Joe, MD, PhD, San Francisco, CA (*Abstract Co-Author*) Nothing to Disclose Benjamin L. Franc, MD, Sacramento, CA (*Abstract Co-Author*) Nothing to Disclose Dexter Hadley, San Francisco, CA (*Abstract Co-Author*) Nothing to Disclose

For information about this presentation, contact:

hari.trivedi@ucsf.edu

PURPOSE

Nearly one in eight U.S. women will develop breast cancer in their lifetimes. Mammography is a safe and effective screening tool; however, it suffers from high recall and biopsy rates, which are costly and traumatic to the patient. The use of deep learning has the potential to improve accuracy, thereby decreasing both the recall and biopsy rate.

METHOD AND MATERIALS

136,253 mammographic accessions corresponding to 755,945 DICOM files were extracted from the radiology picture archiving and communication system (PACS). DICOMs were filtered to include only screening and diagnostic studies and standard, non-magnification views, which resulted in 127,329 accessions corresponding to 660,989 DICOMs. 33,342 pathology reports and 93,727 BI-RADS scores were then extracted from their respective databases for ground truth labeling of DICOM images. Regular expression technique with manual validation was used to assign final pathologic diagnosis to a pilot subset of DICOM files based upon positive pathology results within one year. This was combined with BI-RADS 1, 2, and 6 cases, resulting in 4,738 cases labeled as cancer and 354,837 cases labeled as non-cancer. A deep learning model based on the Inception v3 architecture with pre-trained weights from the Imagenet dataset using the Keras API with TensorFlow backend was fine-tuned on 2,569 cancer and 5,105 non-cancer images at 299 x 299 resolution.

RESULTS

The model achieved an area under the receiver operating characteristic curve (AUC) of 0.83 when predicting on an internal test set of 200 cancer and 200 non-cancer images. Interestingly, on a subset of 50 positive and 50 negative BIRADS-2 cases, the model also achieved an AUC of 0.83, surpassing human readers. When tested on an external validation set of 2000 images with composition reflecting a more clinically accurate prevalence of cancer to non-cancer, i.e., 1% cancer and 99% non-cancer, the model achieved an AUC of 0.96.

CONCLUSION

Deep learning may be an effective tool for detecting breast cancer in mammograms, however training and validation with larger data sets is required. Results may also improve with higher resolution, however this requires modification of existing models and

increased hardware capacity.

CLINICAL RELEVANCE/APPLICATION

Deep learning in mammography has the potential to detect breast cancer using features not yet recognized by human readers, thereby improving accuracy and decreasing false positives.

SSK02-06 Automated Breast Cancer Risk Assessment from FFDM Images

Wednesday, Nov. 29 11:20AM - 11:30AM Room: E451A

Participants

Assaf Hoogi, BMBCh, BMBCh, Palo Alto, CA (*Abstract Co-Author*) Nothing to Disclose Anika Cheerla, Palo Alto, CA (*Abstract Co-Author*) Nothing to Disclose Joe Rothstein, New York, NY (*Abstract Co-Author*) Nothing to Disclose Jan Liphard, Palo Alto, CA (*Abstract Co-Author*) Nothing to Disclose Weiva Sieh, MD,PhD, Stanford, CA (*Abstract Co-Author*) Nothing to Disclose Daniel L. Rubin, MD, MS, Stanford, CA (*Presenter*) Nothing to Disclose Jafi A. Lipson, MD, Stanford, CA (*Abstract Co-Author*) Nothing to Disclose

For information about this presentation, contact:

ahoogi@stanford.edu

PURPOSE

To automatically evaluate future breast cancer risk by computerized analysis of full-field digital mammography (FFDM) images.

METHOD AND MATERIALS

This IRB-approved study included a total of 407 GE FFDM images (12-bit dynamic range). Cases comprised 131 women who underwent screening mammography and were subsequently diagnosed with breast cancer within an average of 2.8±2.4 years. Controls comprised 276 women who did not develop breast cancer over up to 10 years of follow-up screening mammography. We extracted 99 grayscale and texture features such as Haralick and wavelet features, from patches in the CC view of the unaffected breast for cases and LCC view for controls. We applied a Bag of Visual Words method to build the histogram of image features for each breast, and used a random forest classifier to predict case or control status based on the histograms, age, race/ethnicity, menopausal status, parity and body mass index. We evaluated performance using ten-fold cross validation and computed the Area Under the ROC Curve (AUC).

RESULTS

Our method showed better discrimination between cases and controls (AUC, 0.84; 95% CI, 0.81-0.85), than other common techniques such as BIRADS (0.66; 0.62-0.74), Cumulus (0.64; 0.6-0.68), Libra (0.62; 0.55-0.65) and Volpara (0.62; 0.56-0.67). In contrast to these common methods that quantify only the absolute or percentage of dense tissue, we found that the additional image features extracted from non-dense tissue improved the AUC by 0.03 (p<0.05).

CONCLUSION

Our method shows promising results for risk evaluation of future breast cancer. Our novel technique is significantly better than using only area/volume/percentage of breast density, as is done by state of the art methods. Importantly, informative image features are located in both dense and non-dense breast regions.

CLINICAL RELEVANCE/APPLICATION

Our tool can automatically deliver a novel, validated imaging-based risk score to improve the accuracy and reliability of breast cancer risk prediction directly from digital screening mammography.

SSK02-07 Standard-Dose versus Synthetic Digital Mammograms: Are There Differences in Automated Measurements of Breast Parenchymal Patterns?

Wednesday, Nov. 29 11:30AM - 11:40AM Room: E451A

Participants

Aimilia Gastounioti, Philadelphia, PA (*Presenter*) Nothing to Disclose Meng-Kang Hsieh, Philadelphia, PA (*Abstract Co-Author*) Nothing to Disclose Lauren Pantalone, BS, Philadelphia, PA (*Abstract Co-Author*) Nothing to Disclose Eric Cohen, Philadelphia, PA (*Abstract Co-Author*) Nothing to Disclose Emily F. Conant, MD, Philadelphia, PA (*Abstract Co-Author*) Consultant, Hologic, Inc Consultant, Siemens AG Despina Kontos, PhD, Philadelphia, PA (*Abstract Co-Author*) Nothing to Disclose

For information about this presentation, contact:

aimilia.gastounioti@uphs.upenn.edu

PURPOSE

Breast parenchymal pattern measures have demonstrated substantial potential in breast cancer risk assessment. However, as synthetic 2D mammograms (sDMs) are increasingly being used to reduce dose when screening is performed with digital breast tomosynthesis, standard-dose mammograms (DMs) that have widely been used to evaluate breast parenchymal patterns may no longer be acquired. We investigate differences in quantitative parenchymal pattern measures from DMs versus sDMs.

METHOD AND MATERIALS

We retrospectively analyzed 7365 pairs of bilateral "FOR PRESENTATION" DMs and synthetic ("C-View") images corresponding to 3698 women with negative (BI-RADS 1 or 2) routine screening evaluation. Images were acquired with a Selenia Dimensions system (Hologic Inc.) over a 4-month period at our institution for which both DMs and sDMs were available for each screening exam. For each image, 26 established parenchymal pattern descriptors were automatically estimated, including gray-level histogram, co-

occurrence, run-length, and fractal dimension texture features. Feature measurements were compared using paired Wilcoxon signed-ranks tests and Spearman correlation (r). We also compared feature correlations with automated breast percent density (PD) estimates, and evaluated the within woman intraclass feature correlation (ICC) for the two mammogram types.

RESULTS

Most features were strongly (r>0.6 for 12 features) or moderately ($0.4 \le r \le 0.6$ for 11 features) correlated between DMs and sDMs. However, all measurements were significantly different between the two mammogram types (Wilcoxon test, p<0.001). Regardless of the mammogram type, parenchymal texture measures demonstrated weak to moderate correlations with breast PD (- $0.6 \le r \le 0.6$) and strong bilateral symmetry (ICC>=0.6), with significantly increased ICC values for sDMs (average ICC = 0.80 vs average ICC = 0.67, p=0.0003).

CONCLUSION

Breast parenchymal pattern measurements extracted from sDMs are different, yet correlated with those made from DMs. Furthermore, in either mammogram type, there is an inherently strong agreement in bilateral parenchymal symmetry for the extracted texture measures capturing information complementary to the established risk factor of breast density.

CLINICAL RELEVANCE/APPLICATION

Our findings may contribute to integrating computerized parenchymal complexity analysis for breast cancer risk assessment in clinical settings where DMs may be fully replaced by synthetic mammograms.

SSK02-08 Mammographic Parenchymal Analysis with Deep Belief Network for Breast Cancer Risk Prediction

Wednesday, Nov. 29 11:40AM - 11:50AM Room: E451A

Participants

Jun Wei, PhD, Ann Arbor, MI (*Abstract Co-Author*) Nothing to Disclose Heang-Ping Chan, PhD, Ann Arbor, MI (*Presenter*) Institutional research collaboration, General Electric Company Mark A. Helvie, MD, Ann Arbor, MI (*Abstract Co-Author*) Institutional Grant, General Electric Company Songfeng Li, Guangzhou, China (*Abstract Co-Author*) Nothing to Disclose Chuan Zhou, PhD, Ann Arbor, MI (*Abstract Co-Author*) Nothing to Disclose Marilyn A. Roubidoux, MD, Ann Arbor, MI (*Abstract Co-Author*) Research Consultant, Delphinus Medical Technologies, Inc Lubomir M. Hadjiiski, PhD, Ann Arbor, MI (*Abstract Co-Author*) Nothing to Disclose

For information about this presentation, contact:

jvwei@umich.edu

PURPOSE

To develop a quantitative mammographic parenchymal pattern (MPP) descriptor for breast cancer risk prediction using digital mammograms (DM).

METHOD AND MATERIALS

With IRB approval, we performed a matched case-control study to investigate the use of MPP for breast cancer risk prediction. We retrospectively collected data of 398 subjects including 199 paired cancer cases and cancer-free controls. The controls were frequency matched to the cases with respect to the years of screening, age, and race. The screening DMs in the year of cancer diagnosis and up to 5 years of consecutive prior screening DMs were collected for each subject. A total of 2712 CC-views were analyzed in this study. The "for processing" image was first processed by a multiscale method to enhance the fibroglandular densities and parenchymal patterns. Locations of keypoints were identified by a scale-invariant feature transform algorithm. Three ROIs were automatically localized based on the keypoint distribution and used for MPP analysis. The MPP descriptor was formed by a semi-supervised learning scheme, in which an unsupervised deep belief network (DBN) with tied weights was used as MPP feature generator. Layer-wise neurons with ReLU as activation function was first pretrained and then stacked to construct the DBN. The cross-entropy error with *L*2 norm was minimized by an optimization algorithm based on adaptive estimates of lower-order moments. A random forest was then trained to combine the MPP features and estimate the probability of cancer risk. Ten-fold cross validation was used for model selection and evaluation. ROC analysis was performed to assess the prediction accuracy.

RESULTS

The average age for cases and controls were 60.9 ± 10.6 and 60.9 ± 10.5 , respectively. At the year of cancer diagnosis, the AUC was 0.78 ± 0.01 . The AUCs from 1-year to 5-year prior exams were 0.75 ± 0.01 , 0.70 ± 0.01 , 0.64 ± 0.02 , 0.59 ± 0.02 , and 0.61 ± 0.02 , respectively.

CONCLUSION

The MPP can differentiate cases from matched controls and the changes in MPP increased as the time approached cancer diagnosis. Our proposed MPP by machine learning shows promise for cancer risk prediction. Future work is underway to enlarge the data set and to improve the machine learning scheme.

CLINICAL RELEVANCE/APPLICATION

Our MPP analysis on screening DMs shows potential for breast cancer risk assessment and the change in risk over time, which may be useful for personalizing screening regimen and early detection.

SSK02-09 Automatic Identification of Nuanced Imaging Features in Recalled but Biopsy Benign Mammogram Images

Wednesday, Nov. 29 11:50AM - 12:00PM Room: E451A

Awards

Trainee Research Prize - Fellow

Participants Sarah S. Aboutalib, PhD, Pittsburgh, PA (*Presenter*) Nothing to Disclose Aly A. Mohamed, PhD, Pittsburgh, PA (*Abstract Co-Author*) Nothing to Disclose Wendie A. Berg, MD, PhD, Pittsburgh, PA (*Abstract Co-Author*) Nothing to Disclose David Gur, PhD, Pittsburgh, PA (*Abstract Co-Author*) Nothing to Disclose Brenda F. Kurland, PhD, Seattle, WA (*Abstract Co-Author*) Nothing to Disclose Margarita L. Zuley, MD, Pittsburgh, PA (*Abstract Co-Author*) Research Grant, Hologic, Inc; Jules H. Sumkin, DO, Pittsburgh, PA (*Abstract Co-Author*) Institutional research agreement, Hologic, Inc Advisory Board, General Electric Company Hong Peng, MD, Xiangtan, China (*Abstract Co-Author*) Nothing to Disclose Rachel Jankowitz, MD, Pittsburgh, PA (*Abstract Co-Author*) Nothing to Disclose Shandong Wu, PhD, MSc, Pittsburgh, PA (*Abstract Co-Author*) Nothing to Disclose

For information about this presentation, contact:

wus3@upmc.edu

PURPOSE

In digital mammography screening, a main concern is to reduce false recall rates. In this study, we investigate automatic identification of nuanced imaging features to distinguish mammogram images belonging to negative, recalled-benign, and positive cases, aimed to better interpret recalled images with biopsy benign results.

METHOD AND MATERIALS

A retrospective study was performed on a cohort of 1303 patients (5212 mammogram images) who underwent standard digital mammography screening (2007-2014): 552 patients were evaluated as negative in the initial screen, maintaining the cancer-free status in at least a one-year follow-up; 376 patients were recalled and eventually determined to be biopsy-proven benign based on pathology results; 375 patients were evaluated as positive for breast cancer (27% DCIS; 73% Invasive) based on pathology results. Both craniocaudal (CC) and mediolateral oblique (MLO) image views were used for all patients; for the positive cancer cases, only images of the cancer-affected breasts were included. A fully automated computerized method utilizing deep learning with a convolutional neural network was applied to distinguish between the three categories listed above (four binary-class comparisons plus one triple-class comparison). To enhance training of the deep learning network, transfer learning from a large existing imaging database was used followed by fine-tuning with the mammogram images. The receiver operating characteristic (ROC) was generated and the area under the curve (AUC) was calculated as a metric of the classification accuracy.

RESULTS

Full results of all five scenarios are shown in the figure. In all comparisons, the three categories (negative, recalled-benign, and positive) can be distinguished (AUC ranging from 0.66 to 0.81) by automatically identified mammographic imaging nuances. The identified imaging features between recalled-benign and negative are most distinguishing (AUC=0.81), followed by recalled-benign vs. positive (AUC=0.75).

CONCLUSION

Nuanced mammographic imaging features identified by automatic deep learning methods on a large imaging cohort distinguish negative, recalled-benign, and positive cases.

CLINICAL RELEVANCE/APPLICATION

Automatic learning coupled with the distinguishing mammographic imaging nuances can lead to a computerized toolkit to potentially help better interpret recalled-benign images to reduce false recalls.





103rd Scientific Assembly and Annual Meeting November 26 to December 1 McCormick Place, Chicago



SSK03

Cardiac (Coronary Artery Disease: Plaque and Calcium)

Wednesday, Nov. 29 10:30AM - 12:00PM Room: S502AB



AMA PRA Category 1 Credits ™: 1.50 ARRT Category A+ Credit: 1.75

Participants

Harold I. Litt, MD, PhD, Philadelphia, PA (*Moderator*) Research Grant, Siemens AG ; Research Grant, Heartflow, LLC; ; Jens Bremerich, MD, Basel, Switzerland (*Moderator*) Nothing to Disclose Jadranka Stojanovska, MD, MS, Ann Arbor, MI (*Moderator*) Consultant, Guerbet SA

Sub-Events

SSK03-01 Effect of Energy Difference in the Evaluation of Calcification Size and Luminal Diameter in Calcified Coronary Artery Plaque Using Spectral CT

Participants

Hiroto Yunaga, Yonago, Japan (*Presenter*) Nothing to Disclose Yasutoshi Ohta, MD, Yonago, Japan (*Abstract Co-Author*) Nothing to Disclose Shinichiro Kitao, Yonago, Japan (*Abstract Co-Author*) Nothing to Disclose Junichi Kishimoto, Yonago, Japan (*Abstract Co-Author*) Nothing to Disclose Tomomi Watanabe, MD, Yonago, Japan (*Abstract Co-Author*) Nothing to Disclose Kazuhiro Yamamoto, Yonago, Japan (*Abstract Co-Author*) Nothing to Disclose Toshihide Ogawa, MD, Yonago, Japan (*Abstract Co-Author*) Nothing to Disclose

For information about this presentation, contact:

yunagahiroto@gmail.com

PURPOSE

Coronary artery calcification degrades diagnostic accuracy on the evaluation of coronary artery stenosis. It is known that virtual monochromatic image (VMI) at high energy level using dual-energy CT (DECT) reduces blooming artifacts. The aim of our study was to evaluate the calcium blooming effect and the differences of luminal diameter in varying VMI energy using rapid kilovolt switching single-source dual-energy CT (ssDECT).

METHOD AND MATERIALS

We evaluated 45 calcified plaques in 31 patients with suspected coronary artery disease. Coronary artery calcifications were evaluated based on vessel cross-sectional images from 40 to 140 keV in both pre-contrast and contrast-enhanced coronary CT angiography (CCTA) with ssDECT. We measured the diameter of calcifications on non-contrast CT and coronary artery lumens on CCTA using the full-width half maximum method. The calcium blooming effect was evaluated on pre-contrast VMIs. The diameter of calcifications on non-contrast CT and coronary arterial lumens on CCTA in each keV were compared with that of 70 keV VMI that had an equal effective energy of 120kVp as a reference standard.

RESULTS

Only 40 keV VMI showed significantly large calcification diameter than that of 70 keV image $(1.53\pm0.37$ mm vs. 1.48 ± 0.33 mm, p<0.01) on the pre-contrast scan. Meanwhile, the other keV images did not show significant differences in diameter compared to that of 70keV VMI. Regarding coronary artery luminal diameter, no significant differences were observed among all energy levels compared to that of 70keV VMI (40keV, 2.47 ± 0.67 mm; 50keV, 2.47 ± 0.67 mm; 60keV, 2.50 ± 0.67 mm; 70keV, 2.48 ± 0.68 mm; 80keV, 2.48 ± 0.68 mm; 90keV, 2.48 ± 0.68 mm; 100keV, 2.49 ± 0.67 mm; 110keV, 2.51 ± 0.66 mm; 120keV, 2.49 ± 0.68 mm; 130keV, 2.49 ± 0.67 mm; 140keV, 2.48 ± 0.68 mm), on CCTA (all p=N.S).

CONCLUSION

The diameter of coronary artery calcification and the luminal diameter of the coronary artery with calcified plaque would not be changed in almost all VMIs.

CLINICAL RELEVANCE/APPLICATION

The difference of VMI energy would not affect the measurement of luminal diameter of the coronary artery with calcified plaque.

SSK03-02 The Impact of Advanced Modeled Iterative Reconstruction Strength Level on the Image Quality of Calcified Coronary Segments in Coronary CT Angiography

Wednesday, Nov. 29 10:40AM - 10:50AM Room: S502AB

Participants Yuanding Wang, Beijing, China (*Presenter*) Nothing to Disclose Xiangying Du, MD, Beijing, China (*Abstract Co-Author*) Nothing to Disclose Kuncheng Li, MD, Beijing, China (*Abstract Co-Author*) Nothing to Disclose

PURPOSE

To determine the value of advanced model-based iterative reconstruction (ADMIRE) on improving the image quality of coronary CT angiography (CCTA) in coronary segments with/without calcified plaques, by evaluating the image quality at different levels of ADMIRE in comparison with that at filtered back projection (FBP) on a third-generation dual source CT scanner.

METHOD AND MATERIALS

CCTA was performed on a third-generation, dual-source CT with automated tube voltage adaptation. Patients with coronary artery disease and at least one calcified segment on calcium scoring scan were enrolled. Image series were reconstructed with FBP and ADMIRE (strength levels 1 - 5), respectively. Attenuation, image noise, signal-to-noise ratio (SNR), and contrast-to-noise ratio (CNR) were calculated, the volume of the calcified plaques were measurd. Subjective image quality criteria was assessed by two observers using a 5-point Likert scale.

RESULTS

Results: There were no statistically significant differences in attenuation between each ADMIRE group (strengths 1 - 5) and FBP group (p > 0.05). Image noise decreased significantly using ADMIRE compared with FBP and was reduced with increasing ADMIRE strength levels (maximal reduction, 45.4%, p < 0.05). The CNR and SNR of each ADMIRE group were significantly higher than those of FBP group, increasing with higher ADMIRE strength levels (p < 0.05). The volume of calcified plagues were decreased with the increasing ADMIRE strength levels(p < 0.05). Both in segments with calcified plaques and without calcification, subjective image quality was rated best at ADMIRE 4, followed by ADMIRE 5, ADMIRE 3, ADMIRE 2, ADMIRE 1, and FBP.

CONCLUSION

Image quality of CCTA can be significantly improved by the application of ADMIRE, both in coronary segments with and without calcified plaques, while the optimal image quality was achieved at iterative strength level 4.

CLINICAL RELEVANCE/APPLICATION

By increasing the image quality and decreasing the blooming artifacts, the high strength level IR technique decreases the need for unnecessary coronary catheterization or myocardial perfusion studies.

SSK03-03 Coronary Artery Enhancement for Coronary CT Angiography and Plaque Analysis: Optimization with a Test Bolus and Contrast Dilution Protocol

Wednesday, Nov. 29 10:50AM - 11:00AM Room: S502AB

Participants

Veit Sandfort, MD, Bethesda, MD (*Abstract Co-Author*) Nothing to Disclose Mark A. Ahlman, MD, Bethesda, MD (*Abstract Co-Author*) Nothing to Disclose Rolf Symons, MD, Bethesda, MD (*Presenter*) Nothing to Disclose Marissa Mallek, Bethesda, MD (*Abstract Co-Author*) Nothing to Disclose Amir Pourmorteza, PhD, Atlanta, GA (*Abstract Co-Author*) Nothing to Disclose Christopher Sibley, Bethesda, MD (*Abstract Co-Author*) Employed by Merck Joao A. Lima, MD, Baltimore, MD (*Abstract Co-Author*) Research Grant, Toshiba Medical Systems Corporation David A. Bluemke, MD, PhD, Bethesda, MD (*Abstract Co-Author*) Research agreement, Siemens AG; Research support, Siemens AG; Research agreement, Carestream Health, Inc; Research support, Carestream Health, Inc

PURPOSE

Quantification of total coronary plaque index and coronary artery stenosis is markedly affected by attenuation levels of the coronary lumen due to partial volume averaging. Thus, achieving consistent attenuation level of the coronary artery lumen improves quantitative analysis when comparing patient studies. We studied three contrast injection protocols for coronary CT angiography (CCTA) and compared both mean levels and standard deviation of contrast enhancement.

METHOD AND MATERIALS

We evaluated a test-bolus injection protocols in comparison to a weight-based injection (body weight (BW) <60 kg: 50 mL contrast, BW >= 60 kg and BW <= 100 kg: 60 mL contrast and BW > 100 kg: 70 mL, 5 ml/sec, imaging trigger by bolus-tracking). The test bolus injection consisted of injection of 75 ml of diluted contrast (30% iopamidol 370, 4.5 ml/sec) as test bolus. The test bolus peak attenuation was used for scan timing and calculation of the angiography bolus dilution. Aortic and coronary artery attenuation was measured and compared to a pre-defined target attenuation level (375 HU at 120 kVp equivalent).

RESULTS

Overall, 119 subjects were evaluated (66% men, age 62y, BMI 29, heart rate 56/min). The test-bolus guided injection protocol achieved the coronary target attenuation successfully and consistently (mean 373±39 HU, target 375 HU, relative standard deviation (rSD) 10.5 %); inter-study variation of the test-bolus method was significantly lower than that of the body weight injection protocol (mean 362±98, rSD 27%, p<0.0001, also see figure). A similar trend was seen for attenuation in the ascending aorta (rSD 9.4% vs. 30% for the test bolus protocol and the body weight protocol, respectively, p<0.0001). The timing was optimal (highest attenuation in ascending aorta compared with left atrium or descending aorta) in 73% of cases for the test-bolus protocol compared with 27% in the body mass guided injection protocol (p<0.0001).

CONCLUSION

A test-bolus guided injection protocol with variable contrast dilution allowed greatly improved standardization of coronary and aortic attenuation levels for coronary CT angiography.

CLINICAL RELEVANCE/APPLICATION

Consistent coronary lumen attenuation is desirable for plaque and stenosis quantification. A test-bolus guided contrast injection achieves improved consistency in coronary lumen attenuation.

SSK03-04 Half Dose CT Coronary Calcium Score: Impact of Iterative Reconstruction

Awards Student Travel Stipend Award

Participants

Damiano Caruso, MD, Rome, Italy (*Presenter*) Nothing to Disclose Tommaso Biondi, MD, Rome, Italy (*Abstract Co-Author*) Nothing to Disclose Marta Montesano, Latina, Italy (*Abstract Co-Author*) Nothing to Disclose Davide Bellini, MD, Latina, Italy (*Abstract Co-Author*) Nothing to Disclose Marco Rengo, MD, Rome, Italy (*Abstract Co-Author*) Nothing to Disclose Andrea Laghi, MD, Rome, Italy (*Abstract Co-Author*) Nothing to Disclose

For information about this presentation, contact:

dcaruso85@gmail.com

PURPOSE

To evaluate the effectiveness of Iterative Reconstruction (IR) on the coronary artery calcium scores (CACS) by using a half radiation dose CT acquisition protocol compared to standard protocol.

METHOD AND MATERIALS

Based on a power analysis, this prospective study included 57 patients without known coronary artery disease who underwent two CACS acquisition (standard and half radiation dose) with MDCT (128-slice GE-VCT Hino W/VT 2000) within the same examination, following ethical permission. The standard protocol was acquired with tube voltage of 120 KVp and tube current of 170 mA, whereas the half dose protocol was acquired with 50% reduction of mA (85 mA) and the same tube voltage. Raw data of half dose protocols were reconstructed by using IR at all strength levels available, from 10% up to 100%, every 10%. Radiation dose as well as number of plaques, Agatston score, volume and mass were calculated and compared between the two protocols by using dedicated statistical test (Medcalc v17.4, Belgium). A p value <0.05 was considered statistically significant.

RESULTS

From an original population of 57 patients we exclude 6 patients for absence of coronary plaques, thus the final population comprised 51 patients (32 men and 19 women). The mean DLP were 45.447.10 and 21.663.24 for the standard and half dose protocol (p<0.05), respectively. The mean Agatston score for the standard protocol was 595.82±977.09 and 19.27±19.53 plaques were identified. No significant differences for Agatston score were observed between standard protocol and half dose protocol with IR at 40 and 50% (493.35±924.31 and 498.05±959.27, p>0.05), whereas significant differences were observed for all the remaining IR levels (all p<0.05). Moreover, no significant differences were calculated for the number of plaque with IR at 40% (23.67±21.46, p>0.05).

CONCLUSION

Half dose acquisition protocol with IR at 40% and 50% showed reliable results in terms of Agatston score for CACS showing no significan differences with standard protocol.

CLINICAL RELEVANCE/APPLICATION

Patients can benefit of half radiation dose CACS acquisition protocol with IR at 40%, which shows comparable results in the evaluation of Agatston score and number of plaques to the standard protocol.

SSK03-05 250 Micron Resolution Photon-Counting CT: Potential for Improved Imaging of Calcified Coronary Artery Stenoses

Wednesday, Nov. 29 11:10AM - 11:20AM Room: S502AB

Participants

Veit Sandfort, MD, Bethesda, MD (*Abstract Co-Author*) Nothing to Disclose Rolf Symons, MD, Bethesda, MD (*Abstract Co-Author*) Nothing to Disclose Tyler E. Cork, MS, Bethesda, MD (*Abstract Co-Author*) Nothing to Disclose David A. Bluemke, MD, PhD, Bethesda, MD (*Abstract Co-Author*) Research agreement, Siemens AG; Research support, Siemens AG; Research agreement, Carestream Health, Inc; Research support, Carestream Health, Inc Amir Pourmorteza, PhD, Atlanta, GA (*Presenter*) Nothing to Disclose

PURPOSE

Coronary CT angiography using conventional CT leads to overestimation of calcified stenosis due to blooming / partial volume effects. The purpose of this study was to determine the potential utility of ultra-high resolution (UHR) (250 micron) photon-counting detector (PCD) CT using human ex-vivo hearts. We hypothesize that the increased resolution will reduce overestimation of calcified plaque stenosis when compared to (0.50 mm) standard resolution CT.

METHOD AND MATERIALS

We used a whole-body PCD CT scanner. Each PCD pixel consists of 4x4 subpixels whose photon counts are combined in standard resolution (SR) mode to create 0.50 mm isotropic pixels at isocenter. Recently, the system has been upgraded to allow 2x2 binning of subpixels making UHR CT possible with 0.25 mm isotropic pixels at isocenter. 5 human ex-vivo hearts were placed inside an anthropomorphic chest phantom and scanned in dose-matched SR and UHR modes at 140 kVp and 106 mAs. We measured the total cardiac calcium volume to evaluate the effect of higher resolution on calcium volume at a clinically used threshold of 130 HU at 140 kVp. All images were reconstructed with filtered backprojection. We assessed imaging of calcified stenosis in total of 18 coronary locations with at least semi-circumferential calcified plaques. We tested if a previously described method for inner vessel lumen detection based on the 2nd derivative of a cross-sectional Hounsfield Unit (HU) profile was able to detect a stenosed by patient coronary artery lumen.

RESULTS

Calcium volume was 10 % lower in UHR images compared with SR images (424 mm3 vs 469 mm3). Lumen detection rate was

significantly higher in UHR images compared to SR (18/18 [100%] vs. 11/18 [61%], Fisher's test P=0.0076). In addition, the detected lumen diameter was significantly larger in UHR compared to SR images (0.65 mm vs 0.60 mm, Wilcoxon P=0.02).

CONCLUSION

250 micron resolution photon-counting CT resulted in lower calcium volumes, likely reflecting less calcium blooming. It also resulted in larger lumen diameter measurements and enabled successful detection of the lumen in all calcified stenoses while standard resolution failed to depict the lumen in 39% of cases.

CLINICAL RELEVANCE/APPLICATION

One reason for false positive coronary CT angiography is calcium blooming in regions of stenosis. 250 micron photon counting CT may allow better lumen depiction of these difficult lesions.

SSK03-06 Who are the Patients Whose Coronary Artery Calcification Progresses Rapidly? According to Serial CT Measurements of Coronary Artery Calcium

Wednesday, Nov. 29 11:20AM - 11:30AM Room: S502AB

Participants

Hae Young Kim, MD,MS, Seongnam-si, Korea, Republic Of (*Presenter*) Nothing to Disclose Young-Suk Cho, Seongnam-si, Korea, Republic Of (*Abstract Co-Author*) Nothing to Disclose Min Jae Park, Seoul, Korea, Republic Of (*Abstract Co-Author*) Nothing to Disclose Eun Ju Chun, MD, PhD, Seongnam-Si, Korea, Republic Of (*Abstract Co-Author*) Nothing to Disclose

For information about this presentation, contact:

qkfmrp860329@gmail.com

PURPOSE

Coronary artery calcium (CAC) is an established surrogate marker for cardiovascular disease, but little is known about risk factors for the progression of calcium burden. This study assessed the pattern of CAC increment and risk factors for rapid CAC progression.

METHOD AND MATERIALS

515 asymptomatic adults who underwent serial CAC at least 3 times from 2004 to 2016 were included. The patients were categorized into three groups: zero CAC on all serial scans (group 1), eventual CAC formation with initially zero CAC (group 2), and increasing CAC with initial presence of CAC (group 3). Group 3 was subdivided into four groups according to the degree of slope and pattern (linear or exponential slope) of the CAC increment (Figure). Variable risk factors and blood chemistry were analyzed for the each group.

RESULTS

Group 1 (n=310, 60.2%), group 2 (n=59, 11.5%) and group 3 (n=146, 28.3%) were followed up for the mean period of 2760 days. Age, prevalence of male, hypertension, hyperlipidemia, diabetes medication, family history of ischemic heart disease, smoker, systolic and diastolic blood pressure, glucose and triglyceride were higher in the group 3 compared to the group 1 (all p< 0.05). There was no significant difference in any of the risk factor in between the groups with linear (n=63, 43.6%) and exponential slope (n=83, 56.8%). However, there were some risk factors that differed in between the high and low grade slopes, for both linear and exponential groups. In the linear slope group, prevalence of previous ischemic heart disease, hyperlipidemia, triglyceride, glucose, and HbA1c were higher for the group with high grade slope compared to the group with low grade slope (all p< 0.05). On the other hand, in the exponential slope group, initial CACS was higher for the group with high grade slope compared to the group with low grade slope (p=0.03).

CONCLUSION

Patients showed varying CAC progression with differing slope pattern and degree. Although there was no significant relationship of risk factors to the slope pattern (linear vs. exponential), some risk factors and initial CACS were related to the higher degree of slope of CAC progression.

CLINICAL RELEVANCE/APPLICATION

According to our study, appropriate follow up time for CAC measurement should be individualized, under consideration of each patient's risk factors as well as initial CAC score.

SSK03-07 Association between Serum Uric Acid and the Characteristics of Coronary Plaque Burden: Assessment with Coronary CT Angiography

Wednesday, Nov. 29 11:30AM - 11:40AM Room: S502AB

Participants Ruiyi r. Tan SR, ARRT, ARRT, Beijing, China (*Presenter*) Nothing to Disclose Qi Xiao, MD, MBA, Saint Louis, MO (*Abstract Co-Author*) Nothing to Disclose

For information about this presentation, contact:

275577014@qq.com

PURPOSE

It is controversial whether serum uric acid (UA) is an independent risk factor for cardiovascular diseases (CVD). The aim of this study was to investigate the correlation between the serum UA level and coronary plaque burden characteristics evaluated by coronary CT angiography (CCTA).

METHOD AND MATERIALS

In total, 1315 patients who underwent CCTA were divided into the hyperuricemia group and normal serum UA group according to

their serum UA level and stratified by gender. The low-attenuation plaque volume (LPV) and total plaque volume (TPV) were separately measured in each main coronary artery. The correlation of serum UA or hyperuricemia with coronary plaque burden was assessed using multivariate-adjusted logistic and linear regression analyses.

RESULTS

The TPV and LPV significantly differed between males and females (P < 0.0001 each). The TPV values were higher in female subjects with hyperuricemia than in subjects without hyperuricemia (P = 0.0124). The serum UA level significantly correlated with the TPV in both genders (β = 0.4231 and P = 0.0441 for males and β = 0.4996 and P = 0.0149 for females). However, the serum UA and LPV did not correlate with either gender after adjusting for multivariates.

CONCLUSION

The serum UA level was significantly associated with the coronary TPV in both genders. However, the serum UA was not associated with the LPV. We found that the serum UA may play an independent role in the pathophysiology of total plaque burden.

CLINICAL RELEVANCE/APPLICATION

We found that the serum UA plays an independent role in the pathophysiology of the total plaque burden, and we suggest controlling the serum UA level as a meaningful strategy in the management of coronary plaque burden.

SSK03-08 The Diagnosis of Coronary Plaque Stability by Multislice Computed Tomography Coronary Angiography

Wednesday, Nov. 29 11:40AM - 11:50AM Room: S502AB

Participants

Fengxiang Song, Shanghai, China (*Presenter*) Nothing to Disclose Yuesong Yang, Shenzhen, China (*Abstract Co-Author*) Nothing to Disclose Jianjun Zhou, Shanghai, China (*Abstract Co-Author*) Nothing to Disclose Yuxin Shi, PhD, Shanghai, China (*Abstract Co-Author*) Nothing to Disclose Mengsu Zeng, MD, PhD, Shanghai, China (*Abstract Co-Author*) Nothing to Disclose Peng Lv, Shanghai, China (*Abstract Co-Author*) Nothing to Disclose Ruofan Sheng, Shanghai, China (*Abstract Co-Author*) Nothing to Disclose

For information about this presentation, contact:

songfengxiang@shaphc.org

PURPOSE

This study was to investigate and summarize the differential characteristics of non-calcified unstable coronary plaques and stable coronary plaques using MSCT.

METHOD AND MATERIALS

Sixty patients with coronary heart disease were included in our study. 37 unstable plaques and 31 stable plaques were identified. We analyzed the plaque CT attenuation, the napkin-ring sign, napkin-ring thickness, the plaque distribution, the degree of lumen stenosis and the sensitivity, specificity, positive predictive value, negative predictive value of MSCT to identify the plaque stability. The difference and correlation between MSCT and IVUS in the diagnosis of plaque characteristic were also analyzed. All statistical analysis was done using software Stata 10.0. The difference was statistically significant if P<0.05.

RESULTS

The average CT value of unstable plaques (29.7 ± 19.4 HU)was lower than stable plaques (76.4 ± 24.8 HU)(P<0.05), although there was some overlap. The napkin ring sign was more frequently observed in unstable group(91.9%) than stable group (22.6%) (P<0.05). The median thickness of napkin-ring in unstable plaques(0.7mm) was thinner than stable plaques(1.1mm)(P<0.05). The former had more severe lumen stenosis or occlusion (70.3%)than the latter (41.9%)(P<0.05). The plaques were mainly distributed in the left anterior descending artery in both groups. The sensitivity, specificity, positive predictive value and negative predictive value of MSCT to confirm unstable plaques. MSCT and IVUS had no statistically significant difference in the diagnosis of plaque characteristic(P>0.05), while showed a correlation in the identification of plaque stability (P=0.00, r=0.5568).

CONCLUSION

The average CT attenuation of non-calcified unstable plaques was lower than stable plaques although there was some overlap. The incidence of napkin-ring sign in unstable plaques was significantly higher than that in stable plaques; Unstable plaques had more severe lumen stenosis or occlusion than stable plaques. MSCT demonstrated a clinical significance in the identification of coronary plaque stability.

CLINICAL RELEVANCE/APPLICATION

MSCT demonstrated a clinical significance in the identification of coronary plaque stability.

SSK03-09 The Evaluation of Subclinical Coronary Atherosclerosis of Different Therapy Stages in Middle-Aged HIV (+) Chinese Adults

Wednesday, Nov. 29 11:50AM - 12:00PM Room: S502AB

Participants

Juan Huang, Zheng Zhou, China (*Presenter*) Nothing to Disclose Yonggao Zhang, Zhengzhou, China (*Abstract Co-Author*) Nothing to Disclose Shuo Liu, Zhengzhou, China (*Abstract Co-Author*) Nothing to Disclose Jianbo Gao, MD, Zhengzhou, China (*Abstract Co-Author*) Nothing to Disclose

For information about this presentation, contact:

867864639@qq.com

PURPOSE

It is demonstrated that HIV (+) patients have a higher risk for cardiovascular disease, mainly due to HIV infection itself and medication side effect in addition to traditional risk factors. This study is aimed to determine whether the routinely long-term medication treatment using HAART has an impact on total CAC score and plaque formation.

METHOD AND MATERIALS

A total number of 120 HIV (+) patients (52 ± 4 years) was enrolled in the study, who underwent CCTA and besides, who was with normal kidney function and without the history of revascularization. According to the duration of HAART mediation treatment, the patients were divided into three groups: A (less than 2 years), B (2 to 5 years) and C (more than 5 years).

RESULTS

There were 40 patients in each group, and no significant differences in demographic data and risk factors of cardiovascular disease were found between groups. The median Agatston CCS for group A was 74 [25-75th percentile: 0-492], with a range from 0 to 4781;As for group B and group C, the median value was 79 [25-75th percentile: 0-502], with a range from 0 to 5120 and 111 [25-75th percentile: 0-532], with a range from 0 to 7320 respectively, the difference of Agatston CCS between groups were found statistically significant. The number of non-calcified plaques was 17 for group A, 29 for group B and, 33 for group C. And significant difference in the number of non-calcified plaque was also found between groups. The mean segments with plaque for different groups were 15, 23, and 27 respectively. And there was no significant difference found between groups.

CONCLUSION

It is indicated by this study that the longer duration of HAART medication therapy the patients received, the higher level of CAC score and higher incidence of non-calcified plaque would happen. However, larger sample is needed for further validation.

CLINICAL RELEVANCE/APPLICATION

The longer duration of HAART medication therapy the patients received, the higher level of CAC score and higher incidence of noncalcified plaque might happen.





103rd Scientific Assembly and Annual Meeting November 26 to December 1 McCormick Place, Chicago



SSK04

Cardiac (General Topics, MRI)

Wednesday, Nov. 29 10:30AM - 12:00PM Room: S504AB



AMA PRA Category 1 Credits ™: 1.50 ARRT Category A+ Credit: 1.75

Participants

Anil K. Attili, MD, Saline, MI (*Moderator*) Nothing to Disclose Daniel Ocazionez, MD, Houston, TX (*Moderator*) Nothing to Disclose Charles S. White, MD, Baltimore, MD (*Moderator*) Consultant, Koninklijke Philips NV

Sub-Events

SSK04-01 Safety of MRI in Patients with Conditional or Non-Conditional Pacemaker or Other Implantable Cardiac Electronic Devices (ICED): A Systematic Review

Participants

Giovanni Di Leo, San Donato Milanese, Italy (*Presenter*) Travel support, Bracco Group Moreno Zanardo, MSc, Milano, Italy (*Abstract Co-Author*) Nothing to Disclose Simone Schiaffino, MD, Bogliasco, Italy (*Abstract Co-Author*) Nothing to Disclose Francesco Secchi, MD,PhD, Milano, Italy (*Abstract Co-Author*) Nothing to Disclose Francesco Sardanelli, MD, San Donato Milanese, Italy (*Abstract Co-Author*) Speakers Bureau, Bracco Group; Research Grant, Bracco Group; Advisory Board, Bracco Group; Speakers Bureau, Bayer AG; Research Grant, Bayer AG; Advisory Board, General Electric Company

For information about this presentation, contact:

gianni.dileo77@gmail.com

PURPOSE

To review the MRI safety in patients carrying a pacemaker or other ICEDs.

METHOD AND MATERIALS

A search was performed on March 2017 using MEDLINE/EMBASE for articles on the MRI safety in ICED carriers. Keywords included MRI, pacemaker, implantable cardioverter defibrillator, cardiac electronic device, safety, and adverse events (AEs). We extracted: number of patients, age, device dependency, field strength, specific absorption rate (SAR), studied body region, technical ICED parameters, and follow-up time.

RESULTS

Of 493 articles, 53 were analyzed for a total 6,237 exams in 5,394 patients. Design was prospective in 49 (4 randomized). Devices were MRI non-conditional in 32 studies (2,889 patients), conditional in 16 (1,708 patients), mixed in 5 (797 patients). Patients were device-dependent in 1 study, independent in 22, mixed in 18, and not defined in 12. Field strength was 0.2T in 1 study, 0.5T in 3, 1.5T in 45, 2T in 1, 3T in 2, mixed in 1. The studied body region was thoracic in 27 studies, non-thoracic in 16, and mixed in 10. SAR was limited in 39 studies, not limited in 5, not reported in 9. Follow up was 0-6 months in 32 studies, >6 months in 6, and not reported in 15. No fatal events occurred. Five studies reported clinically relevant AEs: atrial arrhythmias (6 patients), intolerable heating (5 patients), perforation (4 patients), lead dislodgements (3 patients), and generator failure with immediate replacement (1 patient), for a total of 19 AEs, 7 in patients with MRI conditional ICED, 9 in patients with non-conditional, and 3 in patients with an undefined ICED, for a total of 19 clinically relevant AEs. Twenty studies reported technical AEs, mainly power-on reset and battery voltage reduction. Two studies showed significant changes of atrial sensing, 4 of ventricular sensing, 3 of atrial pacing capture threshold (PCT), 4 of ventricular PCT, 6 of atrial lead impedance, 7 of ventricular lead impedance, and 9 of battery voltage.

CONCLUSION

Considering 6,237 MRI exams in 5,394 device-dependent or non-dependent carriers of conditional or non-conditional ICED, a very low rate of clinically relevant AEs was reported. The risk/benefit ratio is largely positive, also for non-conditional ICED.

CLINICAL RELEVANCE/APPLICATION

Patients carrying ICED should not be denied thoracic or nonthoracic MRI a priori, included patients with non-conditional devices. MRI may be performed safely under controlled conditions.

SSK04-02 Diagnostic Performance of Minimally Invasive Autopsy for Detection of Ischemic Heart Disease

Wednesday, Nov. 29 10:40AM - 10:50AM Room: S504AB

Participants Ivo Wagensveld, MSc, Leiden, Netherlands (*Presenter*) Nothing to Disclose Britt Blokker, Rotterdam, Netherlands (*Abstract Co-Author*) Nothing to Disclose Andrea Pezzato, Verona, Italy (*Abstract Co-Author*) Nothing to Disclose Piotr A. Wielopolski, PhD, Rotterdam, Netherlands (*Abstract Co-Author*) Nothing to Disclose Jan von der Thusen, Rotterdam, Netherlands (Abstract Co-Author) Nothing to Disclose

Gabriel P. Krestin, MD, PhD, Rotterdam, Netherlands (*Abstract Co-Author*) Research Grant, General Electric Company Research Grant, Bayer AG Research Grant, Siemens AG Consultant, Bracco Group Scientific Advisor, Zebra Medical Vision Ltd Advisory Board, Quantib BV

M.G. Myriam Hunink, MD, PhD, Rotterdam, Netherlands (*Abstract Co-Author*) Nothing to Disclose J.w. Oosterhuis, MD, PhD, Rotterdam, Netherlands (*Abstract Co-Author*) Nothing to Disclose Annick C. Weustink, MD, PhD, Rotterdam, Netherlands (*Abstract Co-Author*) Nothing to Disclose

PURPOSE

In this study we investigated the performance of minimally invasive autopsy (MIA) to diagnose ischemic heart disease in clinically deceased patients

METHOD AND MATERIALS

In 99 adult cases with written consent for conventional autopsy (CA) and MIA, diagnostic accuracy of MIA and CA was calculated for acute and chronic myocardial ischemia. MIA consisted of total-body postmortem MR (PMMR) and CT (PMCT), combined with CT-guided biopsies of myocardial lesions. PMMR and PMCT were independently read by two radiologists with expertise in cardiac radiology. Calcium score (Agatston) and ROC curve for the prediction of acute and chronic ischemia were calculated for each case. CA including macroscopy and microscopy was the gold standard.

RESULTS

CA detected 34 cases of acute ischemia. Sensitivity of PMMR for acute ischemia was 0.50 (CI: 0.33-0.67) and specificity was 0.92 (CI: 0.86-0.99). PMMR combined with biopsy improved sensitivity to 0.97 (CI: 0.91-1.00) and specificity to 0.95 (CI: 0.9-1.00). CA detected 40 cases of chronic ischemia. Sensitivity of PMMR for chronic ischemia was 0.35 (CI: 0.20-0.50) and specificity was 1.00. PMMR combined with biopsy improved sensitivity for chronic ischemia to 0.90 (CI: 0.81-0.99) but specificity was lowered to 0.75 (CI: 0.63-0.86). Calcium score was a fair predictor for chronic ischemia (AUC=0.73, p<0.001), but a poor predictor for acute ischemia (AUC=0.61, p=0.073).

CONCLUSION

MIA shows high diagnostic accuracy for detection of acute and chronic myocardial ischemia. Importantly, our results show that postmortem imaging needs to be combined with CT-guided biopsies to achieve the highest performance.

CLINICAL RELEVANCE/APPLICATION

This study shows that minimally invasive autopsy (MIA) has high diagnostic performance to detect ischemic heart disease which is a very common cause of death in clinically deceased patients.

SSK04-03 Left Bundle Branch Block: Usefulness of MRI in the Evaluation of Regional Left Ventricular Dyssynchrony and in the Detection of Previous Myocardial Infarction with Late Enhancement

Wednesday, Nov. 29 10:50AM - 11:00AM Room: S504AB

Participants

Marco Di Girolamo, MD, Rome, Italy (*Presenter*) Nothing to Disclose Giuseppe Muscogiuri, MD, Charleston, SC (*Abstract Co-Author*) Nothing to Disclose Stefano Fierro, MD, Rome, Italy (*Abstract Co-Author*) Nothing to Disclose Francesco B. Tagliaferro, MD, Rome, Italy (*Abstract Co-Author*) Nothing to Disclose Carlo N. De Cecco, MD, PhD, Charleston, SC (*Abstract Co-Author*) Research Grant, Siemens AG Michele Rossi, MD, Rome, Italy (*Abstract Co-Author*) Nothing to Disclose

For information about this presentation, contact:

digirolamomarco@hotmail.comn

PURPOSE

Left bundle branch block (LBBB) is a common cardiac conduction abnormality diagnosed on ECG. LBBB can be a primary abnormality of the cardiac electrical conduction system or it can be secondary to other cardiogical pathologies such as myocardial infarction and cardiomyopathies. The presence of LBBB per se cannot be used as a single diagnostic criteria for the diagnosis of previous myocardial infarction. Aim of this study was to evaluate the mechanical left ventricular dyssynchrony with high temporal resolution cine MRI and to evaluate the presence of late-enhancement (LE) in order to diagnose previous myocardial infarction.

METHOD AND MATERIALS

38 patient with LBBB underwent cardiac MRI using a 1.5 T magnet (Magnetom Sonata, Siemens). The MRI protocol consisted of a left ventricular trueFISP functional study followed by Late Enhancement data sets acquired 10-15 minutes after iv administration of 0.2mmol/kg BW of extracellular Gd contrast agent. We used a segmented Inversion Recovery Turbo-FLASH sequence (TR:8ms;TE:4ms;TI:250-320ms;sl.thick:8mm). Different pattern of LE were related to the underlying pathology as stated by clinical and other diagnostic imaging features.

RESULTS

We detected a characteristic dyssynchronous ventricular contraction with septal flattening during early ventricular systole in all the patients, tenting of mitral valve apparatus in 5 pts and functional mitral regurgitation in 2 pts. In 1 pt we found the characteristic functional features of dilated cardiomyopathy with no myocardial area of LE. In 8 pts we found areas of LE (transmural in 3 pts and subendocardial in 5 pts) with typical patterns of myocardial infarction (MI). The location of MI was septal in 4 pts, infero-septal in 2 pts, lateral in 1pt, and superior in 1 pt. In 30 patients we found a reduction of the ejection fraction (75%).

CONCLUSION

Cardiac MRI is a useful diagnostic tool in the evaluation of LBBB when the assessment of ventricular dyssynerygy on echocardiography is not technically feasible and when the area of a previous myocardial infarction cannot be determined.

CLINICAL RELEVANCE/APPLICATION

MRI is a useful diagnostic tool in the evaluation of LBBB when US assessment of ventricular dyssynerygy isn't feasible and a previous possible myocardial infarction has to be determined.

SSK04-04 Utility of Native Myocardial T1 Mapping as a Diagnostic Tool for Ischemic and Non-Ischemic Cardiomyopathy

Wednesday, Nov. 29 11:00AM - 11:10AM Room: S504AB

Participants

Krishna S. Kapoor, Austin, TX (*Presenter*) Nothing to Disclose Sanjaya Viswamitra, MD, Bengaluru, India (*Abstract Co-Author*) Nothing to Disclose Sankar Neelakantan, MD, Bangalore, India (*Abstract Co-Author*) Nothing to Disclose Bhavana Nagabhushana Reddy, MBBS, MD, Bangalore, India (*Abstract Co-Author*) Nothing to Disclose Anitha Kini, DMRD,MD, Bangalore, India (*Abstract Co-Author*) Nothing to Disclose Sunitha P Kumaran, MBBS, MD, Toronto, ON (*Abstract Co-Author*) Nothing to Disclose Anju Das Thulasi Das, DMRD, Bangalore, India (*Abstract Co-Author*) Nothing to Disclose Gurudat R. Shenoy, MBBS, Bangalore, India (*Abstract Co-Author*) Nothing to Disclose Aishwarya K. Mahendrakar, MBBS, Bangalore, India (*Abstract Co-Author*) Nothing to Disclose Srikanth Sola, MD, Bangalore, India (*Abstract Co-Author*) Nothing to Disclose

For information about this presentation, contact:

Krishna.kapoor@utexas.edu

PURPOSE

Native myocardial T1 mapping measures interstitial fibrosis and provides prognostic information in patients with cardiomyopathy. We sought to determine the diagnostic utility of native T1 mapping in identifying common cardiomyopathies - ischemic (CAD), dilated cardiomyopathy (DCM), and hypertrophic cardiomyopathy (HCM) - compared with the reference standard late gadolinium enhancement (LGE).

METHOD AND MATERIALS

We enrolled consecutive adult subjects referred for CMR evaluation of ischemic or non-ischemic cardiomyopathy. CMR was performed on a 1.5T magnet using standard cine, LGE, and native T1 mapping using a modified Look-Locker inversion recovery sequence. We compared the diagnostic accuracy of native T1 mapping versus LGE of the mid septum as well as all 16 segments of the left ventricle for etiology of cardiomyopathy.

RESULTS

We evaluated 1,950 myocardial segments in 130 subjects (mean age 48 ± 11 years, 80% male; 90 CAD, 29 DCM, 11 HCM). Mid septal T1 values were similar in CAD vs. DCM and HCM (1051 ± 51 msec, 1064 ± 36 , 1068 ± 22 respectively, p=0.17). T1 values in segments with fibrosis on LGE were significantly lower than segments without fibrosis, regardless of etiology (1057 ± 65 msec with fibrosis vs. 1042 ± 52 without fibrosis, p<.0001). T1 values were markedly reduced in CAD in segments with lipomatous metaplasia (968 ± 17 msec). However, the diagnostic accuracy of native T1 mapping in identifying the etiology of cardiomyopathy was poor. For a threshold T1 value of < 1024 msec in any segment, the AUC for identifying CAD vs. HCM or DCM was 0.565, sensitivity 39%, specificity 78%, PPV 86%, NPV 28%). There was no association between T1 values and standard imaging indices of disease severity (ejection fraction, total myocardial scar, myocardial mass).

CONCLUSION

Compared with LGE, native T1 mapping has limited diagnostic accuracy in distinguishing between etiologies of cardiomyopathy, likely due to considerable overlap of values in CAD, DCM, and HCM. There was no association between T1 values and severity of cardiomyopathy, as measured by ejection fraction, total myocardial scar (CAD), or myocardial mass (HCM).

CLINICAL RELEVANCE/APPLICATION

Native T1 mapping is a useful tool for tissue characterization. However, its utility to distinguish between ischemic, dilated, or hypertrophic cardiomyopathies is limited.

SSK04-05 References Values of Myocardial Strain Measurement Using Cardiovascular Magnetic Resonance Tissue Tracking for Both Ventricles in Asymptomatic Asian Cohort: Association with Cardiovascular Risk Factors

Wednesday, Nov. 29 11:10AM - 11:20AM Room: S504AB

Participants

Hye Na Jung, MD, Seoul, Korea, Republic Of (*Presenter*) Nothing to Disclose Sung Mok Kim, MD, Seoul, Korea, Republic Of (*Abstract Co-Author*) Nothing to Disclose Min Jae Cha, Seoul, Korea, Republic Of (*Abstract Co-Author*) Nothing to Disclose Ji-Won Hwang, Seoul, Korea, Republic Of (*Abstract Co-Author*) Nothing to Disclose Hyun Su Kim, MD, Seoul, Korea, Republic Of (*Abstract Co-Author*) Nothing to Disclose Yeon Hyeon Choe, MD, PhD, Seoul, Korea, Republic Of (*Abstract Co-Author*) Nothing to Disclose

For information about this presentation, contact:

holymosquito@hanmail.net

PURPOSE

To provide the reference values of myocardial deformation parameters of both ventricles using cardiovascular MR with tissue tracking (CMR-TT) in asymptomatic Asian subjects and to evaluate the association of deformation parameters and Framingham risk score (FRS).

METHOD AND MATERIALS

We arrelled 120 asymptometric hashby adults who underwant CMD, and all subjects demonstrated normal left ventricular systelic

we enrolled 129 asymptomatic nearthy adults who underwent CMR, and all subjects demonstrated normal left ventricular systolic function. We assessed the FRS of all study population. Commercial software was used to derive myocardial deformation parameters of both ventricles from short-axis cine views and apical two-, three-, and four-chamber views. The reference value of each strain parameter was determined as mean value of every individual. The linear regression analysis was performed between all strain parameters and FRS. Iota coefficient for the inter-rater agreement of strain parameters was also calculated.

RESULTS

In total 129 patients, the reference values of left ventricle (LV) were 48.90 ± 9.05 for radial, -22.30 ± 2.33 for circumferential and -19.76 ± 2.22 for longitudinal global strain. The reference values of right ventricle (RV) were 18.63 ± 6.52 for radial, -10.60 ± 3.33 for circumferential and -25.06 ± 3.01 for longitudinal global strain. The median FRS was 7 (interquartile range 4-11). The LV strain parameters were significantly associated with FRS in univariate linear regression analysis: radial strain, beta = -0.155, p = 0.002; circumferential strain, beta = 0.56, p = 0.005; longitudinal strain, beta = 0.423, p = 0.043. However, RV strain parameters were not significantly associated with FRS: radial strain, p = 0.74; circumferential strain, p = 0.76; longitudinal strain, p = 0.09. The iota coefficient of all strain parameters were 0.915 for LV (p < 0.001) and 0.715 for RV (p < 0.001), respectively.

CONCLUSION

We present the reference values of strain parameters of both ventricles in asymptomatic Asian subjects. In contrast to RV parameters, LV strain parameters assessed by CMR-TT show significant association with FRS.

CLINICAL RELEVANCE/APPLICATION

We suggest reference values of myocardial strain parameters of both LV and RV assessed by CMR-TT in asymptomatic subjects and LV strain parameters show significant association with Framingham risk scores.

SSK04-06 Cardiac Magnetic Resonance Using Late Gadolinium Enhancement Imaging and T1 Mapping Predicts Poor Outcome in Patients with Atrial Fibrillation after Catheter Ablation Therapy

Wednesday, Nov. 29 11:20AM - 11:30AM Room: S504AB

Participants

Julian A. Luetkens, MD, Bonn, Germany (Presenter) Nothing to Disclose Caroline A. Wolpers, Bonn, Germany (Abstract Co-Author) Nothing to Disclose Thomas Beiert, Bonn, Germany (Abstract Co-Author) Nothing to Disclose Hendrik Meendermann, Bonn, Germany (Abstract Co-Author) Nothing to Disclose Abou Daye Natalie, Bonn, Germany (Abstract Co-Author) Nothing to Disclose Vincent Knappe, Bonn, Germany (Abstract Co-Author) Nothing to Disclose Darius Dabir, Bonn, Germany (Abstract Co-Author) Nothing to Disclose Rami Homsi, Bonn, Germany (Abstract Co-Author) Nothing to Disclose Daniel Kuetting, MD, Bonn, Germany (Abstract Co-Author) Nothing to Disclose Daniel K. Thomas, MD, PhD, Bonn, Germany (Abstract Co-Author) Nothing to Disclose Florian Stockigt, Bonn, Germany (Abstract Co-Author) Nothing to Disclose Markus Linhart, MD, Bonn, Germany (Abstract Co-Author) Nothing to Disclose Georg Nickenig, Bonn, Germany (Abstract Co-Author) Nothing to Disclose Hans H. Schild, MD, Bonn, Germany (Abstract Co-Author) Nothing to Disclose Jan W. Schrickel, Bonn, Germany (Abstract Co-Author) Nothing to Disclose Rene Andrie, Bonn, Germany (Abstract Co-Author) Nothing to Disclose

PURPOSE

Success rates for ablation therapy in patients with atrial fibrillation (AF) vary widely and patient selection criteria are poorly defined. We aimed to determine the pre-procedural value of cardiac magnetic resonance (CMR) and laboratory biomarkers of fibrosis for the prediction of poor response to ablation therapy.

METHOD AND MATERIALS

Left atrial (LA) late gadolinium enhancement (LGE) and LA T1 mapping were performed during pre-procedural CMR. Patients were categorized by four different fibrosis stages based on the percentage of LA wall enhancement on LGE-CMR (Utah stages I-IV). Plasma levels of relaxin and myeloperoxidase (MPO) and serum levels of MMP-mediated cardiac specific titin (TIM) and MMP-mediated collagen type IV (C4M) were obtained prior to ablation therapy. Poor outcome was defined by the reoccurrence of AF during 1-year follow-up (90 days blanking period). Univariate and multivariate cox proportional-hazards regression was used to identify significant predictors of AF recurrence.

RESULTS

A total of 61 patients were included in this prospective study (mean age: 60.3 + 12.5 years, 65.6% male). After 1-year follow-up AF reoccurred in 20 (32.8%) of all patients. Patients with a reoccurrence of AF showed a higher mean percentage of LA wall enhancement ($26.7 \pm 12.5\%$ vs. $17.0 \pm 7.7\%$; P<0.001), higher LA T1 relaxation times (857 ± 112 ms vs. 747 ± 91 ms; P<0.001), and higher plasma level of relaxin (0.7 ± 1.4 pg/ml vs. 0.4 ± 0.9 pg/ml; P=0.010). No significant differences were found in plasma concentrations of MPO and serum concentrations of TIM and C4M. In a multivariate analysis, poor ablation outcome was best predicted by advanced fibrosis stage (stage III and IV) (hazard ratio 5.487; P=0.001) and higher T1 relaxation times (hazard ratio 1.007; P=0.001). Plasma relaxin was not an independent predictor of poor outcome.

CONCLUSION

Pre-procedural CMR is a valuable tool for prediction of poor response to catheter ablation therapy in patients with AF. It offers various imaging techniques for outcome prediction and might be valuable for a better patient selection prior to ablation therapy.

CLINICAL RELEVANCE/APPLICATION

Pre-procedural CMR using LGE and T1 mapping might be useful for the prediction of poor response of patients with AF undergoing ablation therapy.

SSK04-07 Association between Abdominal Adiposity and Subclinical Measures of Left-Ventricular Remodeling and Diastolic Dysfunction in Diabetics, Prediabetics and Normal Controls without History of

Cardiovascular Disease as Measured by MR Imaging

Wednesday, Nov. 29 11:30AM - 11:40AM Room: S504AB

Participants

Carolyn Arndt, Heidelberg, Germany (*Abstract Co-Author*) Nothing to Disclose Roberto Lorbeer, Greifswald, Germany (*Abstract Co-Author*) Nothing to Disclose Sigrid Auweter, Munich, Germany (*Abstract Co-Author*) Nothing to Disclose Juergen Machann, MD, Tuebingen, Germany (*Abstract Co-Author*) Nothing to Disclose Holger Hetterich, MD, Munich, Germany (*Abstract Co-Author*) Nothing to Disclose Wolfgang Rathmann, Duesseldorf, Germany (*Abstract Co-Author*) Nothing to Disclose Hans-Ulrich Kauczor, MD, Heidelberg, Germany (*Abstract Co-Author*) Nothing to Disclose Hans-Ulrich Kauczor, MD, Heidelberg, Germany (*Abstract Co-Author*) Research Grant, Siemens AG; Research Grant, Bayer AG; Speakers Bureau, Boehringer Ingelheim GmbH; Speakers Bureau, Siemens AG; Speakers Bureau, Koninklijke Philips NV; Speakers Bureau, Bracco Group; Speakers Bureau, AstraZeneca PLC; Annette Peters, Neuherberg, Germany (*Abstract Co-Author*) Nothing to Disclose Fabian Bamberg, MD, MPH, Tuebingen, Germany (*Abstract Co-Author*) Speakers Bureau, Bayer AG; Speakers Bureau, Siemens AG; Research Grant, Siemens AG; Christonbar L, Schlett MD, MPH, Heidelberg, Germany (*Persenter*) Nothing to Disclose

Christopher L. Schlett, MD, MPH, Heidelberg, Germany (Presenter) Nothing to Disclose

For information about this presentation, contact:

carolyn.arndt@med.uni-heidelberg.de

PURPOSE

Local, abdominal fat depots may be related to alterations in cardiac function and morphology due to a metabolic linkage, which could be further accelerated in diabetic patients. Therefore we aimed to determine their association with subtle cardiac changes and the potential interaction with hyperglycemic metabolic states.

METHOD AND MATERIALS

Subjects from the general population without history of cardiovascular disease (CVD) underwent 3 Tesla cardiac and body magnetic resonance imaging. Measures of abdominal adiposity such as hepatic proton-density fat fraction (PDFFhepatic), subcutaneous (SAT) and visceral abdominal fat (VAT) as well as established cardiac LV measures including LV remodeling index (LVCI) were derived. Associations and interactions were determined using linear regression analysis based on standard deviation normalized predictors.

RESULTS

Among 374 subjects (56.2 \pm 9.1 years, 58% males), 49 subjects had diabetes, 99 subjects had prediabetes and 226 represented normal controls. Only subtle cardiac alterations were observed (e.g. LVCI: 1.13 \pm 0.30). In multivariable analysis, VAT and PDFFhepatic were independent predictors of increased LVCI (β =0.11 and 0.06, respectively), decreased LV end-diastolic volume (β =-6.70 and 3.23, respectively), and LV stroke volume (β =-3.91 and -2.20, respectively). In contrast, SAT was not associated. Hyperglycemic state or HbA1c-levels did not modify the associations between VAT or PDFF and LV measures (interaction term: all p>=0.29)

CONCLUSION

Particularly VAT, but also fatty liver are independently and incrementally associated with early LV remodeling and diastolic dysfunction in a general western population without history of CVD. Although a metabolic connection is suggestive, no interaction with the diabetic status was revealed for these important associations.

CLINICAL RELEVANCE/APPLICATION

Since LV remodeling and diastolic dysfunction is a precursor of heart failure and worse outcome, imaging-based quantification of VAT or fatty liver in patients without previous CVD could improve risk stratification and thus preventive medicine to avoid complications from heart failure in a very early state.

SSK04-08 Aortic Dimensions and Subclinical Atherosclerosis in Former National Football League Athletes

Wednesday, Nov. 29 11:40AM - 11:50AM Room: S504AB

Participants

Christopher Maroules, MD, Portsmouth, VA (*Presenter*) Nothing to Disclose David Carruthers, Dallas, TX (*Abstract Co-Author*) Nothing to Disclose Parag Joshi, Dallas, TX (*Abstract Co-Author*) Nothing to Disclose Colby Ayers, MS, Dallas, TX (*Abstract Co-Author*) Nothing to Disclose James Gentry, Carrollton, VA (*Abstract Co-Author*) Nothing to Disclose Rory Hachamoitch, Carrollton, VA (*Abstract Co-Author*) Nothing to Disclose Andrew Lincoln, Carrollton, VA (*Abstract Co-Author*) Nothing to Disclose Dermot Phelan, Cleveland, OH (*Abstract Co-Author*) Nothing to Disclose

For information about this presentation, contact:

christopher.maroules@gmail.com

PURPOSE

To evaluate whether past participation in the National Football League (NFL) is associated with increased prevalence of ascending aortic dilation and coronary artery calcium (CAC) on cardiac CT.

METHOD AND MATERIALS

This is a retrospective, cross-sectional study of 206 former National Football League (NFL) athletes compared with 759 matched male subjects from the XXX Heart Study (XHS) older than 40 years old with body mass index \geq 20 kg/m². Mid-ascending aortic dimensions were obtained from non-contrast, multidetector cardiac-gated CT scans performed as part of a screening protocol (NFL)

or as part of the XHS. CAC scores were obtained using the Agatston method. Multivariate logistic regression was performed to evaluate predictors of aortic size > 4.0 cm, CAC>0, and CAC>100 in each cohort.

RESULTS

Compared to the control group, former NFL athletes had significantly larger ascending aortic diameters (3.8 ± 0.5 vs. 3.4 ± 0.4 cm; p<0.0001). A significantly higher proportion of former NFL players had an aorta of >4.0 cm (29.6% versus 8.6%, p<0.0001). After adjusting for age, race, body surface area, systolic blood pressure, history of hypertension, current smoking, diabetes, and lipid profile the former NFL players still had significantly larger ascending aortas (p<0.0001). Former NFL players were twice as likely to have an aorta > 4.0 cm after adjusting for the same parameters. CAC scores were similar in both groups as was the distribution across CAC score categories (CAC=0, 1-100, and >100).

CONCLUSION

While CAC scores are similar between former NFL athletes and controls, ascending aortic dimensions are significantly larger in former NFL athletes even after accounting for their size, age and cardiac risk factors. Whether this translates to an increased risk is unknown and requires further evaluation.

CLINICAL RELEVANCE/APPLICATION

Past exposure to the hemodynamic effects of repetitive strenuous exercise among elite athletes may have lasting effects on aortic dimensions.

SSK04-09 Diagnostic Value of Cardiac Magnetic Resonance Imaging for Cardiac Mass in Children

Wednesday, Nov. 29 11:50AM - 12:00PM Room: S504AB

Participants

Rong-Zhen Ouyang, MD, Shanghai, China (*Presenter*) Nothing to Disclose Ai-Min Sun, MD, Shanghai, China (*Abstract Co-Author*) Nothing to Disclose Qian Wang, Shanghai, China (*Abstract Co-Author*) Nothing to Disclose Li Wei Hu, BEng, Shanghai, China (*Abstract Co-Author*) Nothing to Disclose Xiao Fen Yao, MENG, Shanghai, China (*Abstract Co-Author*) Nothing to Disclose Yumin Zhong, MD, Shanghai, China (*Abstract Co-Author*) Nothing to Disclose

For information about this presentation, contact:

oyrongzhen@163,com

PURPOSE

The aim of this study is to evaluate the diagnostic value of cardiac magnetic resonance imaging(CMR) for cardiac mass in children.

METHOD AND MATERIALS

One hundred and eleven patients who were diagnosed cardiac mass by echocardiography were recommended to perform cardiac MRI from September 2006 to August 2016. Fifty patients (34 boys and 16 girls) who underwent both cardiac MRI, echocardiography and had histopathologic results or confirmed based on clinical diagnosis were enrolled in this study. Patient age ranged from 0.2 months to 183.2 months and the median age was 44.7 months (3.7y). All MRI examinations were performed on a 1.5 T clinical MRI system. A cine balanced steady-state free procession (b-SSFP) imaging, T1and T2 weighted imaging, first-pass perfusion (resting) imaging, post gadolinium T1W and late gadolinium-enhanced imaging were included in the scanning protocol. The characteristics of cardiac masses were reviewed, and the location of cardiac mass was identified. The comparison of diagnostic accuracy between echocardiography and cardiac MR using Chi-square was made.

RESULTS

Thirty-two cases(32/50) were confirmed by histopathologic results and in which twenty-three cases were correctly diagnosed by cardiac MRI, eighteen cases(18/50) were diagnosed based on clinical evidence and in which fourteen cases were correctly diagnosed by cardiac MRI. Benign tumors accounted for 86%(43/50) and malignant tumor accounted for 14%(7/50). Cardiac mass could be located in any part of heart (chamber, wall and epicardium) and most cardiac masses located in the ventricles and outflow tracts. Accurate rate of echocardiography for cardiac mass is 100% (but no characteristic diagnosis except myxoma). Accurate rate of echocardiography for mass characteristics is 6% (3/50) and accurate rate of CMR for mass characteristics is 74% (37/50). CMR provided significantly higher accuracy of pathologic diagnoses compared to echocardiography (p <0.0001).

CONCLUSION

CMR imaging is becoming a major imaging modality for assessment of cardiac mass in children and can provide the tissue characteristics and have higher accuracy for diagnosis of cardiac mass in children.

CLINICAL RELEVANCE/APPLICATION

Cardiac mass is rare in children. The imaging modalities for it mainly include echocardiography and CMR. CMR can provide accurate characteristics and is becoming a major modality for assessment.





103rd Scientific Assembly and Annual Meeting November 26 to December 1 McCormick Place, Chicago



SSK05

Science Session with Keynote: Chest (Diffuse Lung Disease)

Wednesday, Nov. 29 10:30AM - 12:00PM Room: S404CD



AMA PRA Category 1 Credits ™: 1.50 ARRT Category A+ Credit: 1.75

Participants

Jonathan D. Dodd, MD, Dublin 4, Ireland (*Moderator*) Nothing to Disclose Seth J. Kligerman, MD, Denver, CO (*Moderator*) Nothing to Disclose

Sub-Events

SSK05-01 Chest Keynote Speaker: Current Challenges in ILD Analysis

Participants Joseph Jacob, MBBS, MRCP, Rochester, MN (*Presenter*) Consultant, Boehringer Ingelheim GmbH

For information about this presentation, contact:

joseph.jacob@nhs.net

SSK05-02 Assessment of Interstitial Lung Disease Using Lung Ultrasound Surface Wave Elastography (LUSWE) and Validation with Quantitative CT and Pulmonary Function

Wednesday, Nov. 29 10:40AM - 10:50AM Room: S404CD

Participants

Brian J. Bartholmai, MD, Rochester, MN (*Presenter*) License agreement, ImBio, LLC Scientific Advisor, ImBio, LLC Ryan Clay, MD, Rochester, MN (*Abstract Co-Author*) Nothing to Disclose Boran Zhou, PhD, Rochester, MN (*Abstract Co-Author*) Nothing to Disclose Thomas G. Osborn, MD, Rochester, MN (*Abstract Co-Author*) Nothing to Disclose James Greenleaf, Rochester, MN (*Abstract Co-Author*) Nothing to Disclose Sanjay Kalra, MD, Rochester, MN (*Abstract Co-Author*) Nothing to Disclose Xiaoming Zhang, PhD, Rocehster, MN (*Abstract Co-Author*) Nothing to Disclose

For information about this presentation, contact:

bartholmai.brian@mayo.edu

PURPOSE

Lung ultrasound surface wave elastography (LUSWE) may be useful for assessing interstitial lung disease (ILD) as LUSWE measures superficial lung tissue properties. We investigated surface wave speed in ILD and compared results to pulmonary function and quantitative parenchymal features.

METHOD AND MATERIALS

77 subjects with connective tissue disease and 19 healthy, never-smoking volunteers had PFTs within one year of LUSWE. All controls and 54 subjects had CT within 1 year of LUSWE. LUSWE measures are performed in seated upright at full inspiration. A 0.1s vibration at 100 Hz, 150 Hz, and 200 Hz is generated using a handheld indenter, and velocity is measured with an ultrasound probe at the same intercostal space. Bilateral upper lungs were measured anteriorly, mid-lungs laterally and lower lungs posteriorly. CALIPER (computer-aided lung informatics for pathology evaluation and rating) determined percent parenchymal interstitial abnormalities in a 15mm diameter hemisphere in CT regions studied by LUSWE. Categorical data were compared by chi square and continuous data by Wilcoxon Rank Sum.

RESULTS

The cases were significantly older (p < 0.0001) with a higher BMI (p = 0.05) and no difference in sex. Cases had lower FEV1 and FVC (p < 0.0001). Sonographic velocities were higher in all lung regions at all frequencies for cases, however the difference was greatest in the mid-lung at the 200Hz frequency. Median velocity in m/s was 5.84 vs 4.11 and 5.96 vs. 4.27 (p < 0.0001) for case vs. control, left and right middle lung zones, respectively (see Table 1). LUSWE in the right mid-lung negatively correlated with FVC (R = -0.23, 95% CI -0.42 - -0.03) and also positively correlated with CALIPER percent ILA (R = 0.35, 95% CI 0.12 - 0.53). Nominal logistic regression was used in univariate analysis and found that mid-lung LUSWE at 200Hz was predictive of CT-ILD with an AUC of 0.94, p < 0.0001. A multivariate model including age was predictive with AUC of 0.96. For a model including right mid-lung LUSWE velocity at 200Hz, right lower %ILA, FVC and age to predict CT-ILD, the AUC approached 100.

CONCLUSION

LUSWE is a safe and noninvasive technique that may be useful for assessing the presence of ILD and correlates with function and quantitative CT.

CLINICAL RELEVANCE/APPLICATION

LUSWE could potentially be used as a screening tool to detect ILD in patients at risk without use of ionizing radiation or functional

testing.

SSK05-03 Reduced Lung Elasticity in Female Patients with Interstitial Lung Disease: Histogram Analysis and Comparison with Age, Sex-Matched Normal Controls

Wednesday, Nov. 29 10:50AM - 11:00AM Room: S404CD

Participants

Junghoan Park, MD, Seoul, Korea, Republic Of (*Presenter*) Nothing to Disclose Soon Ho Yoon, MD, Seoul, Korea, Republic Of (*Abstract Co-Author*) Nothing to Disclose Jin Mo Goo, MD, PhD, Seoul, Korea, Republic Of (*Abstract Co-Author*) Research Grant, Samsung Electronics Co, Ltd; Research Grant, DRTECH Co, Ltd Helen Hong, PhD, Seoul, Korea, Republic Of (*Abstract Co-Author*) Nothing to Disclose Julip Jung, MS, Seoul, Korea, Republic Of (*Abstract Co-Author*) Nothing to Disclose Jeong-Hwa Yoon, Seoul, Korea, Republic Of (*Abstract Co-Author*) Nothing to Disclose

PURPOSE

To evaluate lung elasticity at the level of vital capacity in female patient with interstitial lung disease (ILD) using a histogram analysis by image registration of paired full inspiratory and expiratory CT scans.

METHOD AND MATERIALS

A total of 16 female patients with ILD and 8 age- and sex-matched normal controls who underwent paired CT scans at full inspiration and full expiration were included. Initially, the paired segmented CT images were aligned using surface-based affine registration. Second, landmark-based registration was sequentially performed using bronchial and pulmonary vascular landmarks (31 to 34 branching points of bronchus and peripheral pulmonary vessel for each lung) which were marked manually by one radiologist using in-house software. Then, lung attenuation-based deformable registration was applied. We obtained the x-, y-, z-axis and 3D distance of movement (mm) of each pixel for image registration between inspiration and expiration CT scans. Histogram analysis of those distances was performed in each axis. Nonparametric repeated-measures ANOVA was used for comparison and Spearman's correlation coefficient was used to assess relationships between the distance of movement and visual fibrosis score and pulmonary function test (PFT) results.

RESULTS

Mean distance error was 1.72 ± 1.32 mm in whole lung. Mean 3D distance of movement was significantly lower in the patient group (27.4 mm vs. 41.8 mm; p=.017), as well as percentile values of 3D distance of movement from 10th to 95th percentile (p<.05). Standard deviation (SD) and Entropy of 3D distance of movement were also significant lower in patient group (p=.017). When analyzed for each axis, mean, SD, entropy and 20th to 95th percentile of distance of movement were significantly lower in the patient group for y-axis (p<.05). The same trend was also observed for x- and z-axis, although not statistically significant. When compared with PFT results, forced vital capacity (FVC) showed significant positive correlation (R2=.271; p=.039) with mean 3D distance of movement.

CONCLUSION

Lung elasticity was significantly decreased in terms of absolute value and heterogeneity at the level of vital capacity in ILD patients.

CLINICAL RELEVANCE/APPLICATION

Decreased lung elasticity in ILD patients can be evaluated quantitatively by full inspiratory and expiratory CT scan, and it can be a potential biomarker of ILD with future investigation.

SSK05-04 HRCT Texture Feature Selection and Imaging Pattern Prediction of IPF using Quantum Particle Swarm Optimization

Wednesday, Nov. 29 11:00AM - 11:10AM Room: S404CD

Participants

Yu Shi, Los Angeles, CA (*Presenter*) Nothing to Disclose Jonathan G. Goldin, MBChB, PhD, Los Angeles, CA (*Abstract Co-Author*) Nothing to Disclose Weng Kee Wong, Los Angeles, CA (*Abstract Co-Author*) Nothing to Disclose Joshua Lai, Los Angeles, CA (*Abstract Co-Author*) Nothing to Disclose Matthew S. Brown, PhD, Los Angeles, CA (*Abstract Co-Author*) Nothing to Disclose Hyung J. Kim, PhD, Los Angeles, CA (*Abstract Co-Author*) Research Consultant, MedQIA

For information about this presentation, contact:

nicoleshi@ucla.edu

PURPOSE

Idiopathic Pulmonary Fibrosis (IPF) is a fatal lung disease with a heterogeneous natural history. Some predictive clinical models have been developed but few incorporate High-resolution Computed Tomography (HRCT) information. We propose an algorithm leveraging HRCT imaging data to build a model that predicts IPF progression at an early stage.

METHOD AND MATERIALS

We collect anonymized longitudinal serial volumetric HRCT scans from patients with IPF. Radiologists visually contoured regions of interest (ROI) and annotated lung morphology types into progression or non-progression, at the previous visits before the changes occurred. Within ROIs at baseline, 71 imaging texture features were extracted from the grid sampled voxels. Quantum particle swarm optimization (QPSO) was used to select important features, coupled with a resampling technique and random forest. In QPSO algorithm, particles iteratively search the space and communicate within swarm so that important features can be found quickly. QPSO was inspired by quantum mechanics in physics and it exhibits superior searching capabilities by using an iterative probability density function. We utilize QPSO to search the feature space and build a random forest classifier based on the QPSO selected features.

RESULTS

The algorithm yields an interpretable model with 19 texture features and achieves 77.27% sensitivity, 85.15% specificity and 83.74% accuracy at ROI level on test set in predicting progression of 6 months to 1 year follow-ups. Compared to other state-of-the-art algorithms, our approach selects a smaller feature subset, has higher prediction accuracy and achieves more balanced classification.

CONCLUSION

We propose an integrated feature selection and pattern recognition algorithm powered by QPSO that achieves superior prediction performance. The algorithm is widely extensible and has great potentials on offering IPF patients timely treatments as HRCT is inherent to the diagnosis of IPF.

CLINICAL RELEVANCE/APPLICATION

Idiopathic pulmonary fibrosis exhibits a heterogeneous natural history. We build a predictive model to anticipate disease courses and help clinicians make timely decisions.

SSK05-05 Evaluating Treatment Response in Patients with Systemic Sclerosis and Diffuse Interstitial Lung Involvement: Quantitative CT as a New Outcome Measure

Wednesday, Nov. 29 11:10AM - 11:20AM Room: S404CD

Participants

Mariaelena Occhipinti, MD, Florence, Italy (*Presenter*) Consultant, ImBio, LLC Silvia Bosello, Rome, Italy (*Abstract Co-Author*) Nothing to Disclose Michael S. Westmore, PhD, Delafield, WI (*Abstract Co-Author*) Employee, ImBio, LLC Giuseppe Cicchetti, Rome, Italy (*Abstract Co-Author*) Nothing to Disclose Leuconoe G. Sisti, Rome, Italy (*Abstract Co-Author*) Nothing to Disclose Chiara De Waure, Rome, Italy (*Abstract Co-Author*) Nothing to Disclose Anna Rita Larici, MD, Rome, Italy (*Abstract Co-Author*) Nothing to Disclose

For information about this presentation, contact:

mariaelena.occhipinti@unifi.it

PURPOSE

To compare semi-quantitative analysis (semi-QA) and quantitative analysis (QA) in the evaluation of treatment response in patients with interstitial lung involvement in systemic sclerosis (SS).

METHOD AND MATERIALS

31 patients with interstitial lung involvement in SS underwent functional evaluation, echocardiography and chest CT scan before and after treatment with rituximab and common anti-inflammatory drugs. Two chest radiologists evaluated the CT scans in consensus for a semi-QA by applying the international Goh score at 5 lung levels. QA was performed by CALIPER, a lung texture analysis program quantifying the relative volume of Normal, Ground-glass(GG), Reticular, and Honeycombing patterns in the whole lungs. Data obtained from semi-QA and QA were compared and correlated with clinical data (Pearson correlation, intraclass correlation coefficient, t-test). Analysis of ROC curves was performed to assess the predictability of a decline in FVC>10% or DLco>15%, commonly used to define lung disease progression.

RESULTS

Most patients (23/31,74.2%) had diffuse disease.By analyzing all 62 CT scans semi-QA and QA had a good reproducibility (ICC:0.67) for GG and only weak (ICC:0.27) for Reticular.Correlations between FVC,TLC,RV,DLco,Kco and semi-QA scores were lower (r=0.3 to 0.4) than QA scores, all statistically significant with the strongest correlations for GG or GG+Reticular and FVC (both r=-0.71).A main pulmonary artery >29mm distinguished patients with higher QA scores in GG, Reticular, GG+Reticular (p<.001),while echographic PASP did not. Δ FVC had a weak correlation with Δ DLco(r=0.4).Semi-QA scores and QA scores were not accurate in predicting a decline in FVC>10%, DLco>15%,or both combined (AUC: 0.33 to 0.70,p>0.05).

CONCLUSION

 Δ FVC and Δ DLco reflect different aspects of disease progression, including impairment of volumes and diffusing capacity. QA allows an objective and reproducible evaluation of both aspects contemporary, quantifying changes in lung patterns during treatment follow-up and correlating with lung function and pulmonary hypertension better than semi-QA. QA is a promising imaging biomarker in evaluating treatment response in patients with SS to add to Δ FVC and Δ DLco, likewise recently recommended in IPF.

CLINICAL RELEVANCE/APPLICATION

QA can help multidisciplinary teams in daily practice in evaluating treatment response in SS patients with interstitial involvement.QA with its reproducibility is a promising outcome measure for RCT.

SSK05-06 Diagnostic Significance of Fibrotic CT Patterns Not Addressed in Current Guidelines

Wednesday, Nov. 29 11:20AM - 11:30AM Room: S404CD

Participants

Jonathan H. Chung, MD, Chicago, IL (*Presenter*) Nothing to Disclose Steven M. Montner, MD, Chicago, IL (*Abstract Co-Author*) Nothing to Disclose Ayodeji Adegunsoye, Chicago, IL (*Abstract Co-Author*) Nothing to Disclose Justin Oldham, Chicago, IL (*Abstract Co-Author*) Nothing to Disclose Aliya N. Husain, Chicago, IL (*Abstract Co-Author*) Nothing to Disclose Imre Noth, MD, Chicago, IL (*Abstract Co-Author*) Nothing to Disclose Imre Noth, MD, Chicago, IL (*Abstract Co-Author*) Speakers Bureau, Sumitomo Dainippon Pharma Co, Ltd Speakers Bureau, F. Hoffmann-La Roche Ltd Speakers Bureau, Boehringer Ingelheim GmbH Consultant, ImmuneWorks, Inc Consultant, Gilead Sciences, Inc Research Grant, F. Hoffmann-La Roche Ltd Research Grant, Boehringer Ingelheim GmbH Rekha Vij, Chicago, IL (*Abstract Co-Author*) Nothing to Disclose

Mary Strek, Chicago, IL (Abstract Co-Author) Nothing to Disclose

For information about this presentation, contact:

jonherochung@uchicago.edu

PURPOSE

A small but substantial proportion of CT scans in patients with pulmonary fibrosis cannot be classified using current guidelines. The purpose of this study was to assess the diagnostic significance of these "indeterminate" cases on CT relative to pathologic findings.

METHOD AND MATERIALS

Subjects with a multidisciplinary diagnosis of IPF, interstitial pneumonia with autoimmune features (IPAF), and hypersensitivity pneumonitis (HP); pathological data from open lung biopsy; and chest CT within one year of biopsy were included in the study. Chest CT scans were analyzed by 2 chest radiologists. Cases were classified as interstitial pneumonia (UIP), possible UIP, or inconsistent with UIP on chest CT as per guidelines. Cases which could not be confidently categorized using strict adherence to current guidelines were additionally annotated as "indeterminate" for subset analysis. Lung biopsies were read by a pathologist with expertise in the diagnosis of interstitial lung diseases.

RESULTS

CT UIP patterns were as follows: UIP (102, 39.4%), possible UIP (54, 21.0%), and inconsistent with UIP (103, 25.4%); 19 (11.9%) CT scans scored as possible UIP were also annotated as "indeterminate," mostly due to diffuse distribution in the axial and/or zonal planes. UIP, possible UIP, and inconsistent with UIP CT patterns were associated with pathological UIP in 90.2%, 81.5%, and 52.4% of subjects; respectively. Those with an "indeterminate" CT pattern showed UIP on pathology in 68.4% of cases, which was not statically different compared to the inconsistent with UIP group on CT (p=0.198) but was different from the CT UIP group (p=0.010). After exclusion of these cases, the high confidence possible UIP subset showed a UIP pattern on pathology in 88.6% of subjects, which was not statistically different compared to the UIP CT group (p=0.784) but did differ from the inconsistent with UIP group (p<0.001). The difference between pathology in the "indeterminate" and high confidence possible UIP CT patterns approached statistical significance (p=0.069).

CONCLUSION

There are a substantial number of cases which cannot be confidently categorized using current CT guidelines in IPF. These cases are often classified as possible UIP but differ from the high confidence cases of possible UIP in regard to their pathological UIP diagnosis.

CLINICAL RELEVANCE/APPLICATION

Our data suggests that a 4th UIP CT category may be necessary for optimal diagnosis in suspected IPF.

SSK05-07 Lung Density Analysis Using Quantitative Chest CT for Early Diagnosis of Chronic Lung Allograft Dysfunction (CLAD)

Wednesday, Nov. 29 11:30AM - 11:40AM Room: S404CD

Awards

Student Travel Stipend Award

Participants

Miho Horie, MSc, Toronto, ON (*Presenter*) Research Grant, Toshiba Medical Systems Corporation Pascal Salazar, Minnetonka, MN (*Abstract Co-Author*) Employee, Toshiba Medical Systems Corporation; Tomohito Saito, MD, PhD, Toronto, ON (*Abstract Co-Author*) Nothing to Disclose Tereza Martinu, Toronto, ON (*Abstract Co-Author*) Nothing to Disclose Shafique Keshavjee, MD, Toronto, ON (*Abstract Co-Author*) Nothing to Disclose Narinder S. Paul, MD, Toronto, ON (*Abstract Co-Author*) Research Grant, Toshiba Medical Systems Corporation; Research Grant, Carestream Health, Inc

For information about this presentation, contact:

miho.horie@uhn.ca

PURPOSE

CLAD and its sub-types, bronchiolitis obliterans syndrome (BOS) and restrictive allograft syndrome (RAS) limit long-term survival following lung transplantation (LTx). Early diagnosis may allow earlier intervention to improve ultimate prognosis. The purpose of this study was to investigate the utility of quantitative CT lung density analysis in early diagnosis of CLAD.

METHOD AND MATERIALS

A retrospective study was conducted of 82 patients having routine periodic surveillance with pulmonary function tests (PFT) and low dose CT (120kV, 25mAs) following LTx. CLAD was defined as FEV1 <80% of baseline. BOS was defined as CLAD with TLC >=90% and RAS was defined as CLAD with TLC <90%. For the CT analyses, following definitions were applied: pre-onset CT when FEV1 <=90% (pre-CLAD). Control (No-CLAD) CT was defined when FEV >90% without Tx lung complications on the latest CT. CT scans were evaluated for 30 single LTx (15 CLAD: 3 RAS and 12 BOS, 15 Control) and 52 bilateral LTx (29 CLAD:12 RAS and 17 BOS, 23 Control). The contributions of low and high-density from each lung were determined from a CT histogram. Nonparametric indices were calculated; including the right tail weight (rqw) and the left tail weight (lqw) of the CT density distribution as well as the ratio: log (rqw0.875/lqw0.125). The area under the Receiver Operating Characteristic curve (AUC) and the Mann-Whitney test were used to evaluate the significance of difference in the metric; log (rqw0.875/lqw0.125) between CLAD and No-CLAD patients before CLAD onset.

RESULTS

Comparison of single LTx: CLAD and No-CLAD, the AUC was 0.80 [95% CI: 0.62- 0.93] (Figure 1a). Bilateral LTx: RAS and No-CLAD, the AUC was 0.80 [95% CI: 0.63-0.91] (Figure 1b), and BOS and No-CLAD, the AUC was 0.78 [95% CI: 0.62-0.89] (Figure 1c). There was a statistical significance between CLAD, RAS, BOS vs No-CLAD (P < 0.05) for both single and bilateral LTx patients.

There was no statistical significance between single and bilateral No-CLAD, tail ratio (P=0.42).

CONCLUSION

Quantitative CT parameters derived from a lung density histogram may help early diagnosis of CLAD in patients with single and bilateral lung transplantation.

CLINICAL RELEVANCE/APPLICATION

A quantitative density metric for CLAD patients might improve early detection of CLAD. It can allow earlier intervention to influence patient management and help to improve clinical outcomes.

SSK05-08 Non-Contrast Computed Tomography in Asthmatics Shows That Sarcopenia Correlates Measured In the Paraspinous Muscle on Non-Contrast CT Is Inversely Correlated With IL-6 and Asthma Exacerbations: Results from the Severe Asthma Research Program

Wednesday, Nov. 29 11:40AM - 11:50AM Room: S404CD

Participants

Mark L. Schiebler, MD, Madison, WI (*Presenter*) Stockholder, Stemina Biomarker Discovery, Inc; Stockholder, HealthMyne, Inc; Michael Peters, MD, San Francisco, CA (*Abstract Co-Author*) Nothing to Disclose John Fahy, MD, San Francisco, CA (*Abstract Co-Author*) Nothing to Disclose Loren Denlinger, MD,PhD, Madison, WI (*Abstract Co-Author*) Nothing to Disclose Clara Chow, MD, Madison, WI (*Abstract Co-Author*) Nothing to Disclose Micheal Evans, PhD, Madison, WI (*Abstract Co-Author*) Nothing to Disclose Nizar Jarjour, MD, Madison, WI (*Abstract Co-Author*) Nothing to Disclose Sean B. Fain, PhD, Madison, WI (*Abstract Co-Author*) Research Grant, General Electric Company Research Consultant, Marvel Medtech, LLC

For information about this presentation, contact:

mschiebler@uwhealth.org

PURPOSE

We sought to determine if a novel imaging biomarker for sarcopenia, found on non contrast CT of the paraspinous musculature, had any relationship to interluekin-6 (IL-6) and asthma exacerbation.

METHOD AND MATERIALS

:This was an IRB approved and HIPAA compliant study involving 173 patients enrolled in the Severe Asthma Research Program. There were 21 normal volunteers, 72 non-severe asthmatics, and 79 severe asthmatics (age range 2 - 72 years). Each patient's diastolic blood pressure, BMI, total cholesterol, triglyceride levels, HDL, LDL, fasting glucose, IL-6 plasma levels, asthma exacerbation frequency and steroid dosage per day were recorded. Region-of-interest Hounsfield unit (HU) measurements were obtained in liver density (LD), trabecular density at vertebrae levels T12 and L1, and paraspinal muscle density. Kruskal-Wallis and Fisher's exact test were used (P<0.05) to compare groups for continuous and discrete variables, respectively.

RESULTS

. For males and females combined (and individually), patients with MetS had lower liver density than those without MetS. Severe and non-severe asthmatics had lower liver HU (p-value = 0.0097), lower trabecular HU (p-value = 0.0006), and lower paraspinal muscle HU (p-value = 0.00002) when compared with normal volunteers. Females had stronger correlations between MetS, asthma severity, and liver density than males. Steroid dosage per day did not correlate with liver density or MetS. A lower LD, lower T12 and L1 BMD, and lower PSMD was found in severe asthmatics. IL6 was strongly correlated with PSMD (Spearman r= -0.62, p< 0.0001) and moderately correlated with hepatic density (Spearman r = -0.35, p < 0.03) Ashtma exacerbations trended to be more common with progressive sarcopenia.

CONCLUSION

IL=6 is strongly correlated with PSMD. The presence of MetS was inversely related to vertebral body BMD and PSMD.. The use of inhaled or oral steroids was not found to be associated with MetS or LD, as there may not be a detectable dose-effect.

CLINICAL RELEVANCE/APPLICATION

A simple imaging biomarker for sarcopenia is now available from routine non contrast CT chest exams that is negatively correlated with IL-6. This is confirmatory evidence that the progressive deposition of intramuscular fat is detrimental to normal health and promotes an underlying increase in inflammatory cytokines.

SSK05-09 Low-dose CT Using Model Based Iterative Reconstruction at Chest Radiography Dose Levels: A Pilot Study in Patients with Cystic Fibrosis Undergoing Treatment with Ivacaftor (Kalydeco)

Wednesday, Nov. 29 11:50AM - 12:00PM Room: S404CD

Participants

Fiachra G. Moloney, MBBCh, MRCPI, Cork, Ireland (*Abstract Co-Author*) Nothing to Disclose Karl James, FFR(RCSI),FRCR, Cork, Ireland (*Presenter*) Nothing to Disclose Maria Twomey, MBChB, FFR(RCSI), Toronto, ON (*Abstract Co-Author*) Nothing to Disclose Niamh Moore, Cork, Ireland (*Abstract Co-Author*) Nothing to Disclose Owen J. O'Connor, MBBCh, Cork, Ireland (*Abstract Co-Author*) Nothing to Disclose Michael M. Maher, MD, FRCR, Cork, Ireland (*Abstract Co-Author*) Nothing to Disclose

PURPOSE

The purpose of this prospective feasibility study was to assess the utility of a modified low-dose CT thorax protocol reconstructed with Model Based iterative reconstruction (MBIR) for the surveillance of pulmonary disease in patients with cystic fibrosis (CF).

METHOD AND MATERIALS

Following institutional review board approval, 15 patients with CF underwent routine quarterly radiological follow-up with low-dose CT thorax for 12 months with a final low-dose CT thorax at 24 months following initiation of Ivacaftor therapy. A modified 7section, low-dose axial CT protocol reconstructed with adaptive statistical iterative reconstruction (IR) (LD-ASIR) was used for the first 12-month quarterly studies. A modified low-dose volumetric protocol reconstructed with model-based IR (LD-MBIR) was used at 24 months. The image quality of both techniques was assessed quantitatively and qualitatively by 2 experienced readers who also quantified disease severity using a validated scoring system (Bhalla score).

RESULTS

15 patients (7 female, 8 male) with a mean age of 26.5 ± 6.1 years of age were included in the study. No significant change was observed in mean Bhalla score over the study period (p=0.51). Body mass index and pulmonary function measures increased significantly after 1 and 2-years of treatment. LD-MBIR studies were performed at a significantly lower mean effective dose (0.09 ± 0.01 mSv) than LD-ASIR studies (0.10 ± 0.02 mSv)(p=0.02). Quantitative measures of image noise and signal-to-noise ratios did not differ significantly between each low-dose protocol. Subjective image assessment of mediastinal structures was significantly worse with the LD-MBIR studies compared to the modified LD-ASIR studies however diagnostic acceptability of lung assessment was similar in both imaging techniques.

CONCLUSION

The use of MBIR with a volumetric low-dose protocol enabled the acquisition of diagnostic quality lung CT images at a dose equivalent to that of a PA and lateral chest radiograph with the added advantage of full volumetric imaging of the entire lungs

CLINICAL RELEVANCE/APPLICATION

This LD MBIR technique provides full volumetric imaging of the lungs and allows earlier and more reliable detection of bronchiectasis, mucus plugging and other subtle findings than with chest radiography at similar radiation doses and is ideally suited for follow-up of younger patients with chronic lung conditions







SSK06

Science Session with Keynote: Gastrointestinal (Advanced Liver MRI Techniques)

Wednesday, Nov. 29 10:30AM - 12:00PM Room: E350

GI MR

AMA PRA Category 1 Credits ™: 1.50 ARRT Category A+ Credit: 1.75

Participants

Hersh Chandarana, MD, New York, NY (*Moderator*) Equipment support, Siemens AG; Software support, Siemens AG; Advisory Board, Siemens AG;

Kathryn J. Fowler, MD, Saint Louis, MO (Moderator) Nothing to Disclose

Scott B. Reeder, MD, PhD, Madison, WI (*Moderator*) Institutional research support, General Electric Company; Institutional research support, Bracco Group; Founder, Calimetrix, LLC; Shareholder, Elucent Medical

Sub-Events

SSK06-01 Gastrointestinal Keynote Speaker: Advances in Liver MRI Techniques

Participants

Scott B. Reeder, MD, PhD, Madison, WI (*Presenter*) Institutional research support, General Electric Company; Institutional research support, Bracco Group; Founder, Calimetrix, LLC; Shareholder, Elucent Medical

SSK06-02 Compressed-Sensing Accelerated Isotropic 3D MRCP: Feasibility Study in Patients with Pancreatobiliary Disorders

Wednesday, Nov. 29 10:40AM - 10:50AM Room: E350

Participants

Liang Zhu, MD, Beijing, China (*Presenter*) Nothing to Disclose Huadan Xue, MD, Beijing, China (*Abstract Co-Author*) Nothing to Disclose Zhao Yong Sun, Beijing, China (*Abstract Co-Author*) Nothing to Disclose Dong Liu, Beijing, China (*Abstract Co-Author*) Nothing to Disclose Tianyi Qian, PhD, Beijing, China (*Abstract Co-Author*) Nothing to Disclose Elisabeth Weiland, Erlangen, Germany (*Abstract Co-Author*) Employee, Siemens AG Zheng Yu Jin, MD, Beijing, China (*Abstract Co-Author*) Nothing to Disclose

For information about this presentation, contact:

zhuliang_pumc@163.com

PURPOSE

to prospectively compare image quality of compressed-sensing (CS) accelerated 3D MR cholangiopancreatography (MRCP) to conventional navigator-triggered (NT) 3D MRCP, in patients with pancreatobiliary disorders.

METHOD AND MATERIALS

Sixty-two patients (38 men and 24 women, median age, 56 years, range, 24-84 years) underwent 3D MRCP at 3T. Three protocols were performed in each patient: a CS-accelerated breath-hold (BH) protocol based on a prototype sequence; a CS-accelerated NT protocol based on a prototype sequence, and a conventional NT protocol. Acquisition time of each protocol was recorded. Image quality of predefined segments of the pancreatobiliary tree was rated on a 5-point scale by two radiologists independently, who were blinded to the acquisition protocols.

RESULTS

Acquisition time for the CS-BH protocol was 17 seconds, for CS-NT was 134.1 ± 33.5 seconds, both significantly shorter than the conventional NT protocol (364.7 ± 78.4 seconds, both p<0.01). Severe respiratory motion artifacts was significantly reduced with the CS- BH protocol (4.8%, compared to 11.3% and 16.1% for CS-NT and conventional NT protocol, respectively), while overall image quality of the biliary tree was higher(p<0.05, compared to both NT protocols). However, CS-BH was less efficient in depicting pancreatic ducts. Overall image quality of the pancreatic duct was better with the CS-NT protocol (p<0.05, compared to CS-BH and conventional NT protocols). Acceptable or better image quality (score>=3) of the entire pancreatic duct (head, body and tail) was achieved in 90.9% patients with CS-NT, 78.2% with CS-BH, and in 83.6% with conventional NT protocol. Acceptable or better image quality for the entire pancreatobiliary tree was achieved with in 95.2% patients with CS-BH +CS-NT protocol, compared to 82.3% with the conventional NT protocol.

CONCLUSION

CS-accelerated 3D MRCP is feasible in routine patients. The protocol is time-efficient and overall image quality is superior than the conventional approach.

CLINICAL RELEVANCE/APPLICATION

CS-accelerated BH and NT 3D MRCP are both feasible in clinical routine. CS-BH-MRCP is free from respiratory movement artifacts and has better image quality for the biliary tree. CS-NT-MRCP can be used to assess pancreatic ducts, when they are not

adequately depicted with CS-BH. The combined CS-BH and CS-NT protocol achieves high success rate for imaging the entire pancreaticobiliary tree, while the acquisition time is still reduced.

SSK06-03 Evaluation of HCC Response to Locoregional Therapy: Validation of MRI-Based Response Criteria Against Explant Pathology

Wednesday, Nov. 29 10:50AM - 11:00AM Room: E350

Participants

Sonja Gordic, MD, New York, NY (*Presenter*) Nothing to Disclose Idoia Corcuera-Solano, MD, New York, NY (*Abstract Co-Author*) Nothing to Disclose Ashley Stueck, MD, New York, NY (*Abstract Co-Author*) Nothing to Disclose Cecilia Besa, MD, New York, NY (*Abstract Co-Author*) Nothing to Disclose Pamela A. Argiriadi, MD, New York, NY (*Abstract Co-Author*) Nothing to Disclose Preethi Guniganti, MD, New York, NY (*Abstract Co-Author*) Nothing to Disclose Michael J. King, MD, New York, NY (*Abstract Co-Author*) Nothing to Disclose Shingo Kihira, BS, New York, NY (*Abstract Co-Author*) Nothing to Disclose James S. Babb, PhD, New York, NY (*Abstract Co-Author*) Nothing to Disclose Swan Thung, New York, NY (*Abstract Co-Author*) Nothing to Disclose Bachir Taouli, MD, New York, NY (*Abstract Co-Author*) Nothing to Disclose

PURPOSE

To evaluate the performance of various magnetic resonance imaging (MRI) response criteria for the prediction of complete pathologic necrosis (CPN) of hepatocellular carcinoma (HCC) post locoregional therapy (LRT) using explant pathology as reference.

METHOD AND MATERIALS

We included 61 patients (M/F 46/15, mean age 60y) who underwent liver transplantation after LRT with transarterial chemoembolization plus radiofrequency or microwave ablation (n=56), or 90Yttrium radioembolization (n=5). MRI was performed within 90 days of liver transplantation. Three independent readers assessed the following criteria: RECIST, EASL, mRECIST, percentage of necrosis on subtraction images, and diffusion-weighted imaging (DWI) [qualitative (signal intensity) and quantitative (apparent diffusion coefficient, ADC)]. Degree of necrosis was retrospectively assessed at histopathology. Intraclass correlation coefficient (ICC) and Cohen's kappa were used to assess inter-reader agreement. Logistic regression and ROC analyses were used to determine imaging predictors of CPN. Pearson correlation was performed between imaging criteria and pathologic degree of tumor necrosis.

RESULTS

97 HCCs (mean size 2.3 \pm 1.3 cm) including 28 with CPN were evaluated. There was excellent inter-reader agreement (ICC 0.77-0.86, all methods). EASL, mRECIST, percentage of necrosis and qualitative DWI were all significant (p<0.001) predictors of CPN, while RECIST and ADC were not. EASL, mRECIST and percentage of necrosis performed similarly (AUCs 0.810-0.815) while the performance of qualitative DWI was lower (AUC 0.622). Image subtraction demonstrated the strongest correlation (r=0.71-0.72, p<0.0001) with pathologic degree of tumor necrosis.

CONCLUSION

EASL/mRECIST criteria and image subtraction have excellent diagnostic performance for predicting CPN in HCC treated with LRT, with image subtraction correlating best with pathologic degree of tumor necrosis. Thus, MR image subtraction is recommended for assessing HCC response to LRT.

CLINICAL RELEVANCE/APPLICATION

Image subtraction is recommended for assessing HCC response to LRT when performing MRI. RECIST and ADC should not be used for prediction of CPN.

SSK06-04 Clinical Feasibility of Implementing DCE-MRI in Routine Liver MRI Using Golden-Angle Radial Sparse Parallel MRI: Preliminary Results

Wednesday, Nov. 29 11:00AM - 11:10AM Room: E350

Participants

Jeong Hee Yoon, MD, Seoul, Korea, Republic Of (*Presenter*) Grant, Bayer AG Speaker, General Electric Company Speaker, Koninklijke Philips NV Speaker, Bayer AG

Jeong Min Lee, MD, Seoul, Korea, Republic Of (*Abstract Co-Author*) Grant, Bayer AG; Grant, General Electric Company; Grant, Koninklijke Philips NV; Grant, STARmed Co, Ltd; Grant, RF Medical Co, Ltd; Grant, Samsung Electronics Co, Ltd; Grant, Guerbet SA;

Robert Grimm, Erlangen, Germany (Abstract Co-Author) Employee, Siemens AG

Robert Gillin, Endigen, Germany (Abstract Co-Adthor) Employee, Siemens AG

Berthold Kiefer, PhD, Erlangen, Germany (Abstract Co-Author) Employee, Siemens AG

Kai Tobias Block, PhD, New York, NY (Abstract Co-Author) Royalties, Siemens AG

Hersh Chandarana, MD, New York, NY (*Abstract Co-Author*) Equipment support, Siemens AG; Software support, Siemens AG; Advisory Board, Siemens AG;

PURPOSE

To investigate clinical feasibility of implementing dynamic contrast enhanced magnetic resonance imaging (DCE-MRI) in routine liver MRI using Golden-angle Radial Sparse Parallel (GRASP) MRI.

METHOD AND MATERIALS

In this IRB-approved ongoing prospective study, 25 patients who were scheduled for liver biopsy or resection have been enrolled and informed consent was obtained from all patients. Liver MRI was performed using incoherent undersampling technique at 3T. A standard dose of extracellular contrast media was injected, and T1-weighted images (T1WI) were obtained using incoherent undersampling technique in free-breathing. Images were reconstructed to achieve either 13.3- or 3.3-second time resolution. On 13.3-second time resolution T1WI with respiratory gating, motion and overall image quality were assessed on four-point scale by two radiologists in consensus, and 3.3-second time resolution T1WI was analyzed using software of dual-input single compartment

RESULTS

In 25 patients, motion artifact was 1.5 ± 0.5 , 2.1 ± 0.3 , 1.0 ± 0.3 and 1.0 ± 0.0 on pre, arterial, portal venous and delayed phase which indicated no significant motion artifact. Overall image quality was 3.9 ± 0.6 , 3.5 ± 0.5 , 3.9 ± 0.3 , and 3.8 ± 0.4 , respectively. In all patients, perfusion analysis was done successfully. After excluding one patient who was treated with chemoembolization, patients with advanced fibrosis (n=7, >=F2) showed substantially high arterial fraction (67.0±17.1%) than patients with no or early fibrosis (n=18, F0-1) who had arterial fraction of 44.7±27.6% (P<0.05).

CONCLUSION

GRASP technique allowed implementation of DCE in routine liver MRI by obtaining high time-resolution and sufficient spatial resolution.

CLINICAL RELEVANCE/APPLICATION

Implementation of DCE-MRI in routine MRI would facilitate its application for various organs and contribute to non-invasive diagnosis and monitoring by displaying hemodynamic information of lesions.

SSK06-05 An Experimental Study on the Assessment of Renal Fibrosis by Using Magnetic Resonance T1rho Imaging

Wednesday, Nov. 29 11:10AM - 11:20AM Room: E350

Participants

Genwen Hu, MD, Shenzhen, China (*Presenter*) Nothing to Disclose Jianming Xu, Shenzhen, China (*Abstract Co-Author*) Nothing to Disclose Xianyue Quan, MD, PhD, Guangzhou, China (*Abstract Co-Author*) Nothing to Disclose Liangping Luo, Guangzhou, China (*Abstract Co-Author*) Nothing to Disclose Yingjie Mei, Guangzhou, China (*Abstract Co-Author*) Nothing to Disclose

For information about this presentation, contact:

hugenwen@163.com

PURPOSE

To correlate magnetic resonance (MR) T1 relaxation time in the rotating frame (T1rho or T1p) with degree of renal fibrosis in a rat model of unilateral ureteral obstruction (UUO).

METHOD AND MATERIALS

This study was approved by the institutional animal care and use committee. UUO was created in each of 36 rats. UUO-A group with 6 rats, longitudinal T1rho value was performed before the UUO (day 0) and on days 1, 3, 5, 10, and 15 after the UUO and was followed by histopathologic analysis (one rat died on 11 days after the UUO). Six rats from UUO-B group (n = 30) were examined at each of five time points on days 0, 1, 3, 5 and 10 after the UUO. Four rats from Sham group (n = 12) were examined on days 1, 5, and 15 after UUO. Hematoxylin-eosin, Masson trichrome staining and a-smooth muscle actin (a-SMA) were performed. T1rho Sequences with Stretched adiabatic as Spin lock pulse type. Spin lock time: 1, 27, 54 ms,with 3.0T clinical MR scanner.

RESULTS

Histopathologic examination revealed typical renal fibrosis on the side with UUO. The T1rho values increased over time on the UUO side, Mean T1rho value with day 0, 1, 3, 5, 10, and 15 after the UUO were 142.23 ± 8.69 , 149.53 ± 9.38 , 172.53 ± 13.53 , 181.05 ± 17.34 , 216.31 ± 22.64 , 228.47 ± 26.95 ms, respectively. Sham rats were 140.28 ± 7.19 , 137.74 ± 9.38 , 138.89 ± 17.76 ms, respectively. Mean T1rho value associated positively (r =0.868 P < 0.001) with a-SMA expression level.

CONCLUSION

Our study shows that the degree of renal fibrosis was correlated with degree of increase with T1rho value in model induced by UUO.

CLINICAL RELEVANCE/APPLICATION

MR-T1rho may become a noninvasive imaging tool for the diagnosis of renal fibrosis.

SSK06-06 Histologic Characteristics of Hepatocellular Carcinoma with Irregular Rim-Like Arterial Phase Enhancement

Wednesday, Nov. 29 11:20AM - 11:30AM Room: E350

Participants

Hyungjin Rhee, MD, Seoul, Korea, Republic Of (*Presenter*) Nothing to Disclose Chansik An, MD, Seoul, Korea, Republic Of (*Abstract Co-Author*) Nothing to Disclose Hye-Young Kim, Seoul, Korea, Republic Of (*Abstract Co-Author*) Nothing to Disclose Jeong Eun Yoo, Seoul, Korea, Republic Of (*Abstract Co-Author*) Nothing to Disclose Young Nyun Park, MD, Seoul, Korea, Republic Of (*Abstract Co-Author*) Nothing to Disclose Myeong-Jin Kim, MD, PhD, Seoul, Korea, Republic Of (*Abstract Co-Author*) Nothing to Disclose

PURPOSE

To examine the histopathologic characteristics of hepatocellular carcinoma (HCC) with irregular rim-like arterial phase enhancement, which has been reported to be associated with more aggressive tumor behavior.

METHOD AND MATERIALS

Institutional review board approved this retrospective study and waived the informed consent. Our subjects were 84 pathologically

confirmed HCCs in 84 patients who underwent curative hepatic resection after gadoxetate-enhanced magnetic resonance (MR) imaging between January 2008 and February 2013. Two abdominal radiologists independently reviewed the MR images and classified HCCs into two categories: HCC showing irregular rim-like arterial enhancement (IRE-HCC) or HCC showing hypovascularity or diffuse arterial enhancement (non-IRE-HCC). We assessed and compared their clinical and pathologic characteristics, using a representative whole-section slide of each case. Differences in disease-free survival were analyzed using the Kaplan-Meier method with the log-rank test. The chi-square, Fisher exact test, or Mann-Whitney test was used to compare the variables.

RESULTS

Of the 84 HCCs, 22 and 51 were classified as IRE-HCCs and non-IRE-HCCs by both reviewers, respectively. Classification was discordant in the remaining 11 patients. IRE-HCC showed, compared to non-IRE-HCC, poorer five-year disease-free survival after curative resection (33.6% vs. 60.3%; P = .030), more frequent microvascular invasion (91% vs. 35%). IRE-HCCs were also associated with lower microvascular density (227 vs. 437 per mm2), more frequent sinusoidal microvascular pattern (55% vs. 0%), larger necrotic area (15% vs. 0%), and larger stromal area (8.3% vs. 2.2%), suggesting more hypoxic and fibrotic microenvironment, and exhibited higher expression of immunomarkers of hypoxia (CAIX, 64% vs. 8%) and stemness (K19 protein, 27% vs. 6%). P-values were < .001 for all comparisons except for K19 (P = .018). Discordant tumors showed intermediate features between IRE-HCC and non-IRE-HCC.

CONCLUSION

Irregular rim-like arterial enhancement of HCC is associated with hypoxic and fibrotic tumor microenvironment which are related with hypoxia and stemness marker expression and poor prognosis.

CLINICAL RELEVANCE/APPLICATION

IRE-HCCs may be associated with worse clinical outcome and histopathologic features related to aggressive biologic behavior, compared to non-IRE-HCCs.

SSK06-07 Impacts of Adding Recent CT Arterial Phase Images On Diagnostic Performances of Gadoxetic Acid-Enhanced MRI in Assessment of HCC

Wednesday, Nov. 29 11:30AM - 11:40AM Room: E350

Participants

Seungbaek Hong, MD, Pusan, Korea, Republic Of (*Presenter*) Nothing to Disclose So Yeon Kim, MD, Seoul, Korea, Republic Of (*Abstract Co-Author*) Nothing to Disclose Young-Suk Lim, Seoul, Korea, Republic Of (*Abstract Co-Author*) Nothing to Disclose Min-Ju Kim, Seoul, Korea, Republic Of (*Abstract Co-Author*) Nothing to Disclose Seung Soo Lee, MD, Seoul, Korea, Republic Of (*Abstract Co-Author*) Nothing to Disclose Seong Ho Park, MD, Seoul, Korea, Republic Of (*Abstract Co-Author*) Nothing to Disclose Grant, Central Medical Service Co, Ltd Moon-Gyu Lee, MD, Seoul, Korea, Republic Of (*Abstract Co-Author*) Nothing to Disclose

For information about this presentation, contact:

sykim.radiology@gmail.com

PURPOSE

To investigate impacts of adding recent CT arterial phase findings on diagnostic performances of gadoxetic acid-enhanced MRI in the assessment of hepatocellular carcinoma (HCC)

METHOD AND MATERIALS

We retrospectively identified 1272 patients (1026 men, 246 women; mean age, 56.6 years) with pathologically confirmed 1490 nodules (1370 HCCs, 60 dysplastic nodules, 39 combined HCC and cholangiocarcinomas, 13 cholangiocarcinomas, 8 nodules with other pathologies) between January 2008 and December 2016 with the following inclusion criteria: patients with chronic hepatitis or liver cirrhosis who had pathologically confirmed focal hepatic lesions; who underwent both multiphase CT and gadoxetic acid-enhanced MR I within 120 days before the pathologic exams; and the size of lesions <= 3 cm. We compared the enhancement patterns on arterial phase imaging between the two imaging modalities. The sensitivity and 95% confidence interval (C.I.) for detecting arterial hyperenhancement in patients with HCCs on a per-nodule basis was compared between the MRI only analyses and the CT+MRI analyses using generalized estimated equations based on a binary logistic regression model to account for data clustering and dependency, as some patients had more than one nodules.

RESULTS

The mean time interval between MRI and CT was 16.5 days. Among the 1490 nodules, 1361 nodules (91.3 %) had the same arterial enhancement patterns both on CT and MRI. In the remaining 129 nodules (105 HCCs and seven non-HCC lesions) with the different enhancement patterns between CT and MRI, arterial hyperenhancement was detected only by CT in the majority of cases (86.8%, 112/129). The sensitivity in detecting arterial hyperenhancement in HCC was significantly improved in the CT+MRI analyses (92.4 %; 95% C.I., 90.9 to 93.7) compared to the MRI only analyses (84.7 %; 95% C.I., 82.2 to 87.0) (P<0.001).

CONCLUSION

Adding recent CT arterial phase findings can improve the detection of arterial hyperenhancement of gadoxetic acid-enhanced MRI in the evaluation of HCC.

CLINICAL RELEVANCE/APPLICATION

Arterial phase findings on recent CT images can serve a substitute for suboptimal arterial phase MR images on gadoxetic acidenhanced MRI in the assessment of HCC.

SSK06-08 A Prospective and Long-Term Follow-Up Study of Non-Hypervascular Hypointense Nodules on the Hepatobiliary Phase of Gadoxetic Acid-Enhanced MRI

Tae Young Lee, MD, Seoul, Korea, Republic Of (*Presenter*) Nothing to Disclose So Yeon Kim, MD, Seoul, Korea, Republic Of (*Abstract Co-Author*) Nothing to Disclose Jae Ho Byun, MD, Seoul, Korea, Republic Of (*Abstract Co-Author*) Nothing to Disclose Min-Ju Kim, Seoul, Korea, Republic Of (*Abstract Co-Author*) Nothing to Disclose So Jung Lee, Seoul, Korea, Republic Of (*Abstract Co-Author*) Nothing to Disclose Hyung Jin Won, MD, Seoul, Korea, Republic Of (*Abstract Co-Author*) Nothing to Disclose Jihyun An, Seoul, Korea, Republic Of (*Abstract Co-Author*) Nothing to Disclose Young-Suk Lim, Seoul, Korea, Republic Of (*Abstract Co-Author*) Nothing to Disclose Seong Ho Park, MD, Seoul, Korea, Republic Of (*Abstract Co-Author*) Nothing to Disclose Seong Ho Park, MD, Seoul, Korea, Republic Of (*Abstract Co-Author*) Nothing to Disclose

For information about this presentation, contact:

sykim.radiology@gmail.com

PURPOSE

Participants

To investigate the incidence of non-hypervascular hypointense nodules on the hepatobiliary phase (HBP) of gadoxetic acidenhanced MRI and to identify the incidence of arterial hypervascular transformation and associated features in a prospective cohort with a long-term follow-up

METHOD AND MATERIALS

A prospective surveillance study included 407 cirrhosis patients at high risk for HCC who underwent one to three, biannual screening examinations with gadoxetic acid-enhanced MRI between November 2011 and August 2014. Among them, 40 patients were identified to have 63 hypovascular hypointense nodules on HBP of gadoxetic acid-enhanced MRI. Follow-up contrastenhanced MRI and CT were reviewed to identify hypervascular transformation (median follow-up period, 45 months). Univariate and multivariable Cox proportional hazards model with robust standard errors for clustered data were used to investigate the association between arterial hypervascular transformation and clinical and imaging features with respect to nodule size, signal intensity on T1-, T2-, diffusion-weighted, portal and delayed phase images, and intratumoral fat.

RESULTS

The incidence of non-hypervascular hypointense nodules on HBP in the prospective cohort was 9.8 % (40/407). On follow-up images, the 1-, 3-, and 5-year cumulative incidences of hypervascular transformation were 6.4, 12.8, and 24.3 %, respectively. Univariate analyses revealed the size >= 1cm and hyperintensity on T1-weighted images as significant risk factors for hypervascular transformation. According to the multivariable analysis, the size >= 1cm was independently associated with hypervascularization with a hazard ratio HR of 12.6 (P=.02). The 5 year-cumulative incidence of nodules >= 1cm in size (52.5%) was more than 10 folds compared to that of nodules smaller thant 1cm (4.4%).

CONCLUSION

Our study demonstrates the incidence of non-hypervascular hypointense nodules on HBP and hypervascular transformation in a prospective cohort. Non-hypervascular hypointense nodules >= 1cm in size are strongly associated with hypervascular transformation.

CLINICAL RELEVANCE/APPLICATION

Non-hypervascular hypointense nodules on HBP >= 1cm in size should be cautiously followed up with their culmulative incidence of hypervascular transformation in mind.

SSK06-09 High-Precision Computed Diffusion Weighted Images for the Diagnosis of Hepatocellular Carcinoma

Wednesday, Nov. 29 11:50AM - 12:00PM Room: E350

Participants

Motonori Akagi, MD, Hiroshima, Japan (*Presenter*) Nothing to Disclose Yuko Nakamura, MD, Hiroshima, Japan (*Abstract Co-Author*) Nothing to Disclose Toru Higaki, PhD, Hiroshima, Japan (*Abstract Co-Author*) Nothing to Disclose Makoto Iida, Hiroshima, Japan (*Abstract Co-Author*) Nothing to Disclose Masaaki Umeda, Otawara, Japan (*Abstract Co-Author*) Nothing to Disclose Masaaki Umeda, Otawara, Japan (*Abstract Co-Author*) Employee, Toshiba Medical Systems Corporation Kazuo Awai, MD, Hiroshima, Japan (*Abstract Co-Author*) Research Grant, Toshiba Corporation; Research Grant, Hitachi, Ltd; Research Grant, Bayer AG; Research Grant, Daiichi Sankyo, Ltd; Research Grant, Eisai, Ltd; Medical Adviser, GE Healthcare; Research Grant, Fujitsu Ltd; ; ; ; ; ;

PURPOSE

Diffusion-weighted images (DWI) obtained with higher b-values yield better contrast between tumor and background normal tissue. Computed DWI (c-DWI) can calculate high b-value images from DWI obtained at lower b-values. However, the image quality of c-DWI may be degraded due to mis-registration between image acquisitions with different b-values. We developed high-precision c-DWI (hc-DWI) in which mis-registration was reduced by applying non-rigid registration technique to real DWI (r-DWI) with different b values. We tested our hypothesis that hc-DWI can improve image quality in diagnosing hepatocellular carcinoma (HCC) compared to conventional c-DWI (cc-DWI).

METHOD AND MATERIALS

In 75 patients with HCCs we acquired r-DWIs with b-value at 150, 600, and 1000 s/mm2. We defined the r-DWI acquired with b = 1000 s/mm2 as standard. C-DWIs with b-value at 1500 s/mm2 were calculated with DWIs at b-values of 150 and 600 s/mm2. For generating hc-DWI we used a non-rigid image registration for avoiding mis-registration of two different b-value images and an image filter to remove abnormal values from the apparent diffusion coefficient map.Two radiologists evaluated the image quality of each DWI by consensus reading using a 3-point scale where 1 = poor (non-diagnostic), 2 = fair (diagnostic but blurred margin), 3 = good (good quality and sharp margin). They also evaluated the signal intensity of HCC using a 3-point score where 1 = not visible, 2 = discernible, and 3 = clearly visible and calculated the contrast ratio (CR) between HCC and the surrounding liver parenchyma.

RESULTS

Image quality was better with hc-DWI compared to cc-DWI (p < 0.01). The visual score of HCC was also better with hc-DWI compared to cc-DWI (p < 0.01). In addition, the CR for HCC was significantly higher in hc-DWI compared to cc-DWI (mean value: 2.6 and 2.1 for hc-DWI and cc-DWI, p < 0.01).

CONCLUSION

Image quality, subjective visual score, and CR of HCC was higher in hc-DWI compared to cc-DWI.

CLINICAL RELEVANCE/APPLICATION

Hc-DWI may be useful for characterization of HCC compared to cc-DWI.







SSK07

Science Session with Keynote: Gastrointestinal (Quantitative Imaging and Machine Learning)

Wednesday, Nov. 29 10:30AM - 12:00PM Room: E353A

BQ GI IN MR

AMA PRA Category 1 Credits ™: 1.50 ARRT Category A+ Credit: 1.75

FDA Discussions may include off-label uses.

Participants

Srinivasa R. Prasad, MD, Houston, TX (*Moderator*) Nothing to Disclose Aya Kamaya, MD, Stanford, CA (*Moderator*) Nothing to Disclose

Sub-Events

SSK07-01 Gastrointestinal Keynote Speaker: Is There a Role of Machine Learning in Oncology?

Participants

Garry Choy, MD, MS, Boston, MA (Presenter) Nothing to Disclose

SSK07-02 Machine Learning-Based Radiogenomics in Metastatic Colon Cancer: Association between Quantitative Tumor MRI Radiomic Features and KRAS Mutation Status

Wednesday, Nov. 29 10:40AM - 10:50AM Room: E353A

Participants

Dania Daye, MD, PhD, Boston, MA (*Presenter*) Nothing to Disclose Azadeh Tabari, Boston, MA (*Abstract Co-Author*) Nothing to Disclose Sophia C. Kamran, MD, Boston, MA (*Abstract Co-Author*) Nothing to Disclose Theodore S. Hong, MD, Boston, MA (*Abstract Co-Author*) Nothing to Disclose Michael S. Gee, MD, PhD, Jamaica Plain, MA (*Abstract Co-Author*) Nothing to Disclose

For information about this presentation, contact:

dania.daye@gmail.com

PURPOSE

Assessment of KRAS mutation status is essential for prognosis assessment and for guiding treatment decisions in patients with metastatic colon cancer. This study investigates the association between quantitative tumor MRI features and KRAS mutation status in this patient population.

METHOD AND MATERIALS

In this IRB-approved retrospective study, we identified 52 patients with stage 4 colon cancer with hepatic metastases reported on abdominal MRI studies performed from 2007-2013. KRAS mutation status was ascertained from the medical record. The largest hepatic lesion was identified on the portal venous phase T1-weighted fat-suppressed post-contrast images and manually segmented. MR radiomic feature vectors were extracted from each lesion using quantitative morphological and texture analysis. Univariate logistic regression analysis was used to assess for independent contribution of 18 extracted morphological features and 32 extracted texture features to mutation status prediction. A linear support vector machine (SVM) machine learning technique was applied to the extracted imaging phenotype vector to predict tumor mutation status. The classifier was trained and tested using 10-fold cross validation to avoid overfitting. ROC analysis and the area under the curve (AUC) were used to assess classification performance.

RESULTS

60% (19/31) of patients had tumors with KRAS mutations. Tumor circularity and tumor coarseness exhibited significant differences in mean values between KRAS-wildtype and KRAS-mutated tumors (p<0.001 and p=0.01, respectively). Univariate regression revealed six features independently association with KRAS mutation status: tumor circularity (p=0.003), solidity (p=0.006), eccentricity (p=0.03), coarseness (p=0.03), shade (p=0.01), and GLCM matrix standard deviation (p=0.04). A trained SVM model that included the tumor morphologic and texture features resulted in an area under the ROC curve of 0.95.

CONCLUSION

Quantitative tumor MRI features exhibit significant association with KRAS mutation and may contribute to predicting KRAS status in colon cancer patients.

CLINICAL RELEVANCE/APPLICATION

Tumor MRI radiomic analysis may aid in non-invasively assessing tumor genetic status and may aid in informing treatment choices and personalizing therapeutic decisions in patients with colon cancer.

SSK07-03 A Deep Neural Network for Liver Volumetry in Contrast Enhanced MRI

Awards Student Travel Stipend Award

Participants

Niklas Verloh, MD, Regensburg, Germany (*Presenter*) Nothing to Disclose Julian H. Juergens, Magdeburg, Germany (*Abstract Co-Author*) Nothing to Disclose Christian Hundt, DIPLPHYS, PhD, Mainz, Germany (*Abstract Co-Author*) Nothing to Disclose Kristina I. Ringe, MD, Hannover, Germany (*Abstract Co-Author*) Nothing to Disclose Lukas Beyer, MD, Regensburg, Germany (*Abstract Co-Author*) Nothing to Disclose Philipp Wiggermann, Regensburg, Germany (*Abstract Co-Author*) Nothing to Disclose Hinrich B. Winther, MD, Hannover, Germany (*Abstract Co-Author*) Nothing to Disclose

For information about this presentation, contact:

niklas.verloh@ukr.de

PURPOSE

To establish a fully automated, reliable, and novel liver volumetry in contrast enhanced MRI based on deep learning algorithms.

METHOD AND MATERIALS

Data-sets of Gd-EOB-DTPA-enhanced liver MR images of 48 participants were assembled, consisting of 44 training and 4 validation cases. All imaging was performed using a clinical whole-body 3-T system (Magnetom Skyra, Siemens Healthcare). For segmentation, a T1-weighted volume-interpolated breath-hold examination (VIBE) sequences with fat suppression covering the entire liver, acquired during one breath-hold during the hepatobiliary phase (20 min after contrastinjection), was used. The current gold standard of manual liver segmentation was accepted as ground truth. Image Segmentation was performed by a resident physician with 5 years of experience in hepatobiliary imaging. Furthermore, 9 of the training images have been segmented by a second reader (5 years of experience) to determine the expert intraclass correlation coecient (ICC), dice index, and overlap. The neural network topology is loosely based on U-Net.

CONCLUSION

This study presents a fully automated liver volumetry scheme in MR imaging. It is evaluated in comparison to the gold standard manual volumetry. The neural network achieves a higher concordance with the ground truth than two expert readers agree in terms of ICC, dice index, and overlap. The results are highly competitive to current studies, in example Huynh et al. found an ICC of 0.94.

CLINICAL RELEVANCE/APPLICATION

This scheme provides an accurate automatic liver segmentation in MRI; hence it would serve as a useful tool for radiologists for treatment planning, especially for patients undergoing liver surgery.

SSK07-04 The Value of Texture Analysis on Perfusion-Weighted Magnetic Resonance Imaging for Malignancy Characterization of Hepatocellular Carcinoma

Wednesday, Nov. 29 11:00AM - 11:10AM Room: E353A

Participants

Jie Chen, Chengdu, China (*Presenter*) Nothing to Disclose Ting Duan, Chengdu, China (*Abstract Co-Author*) Nothing to Disclose Xin Li, Shanghai, China (*Abstract Co-Author*) Nothing to Disclose Bin Song, MD, Chengdu, China (*Abstract Co-Author*) Nothing to Disclose

PURPOSE

To explore the performance of texture analysis on perfusion-weighted magnetic resonance imaging (PW-MRI) in evaluating the malignancy of hepatocellular carcinoma (HCC).

METHOD AND MATERIALS

Thirty-one surgically confirmed HCC patients were prospectively included and examined using a 3.0 Tesla MR scanner. The perfusion data was acquired using a prototype radial stack-of-stars three-dimensional spoiled gradient echo pulse sequence with goldenangle radial sampling schemes over the course of 6.25 minutes. Post-processing of PW-MRI data was performed on an in-housed software (Omini-Kinetics, GE Healthcare) to generate the Ktrans, Kep, Ve and AUC parametric maps using the Extended Tofts liner model. Texture analysis was then performed on those parametric maps using the same software. A total of 75 texture features were calculated for each perfusion results. The Edmondson-Steiner classification of HCC were histopathologically determined. Texture parameters were correlated with the Edmondson-Steiner grade of HCC. Receiver operation characteristic (ROC) analysis of discriminating low-grades (grade 1 and 2) from high-grades (grade 3 and 4) HCC was conducted for identified texture parameters.

RESULTS

The MinIntensity of Ktrans (r=-0.433, P=0.015), Kep (r=-0.409, P=0.022) and Ve (r=-0.384, P=0.033) maps, and the MinIntensity (r=-0.451, P=0.011), skewness (r=0.623, P<0.001), kurtosis (r=0.412, P=0.021) and uniformity (r=-0.55, P=0.001) of AUC maps showed week to moderate correlations with the Edmondson-Steiner grades of HCC. The skewness and kurtosis of AUC were significantly lower in low-grades HCC than in high-grades HCC, while the uniformity of AUC were significantly higher in low-grades HCC than in high-grades HCC. The areas under the ROC curve for the skewness, kurtosis and uniformity of AUC in differentiating high-grades from los-grades HCC were 0.868, 0.789 and 0.719, respectively.

CONCLUSION

Texture features based on PW-MRI, in particular the skewness of AUC, offer a potential avenue toward preoperative evaluation of HCC malignancy.

CLINICAL RELEVANCE/APPLICATION

The first of the f

I exture reatures of pertusion imaging can reflect the intratumoral neterogeneity of blood supply and cellular density, thereby providing a reliable marker of lesion's potential malignancy.

SSK07-05 Hepatocellular Carcinoma: Texture Analysis of Preoperative CT Images as a Potential Marker of Disease-Free Survival

Wednesday, Nov. 29 11:10AM - 11:20AM Room: E353A

Participants

Jiseon Oh, MD, Seoul, Korea, Republic Of (Presenter) Nothing to Disclose

Jeong Min Lee, MD, Seoul, Korea, Republic Of (*Abstract Co-Author*) Grant, Bayer AG; Grant, General Electric Company; Grant, Koninklijke Philips NV; Grant, STARmed Co, Ltd; Grant, RF Medical Co, Ltd; Grant, Samsung Electronics Co, Ltd; Grant, Guerbet SA; Jeong Hee Yoon, MD, Seoul, Korea, Republic Of (*Abstract Co-Author*) Grant, Bayer AG Speaker, General Electric Company Speaker, Koninklijke Philips NV Speaker, Bayer AG

Ijin Joo, MD, Seoul, Korea, Republic Of (Abstract Co-Author) Nothing to Disclose

Junghoan Park, MD, Seoul, Korea, Republic Of (Abstract Co-Author) Nothing to Disclose

Balaji Ganeshan, PhD, London, United Kingdom (*Abstract Co-Author*) CEO, TexRAD Ltd; Director, Feedback plc; Director, Stone Checker Software Ltd; Director, Prostate Checker Ltd

Joon Koo Han, MD, Seoul, Korea, Republic Of (Abstract Co-Author) Nothing to Disclose

PURPOSE

To investigate the performance of CT textural analysis (CTTA) in characterizing malignancy of hepatocellular carcinoma and predicting disease-free survival (DFS).

METHOD AND MATERIALS

Institutional review board approved this retrospective study, with a waiver of informed consent. From January 2009 to January 2015, 81 patients with single HCC underwent preoperative contrast-enhanced CT with same protocol and vender. Texture features of the largest tumor cross-sectional area from portal phase liver CT images were assessed by using TexRAD software which employed a filtration-histogram technique. Mean value of positive pixels (MPP), entropy, kurtosis, skewness, and standard deviation (SD) of the pixel distribution histogram were derived from the images without filtration and with filter values corresponding to fine, medium, and coarse texture scale. The texture features were compared between groups with different histologic grade using Student's t-test and Mann-Whitney test. Kaplan-Meier analysis was performed to determine the relationship between CTTA and DFS. The Cox proportional hazards model was used to assess the independence of texture parameters from other known clinical and imaging parameters.

RESULTS

SD and MPP quantified from fine to coarse texture on CT images showed significant associations with the histologic grade (P<.05). Univariate analysis identified most CT texture features across the different filters - fine, medium and coarse texture scales were significant univariate markers of DFS. Also a number of known clinical and imaging parameters such as tumor size, vascular invasion, the average intensity of tumor, the level of AFP and PIVKA were significant univariate markers of DFS. A Cox regression model including all significant univariate markers identified that CTTA (fine texture scale - kurtosis: p=0.037, skewness: p=0.015), and tumor size (P<0.001) were independent predictors of DFS.

CONCLUSION

CTTA could act as a prognostic biomarker in HCCs and play a key complementary role as an adjunct with other known clinical and imaging markers in better risk stratification of these patients.

CLINICAL RELEVANCE/APPLICATION

CTTA is a significant marker of disease-free survival in patients with HCCs. Their role as a prognostic biomarker can be a useful adjunct to improve stratification of HCC patients.

SSK07-06 HCC Treated With 90Yttrium Radioembolization: Can Pre-Treatment and 6week Post-Treatment Volumetric ADC Histogram Measurements Predict Subsequent Tumor Response?

Wednesday, Nov. 29 11:20AM - 11:30AM Room: E353A

Participants

Sonja Gordic, MD, New York, NY (*Presenter*) Nothing to Disclose Mathilde Wagner, MD, PhD, Paris, France (*Abstract Co-Author*) Consultant, Toshiba Medical Systems Corporation Riccardo Zanato, Padova, Italy (*Abstract Co-Author*) Nothing to Disclose Stefanie Hectors, PhD, New York, NY (*Abstract Co-Author*) Nothing to Disclose Cecilia Besa, MD, New York, NY (*Abstract Co-Author*) Nothing to Disclose Shingo Kihira, BS, New York, NY (*Abstract Co-Author*) Nothing to Disclose Edward Kim, MD, East Meadow, NY (*Abstract Co-Author*) Consultant, Koninklijke Philips NV Advisory Board, Onyx Pharmaceuticals, Inc Advisory Board, Sterigenics International LLC Bachir Taouli, MD, New York, NY (*Abstract Co-Author*) Consultant, MEDIAN Technologies ; Grant, Guerbet SA

PURPOSE

To assess the potential of volumetric ADC (vADC) histogram measurements obtained before and 6 weeks (6w) post-treatment for prediction of hepatocellular carcinoma (HCC) response to 90Yttrium radioembolization (RE).

METHOD AND MATERIALS

22 patients (M/F 15/7, mean age 65y) who underwent lobar RE (right lobe n=15; left lobe n=7) were included. All patients underwent MRI pre-treatment and 6w and 6 months (6m) after RE using a routine liver MRI protocol including DWI. Two readers assessed tumor response 6m after RE in consensus. Definition of complete tumor response, partial tumor response, stable disease, and progression of HCC lesions was based on modified RECIST criteria (mRECIST) for each index tumor. vADC histogram parameters (mean, median, mode, min, max, kurtosis and skewness) were obtained by placing regions of interest (ROIs) on the ADC map covering the whole index tumors. One reader placed the ROIs at baseline and 6w after treatment. Changes in tumor vADC (ΔvADC) histogram parameters were calculated. Data was evaluated using Mann-Whitney U test and receiver operating characteristics

RESULTS

26 HCC lesions (mean size 3.4 ± 2.4 cm) were assessed (18 patients with 1 tumor, 4 patients with 2 tumors). Response at 6m was as follows: complete response (CR, 8 tumors), partial response (PR, 3 tumors), stable disease (SD, 13 tumors) and progression (PD, 2 tumors). vADC mean, median, mode (1.76-1.81 vs. 1.23-1.34 x10-3 mm2/s) and Δ vADC median and Δ vADC max (30-43% vs. 2-9%) at 6w were significantly higher in CR/PR vs. SD/PD (p=0.013-0.032), while there was no significant difference at baseline. vADC mean, median, Δ vADC mean and Δ vADC max at 6w were significant predictors of CR/PR (AUC 0.752-0.788; p=0.014-0.031) and of CR (AUC 0.750-0.861; p=0.004-0.046) after RE. vADC median threshold of 1.377 x10-3 mm2/s at 6w had a sensitivity of 81.8% and a specificity of 66.7% for prediction of PR/CR and Δ vADC median threshold of 19.2% had a sensitivity of 87.5% and a specificity of 83.3% for prediction of CR.

CONCLUSION

vADC mean, median, Δ vADC mean and Δ vADC max at 6w are significant predictors of subsequent response in HCCs treated with RE, while pre-treatment vADC did not have any predictive value.

CLINICAL RELEVANCE/APPLICATION

Our results suggest that vADC histogram measurements at 6w post RE are early biomarkers and allow prediction of treatment response.

SSK07-07 Development of CT Derived Biomarker for Gastrointestinal Stromal Tumor; Comparison with FDG-PET and DWI

Wednesday, Nov. 29 11:30AM - 11:40AM Room: E353A

Participants

Yoshihiro Kurata, Chiba, Japan (*Presenter*) Nothing to Disclose Koichi Hayano, MD, Chiba, Japan (*Abstract Co-Author*) Nothing to Disclose Takeshi Fujishiro, Chiba, Japan (*Abstract Co-Author*) Nothing to Disclose Hiroki Watanabe, Chiba, Japan (*Abstract Co-Author*) Nothing to Disclose Yumiko Takahashi, MD, Chiba, Japan (*Abstract Co-Author*) Nothing to Disclose Kazuo Narushima, MD, PhD, Chiba, Japan (*Abstract Co-Author*) Nothing to Disclose Gaku Ohira, Chiba, Japan (*Abstract Co-Author*) Nothing to Disclose Kiyohiko Shuto, MD, PhD, Chiba, Japan (*Abstract Co-Author*) Nothing to Disclose Hisahiro Matsubara, MD, PhD, Chiba, Japan (*Abstract Co-Author*) Nothing to Disclose

PURPOSE

Gastrointestinal stromal tumor (GIST) is the most common mesenchymal tumor of the gastrointestinal tract. It has been reported that 18F-Fluorodeoxyglucose-positron emission tomography (FDG-PET) and diffusion-weighted MRI (DWI) can be biomarkers to evaluate malignant potential of GIST. But considering availability of FDG-PET and DWI, development of CT derived biomarker would be valuable. The texture analysis such as fractal analysis of the medical image has been reported to be a potential biomarker for malignancies, reflecting structural heterogeneity of the tumor. The purpose of this study is to evaluate the usefulness of CT fractal analysis in preoperative assessment of malignant potential of GIST, comparing with FDG-PET and DWI.

METHOD AND MATERIALS

We retrospectively identified 43 patients (20 M / 23W; median age: 65) with GISTs who received FDG-PET, DWI, and contrastenhanced (CE) CT before surgery. Tumor SUV and ADC were measured from FDG-PET and DWI. Regarding CT analysis, fractal analysis was applied to portal-phase CE-CT image with use of a plugin software of ImageJ (NIH), and fractal dimension (FD) of the tumor was measured. These tumor parameters were compared with the risk classification of GIST, and diagnostic values of these parameters for malignant potential of GIST were evaluated.

RESULTS

According to modified Fletcher classification, 9 patients were categorized as the high risk, and the other 34 cases were categorized as the very low or low risk (26) or the intermediate risk (8). Tumor FD of high risk group was significantly higher than that of the other risk groups (very low, low, and intermediate risk) (P<0.05). The areas under the ROC curves (AUCs) of tumor FD, ADC and SUV for prediction of high risk group were 0.84, 0.86 and 0.82, respectively. From this ROC curve analysis, 1.11(FD), 1.21(ADC), and 4.16(SUV) were the best cut-off value to predict the high risk GIST patients with a highest accuracy (85.7%, 71.4% and 83.3%, respectively).

CONCLUSION

Diagnostic value of CT fractal analysis for prediction of high risk GIST is comparable with FDG-PET and DWI. In terms of cost and availability, CT fractal analysis can be a most beneficial imaging biomarker for the management of GIST.

CLINICAL RELEVANCE/APPLICATION

CT fractal analysis can be a noninvasive, economical and widely applicable biomarker for preoperative risk stratification of GIST, and it would help select an optimal therapy for patients with GISTs.

SSK07-08 CT-Based Radiomic Signature Preoperatively Predicts Lymphovascular Invasion in Patients with Advanced Gastric Cancer

Wednesday, Nov. 29 11:40AM - 11:50AM Room: E353A

Participants

Mengjie Fang, Beijing, China (*Presenter*) Nothing to Disclose Zaiyi Liu, MD, Guangzhou, China (*Abstract Co-Author*) Nothing to Disclose Zelan Ma, Guangzhou, China (*Abstract Co-Author*) Nothing to Disclose Di Dong, Beijing, China (*Abstract Co-Author*) Nothing to Disclose Dongdong Yu, Beijing, China (*Abstract Co-Author*) Nothing to Disclose For information about this presentation, contact:

jie.tian@ia.ac.cn

PURPOSE

To develop and validate a machine learning based radiomics signature for preoperative prediction of lymph vascular invasion (LVI) in patients with advanced gastric cancer (AGC).

METHOD AND MATERIALS

In this ethical-approved retrospective study, we collected a primary cohort consisting of 152 patients gathered from July 2011 to December 2013 and a time-independent validation cohort consisting of 95 patients from January 2014 to July 2015. 273 texture features were extracted from venous-phase CT of AGC. Then, we adopted minimum redundancy maximum relevance (mRMR) algorithm to reduce the feature dimension as well as identify a radiomics signature for predicting LVI. We built a support vector machine (SVM) model to yield a quantitative risk score for LVI. The classification performance of the SVM model was evaluated by univariate analysis, multivariate analysis and receiver operator characteristics (ROC) analysis in the primary cohort and validated in the time-independent validation cohort.

RESULTS

The 5-feature-based radiomics signature was an independent predictor for LVI in AGC (P<0.001 for both primary and validation cohorts). The radiomics signature showed strong discriminatory power for LVI prediction with an AUC of 0.764 (95% CI: 0.685-0.843; sensitivity: 0.844; specificity: 0.618) in the primary cohort. In addition, the radiomics analysis achieved competitive generalization performance with an AUC of 0.744 (95% CI: 0.640-0.848; sensitivity: 0.818; specificity: 0.600) in validation cohort.

CONCLUSION

Machine learning by means of SVM in combination with texture features can be used to associate with the status of LVI. The radiomics signature may serve as a potential non-invasive tool for the preoperative LVI prediction in patients with AGC.

CLINICAL RELEVANCE/APPLICATION

Machine learning based radiomics signature has potential in the preoperative non-invasive prediction of lymphvascular invasion and facilitate the clinical strategy.

SSK07-09 Comparison of Current Response Criteria in Patients with HCC Treat with Targeted Therapy Using a 3D Quantitative Analysis

Wednesday, Nov. 29 11:50AM - 12:00PM Room: E353A

Participants

Guobin Hong, MD,PhD, Zhuhai, China (*Abstract Co-Author*) Nothing to Disclose Yijie Fang, Zhuhai, China (*Presenter*) Nothing to Disclose YI ZHANG, ZHUHAI, China (*Abstract Co-Author*) Nothing to Disclose Wenjuan Li, Zhuhai, China (*Abstract Co-Author*) Nothing to Disclose Yunpeng Liu, Boston, MA (*Abstract Co-Author*) Nothing to Disclose Wenli Cai, PhD, Boston, MA (*Abstract Co-Author*) Stockholder: IQ Medical Imaging LLC Min Pan, MD, Boston, MA (*Abstract Co-Author*) Nothing to Disclose

For information about this presentation, contact:

honggb@mail.aysu.edu.cn

PURPOSE

The aim of this study was to compare existing available non-three-dimensional methods (Response Evaluation Criteria in Solid Tumors [RECIST], modified RECIST [mRECIST], European Association for Study of the Liver [EASL]) with three-dimensional (3D) quantitative methods of the index tumor as early response markers in predicting patient survival after targeted therapy.

METHOD AND MATERIALS

This study was a retrospective single-institution HIPAA-compliant. A total of 88 patients with hepatocellualr carcinoma (HCC) treated with targeted therapy was enrolled (in 76 men and 12 women; mean age, 61 years \pm 7 [standard deviation]; Range, 22-88 years). CT scans before and after targeted therapy were analyzed. Six response assessment methods (RECIST, mRECIST, EASL and 3D methods of volumetric RECIST [vRECIST], modified vRECIST [vmRECIST] and quantitative EASL [qEASL]) were used to classify all patients as responders or nonresponders by following standard guidelines for the uni- and bidimensional measurements and by using the formula for a sphere for the 3D measurements. 3D quantitative tumor assessments were performed using an inhouse software prototype (3D Quantitative Imaging, MGH, USA).The Kaplan-Meier method with the log-rank test was performed for each method to evaluate its ability to help predict survival of responders and nonresponders. Uni- and multivariate Cox proportional hazard ratio models were used to identify covariates that had significant association with survival.

RESULTS

The 3D quantitative tumor assessments of vRECIST (hazard ratio,0.6; 95% confidence interval [CI]: 0.4, 1.2; P=0.03), vmRECIST (hazard ratio,0.6; 95% CI: 0.3, 0.6; P=0.002) showed a significant difference in survival between responders and nonresponders groups, whereas the uni- and bidementional measurements of RECIST (hazard ratio,0.5; 95% CI: 0.3, 0.5; 95% CI: 0.3, 0.9; P=0.08), mRECIST (hazard ratio,0.6; 95% CI: 0.3, 1.0; P=0.07), and EASL(hazard ratio,0.7; 95% CI: 0.3, 0.8; P=0.06) did not show a significant difference between these groups.

CONCLUSION

Compared with the uni- and bidementional measurements, the 3D-based imaging biomarkers vRECIST, vmRECIST and qEASL could

be used to predict patient survival early after targeted therapy.

CLINICAL RELEVANCE/APPLICATION

Volumetric quantification is sensitive to detect early change of HCC and to accurately assess treatment response.





103rd Scientific Assembly and Annual Meeting November 26 to December 1 McCormick Place, Chicago



SSK08

Gastrointestinal (Colon Cancer and CT Colonography)

Wednesday, Nov. 29 10:30AM - 12:00PM Room: E353B



AMA PRA Category 1 Credits ™: 1.50 ARRT Category A+ Credit: <u>1.75</u>

FDA Discussions may include off-label uses.

Participants

Judy Yee, MD, Bronx, NY (*Moderator*) Research Grant, EchoPixel, Inc David J. Lomas, MD, Cambridge, United Kingdom (*Moderator*) Nothing to Disclose Lorenzo Mannelli, MD, PhD, New York, NY (*Moderator*) Speaker, Bracco Group Speaker, General Electric Company

Sub-Events

SSK08-01 Multilevel Determinants of Adenoma Detection Rate at CT Colonography (CTC) Screening: Association with Radiologist Experience and Patient-Related Factors

Participants

Daniele Regge, MD, Torino, Italy (*Abstract Co-Author*) Speakers Bureau, General Electric Company Loredana Correale, PhD, Turin, Italy (*Abstract Co-Author*) Researcher, im3D SpA Carlo Senore, MD, Torino, Italy (*Abstract Co-Author*) Nothing to Disclose Cesare Hassan, Rome, Italy (*Abstract Co-Author*) Nothing to Disclose Lia Morra, PhD, Torino, Italy (*Abstract Co-Author*) Nothing to Disclose Nereo Segnan, Torino, Italy (*Abstract Co-Author*) Nothing to Disclose Davide Bellini, MD, Latina, Italy (*Presenter*) Nothing to Disclose

For information about this presentation, contact:

daniele.regge@ircc.it

PURPOSE

In a large randomized trial the overall adenoma detection rate appeared to be similar between CTC and sigmoidoscopy (FS). CTC achieved a higher detection than FS in the proximal colon, while the reverse was true for the distal colon. To assess the relationship between radiologist experience and adenoma detection rate at CTC screening.

METHOD AND MATERIALS

Post-hoc analysis of a RCT, examining the diagnostic performance of radiologists in relation with previous CTC experience. Radiologist experience was classified according to the total number of CTC performed before the trial (i.e, <200, 200-1,000, >1,000). Multilevel logistic regression was used to model the influence of reading volumes and patient characteristics on the probability to detect adenomas. Patient factors included gender, previous CRC screening, CRC family risk, and image/distension quality. Analyses were performed separately for each of the following lesions: all adenomas (ADR), distal adenomas (DADR), proximal adenomas (PADR), advanced histology (i.e. >=10-mm, villous histology or high grade dysplasia). A 6-mm cut-off was used for post-CTC referral to colonoscopy.

RESULTS

2593 CTC (1266 F; age, 58-60) were read by 7 radiologists. In detail, 1337 (51.5%), 584 (22.5%), and 672 (26.0%) were read by radiologists with reading volumes<200, 200-1000, and >1000, respectively. The average ADR, DADR and PADR were 8.0% (95% CI: 7.0-9.1%; range, 5.8-8.7%), 5.0% (95% CI:4.3-5.9%, range, 2.1-8.4%), and 5.1% (95% CI:4.2-6.3, range, 4.4-5.4%), respectively. Radiologist experience appeared to be related with DADR (OR, >1000 vs <=1000:1.49; 95% CI: 1.04-2.13), but not with PADR (OR,>1000 vs. <=1000:0.91; 95% CI:0.64-1.29). The association of radiologist experience with distal location appeared to be statistically significant also for advanced adenomas (OR,>1000 vs. <=1000, 1.73; 95% CI:1.08-2.88). In multivariate analysis, volumes>1000, male gender, excellent/good image quality and no previous colonoscopy were significantly associated with greater odds of detecting distal adenomas.

CONCLUSION

According to our data, distal adenomas, including those with advanced histology, could be missed by less experienced radiologists (<1000 CTC).

CLINICAL RELEVANCE/APPLICATION

High reading volumes, greater than 1000 CTCs, may be required to achieve high adenoma detection rates in the distal colon. Optimization of training methods is critical to ensure a consistent high-quality level at CTC screening.

SSK08-02 Effect of Iterative Model Reconstruction algorithm on Radiologist's Performance in CT Colonography

Wednesday, Nov. 29 10:40AM - 10:50AM Room: E353B

Yanbang Lian, Zhengzhou, China (*Presenter*) Nothing to Disclose Zhiyang Zhou, PhD, Guangzhou, China (*Abstract Co-Author*) Nothing to Disclose Jianbo Gao, MD, Zhengzhou, China (*Abstract Co-Author*) Nothing to Disclose Junqiang Dong, MD, Zhengzhou, China (*Abstract Co-Author*) Nothing to Disclose Shangwen Geng, MD, Zhengzhou, China (*Abstract Co-Author*) Nothing to Disclose Yuanwei Pan, PhD, Zhengzhou, China (*Abstract Co-Author*) Nothing to Disclose

PURPOSE

To assess radiation dose and image quality of CT colonography (CTC) at 100 kVp with iterative model reconstruction algorithm (IMR) at 20 mAs compared with filtered back projection (FBP) at 50 mAs.

METHOD AND MATERIALS

Thirty-two patients suspected with colon adenomatous polyp or adeno-carcinoma were enrolled in this study. All of patients underwent CTC examination at 50mAs in supine position and 20mAs with prone position with the same tube voltage at 100 kVp about two hours before fibro-colonoscope. Images were reconstructed using FBP and IMR. Two radiologists independently evaluated image quality. Qualitative image quality was assessed with a five-score scale. Image noise, signal-to-noise ratio (SNR), contrast-to-noise ratio (CNR), and effective radiation dose were recorded and calculated. Qualitative and quatitative values were analysed by using Wilcoxon signed rank test and the paired t test, respectively.

RESULTS

Totally 38 colon polyps or adeno-carcinoma were detected in fibro-colonoscope examination. For 20 mAs with IMR (A group) and 50 mAs with FBP (B group), there is no statistically significant difference in lesion detection (reader 1: 35/38 vs 36/38, and reader 2: 31/38 vs. 33/38, p>0.05). However, qualitative image quality scores (3.9 vs 2.5), image noise ([12.77 ± 0.91] HU vs. [50.04 ± 5.45] HU), SNRs (3.13 ± 0.28 vs. 1.02 ± 0.20) and CNRs (81.42 ± 6.11 vs. 19.93 ± 1.46) were significantly superior of 20 mAs with IMR, respectively (p<0.05). Compared with B group, radiation dose of A group decreased significantly (0.42 ± 0.03 mSv vs. 1.07 ± 0.12 mSv).

CONCLUSION

Image quality of CTC using 20 mAs with IMR reconstruction could be comparable to 50 mAs with FBP at the same tube voltage while with no significant detection of poply, and radiation dose of the former was only 0.42 mSv, which was reduced by about 39.3%.

CLINICAL RELEVANCE/APPLICATION

This preliminary study helps to reduce the radiation dose of patients undergoing CTC examination with IMR algorithm.

SSK08-03 Feasibility of Computer-Aided CT Colonography in a Single-Position Reading

Wednesday, Nov. 29 10:50AM - 11:00AM Room: E353B

Participants

Yasuji Ryu, MD, Boston, MA (*Presenter*) Nothing to Disclose

Chinatsu Watari, MD, Boston, MA (Abstract Co-Author) Nothing to Disclose

Janne J. Nappi, PhD, Boston, MA (Abstract Co-Author) Royalties, Hologic, Inc; Royalties, MEDIAN Technologies;

Hiroyuki Yoshida, PhD, Boston, MA (Abstract Co-Author) Patent holder, Hologic, Inc; Patent holder, MEDIAN Technologies;

For information about this presentation, contact:

yoshida.hiro@mgh.harvard.edu

PURPOSE

To evaluate the performance of computer-aided single-position reading of full-cathartic CT colonography (CTC) in detecting polyps from patients at average or high risk of colorectal cancer.

METHOD AND MATERIALS

A total of 266 CTC cases were sampled from a multi-center CTC trial for patients at average or high risk of colorectal cancer. The patients underwent cathartic bowel preparation with 2L polyethylene glycol solution and fecal tagging by 20mL sodium diatrizoate, followed by automated CO2 insufflation. A computer-aided detection (CADe) system trained with cases independent from this study was used to review the CTC cases. Two experienced readers (>=600 CTC cases reading experience) reviewed the cases for >=6 mm lesions in supine-only reading mode, in which only the supine scans of these cases were interpreted and CADe was used as a second reader. The per-patient sensitivity and area under the receiver operating characteristic curve (AUC) were compared in the detection of adenomas and carcinomas between the unaided and CADe-aided supine-only readings, and between the CADe-aided supine-only reading and the conventional unaided dual-position reading result of the original trial.

RESULTS

There were 35 and 28 patients with 6-9 mm and >=10 mm adenomas/carcinomas, respectively. The corresponding average perpatient sensitivities (AUCs) for CADe-aided supine-only reading were 82.9% (0.89) and 90.9% (0.95), respectively, whereas those of unaided dual-position reading were 82.9% (0.88) and 92.9% (0.96), respectively. The differences of sensitivities and AUCs at each size range were not statistically significant (sensitivities: Fisher's exact test, P>0.7; AUCs: two-sided t-test, P>0.3). For 6-9 mm lesions, the per-patient sensitivity (AUC) of CADe-aided supine-only reading was 82.9% (0.89), higher than that of unaided supine-only reading of 71.4% (0.85) (sensitivity: McNemar's test, P<0.01; AUC: one-sided t-test, P<0.05).

CONCLUSION

In full-cathartic CTC, CADe-aided single-position reading yields an equally high performance in detecting adenomas and carcinomas as that of conventional supine-prone reading. In single-position reading, the use of CADe significantly improves the detection of polyps 6-9 mm in size.

CLINICAL RELEVANCE/APPLICATION

Computer-sided single-nosition reading has notential to allow one-nosition scanning in CTC thereby effectively halving the radiation

computer-allow single-position reading has potential to allow one-position scatting in CTC, thereby enectively haiving the radiation dose and reading time of conventional dual-position reading.

SSK08-04 Dual-Energy CT Colonography Using Dual-Layer Spectral Detector Computed Tomography: Feasibility of Virtual Monochromatic Imaging for Electronic Cleansing

Wednesday, Nov. 29 11:00AM - 11:10AM Room: E353B

Participants

Narumi Taguchi, Kumamoto, Japan (*Presenter*) Nothing to Disclose Seitaro Oda, MD, Kumamoto, Japan (*Abstract Co-Author*) Nothing to Disclose Masanori Imuta, MD, Kumamoto, Japan (*Abstract Co-Author*) Nothing to Disclose Sadahiro Yamamura, Kumamoto-shi, Japan (*Abstract Co-Author*) Nothing to Disclose Takeshi Nakaura, MD, Kumamoto, Japan (*Abstract Co-Author*) Nothing to Disclose Daisuke Utsunomiya, MD, Kumamoto, Japan (*Abstract Co-Author*) Nothing to Disclose Yasunori Nagayama, MD, Kumamoto, Japan (*Abstract Co-Author*) Nothing to Disclose Yoshinori Funama, PhD, Kumamoto, Japan (*Abstract Co-Author*) Nothing to Disclose Tadatoshi Tsuchigame, MD, Kumamoto, Japan (*Abstract Co-Author*) Nothing to Disclose Yasuyuki Yamashita, MD, Kumamoto, Japan (*Abstract Co-Author*) Nothing to Disclose

PURPOSE

We investigated the utility of virtual monochromatic imaging (VMI) using dual-layer spectral detector CT on the electronic cleansing in fecal-tagging CT colonography.

METHOD AND MATERIALS

This study included 30 patients who underwent fecal-tagging CT colonography performed on a novel dual-layer detector spectral CT scanner. Conventional 120-kVp images and VMI at 40-, 50-, and 60-keV were reconstructed. Quantitative image quality parameters, i.e. CT attenuation of tagged fluid and image noise, were compared and the visual image quality was scored on a four-point scale. We recorded the number of the colon segments with appropriate CT attenuation of tagged fluid (>= 300 HU) for each patient and used these data to compare the reconstructions. The performance of the electronic cleansing was also assessed semi-quantitatively using a four-point scale.

RESULTS

The mean CT attenuation of tagged fluid was significantly higher on VMI than conventional 120-kVp images. There was no significant difference in image noise among the reconstructions. The number of colon segments with appropriate CT attenuation of tagged fluid was significantly higher on VMI than conventional 120 kVp images. Significant higher score of the subjective image quality and the performance of the electronic cleansing were observed on VMI than conventional 120 kVp images.

CONCLUSION

With dual-layer spectral detector CT, the use of VMI can yield significantly better image quality of fecal-tagging CT colonography and improve the performance of the electronic cleansing.

CLINICAL RELEVANCE/APPLICATION

VMI using dual-layer spectral detector CT can improve image quality of fecal-tagging CT colonography and provide more accurate diagnostic information.

SSK08-05 Inter-Observer Agreement Using a Coding System for Reporting Virtual Colonoscopy

Wednesday, Nov. 29 11:10AM - 11:20AM Room: E353B

Participants

Stephen Sammut, MBChB, Stoke-on-Trent, United Kingdom (*Presenter*) Nothing to Disclose Vincent Leung, MBCHB, Stoke-on-Trent, United Kingdom (*Abstract Co-Author*) Nothing to Disclose Nicola J. Cook, MBChB, Stoke-on-Trent, United Kingdom (*Abstract Co-Author*) Nothing to Disclose Paul Clarke, Stoke-on-Trent, United Kingdom (*Abstract Co-Author*) Nothing to Disclose Ingrid Britton, MBBS, FRCR, Stoke On Trent, United Kingdom (*Abstract Co-Author*) Nothing to Disclose

PURPOSE

A coding system is utilised at our UK institution for reporting virtual colonoscopy/CT colonography (CTC) examinations. The C coding refers to the intra-colonic findings, whereas the E coding refers to extra-colonic findings, both on a scale from 1 to 5. The purpose of this study was to validate the coding system by assessing the inter-observer variability of two independent readers using the same coding system to summarise the CTC findings.

METHOD AND MATERIALS

A retrospective study was performed of all CTCs in our University Teaching Hospitals NHS Trust in the UK, which performs the largest number of examinations at any single institution throughout Europe, over a 3 month period (01/07/16 - 30/09/16). Our standard practice is for each study to be read initially by an advanced practitioner radiographer with a final report issued by a consultant radiologist. The report coding issued by the different readers was analysed and compared.

RESULTS

626 CTCs (mean age 69 years) were selected for inclusion. 57 studies were excluded either as they were not coded, not read by a radiographer prior to consultant report or rated as an inadequate study by either reader. The percentage agreement between radiographer findings and radiologist report was 92.3% for C coding and 50.6% for E coding. Interobserver agreement Kappa statistic was calculated to be 0.77 (95% CI 0.703-0.830) for C coding and 0.27 (95% CI 0.206-0.324) for E coding.

CONCLUSION

There is high inter-observer agreement between medical and non-medical readers for C coding suggesting it is a precise and easy to follow method of classifying colonic findings. The greater variability for E coding may be due to difficulty in classifying extra-

colonic findings but also reflective of the skill set between the two types of readers.

CLINICAL RELEVANCE/APPLICATION

The use of a report scoring system highlights important CTC findings so that the clinical teams can expedite arrangement of the appropriate further management and if necessary multi-disciplinary team discussion. The study shows that our scoring system is easy to use and demonstrates high inter-observer agreement for the intr-colonic findings, which is required for the system to be valid.

SSK08-06 Assessment of the Neoadjuvant Chemoradiation Outcomes in Patients with Clinical T1/T2 Rectal Cancer Using the MRI Tumor Regression Grade

Wednesday, Nov. 29 11:20AM - 11:30AM Room: E353B

Participants

Heejin Bae, Seoul, Korea, Republic Of (*Presenter*) Nothing to Disclose Joonseok Lim, MD, Seoul, Korea, Republic Of (*Abstract Co-Author*) Nothing to Disclose

PURPOSE

To analyze magnetic resonance imaging (MRI) tumor regression grade (mrTRG) for predicting the outcomes after the neoadjuvant chemoradiation in patients with clinical T1/T2 rectal cancer.

METHOD AND MATERIALS

Between 2012 and 2016, we retrospectively registered 39 patients with clinical T1/T2 rectal cancer who had undertaken either the total mesorectal excision (TME) or local excision after the neoadjuvant chemoradiation. Initial rectal MRI was analyzed to determine the mural involvement of the primary tumor (partial or transmural involvement) and both initial and post-treatment rectal MRI were reviwed for mrTRG. Surgical pathologic assessment including Mandard grade was used to evaluate the tumor regression after the neoadjuvant treatment and Mandard grade 1 was considered as pathologic complete response (pCR). Associations of mrTRG and the degree of mural involvement with Mandard grade and pathologic T stage (pT) were analyzed.

RESULTS

Out of 39 patients, 20 patients had mrTRG 1 and 19 patients had mrTRG 2-4 (mrTRG2=11, mrTRG3=6, mrTRG4=2). Sixty-five percent (13/20) of mrTRG 1 patients showed pCR, and this positive predictive value of mrTRG 1 was higher than observed pCR rate (18/39, 46.2%). The odds of accomplishing pCR were 5.2 times higher for mrTRG 1 than they were for mrTRG 2-4 (95% confidence interval (CI): 1.3 - 20.5, p=0.019). Univariate analysis of the degree of mural involvement indicated that the difference in probability of pCR did not reach the significance (odds ratio (OR)=1.1, 95% CI=0.3-3.9, p=0.882). Ninety percent (18/20) of mrTRG 1 patients had early stage cancer (pT0, pTis and pT1) after the preoperative chemoradiation. Univariate analysis demonstrated that mrTRG1 group was significantly more likely to have early stage cancer than was mrTRG2-4 group (OR=8.1, 95% CI=0.5-45.1, p=0.017), while the OR of partial involvement of the primary tumor was not statistically significant (OR=3.6, 95% CI=0.8-16.3, p=0.103).

CONCLUSION

mrTRG 1 can be used as a supportive factor to predict the complete response after the neoadjuvant chemoradiation in patients with clinical T1/T2 rectal cancer. Moreover, mrTRG seem to deduce pathologic early stage rectal cancer which can be the candidate for local excision rather than TME.

CLINICAL RELEVANCE/APPLICATION

mrTRG can be a supportive tool to predict the complete response and to identify pathologic early stage cancer after the neoadjuvant chemoradiation in clinical T1/T2 rectal cancer patients.

SSK08-07 Influence of Iterative Reconstruction and Slice Thickness on Texture Analysis

Wednesday, Nov. 29 11:30AM - 11:40AM Room: E353B

Participants

Paul Gillard, Paris, France (Abstract Co-Author) Nothing to Disclose
Emilie Hubert, Paris, France (Abstract Co-Author) Nothing to Disclose
Pierre-Adrien Lampson, MD, Paris, France (Abstract Co-Author) Nothing to Disclose
Olivier Lucidarme, MD, Paris, France (Abstract Co-Author) Consultant, Bracco Group Consultant, F. Hoffmann-La Roche Ltd
Consultant, Boehringer Ingelheim GmbH
Mathilde Wagner, MD, PhD, Paris, France (Presenter) Consultant, Toshiba Medical Systems Corporation

For information about this presentation, contact:

mathilde.wagner@aphp.fr

PURPOSE

To assess the variability of texture analysis parameters on CT scans depending on the iterative reconstruction technique and the slice thickness.

METHOD AND MATERIALS

To date, ten patients (M/F=4/6, mean age 71 yo) with liver metastases were retrospectively included in this study (1 patient with a GIST, 1 patient with a pancreatic cancer, 8 patients with a colorectal cancer). All patients had a CT-scan at a portal venous phase after injection of Iomeron 350, using a Philips system (ICT256). The standard reconstruction parameters included an iDose4 reconstruction with a 2 mm-slice thickness. Four additional reconstructions were performed: iDose4 with 1 and 5 mm-slice thickness, and iDose2 and 6 with a 2 mm-slice thickness. Using LIFEx software v3.0, a region of interest (ROI) was drawn by one radiologist, on one of the reconstruction. The ROI contained the largest diameter of the liver metastases (max 5 lesions /patient, lesion diameter > 1cm). The ROI was copied and pasted on the images from other reconstructions. Mean, standard deviation, skewness, kurtosis and entropy of each ROI were obtained. Variability between iterative reconstructions and slice thicknesses was

assessed using coefficient of variation (CV), and Bland and Altman limits of agreement (BALA) (percentage of difference).

RESULTS

Forty-eight liver metastases were analyzed. Between iterative reconstructions, all the parameters, except skewness, had a good reproducibility (CV<8%). The mean was the less variable parameter with a CV<1% and BALA thinner than [-4.38%; 2.36%], while skewness was the less reproducible parameter with a CV of 25.5% and BALA until [-135.3%; 48.18%]. For all texture parameters, the variability was higher between slice thicknesses than between iterative reconstructions, but still acceptable for all parameters (CV<18%) except for skewness. Skewness had a very low reproducibility between slice thicknesses with a CV of 954% and BALA until [-846.5%; 1103%].

CONCLUSION

Texture parameters, mostly skewness, show some variability depending on the iterative reconstruction and moreover on the slice thickness.

CLINICAL RELEVANCE/APPLICATION

Texture analysis is a more and more used method, especially for tumor follow-up and assessment of treatment response. Variability related to the CT acquisition parameters needs to be taken into account to avoid incorrect conclusion.

SSK08-08 Changes in the Diagnostic Accuracy of Radiologists and Residents for Rectal Cancer Staging by using Diffusion Weighted Imaging

Wednesday, Nov. 29 11:40AM - 11:50AM Room: E353B

Participants

Roberto Fornell-Perez, MD, Las Palmas de Gran Canaria, Spain (*Presenter*) Nothing to Disclose Esteban Perez Alonso, Las Palmas de Gran Canaria, Spain (*Abstract Co-Author*) Nothing to Disclose Juan F. Loro Ferrer, PhD,MD, Las Palmas de Gran Canaria, Spain (*Abstract Co-Author*) Nothing to Disclose Patricia Aleman Flores, Las Palmas de Gran Canaria, Spain (*Abstract Co-Author*) Nothing to Disclose Alvaro Lozano Rodriguez, MD, Las Palmas de Gran Canaria, Spain (*Abstract Co-Author*) Nothing to Disclose Gabriela Porcel De Peralta, Las Palmas de Gran Canaria, Spain (*Abstract Co-Author*) Nothing to Disclose Alfonso Duran Castellon, MD, Las Palmas de Gran Canaria, Spain (*Abstract Co-Author*) Nothing to Disclose Maria Del Carmen Gonzalez Dominguez, PhD, Firgas, Spain (*Abstract Co-Author*) Nothing to Disclose Jano M. Rubio Garcia, MD, Las Palmas de Gran Canaria, Spain (*Abstract Co-Author*) Nothing to Disclose Maria V. Vivas Escalona, MD, Las Palmas, Spain (*Abstract Co-Author*) Nothing to Disclose Joel J. Aranda Sanchez Sr, MD, Las Palmas, Spain (*Abstract Co-Author*) Nothing to Disclose Maria Elena Orihuela de la Cal, MD, Las Palmas de Gran Canaria, Spain (*Abstract Co-Author*) Nothing to Disclose

PURPOSE

To analyze the influence of Diffusion Weighted Imaging (DWI) on the diagnostic accuracy for the staging of Rectal Cancer (RC), regional lymph nodes (LN) and primary tumor (T) in Radiologists with different degree of expertize

METHOD AND MATERIALS

The study included 50 patients with Magnetic Resonance Imaging (MRI) for RC staging, all with same technique (1.5 T) and later total mesorectal excision. Initial diagnosis (32) and post-neoadyuvancy cases (28, MRI after treatment) were included (ID and PN respectively). The histological stage was used as Gold Standard. 10 Radiologist reviewed individually all cases, blinded to any data but the presence of RC: 3 experienced in RC staging (ER); 3 experienced in other areas (NER); and 4 Residents (RR). Each reading had 2 phases: 1st analyzing just T2 and T2 High Definition sequences (T2HD); after a month washout period, 2nd reading with DWI and T2HD. The staging followed AJCC 7th ed. guidelines. Malignant LN were defined as heterogeneous internal signal/irregular borders. The results were pooled by experience groups for statistical analysis. Area under ROC curves were used to determine accuracy of positive LN, stage greater than I and T greater tan 2. Also, ponderated Kappa with respect to the histological results. All calculations were made in the different reviews and then made again after spliting them into ID and PN patients groups.

RESULTS

Due to their length the results have been summarized in the attached charts. Differences after use of DWI (increase/decrease) in group accuracy and Kappa regarding Gold Standard are shown.

CONCLUSION

There is a significant decrease of accuracy for local and N staging in all Radiologists with the use of DWI (also present in Kappas), more uniform in the experienced ones but for local stage in PN cases. Residents' accuracy for N highly increase in ID cases, while decreasing in PN. This could be due to a better detection of the LN, but with difficult interpretation of the changes secondary to treatment. On the contrary, all Radiologists show an increase in accuracy for T stage with DWI in ID cases (also PN in experienced ones), while decreasing in the rest. This could be due to a decrease in the overstaging of desmoplastic reaction or fibrosis in PN, with difficult interpretation of the latter for unexperienced ones.

CLINICAL RELEVANCE/APPLICATION

DWI could be functioning as a confounding factor in RC, especially in N and global staging.

SSK08-09 Role of CT-Colonography for Detection and Characterization of Synchronous Proximal Colonic Lesions in Patients with Stenosing Colorectal Cancer

Wednesday, Nov. 29 11:50AM - 12:00PM Room: E353B

Participants

Maria Jose Martinez-Sapina LLanas, A Coruna, Spain (*Presenter*) Nothing to Disclose Diego Dominguez Conde, MD, A Coruna, Spain (*Abstract Co-Author*) Nothing to Disclose Carmen Rodriguez Lopez, A Coruna, Spain (*Abstract Co-Author*) Nothing to Disclose Concepcion Crespo Garcia, A Coruna, Spain (*Abstract Co-Author*) Nothing to Disclose Ariana Prado Prado, A Coruna, Spain (*Abstract Co-Author*) Nothing to Disclose Sergio Garcia Dubra, A Coruna, Spain (*Abstract Co-Author*) Nothing to Disclose Fatima Vidal, A Coruna, Spain (*Abstract Co-Author*) Nothing to Disclose

PURPOSE

To evaluate the clinical usefulness of CT Colonography (CTC) immediately after incomplete Optical Colonoscopy (OC) for occlusive colorectal cáncer (CCR), in the detection of synchronous carcinomas and advanced adenomas and their impact in the management of patients.

METHOD AND MATERIALS

Posterior to incomplete OC,165 patients (mean age of 71 years) with occlusive colonic carcinoma underwent subsequent CTC. 135 patients had distal CRC and 29 proximal. Experienced radiologists prospectively analyzed the presence of syncronous carcinomas and colorectal polys. 164 patients underwent colorectal resection. We retrospectively analyzed the surgical outcome and the follow-up of patients.

RESULTS

Seventeen syncronous tumors were detected in 11 patients (6,6%). Eight in the proximal and nine in distal colon. Eight patients had only one synchronous tumor and three patients had several tumors (2, 3 and 4 synchronous carcinomas, respectively). Nineteen polypoid lesions > 2 cm were detected in 10 patients, seventeen were tubulo-villous adenomas with high-grade displasia and two were tubulo-villous adenomas with low-grade displasia. Twenty one patient (12.72%) had pediculated and sesil polyps in the remainig colorectum not explored in the OC, that required OC and exeresis between 1 and 6 months after surgery. After CTC, surgeons modified initial surgical plan in 22 patients (13,3%) and the follow-up in 25 patients (15,15%). 13 patients with obstructive cancer couldnt be correctly assesed, 8 because of defficient colonic distension and 5 due to great amount of feces. Gross lesions were discharged, nevertheless we recommended vigilance during surgical procedure and posterior.

CONCLUSION

Detection of all synchronous CRC and adenomatous polys, before surgery is very important, as the number and location of tumors may affect the surgical procedure and the subsequent management of patients. In our series, CTC changed surgical management and surveillance in 47 patients (28,45%). CTC is a technically robust and the most practical method to evaluate the colon proximal to an occlusive cancer, even in patients with metallic stent placement in acute neoplastic colonic obstruction.

CLINICAL RELEVANCE/APPLICATION

This exhibit exposes the use of CT-Colonography to evaluate all the colon in obstructing colorectal cancers with incomplete Optical Colonoscopy and their ability to detect synchronous cancers and advanced adenomas.





103rd Scientific Assembly and Annual Meeting November 26 to December 1 McCormick Place, Chicago



SSK09

Genitourinary (New Methods in Prostate Imaging and Intervention)

Wednesday, Nov. 29 10:30AM - 12:00PM Room: E450B



AMA PRA Category 1 Credits ™: 1.50 ARRT Category A+ Credit: 1.75

FDA Discussions may include off-label uses.

Participants

Andrew B. Rosenkrantz, MD, New York, NY (*Moderator*) Nothing to Disclose Ronaldo H. Baroni, MD, Sao Paulo, Brazil (*Moderator*) Nothing to Disclose Temel Tirkes, MD, Indianapolis, IN (*Moderator*) Nothing to Disclose

Sub-Events

SSK09-01 A New System to Spatially Align In Vivo MRI with Ex Vivo MRI and Whole-Mount Histopathology for Integrated Prostate Cancer Research

Participants

Holden H. Wu, PhD, Los Angeles, CA (*Presenter*) Institutional research support from Siemens
Alan Priester, MS, Los Angeles, CA (*Abstract Co-Author*) Nothing to Disclose
Pooria Khoshnoodi, MD, Los Angeles, CA (*Abstract Co-Author*) Nothing to Disclose
Preeti Ahuja, PhD, Los Angeles, CA (*Abstract Co-Author*) Nothing to Disclose
Zhaohuan Zhang, Los Angeles, CA (*Abstract Co-Author*) Nothing to Disclose
Nazanin H. Asvadi, MD, Los Angeles, CA (*Abstract Co-Author*) Nothing to Disclose
Kyunghyun Sung, PhD, Los Angeles, CA (*Abstract Co-Author*) Nothing to Disclose
Shyam Natarajan, Los Angeles, CA (*Abstract Co-Author*) Nothing to Disclose
Shyam Natarajan, Los Angeles, CA (*Abstract Co-Author*) Nothing to Disclose
Robert E. Reiter, MD, Los Angeles, CA (*Abstract Co-Author*) Nothing to Disclose
Steven S. Raman, MD, Santa Monica, CA (*Abstract Co-Author*) Nothing to Disclose
Dieter R. Enzmann, MD, Los Angeles, CA (*Abstract Co-Author*) Research support, Siemens AG

For information about this presentation, contact:

HoldenWu@mednet.ucla.edu

PURPOSE

The development and validation of multi-parametric MRI (mp-MRI) for prostate cancer (CaP) diagnosis relies on comparisons with histopathology (HP) and accurate spatial alignment is critical. In this study, we develop and evaluate a new system that combines patient-specific molds and ex vivo MRI of the resected prostate to align in vivo (InV) MRI, ex vivo (ExV) MRI, and whole-mount (WM) HP in CaP patients.

METHOD AND MATERIALS

Patients who underwent radical prostatectomy were studied. InV-MRI was obtained prior to surgery (mean = 77 days) at 3 T (Trio/Verio/Skyra/Prisma, Siemens) using an external array and an endorectal coil. The protocol included 3D T2w MRI, on which the prostate was contoured in 3D to print a patient-specific mold before surgery. Within 30 min after surgery, the fresh whole prostate specimen was placed in a patient-specific mold and underwent ExV-MRI at 3 T (Prisma, Siemens) using a knee coil. The protocol included high-resolution T2w MRI to evaluate spatial alignment with in vivo 3D T2w MRI and WM slides. Immediately afterwards, the prostate was sectioned in the mold along slits (4.5-mm steps) to create WM slides. InV-MRI was registered to ExV-MRI using a mutual information based rigid 3D algorithm. A non-rigid algorithm was used to register WM slides to ExV and InV MRI. A radiologist matched 2D slice locations and annotated corresponding non-cancerous landmarks on all three image sets. The WM to ExV-MRI slices offset error was recorded. In the matched slices, 2D target registration error (TRE) between the landmarks was calculated.

RESULTS

In all patients (N=10, mean 64.7 years, mean PSA 6.17 ng/ml), ExV-MRI was successfully completed (mean time 116 min). The mold and ExV-MRI had no adverse impact on WM HP. The mean slice offset error was 1.36 mm (<1.5-mm MRI slice thickness). Mean 2D TRE was (mean \pm SD): 1.9 \pm 1.1 mm for INV vs. ExV MRI, 1.6 \pm 0.9 mm for WM vs. ExV MRI, and 2.1 \pm 1.4 mm for WM vs. InV MRI.

CONCLUSION

We have successfully integrated the new system with our clinical workflow to achieve excellent spatial alignment among InV-MRI, ExV-MRI, and WM slides with 2D TRE of 1-2 mm. This can enable MRI-WM comparisons and integrated research in CaP.

CLINICAL RELEVANCE/APPLICATION

The new system achieves excellent spatial alignment among in vivo MRI, ex vivo MRI, and whole-mount histopathology for integrated research in prostate cancer.

SSK09-02 An Objective Tool for Diagnosing Prostate Cancer and Benign Prostatic Hyperplasia: Radiomics Features Extracted from Diffusion-Weighted Imaging

Participants

Chen Lihua, Dalian, China (*Presenter*) Nothing to Disclose Ailian Liu, MD, Dalian, China (*Abstract Co-Author*) Nothing to Disclose Yan Guo, Shenyang, China (*Abstract Co-Author*) Nothing to Disclose Xin Li, Shanghai, China (*Abstract Co-Author*) Nothing to Disclose Dan Guo, Dalian, China (*Abstract Co-Author*) Nothing to Disclose

PURPOSE

To evaluate the usefulness of radiomics features indistinguishing prostate cancer (PCa) from benign prostatic hyperplasia (BPH) based on diffusion-weighted imaging (DWI) sequence without subjective factors.

METHOD AND MATERIALS

This retrospective study was approved by local IRB, and written informed consent was waived. 200patientswere enrolled followed by surgery or biopsy within one month in this study(100 were PCa and 100 were BPH)High-throughput extraction and analysis of the radiomics features based on DWI included five procedures: 1) 2D region of interest (ROI) was sketched along the edge of the whole prostate at the slice with the maximum diameter of the lesion by a 3-year experienced radiologist.2) 396 radiomics features, including size and shape based-features, histogram, GLCM as well as GLRLM texture features were automatically generated from A.K.(Analysis-Kinetics, GE Healthcare). 3) Feature reduction was conducted based on Kruskal-Wallis test and auto-correlation analysis with |r| > 0.9 using R.4)90 PCa and 90 BPH selected randomly in 200 patients were used for supervise Model-learning using Logistic Regression. 5)10 PCa and 10 BPH were used and compared with pathologic diagnosis and receiver operating characteristics (ROC) were used to assess the efficiency of model.

RESULTS

K-W test showed that 233 radiomic parameters had significant difference between PCa and BPH groups, auto-correlationanalysis reduced them into 47 potential predictors which used for diagnostic model building. The area under the curve (AUC) of Logisticregression model in discriminating the two groups was 0.894, sensitivity and specificity were respectively 92.2% and 86.7%, with 85% diagnosis accuracy rate.

CONCLUSION

Radiomics features of DWI performed well indistinguishing PCa from BPH, which could help objectively and quantitatively evaluate tumor heterogeneity, and have prospect of being an independent &non-invasive efficient diagnostictool.

CLINICAL RELEVANCE/APPLICATION

Compared with traditional manual method, Radiomics features not only could lighten the visual fatigue for radiologist but also raise the precision of diagnosis.

SSK09-03 Diagnosing Prostate Cancer through Non-Invasive Estimation of Prostate Tissue Composition Using Hybrid Multidimensional MRI

Wednesday, Nov. 29 10:50AM - 11:00AM Room: E450B

Awards

Student Travel Stipend Award

Participants

Aritrick Chatterjee, PhD, Chicago, IL (*Presenter*) Nothing to Disclose Roger Bourne, PhD, Sydney, Australia (*Abstract Co-Author*) Nothing to Disclose Shiyang Wang, PhD, Chicago, IL (*Abstract Co-Author*) Nothing to Disclose Alexander Gallan, MD, Chicago, IL (*Abstract Co-Author*) Nothing to Disclose Gregory S. Karczmar, PhD, Chicago, IL (*Abstract Co-Author*) Nothing to Disclose Aytekin Oto, MD, Chicago, IL (*Abstract Co-Author*) Research Grant, Koninklijke Philips NV; Research Grant, Guerbet SA; Research Grant, Profound Medical Inc; Medical Advisory Board, Profound Medical Inc; Speaker, Bracco Group; ; Tatjana Antic, Chicago, IL (*Abstract Co-Author*) Nothing to Disclose

For information about this presentation, contact:

aritrick@uchicago.edu

PURPOSE

This study proposes to use Hybrid Multidimensional MRI (HM-MRI) to measures the change in ADC and T2 as a function of TE and *b*-value, respectively. This interdependence is used as a source of information about the underlying tissue microstructure. Specifically, we analyzed HM-MRI data to identify signal contribution from epithelial, stromal and luminal compartments in each image voxel. We evaluated whether this compartmental analysis can distinguish prostate cancer (PCa) from normal tissue.

METHOD AND MATERIALS

Patients (n=21) with confirmed PCa underwent preoperative 3T MRI. Axial images using HM-MRI were acquired with TE = 47, 75, 100 ms and *b*-values of 0, 750, 1500 s/mm2, resulting in a 3×3 array of data associated with each voxel. Volumes of tissue components- stroma, epithelium and lumen were calculated by fitting the hybrid data to a three compartment signal model, with distinct ADC and T2 associated with each compartment. Volume fractions, and conventional ADC and T2 were measured for ROIs on sites of prostatectomy verified malignancy (n=28) and normal tissue (n=71). ROC analysis was used to evaluate the performance of various parameters in differentiating PCa from benign tissue.

RESULTS

HM-MRI data from PCa showed significantly increased fractional volumes of epithelium (48.8 ± 9.2 vs $23.2\pm7.1\%$) and reduced lumen (14.0 ± 5.2 vs $26.4\pm14.1\%$), stroma (37.2 ± 9.1 vs $50.5\pm15.7\%$), ADC (0.86 ± 0.18 vs $1.30\pm0.23\mu$ m2/ms) and T2 (76.3 ± 22.9 vs

104.2 \pm 47.1ms) as compared to normal tissue. These trends and values measured by HM-MRI are similar to those reported in previous histological studies. The volume fractions of epithelium (0.65), stroma (-0.44) and lumen (-0.39) show significantly higher Spearman correlation coefficient with Gleason score as compared to T2 (-0.29) and ADC (-0.32). Area under the ROC curve was highest for epithelium (0.99), followed by lumen (0.80), stroma (0.79) and T2 (0.71).

CONCLUSION

Fractional volumes of prostatic lumen, stroma, and epithelium change significantly when cancer is present. These parameters can be measured non-invasively using HM-MRI and these novel quantitative parameters have the potential to improve PCa diagnosis and determine the aggressiveness of PCa.

CLINICAL RELEVANCE/APPLICATION

Prostate tissue composition estimated non-invasively using HM-MRI has better diagnostic accuracy of detecting PCa compared to conventional T2 and ADC values.

Honored Educators

Presenters or authors on this event have been recognized as RSNA Honored Educators for participating in multiple qualifying educational activities. Honored Educators are invested in furthering the profession of radiology by delivering high-quality educational content in their field of study. Learn how you can become an honored educator by visiting the website at: https://www.rsna.org/Honored-Educator-Award/ Aytekin Oto, MD - 2013 Honored EducatorAytekin Oto, MD - 2017 Honored Educator

SSK09-04 Temporal Changes in MRI Appearance of the Prostate after Focal Ablation

Wednesday, Nov. 29 11:00AM - 11:10AM Room: E450B

Participants

Andreas M. Hoetker, MD, Mainz, Germany (*Presenter*) Nothing to Disclose Andreas A. Meier, MD, New York, NY (*Abstract Co-Author*) Nothing to Disclose Yousef Mazaheri, PhD, New York, NY (*Abstract Co-Author*) Nothing to Disclose Junting Zheng, New York, NY (*Abstract Co-Author*) Nothing to Disclose Marinela Capanu, New York, NY (*Abstract Co-Author*) Nothing to Disclose Ramon E. Sosa, BA, New York, NY (*Abstract Co-Author*) Nothing to Disclose Jonathan A. Coleman, MD, New York, NY (*Abstract Co-Author*) Speakers Bureau, Amgen Inc Speakers Bureau, Steba-Biotech NV Hedvig Hricak, MD, PhD, New York, NY (*Abstract Co-Author*) Board of Directors, Ion Beam Applications, SA Oquz Akin, MD, New York, NY (*Abstract Co-Author*) Nothing to Disclose

PURPOSE

The purpose of our study was to retrospectively evaluate and categorize temporal changes in MRI appearances of the prostate in patients who underwent focal therapy with MRI follow up.

METHOD AND MATERIALS

The Institutional Review Board approved this retrospective study and waived the requirement for informed consent. Forty-two patients (median age 61; 48-76 years) with low-to-intermediate-risk, clinically organ-confined prostate cancer underwent focal ablation therapy from 2009 through 2014. Two radiologists reviewed post-treatment MRIs (n=88) and categorized imaging features blinded to the time interval between the focal therapy and the follow-up MRI. Inter-reader agreement was assessed (kappa) and generalized linear regression was used to examine associations between imaging feature being present/absent and days between ablation and MRI.

RESULTS

Inter-reader agreement on MRI features ranged from fair to substantial. The presence of edema on MRI was found at the shortest median time interval after ablation (15-22d; p<0.001), followed by rim enhancement of the ablation zone (18-23d), a hypointense rim around the ablation zone on T2-weighted images (49-54d) and the presence of an appreciable ablation cavity (49-55d; all p<0.05). The formation of a T2-hypointense scar (446-461d) and enhancement of the ablation zone/scar (216-610d) were found to be present on later MRI scans for one reader.

CONCLUSION

The MRI appearance of the prostate after focal ablation changes substantially over time. Identification of temporal patterns in the appearance of imaging features should help radiologists distinguish normal MRI findings from possible recurrence and reduce image interpretation variability and errors when assessing post-therapeutic scans.

CLINICAL RELEVANCE/APPLICATION

The identification of distinct imaging features on prostate MRI after ablation with distinct temporal patterns allows for a more consistent language among radiologists and could reduce variability and errors when assessing post-therapeutic scans.

SSK09-05 Multiplexed Sensitivity-Encoding (MUSE) Reconstructed Multi-Shot Diffusion Weighted Imaging in Patients with Prostate Cancer: Preliminary Study on Image Quality and Apparent Diffusion Coefficient

Wednesday, Nov. 29 11:10AM - 11:20AM Room: E450B

Participants

Makoto Sakane, MD, Suita, Japan (*Presenter*) Nothing to Disclose Masatoshi Hori, MD, Suita, Japan (*Abstract Co-Author*) Nothing to Disclose Hiromitsu Onishi, MD, Suita, Japan (*Abstract Co-Author*) Nothing to Disclose Tetsuya Wakayama, PhD, Hino-Shi, Japan (*Abstract Co-Author*) Employee, General Electric Company Hiroyuki Tarewaki, Osaka, Japan (*Abstract Co-Author*) Nothing to Disclose Noriyuki Tomiyama, MD, PhD, Suita, Japan (*Abstract Co-Author*) Nothing to Disclose Mitsuaki Tatsumi, MD, PhD, Suita, Japan (*Abstract Co-Author*) Nothing to Disclose Takahiro Tsuboyama, MD, Suita, Japan (*Abstract Co-Author*) Nothing to Disclose Takashi Ota, Suita, Japan (*Abstract Co-Author*) Nothing to Disclose Yoshihiro Koyama, BS, Suita, Japan (*Abstract Co-Author*) Nothing to Disclose Motohide Uemura, Suita, Japan (*Abstract Co-Author*) Nothing to Disclose Norio Nonomura, Suita, Japan (*Abstract Co-Author*) Nothing to Disclose

PURPOSE

Multiplexed Sensitivity-Encoding (MUSE) is a new reconstruction algorithm for multi-shot diffusion weighted image (msDWI) without using navigator echo to correct motion-induced phase error. The purpose of this study was to prospectively evaluate the image quality and apparent diffusion coefficient (ADC) of high-spatial resolution msDWI reconstructed with MUSE in patients suspected with prostate cancer.

METHOD AND MATERIALS

Fifteen consecutive patients clinically suspected with prostatic cancer (median 72 years old, range 55 - 80) underwent 3-T MR imaging using T2 weighted image, single-shot DWI (ssDWI; matrix, 96 x 96) and MUSE-reconstructed msDWI (matrix, 192 x 192) acquired with 4-shot interleaved echo-planar imaging. Both DWI were acquired with FOV of 22 cm, thickness of 4 mm, and b-value of 50 and 800 mm2/s. ADC maps were constructed for both DWI. Two radiologists blindly and independently assessed the image quality of DWI (b = 50, 800) and ADC map by comparing ssDWI and msDWI on image noise, anatomic delineation, distortion, artifact, and overall image quality with a 5-point scale. ADC values were measured in transitional and peripheral zone (TZ and PZ). Wilcoxon rank-sum test, kappa coefficient and paired t test was used to compare the score, inter-observer concordances and ADC value.

RESULTS

The scores of anatomic delineation of msDWI (b = 50, 800) and msADC map were significantly better than a single-shot image, and the scores of image noise were significantly worse for multi-shot image by 2 radiologists (p < .05, respectively). The score of overall image quality of msDWI (b = 50) was significantly better than ssDWI by 2 radiologists (p = .001, for both), but there were no significant differences for DWI (b = 800) and ADC map. Distortion and artifact were not significantly different between msDWI and ssDWI. The inter-observer concordances were poor to good (k = .074 - .770). ADC values of msDWI and ssDWI were not significantly different for TZ and PZ (p = 0.47 and 0.70).

CONCLUSION

The msDWI reconstructed with MUSE and its ADC map significantly improved anatomical delineation of the prostate, although the technique increased image noise. ADC values were not significantly different between ssDWI and msDWI.

CLINICAL RELEVANCE/APPLICATION

Evaluation of the prostate can be improved with high-spatial resolution msDWI reconstructed with MUSE, which is a promising technique for the detection and diagnosis of prostate cancer.

SSK09-06 Radiomics on Contrast-Free Bi-Parametric MRI Achieves Improves Prediction of Significant Prostate Cancer Compared to Clinical PI-RADS Version 2 Interpretation

Wednesday, Nov. 29 11:20AM - 11:30AM Room: E450B

Participants

David Bonekamp, MD, PhD, Heidelberg, Germany (*Presenter*) Speaker, Profound Medical Inc Manuel Wiesenfarth, PhD, Heidelberg, Germany (*Abstract Co-Author*) Nothing to Disclose Jan P. Radtke, Heidelberg, Germany (*Abstract Co-Author*) Nothing to Disclose Michael Gotz, Heidelberg, Germany (*Abstract Co-Author*) Nothing to Disclose Philipp Kickingereder, Heidelberg, Germany (*Abstract Co-Author*) Nothing to Disclose Kaneschka Yaqubi, Heidelberg, Germany (*Abstract Co-Author*) Nothing to Disclose Bertram Hitthaler, Heidelberg, Germany (*Abstract Co-Author*) Nothing to Disclose Nils Gahlert, Heidelberg, Germany (*Abstract Co-Author*) Nothing to Disclose Martin T. Freitag, MD, Heidelberg, Germany (*Abstract Co-Author*) Nothing to Disclose Markus Hohenfellner, MD, PhD, Heidelberg, Germany (*Abstract Co-Author*) Nothing to Disclose Boris Hadaschik, Heidelberg, Germany (*Abstract Co-Author*) Nothing to Disclose Heinz-Peter W. Schlemmer, MD, Heidelberg, Germany (*Abstract Co-Author*) Nothing to Disclose Klaus Maier-Hein, Heidelberg, Germany (*Abstract Co-Author*) Nothing to Disclose

PURPOSE

To apply radiomics and machine learning (ML) to PI-RADS version 2 lesions and assess whether radiomics alone or the addition of radiomics improves predictive performance.

METHOD AND MATERIALS

In 194 consecutive patients examined on a 3T MRI system 253 PIRADSv2 lesions were identified and manually segmented on ADC/bvalue of 1500 s/mm2 and T2-weighted images (segP). Patient were subsequently undergoing MRI-TRUS fusion biopsy with median 23 systematic cores and 4 targeted cores per lesion. In addition, on the basis of the biopsy results, retrospective PI-RADS assessment (PIRADSv2R) and manual lesions segmentation of the MR index lesion was performed manually by an experienced radiologist (segR). A total of 1073 quantitative radiomics features [including first-order, volume shape features, and texture features] were automatically extracted. The prediction of clinically significant Cancer (csPC) (GS 3+4 and 4+3 or higher) by PIRADSv2 assessment was compared to different ML approaches to integrate radiomics data (random forest, parameter normalization, training on segP/segR). Performance was assessed using bootstrap. The number of biopsies spared was assessed on a lesion and patient level.

RESULTS

A cut-off >=3 for PIRADSv2 was used. Radiomics Models were evaluated at the PIRADSv2 sensitivity, which was 96-97% in all cases. On a per-lesion basis PIRADSv2 achieved a specificity of 20% compared to 39% for the best ML model (RF trained using segR at PIRADSv2R cut-off of 4 including normalization, for GS4+3 prediction), which would have saved 42.3 biopsies. On a per-patient basis the model increased specificity from 23% to 37% which would have saved 23 patients a biopsy. Excluding the transitional zone, specificity increased from 41% to 52% for lesions, saving 11.2 biopsies and from 48% to 59% for patients saving

14.2 biopsies for GS3+4 prediction. Figure 1 demonstrates improved performance of the best ML model over PI-RADSv2, especially in the important high sensitivity range.

CONCLUSION

Radiomics and ML improve predictive performance compared to PI-RADS version 2 when applied to clinically selected lesions. The potential of radiomics to support clinical decision making is shown. Our results motivate the evaluation of this approach in larger and prospective cohorts.

CLINICAL RELEVANCE/APPLICATION

The potential application of the addition of radiomics to the clinical evaluation of PI-RADS lesions should be evaluated in a prospective setting.

SSK09-07 Towards Improved Gleason Score Prediction Using 18F-FACBC (Fluciclovine) PET and MRI: Evaluation of Advanced Post-Processing Methods Using Machine Learning

Wednesday, Nov. 29 11:30AM - 11:40AM Room: E450B

Awards

Trainee Research Prize - Resident

Participants

Ivan Jambor, MD, Turku, Finland (*Presenter*) Speakers Bureau, Koninklijke Phillips NV Parisa Movahedi, Turku, Finland (*Abstract Co-Author*) Nothing to Disclose Harri Merisaari, Turku, Finland (*Abstract Co-Author*) Nothing to Disclose Jukka Kemppainen, MD, PhD, Turku, Finland (*Abstract Co-Author*) Nothing to Disclose Pekka Taimen, Turku, Finland (*Abstract Co-Author*) Nothing to Disclose Heikki R. Minn, MD, PhD, Turku, Finland (*Abstract Co-Author*) Nothing to Disclose

PURPOSE

To evaluate the potential of advanced post-processing methods for 18F-FACBC (Fluciclovine) PET and MRI in the characterization of prostate cancer.

METHOD AND MATERIALS

Twenty one patients with histologically confirmed prostate cancer (PCa) scheduled for robotic-assisted prostatectomy underwent PET/CT immediately after injection of 369 \pm 10 MBq 18F-FACBC followed by PET/MRI (ClinicalTrials.gov Identifier: NCT02002455). MRI of PET/MRI consisted of T2-weighted imaging (T2w), two separate diffusion weighted imaging (DWI) acquisitions, second order rotating frame (RAFF) imaging, and T2 mapping. A separate 3T mpMRI consisting of T2w, three DWI acquisitions, proton magnetic resonance spectroscopy (1H-MRS) and dynamic contrast enhanced (DCE) imaging was acquired within a week of the PET scans. DWI was post-processed using kurtosis (ADCk, K), mono- (ADCm), and biexponential functions (f, Dp, Df) while Logan plots were used to calculate volume of distribution (VT). Logistic Regression with I2 normalization and leave-pair out cross validation (LPOCV) based area under the curve (AUC) values were used to estimate the potential of the quantitative parameters and their combination to predict Gleason score group (3+3 vs >3+3). Recursive feature elimination technique in the cross-validation loop was applied to exclude the bias of the model performance. In total, 16 unique PET (Vt, SUV) and MRI derived quantitative parameters were evaluated. Whole mount prostatectomy sections were used as "ground true".

RESULTS

The RAFF, monoexponential and kurtosis derived parameters had LPOCV AUC in the range of 0.72 to 0.82 while the corresponding value for VT was 0.85. T2 mapping, 1H-MRS ((choline+creatine)/citrate)) and DCE-MRI (Ktrans, Ve) derived parameters had the lowest LPOCV AUC in the range of 0.33 to 0.60. Most frequently selected parameters in each round of the cross-validation were VT, ADCk (0-2000 s/mm2, 12 b values), ADCm (0-1500 s/mm2, 2 b values), ADCm (0-500 s/mm2, 5 values), and K (0-2000 s/mm2, 12 b values) which demonstrated LPOCV AUC of 0.91.

CONCLUSION

Quantitative models using DWI and RAFF derived parameters led to improved PCa characterization. The added value of 18F-FACBC PET appears to be limited.

CLINICAL RELEVANCE/APPLICATION

18F-FACBC (Fluciclovine) PET has a power to predict Gleason score but adds little value to DWI and RAFF derived parameters.

SSK09-08 Computer-Aided Diagnosis for Prostate Cancer Detection in Multiparametric MRI: Influence on Reader Performance

Wednesday, Nov. 29 11:40AM - 11:50AM Room: E450B

Participants

Ge Gao, MD, Beijing, China (*Presenter*) Nothing to Disclose Huihui Wang, MD, Beijing, China (*Abstract Co-Author*) Nothing to Disclose Min Cao, MBBCh, MD, Beijing, China (*Abstract Co-Author*) Nothing to Disclose Rui Wang, PhD, Beijing, China (*Abstract Co-Author*) Nothing to Disclose Xiaoying Wang, MD, Beijing, China (*Abstract Co-Author*) Nothing to Disclose Yi Liu, Beijing, China (*Abstract Co-Author*) Nothing to Disclose

For information about this presentation, contact:

effie_gao@163.com

PURPOSE

To determine the interaction between computer-aided diagnosis (CAD) and readers with varying levels of experience in the interpretation of multiparametric prostate MR imaging with PIRADS v2.

METHOD AND MATERIALS

The institutional review board waived the need for informed consent. 64 patients (PCa=35; nonPCa=29) who were suspected of PCa and underwent mpMRI with subsequent biopsy or prostatectomy within 3 months were involved in this retrospective study. 6 readers were divided into 3 groups according to their experience in prostate imaging. Unknown the pathologic diagnosis, readers were asked to detect up to 3 lesions and graded 1-5 score according to PI-RADS v2 separately first without CAD and subsequently with CAD. Interreader agreement was assessed. According to histologic-radiologic correlation, the effect of CAD was evaluated by using ROC curve and Z test on patients and lesions basis. Wilcoxon signed ranks test were used to compare the diagnostic time and confidence with and without CAD. Furthermore, the requirement for CAD was also evaluated.

RESULTS

the AUC of stand-alone CAD was 0.918±0.036, and the spearman correlation coefficient between predictive values and PI-RADS scores was 0.706(P<0.01). Based on lesions, the AUCs of 6 readers were improved from 0.697-0.868 to 0.778-0.921 and the improvements were better than patient basis analysis. While the difference wasn't significant(P>0.05). Among 3 groups, the difference of AUCs between less experienced and experienced readers was significant without CAD, while with CAD, the difference was not significant. Besides, the interreader agreement and diagnostic confidence was improved significantly with CAD assisted. The rates of requirement for CAD were rising with reader's experience reduce. The average interpretation time of each case required an additional 0.8 minutes.

CONCLUSION

Integrating CAD into PCa mpMRI diagnostic process as a second reader, the performance of less experienced readers could be improved and similar with experienced readers. Additionally, with the reducing of experience, the requirement for CAD was rising.

CLINICAL RELEVANCE/APPLICATION

The CAD assisted can significantly improve the performance of less experienced readers in prostate mpMRI interpretation, and much better in lesion detection and evaluation than it in patient, which indicate that CAD could be a promising method for detecting a target lesions for prostate biopsy.

SSK09-09 Detection of MRI "Index Lesion" with mpMRI-TRUS Fusion-Targeted Prostate Biopsy: Does it Correspond to Histopathology?

Wednesday, Nov. 29 11:50AM - 12:00PM Room: E450B

Participants

Maurizio Del Monte, Montelanico, Italy (*Presenter*) Nothing to Disclose Marcello Domenico Grompone, MD, Roma, Italy (*Abstract Co-Author*) Nothing to Disclose Vincenzo Salvo, MD, Roma, Italy (*Abstract Co-Author*) Nothing to Disclose Martina Pecoraro, MD, Roma, Italy (*Abstract Co-Author*) Nothing to Disclose Carlo Catalano, MD, Rome, Italy (*Abstract Co-Author*) Nothing to Disclose Valeria Panebianco, MD, Rome, Italy (*Abstract Co-Author*) Nothing to Disclose

For information about this presentation, contact:

delmontemaurizio250285@gmail.com

PURPOSE

To determine the histopathological correspondence of MRI "index lesion" between multiparametric magnetic resonance imaging (mpMRI)/Transrectal ultrasonography (TRUS) fusion biopsy and radical prostatectomy.

METHOD AND MATERIALS

Institutional review board approval; Informed consent was obtained from all individual participants included in the study. This prospective study has been performed on a cohort of 142 biopsy naive patients aged 45-76 years, with elevated PSA level, recruited from October 2015. Diagnostic 3T MRI was performed and the index lesion is identified as being the one with the highest PI-RADS v.2 score and 1-3 additional "potential lesion" with a lower PI-RADS (v.2) and/or smaller volume are defined as 'Non Index lesion'. A maximum of 2-3 biopsies per lesion have been carried out and pathologic results acquired. Patients found to be positive undergo radical prostatectomy.

RESULTS

Prostate cancer was detected in 142/142 patients with a cancer detection rate being 100%. MR index lesion and the pathology report show a 100% correspondence concerning the lesion dimensions. MR/TRUS guided biopsy and the pathology report show a 86% correspondence with a relative risk of 0.94 and a p value <0.01, concerning Gleason Score Determination; and a 72% correspondence with a relative risk of 0.69 a p value <0.01, concerning the highest Gleason Score. Missed lesions on MRI proved to be low risk , Gleason Score 6 area, with a volume < 0.5 cc, which can be defined as «Insignificant» disease, with a negative predictive value (NPV) equal to 95-98%.

CONCLUSION

MRI/TRUS fusion biopsy shows a good correlation between "MRI index lesion" and definitive histopathological diagnosis on radical prostatectomy, in terms of dimensions, histological aggressiveness and highest Gleason Score of the pathology report.

CLINICAL RELEVANCE/APPLICATION

Among the new approaches to prostate biopsy, MR Imaging-Transrectal US Fusion has the potential to significantly increase the detection of csPCA.



KSNA° 2017

103rd Scientific Assembly and Annual Meeting November 26 to December 1 McCormick Place, Chicago



SSK10

Science Session with Keynote: Genitourinary (DECT)

Wednesday, Nov. 29 10:30AM - 12:00PM Room: N228



AMA PRA Category 1 Credits ™: 1.50 ARRT Category A+ Credit: 1.75

FDA Discussions may include off-label uses.

Participants

Benjamin M. Yeh, MD, San Francisco, CA (*Moderator*) Research Grant, General Electric Company; Author with royalties, Oxford University Press; Shareholder, Nextrast, Inc; Research Grant, Koninklijike Philips NV; ; Daniele Marin, MD, Durham, NC (*Moderator*) Research support, Siemens AG

Sub-Events

SSK10-01 Genitourinary Keynote Speaker: Vivid Material Separation at Multi-energy CT

Participants

Benjamin M. Yeh, MD, San Francisco, CA (*Presenter*) Research Grant, General Electric Company; Author with royalties, Oxford University Press; Shareholder, Nextrast, Inc; Research Grant, Koninklijike Philips NV; ;

For information about this presentation, contact:

ben.yeh@ucsf.edu

SSK10-02 A Probabilistic Approach to the Assessment of Renal Stone Mineral Composition Using Dual-Energy CT

Wednesday, Nov. 29 10:40AM - 10:50AM Room: N228

Participants Andrea Ferrero, PhD, Rochester, MN (*Presenter*) Nothing to Disclose Aeli Olson, St. Paul, MN (*Abstract Co-Author*) Nothing to Disclose Jayse Weaver, Rochester, MN (*Abstract Co-Author*) Nothing to Disclose Cynthia H. McCollough, PhD, Rochester, MN (*Abstract Co-Author*) Research Grant, Siemens AG

For information about this presentation, contact:

ferrero.andrea@mayo.edu

PURPOSE

In dual-energy CT (DECT) a threshold in the ratio between the average CT number within the stone from a low kV and a high kV image is generally used to differentiate stone types. This approach has demonstrated near 100% accuracy in separating uric acid (UA) from non-uric acid (NUA) stones, however it has failed to yield acceptable performance in separating NUA subtypes, such as calcium oxalate and apatite stones. In this study, we investigated a probabilistic approach that replaced discrete classification of stone mineral composition with a likelihood estimation.

METHOD AND MATERIALS

Patients with a DECT scan of the abdomen followed by an ex vivo analysis of the removed stone were retrospectively evaluated with IRB approval. Of these, only the cases with pure stones (i.e. >90% purity) were included in the study. Each stone was segmented using automated in-house software, and histograms of the distribution of CT number ratios for each stone were generated. Each histogram was compared to simulated histograms for 5 mineral compositions: uric acid (UA), cystine (CYS), struvite (STR), calcium oxalate / brushite (COM/COD/BRU) and apatite (APA). The likelihood of each mineral composition was computed as the overlap of the area between each histogram. The most likely mineral composition was compared to the conventional, threshold based approach currently used in clinical practice. Accuracy for the two methods was computed as the percentage of patient cases whose stone was correctly classified, using the ex vivo composition analysis as reference.

RESULTS

228 patients were retrospectively identified. 112 patients that had a pure stone (as determined ex vivo through infrared spectroscopy) of at least 10 mm3 were included in the study. The threshold-based method correctly classified 70% of the stones, whereas the probabilistic method correctly classified 73% - 88% if the two most likely compositions were considered. Of note is that the average confidence for the correct cases was 65%, whereas it was below 50% for the incorrect cases.

CONCLUSION

A probabilistic approach that provides an estimation of composition likelihood has been shown to more accurately characterize renal stones compared to threshold-based methods.

CLINICAL RELEVANCE/APPLICATION

The proposed method would increase clinician confidence in the in vivo determination of urinary stone composition using DECT,

appropriately identifying cases where the assessment is more uncertain.

SSK10-03 Characterization of Small (<4 cm) Focal Renal Lesions: Diagnostic Accuracy of Spectral Analysis using Single-Phase Contrast-enhanced Dual-energy CT

Wednesday, Nov. 29 10:50AM - 11:00AM Room: N228

Participants

Bhavik N. Patel, MD, MBA, Stanford, CA (*Presenter*) Consultant, General Electric Company; Research support, General Electric Company

Kingshuk Choudhury, PhD, Durham, NC (*Abstract Co-Author*) Nothing to Disclose Rendon C. Nelson, MD, Durham, NC (*Abstract Co-Author*) Research Consultant, General Electric Company; Research Consultant, Nemoto Kyorindo, Ltd; Consultant, VoxelMetrix, LLC; Co-owner, VoxelMetrix, LLC; Advisory Board, Bracco Group; Advisory Board, Guerbet, SA; Research grant, Nemoto Kyorindo, Ltd; Speaker Bureau, Bracco Group; Royalties, Wolters Kluwer nv Daniele Marin, MD, Durham, NC (*Abstract Co-Author*) Research support, Siemens AG

PURPOSE

To determine whether single-phase contrast-enhanced dual-energy quantitative spectral analysis improves the accuracy of diagnosis for small (< 4.0 cm) renal lesions, compared to conventional single-energy attenuation measurements.

CONCLUSION

Single-phase contrast-enhanced dual-energy quantitative spectral analysis significantly improves the specificity for characterization of small (< 4.0 cm) renal lesions, compared to conventional single-energy attenuation measurements.

CLINICAL RELEVANCE/APPLICATION

Single-phase contrast enhanced dual energy quantitative spectral analysis can reliably characterize small renal lesions thereby reducing the need for additional subsequent dedicated renal lesion evaluation protocol imaging.

SSK10-04 Analysis of Dual Energy Spectral CT and Pathological Grading of Clear Cell Renal Cell Carcinoma

Wednesday, Nov. 29 11:00AM - 11:10AM Room: N228

Participants

Jinyan Wei, Lanzhou, China (*Presenter*) Nothing to Disclose Junlin Zhou, Lanzhou, China (*Abstract Co-Author*) Nothing to Disclose Jianhong Zhao, Lanzhou, China (*Abstract Co-Author*) Nothing to Disclose

For information about this presentation, contact:

weijinyan501@163.com

PURPOSE

To discuss the dual energy spectral CT imaging features of the pathological grading of clear cell renal cell carcinoma (ccRCC) and the correlation between spectral CT imaging features and pathology.

METHOD AND MATERIALS

We performed retrospective analyses of 62 patients with confirmed diagnosis of ccRCC. All patients underwent non-enhanced CT and dual-phase(cortex phase, CP and parenchyma phase, PP) contrast-enhanced CT with dual energy spectral mode. The subjects were pathologically divided into two groups: low-grade group (Fuhrman 1/2) and high-grade group (Fuhrman 3/4). The CT value of each lesion was measured on the monochromatic image of 70keV; the normalized iodine concentrations (NIC) and the slope of spectrum curve were calculated. The qualitative morphological parameters, including tumor shape, calcification, pseudocapsule, necrosis, and enhancement mode were compared between the two groups.

RESULTS

The CT value, NIC, and the mean slope of the low-grade group were higher than that of the high-grade group during CP(P=0.001, P=0.043, P<0.001, respectively). The CT did not differ significantly during PP(P=0.134); however, the NIC and mean slope varied considerably in the low grade than the high-grade group (P=0.048, P=0.017, respectively). The CT threshold value, NIC, and slope had high sensitivity and specificity in differentiating well-differentiated ccRCC from the poorly differentiated.The tumor shape, pseudocapsule, and necrosis differed significantly between the two groups (P<0.01).

CONCLUSION

Dual energy spectral CT with the quantitative analysis of iodine concentration and qualitative analysis of morphological characteristics increase the accuracy of diagnosing pathological grading of ccRCC.

CLINICAL RELEVANCE/APPLICATION

Clinnical relevance/application Dual energy spectral CT with the analysis of iodine concentration and the correlation between spectral CT imaging features and pathology may help increase the accuracy in differentiating the pathological grading of ccRCC

SSK10-05 Impact of Noise-Optimized Virtual Monoenergetic Dual-Energy Computed Tomography on Image Quality in Patients With Renal Cell Carcinoma

Wednesday, Nov. 29 11:10AM - 11:20AM Room: N228

Awards Student Travel Stipend Award

Participants Simon S. Martin, MD, Frankfurt, Germany (*Presenter*) Nothing to Disclose Julian L. Wichmann, MD, Frankfurt, Germany (*Abstract Co-Author*) Speaker, General Electric Company; Speaker, Siemens AG Lukas Lenga, Frankfurt, Germany (*Abstract Co-Author*) Nothing to Disclose Tommaso D'Angelo, MD, Messina, Italy (*Abstract Co-Author*) Nothing to Disclose Thomas J. Vogl, MD, PhD, Frankfurt, Germany (*Abstract Co-Author*) Nothing to Disclose Moritz H. Albrecht, MD, Charleston, SC (*Abstract Co-Author*) Nothing to Disclose Doris Leithner, MD, Frankfurt Am Main, Germany (*Abstract Co-Author*) Nothing to Disclose Christian Booz, MD, Frankfurt am Main, Germany (*Abstract Co-Author*) Nothing to Disclose

For information about this presentation, contact:

simartin@outlook.com

PURPOSE

To perform a quantitative and qualitative image analysis of noise-optimized virtual monoenergetic images (VMI+) in patients with renal cell carcinoma (RCC) undergoing dual-energy computed tomography (DECT).

METHOD AND MATERIALS

Fifty-two patients (33 men; 61.5 ± 13.6 years) with RCC underwent contrast-enhanced DECT during the corticomedullary and nephrogenic phase of renal enhancement. DECT datasets were reconstructed with standard linearly-blended (M_0.6) as well as traditional virtual monoenergetic (VMI) and VMI+ algorithms in 10-keV increments from 40 to 100 keV. Contrast-to-noise (CNR) and tumor-to-cortex ratios for corticomedullary- and nephrogenic-phase images were objectively measured. Subjective image quality and RCC delineation were evaluated by three radiologists.

RESULTS

Greatest CNR values were found for 40-keV VMI+ series in both corticomedullary- (8.9 ± 4.9) and nephrogenic-phase (7.1 ± 4.6) images and were significantly higher compared to all other reconstructions (P<0.001). Furthermore, tumor-to-cortex ratios were highest for 40-keV nephrogenic-phase VMI+ $(2.1\pm3.5; P<=0.016)$, followed by 50-keV and 60-keV VMI+ $(2.0\pm3.2 \text{ and } 1.8\pm2.8)$, respectively). Qualitative image quality scored highest for 50-keV VMI+ series in corticomedullary-phase reconstructions and 60-keV in nephrogenic-phase reconstructions (P<=0.031). Highest scores for lesion delineation were assigned for 40-keV VMI+ reconstructions (P<=0.074).

CONCLUSION

Low-keV VMI+ reconstructions lead to improved image quality and lesion delineation of corticomedullary- and nephrogenic-phase DECT datasets in patients with RCC.

CLINICAL RELEVANCE/APPLICATION

In summary, our results demonstrate that the noise-optimized VMI+ algorithm substantially improves subjective and objective image quality of abdominal DECT examinations in patients with RCC compared to traditional VMI and standard linearly-blended images. Furthermore, low-keV VMI+ reconstructions have the potential to improve delineation of RCC lesions

SSK10-06 Dual-Source Single-Energy Multidetector CT Urography with Multiple Radiation Exposures within the Same Patient: Comparison of Full-Dose and Half-Dose Images Reconstructed with FBP and Half-Dose Images with SAFIRE

Wednesday, Nov. 29 11:20AM - 11:30AM Room: N228

Participants

See Hyung Kim, Daegu, Korea, Republic Of (*Abstract Co-Author*) Nothing to Disclose Donghyeon Kim, Daegu, Korea, Republic Of (*Presenter*) Nothing to Disclose

For information about this presentation, contact:

kseehdr@dsmc.or.kr

PURPOSE

To prospectively compare image quality and lesion confidence of CTU images acquired at FBP with 100% radiation dose with those of CTU images simultaneously acquired at FBP and SAFIRE-3 with 100% and 50% radiation dose in patients with high risk for urothelial carcinomas.

METHOD AND MATERIALS

The institutional review board approved the study with written informed patient consent. 150 patients underwent CTU examinations using a dual-source single-energy scanner. Data from both tubes were reconstructed with FBP, and data from the primary tube only were reconstructed with SAFIRE. Seven radiologists subjectively assessed image quality and lesion confidence for 1200 total datasets. Nonparametric methods for cluster data were used to estimate the areas under the receiver operating characteristic curves (AUCs) for variance methods on the basis of a noninferiority margin of 0.05.

RESULTS

Mean AUCs of image quality in SAFIRE-3 at 25% radiation dose was significantly lower than those of FBP at 100% radiation dose (all P <0.05). The mean AUCs for the presence of lesion were 0.907 and 0.894 for FBP at 100% and 50% radiation doses, and 0.900 and 0.799 for SAFIRE-3 at 50% and 25% radiation doses. However, SAFIRE-3 at 25% radiation dose was significantly inferior to FBP at 100% radiation dose.

CONCLUSION

CTU images acquired at SAFIRE-3 with 25% radiation dose were inferior to those of FBP with 100% radiation dose for image quality and confidence for the presence of lesion, regardless of the radiologists' experience.

CLINICAL RELEVANCE/APPLICATION

CTU images acquired at SAFIRE-3 with 25% radiation dose were inferior to those of FBP with 100% radiation dose for image quality

and confidence for the presence of lesion, regardless of the radiologists' experience.

SSK10-07 The Application Value of Spectral CT Imaging in Distinguishing Renal Cell Carcinoma and Renal Angiomyolipomas

Wednesday, Nov. 29 11:30AM - 11:40AM Room: N228

Participants

Ma Guangming, MMed, Xianyang City, China (*Presenter*) Nothing to Disclose Zhang Xirong, MMed, Xianyang City, China (*Abstract Co-Author*) Nothing to Disclose He Taiping, MMed, Xian Yang City, China (*Abstract Co-Author*) Nothing to Disclose Chuangbo Yang, MMed, Xianyang City, China (*Abstract Co-Author*) Nothing to Disclose Haifeng Duan, Xianyang City, China (*Abstract Co-Author*) Nothing to Disclose

For information about this presentation, contact:

416725386@qq.com

PURPOSE

To assess the value of dual-energy spectral CT imaging in differentiating renal cell carcinoma (RCC) from Renal Angiomyolipomas (RAML).

METHOD AND MATERIALS

53 patients with suspected renal tumors who underwent plain and contrast-enhanced CT in cortical phase and medulla phase with dual-energy Spectral imaging mode were retrospectively analyzed. There were 31 cases of RCC and 22 cases of RAML. Images were analyzed on an AW4.6 workstation with GSI Viewer software to measure the effective-Z and fat concentration for lesions with the plain scan, CT values in 70keV images and iodine concentration (IC) in the cortical and medulla phases for lesions. The iodine concentration was normalized to that of the aorta to obtain normalized iodine concentration (NIC), and the difference of NIC between medulla and cortical phases was calculated. The above quantitative parameters from lesions were compared using independent sample t test, and ROC analysis was used to evaluate their diagnosis efficiency in differentiating RCC from RAML.

RESULTS

The Effective-Z, fat concentration, NIC in cortical phase, medulla phase, NIC difference, CT value in cortical phase and medulla phase for RCC were 7.60 ± 0.13 , -143.03 ± 32.75 g/L, 0.64 ± 0.13 , 0.49 ± 0.15 , 0.14 ± 0.18 , 116.53 ± 14.29 HU, 94.8 ± 12.34 HU, respectively; while the corresponding values for RAML were 7.74 ± 0.11 , -103.24 ± 9.84 g/L, 0.50 ± 0.88 , 0.58 ± 0.12 , -0.08 ± 0.13 , 96.47 ± 18.46 HU, 105.58 ± 14.14 HU, respectively. The differences for these parameters between the two lesion types were statistically significant (all p<0.05). Using the threshold value of -112.8g/L for the fat concentration in ROC analysis, one would obtain a sensitivity of 90.9% and specificity of 77.4% for differentiating RCC from RAML and the area under the curve was 0.89.

CONCLUSION

The parameters obtained in dual-energy spectral CT scans demonstrated appreciable clinical values for differentiating RCC from RAML, with the fat concentration providing the highest diagnostic performance.

CLINICAL RELEVANCE/APPLICATION

Dual-energy spectral CT is a promising method in differentiate RCC from RAML.

SSK10-08 Does Dual Energy CT Have the Ability to Differentiate Benign vs Malignant Ovarian Tumors?

Wednesday, Nov. 29 11:40AM - 11:50AM Room: N228

Awards

Student Travel Stipend Award

Participants

Steven W. Zheng, MD, Houston, TX (*Presenter*) Nothing to Disclose Dhakshina M. Ganeshan, MBBS, FRCR, Houston, TX (*Abstract Co-Author*) Nothing to Disclose Revathy B. Iyer, MD, Houston, TX (*Abstract Co-Author*) Nothing to Disclose Wei Wei, Houston, TX (*Abstract Co-Author*) Nothing to Disclose Priya R. Bhosale, MD, Bellaire, TX (*Abstract Co-Author*) Nothing to Disclose

For information about this presentation, contact:

steven.w.zheng@uth.tmc.edu

PURPOSE

To assess the ability of dual energy CT (DECT) to distinguish benign from malignant ovarian tumors (OT).

METHOD AND MATERIALS

Following approval of the institutional-review-board, institutional database was mined for treatment naïve patients who underwent primary cytoreduction for OT. 35 patients were included in the study. 17 patients had high grade, 8 had low grade, and 10 had benign tumors. Age, gender pathological diagnosis following surgical resection and tumor grade was documented. Advanced processing using the Advantage Work (AW) station was performed on the preoperative dual energy CT scan. ROIs were drawn on the ovarian mass on the AW. Pixel level data of the tumor was recorded for different energy levels 50 keV, 70 keV and 120 keV. The effective-Z (atomic number) amount of water and iodine present in the ovarian mass was recorded. Kruskal; Wallis test was used to compare the differences between three types of OT. All tests were two; sided and p < 0.05 were considered statistically significant.

RESULTS

Patients with high grade OTs were older than those with the low grade and the benign OTs (p = 0.02). High grade OT had higher

Hounsfield values than low grade and benign OT at 50 keV (p = 0.001), 70 keV (p = 0.0006), 120 keV (p = 0.0009), and higher amount of water g/cm3 (p < 0.005). Benign OT had significantly lower atomic number (p = 0.002) and amount of iodine g/cm3 (p = 0.002) compared to malignant OT.

CONCLUSION

Dual energy CT has the potential to distinguish between high grade, low grade and benign ovarian tumors. Given the small sample size, future trials may be helpful in confirming our findings.

CLINICAL RELEVANCE/APPLICATION

DECT has the potential to differentiate between benign and malignant tumors and may be helpful in avoiding unneccessary surgery.

Honored Educators

Presenters or authors on this event have been recognized as RSNA Honored Educators for participating in multiple qualifying educational activities. Honored Educators are invested in furthering the profession of radiology by delivering high-quality educational content in their field of study. Learn how you can become an honored educator by visiting the website at: https://www.rsna.org/Honored-Educator-Award/ Priya R. Bhosale, MD - 2012 Honored Educator

SSK10-09 Dual Layer Spectral CT: Non-Inferiority Assessment Compared To Dual Source Dual Energy CT in Discriminating Uric Acid from Non-Uric Acid Stones in a Phantom Model

Wednesday, Nov. 29 11:50AM - 12:00PM Room: N228

Participants

Lakshmi Ananthakrishnan, MD, Dallas, TX (*Presenter*) Nothing to Disclose Xinhui Duan, PhD, Dallas, TX (*Abstract Co-Author*) Nothing to Disclose Yin Xi, Dallas, TX (*Abstract Co-Author*) Nothing to Disclose Harold Goerne, MD, Zapopan, Mexico (*Abstract Co-Author*) Nothing to Disclose John R. Leyendecker, MD, Dallas, TX (*Abstract Co-Author*) Nothing to Disclose Julia R. Fielding, MD, Dallas, TX (*Abstract Co-Author*) Nothing to Disclose Suhny Abbara, MD, Dallas, TX (*Abstract Co-Author*) Nothing to Disclose Suhny Abbara, MD, Dallas, TX (*Abstract Co-Author*) Author, Reed Elsevier; Editor, Reed Elsevier; Institutional research agreement, Koninklijke Philips NV; Institutional research agreement, Siemens AG Matthew A. Lewis, PhD, Dallas, TX (*Abstract Co-Author*) Research collaborations, CMR Naviscan Corporation and QT Ultrasound Labs Robert E. Lenkinski, PhD, Dallas, TX (*Abstract Co-Author*) Research Grant, Koninklijke Philips NV Research Consultant, Aspect Imaging Jodi A. Antonelli, MD, Dallas, TX (*Abstract Co-Author*) Scientific Advisory Board, Boston Scientific Corporation Margaret S. Pearle, Dallas, TX (*Abstract Co-Author*) Nothing to Disclose Elysha M. Kolitz, Dallas, TX (*Abstract Co-Author*) Nothing to Disclose

For information about this presentation, contact:

lakshmi.ananthakrishnan@utsouthwestern.edu

PURPOSE

To assess non-inferiority of novel dual layer spectral detector CT (SDCT) technology in comparison to dual source dual energy CT (dsDECT) in discriminating between uric acid (UA) and non-UA stones

METHOD AND MATERIALS

In this phantom study, 57 surgically extracted urinary calculi were placed in individual tubes within a cylindrical phantom in a water bath. CT images were obtained at 1 mm slice thickness and 0.5 mm intervals on a prototype SDCT scanner (IQon, Philips Healthcare), and second and third generation dsDECT scanners (Somatom Flash and Force, Siemens Healthcare) under matched scan parameters. For SDCT data, effective Z images and virtual monoenergetic images (40, 62, 92, 100, and 200 keV) were created. For SDCT data, 3D growing region segmentation tool using custom pyOsirix software was used to segment each stone on the various reconstructions for pixel by pixel analysis. Median virtual monoenergetic ratios (VMR) of 40/200, 62/92, and 62/100 (chosen as VMR theoretically yielding best spectral separation, equivalent of 100/140Sn, and 100/150Sn kVp ratios used in dsDECT) and effective Z (Zeff) values for each stone were recorded. For dsDECT data, dual energy ratio (DER) for each stone was recorded from vendor specific post-processing software (Syngo Via) using the Kidney Stones Application. The clinical reference standard of x-ray diffraction analysis was used to assess non-inferiority. Pearson's correlation coefficient was calculated to assess correlation between the 3 VMRs and 2 DERs.

RESULTS

6 pure UA, 47 pure calcium based, 1 pure cystine, and 3 mixed struvite stones were scanned. All pure UA stones were correctly separated from non-UA stones using SDCT and dsDECT. For UA stones, median VMR was 0.95-0.99, Zeff 7.2, DER 1.00-1.02. For non-UA stones, median VMR was 1.65-4.1, Zeff 10.76, and DER 1.54-1.69. VMR ratio 40/200 provided the greatest difference between UA and non-UA stones. There was excellent correlation between the 3 VMRs and DERs (Pearson's correlation coefficient 0.89-0.94, p<.0001). More variability was noted using Zeff.

CONCLUSION

SDCT spectral reconstructions demonstrate similar performance to dsDECT in discriminating UA from non-UA stones in a phantom model.

CLINICAL RELEVANCE/APPLICATION

Uric acid stones may be differentiated from non uric acid stones using novel dual layer spectral detector CT technology in a phantom model.

Honored Educators

Presenters or authors on this event have been recognized as RSNA Honored Educators for participating in multiple qualifying educational activities. Honored Educators are invested in furthering the profession of radiology by delivering high-quality

educational content in their field of study. Learn how you can become an honored educator by visiting the website at: https://www.rsna.org/Honored-Educator-Award/ Suhny Abbara, MD - 2014 Honored EducatorSuhny Abbara, MD - 2017 Honored Educator





103rd Scientific Assembly and Annual Meeting November 26 to December 1 McCormick Place, Chicago



SSK11

Science Session with Keynote: Health Service, Policy and Research (Education)

Wednesday, Nov. 29 10:30AM - 12:00PM Room: S105AB



AMA PRA Category 1 Credits ™: 1.50 ARRT Category A+ Credit: 1.75

Participants

Marc H. Willis, DO, Houston, TX (*Moderator*) Nothing to Disclose Leif Jensen, MD,MPH, Salt Lake City, UT (*Moderator*) Nothing to Disclose

Sub-Events

SSK11-01 In the Era of Tumor Genotyping, Molecular Imaging and Immunotherapy, Should Dedicated Cancer-Imaging Training Be Added to the Radiology Residency Curriculum?

Awards

Student Travel Stipend Award

Participants

Shanna A. Matalon, MD, Boston, MA (*Presenter*) Nothing to Disclose Michael H. Rosenthal, MD, PhD, Boston, MA (*Abstract Co-Author*) Equipment support, Toshiba Medical Systems Corporation Stephanie A. Howard, MD, Boston, MA (*Abstract Co-Author*) Nothing to Disclose

For information about this presentation, contact:

smatalon@partners.org

PURPOSE

Cancer treatment has recently undergone a dramatic shift toward personalized care, with new therapies significantly prolonging life, often in the setting of advanced disease. The imaging of treatment response and toxicity has dramatically changed with the advent of molecular targeted agents and immune modulating drugs. Despite these changes, there are currently no specific guidelines regarding the teaching of cancer-imaging to radiology residents. This study surveyed radiology chief residents (CRs) and program directors (PDs) to determine the current state of cancer-imaging teaching in residency.

METHOD AND MATERIALS

An IRB-exempt survey was provided to CRs and PDs at the Association of University Radiologists (AUR) meeting in 2014. Survey results were summarized using frequency and percentages. Chi-square tests and Fisher's exact test were used for statistical analysis.

RESULTS

102 CRs and 64 PDs responded. Most respondents were from university-based residency programs (80% of CRs, 70% of PDs) and most reported program size >30 residents (64% of CRs, 44% of PDs). Most CRs and PDs report incorporation of cancer imaging into residency education by body part (70% and 75%, respectively), with very few having a dedicated cancer-imaging block (6% and 8%, respectively). While most CRs report 6 or more cancer-imaging lectures annually (69%), fewer than half have dedicated lectures on treatment response, side effects and genomics (43%, 37% and 34%, respectively). Just over half of CRs and PDs would like a dedicated, standardized cancer-imaging curriculum added to the ABR residency curriculum guidelines (52% and 57%, respectively). CRs that had lectures on treatment response were significantly more likely to want added curricula (P=.0053).

CONCLUSION

Despite radiologists' integral role in cancer care, most residencies do not currently incorporate dedicated cancer-imaging teaching blocks, with curricula lacking in topics such as cancer treatment response, side effects and genomics.

CLINICAL RELEVANCE/APPLICATION

Despite dramatic advances in cancer treatment, cancer-imaging education may be lagging behind; radiology residencies must adapt to include dedicated cancer-imaging teaching, in order to ensure imagers remain essential members of the oncologic team.

SSK11-02 Medicolegal Issues in Radiology Training

Wednesday, Nov. 29 10:40AM - 10:50AM Room: S105AB

Participants Sarvenaz Pourjabbar, MD, New Haven, CT (*Presenter*) Nothing to Disclose Amir Imanzadeh, MD, Shelton, CT (*Abstract Co-Author*) Nothing to Disclose Jonathan Mezrich, MD, New Haven, CT (*Abstract Co-Author*) Nothing to Disclose

For information about this presentation, contact:

sarvenaz.pourjabbar@yale.edu

PURPOSE

Radiologists comprise approximately 3.6% of US physicians while ranked 6th in medicolegal claims. Studies suggest that by age of 60, 50% of radiologists will be sued at least once. Given this inevitability, it is surprising how little attention is paid to teaching of medicolegal and malpractice issues during training and practice. Most trainees emerge from residency with only a vague notion of the medicolegal issues inherent in radiology, and it is hypothesized that most radiologists would benefit from additional training on these topics.

METHOD AND MATERIALS

All the radiology attending, trainees and alumni in our tertiary care 1500-bed teaching hospital were surveyed via an electronic questionnaire. Respondents were surveyed on their overall knowledge of job-related medicolegal issues and willingness to receive additional education. The survey also included two real life medicolegal scenarios and the radiologists were asked to choose the most likely result.

RESULTS

A 9-item questionnaire was sent to total of 332 trainees, attending and alumni. There were 104 responses constituting a response rate of 31% (104/332) from 60% (62/104) academic and 40%(42/104) private practice radiologists, F:M 29:75. Only 36% of the respondents were aware that by age of 60, half of them would be involved in at least one lawsuit. All knew the most common causes of malpractice claims in the United States, however, only one-third were aware of available resources offered by ACR. 80% never received training on medicolegal issues during residency and 97% believed that additional education would be useful; 87% showed willingness to attend post-residency medicolegal CME courses. All the residents believed that medicolegal lectures should be included in the didactics.

CONCLUSION

There is a dearth of knowledge among radiologists on job-related medicolegal topics, and radiologists are willing to acquire additional training in the form of targeted didactic sessions for trainees or CME for the graduates. This survey suggests that, at a minimum, incorporating additional medicolegal topics into the non-interpretive skills curriculum of residents would be well received.

CLINICAL RELEVANCE/APPLICATION

As medicolegal issues are numerous in radiology this topic should be of interest to all radiologists in active practice.

SSK11-03 Health Service, Policy and Research Keynote Speaker: Understanding the Cost of Care

Wednesday, Nov. 29 10:50AM - 11:00AM Room: S105AB

Participants

Yoshimi Anzai, MD, Salt Lake City, UT (Presenter) Nothing to Disclose

SSK11-04 Global Lecture Sharing from United States Radiology Residency Programs: A Vital Branch of Improving Radiology Outreach

Wednesday, Nov. 29 11:00AM - 11:10AM Room: S105AB

Participants

Krystal C. Buchanan, MD, New Haven, CT (*Presenter*) Nothing to Disclose Fabian Laage-Gaupp, MD, New Haven, CT (*Abstract Co-Author*) Nothing to Disclose Melissa L. Yearwood, MD, Kingston 7, Jamaica (*Abstract Co-Author*) Nothing to Disclose Kirsten Cooper, MD, New Haven, CT (*Abstract Co-Author*) Nothing to Disclose Syed A. Bokhari, MD, New Haven, CT (*Abstract Co-Author*) Nothing to Disclose William B. Zucconi, DO, New Haven, CT (*Abstract Co-Author*) Nothing to Disclose Jitendra Bhawnani, New Haven, CT (*Abstract Co-Author*) Nothing to Disclose

For information about this presentation, contact:

krystal.buchanan@yale.edu

PURPOSE

Education is an important component of any successful and sustainable radiology program, which warrants continuous and methodical improvement. However, there is often a lack of structured radiology training in countries with limited resources. In addition to clinical teaching, which can only be provided in person, sharing of educational material is feasible nearly everywhere around the world. While utilizing publicly accessible materials from the internet is one option to supplement learning, we hypothesized that participating remotely in lectures provided by a well-established training program with a more structured didactic system may provide additional benefits to all, especially as outreach to less resourced establishments within developing countries. The purpose of this study was to assess whether live streaming of educational resident lectures to a partner program in a developing country can have an impact on radiology training and patient care.

RESULTS

The pre-survey demonstrated that 80% of the residents stated they currently have educational lectures once a week or less. 90% believe that live-streamed lectures could be useful for their daily work and case spectrum, 65% percent believe there will be an immediate impact on local patient care, while 35% percent believe there will be no immediate impact, but potential long-term impact. Areas of particular interest included Musculoskeletal radiology, Neuroradiology, Chest Imaging, and Breast Imaging. After implementation of the lecture-sharing program, preliminary feedback from 13 residents demonstrated that 100% of residents thought the lectures have assisted them in learning radiology and 53% of them felt that they were exposed to new material.

CONCLUSION

Lecture sharing as an initiative to improve education in resource limited settings has substantial potential to impact radiology training programs and has proven beneficial during this outreach project. The future goal is to stream at least one lecture per week use follow-up surveys to continually assess any improvement in learning habits, local didactic culture and eventually patient care. As the project progresses, the frequency of streamed lectures will be increased and the program will be expanded to other partner-

institutions in other developing countries. Long-term impact on examination performance will be studied annually to assess any change in overall performance of trainees, which could be attributed to lecture sharing. Ultimately, maintaining a robust relationship is the most important goal, which would facilitate residents' access to a stored lecture database and also facilitate developing direct resident exchange programs between countries.

METHODS

Twenty residents from a radiology residency program in the country of Jamaica, were surveyed about their interests in participating in streamed lectures from our institution. Survey questions included gathering information about their current learning tools and resources, their current lecture system and logistics of participating in lectures remotely. Members of our institutional faculty were also surveyed about willingness to participate and feasibility of this concept. The current lecture infrastructure was expanded to include remote communication capabilities, which included using a web conferencing software platform. A preset link was generated for access to the sessions and this was distributed in advance to the residents after they signed applicable waivers. After implementation of the project, residents were surveyed to assess impression of the lecture system.

PDF UPLOAD

https://abstract.rsna.org/uploads/2017/17017751/17017751_mxxx.pdf

SSK11-05 Factors that Influence the Choice of Radiology as a Specialty and Analysis of Factor Relationships with Job and Career Satisfaction During Residency

Wednesday, Nov. 29 11:10AM - 11:20AM Room: S105AB

Awards

Student Travel Stipend Award

Participants

Jeffrey P. Guenette, MD, Boston, MA (*Presenter*) Nothing to Disclose Shanna A. Matalon, MD, Boston, MA (*Abstract Co-Author*) Nothing to Disclose Alicia S. Chua, MS, Boston, MA (*Abstract Co-Author*) Nothing to Disclose Stacy E. Smith, MD, Weston, MA (*Abstract Co-Author*) Nothing to Disclose Sara M. Durfee, MD, Boston, MA (*Abstract Co-Author*) Nothing to Disclose

For information about this presentation, contact:

jpguenette@bwh.harvard.edu

PURPOSE

Improve radiology recruitment efforts by identifying what factors influence medical students' choice of radiology and what factors correlate with job and career satisfaction.

METHOD AND MATERIALS

An IRB-exempted online survey was distributed to United States radiology residents by email between December 7, 2016 and March 31, 2017. Respondents identified what aspect of radiology was most appealing during medical school and what experience was most influential in choosing radiology. Respondents also completed visual analog scale measures of career choice satisfaction and current job satisfaction. Descriptive statistics were performed to evaluate relative factor importance. Analysis of variance with post hoc Tukey honest significance difference test was performed to compare career and job satisfaction scores across factors.

RESULTS

A total of 488 radiology residents (age 30.8 ± 3.2 years; 358 male, 129 female, 1 non-responder; 144 PGY1, 123 PGY2, 103 PGY3, 118 PGY4) responded. Respondents were most drawn to the intellectual component (n=187, 38%), imaging component (n=100, 20%), procedure component (n=96, 20%), and potential lifestyle (n=69, 14%) of radiology. Individuals were most influenced by radiology clerkship reading room shadowing (n=143, 29%), radiologist mentor (n=98, 20%), non-radiology clerkship imaging exposure (n=77, 16%), and radiology clerkship interventions exposure (n=75, 15%). Residents who chose radiology primarily for potential lifestyle recorded less career satisfaction and less job satisfaction than residents who chose radiology for its intellectual (p=0.00005 and 0.0004) and imaging (p=0.00002 and 0.0003) components. There was no significant relationship of influential experiences with career or job satisfaction.

CONCLUSION

Effective recruitment of medical students into radiology may best be achieved by radiology clerkships that emphasize the intellectual and imaging components of radiology through reading room shadowing and exposure to interventions. Those who choose radiology for potential lifestyle appear less likely to have job and career satisfaction, at least during residency.

CLINICAL RELEVANCE/APPLICATION

Optimal recruitment of medical students into radiology may be achievable through radiology clerkships that emphasize the intellectual and imaging components of radiology.

SSK11-06 Development, Implementation, and Evaluation of a Medical Student Radiology Elective

Wednesday, Nov. 29 11:20AM - 11:30AM Room: S105AB

Participants

Natasha Larocque, MD, Hamilton, ON (*Presenter*) Nothing to Disclose Stefanie Y. Lee, MD,FRCPC, Hamilton, ON (*Abstract Co-Author*) Nothing to Disclose Sandra Monteiro, PhD, Hamilton, ON (*Abstract Co-Author*) Nothing to Disclose Karen Finlay, MD, Burlington, ON (*Abstract Co-Author*) Nothing to Disclose

For information about this presentation, contact:

PURPOSE

To re-structure a medical student Radiology elective based on the results of a needs assessment and to prospectively evaluate implemented interventions.

METHOD AND MATERIALS

An online retrospective survey was sent to medical students who completed a Radiology elective during the 2015 calendar year. Students were asked to evaluate current and potential elective activities using dichotomous, ranking, and 5-point Likert scale questions (5=excellent, 4=very good, 3=good, 2=fair, 1=poor). The Salant-Dillman survey protocol was used to maximize response rate. Based on these results, three new interventions were piloted: a more structured schedule, bi-weekly resident-led medical student rounds and the creation of a medical student case bank. These changes were implemented from July 1- December 31, 2016 and were prospectively assessed using the same methodology as the needs assessment. Responses were analyzed using descriptive statistics and t-tests.

RESULTS

Response rate for both the needs assessment and prospective survey was good (62% and 90%). In the needs assessment, mean score for overall elective experience was 3.4/5 (SD=1.08) and self-rated knowledge gained was 3.4/5 (SD=0.99). The highest rated educational activities were: working with residents (mean=4.1/5, SD=1.24) and attending resident rounds/self-study time (mean=3.6/5, SD=1.11/1.26). Prospective evaluation of the three interventions showed an increased score for overall elective experience of 4.24/5 (SD=0.90, p=0.022) and for perceived knowledge gained (mean=3.76/5, SD=0.83, p=0.11). The resident-led rounds and case bank were the highest rated activities students encountered in the new elective with scores of 4.87/5 (SD=0.35) and 4.67/5 (SD=0.49) respectively.

CONCLUSION

This study describes the successful re-structuring of a medical student Radiology elective with improved scores in student satisfaction and knowledge gained.

CLINICAL RELEVANCE/APPLICATION

These results are important to medical educators and may facilitate the creation of higher quality electives for medical students.

SSK11-07 Resident Perception of the Use of Peer Teachers for Hands-On Ultrasound Training

Wednesday, Nov. 29 11:30AM - 11:40AM Room: S105AB

Participants

Netanel Berko, MD, Bronx, NY (*Presenter*) Nothing to Disclose Mordecai Koenigsberg, MD, Flushing, NY (*Abstract Co-Author*) Nothing to Disclose Thomas G. Hoffman, RT,BS, Bronx, NY (*Abstract Co-Author*) Nothing to Disclose Beverly A. Thornhill, MD, Bronx, NY (*Abstract Co-Author*) Nothing to Disclose E. Stephen Amis JR, MD, Bronx, NY (*Abstract Co-Author*) Nothing to Disclose

For information about this presentation, contact:

Netanel.Berko@uphs.upenn.edu

PURPOSE

To determine resident perceptions of the use of peer teachers for hands-on radiology resident education.

METHOD AND MATERIALS

Hands-on musculoskeletal and abdominal ultrasound scanning workshops were designed for radiology residents. Prior to the workshops several senior residents received three hours of training, and then served as instructors ("peer teachers") during the workshops. During the workshops, demonstrations were performed by an attending radiologist or senior sonographer, followed by small-group hands-on scanning led by the peer teachers. Following the workshops resident participants and peer teachers completed surveys with 5-point Likert scale statements regarding their experience. Median scores and interquartile ranges (IQR, 25-75%) were calculated.

RESULTS

40 residents from all years of training and 9 senior resident peer teachers participated in 6 workshops. Participants thought that peer teachers were effective (median score 5, IQR 4-5), would like to be taught by peer teachers again (5, 4-5) and were interested in serving as peer teachers (4, 3-5). Peer teachers highly rated the overall experience (5, 5-5), were interested in serving as peer teachers again (5, 5-5), and found peer teaching enjoyable (5, 5-5). Peer teachers felt comfortable with the material (4, 4-5) and were able to answer most questions posed to them (4, 3-5). Peer teaching resulted in increased understanding of ultrasound technique and anatomy (5, 5-5). 78% of peer teachers thought that 3 hours of training was sufficient, while all thought that group size (3-4 residents per small group) was appropriate.

CONCLUSION

Use of peer teachers for hands-on ultrasound training is viewed extremely positively by resident participants and peer teachers. Residents found peer teaching educational, enjoyable and highly rated the overall experience. Both resident participants and peer teachers were interested in participating in peer teaching again. A ratio of 1 peer teacher for 3-4 trainees is appropriate for effectively teaching ultrasound scanning technique, and approximately 3 hours of peer teacher training is required.

CLINICAL RELEVANCE/APPLICATION

Peer teaching is viewed extremely positively by residents and can play a role in hands-on training of radiology residents.

SSK11-08 Procedural Training in Radiology Residency: Variability in the Use of Simulation

Wednesday, Nov. 29 11:40AM - 11:50AM Room: S105AB

Participants Shanna A. Matalon, MD, Boston, MA (*Presenter*) Nothing to Disclose Sona A. Chikarmane, MD, Boston, MA (*Abstract Co-Author*) Nothing to Disclose Eren D. Yeh, MD, Boston, MA (*Abstract Co-Author*) Reader, Hologic, Inc; Reader, Statlife SAS Stacy E. Smith, MD, Weston, MA (*Abstract Co-Author*) Nothing to Disclose William W. Mayo-Smith, MD, Boston, MA (*Abstract Co-Author*) Author with royalties, Reed Elsevier; Catherine S. Giess, MD, Wellesley, MA (*Abstract Co-Author*) Nothing to Disclose

For information about this presentation, contact:

smatalon@partners.org

PURPOSE

Increased attention to quality and safety has cast doubt on the classic "see one, do one" model of procedural training. Many have proposed simulation training as an additional teaching tool in procedural training. This study surveyed radiology residents to determine if and how simulation-based training is being utilized during residency.

METHOD AND MATERIALS

An IRB-exempt online survey was distributed to current radiology residents in the United States by e-mail. Survey results were summarized using frequency and percentages. Chi-square tests were used for statistical analysis where appropriate.

RESULTS

353 residents completed the survey. Thirty-seven percent (n=129/353) of residents have not participated in procedure simulation (37%, n=129/353). Of the residents who have used simulation, most did not do so until after having already performed procedures on patients (59%, n=132/223). Vascular/interventional (VIR) radiology is the most common subspecialty in which residents get hands-on exposure to procedures (96%, n=336/352), but only 26% (n=57/222) reported procedural simulation use in VIR. Simulation was most commonly utilized by breast and abdominal divisions (n=97/222, 44%, and n=95/222, 42%, respectively). The presence of a dedicated simulation center was reported by over half of residents (56%, n=196/353) and was associated with prior simulation experience (P=.007). Simulation training was associated with higher comfort levels in performing procedures (P<.001).

CONCLUSION

Although procedural simulation training is associated with higher comfort levels in performing procedures, there is variable use in radiology resident training and its use may not be currently optimized. Results suggest the need to increase procedural simulation use throughout US residencies, including earlier introduction to simulation during residency, particularly within the vascular/interventional division.

CLINICAL RELEVANCE/APPLICATION

Simulation training is associated with higher resident comfort levels in performing procedures, but its use is variable in resident training and increased use may benefit both resident training and ultimately, patient care.

SSK11-09 Integrating Simulated Clinical Decision Support at the Point-of-Order into Physician Assistant Students' Radiology Curriculum

Wednesday, Nov. 29 11:50AM - 12:00PM Room: S105AB

Participants Marc H. Willis, DO, Houston, TX (*Presenter*) Nothing to Disclose Alana D. Newell, Houston, TX (*Abstract Co-Author*) Nothing to Disclose Tamara Ortiz-Perez, MD, Houston, TX (*Abstract Co-Author*) Nothing to Disclose Jay Lin, MD, Bellaire, TX (*Abstract Co-Author*) Nothing to Disclose Karla A. Sepulveda, MD, Houston, TX (*Abstract Co-Author*) Nothing to Disclose

For information about this presentation, contact:

mwillis@bcm.edu

PURPOSE

Improving appropriateness of imaging is a national focus, including imaging requested by advanced practice providers (Hughes et al, JAMA Intern Med 2015;175(1):101-107). Given our experience in this arena, we engaged leadership from our physician assistant program to innovate the radiology education curriculum. We introduced a cutting-edge clinical tool (ACR Select) through an education simulation portal. In an era of evolving decision support for medical providers, this simulation portal exposes future ordering providers to evidence-based medicine and clinical decision support.

METHOD AND MATERIALS

We utilized an education portal integrated with ACRSelect to allow learners to simulate ordering imaging studies with clinical decision support. Learners received instant feedback during their simulation. Our program utilized a hybrid classroom experience. The learners met with key members of our radiology team in a traditional classroom before and after the simulation education. Assessment was via a pre/post-assessment a qualitative survey.

RESULTS

In 2015, sixteen students completed both tests, and on average, showed a gain of 11% from one test to the next. A paired t-test between students' pre- and posttest scores was statistically significant - t(15)=4.664, p<0.001, with a large effect size (Cohen's d = 1.166). In 2016, the module cases were updated and refined. The test items were accordingly updated. Thus, comparisons cannot be made directly between the two groups. However, similar to the 2015 cohort, the 2016 cohort, also had about an 11% increase from pre- to posttest, which was a statistically significant average content knowledge gain t(17)=3.4436, p=0.003, with a

CONCLUSION

The role of advanced practice providers is expected to expand within our evolving health care system. Their radiology curricula need to empower these future providers to request the "right test at the right time". Evidence-based, simulated ordering of imaging exams with integrated clinical decision support is a promising resource. This web-based platform is easily scalable which enhances the potential to have a broad and meaningful impact on medical education.

CLINICAL RELEVANCE/APPLICATION

Given the challenges of our current health care situation and national trends in medicine, it is imperative that we find more efficient and effective mechanisms to better educate and prepare medical providers for the future.





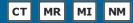
103rd Scientific Assembly and Annual Meeting November 26 to December 1 McCormick Place, Chicago



SSK12

Molecular Imaging (Infection and Inflammation)

Wednesday, Nov. 29 10:30AM - 12:00PM Room: S504CD



AMA PRA Category 1 Credits ™: 1.50 ARRT Category A+ Credit: 1.75

FDA Discussions may include off-label uses.

Participants

Kathryn A. Morton, MD, Salt Lake City, UT (*Moderator*) Nothing to Disclose Vikas Kundra, MD, PhD, Houston, TX (*Moderator*) Institutional license agreement, Introgen Therapeutics, Inc; Research Grant, General Electric Company

Sub-Events

SSK12-01 Fluorescence Molecular Imaging of Cathepsin Activity as a Novel Biomarker for Giant Cell Arteritis

Participants

Marcus Both, MD, Kiel, Germany (*Presenter*) Nothing to Disclose Jana Humbert, MS, Kiel, Germany (*Abstract Co-Author*) Nothing to Disclose Antje Muller, PhD, Lubeck, Germany (*Abstract Co-Author*) Nothing to Disclose Dirk Duwendag, Kiel, Germany (*Abstract Co-Author*) Nothing to Disclose Konstanze Holl-Ulrich, MD, Lubeck, Germany (*Abstract Co-Author*) Nothing to Disclose Carola Heneweer, Cologne, Germany (*Abstract Co-Author*) Nothing to Disclose Patrick Meyer, MD, Kiel, Germany (*Abstract Co-Author*) Nothing to Disclose Elfriede Fritzer, Kiel, Germany (*Abstract Co-Author*) Nothing to Disclose Johann O. Schroder, MD, Kiel, Germany (*Abstract Co-Author*) Nothing to Disclose Georg Lutter, Kiel, Germany (*Abstract Co-Author*) Nothing to Disclose Claus C. Glueer, PhD, Kiel, Germany (*Abstract Co-Author*) Nothing to Disclose Olav Jansen, MD, PhD, Kiel, Germany (*Abstract Co-Author*) Nothing to Disclose Sanjay Tiwari, PhD, Kiel, Germany (*Abstract Co-Author*) Nothing to Disclose

For information about this presentation, contact:

mboth@rad.uni-kiel.de

PURPOSE

The aim of this study was to investigate whether cathepsin activity can be utilized as a novel biomarker for presence and inflammatory status of giant cell arteritis (GCA).

METHOD AND MATERIALS

Biopsy specimen of the temporal artery from patients (n=91, average age: 74 years) with a suspected giant cell arteritis were partially subjected to immunohistological analyses of the expression of Cathepsin K, L and B. The enzymatic activity of the specimen was assessed in n=61 cases with a fluorometric essay sensitive to cathepsin K. Ex vivo fluorescence imaging using a pancathepsin activatable fluorescent imaging agent was performed in n=45 temporal artery biopsy specimen and in n=13 segments of the internal thoracic artery from non-vasculitis patients (control group) undergoing cardiac bypass surgery. Cathepsin-based methods were compared to standard clinical diagnostics, serology, presurgical MRI and routine histology.

RESULTS

The clinical reference diagnosis revealed n=18 negative cases, n=45 positive cases and n=28 cases with inconclusive results. Immunohistochemistry (Figure) showed significantly increased (p<0.001) expression of cathepsins B, K and L in patients diagnosed with GCA versus negative diagnoses. GCA positive biopsy specimen also had significantly increased cathepsin activity compared to negative biopsy specimen (p<0.01) and compared to control arteries from bypass surgery (p<0.05) as determined by ex vivo fluorescent imaging. Supporting a pathogenic role for cathepsin K, tissue lysates showed increased Cathepsin K enzymatic activity (p<0.001). The ex vivo fluorescent signal moderately but significantly correlated with cathepsin K activity (R^2 =0.63, p<0.001), and strongly with the histological scores of all cathepsin stainings (Cathepsin B: R^2 =0.74; Cathepsin K: R^2 =0.72; Cathepsin L: R^2 =0.76; p<0.001).

CONCLUSION

These in vitro findings demonstrate that cathepsins can be utilized as an immunohistological and imaging biomarker for the diagnosis of GCA.

CLINICAL RELEVANCE/APPLICATION

Cathepsins possibly offer a translational approach towards in vivo fluorescent imaging for the non-surgical diagnosis of GCA.

SSK12-02 Comparison of Different Semi-quantitative Approaches for the Diagnosis of Graft Infection after Thoracic or Abdominal Aortic Repair Using [F-18]-FDG PET/CT

Wednesday, Nov. 29 10:40AM - 10:50AM Room: S504CD

Participants

Ingo Einspieler, Munich, Germany (*Presenter*) Nothing to Disclose Victor Mergen, Munich, Germany (*Abstract Co-Author*) Nothing to Disclose Heiko Wendorff, Munich, Germany (*Abstract Co-Author*) Nothing to Disclose Markus Schwaiger, MD, Munich, Germany (*Abstract Co-Author*) Research Grant, Siemens AG; Speaker, Siemens AG Mona Mustafa, Munich, Germany (*Abstract Co-Author*) Nothing to Disclose

PURPOSE

The aim of this study was the evaluation and comparison of different semiquantitative parameters for the diagnosis of graft infection after thoracic or abdominal aortic repair applying [18F]fluorodeoxyglucose (FDG) positron emission tomography (PET)/computed tomography (CT).

METHOD AND MATERIALS

50 patients who underwent [18F]-FDG PET/CT for suspected aortic graft infection were retrospectively analysed. Besides, 13 oncological patients with aortic repair but without graft infection were included in the analysis. Maximum standardized uptake values (SUVmax) were obtained for all patients and different graft to background ratios were calculated. The diagnostic accuracy of SUVmax and different target-to-background ratios (TBRs) was assessed by receiver-operating-characteristic (ROC) analysis. Overall, 8 different background regions were defined and analysed (blood pool activity within the left cardiac ventricle, 4 different aortic segments, the vena cava and the pulmonary trunk as well as FDG wall uptake in non inflammatory aortic segments). A combination of clinical follow-up, imaging (including PET/CT) and/or microbiological/histopathological results, if available, served as the standard of reference for the final diagnosis.

RESULTS

28 infected and 35 uninfected grafts were identified. SUVmax was the most powerful predictor for the diagnosis of graft infection according to the ROC analysis (area under the curve: 0.978, CI: 0.904-0.999). ROC analysis suggested an SUVmax cut off value of >4.48 to differentiate between infected and non-infected grafts (p<0.0001). Notably, there was no substantial difference between SUVmax and other semiquantitative approaches (TBR) according to the area under the curve.

CONCLUSION

Semiquantitative approaches and in particular SUVmax provide a good reference to assess graft infection after thoracic or abdominal aortic repair and may increase the diagnostic accuracy of [18F]-FDG-PET/CT in the setting of suspected graft infection.

CLINICAL RELEVANCE/APPLICATION

[18F]-FDG-PET/CT is increasingly used in the setting of suspected aortic graft infection. However, data is limited with respect to different semiquantitative approaches for the diagnosis of graft infection. According to our results, SUV max showed the best performance to differentiate between infected and non-infected grafts and may increase the diagnostic accuracy of [18F]-FDG-PET/CT.

SSK12-03 Ultrasound-detectable O2 Microbubbles Generated from Catalase-Containing Silica Nanoshells (CSNs) in Determining Infected from Non-infected Fluid Collections in Humans

Wednesday, Nov. 29 10:50AM - 11:00AM Room: S504CD

Participants Christopher D. Malone, MD, San Diego, CA (*Abstract Co-Author*) Nothing to Disclose David T. Fetzer, MD, Dallas, TX (*Presenter*) Nothing to Disclose Jacques Lux, Dallas, TX (*Abstract Co-Author*) Nothing to Disclose Robert F. Mattrey, MD, Dallas, TX (*Abstract Co-Author*) Nothing to Disclose

For information about this presentation, contact:

cmalone05@gmail.com

PURPOSE

Elevated levels of hydrogen peroxide (H2O2) play a key role in neutrophil oxidative defense against infection. Catalase-containing silica nanoshells (CSNs) are novel nanoparticles that generate oxygen microbubbles (O2 MBs) in the presence of elevated levels of H2O2. We aim to determine whether ultrasound detectable O2 MBs produced by CSNs can distinguish infected from non-infected fluid collections drained from patients.

METHOD AND MATERIALS

During this HIPAA-compliant, IRB-approved study, 52 human fluid samples were collected from clinically-required, image-guided percutaneous drainage procedures. Each sample was placed in a 3 mL transfer pipette imbedded in a tissue mimicking agarose/corn starch holder. Both the holder and the face of a Siemens Sequoia 512; 15L8-S linear transducer were submerged and mechanically held in a 37 °C water bath. CSNs were added to the fluid samples while imaging in real-time using the CPS microbubble-only imaging technique. Production of detectable MBs was graded subjectively as negative (not infected), or mild, moderate, or marked (infected) by a single observer blinded to all clinical data. The truth standard was culture results performed by the Microbiology laboratory. Performance characteristics including ROC curves were calculated.

RESULTS

Presence of MB formation to distinguish infected from non-infected fluids was 84% sensitive and 72% specific, and offered positive and negative predictive values of 64% and 89%, respectively. The area under the ROC curve (AUC) was 0.79. All nine false positive cases were peritoneal fluid collections, which could be indicative oxidative stress rather than infection.

CONCLUSION

The presence of elevated H2O2 recognized by MB formation in the presence of CSNs is sensitive in distinguishing infected from noninfected fluids with a relatively high negative predictive value. CSNs may offer a novel point of care method at the time of percutaneous drainage, potentially obviating placement of drains in otherwise sterile collections to minimize risk of colonization and secondary infection.

CLINICAL RELEVANCE/APPLICATION

CSN technology can be administered through a needle or potentially incorporated on existing needles/catheters, functioning as a point of care device during percutaneous drainage or aspiration.

SSK12-04 Utility of F18 FDG PET/CT in Evaluation of Pyrexia of Unknown Origin

Wednesday, Nov. 29 11:00AM - 11:10AM Room: S504CD

Participants

Rasika Kabnurkar, MBBS, MD, Thane, India (*Presenter*) Nothing to Disclose Namrata Tuteja, MBBS, Mumbai, India (*Abstract Co-Author*) Nothing to Disclose M.I Rokade, MD, Thane, India (*Abstract Co-Author*) Nothing to Disclose Nikhil Kamat, MD, Thane, India (*Abstract Co-Author*) Nothing to Disclose

PURPOSE

Pyrexia of Unknown Origin (PUO) often poses diagnostic challenge. Timely diagnosis helps in guiding appropriate treatment. The aim of this retrospective study was to asses the contribution of Fluorine-18 Fluorodeoxyglucose (18F-FDG) Positron Emission Tomography /Computed Tomography (PET/CT) in the diagnostic evaluation of PUO.

METHOD AND MATERIALS

46 consecutive patients of PUO (23 men and 23 females, Age Range: 5 to 75 years) referred for 18F-FDG PET/CT between December 2015 to March 2017 were evaluated. Biopsy confirmation was available in 12 patients. Remaining patients underwent biochemical, microbiological, clinical and imaging follow up.

RESULTS

FDG PET/CT identified hypermetabolic foci in 42 patients (91.30%). Out of these, 14/42 patients revealed non-specific FDG uptake which did not contribute to final diagnosis. No abnormal focal FDG uptake was seen in 4 patients. No pathological disease was diagnosed in these 18 patients on subsequent work-up and were afebrile on follow up. Among the definite positive scans in 66.67% patients(28/42), various etiologies identified were as follows: A) Infectious etiology (n=15) including tuberculous lymphadenitis(7/15), septic arthritis (1/15), otitis media (1/15), acute hepatitis (1/15), infected prosthesis (2/15), spondylodiskitis (2/15), gluteal pyogenic abscess(1/15); B) Inflammatory etiology (n=10) such as Interstitial lung disease (2/10), Inflammatory mesenteric lymphadenopathy (2/10), Synovitis (2/10), Polymyositis and Dermatomyositis (2/10)Vasculitis (2/10); C) Malignancy (n=3) in colon carcinoma, adrenocortical carcinoma of lung, liver metastases from unknown primary.

CONCLUSION

18F-FDG PET/CT has a useful role in identification of pathological focus in PUO. Negative FDG PET/CT scan reliably rules out focal etiologies for PUO. Further prospective studies are warranted for confirmation.

CLINICAL RELEVANCE/APPLICATION

18F-FDG PET/CT has higher sensitivity to identify occult pathologies in PUO.

SSK12-05 Ultra-small Superparamagnetic Iron Oxide Nanoparticle as a Surrogate Marker of Aortic Wall Inflammation Following Radiation Therapy for Pancreatic Cancer

Wednesday, Nov. 29 11:10AM - 11:20AM Room: S504CD

Participants

Sandeep S. Hedgire, MD, Boston, MA (*Presenter*) Nothing to Disclose Cicely Krebill, Boston, MA (*Abstract Co-Author*) Nothing to Disclose Gregory R. Wojtkiewicz, MSc, Boston, MA (*Abstract Co-Author*) Nothing to Disclose Irai S. Oliveira, MD, Boston, MA (*Abstract Co-Author*) Nothing to Disclose Brian B. Ghoshhajra, MD, Waban, MA (*Abstract Co-Author*) Consultant, Siemens AG; Consultant, Medtronic plc Udo Hoffmann, MD, Boston, MA (*Abstract Co-Author*) Research Grant, HeartFlow, Inc Mukesh G. Harisinghani, MD, Boston, MA (*Abstract Co-Author*) Nothing to Disclose

For information about this presentation, contact:

Hedgire.Sandeep@mgh.harvard.edu

PURPOSE

Radiation therapy for cancer can lead to atherosclerosis by inducing inflammatory changes in the vascular wall. Though atherosclerotic changes can be seen with CT and MRI techniques, it is difficult to quantitatively measure inflammation on CT and MR imaging studies. The purpose of this study was to assess the use of ferumoxytol- an ultrasmall superparamagnetic iron oxide nanoparticle, as a surrogate marker of vessel wall inflammation secondary to radiation therapy in pancreatic cancer patients in comparison with healthy volunteers.

METHOD AND MATERIALS

MRI of upper abdomen (T1, T2, multi-echo T2*-weighted imaging) was performed on 3T magnet before and 48 hours after intravenous administration of ferumoxytol in pancreatic cancer patients who underwent radiation therapy (n=8) and healthy volunteers (n=8). R2* value was obtained by drawing regions of interest (ROIs) outlining the aortic wall directly on the T2* medic image and subsequently transposed to the R2* image using Amira software (Version 5.3.2, FEI, Bordeaux, France). The change in R2* values was analyzed by student's t-test.

RESULTS

The average change in R2* value of the pancreatic cancer patients was determined to be 216.18 1/ms. The average change R2*

value of the control patients was determined to be 54.67 1/ms. This indicates that the pancreatic cancer patients following radiation therapy had a greater uptake of ferumoxytol (p=0.0082) in their aortic wall.

CONCLUSION

Ferumoxytol can offer a non invasive, quantitative assessment of vascular inflammation following radiation therapy in cancer patients.

CLINICAL RELEVANCE/APPLICATION

Radiation therapy induced atherosclerosis could potentially be diagnosed earlier on due to its inflammatory nature. Ferumoxytol enhanced MRI offers a novel, radiation-free imaging marker of inflammation, would augment risk stratification, inform therapeutic decisions, and allow safe, robust, and quantitative monitoring of therapy-mediated changes.

SSK12-06 Anti-Inflammatory Therapeutic Effects in Swine Acute Ileitis: Longitudinal Monitoring with Ultrasound Molecular Imaging

Wednesday, Nov. 29 11:20AM - 11:30AM Room: S504CD

Participants

Huaijun Wang, MD, PhD, Stanford, CA (*Presenter*) Nothing to Disclose Stephen A. Felt, DVM, MPH, Stanford, CA (*Abstract Co-Author*) Nothing to Disclose Jean-Marc Hyvelin, Geneva, Switzerland (*Abstract Co-Author*) Employee, Bracco Group Ismayil Guracar, Mountain View, CA (*Abstract Co-Author*) Employee of Siemens Medical Solutions, USA Inc. Samir Cherkaoui, Geneva, Switzerland (*Abstract Co-Author*) Nothing to Disclose Thierry Bettinger, Geneva, Switzerland (*Abstract Co-Author*) Nothing to Disclose Juergen K. Willmann, MD, Stanford, CA (*Abstract Co-Author*) Research Consultant, Bracco Group Research Grant, Siemens AG Research Grant, Bracco Group Research Grant, Koninklijke Philips NV Research Grant, General Electric Company Advisory Board, Lantheus Medical Imaging, Inc Advisory Board, Bracco Group

For information about this presentation, contact:

willmann@stanford.edu

PURPOSE

Ultrasound molecular imaging (USMI) using P- and E-selectin targeted microbubbles (MBselectin) has been shown to accurately quantify inflammation at molecular level in rodent and swine models of inflammatory bowel disease (IBD). This study aimed to assess whether USMI allows longitudinal monitoring of anti-inflammatory treatments in a swine model of IBD.

METHOD AND MATERIALS

Fourteen female swine with acute terminal ileitis induced by TNBS/ethanol solution at day 0 were randomized into 1) an antiinflammatory treatment group (n=8 with meloxicam at 0.25mg/kg and prednisone at 0.5mg/kg; oral or intravenous, twice daily) and 2) a control group (n=6 without treatment). USMI was performed with a clinical machine (Acuson Sequoia 512; 15L8W, 7MHz; Siemens) after intravenous injection of MBselectin (5x108/kg). Three bowel segments per swine were imaged each at baseline, day 1, 3 and 6 after inflammation induction. Imaging signal was quantified as the difference between pre- and post-destructive signal intensity with VueBox software (Bracco) and normalized to day 1. At day 6 after imaging, scanned ileal segments were analyzed ex vivo for expression level of P-selectin using immunofluorescence staining.

RESULTS

Background USMI signals at baseline day 0 were not significantly different (P=0.09) between the two groups. At day 1, USMI signals significantly (P<0.05) increased in both groups and were not significantly different (P=0.9) between both groups. At day 3, signals significantly (P=0.02 vs. day 1) decreased in the treatment group, while it remained high in controls (P=0.25) and was significantly higher (P=0.001) compared to the treatment group. At day 6, signals further decreased in the treatment group; signals also dropped in controls due to known spontaneous decrease of inflammation in this model, but it remained significantly higher (P=0.046) compared to the treatment group. Immunofluorescence staining demonstrated significantly (P=0.004) higher P-selectin expression level in control versus treated ileum.

CONCLUSION

Dual-selectin targeted USMI allows longitudinal monitoring of anti-inflammatory treatment effects in a swine model of acute ileitis.

CLINICAL RELEVANCE/APPLICATION

This study paves the way for clinical translation of this radiation-free technique for monitoring IBD in patients.

SSK12-07 Sepsis of Unknown Origin: A Role of 18F-FDG-PET/MRI in Immunocompromised Patients

Wednesday, Nov. 29 11:30AM - 11:40AM Room: S504CD

Participants

Jiri Ferda, MD, PhD, Plzen, Czech Republic (*Presenter*) Nothing to Disclose Eva Ferdova, MD, Plzen, Czech Republic (*Abstract Co-Author*) Nothing to Disclose Jan Baxa, MD, PhD, Plzen, Czech Republic (*Abstract Co-Author*) Nothing to Disclose

For information about this presentation, contact:

ferda@fnplzen.cz

PURPOSE

To evaluate a diagnostic value of the PET/MRI in detection of cause of the septic state in patients with immunodeficiency

METHOD AND MATERIALS

There were performed 20 18F-FDG-PET/MRI examinations in patients including two children (the age 7-69 year. 13 females. 8

males) who suffered from signs of sepsis, and the cause was remained unclear after routine examinations. The procedures were performed using integrated PET/MRI system after application of the 18F-FDG with the dose of 2.5 MBq/kg. The examinations had to be performed under general anesthesia in 5 patients. The imaging protocol contained gradient echo T1 (VIBE) and T2 STIR sequences before application of the gadolinium contrast. The application of macrocyclic gadolinium containing contrast agent was used with the dose of 0.1 mmol/kg in those patients in whom the renal impairment was not present. PET data acquisition took 4 minutes in each position. When the suspected inflammation of the brain or spine was suspicious, the targeted imaging was performed. The imaging findings were compared with microbiology investigations or histological assessments

RESULTS

There were eleven patients immunocompromised after therapy of the hemato-oncological disease, four patients with advanced diabetes, three patients on long-term dialysis and two patients with congenital impairment of cellular immunity. The cause of the septic state was found in 90% of all cases. There were found seven cases of musculoskeletal infections caused by Staphylococcus (5), Enterococcus sp. (1), and Pseudomonas (1) infections. In four patients were found central nervous system infections including one patient with granulomatous inflammation of unknown agens and one patient with Toxoplasma meningitis. Other single causes included lung aspergillosis, abdominal Salmonella abscess, mycobacterial lymphadenitis. In three patients, the recurrent hematological malignancy was found, the disseminated renal cell carcinoma was found in one patient. The cause of septic state remained undetected in two patients. The results of imaging trigger therapy in 16 patients.

CONCLUSION

18F-FDG-PET/MRI could play an important role in detection of the cause of septic state in immunocompromised patients and in the therapy decisions.

CLINICAL RELEVANCE/APPLICATION

The advantage of the combination of PET and MRI lies especially in the detection of central nervous system and musculoskeletal infections.

SSK12-08 MRI Detection of Brain Abscesses and Monitoring of Antibiotic Treatment Using Endogenous Bacterial CEST Contrast

Wednesday, Nov. 29 11:40AM - 11:50AM Room: S504CD

Participants

Jing Liu, Baltimore, MD (*Presenter*) Nothing to Disclose Peter C. Van Zijl, PhD, Baltimore, MD (*Abstract Co-Author*) Nothing to Disclose Guanshu Liu, PhD, Baltimore, MD (*Abstract Co-Author*) Nothing to Disclose Shui Xing Zhang Sr, MD, Guangzhou, China (*Abstract Co-Author*) Nothing to Disclose Yuguo Li, PhD, Baltimore, MD (*Abstract Co-Author*) Nothing to Disclose Renyuan Bai, Baltimore, MD (*Abstract Co-Author*) Nothing to Disclose Verena Staedtke, Baltimore, MD (*Abstract Co-Author*) Nothing to Disclose

For information about this presentation, contact:

jliu142@jhmi.edu

PURPOSE

To develop an endogenous CEST MR imaging strategy to detect bacterial infections and to monitor their antibiotic treatment in deep organs, and to evaluate it in a preclinical animal model.

METHOD AND MATERIALS

Brain abscesses were developed by stereotactically injecting $6x106 \ S. \ aureus$ in the brains of F344 rats (3 mm left, 2 mm anterior of Bregma). After well circumscribed lesions were formed on ~ 9 days [1], rats received the ampicillin treatment at a daily dose of 30 mg/kg (*i.p.*) twice a day for 10 days. A F98 brain tumor model was established by injecting 5x104 F98-luc cells (3 mm right, 2 mm anterior of Bregma). MRI assessments were conducted before, 4 days and 10 days after the treatment. CEST MRI weighted images were acquired using a 3-sec CW pulse (B1= 1 and 3 μ T) according to previously published methods [2].

RESULTS

As shown in Fig.1A, endogenous CEST contrast at 2.6 ppm allowed the *in vitro* MRI detection of three types of gram positive bacteria (*C. novyi-NT* [2], *S. aureus* and *S. epidermidis*) with slightly differing CEST patterns, as well as the *in vivo* visualization of brain abscesses formed by *S. aureus* (Fig.1C). Currently, differentiation of bacterial infection and brain tumors remains a formidable clinical challenge. In CEST MRI, while both type lesions showed higher CEST contrast than brain parenchyma, bacteria and tumors cells showed different CEST-dependence on the B1 strengths used for RF irradiation in CEST, likely attributed to the difference in cell composition and metabolism, which was utilized to differentiate them successfully (Figs. E-H). Finally, we investigated the longitudinal CEST signal changes during antibiotic treatment. As shown in Figs. I&J, CEST signal decreased markedly in the animals receiving amoxicillin treatment and, in contrast, remained constantly in the control group.

CONCLUSION

The endogenous CEST contrast of bacteria cells enables the direct and specific MRI assessment of bacterial infections of *S. aureus* in animal models. Moreover, this method allows non-invasive monitoring of bacteria responses to antibiotic treatments. References (1) Flaris, N. A.; Hickey, W. F. Am J Pathol 1992, 141, 1299-307. (2) Liu, G., et al. Magn. Reson. Med. 2013, 70, 1690-8.

CLINICAL RELEVANCE/APPLICATION

Endogenous CEST MRI contrast of bacterial cells provides a new clinically compatible imaging strategy for the diagnosis and treatment monitoring of bacterial infections in deep-seated organs.

SSK12-09 Developing a Novel Paramagnetic Fluorinated Nanoemulsion for Sensitive Imaging of Inflammation by Fluorine-19 Magnetic Resonance Imaging

Awards Trainee Research Prize - Resident

Participants

Amin Haghighat Jahromi, MD, PhD, San Diego, CA (*Presenter*) Nothing to Disclose Stephen R. Adams, PhD, La Jolla, CA (*Abstract Co-Author*) Nothing to Disclose Kazim Narsinh, MD, San Diego, CA (*Abstract Co-Author*) Nothing to Disclose Hongyan Xu, San Diego, CA (*Abstract Co-Author*) Nothing to Disclose Wenlian Zhu, PhD, Baltimore, MD (*Abstract Co-Author*) Nothing to Disclose Eric T. Ahrens, PhD, La Jolla, CA (*Abstract Co-Author*) Nothing to Disclose

For information about this presentation, contact:

ajahromi@ucsd.edu

PURPOSE

Imaging of macrophages holds tremendous promise to address a variety of unmet diagnostic needs, such as imaging of cancer, cardiovascular disease, inflammatory disease, or tracking cells in vivo. 19F MRI of inflammation has emerged as an approach to locate macrophages using exogenous 19F probes in a highly specific and quantitative manner. We propose a novel nanoemulsion (NE) imaging probe for sensitive imaging of inflammation in vivo.

METHOD AND MATERIALS

We designed and synthesized a highly stable hexadentate chelating agent for iron (III). The structure of this complex was confirmed by NMR and x-ray crystallography. We added the iron (III) complex to perfluorooctyl bromide (PFOB) to form paramagnetic PFOB (P-PFOB) NE. (PFOB has been used previously in the clinic as a 19F tracer.) The NE was formed using high shear microfluidization to yield a monodispersed oil-in-water NE. Relaxation time 19F NMR measurements (9.4 T and 3 T) and in vitro cell apoptosis assays where used to characterize the nanoemulsion. Inflammation was induced in a murine model via a subcutaneous plug of Matrigel mixed with lipopolysaccharide in the neck. NE was subsequently injected intravenously and 11.7 T MRI data were acquired 24 h later using 2D chemical shift imaging (CSI).

RESULTS

Addition of Fe3+ chelate to PFOB dramatically enhanced 19F MRI detection sensitivity by reducing the 19F T1 by an order of magnitude. T1 values at 3 T are reduced from 1266 ms (PFOB) to 199 ms (P-PFOB, [Fe3+]= 3.5 mM) with minimal T2 line broadening; the effect diminishes at higher fields. In vitro cell assays confirmed viability of NE-labeled macrophages. Upon intravenous injection of P-PFOB NE, accumulation of the agent in the Matrigel plug was observed by 19F MRI, corresponding to the inflammation site. A linear [Fe3+]-dependent chemical shift was also observed in the PFOB fluorine peaks, which enables simultaneous tracking of various subtypes of cells via CSI.

CONCLUSION

We developed P-PFOB, capable of forming NE, with enhanced 19F MRI detection sensitivity over PFOB. By shortening T1, more signal averaging in a given scan time is possible. P-PFOB can also serve as a chemical shift agent for tracking various subtypes of immune cells.

CLINICAL RELEVANCE/APPLICATION

P-PFOB NE is a novel 19F MRI probe with greatly enhanced sensitivity for imaging inflammation and can be used to track various subtypes of immune cells in vivo.



KSNA[®] 2017

103rd Scientific Assembly and Annual Meeting November 26 to December 1 McCormick Place, Chicago



SSK13

Musculoskeletal (Intervention)

Wednesday, Nov. 29 10:30AM - 12:00PM Room: E353C



AMA PRA Category 1 Credits ™: 1.50 ARRT Category A+ Credit: 1.75

FDA Discussions may include off-label uses.

Participants

Luca Maria Sconfienza, MD, PhD, Milano, Italy (*Moderator*) Travel support, Bracco Group; Travel support, Esaote SpA; Travel support, ABIOGEN PHARMA SpA

Daria Motamedi, MD, Washington, DC (Moderator) Nothing to Disclose

Sub-Events

SSK13-01 CT Guided Pulsed Radiofrequency Treatment of the Lumbar Dorsal Root Ganglion in Patients with Acute Radicular Lower Back Pain

Participants

Alessandro Napoli, MD, Rome, Italy (*Presenter*) Nothing to Disclose Roberto Scipione, MD, Rome, Italy (*Abstract Co-Author*) Nothing to Disclose Hans Peter Erasmus, Rome, Italy (*Abstract Co-Author*) Nothing to Disclose Cristina Marrocchio, Rome, Italy (*Abstract Co-Author*) Nothing to Disclose Susan Dababou, Rome, Italy (*Abstract Co-Author*) Nothing to Disclose Carlo Catalano, MD, Rome, Italy (*Abstract Co-Author*) Nothing to Disclose

For information about this presentation, contact:

alessandro.napoli@uniroma1.it

PURPOSE

To determine the clinical impact of CT-guided Pulsed Radiofrequency in the management of patients with acute or sub-acute neuro-radicular pain from lumbar disc herniation, refractory to usual therapeutic strategies.

METHOD AND MATERIALS

Patients were eligible for this single-center prospective study if they presented acute or sub-acute neuro-radicular low back pain (EMG confirmed), refractory to usual treatments (drugs and injections), and if they could safely undergo Pulsed Radiofrequency procedure. Treatment was performed using a 22-20 G needle-electrode with probe tip directed to the symptomatic DRG under CT guidance; E-pulsed radiofrequency (Cosman G4) was administered for 10 min at 45V with constant local temperature of 42°C. Clinical evaluation was conducted with Visual Analogue Scale (VAS), Owestry Disability Index (ODI) and Roland-Morris (RM) score for quality of life assessment; all questionnaires were obtained at baseline and at 1-week, 1-month and 3-month follow-up. Analyses were performed on a per-protocol basis.

RESULTS

Over a 3-year period, 80 patients were treated with Pulsed RadiofrequencyMedian VAS scores decreased from 7.8 at baseline to 3.5 at 1week after treatment, to 2.6 at 1 month and 1.3 at 3 months; median ODI scores decreased from 78.0 at baseline to 12.5 at 1 week, to 6.0 at 1 month and 5.5 at 3 months; RM score decreased from 16 at baseline to 3 at 1 month and 1.5 at 3 months (p<0.001). Overall, 90.0% of patients reached a 0 VAS score within the first month after treatment; 97.5% of patients had a decrease of at least 20 points in ODI score in the same interval. There were 6 patients considered partial responders that required a second PRF session.

CONCLUSION

CT-guided Pulsed Radiofrequency has shown to be a minimally invasive, effective and repeatable percutaneous treatment option for patients with acute or sub-acute neuro-radicular low back pain.

CLINICAL RELEVANCE/APPLICATION

the results of this study are superior to those reported from literature for usual care strategies and injections and may avoid surgery for a substantial number of patients with sciatic disc compression.

SSK13-02 Effects of Allogeneic Human Chondrocytes Expressing TGF-B1 (TG-C) On Structural Progression of MRI Features Of Knee Osteoarthritis: A Randomized Clinical Trial

Wednesday, Nov. 29 10:40AM - 10:50AM Room: E353C

Participants

Ali Guermazi, MD, PhD, Boston, MA (*Presenter*) President, Boston Imaging Core Lab, LLC; Research Consultant, Merck KGaA; Research Consultant, sanofi-aventis Group; Research Consultant, TissueGene, Inc; Research Consultant, OrthoTrophix, Inc; Research Consultant, AstraZeneca PLC; Research Consultant, General Electric Company; Research Consultant, Pfizer Inc

Gurdyal Kalsi, Rockville, MD (*Abstract Co-Author*) Officer, TissueGene, Inc Michel D. Crema, MD, Boston, MA (*Abstract Co-Author*) Shareholder, Boston Imaging Core Lab, LLC Ogden Copeland, Rockville, MD (*Abstract Co-Author*) Director, TissueGene, Inc Moon J. Noh, Rockville, MD (*Abstract Co-Author*) Vice President, TissueGene, Inc Frank W. Roemer, MD, Erlangen, Germany (*Abstract Co-Author*) Chief Medical Officer, Boston Imaging Core Lab LLC; Director of Research, Boston Imaging Core Lab LLC; Shareholder, Boston Imaging Core Lab LLC; ;

For information about this presentation, contact:

guermazi@bu.edu

PURPOSE

To determine effects of allogeneic human chondrocytes expressing TGF-B1 (TG-C) on structural progression of MRI features of knee osteoarthritis over a 1 year period.

METHOD AND MATERIALS

This phase II randomized controlled trial of TG-C included patients with moderate to advanced osteoarthritis. Patients were randomized to receive an intraarticular 3:1 mixture of non-transduced allogeneic human chondrocytes and TG-C or placebo. 3T MRI was acquired for all patients at baseline and follow-up (3, 6 and 12 months). MRIs were assessed using the WORMS system including cartilage damage, bone marrow lesions (BMLs), meniscal damage/extrusion, Hoffa-, effusion-synovitis, and osteophytes. Analyses were performed on a whole knee level, compartmental level, and subregional level. Binary logistic regression with Generalized Estimating Equation was used to compare risks of progression, adjusting for baseline age and gender. Mann-Whitney-Wilcoxon tests were used to assess differences for continuous variables.

RESULTS

57 Patients were included in the TG-C group and 29 in the placebo group. At 12 months, knees in the TG-C group showed less progression of cartilage damage compared to placebo on a whole knee level (34.6% vs. 47.9%; adjusted RR 0.7, 95%CI [0.5-1.1], p=0.077). Less progression of Hoffa-synovitis and effusion-synovitis was observed in the TG-C group compared to placebo (9.6% vs. 21.1%, adjusted RR 0.5, 95%CI [0.2,1.2], p=0.115). No statistically significant differences were seen for BMLs, meniscal damage and osteophytes.

CONCLUSION

Intraarticular treatment with TG-C showed fewer patients in the treated group with progression in structural OA features and other MRI-defined inflammatory markers such as Hoffa-synovitis and effusion-synovitis. However, no differences were observed in regard to progression of BMLs and meniscal damage, or hypertrophic osteophyte formation.

CLINICAL RELEVANCE/APPLICATION

Intraarticular treatment with TG-C may potentially show benefits on delayed progression of cartilage damage and MRI markers of inflammation in osteoarthritis.

Honored Educators

Presenters or authors on this event have been recognized as RSNA Honored Educators for participating in multiple qualifying educational activities. Honored Educators are invested in furthering the profession of radiology by delivering high-quality educational content in their field of study. Learn how you can become an honored educator by visiting the website at: https://www.rsna.org/Honored-Educator-Award/ Ali Guermazi, MD, PhD - 2012 Honored Educator

SSK13-03 MR Guided High Intensity Focused Ultrasound (MRgFUS) for the Treatment of Oligometastatic Prostate Cancer Bone Metastasis: Can Soundwaves Downstage Cancer Spread?

Wednesday, Nov. 29 10:50AM - 11:00AM Room: E353C

Participants

Carola Palla, MD, Rome, Italy (*Presenter*) Nothing to Disclose Alessandro Napoli, MD, Rome, Italy (*Abstract Co-Author*) Nothing to Disclose Cristina Marrocchio, Rome, Italy (*Abstract Co-Author*) Nothing to Disclose Lorenzo Chiurchioni, Rome, Italy (*Abstract Co-Author*) Nothing to Disclose Fabrizio Andrani, MD, Roma, Italy (*Abstract Co-Author*) Nothing to Disclose Carlo Catalano, MD, Rome, Italy (*Abstract Co-Author*) Nothing to Disclose

PURPOSE

With improvements in diagnostic modalities such as functional imaging, oligometastatic prostate cancer is being diagnosed with greater frequency than ever before. Our aim was to determine MRgFUS ability to downstage patients with oligometastatic bone disease with single session of non-invasive metastasis-directed therapy.

METHOD AND MATERIALS

The study was designed with intention-to-treat metastatic bone lesions. Patients were enrolled if they had accessible bone metastasis and could safely undergo MRgFUS (InSightec, Israel). Baseline measurable characteristics included dynamic contrast enhanced MRI study (Gd-BOPTA, Bracco; GE 750 3T magnet) with semiquantitative perfusion analysis, PSA level (ng/ml) and choline PET (SUV). Measurable variables were obtained at treatment time, 3 months, 12 months and 24 months follow-up.

RESULTS

18 patients fulfilled the inclusion criteria and safely underwent MRgFUS procedure of metastatic bone ablations. Lesions were located in the pelvis (11), scapula (3) and long bones (4). At baseline all lesions showed a significant DCE perfusion (highly vascular) with mean perfusion reduction of 88% at 3 months follow-up (CI: 100-50; p<0.001) stable at subsequent follow-up scans. Similarly PSA levels decreased from a mean baseline of 19 (ng/ml) to 7.1, 2.9 and 2.1, at 3-12 and 24 moths respectively. SUV values showed similar trend with reduction from baseline (mean 8.9 to 3.0, 2.3 and 1.7: p<0.001). In all patients single MRgFUS session was appropriate without any major or minor adverse events reported.

CONCLUSION

MRgFUS is a totally non-invasive procedure that can obtain nearly complete bone ablation in patients with oligometastatic prostate disease. The technique features a radiation-free approach that can be of incremental value in long-survivor subset on oncological patients, significantly reducing risk of toxic effects.

CLINICAL RELEVANCE/APPLICATION

MRgFUS could be routinely introduced as a treatment option for oligometastatic bone disease non responding to conventional treatment.

SSK13-04 Image-guided Spine Injections: Paradoxical Particle Formation of Ropivacaine and Non-Particulate Dexamethasone Poses a Risk for Spinal Cord Infarction Events

Wednesday, Nov. 29 11:00AM - 11:10AM Room: E353C

Participants

Brandon Childers, MD, Baltimore, MD (*Presenter*) Nothing to Disclose II Minn, Baltimore, MD (*Abstract Co-Author*) Nothing to Disclose Jace Jones, Baltimore, MD (*Abstract Co-Author*) Nothing to Disclose Maureen Kane, Baltimore, MD (*Abstract Co-Author*) Nothing to Disclose Jan Fritz, MD, Baltimore, MD (*Abstract Co-Author*) Research Grant, Siemens AG; Scientific Advisor, Siemens AG; Scientific Advisor, Alexion Pharmaceuticals, Inc; Speaker, Siemens AG

PURPOSE

Image-guided epidural steroid injections are frequently performed radiologic procedures using local anesthetics and steroids. Because particulate steroids can embolize into the arterial system and cause rare cord infarction events, non-particulate steroids are now recommended. However, we have observed paradoxical particulation when mixing the non-particulate steroid dexamethasone and the local anesthetic ropivacaine, posing a risk for cord infarction events despite using recommended nonparticulate injectables. Therefore, we investigated the occurrence of particulation between different local anesthetics and nonparticulate dexamethasone formulations, as well as the mechanism of action.

METHOD AND MATERIALS

We evaluated clinically relevant dilution series (1:1 - 1:10) of commercially available ropivacaine (2), lidocaine (2) and bupivacaine (1) formulations mixed with three different commercially available dexamethasone formulations. The outcome variables were the pH of the native drugs and mixtures as well as the presence of precipitation using macroscopic inspection and microscopic photography. Mass spectroscopy was used to analyze the composition of ropivacaine-dexamethasone precipitate.

RESULTS

The pH of the native formulations and mixtures were acidic for ropivacaine, and near neutral for bupivacaine, lidocaine, and dexamethasone. All mixtures were pH neutral. Both ropivacaine formulations demonstrated particulation at all concentrations when combined with two dexamethasone formulations, whereas only minimal particulation occurred at concentrations of 1:1-2 of ropivacaine and the third dexamethasone formulation. Bupivacaine showed minimal, wall-adherent crystal formation with only one dexamethasone formulation of 1:1-2. Lidocaine did not form any particles. Mass spectroscopy identified the particles as pure ropivacaine precipitate.

CONCLUSION

Ropivicaine precipitates out of solution and forms particles when combined with dexamethasone, owing to a change from acidic to neutral pH. However, the degree of particulation varies based upon the commercially-available formulations, suggesting that other factors may also play a role.

CLINICAL RELEVANCE/APPLICATION

The combination of non-particulate ropivacaine and non-particulate dexamethasone formulations should be avoided when performing epidural steroid injections to prevent particle formation and minimize the risk of embolic cord infarction events.

SSK13-05 Greater Occipital Nerve Infiltration under MR Guidance: Feasibility Study and Preliminary Results

Wednesday, Nov. 29 11:10AM - 11:20AM Room: E353C

Participants

Adrian I. Kastler, MD,PhD, Grenoble, France (*Abstract Co-Author*) Nothing to Disclose Romain Perolat, Grenoble, France (*Presenter*) Nothing to Disclose Bruno A. Kastler, MD, PhD, Besancon, France (*Abstract Co-Author*) Nothing to Disclose Jan Fritz, MD, Baltimore, MD (*Abstract Co-Author*) Research Grant, Siemens AG; Scientific Advisor, Siemens AG; Scientific Advisor, Alexion Pharmaceuticals, Inc; Speaker, Siemens AG Caroline Maindet, Grenoble, France (*Abstract Co-Author*) Nothing to Disclose Stephan Chabardes, Grenoble, France (*Abstract Co-Author*) Nothing to Disclose Alexandre Krainik, MD, PhD, Grenoble Cedex, France (*Abstract Co-Author*) Nothing to Disclose

PURPOSE

To assess the feasibility of greater occipital nerve (GON) intermediate site infiltration with MRI guidance

METHOD AND MATERIALS

Eleven consecutive patients suffering from chronic refractory cranio-facial pain who underwent 16 GON infiltrations between November 2016 and January 2017 were included in this prospective study. All of the procedures were performed on an outpatient basis in the research facility of our institution, equipped with a widebore 1.5T scanner. The fatty space between inferior obliquus and semispinalis muscles at C1-C2 level was defined as the infiltration target. Technical success was defined as the ability to accurately inject the products in the pre-defined target, assessed by post procedure axial and sagittal proton density weigthed sequences. Clinical success was defined as a 50% pain decrease at one month follow up.

RESULTS

Technical success as defined above was 100%. GON was depicted in 6 of 11 cases on planning MRI sequences. Mean duration of procedure was 22.5 minutes (range-16-41). Clinical success as previously defined was obtained in 7 of 11 included patients (63.6%) with a mean self reported improvement of 78%.

CONCLUSION

Interventional MR guidance for GON infiltration is a feasible technique offering similar results to an already established effective procedure. It may appear as a useful tool in specific populations, such as young patients and repeat infiltrations, and should be considered in these settings.

CLINICAL RELEVANCE/APPLICATION

• MR guidance for GON infiltration is a feasible technique • Preliminary results are in agreement with other guidance modalities • MR guidance may be seen as a useful tool in specific populations

SSK13-06 Cementoplasty of Pelvic Bone Metastases: Lesion Filling and Other Factors Influencing the Therapeutic Response

Wednesday, Nov. 29 11:20AM - 11:30AM Room: E353C

Participants Thomas Moser, MD, Montreal, QC (*Presenter*) Nothing to Disclose Marta Onate Miranda, MD, Madrid, Spain (*Abstract Co-Author*) Nothing to Disclose Katia Achour, MD, Laval, QC (*Abstract Co-Author*) Nothing to Disclose Veronique Freire II, MD, Montreal, QC (*Abstract Co-Author*) Nothing to Disclose

For information about this presentation, contact:

thomas.moser@umontreal.ca

PURPOSE

To determine the parameters likely to influence the therapeutic response in cementoplasty of pelvic metastases.

METHOD AND MATERIALS

We retrospectively reviewed a series of pelvic bone cementoplasties performed for symptomatic metastatic involvement in the last 7 years. In addition to demographics, primary tumor and associated treatments, we collected information on the lesion treated: localization, dimensions, cortical destruction graded 0-6, soft tissue mass and pathological fracture; and procedural information: number of needles, cement volume, filling percentage and extra-osseous leakage. The pain scores were evaluated on a visual analog scale before treatment and at the 1 month follow-up visit.

RESULTS

We included 44 procedures in 40 patients (21 females and 19 males, mean age 63 years). The primary tumor was lung (n = 15), breast (n = 9), kidney (n = 7), thyroid (n = 2) or other (n = 7). There were 38 osteolytic and 6 mixed lesions. Localization was acetabular (n = 30), iliac (n = 11) or sacral (n = 3). The maximal lesion diameter was on average 43 mm. The cortical destruction was on average 2.4 / 6 with soft tissue extension in 7/35 and pathological fracture in 7/35. The number of needles was one in 32/44, two in 10/44 and three in 2/44. The volume of cement injected was on average 10 ml with an average filling of 55%. A cement leak was minimal in 11/44, moderate in 9/44. Pain relief was observed in 74% of patients with an average score of 84/100 before the procedure and 46/100 after. The pain relief did not appear correlated to lesion volume (p = 0.2), presence of pathological fracture (p = 0.3), soft tissue extension (p = 0.21), filling percentage (p =0,42), cement leak (p = 0,26), or previous radiation therapy (p = 0,8).

CONCLUSION

Cementoplasty of pelvic bone metastases provides pain relief in a majority of patients. The lesion filling can be optimized by injection through multiple needles but this parameter does not appear correlated with the therapeutic response.

CLINICAL RELEVANCE/APPLICATION

Cementoplasty is a valuable adjunct in the management of symptomatic pelvic bone metastases.

SSK13-07 Hip Steroid/Anesthetic Injections: Is there an Increased Incidence of Hip Osteoarthritis Progression, Femoral Head Osteonecrosis and Collapse?

Wednesday, Nov. 29 11:30AM - 11:40AM Room: E353C

Participants

Frank J. Simeone, MD, Boston, MA (*Abstract Co-Author*) Nothing to Disclose Joao Rafael T. Vicentini, MD, Sao Paulo, Brazil (*Abstract Co-Author*) Nothing to Disclose Susan V. Kattapuram, MD, Boston, MA (*Abstract Co-Author*) Nothing to Disclose Connie Y. Chang, MD, Boston, MA (*Presenter*) Nothing to Disclose

For information about this presentation, contact:

cychang@mgh.harvard.edu

PURPOSE

To evaluate incidence of osteoarthritis progression, femoral head osteonecrosis and articular surface collapse in hip steroid/anesthetic injection patients.

METHOD AND MATERIALS

Our study was IRB-approved and HIPAA compliant. A total of 123 hip steroid/anesthetic(40 mg triamcinolone, 4 mL 0.5%

preservative free ropivicaine) injections were performed from 01/2014 to 07/2015. Inclusion criterion was follow-up radiography of the native hip 3-9 months after the injection. Two musculoskeletal radiologists performed retrospective, blinded reviews of the preand post-injection radiography of hip injection patients (HIPs) and 2 demographic and follow-up duration matched control groups: 1, patients undergoing hip x-rays without injection; 2, glenohumeral joint injection patients. Groups were compared with Fisher exact test.

RESULTS

There were 102 HIPs (age 65 ± 13 (range 19-92) years; 62 F, 40 M; 41 L, 61 R), who were followed for 26 ± 10 (12-66) weeks. For Reader 1, 38/102 (37%) of HIPs had increased osteoarthritis after steroid injection, compared with 27/102 (26%) of hip controls and 14/44 (32%) of shoulder injection patients. For Reader 2, 42/102 (41%) of HIPs had increased osteoarthritis after steroid injection, compared with 20/102 (20%) of hip controls and 10/44 (23%) of shoulder injection patients. There was no significant difference between these groups (P>0.05). For Reader 1, 24/102 (24%) of HIPs had new osteonecrosis and 15/102 (15%) had new collapse after the steroid injection, compared with 9/102 (9%) and 4/102 (4%) of hip controls and 2/44 (5%) and 1/44 (2%) of shoulder injection patients. There was significantly more osteonecrosis and collapse in HIPs, compared with hip controls (P=0.001 and 0.01) and shoulder injection patients (P = 0.005 and 0.04). For Reader 2, 22/102 (22%) of HIPs had new osteonecrosis and 2/44 (5%) and 2/44 (5%) and 1/44 (2%) of hip controls and 2/44 (5%) and 1/44 (2%) of shoulder injection patients. There was significantly more osteonecrosis and collapse in HIPs, compared with hip controls and 2/44 (5%) and 1/44 (2%) of shoulder injection patients (P = 0.005 and 0.04). For Reader 2, 22/102 (22%) of HIPs had new osteonecrosis and 17/102 (17%) had new collapse after the steroid injection, compared with 9/102 (9%) and 4/102 (4%) of hip controls and 2/44 (5%) and 1/44 (2%) of shoulder injection patients. There was significantly more osteonecrosis and collapse in HIPs, compared with hip controls and 2/44 (5%) and 1/44 (2%) of shoulder injection patients. There was significantly more osteonecrosis and collapse in HIPs, compared with hip controls (P=0.01 and 0.01) and shoulder injection patients (P = 0.03 and 0.005).

CONCLUSION

Hip injection patients have a greater incidence of osteonecrosis and collapse compared with hip controls and shoulder injection patients.

CLINICAL RELEVANCE/APPLICATION

Further evaluation of hip injectates and the injection population is warranted, given these findings.

SSK13-08 MRI-Guided High Intensity Focused Ultrasound: A New First-Line Technique in the Treatment of Osteoid Osteoma?

Wednesday, Nov. 29 11:40AM - 11:50AM Room: E353C

Awards

Trainee Research Prize - Resident

Participants Roberto Scipione, MD, Rome, Italy (*Presenter*) Nothing to Disclose Alessandro Napoli, MD, Rome, Italy (*Abstract Co-Author*) Nothing to Disclose Alberto Bazzocchi, MD, Bologna, Italy (*Abstract Co-Author*) Nothing to Disclose Andrea Leonardi, MD, Roma, Italy (*Abstract Co-Author*) Nothing to Disclose Susan Dababou, Rome, Italy (*Abstract Co-Author*) Nothing to Disclose Carlo Catalano, MD, Rome, Italy (*Abstract Co-Author*) Nothing to Disclose

For information about this presentation, contact:

roberto.scipione@uniroma1.it

PURPOSE

to demonstrate that completely non-invasive radiation-free ablation of osteoid osteoma with MRI-guided high intensity focused ultrasound (MRgFUS) is a safe, effective and durable treatment option.

METHOD AND MATERIALS

Patients with typical clinical and radiological diagnostic findings of osteoid osteoma (non-vertebral), suitable for MRgFUS and anaesthesia, were enrolled in this dual-centre prospective observational study. Vertebral locations were excluded as considered inaccessible. MrgFUS was performed using InSightec ExAblate 2100 system. Safety (rate of complications), clinical effectiveness (Visual Analogue Scale [VAS] pain score reduction) and durability (stability of results over time) of MRgFUS were evaluated as primary outcomes; tumour control (nidus ablation) at dynamic contrast enhanced MR imaging (Discovery 750, GE; Gd-BOPTA, Bracco) was considered as secondary outcome. All patients underwent a minimum follow-up period of 4 years.

RESULTS

Out of 50 subjects screened for recruitment, 45 were enrolled and submitted to MRgFUS. No treatment-related complications were observed. A complete and durable response was achieved in 80% of cases. Median VAS pain score dropped from 8 (IQR 7-9) to 0 at 1-week, and at all subsequent follow-up check points (1 month, 6, 12, 24, 36 and 48 months). Scores evaluating interference of pain with sleep, physical and daily activities showed similar improvement after treatment. Among subjects with partial response (20%), 4 received a second treatment (3 with CT-guided Radiofrequency Ablation, 1 with MRgFUS), and 5 did not need any other treatment. All re-treated patients achieved 0 VAS score. Overall, 87% of patients after MRgFUS treatment reached and maintained a stable 0 VAS score during follow-up. At 3-year MRI osteoid osteoma showed no vascularization in 32/42 patients (76%) treated with MRgFUS alone.

CONCLUSION

MRgFUS is a safe, effective and durable option in the treatment of non-spinal osteoid osteoma.

CLINICAL RELEVANCE/APPLICATION

This technique provides relevant advantages in the treatment of this impairing disease affecting mostly young population: no ionizing radiation, no incisions or needles, and, so far, no complications. Our results support the role of MRgFUS as first-line treatment option for accessible osteoid osteoma.

SSK13-09 Imaging and Clinical Risk Factor Correlation with Rate of Conversion to Surgery Following Fluoroscopically Guided Facet Cyst Rupture

Participants

Andrew J. Hill IV, MD, Charlottesville, VA (*Abstract Co-Author*) Nothing to Disclose Michael Hadeed, MD, Charlottesville, VA (*Abstract Co-Author*) Nothing to Disclose Adam Shimer, MD, Charlottesville, VA (*Abstract Co-Author*) Speaker, Stryker Corporation; Consultant, NuVasive, Inc; Royalties, NuVasive, Inc Wendy Novicoff, PhD, Charlottesville, VA (*Abstract Co-Author*) Nothing to Disclose Nicholas C. Nacey, MD, Charlottesville, VA (*Presenter*) Nothing to Disclose

For information about this presentation, contact:

hillaj1@gmail.com

PURPOSE

Facet cysts may be encountered at magnetic resonance imaging (MRI) in patients with back pain and radicular symptoms. The purpose of this study was to evaluate the conversion rate to surgery following cyst rupture, and to assess associated clinical, imaging and procedural variables.

METHOD AND MATERIALS

A retrospective review was completed of all patients who underwent fluoroscopically guided facet cyst rupture through access of the inferior facet recess from 2000-2016. Primary outcome was conversion to surgery. Secondary outcomes included clinical, MRI, and procedural variables possibly associated with conversion. Clinical variables included sex, age, # of comorbidities, symptoms (pain, motor, sensory), pain laterality, and if pain involved the leg, back or both. MRI variables included cyst size, shape, internal signal, rim signal, spine level, laterality, spondylolisthesis, canal or lateral recess stenosis, presence of facet fluid +/- unilateral vs. bilateral, bone edema and erosion. Procedural variables included cyst opacification, successful epidural rupture and pre vs. post procedure pain.

RESULTS

49 patients met the inclusion criteria. 4 were excluded because they had either no clinical notes or no MRI available for review. 13/45 (29%) of patients converted to surgery. Successful epidural rupture was observed fluoroscopically in 33/45 (73%), of whom 7/33 (21%) converted to surgery. No epidural rupture was seen in 12/45 (27%), of whom 6/12 (50%) converted to surgery. The average interval to surgery was 95 days and average follow up was 889 days after cyst rupture. Of the clinical, imaging and procedural variables evaluated, only the number of comorbidities was significantly associated with conversion to surgery (p = 0.03).

CONCLUSION

Facet cysts have been recognized as a cause of spinal stenosis. Fluoroscopically guided facet cyst rupture may be attempted prior to surgery, though 29% our patients eventually required surgery. No significant correlation was found between facet cyst features at MRI and conversion rate to surgery to aid in determining which patients may be benefit from intervention.

CLINICAL RELEVANCE/APPLICATION

Fluoroscopic guided facet cyst rupture is a minimally invasive procedure worth attempting in symptomatic patients as it has a high rate of technical success, with most patients avoiding surgery.



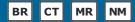




SSK14

Nuclear Medicine (Breast and Gynecologic Imaging)

Wednesday, Nov. 29 10:30AM - 12:00PM Room: S505AB



AMA PRA Category 1 Credits ™: 1.50 ARRT Category A+ Credit: 1.75

FDA Discussions may include off-label uses.

Participants

Gary A. Ulaner, MD, PhD, New York, NY (*Moderator*) Research support, General Electric Company; Research support, F. Hoffmann-La Roche Ltd

Don C. Yoo, MD, E Greenwich, RI (Moderator) Consultant, Endocyte, Inc

Sub-Events

SSK14-01 Bridging the Gap between Digital Mammography and Molecular Breast Imaging

Awards

Student Travel Stipend Award

Participants

Lucas R. Borges, Sao Carlos, Brazil (*Presenter*) Consultant, Photon Tech Solutions; Consultant, Real Time Tomography, LLC; Consultant, Noiseless Imaging Oy

Carrie B. Hruska, PhD, Rochester, MN (Abstract Co-Author) Institutional license agreement, Gamma Medica, Inc

Michael K. O'Connor, PhD, Rochester, MN (Abstract Co-Author) Royalties, Gamma Medica, Inc

Marcelo A. Vieira, PhD, Sao Carlos, Brazil (Abstract Co-Author) Nothing to Disclose

Andrew D. Maidment, PhD, Philadelphia, PA (*Abstract Co-Author*) Research support, Hologic, Inc; Research support, Barco nv; Research support, Analogic Corporation; Spouse, Employee, Real-Time Tomography, LLC; Spouse, Stockholder, Real-Time Tomography, LLC; Scientific Advisory Board, Real-Time Tomography, LLC; Scientific Advisory Board, Inc

For information about this presentation, contact:

lucas.rodrigues.borges@usp.br

PURPOSE

To develop image processing algorithms and visualization tools to assist with the interpretation of molecular breast imaging (MBI).

METHOD AND MATERIALS

MBI images were first denoised using a state-of-the-art denoising pipeline. The pipeline consists of a variance stabilization step, followed by noise suppression using the block-matching 3D (BM3D) filter. Optimal denoising parameters were defined based on a subset of cases; a graphical user interface allows for dynamic adjustment of the sharpness and noise by the reader. The visualization software includes a computer-aided diagnosis (CAD) feature, which searches for bright regions on the denoised image and automatically highlights their positions for further investigation. To assist the translation between MBI and digital mammography (DM), a registration algorithm is used to determine an affine algebraic transformation that maps coordinates from the MBI images into coordinates on the DM images. The transformation can be used to highlight a region on the DM image based on a user selected location on an MBI image. Alternatively, the MBI may be fused with the corresponding DM images and displayed similar to PET CT images. A software prototype was implemented using MATLAB and evaluated using 18 patient cases.

RESULTS

The denoising algorithm improved the visualization of lesions with subtle uptake by suppressing noise with minimal signal smoothing. The CAD was capable of identifying areas of increased uptake in faint lesions. In this small test set, all lesions were marked; falsepositive marks at the chest wall were noted in a minority of cases. The MBI registration resulted in good matches between MBI and DM images, based upon visual inspection of anatomic landmarks.

CONCLUSION

We have developed image processing algorithms and visualization tools for improving the interpretation of MBI images. It is important that MBI is combined with current technologies, such as DM and tomosynthesis, to improve the detection and characterization of lesions.

CLINICAL RELEVANCE/APPLICATION

Denoising may offer the potential to reduce MBI radiation dose and imaging time and increase tumor detectability. By co-registering MBI and DM images, ambiguities between the modalities are reduced, offering the potential to reduce false positive findings.

SSK14-02 Supine Breast PET-MR Imaging in a Whole-Body Approach: How Good is it Compared to Dedicated **Breast PET MR Imaging**

Wednesday, Nov. 29 10:40AM - 10:50AM Room: S505AB

Participants

Julian Kirchner, Dusseldorf, Germany (Abstract Co-Author) Nothing to Disclose Johannes Grueneisen, Essen, Germany (Presenter) Nothing to Disclose Alexander Tschischka, Duesseldorf, Germany (Abstract Co-Author) Nothing to Disclose Philipp Heusch, MD, Duesseldorf, Germany (Abstract Co-Author) Nothing to Disclose Ken Herrmann, Essen, Germany (Abstract Co-Author) Co-founder, SurgicEye GmbH Stockholder, SurgicEye GmbH Consultant, Sofie Biosciences Consultant, Ipsen SA Consultant, Siemens AG Research Grant, Advanced Accelerator Applications SA Research Grant, Ipsen SA

Lale Umutlu, MD, Essen, Germany (Abstract Co-Author) Consultant, Bayer AG

For information about this presentation, contact:

Julian.Kirchner@med.uni-duesseldorf.de

PURPOSE

To evaluate the detection rate of breast tumor in supine breast MRI and supine breast 18F-FDG PET/MRI compared to diagnostic breast MRI and diagnostic breast 18F-FDG PET/MRI.

METHOD AND MATERIALS

A total of 32 patients (31 women, 1 man, mean age 38 years) with histopathologically confirmed breast cancer were included in this study. Each patient underwent a whole-body 18F-FDG PET/MR examination including dedicated diagnostic breast imaging in prone position and subsequently a whole-body MRI in supine position. We analysed the diagnostic performance of (1) dedicated prone breast MRI, (2) dedicated prone breast 18F-FDG PET/MRI (3) supine breast MRI and (4) supine breast 18F-FDG PET/MRI derived from a whole-body staging examination, on a per-patient and per-lesion basis.

RESULTS

Dedicated prone breast MRI and dedicated prone breast 18F-FDG PET/MRI correctly identified all 32 patients with breast cancer (100%). Supine breast MRI correctly identified 28/32 patients (87.5%), while supine breast 18F-FDG PET/MRI correctly identified 29/32 patients (90%). Based on the reference standard a total of 51 lesions were included for analysis. In both dedicated breast imaging examinations all lesions (100%) were identified with 2 additional false-positive findings. Supine breast MR imaging identified 36/51 lesions (70%) with 5 additional false-positive findings and supine breast 18F-FDG PET/MRI identified 40/51 lesions (78%) with 6 additional false-positive findings. The mean SUVmax for lesions in prone 18F-FDG PET/MRI was 3.4 and 4.2 in supine 18F-FDG PET/MRI.

CONCLUSION

Dedicated breast imaging in prone positioning with or without 18F-FDG information is superior to examinations in supine position. While 18F-FDG information did not improve the diagnostic value of dedicated prone breast MRI, adding 18F-FDG information to supine breast examination led to an increase of tumor detection but also of false positive findings.

CLINICAL RELEVANCE/APPLICATION

Dedicated prone breast (PET)MRI is superior to supine breast imaging, as supine breast (PET)MR imaging identifies less tumor lesions and elicits an increase of false-positive findings leading to potentially harmful biopsies.

SSK14-03 Correlation of Bone Marrow Fat Fraction Content using T1 Dixon and Changes in FDG with PET/MR in **Breast Cancer Patients with Bone Metastases**

Wednesday, Nov. 29 10:50AM - 11:00AM Room: S505AB

Participants

Jerrin Varghese, MD, Stony Brook, NY (Presenter) Nothing to Disclose Robert Matthews, MD, Stony Brook, NY (Abstract Co-Author) Nothing to Disclose Lev Bangiyev, DO, Stony Brook, NY (Abstract Co-Author) Nothing to Disclose Annapurneswara R. Chimpiri, MD, Stony brook, NY (Abstract Co-Author) Nothing to Disclose James Bai, MD, Stony Brook, NY (Abstract Co-Author) Nothing to Disclose Dinko Franceschi, MD, Stony Brook, NY (Abstract Co-Author) Nothing to Disclose

For information about this presentation, contact:

jerrin.varghese@stonybrookmedicine.edu

PURPOSE

Bone metastases replace the normal fat of bone marrow which can easily be imaged with Dixon sequence. However, there is a lack of quantitative evaluation in the literature. We utilized Dixon sequence with FDG PET/MR to determine if change in fat content correlated with change in metabolic activity and if it could be used to assess treatment response.

METHOD AND MATERIALS

We retrospectively identified 7 females with osseous metastases from breast cancer who had pre- and post-treatment FDG PET/MR scans. Regions of interest were drawn around metastases on coronal T1 Dixon fat only images. Fat fraction of each lesion was measured using the ratio of signal intensity of metastases to signal intensity of the patient's normal psoas muscle as well as normal vertebral body. Change in fat fraction was then compared with change in PET SUV of each lesion.

RESULTS

32 bone metastases were identified on PET/MR scans in 7 females with breast cancer. 63% (n=20) of the lesions were in the spine, 22% (n=7) in the pelvis, and 15% (n=5) in the extremities. The average time between studies was 6 months. From pre-treatment

to post-treatment study, 25 lesions increased in FDG activity and 7 lesions decreased in FDG activity. 89% (22/25) of lesions with increasing metabolic activity demonstrated a decrease in fat fraction, with an overall average change in fat fraction of -56%. To the contrary, lesions with decreasing metabolic activity had an average change of +153% in fat fraction. A Wilcoxon rank-sum test revealed a significant difference in the change of fat fraction between the two groups with a p-value of 0.01. A Pearson correlation test between the percent change in SUV and change in fat fraction of each lesion revealed an r-value of -0.3. More specifically, 100% (7/7) of pelvic and 85% (11/13) of vertebral lesions with increased metabolic activity demonstrated a decrease in fat fraction.

CONCLUSION

Quantitative analysis of bone metastases in breast cancer patients reveals that fat fraction of lesions increases with significance as metastases improve and vice versa. However, a strong negative linear correlation did not exist between changes in metabolism and changes in fat fraction.

CLINICAL RELEVANCE/APPLICATION

Many breast cancer patients present in the late stages with osseous metastases. Measuring quantitative fat fraction changes in lesions can help follow up treatment response in bone metastases, especially when PET imaging is not available.

SSK14-04 Quantitative Evaluation of Metabolic Tumor Burden in Molecular Subtypes of Primary Breast Cancer with FDG PET/CT

Wednesday, Nov. 29 11:00AM - 11:10AM Room: S505AB

Participants

Wei Chen, PhD,MD, Tianjin, China (*Presenter*) Nothing to Disclose Wengui Xu, Tianjin, China (*Abstract Co-Author*) Nothing to Disclose Ping Wang, Tianjin, China (*Abstract Co-Author*) Nothing to Disclose

For information about this presentation, contact:

weichen@tmu.edu.cn

PURPOSE

To quantitatively evaluate volume-based metabolic tumor burden including metabolic tumor volume and total lesion glycolysis in different molecular subtypes of breast cancer and to compare the total lesion glycolysis before and after normalizing for lean body mass on 18F-FDG PET/CT.

METHOD AND MATERIALS

This study involved 99 female patients who were pathologically diagnosed with primary breast cancer and 18F-FDG PET/CT were performed before any therapy. The patients were divided into 4 subtypes including Luminal A, Luminal B, ERBB2+ and Basal-like according to the immunohistochemistry results. Metabolic tumor volume (MTV) and total lesion glycolysis (TLG) before and after correction for lean body mass (LBM) were achieved and compared. Correlations between metabolic tumor burden and the expression level of Ki-67 and p53 were analyzed. Diagnostic performance of volume-based metabolic parameters was evaluated using the receiver operating characteristic curve.

RESULTS

Group differences of the total lesion glycolysis were found between each molecular subtype of breast cancer, with the highest value in the subtype of Basal-like but there was no significant difference in metabolic tumor volume in subtypes of breast cancer. Values of total lesion glycolysis before and after correction for LBM were highly associated and significant reduction was found after correction of LBM for all subtypes of breast cancer. TLG after correction for LBM showed more close correlations with the expression level of Ki-67 and it presented higher diagnostic ability in identifying patients of Basal-like from those of non-Basal-like than that before correction.

CONCLUSION

Metabolic tumor burden could reflect the metabolic differences and predict prognosis of different molecular subtypes of breast cancer, especially total lesion glycolysis after correction for LBM. It could be used to help with differentiating patients in the subtype of Basal-like.

CLINICAL RELEVANCE/APPLICATION

Metabolic tumor burden is superior to daily used SUV and could comprehensively reflect the metabolic differences and predict prognosis of different molecular subtypes of breast cancer,

SSK14-05 Relationship between SUV Max and Gene Expression in FDG-PET/CT in Invasive Ductal Breast Cancer

Wednesday, Nov. 29 11:10AM - 11:20AM Room: S505AB

Participants

Charles M. Intenzo, MD, Philadelphia, PA (*Presenter*) Nothing to Disclose Sung M. Kim, MD, Philadelphia, PA (*Abstract Co-Author*) Nothing to Disclose Paras Lakhani, MD, Philadelphia, PA (*Abstract Co-Author*) Nothing to Disclose Daly Colarossi, Collegeville, PA (*Abstract Co-Author*) Nothing to Disclose Rebecca Jaslow, MD, Philadelphia, PA (*Abstract Co-Author*) Nothing to Disclose

For information about this presentation, contact:

Charles.intenzo@jefferson.edu

PURPOSE

To compare 18FDG uptake within invasive ductal breast carcinoma (IDC) with estrogen and progesterone receptor status, as well as epidermal growth factor (HER-2) gene expression.

METHOD AND MATERIALS

Over a 5-year interval, a total of 142 women with IDC, 1 cm or larger, underwent PET/CT imaging for staging purposes. From histopathology reports, all estrogen receptor (ER) and progesterone receptor (PR) status results were collected, as well as results of the human epidermal growth receptor 2 (HER-2) gene expression status. Four patient subgroups were formed. Group A (N=43) were ER negative/PR negative/HER-2 negative (i.e. 'triple negative'), group B (N=50) were ER positive/PR positive/HER-2 negative, group C (N=45) were ER positive/PR positive/HER-2 positive, group D (N=9) consisted of any other combination.

RESULTS

The triple-negative tumors had the highest SUV Max, ranging from 2.24 to 26.7, with a mean of 14.69. The ER positive/PR positive/HER-2 positive had the lowest SUV Max, ranging from 0.85-6.86, with a mean of 3.85.

CONCLUSION

As expected, triple negative IDC, as the most aggressive, demonstrated the highest glucose comsumption rate. By contrast, those tumors with combined estrogen, progesterone and HER-2 receptor activity demonstrates the lowest glucose consumption.

CLINICAL RELEVANCE/APPLICATION

There is a direct correlation between hormone and HER-2 receptor status and 18FDG uptake in invasive ductal breast cancers.

SSK14-06 A Patient-Centered Quality Initiative: Stepwise Modification of Departmental Protocol Culminating in a Single Periareolar Radiotracer Injection with Equally Effective Sentinel Node Detection While Reducing Procedural Pain

Wednesday, Nov. 29 11:20AM - 11:30AM Room: S505AB

Awards

Student Travel Stipend Award

Participants

Janice Thai, MD, Staten Island, NY (*Presenter*) Nothing to Disclose Michael Shamis, MD, Staten Island, NY (*Abstract Co-Author*) Nothing to Disclose Ami Gokli, MD, Staten Island, NY (*Abstract Co-Author*) Nothing to Disclose Arnold Brenner, DO, Staten Island, NY (*Abstract Co-Author*) Nothing to Disclose

PURPOSE

To evaluate the effectiveness of multiple technical modifications of technique in performing preoperative axillary sentinel lymph node (SLN) mapping in breast cancer patients, with the endpoints of nodal detection sensitivity and perceived procedural pain.

METHOD AND MATERIALS

A superficial injection of radiotracer 99Tc- ultra-filtered sulfur colloid was used. Stepwise optimization of this technique resulted in a standardized injection protocol with a tracer dose of 1 mCi, administered through a single periareolar intradermal injection of 0.1 mL using a TB syringe and a 26G needle. Additional modification included the use of benzocaine topical anesthetic spray. Over a 6 year period (2011 - 2017), the number of periareolar injections performed was reduced stepwise from 4 injection sites to 1 injection site and this final refinement was analyzed for SLN detection sensitivity and perceived pain, using our institutional pain scale ranging from 0-10.

RESULTS

682 women with invasive breast cancer who underwent consecutive preoperative axillary SLN mapping were included (mean age 63, range 31-90). Laterality of breast injection site included 263 in the right breast, 287 in the left breast and 132 in bilateral breasts. Axillary SLN was visualized with detection sensitivity of 100%. In women who had 4 injection sites in a unilateral breast or 8 injections in bilateral breasts (n= 180), the mean reported pain score was 4.6 (range 0-10). Women with 3 injection sites in a unilateral breast or 6 injections in bilateral breasts (n= 214) and 2 injection sites in a unilateral breast or 4 injections in bilateral breasts (n= 196) have a mean reported pain score of 3.7 and 3.2, respectively (range 0-10). Women who had only 1 injection in a unilateral breast or 2 injections in bilateral breasts (n= 92) reported a mean pain score of 2.4 (range 0-8). A decrease in the number of injection sites from 4 to 1 reduced the mean pain score by 48% (p-value < 0.0001).

CONCLUSION

Multiple sequential technical modifications culminating in a single periareolar injection technique for axillary SLN mapping reduces periprocedural pain while maintaining 100% SLN detection sensitivity.

CLINICAL RELEVANCE/APPLICATION

A stepwise modification of technique resulting in a single periareolar intradermal injection reduces periprocedural pain while maintaining 100% axillary sentinel lymph node detection sensitivity.

SSK14-07 Value of Intratumoral Metabolic Heterogeneity and Quantitative 18F-FDG PET/CT Parameters to Predict Prognosis in Patients with Cervical Cancer

Wednesday, Nov. 29 11:30AM - 11:40AM Room: S505AB

Participants

Daniella F. Pinho, MD, Dallas, TX (*Presenter*) Nothing to Disclose Brent King, MD, Dallas, TX (*Abstract Co-Author*) Nothing to Disclose Rathan M. Subramaniam, MD, PhD, Dallas, TX (*Abstract Co-Author*) Nothing to Disclose

For information about this presentation, contact:

daniella.pinho@utsouthwestern.edu

PURPOSE

To evaluate the impact of intratumoral metabolic heterogeneity and quantitative FDG PET/CT parameters for predicting patient outcomes in cervical cancer.

METHOD AND MATERIALS

This ongoing IRB and HIPPA complaint retrospective study included a total of 120 patients with biopsy proven squamous cell carcinoma of the cervix who had a FDG PET/CT for initial staging. Automated gradient-based segmentation method was used to assess the primary tumor standardized uptake value maximum and peak (SUV max and SUV peak), metabolic tumor volume (MTV) and metabolic intratumoral heterogeneity index, calculated as the area under cumulative SUV-volume histograms (AUC-CSH), with lower AUC-CSH indexes corresponding to higher degrees of tumor heterogeneity. Patient's demographics and tumor staging were also collected. Median follow up time was 27.5 months. Overall survival (OS) and progression free survival (PFS) were calculated using multivariate cox proportion hazard regression model and log-rank (Mantel-Cox) test to generate Kaplan-Meier survival plots.

RESULTS

The patients' mean age was 54.4 ± 13.1 years and there were 27 patients with stage I, 53 with stage II, 23 with stage III and 17 with stage IV disease. Median survival was 74.9 months. Thirty three patients died and 82 were alive (for 5 patient no information on survival available). Higher MTV was significantly associated with reduced OS in the multivariate analysis for every 10 mL increase in volume (HR=1.084, 95% CI=1.036-1.134, p=0.0005). Higher AUC-CSH (lower tumor heterogeneity) was significantly associated with increased PFS in the multivariate analysis for every 1000 increase in the area under the curve (HR=0.679, 95% CI=0.468-0.968, p=0.042). Kaplan-Meier survival analysis using the median value for MTV (74.7 mL) significantly predicted OS (HR = 2.839; 95% CI =1.33-6.02; p=0.0045) and using median value for AUC-CSH of 5602 significantly predicted PFS (HR = 0.469; 95% CI =0.226-0.973; p=0.03).

CONCLUSION

MTV segmented by gradient method is significantly associated with overall survival and tumor heterogeneity is associated with progression free survival for patients with cervical cancer.

CLINICAL RELEVANCE/APPLICATION

FDG PET/CT quantitative parameters can provide prognostic information on initial staging scan, potentially leading to a more personalized approach for patient's treatment.

SSK14-08 18F-FDG PET/MRI vs MRI Alone in Whole-Body Staging of Seventy-One Patients with Suspected Recurrent Gynecologic Pelvic Cancers

Wednesday, Nov. 29 11:40AM - 11:50AM Room: S505AB

Participants

Lino Sawicki, MD, Dusseldorf, Germany (*Presenter*) Nothing to Disclose Julian Kirchner, Dusseldorf, Germany (*Abstract Co-Author*) Nothing to Disclose Johannes Grueneisen, Essen, Germany (*Abstract Co-Author*) Nothing to Disclose Verena Ruhlmann, Essen, Germany (*Abstract Co-Author*) Nothing to Disclose Gerald Antoch, MD, Duesseldorf, Germany (*Abstract Co-Author*) Nothing to Disclose Lale Umutlu, MD, Essen, Germany (*Abstract Co-Author*) Consultant, Bayer AG

PURPOSE

To evaluate the diagnostic performance of whole-body 18F-fluordesoxyglucose positron emission tomography/magnetic resonance imaging (18F-FDG PET/MRI) for whole-body staging of suspected recurrent gynecologic pelvic cancer in comparison with whole-body MRI alone.

METHOD AND MATERIALS

Seventy-one consecutive female patients (54 ± 13 years) with suspected recurrence of cervical (32), ovarian (26), endometrial (7), vulvar (4), and vaginal (2) cancer prospectively underwent whole-body PET/MRI including a diagnostic contrast-enhanced MRI protocol. PET/MRI and MRI datasets were separately evaluated regarding lesion count, localization, categorization (benign/malignant), and diagnostic confidence (4-point scale; 0 - 3) by two radiologists. The reference standard was based on histopathological results and follow-up imaging. Proportions of lesions rated correctly were compared on a per-patient and per-lesion basis using McNemar's chi2 test. Differences in diagnostic confidence were assessed by Wilcoxon test.

RESULTS

Fifty-five patients had cancer recurrence. PET/MRI and MRI alone correctly identified 55/55 (100 %) and 46/55 (83.6 %) patients with cancer recurrence, respectively. A total of 241 lesions were described on the reference standard, including 181 malignant and 60 benign lesions. PET/MRI detected all 241 lesions, whereas only 186/241 lesions (77.2 %) were detectable on MRI alone. PET/MRI provided correct identification of all 181 malignant lesions. Instead, MRI alone correctly identified only 126/181 (69.6 %) malignant lesions, which was significantly less compared with PET/MRI (p < 0.001). PET/MRI offered significantly higher diagnostic confidence in the categorization of malignant lesions compared with MRI alone (p < 0.001).

CONCLUSION

PET/MRI demonstrates excellent diagnostic performance and outperforms MRI alone in staging of patients with suspected recurrent gynecologic pelvic cancers.

CLINICAL RELEVANCE/APPLICATION

PET/MRI enables exact assessment of recurrence of female pelvic malignancies and should be considered a valuable alternative for whole-body staging of patients with suspected recurrent disease.

SSK14-09 First-in-Human Biodistribution and Dosimetry of In-111/Y-90-FF-21101: A Radioimmunotherapeutic Agent Targeting P-cadherin

Wednesday, Nov. 29 11:50AM - 12:00PM Room: S505AB

Participants

William D. Erwin, MS, Houston, TX (*Presenter*) Research Grant, FUJIFILM Holdings Corporation; Research Grant, Leadiant Biosciences SpA;

Vivek Subbiah, MD, Houson, TX (Abstract Co-Author) Nothing to Disclose

Osama R. Mawlawi, PhD, Houston, TX (*Abstract Co-Author*) Research Grant, General Electric Company Research Grant, Siemens AG Carlos Gonzalez-Lepera, PhD, Houston, TX (*Abstract Co-Author*) Nothing to Disclose

Masahiko Tokura, MS, Tokyo, Japan (Abstract Co-Author) Employee, FUJIFILM Holdings Corporation

Michele Rosner, Spring, TX (Abstract Co-Author) Nothing to Disclose

Louis DePalatis, PhD, Spring, TX (Abstract Co-Author) Employee of Strategia Therapeutics

Linda Paradiso, DVM, MBA, Spring, TX (Abstract Co-Author) Employee of Strategia Therapeutics, Inc.

Elmer B. Santos, MD, PhD, Houston, TX (Abstract Co-Author) Nothing to Disclose

Gregory C. Ravizzini, MD, Houston, TX (Abstract Co-Author) Research grant, Strategia Therapeutics; Research grant, Endocyte, Inc

For information about this presentation, contact:

werwin@mdanderson.org

PURPOSE

To assess the human biodistribution and dosimetry of 111In/90Y-FF-21101, a human-mouse chimeric monoclonal antibody directed against P-cadherin, encoded by CDH3 gene-overexpressing solid tumors.

METHOD AND MATERIALS

Ten patients (4 male, 6 female) in a first-in-human dose-escalation (5, 10, 15, 20, 25 mCi/m2 <= 60 mCi) 90Y-FF-21101 clinical trial, underwent a 5 mCi 111In-FF-21101 pre-treatment dosimetry study. Whole-body planar (WB) scans were acquired at 0.25, 4, 24, 72 and 144 h on a Siemens Symbia S camera. A two-bed SPECT scan was acquired at 24-h, calibrated with a 10 ml vial containing 50 µCi of 111In, to compute organ absolute activity. (A CT scan was acquired on a General Electric 750 HD scanner for SPECT attenuation correction and fusion.) Blood samples were collected at 0.5, 1, 2, 4, 24, 72 and 144 h, for estimating marrow dose. Time-activity curves (TACs) were generated from two-dimensional regions of interest drawn on the WB images around the heart contents, lungs, liver, spleen, kidneys, testes and total body. Three-dimensional volumes of interest for the lungs, liver, spleen and kidneys were defined on the SPECT/CT images, to activity-correct planar TACs and estimate organ masses for the dosimetric analysis. Source organ and marrow 111In and 90Y residence times derived from TAC exponential fits were entered into OLINDA/EXM v1.1 for dose calculation (mSv/MBq), with mass correction for liver, kidneys, spleen and lungs. Tumor uptake was assessed qualitatively.

RESULTS

The five highest mSv/MBq for 111In were: spleen (M:2.55,F:2.66); kidneys (M:0.77,F:0.76); testes (M:0.62) and liver (F:0.64); liver (M:0.62) and lungs (F:0.52); and pancreas (M:0.57,F:0.47); and for 90Y were: spleen (M:23.4,F:28.5); testes (M:8.56) and kidneys (F:6.42); kidneys (M:6.48) and lungs (F:5.09); liver (M:4.34,F:4.66); and lungs (M:4.12) and heart wall (F:2.66). Tumor uptake was visualized in 6 of 10 patients; with the highest uptake seen in tumors of epithelial origin, including metastatic vaginal, ovarian and colon carcinomas, and liposarcoma, consistent with anti-P-cadherin targeting.

CONCLUSION

FF-21101 exhibits favorable biodistribution and dosimetry, enhancing its attractiveness as an imaging and therapeutic agent targeting P-cadherin overexpression.

CLINICAL RELEVANCE/APPLICATION

FF-21101 demonstrates P-cadherin targeting and favorable biodistribution, and thus may be a viable radioimmunotherapeutic agent for P-cadherin-overexpressing cancers.







SSK15

Neuroradiology (Striking at the Heart of Stroke)

Wednesday, Nov. 29 10:30AM - 12:00PM Room: N226



AMA PRA Category 1 Credits ™: 1.50 ARRT Category A+ Credit: 1.75

FDA Discussions may include off-label uses.

Participants

Bharathidasan Jagadeesan, MD, Minneapolis, MN (*Moderator*) Research Consultant. MicroVention Inc; Research Consultant, Medtronic plc; Research Consultant, CVRx

Joseph J. Gemmete, MD, Northville, MI (*Moderator*) Consultant, Terumo Corporation; Stockholder, Ablative Solutions, Inc; Stockholder, Innovative Cardiovascular Solutions; Stockholder, InNeuro; Stockholder, FlexDex Inc; Stockholder, Kalypso

Sub-Events

SSK15-01 Prediction of Malignant Cerebellar Edema Occurrence and Clinical Outcome after Ischemic Cerebellar Stroke Using Multiparametric CT

Participants

Wolfgang G. Kunz, MD, Munich, Germany (*Abstract Co-Author*) Nothing to Disclose Kolja M. Thierfelder, MD,MSc, Munich, Germany (*Abstract Co-Author*) Nothing to Disclose Pierre Scheffler, Munich, Germany (*Abstract Co-Author*) Nothing to Disclose Maximilian F. Reiser, MD, Munich, Germany (*Abstract Co-Author*) Nothing to Disclose Wieland H. Sommer, MD, Munich, Germany (*Abstract Co-Author*) Founder, Smart Reporting GmbH Matthias P. Fabritius, MD, Munich, Germany (*Presenter*) Nothing to Disclose

For information about this presentation, contact:

wolfgang.kunz@med.lmu.de

PURPOSE

Malignant cerebellar edema (MCE) is a life-threatening complication after acute cerebellar stroke. The aim of this study was to identify imaging predictors for the occurrence of MCE using multiparametric CT including whole-brain CT perfusion (WB-CTP).

METHOD AND MATERIALS

We selected all subjects with cerebellar WB-CTP perfusion deficit and follow-up-confirmed infarction from a cohort of 3,254 consecutive patients who underwent multiparametric CT. Follow-up imaging was assessed for the presence (MCE+) or absence (MCE-) of MCE, measured using an established 10-point scale by Jauss et al., of which scores >=4 are considered malignant. Posterior-circulation-Acute-Stroke-Prognosis-Early-CT-Score (pc-ASPECTS) was determined to assess ischemic changes on non-contrast CT (NCCT), CT angiography (CTA), and on parametric WB-CTP maps (cerebral blood flow, CBF; cerebral blood volume, CBV; mean transit time, MTT; time to drain, TTD). The volumes of CBF, CBV, MTT, and TTD deficits were quantified. Chi-square, Mann-Whitney-U tests and receiver operating characteristics (ROC) analyses were performed.

RESULTS

Fifty-one patients were included. 42 patients (82.4%) were categorized as MCE- and 9 (17.6%) as MCE+. MCE+ patients had larger CBF, CBV, MTT and TTD deficit volumes (each with p<0.001) and showed significantly lower median pc-ASPECTS assessed using WB-CTP (CBF: 5 vs. 8; CBV: 8 vs. 9; MTT: 5 vs. 8; TTD: 5 vs. 8; each with p<0.001) compared to MCE- patients, while median pc-ASPECTS on NCCT was not significantly different (9 vs. 10, p=0.097). ROC analyses for MCE yielded the largest area-under-the-curve (AUC) values for CBF (0.984), followed by CBV deficit volumes (0.972) and pc-ASPECTS on CBF (0.949), whereas pc-ASPECTS on NCCT (0.664) and CTA (0.699) provided less diagnostic value. Regarding mortality, ROC analyses revealed the highest AUC values for pc-ASPECTS CBV (0.853) and CBV deficit volume (0.837), and the lowest AUC values for pc-ASPECTS on NCCT (0.610) and CTA (0.643).

CONCLUSION

WB-CTP provides added diagnostic value regarding the prognosis of MCE occurrence and clinical outcome after cerebellar stroke compared to NCCT and CTA.

CLINICAL RELEVANCE/APPLICATION

WB-CTP performed in acute cerebellar stroke has the potential to impact clinical decision making based on an early identification of patients that are at high risk of developing MCE.

SSK15-02 Utility of Serial and Ancillary Neuroimaging in Assessment of Suspected Hypertensive Hemorrhage

Wednesday, Nov. 29 10:40AM - 10:50AM Room: N226

Richelle Roelandt L. Homo, Irvine, CA (*Abstract Co-Author*) Nothing to Disclose Dana Stradling, RN, Orange, CA (*Abstract Co-Author*) Nothing to Disclose Hermelinda G. Abcede, Orange, CA (*Abstract Co-Author*) Nothing to Disclose Seyed M. Shafie, Orange, CA (*Abstract Co-Author*) Nothing to Disclose Wengui Yu, Orange, CA (*Abstract Co-Author*) Nothing to Disclose David Floriolli, MD, Orange, CA (*Abstract Co-Author*) Nothing to Disclose Daniel S. Chow, MD, Orange, CA (*Abstract Co-Author*) Nothing to Disclose

For information about this presentation, contact:

ekuoyatucidotedu

PURPOSE

To assess the utility of serial and ancillary neuroimaging in the work-up of primary intracerebral hemorrhage involving characteristic hypertensive regions, including basal ganglia, thalamic, pontine and cerebellar hemorrhages. Lobar hemorrhages were included in the study, although these are more classically seen with cerebral amyloid angiopathy in non-hypertensive patients.

METHOD AND MATERIALS

This IRB-approved study retrospectively reviewed hypertensive patients presenting to the emergency room or transferred from an outside facility with imaging findings of primary intracerebral hemorrhage from October 2013 - October 2015. Patients were excluded if they had known CNS malignancy. Age, admitting systolic blood pressure, the location of bleed, and findings from follow-up imaging were recorded.

RESULTS

A total of 135 patients were identified, of which 73.6% (98/135) and 51.9% (70/135) had follow-up CTA/MRA or MRI, respectively. Sites of involvement included basal ganglia (42.9%, 56), thalamic (24.4%, 36), lobar (20%, 27), and the remaining within the brainstem or cerebellum. Of patients who underwent ancillary imaging, CTA/MRA revealed a vascular abnormality in a single patient, an arteriovenous malformation within the cerebellum. MRI also revealed a vascular abnormality in a single patient, vasculitis resulting in lobar hemorrhage. All remaining follow-up imaging reviewed was negative for additional pathology. With regards to location, all cases of basal ganglia and thalamic hemorrhages were consistent with hypertensive hemorrhage only.

CONCLUSION

In the setting of hypertension, ancillary imaging for basal ganglia and thalamic hemorrhages did not reveal alternative etiologies. In the absence of initial findings to warrant operative management, serial CT imaging in otherwise clinically stable patients did not result in findings warranting a change in management.

CLINICAL RELEVANCE/APPLICATION

In the absence of clinical concerns and findings on initial imaging, there is low utility in ancillary and serial neuroimaging for primary intracerebral hemorrhage involving the basal ganglia and thalamus in patients presenting with hypertension.

SSK15-03 The Ischemic Penumbra Assessment Using 3D ASL at Different Post Labeling Delays in Patients with Unilateral Middle Cerebral Artery Severe Stenosis or Occlusion

Wednesday, Nov. 29 10:50AM - 11:00AM Room: N226

Participants

Hui Du, MA,MA, DaLian, China (*Presenter*) Nothing to Disclose Jin Shang, Dalian, China (*Abstract Co-Author*) Nothing to Disclose Mengchen Wang Jr, MEd, Dalian, China (*Abstract Co-Author*) Nothing to Disclose Dunchao Chen, Xiangyang, China (*Abstract Co-Author*) Nothing to Disclose Yanwei Miao, Dalian, China (*Abstract Co-Author*) Nothing to Disclose

For information about this presentation, contact:

1161468090@qq.com

PURPOSE

To evaluate ischemic penumbra (IP) using three-dimensional pseudo continuous arterial spin labeling (3D pCASL) at PLD of 1.5 s and 2.5 s in patients with ischemic cerebrovascular disease.

METHOD AND MATERIALS

Twenty-six patients (mean age, 60±12 years; 16 men and 10 females) with unilateral middle cerebral artery (MCA) severe stenosis or occlusion were enrolled into the present study, underwent MRI scan especially 3D pCASL with PLDs of 1.5s and 2.5s and DWI. The IP was first observed according to mismatched CBF-DWI region. The mean CBF (CBF1.5 vs. CBF2.5, mL/100g per minute) values and the mean area (mm2) of IP were measured at PLDs of 1.5s and 2.5s. Comparisons of the mean CBF values and the mean IP area between the two PLDs were analyzed using paired T test. Compared with the positive detection rate of IP by Chi-square test.

RESULTS

The detection rate of IP increased at the PLD of 1.5s (21/26, 80.77%) than 2.5s (6/26, 23.08%) (P=0.000). The mean CBF1.5 and CBF2.5 values of IP were 12.32±1.66 vs.18.84±1.44 (P=0.002). The mean IP area was also significantly widened at the PLD of 1.5s (4273.17 ± 611.17) than 2.5s (1074.50 ± 955.32 , P=0.01).

CONCLUSION

IP detection and areas result from different PLD using 3D ASL and DWI in patients with ischemic cerebrovascular disease. The higher detection, decreased CBF and wider region of IP are present at the PLD of 1.5s.

CLINICAL RELEVANCE/APPLICATION

It is necessary to consider the different PLDs to assess IP by 3D pCASL in ischemic cerebrovascular disease.

SSK15-04 Early Identification of Tissue at Risk of Infarction after Acute Ischemic Stroke Using Convolutional Neural Networks

Wednesday, Nov. 29 11:00AM - 11:10AM Room: N226

Awards

Trainee Research Prize - Resident

Participants

Stefan Winzeck, MSc, Charlestown, MA (Presenter) Nothing to Disclose Mark J. Bouts, PhD, Charlestown, MA (Abstract Co-Author) Nothing to Disclose Elissa McIntosh, Charlestown, MA (Abstract Co-Author) Nothing to Disclose Raquel Bezerra, MD, Houston, TX (Abstract Co-Author) Nothing to Disclose Izzuddin Diwan, Charlestown, MA (Abstract Co-Author) Employee, Abcam plc Steven Mocking, Charlestown, MA (Abstract Co-Author) Employee, Google, Inc Priya Garg, Charlestown, MA (Abstract Co-Author) Nothing to Disclose William T. Kimberly, MD, PhD, Boston, MA (Abstract Co-Author) Research Grant, Remedy Pharmaceuticals, Inc William A. Copen, MD, Boston, MA (Abstract Co-Author) Nothing to Disclose Pamela W. Schaefer, MD, Boston, MA (Abstract Co-Author) Nothing to Disclose Aneesh B. Singhal, MD, Boston, MA (Abstract Co-Author) Scientific Advisory Board, Biogen Idec Inc; Consultant, Biogen Idec Inc; Spouse, Employee, Biogen Idec Inc; Institutional research support, Boehringer Ingelheim GmbH; Consultant, Doch Technologies; Royalties, Medicolegal Consultation; Royalties, UpToDate, Inc; Royalties, Medlink Imaging, Inc; Consultant, Omniox; Consultant, Boston Clinical Research Institute, LLC Ona Wu, PhD, Charlestown, MA (Abstract Co-Author) Royalties, General Electric Company; Royalties, Toshiba Medical Systems Corporation; License agreement, General Electric Company; License agreement, Toshiba Medical Systems Corporation; Research Consultant, Penumbra, Inc

PURPOSE

Early identification of potentially salvageable tissue after acute ischemic stroke (AIS) is increasingly being used to guide treatment decisions. Deep learning algorithms, e.g. convolutional neural networks (CNN), have been employed for chronic stroke lesion segmentation. We investigated the utility of CNN algorithms for predicting tissue infarction on follow-up MRI based on acute DWI and PWI MRI.

METHOD AND MATERIALS

The study included 50 AIS patients not treated with reperfusion therapy with DWI and PWI acquired <12h from the time when patients were last known to be well. Patients were also required to have follow-up (F/U) imaging performed >= 4 days after stroke. Apparent diffusion coefficient maps, T2WI, isotropic DWI, MTT, and Tmax were used as covariates to train a CNN (5-fold cross validation). The CNN was trained via the open source framework DeepMedic using the default architecture. The CNN segmentation maps were evaluated for each patient individually. Performance metrics were based on Dice score, sensitivity, and precision.

RESULTS

The CNN prediction of F/U lesions resulted in a mean \pm SD Dice score of 42% \pm 26%, sensitivity 39% \pm 27% and precision 60% \pm 30%. The CNN resulted in fair results for lesion volumes >= 10ml, however it underperformed for smaller lesions <10 mL (Dice score 24% \pm 20%, Sensitivity 25% \pm 25%, Precision 38% \pm 30%). Visual inspection showed compelling results for large lesions (Figure). The lesion size group analysis and the correlations of lesion volumes revealed that performance was dependent on lesion extent.

CONCLUSION

Our results showed that CNN can be used to combine acute multiparametric MRI for predicting tissue infarction on F/U, which hold especially true for large lesions. Although the CNN performed best for large lesion volumes, the focus of many early decision-making for AIS patients is whether or not the patient is at high risk of infarct growth. Therefore, CNN algorithms that can identify which patients will experience large infarct volumes without intervention hold promise for guiding AIS treatment decision strategies on an individual patient basis.

CLINICAL RELEVANCE/APPLICATION

Convolutional neural networks can be used to combine acute multiparametric MRI to predict follow-up tissue infarction with high accuracy, and therefore has potential for guiding treatment decisions on an individual patient basis.

SSK15-05 Regional Detection of Hemorrhagic Transformation using Kernel Spectral Regression and a Neural Network on Multi-modal MRI for Acute Ischemic Stroke

Wednesday, Nov. 29 11:10AM - 11:20AM Room: N226

Participants

Samantha J. Ma, Los Angeles, CA (*Presenter*) Nothing to Disclose Songlin Yu, Beijing, China (*Abstract Co-Author*) Nothing to Disclose David S. Liebeskind, Los Angeles, CA (*Abstract Co-Author*) Nothing to Disclose Lirong Yan, BSc, Beijing, China (*Abstract Co-Author*) Nothing to Disclose Fabien Scalzo, PhD, Los Angeles, CA (*Abstract Co-Author*) Nothing to Disclose Danny Wang, PhD, Los Angeles, CA (*Abstract Co-Author*) Shareholder, Hura Imaging, LLC

PURPOSE

Hyperperfusion detected on arterial spin labeling (ASL) cerebral blood flow (CBF) images acquired after acute ischemic stroke (AIS) onset has been shown to be significantly associated with development of intracerebral hemorrhage. The purpose of this study was to develop a machine model for the voxel-based detection of tissue at risk for hemorrhagic transformation (HT) given multiple MRI modalities as input.

The present study utilized routine clinical MRI and ASL image data acquired from 67 AIS patients shortly after endovascular therapy or clot retrieval. A novel regional cuboid sampling framework was developed for machine learning training, in which local cuboids were extracted from the CBF map, DWI, FLAIR, and T2 TSE before being matched with GRE-based manually drawn bleed groundtruth delineations. Kernel spectral regression (KSR) uses the information in the eigenvectors of the graph representation to reveal low dimensional structure in high dimensional data. After determining optimal kernel input parameters with KSR, we built a two-layer feed-forward neural network with 10 neurons in the sigmoid hidden layer and trained with scaled conjugate gradient backpropagation to classify cuboid inputs into likelihood of HT.

RESULTS

The proposed multimodal regional framework reached an accuracy of $80.59 \pm 3\%$ in detecting hemorrhage with KSR on our dataset (better than any single image modality alone); while a simple voxel-based prediction was $72.80 \pm 5\%$ accurate. Using the neural network training, the framework reached an improved accuracy of $95.1\% \pm 0.6\%$. Figure 1 shows a few predictive images based on the probabilities determined by the neural network. One can appreciate how the regions with high likelihood of hemorrhage determined by machine learning match well with the manually drawn regions in the reference GRE map.

CONCLUSION

Machine learning using kernel spectral regression or neural networks in particular can provide more accurate detection of tissues at risk for HT. Although CBF can inform AIS patient clinical outcome, the addition of multi-modal MRI data into the regional cuboid framework substantially improves the voxel-based HT detection accuracy.

CLINICAL RELEVANCE/APPLICATION

The proposed multi-modal regional framework for HT detection can improve stroke physicians' utilization of perfusion data in AIS treatment planning and monitoring.

SSK15-06 The Detectability of Forward Projected Model-Based Iterative Reconstruction for Low Contrast Lesions: Acute Cerebral Infarction-Phantom Study

Wednesday, Nov. 29 11:20AM - 11:30AM Room: N226

Participants

Toru Higaki, PhD, Hiroshima, Japan (*Presenter*) Nothing to Disclose Yoko Kaichi, Hiroshima, Japan (*Abstract Co-Author*) Nothing to Disclose Fuminari Tatsugami, Hiroshima, Japan (*Abstract Co-Author*) Nothing to Disclose Hiroki Taguchi, Otawara, Japan (*Abstract Co-Author*) Employee, Toshiba Mediical Systems Corporation Makoto Iida, Hiroshima, Japan (*Abstract Co-Author*) Nothing to Disclose Kazuo Awai, MD, Hiroshima, Japan (*Abstract Co-Author*) Nothing to Disclose Kazuo Awai, MD, Hiroshima, Japan (*Abstract Co-Author*) Research Grant, Toshiba Corporation; Research Grant, Hitachi, Ltd; Research Grant, Bayer AG; Research Grant, Daiichi Sankyo, Ltd; Research Grant, Eisai, Ltd; Medical Adviser, GE Healthcare; Research Grant, Fujitsu Ltd; ; ; ; ; ;

PURPOSE

Low-contrast areas in acute cerebral infarction are often difficult to be detected by computed tomography (CT) despite use of hybrid iterative reconstruction techniques such as adaptive iterative dose reduction 3D (AIDR 3D, Toshiba Medical Systems). Forward projected model-based Iterative Reconstruction SoluTion (FIRST, Toshiba Medical Systems), a novel iterative reconstruction technique, can strongly reduce noise and beam hardening artifact and improve spatial resolution. We compared the detectability of low contrast lesions on AIDR 3D- and FIRST images using a head phantom including simulated acute cerebral infarction.

METHOD AND MATERIALS

We developed dedicated head phantoms including simulated acute cerebral infarction using a 3D printer (Agilista 3200, Keyence). This study included 36 images of various models of acute cerebral infarction and 24 images of normal brain model. Half of these images were reconstructed with AIDR 3D and the rest were reconstructed with FIRST. Two radiologists separately specified the location of the low-contrast lesions in which subtle contrast between the gray and white matter diappeared. They rated the probability of the presence using an analog confidence scale. For the evaluation ROC analysis was performed. Statistical difference between AIDR 3D and FIRST was tested by DeLong's method.

RESULTS

ROC analysis showed that the difference between AIDR 3D (reader1: Az- value 0.773, reader2: Az- value 0.706) and FIRST (reader1: Az- value 0.935, reader2: Az- value 0.880) was significant in favour of FIRST (p = 0.037, 0.041, respectively).

CONCLUSION

Our study demonstrates a significant advantage of FIRST in the detection of low contrast lesions compared with AIDR 3D, one of the conventional iterative reconstruction techniques.

CLINICAL RELEVANCE/APPLICATION

FIRST may improve detectability of low contrast lesions in acute cerebral infarction.

SSK15-07 Intra-Arterial Thrombectomy in Patients with Cervical Dissections in the MR CLEAN Trial: A Descriptive Analysis

Wednesday, Nov. 29 11:30AM - 11:40AM Room: N226

Participants

Kars Compagne, BSC, Rotterdam, Netherlands (*Abstract Co-Author*) Nothing to Disclose Olvert A. Berkhemer, MD, Amsterdam, Netherlands (*Abstract Co-Author*) Nothing to Disclose Ad Van Es, Rotterdam, Netherlands (*Abstract Co-Author*) Nothing to Disclose Aad Van Der Lugt, MD, PhD, Rotterdam, Netherlands (*Abstract Co-Author*) Research Grant, Stryker Corporation; Research Grant, General Electric Company Bart J. Emmer, MD, Leiden, Netherlands (*Presenter*) Nothing to Disclose

PURPOSE

Several treatment strategies have been proposed in patients presenting with acute stroke and an extracranial dissection of the internal carotid artery (ICA). The aim of this study is to describe the outcome and variation of treatment strategies in intra-arterial thrombectomy (IAT) in patients with dissection of extracranial ICA and a proximal intracranial occlusion.

METHOD AND MATERIALS

Data (n=500) of the randomized controlled MR CLEAN trial on the effectiveness of IAT were analyzed. Carotid dissection was identified on CTA scans at baseline. Primary outcome was a favorable functional outcome defined as an modified Rankin Scale (mRS) score of <=2. Secondary outcomes were mRS <=3 and serious adverse events (SAE).

RESULTS

Carotid dissection was identified in 24 patients (21 male; median age 50.5) of which 15 in IAT group and 9 in non-IAT group. No differences at baseline NIHSS (p 0.74) and collateral score (p 0.29) was observed. In two patients stent placement was performed during IAT. A good functional outcome was observed at 7 (47%) in the IAT group versus 1 patient (11%) but was not statistically different (p 0.18). With respect to secondary outcomes, mRS <=3 and SAE were significantly different in favor of IAT (resp. p 0.03 and 0.04).

CONCLUSION

IAT is feasible in patients with extracranial dissections of the ICA and good outcomes have also been observed without carotid stenting.

CLINICAL RELEVANCE/APPLICATION

Carotid dissection is not a reason the withhold IAT in acute stroke patients.

SSK15-08 Diagnostic Accuracy of 3D black blood MRI with High Resolution T1 SPACE in the Evaluation of Intracranial Arterial Thrombosis

Wednesday, Nov. 29 11:40AM - 11:50AM Room: N226

Participants

Anas Al-Smadi, MD, Chicago, IL (*Presenter*) Nothing to Disclose Ali H. Elmokadem, MD,PhD, Mansoura, Egypt (*Abstract Co-Author*) Nothing to Disclose Ali Shaibani, MD, Chicago, IL (*Abstract Co-Author*) Nothing to Disclose Michael C. Hurley, MBBCh, Dublin, Ireland (*Abstract Co-Author*) Nothing to Disclose Matthew B. Potts, MD, Chicago, IL (*Abstract Co-Author*) Nothing to Disclose Babak S. Jahromi, MD,PhD, Chicago, IL (*Abstract Co-Author*) Nothing to Disclose Sameer A. Ansari, MD,PhD, Chicago, IL (*Abstract Co-Author*) Nothing to Disclose

PURPOSE

3D black blood (BB) MRI using a T1 sampling perfection with application-optimized contrast using different flip angle evolutions (SPACE) sequence allows high resolution, vessel wall imaging to evaluate the intracranial arterial wall and its associated pathologies. We investigated the diagnostic features and accuracy of 3D BB MRI in the detection of arterial thrombosis.

METHOD AND MATERIALS

We retrospectively identified fifteen patients with intracranial arterial thrombosis that underwent 3D BBMRI with non-enhanced and contrast enhanced high resolution T1 SPACE sequences. 3D BBMRI findings were evaluated by 2 independent neuro-radiologists blinded to all other angiographic studies, conventional MRI sequences, and clinical indications for imaging. Nineteen total intracranial vessel segments per patient were evaluated and graded on a three-point scale (grade 0-2) [Table] for intraluminal TI SPACE hyperintensity and contrast enhancement. Images were considered positive for arterial thrombosis when focal intraluminal T1 SPACE hyper-intense signal and/or enhancement on 3D BBMRI was graded as 1 or 2. Arterial occlusion was confirmed by digital subtraction angiography (DSA) or computed tomographic angiography (CTA). In limited cases (n=4) without DSA/CTA availability, susceptibility weighted imaging (SWI) in combination with time of flight (TOF) MR angiography (MRA) confirmed the diagnosis of complete vessel occlusion.

RESULTS

Fifteen patients with 18 intracranial arterial occlusions were studied. Fair inter-observer agreement for intraluminal T1 SPACE hyperintensity (Kappa = 0.50) and excellent inter-observer agreement for contrast enhancement (Kappa = 0.84) was noted. The sensitivity and specificity for intracranial arterial thrombosis of intraluminal T1 hyperintensity was 88.89% and 100% respectively and that of contrast enhancement was 94.45% and 100% respectively, taking Observer 1 as gold standard and Observer 2 as test when both partial and clear visualization (combined grades 1 and 2) suggested vessel thrombosis/occlusion.

CONCLUSION

3D BBMRI with T1 SPACE imaging is a valuable sensitive and specific technique for the evaluation of intracranial arterial thrombosis.

CLINICAL RELEVANCE/APPLICATION

This technique provides an adjunctive mechanism to confidently diagnose complete arterial occlusions in the setting of low resolution conventional MRI findings and absent flow enhancement on TOF-MRA imaging prone to overestimation.

SSK15-09 Actionable Vascular and Other Incidental Findings on CTA in Patients Undergoing Acute Stroke Intervention: Findings in 225 Patients

Wednesday, Nov. 29 11:50AM - 12:00PM Room: N226

Participants

Riti M. Kanesa-Thasan, MD, Philadelphia, PA (*Presenter*) Nothing to Disclose Mougnyan Cox, MD, Philadelphia, PA (*Abstract Co-Author*) Nothing to Disclose Brian R. Curtis, MD, Philadelphia, PA (*Abstract Co-Author*) Nothing to Disclose Manisha C. Patel, MD, Philadelphia, PA (*Abstract Co-Author*) Nothing to Disclose Adam E. Flanders, MD, Narberth, PA (*Abstract Co-Author*) Nothing to Disclose Robert W. Hurst, MD, Bryn Mawr, PA (*Abstract Co-Author*) Nothing to Disclose

For information about this presentation, contact:

ritikanesa@gmail.com

PURPOSE

The detection and appropriate management of incidental findings is an important part of any clinical radiology practice. The intricate anatomy covered by CTAs of the head and neck coupled with the time pressures of acute stroke diagnosis creates an environment for missing important unrelated findings. The purpose of our study was to document incidental findings on CTA in 225 patients undergoing acute stroke intervention.

METHOD AND MATERIALS

Under IRB approval and HIPAA compliance, 225 CTAs of the head and neck in patients undergoing acute stroke intervention from 2011-2016 were reviewed for important incidental findings. Average patient age was 65 (range 16-95 years). Findings were separated into vascular (mainly aneurysms) and non-vascular entities (such as tumor and infection), with results tabulated.

RESULTS

There were 19 vascular and 31 non-vascular important incidental findings. Intracranial aneurysms were the most common vascular finding, with 18 aneurysms present in 16 patients (7% of patients). All aneurysms were unknown prior to imaging, with average size of 5mm(range of 2-10mm). 5 malignancies, most of which were unknown, included 2 lung cancers and an erosive nasopharyngeal skull base tumor. 2 patients with malignancy had pathologic cervical spine fractures. Critical pulmonary findings included 3 malpositioned endotracheal tubes in their right main stem bronchus, and 1 moderate pneumothorax. 6 patients had pulmonary edema, and 3 had pneumonia.

CONCLUSION

Providing fast and accurate diagnosis of acute large vessel occlusion on CTA is essential for good stroke outcomes. However, important and even urgent findings are surprisingly frequent in this patient population, and should be looked for with equal fervor.

CLINICAL RELEVANCE/APPLICATION

CTAs of the head and neck in patients undergoing acute stroke intervention harbor important and urgent findings with surprising frequency, and should not be overlooked even in this time-sensitive clinical scenario.





103rd Scientific Assembly and Annual Meeting November 26 to December 1 McCormick Place, Chicago



SSK16

Neuroradiology (Epilepsy Imaging: Finding the Spark)

Wednesday, Nov. 29 10:30AM - 12:00PM Room: N229



AMA PRA Category 1 Credits ™: 1.50 ARRT Category A+ Credit: 1.75

FDA Discussions may include off-label uses.

Participants

Girish M. Fatterpekar, MBBS, New York, NY (*Moderator*) Nothing to Disclose Greg D. Avey, MD, Madison, WI (*Moderator*) Nothing to Disclose

Sub-Events

SSK16-01 Comparison of Arterial Spin Labeling MRI With EEG and Structural MRI in Patients With Epilepsy

Awards

Student Travel Stipend Award

Participants

Shankhneel Singh, MBBS,MD, Chandigarh, India (*Presenter*) Nothing to Disclose Paramjeet Singh, MBBS,MD, Chandigarh, India (*Abstract Co-Author*) Nothing to Disclose Niranjan Khandelwal, MD, Chandigarh, India (*Abstract Co-Author*) Nothing to Disclose Parampreet S. Kharbanda, MBBS,MD, Chandigarh, India (*Abstract Co-Author*) Nothing to Disclose

For information about this presentation, contact:

shankhneel@gmail.com

PURPOSE

The purpose of our study was to compare the results of interictal EEG and structural MRI with ASL-MRI findings in patients with epilepsy in the peri-ictal period and inter-ictal period and try to localize the epileptogenic zone.

METHOD AND MATERIALS

Two groups of patients were selected. The first group consisted of 21 patients having seizure episode in the hospital premises (selected randomly as per availability of MRI machine at time of seizure) who underwent structural MRI with an additional ASL sequence in the peri-ictal period (arbitrarily fixed at 2 hours from seizure onset). The patients also underwent an inter-ictal scalp EEG. The second group included 30 patients with refractory seizures who underwent inter-ictal structural MRI with additional ASL sequence (selected randomly from out-patient referrals for MRI from a dedicated seizure clinic). Inter-ictal scalp EEG was also performed for these patients. Hyperperfusion or hypoperfusion was recorded and localized to the hemisphere and if possible the anatomical lobe.

RESULTS

In the 'peri-ictal' group, 'structural MRI positive' patients had 87.5% concordance of ASL findings with the structural MRI abnormalities (50% showed localization to ipsilateral hemisphere -partial concordance, and an additional 37.5% to ipsilateral lobe and the hemisphere -complete concordance) whereas the 'structural MRI negative' patients had 71.3% concordance between ASL and structural MRI findings (57% having complete concordance and an additional 14.3% showing partial concordance). In the 'inter-ictal' group, 'structural MRI positive' patients showed 75% concordance between ASL and structural MRI findings (50% complete concordance) and 'structural MRI negative' patients had a 78.5% concordance between ASL and structural MRI findings (71.4% complete concordance and additional 7.1% partial concordance).

CONCLUSION

Perfusion abnormalities are intricately linked with seizures in both inter-ictal and peri-ictal phase with localized hyperperfusion being the most frequent pattern in peri-ictal and hypoperfusion predominating in the inter-ictal phase.

CLINICAL RELEVANCE/APPLICATION

ASL imaging can be a promising complementary imaging tool and can be contributory to the clinical scenario irrespective of the time of imaging, including in follow-up imaging and in increasing confidence in lesion localization for possible surgical work-up.

SSK16-02 Multi-Regional Volumetric Patterns are Associated with Post-Surgical Outcomes in Patients with Medically Refractory Temporal Lobe Epilepsy

Wednesday, Nov. 29 10:40AM - 10:50AM Room: N229

Participants

Anil K. Vasireddi, BS,MD, Pittsburgh, PA (*Presenter*) Nothing to Disclose R. Mark Richardson, MD,PhD, Pittsburgh, PA (*Abstract Co-Author*) Nothing to Disclose Joseph M. Mettenburg, MD, Pittsburgh, PA (*Abstract Co-Author*) Nothing to Disclose

For information about this presentation, contact:

avasireddi@gmail.com

PURPOSE

To investigate patterns of regional pre-operative volumetric differences that may be associated with post-operative outcome using lasso regression analysis (LRA) in patients with medically refractory temporal lobe epilepsy (TLE) who underwent anterior temporal lobectomy (ATL).

METHOD AND MATERIALS

69 subjects with TLE treated with ATL are classified as either seizure-free (ILAE 1-2) or as having continued seizures (ILAE 3-6) postoperatively. Preoperative T1-weighted MRI were analyzed for volumetric measurements. LRA was performed to identify groups of regions associated with postoperative outcomes and results were cross-validated to quantify the selected model's ability to predict outcome classification. A sub-group of patients with pathology proven mesial temporal sclerosis (MTS) was analyzed in a similar manner (n=26).

RESULTS

LRA identified smaller volumes in the contralateral occipital lobe as being associated with the seizure-free group (p = 0.0179); cross-validation revealed sensitivity of 0.27 and specificity of 0.77 in correctly identifying patients with continued postoperative seizures. In the sub-group of patients with MTS, LRA selected the contralateral occipital lobe, ipsilateral hippocampus, ipsilateral caudate, contralateral cerebellum, and contralateral frontal lobe in the model associated with postoperative outcomes (p<0.001). Cross-validation yielded better results in the more focused sub-group (sensitivity = 0.7, specificity=0.81). Hippocampal volumes alone were not significantly different between the seizure-free and continued seizures groups in either analysis.

CONCLUSION

LRA identified temporal and extra-temporal regions associated with postoperative seizure outcome. The model selected by LRA was more descriptive and more robust in cross-validation when limited to subjects identified by a single pathology such as MTS indicating that the underlying pathology should be accounted for in such analyses. Involvement of extra-temporal regions may be related to extra-temporal seizure activity, chronic sequela of anti-epileptic drug usage and/or history of frequency/severity and generalization of seizures.

CLINICAL RELEVANCE/APPLICATION

Approximately 40% of patients who undergo temporal lobectomy for TLE may continue to experience seizures postoperatively. Thus, further stratification of potential surgical candidates using pre-operative data may improve outcomes.

SSK16-03 The Clinical Impact of Emergency CT Brain Scan in Seizure

Wednesday, Nov. 29 10:50AM - 11:00AM Room: N229

Participants

Bodo P. Kress, MD, Frankfurt, Germany (*Presenter*) Research Grant, Guerbet SA; Research Grant, Bayer AG Eduardo Lazo-Gonzalez, Heidelberg, Germany (*Abstract Co-Author*) Nothing to Disclose Uta Meyding, Frankfurt, Germany (*Abstract Co-Author*) Nothing to Disclose

For information about this presentation, contact:

Kress.bodo@khnw.de

PURPOSE

Does emergency CT brain in patients with seizures have an immediate clinical impact?

METHOD AND MATERIALS

In a retrospective analysis we evaluated 1785 CT brain scans performed between 2006 and 2013 in patients after seizures. The indication for this exam has been to exclude pathological lesions being focus of seizures or being caused by seizures. Study design and protocol has been approved by our local ethic comitee (S071/2017).

RESULTS

1088 male, 697 female, average age 58 years. In 173 (9,6%) patients the CT scan revealed a significant pathological finding. In 104 (5%) patients a either tumorous or metastatic lesion was found, in 62 (3,5%) hemorrhages (subdural, epidural, parenchymal or subarachnoidal) and in 14 (0,7%) signs of a subacute infarct. 1 patient revealed signs of a acute hydrocephalus. All patients with infarcts were outside the lysis time window or time window for thrombectomy. No patient with tumorous or metastatic lesion needed immediate treatment. 6 (0,3%) of 62 patient with hemorrhage were transfered for immediate treatment. All 6 patients had clinical symptoms additionally to seizures such as clinical history of acute headache, midface fracture, hypertension (>220mmHg). No patient with isolated clinical symptom of seizure needed emergency treatment.

CONCLUSION

In this study no CT scan revealed pathological findings with immediate clinical impact if patient had only clinical history of seizure. It should be discussed whether patient with additional clinical symptoms such as acute headache, severe head trauma or hypertension need CT scan in the acute setting and whether the other patients -taken to the ward for surveillance- are evaluated only by MR scan in between 24 hours.

CLINICAL RELEVANCE/APPLICATION

Retrospective design is ia limitation, however all other studies published in the literature evaluated less than 200 exams (while we evaluated 1785), therefore this is the study with by far the biggest number of cases.

SSK16-04 Abnormality of Cerebral White Matter Microstructure in Children with New-Onset, Untreated Idiopathic Generalized Epilepsy

Participants

Lihua Qiu, PhD, MD, Yibin, China (*Presenter*) Nothing to Disclose Ran Long, Luzhou, China (*Abstract Co-Author*) Nothing to Disclose Lizhou Chen, Chengdu, China (*Abstract Co-Author*) Nothing to Disclose Guangcai Tang, Luzhou, China (*Abstract Co-Author*) Nothing to Disclose Qiyong Gong, MD, PhD, Chengdu, China (*Abstract Co-Author*) Nothing to Disclose

For information about this presentation, contact:

qiulihuah@gmail.com

PURPOSE

Epilepsy, as one of the most prevalent, noncommunicable neurologic conditions and a significant cause of disability and mortality, affects approximately 70 million people worldwide. Microstructural change of idiopathic generalized epilepsies (IGE) has been widely reported in children and adult patients. However, previous studies were focused on the chronic patients with antiepileptic drugs. This study aims at using the diffusion tensor imaging (DTI) technique to investigate the microstructural abnormalities of white matter in children with new-onset, untreated IGE.

METHOD AND MATERIALS

A total of 45 IGE patients (age range: 5-18 years, males: females=26:19) and 32 healthy controls (age range: 5-18 years, males: females=21:11) were included in our present study. Voxel-based analysis was used to compare the differences of DTI metrics including fractional anisotropy (FA) and mean diffusivity (MD) between patients and controls. Pearson correlation analysis was used to investigate the relationships between altered DTI metrics and clinical parameters.

RESULTS

After multiple comparison correction using family-wise error method, only the parameter of mean diffusivity (MD) showed significant decrease in the left paracentral lobule, right precuneus and right superior parietal lobule (SPL) in IGE patients compared to healthy controls. Increased factional anisotropy (FA) was found in the deep white matter of bilateral prefrontal lobe in IGE patients at a less conservative level using AlphaSim correction. There was no correlation between the altered diffusion parameters and the clinical measures.

CONCLUSION

Our study demonstrated microstructural impairments in children with new-onset, untreated IGE and that the MD might be more sensitive to detect the microstructural changes in the early stage of IGE than FA. Furthermore, the increased FA and decreased MD in the IGE group might suggest an initiating or compensatory mechanism prior to cognitive decline in IGE patients. Longitudinal studies are needed to clarify the maturational and seizure-related nature of these alterations of brain anatomy, their potential progression over the course of illness in IGE patients, and the potential impact of therapeutic intervention on these processes.

CLINICAL RELEVANCE/APPLICATION

Microstructural abnormalities exist from the very beginning of IGE and MD may be more affected than FA in the initial stage of children with IGE.

SSK16-05 Utility of MRI Brain Epilepsy Protocol in New Onset Seizures: How is it Different in Developing Countries?

Wednesday, Nov. 29 11:10AM - 11:20AM Room: N229

Participants

Janardhana Ponnatapura Satyanarayana, MBBS, MD, Bangalore, India (*Presenter*) Nothing to Disclose Avisha Singla, Bangalore, India (*Abstract Co-Author*) Nothing to Disclose

For information about this presentation, contact:

PSJANARDHAN@YAHOO.COM

PURPOSE

1. To evaluate the diagnostic efficacy of a standard MRI of the brain in patients with first onset seizures. 2. To identify whether there is an increase in the diagnostic yield with the addition of high-resolution sequences with a dedicated seizure protocol. 3. To compare the diagnostic yields of MRI and EEG individually and in combination.

METHOD AND MATERIALS

Patients presenting with a history of first onset seizures who underwent MRI of the brain and EEG. Totally 129 cases were studied for a period of 18 months. Chi square test of significance (p<0.005) was used to test for the difference in proportion. The correlation between MRI brain and EEG was studied using McNemer test. All the patients underwent both standard protocol and dedicated epilepsy protocol MRI brain scanning on 1.5T within seven days from the onset of seizures. A routine electroencephalogram is recorded from the scalp electrodes obtained three days before or after the MRI and as soon as practical after presentation with the index seizure, preferably within 48 hours.

RESULTS

The diagnostic yield of MRI in detecting epileptogenic lesion was 47% in our study. Among the potentially epileptogenic lesion, infection and inflammation was most common 17 (28%). Of the 59 patients with potential epileptogenic lesions in our study, 37 (63%) epileptogenic lesions were detected using "standard protocol" MRI and remaining 22 (37%) lesions were detected using "dedicated epilepsy protocol" MRI. Of the epileptogenic lesions, all 11 patients (100%) with hippocampal sclerosis were detected by using "epilepsy protocol" MRI which would have been missed if only "standard protocol" MRI was done. Patients who presented with focal-onset seizures (27) had a higher proportion of potentially epileptogenic lesions 22 (81%) compared with the patients with generalized clonic tonic seizures. There were 22 patients (18%) with an abnormality on both MRI and EEG. So, abnormal MRI and

EEG were concordant in18% of patients in our study.

CONCLUSION

A dedicated epilepsy protocol MRI should be done in all patients who presents with first-onset seizures. MRI in first-onset seizure patients allows the identification of a lesion and earlier consideration of epilepsy surgery especially in patients presenting with focal-onset seizures.

CLINICAL RELEVANCE/APPLICATION

A dedicated epilepsy protocol MRI should be done in all patients who presents with first-onset seizures.

SSK16-06 PET-MRI Value in Detecting 'Occult' Anterior-Inferior Temporal Lobe Encephaloceles in Medically Refractory Focal Temporal Lobe Epilepsy

Wednesday, Nov. 29 11:20AM - 11:30AM Room: N229

Participants

Karl N. Krecke, MD, Rochester, MN (*Presenter*) Nothing to Disclose Robert J. Witte, MD, Rochester, MN (*Abstract Co-Author*) Nothing to Disclose Robert E. Watson JR, MD, PhD, Rochester, MN (*Abstract Co-Author*) Nothing to Disclose

PURPOSE

Temporal lobe anterior-inferior encephaloceles are increasingly recognized as a surgically amenable cause of adult medicallyrefractory temporal lobe epilepsy. The anatomic defect on MRI exam can be quite subtle and these lesions are frequently overlooked for multiple years and exams. Two such cases led to a review of our PET-MRI experience in imaging-occult medically refractory focal epilepsy.

METHOD AND MATERIALS

PET-MRI has been part of our epilepsy imaging armament since December 2015. A PET-MRI database was created that included patients with refractory focal epilepsy that were considered non-lesional, based on prior MRI exams. The PET-MRI exams were reviewed without knowledge of the specific clinical history or signs and symptoms with a goal of identifying additional cases of anterior inferior temporal lobe encephalocele. Separately, we collected demographic and clinical data from the medical record including age of seizure onset, semiology, EEG and interpretation of prior imaging exams.

RESULTS

Sixty-eight patients were catalogued in our epilepsy PET-MRI database including examinations through March 31, 2017. Four patients were identified with anterior-inferior temporal lobe encepahlocele. Two patients had been identified through clinical evaluation for epilepsy surgery and two additional patients were identified though this retrospective review. The key PET-MRI findings were 1. Decreased FDG uptake in anterior temporal lobe, ipsilateral to the clinical region of concern, 2. FDG activity extending beyond the expected confines of the middle cranial fossa and sphenoid wing, 3. MRI findings of CSF or brain extending into a defect in sphenoid wing, unrecognized on prior exams. Demographic items include: 3 female patients (75%), age: mn= 28 (15-43 range), age from seizure onset mn=9 years (3-18 range). The three female patients demonstrated MRI findings of incranial hypertension or dural ectasia.

CONCLUSION

PET-MRI can be useful as a next-step in evaluation of medically refractory focal temporal lobe epilepsy, particularly in the surgical candidate. Anterior-inferior temporal lobe encephalocele, as a cause of refractory epilepsy, is unusual but a combination of co-localizable findings can identify patients who may benefit from a focal resection.

CLINICAL RELEVANCE/APPLICATION

Temporal lobe encephalocele is emerging as an important, surgically amenable cause of epilepsy. PET-MRI can help with detection.

SSK16-07 Hippocampal Sclerosis with Negative MR Findings: Diagnostic Usefulness of Subfield Volumetric Analysis

Wednesday, Nov. 29 11:30AM - 11:40AM Room: N229

Participants

Hiromi Masaki, MD, Kitakyushu, Japan (*Presenter*) Nothing to Disclose Shingo Kakeda, MD, Kitakyushu, Japan (*Abstract Co-Author*) Nothing to Disclose Koichiro Sugimoto, MD, Kitakyushu, Japan (*Abstract Co-Author*) Nothing to Disclose Issei Ueda, Kitakyusyu, Japan (*Abstract Co-Author*) Nothing to Disclose Keita Watanabe, Fukuoka, Japan (*Abstract Co-Author*) Nothing to Disclose Yukunori Korogi, MD, PhD, Kitakyushu, Japan (*Abstract Co-Author*) Nothing to Disclose

PURPOSE

In previous studies, up to 15% of the patients with diagnosis of hippocampal sclerosis (HS) showed normal findings on conventional MRI (neg-MR). Recently, subfield volumetry of hippocampus (SVH) using the open-source automatic segmentation software has been utilized. Our aims were; (a) to study the volume changes of the hippocampal subfields in HS patients using SVH, and (b) to determine the diagnostic accuracy of the SVH for the HS patients with neg-MR.

METHOD AND MATERIALS

We assessed 46 unilateral HS patients and 54 controls; all HS cases had histopathologic confirmation by surgery. Two neuroradiologists divided the HS patients into two groups based on the presence (pos-MR, n=26) or absence (neg-MR, n=20) of following MR findings at the affected hippocampus; reduced volume or increased T2 signal. For SVH analysis, 3D-volume T1-weighted images were processed with FreeSurfer (ver.5.3, ver.6.0) in all patients and controls. The ratio to total intracranial volume were calculated for each subfield and compared among the two groups. The diagnostic accuracy (AUC) were calculated using cutoff values for the hippocampal subfield volumes that were obtained in a ROC analysis.

RESULTS

In the pos-MR group, 8 of 9 subfields at the affected side (CA1, CA3, CA4-DG, fimbria, hippocampal-amygdala transitional area, presubiculum, hippocampal tail, and subiculum) were significantly smaller than in the controls. In the neg-MR group, however, only 2 of 9 subfields (CA3 and CA4-DG) were significantly smaller than in the controls. The diagnostic accuracy of the discrimination of the HS patients with neg-MR was better for the SVH based on the volumes of CA3 and CA4-DG (AUC: 0.719) than for the volume of the whole hippocampus (AUC: 0.614).

CONCLUSION

In the MR-negative HS patients, the subfield volumetry detected the localized atrophy within CA3 and CA4-DG, and showed better diagnostic performance than the whole hippocampal volume.

CLINICAL RELEVANCE/APPLICATION

In the mesial temporal epilepsy patients with normal findings on conventional MRI, SVH may be used not only for the diagnosis of HS but also for the assessment of its histopathologic subtypes.

SSK16-08 Longitudinal Functional Connectivity of Language Networks in Surgical Epilepsy Patients: Preliminary Results

Wednesday, Nov. 29 11:40AM - 11:50AM Room: N229

Participants

Olivia Fosleitner, Vienna, Austria (*Presenter*) Nothing to Disclose Karl-Heinz Nenning, PhD, Vienna, Austria (*Abstract Co-Author*) Nothing to Disclose Silvia Bonelli, Vienna, Austria (*Abstract Co-Author*) Nothing to Disclose Christoph Baumgartner, MD, Vienna, Austria (*Abstract Co-Author*) Nothing to Disclose Susanne Pirker, Vienna, Austria (*Abstract Co-Author*) Nothing to Disclose Ekaterina Pataraia, Vienna, Austria (*Abstract Co-Author*) Nothing to Disclose Thomas Czech, Vienna, Austria (*Abstract Co-Author*) Nothing to Disclose Christian Dorfer, MD, Vienna, Austria (*Abstract Co-Author*) Nothing to Disclose Georg Langs, Vienna, Austria (*Abstract Co-Author*) Nothing to Disclose Georg Langs, Vienna, Austria (*Abstract Co-Author*) Nothing to Disclose Gregor Kasprian, MD, Vienna, Austria (*Abstract Co-Author*) Nothing to Disclose

For information about this presentation, contact:

olivia.foesleitner@muv.ac.at

PURPOSE

Investigating the reorganization of language networks in temporal lobe epilepsy (TLE) patients with task-based functional MRI (fMRI) before and after selective amygdalohippocampectomy or anterior temporal lobectomy (ATLR).

METHOD AND MATERIALS

Eighteen TLE patients (8 left TLE, 10 right TLE) performed task-based fMRI using a verb generation and a semantic paradigm before and after neurosurgery (9 ATLR; mean age at surgery: 38y, range: 26-53y). Mean time between surgery and postoperative scan was 14.9 months (range: 3-44m). Neuropathology revealed hippocampal sclerosis in 13 patients, focal cortical dysplasia in 4 patients and ganglioglioma in one patient. Ten healthy right-handed subjects underwent the same fMRI protocol on the same 3T scanner (mean age: 38y, range: 31-49y). FMRI activation maps and functional connectivity (FC) were analyzed on SPM12 for intraand intergroup comparisons (p<0.005 uncorr.).

RESULTS

Compared to controls, patients showed decreased FC ipsilateral to their epileptogenic focus before and after surgery. In comparison to scans before surgery, postoperative left TLE patients had markedly decreased FC involving the left TL with particularly less connections to the right frontal lobe, stronger connections were visible including the residual left posterior TL and the right TL. In postsurgical right TLE, inter- and intrahemispheric FC to the right TL was decreased with only few stronger postsurgical connections exclusively found in the left hemisphere.

CONCLUSION

Task-based fMRI functional connectivity analysis visualizes extensive language related reorganization processes in TLE patients following surgery. Patterns of reorganization in language FC differ between left- and right-sided TLE with more extensive changes in left TLE patients.

CLINICAL RELEVANCE/APPLICATION

Temporal lobe epilepsy (TLE) surgery triggers widespread changes of language-related functional connectivity (FC). FC analysis allows us to link specific clinical deficits with certain neuroanatomical and imaging substrates. This will help to optimize surgical approaches and minimize postoperative language deficits in individual TLE patients.

SSK16-09 DTI-Derived Textural Features Can Improve Detectability of Epileptogenic Tubers in Tuberous Sclerosis Complex

Wednesday, Nov. 29 11:50AM - 12:00PM Room: N229

Participants

Hajime Yokota, MD, Los Angeles, CA (*Presenter*) Nothing to Disclose Yoko Hirata, Los Angeles, CA (*Abstract Co-Author*) Nothing to Disclose Emiko Morimoto, MD, PhD, Los Angeles, CA (*Abstract Co-Author*) Nothing to Disclose Iren Orosz, MD,PhD, Los Angeles, CA (*Abstract Co-Author*) Nothing to Disclose Noriko Salamon, MD, Los Angeles, CA (*Abstract Co-Author*) Nothing to Disclose

PURPOSE

Diffusion tensor imaging (DTI)-derived quantitative values such as maximum apparent diffusion coefficient (ADC) were reported as predictors of epileptogenic tubers in tuberous sclerosis complex (TSC). Texture of tubers, volume and location were also known predictors of epileptogenicity. The purpose of this study was to document detectability of texture analysis for DTI, which can combine the information of DTI and textural heterogeneity.

METHOD AND MATERIALS

Twenty-five consecutive studies involving 23 patients were involved in this study. Epileptogenic tubers were characterized using video-encephalographyEEG, structural MRI, FDG-PET, magnetoencephalography, magnetic source imaging (MSI) and intraoperative electro-corticography. A total of 558 tubers, 32 epileptogenic and 526 nonepileptogenic, were identified. The volume of interest (VOI) of tubers was drawn on an ADC map based using T2-weighted and FLAIR images. The original VOI was inflated to include 4-mm-thick ring-shaped tissues surrounding the tuber. Histogram- and 3-dimentional 13-direction gray-level co-occurrence matrix (GLCM)-based textural features were extracted from the VOIs using ADC, fractional anisotropy, axial diffusivity and radial diffusivity maps. Mann-Whitney U-test with false discovery rate control was used to compare the features. The diagnostic model was constructed with an elastic net model to avoid overfitting. The model was compared with known predictors using receiver operating characteristic analysis and DeLong test.

RESULTS

A total of 122 features was derived from each VOI. There were no significant difference in features derived from the original VOI between epileptogenic vs non epileptogenic tubers. By contrast, 32 of 122 features showed significant differences on the inflated VOI. The diagnostic model was significantly better than the ROC curves of maximum ADC, volume and location (area under curve = 0.75 vs. 0.67 and 0.55; P = 0.042 and 0.001). The model did not significantly surpass tuber volume (0.75 vs. 0.71, P = 0.119).

CONCLUSION

Texture analysis using inflated VOI showed improved diagnostic performance to differentiate between epileptogenic and nonepileptogenic tubers. The VOI within the tuber was not useful for DTI-based texture analysis.

CLINICAL RELEVANCE/APPLICATION

DTI-derived texture analysis with VOI including perituber tissue can improve detectability of epileptogenic tubers in tuberous sclerosis complex.





103rd Scientific Assembly and Annual Meeting November 26 to December 1 McCormick Place, Chicago



SSK17

Physics (MR: New Techniques, System Evaluation)

Wednesday, Nov. 29 10:30AM - 12:00PM Room: S404AB



AMA PRA Category 1 Credits ™: 1.50 ARRT Category A+ Credit: 1.75

Participants

R. Jason Stafford, PhD, Houston, TX (*Moderator*) Nothing to Disclose Seth A. Smith, PhD, Nashville, TN (*Moderator*) Nothing to Disclose

Sub-Events

SSK17-01 Blipped Radial CAIPIRINHA for Simultaneous Multislice pseudo-SSFP Magnetic Resonance Fingerprinting

Participants

Nikolai Mickevicius, Milwaukee, WI (*Presenter*) Nothing to Disclose Eric Paulson, PHD, Milwaukee, WI (*Abstract Co-Author*) Nothing to Disclose

For information about this presentation, contact:

nmickevicius@mcw.edu

PURPOSE

The purpose of the present work is to accelerate pseudo steady-state free-precession magnetic resonance fingerprinting (pSSFP-MRF) T1 and T2 mapping sequences with simultaneous multislice (SMS) imaging methods.

METHOD AND MATERIALS

Controlled aliasing (CAIPI) techniques are useful for improving the image quality from SMS acquisitions. For multi-shot non-Cartesian k-space trajectories, as is the case for most MRF acquisitions, CAIPI takes the form of modulating the phase of one or more SMS slices relative to the others from readout-to-readout. This is usually accomplished by means of RF phase cycling. An underlying assumption of the pSSFP-MRF method, however, is that all slices experience a sign change of RF phase in consecutive excitations, thus prohibiting the use of RF phase cycled CAIPI. Gradient blips along the slice-selection axis allow similar CAIPI phase modulation without the use of RF phase patterns. This work employs a blipped-CAIPI acquisition with a radial trajectory for pSSFP-MRF. The SMS pSSFP-MRF sequence was implemented on a Siemens 3T scanner. The gradient blips were applied to induce a phase difference of pi/2 between two simultaneously excited slices. The sign of the gradient blip changed in each subsequent spoke which rotates with the golden angle of ~111.246 degrees. A total of 881 spokes were acquired in approximately 5 seconds. To reconstruct images of each slice, the conjugate of the blip-induced phase of the slice-of-interest was added to each spoke. A dictionary was simulated, and T1 and T2 maps were reconstructed using the low rank (R=5) alternating direction method of multipliers (ADMM) technique. The brain of a glioblastoma patient who consented to be a part of an institutional review board approved study was scanned.

RESULTS

The T1 and T2 maps of two simultaneously excited slices are shown in the figure. Total acquisition time was 5 seconds. No slice-leakage is apparent. The relaxation times outside of the tumor agree with literature values for healthy brain tissue. Lengthened T1 and T2 values can be seen within the lesion.

CONCLUSION

A blipped radial CAIPI pSSFP-MRF sequence permits rapid T1 and T2 mapping for use in disease diagnosis, treatment planning, and response assessment.

CLINICAL RELEVANCE/APPLICATION

This work aims to further push the acceleration of pSSFP magnetic resonance fingerprinting scans to aid in the clinical adoption of fully quantitative imaging protocols.

SSK17-02 First Clinical Assessment of kT-Points Dynamic RF Shimming on Abdominal DCE-MRI in a Commercial 3T MRI Scanner

Wednesday, Nov. 29 10:40AM - 10:50AM Room: S404AB

Participants

Raphael Tomi-Tricot, MSc, Gif-Sur-Yvette, France (*Presenter*) Nothing to Disclose Vincent Gras, Gif-sur-Yvette Cedex, France (*Abstract Co-Author*) Nothing to Disclose Franck Mauconduit, Saint-Denis, France (*Abstract Co-Author*) Employee, Siemens AG Francois Legou, MD, Creteil, France (*Abstract Co-Author*) Nothing to Disclose Nicolas Boulant, Gif-sur-Yvette Cedex, France (*Abstract Co-Author*) Nothing to Disclose Matthias Gebhardt, Erlangen, Germany (*Abstract Co-Author*) Employee, Siemens AG Dieter Ritter, Erlangen, Germany (*Abstract Co-Author*) Employee, Siemens AG Berthold Kiefer, PhD, Erlangen, Germany (*Abstract Co-Author*) Employee, Siemens AG Pierre Zerbib, Creteil, France (*Abstract Co-Author*) Nothing to Disclose Alain Rahmouni, MD, Nogent Sur Marne, France (*Abstract Co-Author*) Nothing to Disclose Alexandre Vignaud, PhD, Gif Sur Yvette, France (*Abstract Co-Author*) Consultant, Siemens AG Alain Luciani, MD,PhD, Creteil, France (*Abstract Co-Author*) Research Consultant, Bracco Group; Research Grant, Bracco Group; Research Consultant, General Electric Company; Research Consultant, Siemens AG Alexis Amadon, Gif-sur-Yvette Cedex, France (*Abstract Co-Author*) Nothing to Disclose

For information about this presentation, contact:

raphael.tomi-tricot@cea.fr

PURPOSE

The 'B1 artefact' is an important challenge for abdominal MRI at 3T. Our aim was to assess excitation homogeneity and image quality achieved in the liver by kT-points pulses, compared to patient-tailored static RF-shimming.

METHOD AND MATERIALS

The prototypical non-selective kT-points pulse design was compared with patient-tailored static RF shimming for 3D breath-hold liver DCE-MRI on a product dual-transmit MAGNETOM Skyra MRI (Siemens Healthcare). 50 consecutive patients referred for liver MRI at a single institute were included in this IRB-approved study. Quantitative analysis was carried out via simulation to estimate flip angle homogeneity. Signal homogeneity, T1 contrast, enhancement quality, structure details and global degree of trust provided by each technique were qualitatively assessed on a 4-level scale (0 to 3) by 2 radiologists on in vivo pre-injection and late-phase images from 20 acquisitions selected from the pool. An exact matched-pairs one-tailed Wilcoxon signed-rank test was used to compare the methods.

RESULTS

Average excitation inhomogeneity was significantly reduced with kT-points compared to static RF-shimming (mean flip angle error \pm standard deviation: 8.5 \pm 1.5% vs 20.4 \pm 9.8% respectively; p<0.0001). The worst case (heavy ascites) was 13.0% (kT-points) vs 54.9% (RF-shim). KT-points qualitative grades were higher for all criteria. Global image quality was significantly higher for kT-points than for RF-shimming (mean grade \pm standard deviation: 2.3 \pm 0.5 vs 1.9 \pm 0.6; p=0.008). One subject's examination was judged unusable (0/3 for all criteria) with RF-shim by one reader and none with kT-points. 85% of kT-points acquisitions were graded at least 2/3, compared to only 55% in the static RF-shim case.

CONCLUSION

KT-points significantly reduce excitation inhomogeneity both quantitatively and qualitatively, especially in patients with ascites and prone to 'B1 artefact'.

CLINICAL RELEVANCE/APPLICATION

Proper excitation homogeneity is crucial to take advantage of the high signal-to-noise ratio available at 3T. KT-points improve 3T MRI for abdominal imaging of all patients.

SSK17-03 Multi-Compartmental Analysis Using a Fast Multi-Echo TSE Sequence for Prostate Cancer Diagnosis

Wednesday, Nov. 29 10:50AM - 11:00AM Room: S404AB

Participants

Shiyang Wang, PhD, Chicago, IL (*Presenter*) Nothing to Disclose Ajit Devaraj, PhD, Chicago, IL (*Abstract Co-Author*) Nothing to Disclose Roger Bourne, PhD, Sydney, Australia (*Abstract Co-Author*) Nothing to Disclose Aritrick Chatterjee, PhD, Chicago, IL (*Abstract Co-Author*) Nothing to Disclose Tatjana Antic, Chicago, IL (*Abstract Co-Author*) Nothing to Disclose Aytekin Oto, MD, Chicago, IL (*Abstract Co-Author*) Research Grant, Koninklijke Philips NV; Research Grant, Guerbet SA; Research Grant, Profound Medical Inc; Medical Advisory Board, Profound Medical Inc; Speaker, Bracco Group; ; Gregory S. Karczmar, PhD, Chicago, IL (*Abstract Co-Author*) Nothing to Disclose Harsh K. Agarwal, PhD, Briarcliff, NY (*Abstract Co-Author*) Employee, Koninklijke Philips NV Ambereen Yousuf, MBBS, Chicago, IL (*Abstract Co-Author*) Nothing to Disclose

For information about this presentation, contact:

shiyang@uchicago.edu

PURPOSE

Prostate tissue has three major histological components: stroma, glandular lumen and epithelial cells. These volume fractions change when cancer is present. This study evaluates the feasibility of measuring the volume fractions of these compartments quantitatively in normal prostate and prostate cancer (PCa) using multi-compartment T2 decay modeling. A fast multi-echo TSE T2 MRI (k-t-T2) was applied to obtain high resolution T2 maps in clinically feasible scan time. Signal contributions from the three compartments were compared with pathological slices as a gold standard.

METHOD AND MATERIALS

k-t-T2 data were acquired on 17 patients on Philips 3T Achieva scanner; this method uses k-space under sampling for image acquisition to accelerate the scan. TR=3.1-10s; 32 echoes; $\Delta TE=12ms$ (TE=24-396ms); 1.0x1.0x3 mm3 in-plane resolution, scan time=4.5-9.6min. Regions of-interest (ROIs) including PCa (n=28) and normal prostate (n=43) were identified through histologic and MRI consensus review. Voxel-based three compartment analysis was used to extract the epithelial, lumen and stromal volume fractions, and T2 value of each compartment, in each ROI. Kruskall-Wallis test and Welch two sample t-test were used to evaluated the statistical significance between ROI groups. Spearman correlation coefficient was calculated between the image features and ROI-specific Gleason scores (GS).

RESULTS

ROI based analysis results showed the volume fraction of epithelium (50±12% vs. 37±10%) and lumen (11±6% vs. 21±7%) are

significantly different between PCa and normal prostate (p<0.01). There is no significant difference in stromal volume fraction (39±9% vs. 41±8%) between PCa and normal prostate (p>0.5). The volume fractions measured by MRI are close to those reported in previous histological studies. The volume fractions of epithelial cells and lumen are strongly correlated with GS (p =0.53; -0.41, p<0.05). Epithelial volume fraction in PCa correlates better with GS compared to T2 values (p=-0.41, p=0.02).

CONCLUSION

Multi-echo k-t-T2 sequence is feasible in clinical setting. Volume fractions obtained from three compartment model fitting of spin echo signal decay sampled at multiple TE's may help to characterize prostate lesions and may be sensitive to Gleason grade.

CLINICAL RELEVANCE/APPLICATION

New features extracted from multi-echo TSE images are more sensitive to prostate cancer and Gleason score than T2 values alone which may improve prostate cancer diagnosis.

Honored Educators

Presenters or authors on this event have been recognized as RSNA Honored Educators for participating in multiple qualifying educational activities. Honored Educators are invested in furthering the profession of radiology by delivering high-quality educational content in their field of study. Learn how you can become an honored educator by visiting the website at: https://www.rsna.org/Honored-Educator-Award/ Aytekin Oto, MD - 2013 Honored EducatorAytekin Oto, MD - 2017 Honored Educator

SSK17-04 Comparison between Readout Segmented Diffusion Weighted Imaging and Single Shot Echo Planar Imaging in Image Quality

Wednesday, Nov. 29 11:00AM - 11:10AM Room: S404AB

Participants

Chuangbo Yang, MMed, Xianyang City, China (*Abstract Co-Author*) Nothing to Disclose Hui Zhong, Xianyang, China (*Presenter*) Nothing to Disclose Nan Yu, MD, Xian Yang, China (*Abstract Co-Author*) Nothing to Disclose Guangming Ma, Xianyang, China (*Abstract Co-Author*) Nothing to Disclose Haifeng Duan, Xianyang City, China (*Abstract Co-Author*) Nothing to Disclose Yongjun Jia, MMed, Xianyang City, China (*Abstract Co-Author*) Nothing to Disclose Qi Yang, Xianyang, China (*Abstract Co-Author*) Nothing to Disclose Chenglong Ren, Shanxi, China (*Abstract Co-Author*) Nothing to Disclose He Taiping, MMed, Xian Yang City, China (*Abstract Co-Author*) Nothing to Disclose Yuhuan Chen, MD, Xianyang, China (*Abstract Co-Author*) Nothing to Disclose

For information about this presentation, contact:

937874041@qq.com

PURPOSE

To compare difference of readout segmented diffusion weighted imaging (RS-EPI) and single shot echo planar imaging (SS-EPI) on image quality with ultra-high b value for prostate cancer detection.

METHOD AND MATERIALS

37 patients with prostate disease who underwent both RS-EPI and SS-EPI were enrolled in this study. All data were collected on a MAGNETOM Skyra 3T MR scanner (Siemens AG, Erlangen, Germany) with the b value of 0,1000,2000,3000s/mm2. The image quality including lesions clarity, anatomical distortion, image sharpness, detail display based on diffusion weighted imaging (DWI) were classified according to Likert score into 1 to 5 grade.(Grade 1 : cannot be used for diagnosis; Grade 2: poor; Grade 3: acceptable; Grade 4: good; Grade 5: very good.) All the images were analyzed by two experienced radiologists blinded to any clinical information as well as MR sequence information. The classification was provided from two radiologists separately. The signal-to-noise ratio (SNR), and contrast ratio, and contrast to noise ratio (CNR) were also measured on workstations by the radiologist.

RESULTS

The scores concluded by the two radiologists have good consistency, Kappa value>0.80. The image quality including lesions clarity, anatomical distortion, image sharpness, detail display obtained from RS-EPI sequences were higher than those obtained from SS-EPI regardless of 1000,2000,3000s/mm2 (P<0.001). The signal-to-noise ratio (SNR), and contrast ratio, and contrast to noise ratio (CNR) measured on RS-EPI sequences were also higher than those measured on SS-EPI (P<0.001) (table1).

CONCLUSION

Compared with the SS-EPI sequence, ultra high b value RS-EPI sequence significantly improves the image quality, which is more conducive to the detection of prostate lesions.

CLINICAL RELEVANCE/APPLICATION

Compared with the SS-EPI sequence, ultra high b value RS-EPI sequence significantly improves the image quality, which is more conducive to the detection of prostate lesions.

SSK17-05 Magnetic Resonance Water-Fat Separation using Deep Machine Learning

Wednesday, Nov. 29 11:10AM - 11:20AM Room: S404AB

Participants

James W. Goldfarb, PhD, Roslyn, NY (Presenter) Nothing to Disclose

PURPOSE

The goal of this study was to develop, train and evaluate a convolutional neural network for decomposition of cardiovascular MR images into separate water and fat images with additional calculation of $R2^*$ and off-resonance.

METHOD AND MATERIALS

1204 cardiac images in multiple anatomical orientations from 90 imaging sessions acquired at 1.5T using a dark blood double inversion recovery multiple spoiled gradient-echo sequence (TR=20ms; 12 TEs=2.4-15.5ms (1.2ms spacing), bipolar gradient acquisition) were included in this study. This included 15 acute myocardial infarction (MI), 24 sub-acute MI, 34 chronic MI subjects and 17 normal subjects. Water-fat separation was initially performed with a conventional model based technique providing water, fat, R2* and off-resonance images for deep learning training. A U-Net convolutional neural network (CNN) was used for deep learning. The input to the CNN was 24 real and imaginary images from 12 TEs. The output of the CNN was four images (water, fat, R2* and off-resonance). The implementation was done using open source software written in Python v2.7 with the TensorFlow v1.1 and Keras v2.0 machine learning libraries. Training on 900 (x12 echo-times) complex images with 50 epochs was performed using the Adam optimizer with Nestrov momentum. Water and fat images from the data not used for training (n=304) were predicted using the trained CNN. Water-fat fraction images were constructed for both the conventional and deep learning approaches.

RESULTS

Water-fat separation performed well across all image slice orientations. Signal-to-noise was better in the deep learning images when compared to conventional images, p<0.001. Fine details were preserved in the deep learning images when compared to conventional images. There was an excellent correlation (R2=0.97, p<0.001) between the conventional and deep learning fat fraction measurements. Multiple pathologies were visualized with deep learning, including fatty metaplasia (Fig 1a) and intramyocardial hemorrhage (IMH) Fig 1b.

CONCLUSION

Deep learning is a robust, efficient, feasible method for water-fat separation. After the learning phase, utilization is computationally efficient and can make use of echoes with bipolar gradients.

CLINICAL RELEVANCE/APPLICATION

Deep machine learning can provide fat suppressed images and quantitative fat fraction maps with $R2^*$ and off-resonance corrections in challenging situations such as cardiovascular imaging.

SSK17-06 Analysis of Different Image Registration Algorithms for Fourier Decomposition MRI in Functional Lung Imaging

Wednesday, Nov. 29 11:20AM - 11:30AM Room: S404AB

Participants

Alexandra Ljimani, MD, Duesseldorf, Germany (*Abstract Co-Author*) Nothing to Disclose Rotem S. Lanzman, MD, Duesseldorf, Germany (*Abstract Co-Author*) Nothing to Disclose Gerald Antoch, MD, Duesseldorf, Germany (*Abstract Co-Author*) Nothing to Disclose Hans-Jorg Wittsack, Duesseldorf, Germany (*Abstract Co-Author*) Nothing to Disclose Julian Kirchner, Dusseldorf, Germany (*Presenter*) Nothing to Disclose

PURPOSE

To evaluate different image registration algorithms for Fourier decomposition MRI (FD-MRI) in functional lung imaging in healthy subjects.

METHOD AND MATERIALS

Fifteen healthy volunteers (mean age 33.0 ± 10.1 years) were examined on a 1.5 T whole-body MR-scanner (Magnetom Avanto, Siemens AG) with a non-contrast enhanced 2D-TrueFISP pulse sequence in coronal view (TR/TE 2.06/0.89 ms, acquisition time 180 ms/image, 250 images). No ECG or respiratory triggering was used. Three different image registration algorithms (fMRLung 3.0, Siemens Corporate Research; diffeomorphism based ANTs by Avants et al. NeuroImage 2011; Elastix by Staring et al. Medical Physics 2007) were used to compensate the spatial variation of the lung structure. Quality control for the image registration was performed by quotient images (Δ Q) and dice similarity coefficient (Δ D). The impact of the used registration algorithms on the calculated perfusion and ventilation values by Fourier decomposition method was evaluated.

RESULTS

The average time for motion correction by the different image registration algorithms were for fMRILung 1.0±1.6 min, ANTs 38±13.5 min and Elastix 5.9±1.3 h, respectively. No significant (p>0.05) difference in the quality of the motion correction provided by different image registration algorithms (Δ Q fMRILung 0.12, ANTs 0.11, Elastix 0.11; Δ D fMRILung 0.06, ANTs 0.07, Elastix 0.06) occurred. Further no significant difference of the calculated ventilation and perfusion values between the different registration algorithms (p>0.05) were determined. The calculated ventilation values were 119±12 for fMRILung, 110±14 for ANTs and 118±12 ml/min/100 ml for Elastix, respectively. The perfusion values for fMRILung, ANTs and Elastix were 156±41, 166±46 and 185±66 ml/min/100 ml, respectively.

CONCLUSION

The mandatory motion correction for the calculation of perfusion and ventilation images by FD-MRI is possible with different image registration algorithms without significant influence on the quality of the motion correction or changes of the calculated functional lung values. fMRILung 3.0 (Siemens Corporate Research) provides the fastest way of motion correction.

CLINICAL RELEVANCE/APPLICATION

Motion correction for FD-MRI is possible with different image registration algorithms without loss of accuracy of perfusion and ventilation results.

SSK17-07 MRI Quantitative Quality Control and Calibrated Measurement with DTI and Reference Fluid Phantom Novel Phantom for Quantitate Assessment of DTI Inters Canner Variability

Wednesday, Nov. 29 11:30AM - 11:40AM Room: S404AB

Participants

Walter Schneider, PhD, Pittsburgh, PA (Abstract Co-Author) Consultant, Psychology Software Tools, Inc

James M. Provenzale, MD, Durham, NC (*Abstract Co-Author*) Consultant, ArmaGen; Research Grant, Bayer AG; Consultant, Bayer AG; Consultant, Biomedical Systems; Consultant, Laboratory Corporation of America Holdings; Consultant, CurAccel, LLC; Research Grant, General Electric Company; Consultant, sanofi-aventis Group; Consultant, Guerbet SA; Consultant, Takeda Pharmaceutical Company Limited; Consultant, F. Hoffmann-La Roche Ltd

Michael Boss, PhD, Boulder, CO (*Presenter*) Nothing to Disclose Elisabeth Wilde, PhD, Houston, TX (*Abstract Co-Author*) Nothing to Disclose Brian A. Taylor, PhD, Houston, TX (*Abstract Co-Author*) Nothing to Disclose

For information about this presentation, contact:

wws@pitt.edu

CONCLUSION

Current DTI scanning has substantial systematic error, distorting measurement and impairing clinical diagnostic stability. Phantom calibration can quantify such errors and may provide a means for a correction factor to reduce variability across scanners.

Background

We used a novel DTI and isotropic fluid phantom funded by the Chronic Effects of Neurotrauma Consortium, VA, DoD & NIH QIBA programs to provide "ground truth" reference measurement and quality assurance metrics.

Evaluation

The phantom contains anisotropic diffusion components of hollow textiles termed Taxons (axon-shaped tubes, 12-µm inner diameter diffusion chambers) arranged in water-filled bundles of > 100,000. To quantify loss of tract integrity and size, we created tracts with densities of 12.5%- 100% and tract cross-sections of 4-100 mm2. The phantom includes 32 NIST reference fluids (T1, T2, PD, ADC) for isotropic reference metric correction. We imaged on 11 scanners (1.5T and 3T, Siemens, GE & Phillips) with head coils 12-64 channels. Scans detected tracts with high spatial detail at all sizes (average correlation of FA to tract density r=0.992). We found tight repeat measurements, with small changes between scans on the same magnet within a few weeks. However, substantial (35%) inter-scanner systematic error/biases in measurements of FA were seen, greatly exceeding presumed effect size of TBI-induced FA change and 2.85 times the variance within scanner. We applied a reference measurement correction by estimating scanner-specific systematic error on one scan and applying that correction to a second scan weeks later to calculate calibrated FA relative to the mean cross-scanner FA to reference density metrics. The correction reduced the across-scanner spread error by 94%.

Discussion

The phantom provides a reliable and reproducible method to determine degree to which DTI scans on a MR scanner differ from a reference standard that simulates the microstructure of brain white matter. The phantom also allows a means to determine the degree to which DTI scans from multiple scanners differ from one another and, potentially, a method to correct for inter-scanner differences.

SSK17-08 A Quality Improvement (QI) Initiative to Evaluate MR QA Training Strategies for MR Technologists to Enable Them to Undertake Quality Assurance (QA) Testing in MRI

Wednesday, Nov. 29 11:40AM - 11:50AM Room: S404AB

Participants

Walaa M. Alsharif, MSc, dublin, Ireland (*Presenter*) Nothing to Disclose Michaela Davis, Dublin, Ireland (*Abstract Co-Author*) Nothing to Disclose Patrick Kenny, Dublin, Ireland (*Abstract Co-Author*) Nothing to Disclose David P. Costello, BSC,MSc, Dublin, Ireland (*Abstract Co-Author*) Nothing to Disclose Andrea Cradock, Dublin, Ireland (*Abstract Co-Author*) Nothing to Disclose Ciara M'Centee, Dublin, Ireland (*Abstract Co-Author*) Nothing to Disclose Allison Mc Gee, Dublin, Ireland (*Abstract Co-Author*) Nothing to Disclose

For information about this presentation, contact:

WALAA_ALSHARIF@HOTMAIL.COM

PURPOSE

The American College of Radiology (ACR) standard recommends that quality assurance (QA) testing of MR systems is the responsibility of both technologists and medical physicists to ensure efficient scanner performance. However, in the Kingdom of Saudi Arabia (KSA), meeting this standard is challenging due to a shortage of medical physicists, variable MR-specific education amongst technologists, and difficulties in achieving standardisation across centres providing MR imaging services. These factors have contributed to low compliance with recommendations for the performance of MR QA tests. This study explored the development of an education-based Quality Improvement (QI) initiative to enable MR technologists across multiple clinical sites to consistently perform MR system QA testing. The authors aimed to develop an educational tool to provide MR QA training to technologists enabling them to undertake this activity in their departments.

RESULTS

There was 95% agreement between the expert-determined and technologist-determined MR QA test results. Interview findings revealed that all technologists reported that the test methods presented in the training video were clear and logical, and enabled them to perform practical QA testing of their scanner. 12% of technologist participants (n=1) acknowledged some difficulty positioning the QA phantom, and 50% (n=4) indicated challenges interpreting the test pattern appearances due to the inherent subjectivity of the low contrast detectability QA test. All participants indicated that their experience of MR QA training was positive, using expressions such as "I enjoyed it", "It was a positive experience", and "very good experience", "It showed me what I can do with the right training". Technologists indicated they had learned a new skill to help them improve the quality of the MR imaging service they provide, and were willing to continue undertaking QA testing, seeing this as one way to expand their professional role.

CONCLUSION

with the ongoing shortage of medical physicists in KSA and other countries, the training video introduced as a QLIIIItative demonstrated the effectiveness of an appropriately designed educational resource combining both technical information and practical skills demonstration. The ease of access and display means that this educational tool can readily be made available to MR technologists across multiple centres in KSA, as a strategy to prevent a shortage in expert personnel limiting the implementation of practices to optimise MR service quality. The broader application of the methods applied during this education-based QI is apparent.

METHODS

Educational Tool Design: A training video was designed to demonstrate MR OA test methods and provide background explanatory information. sing a focus group discussion framework, the research team, comprising two medical physicists and four MR technologists, reached consensus regarding the essential content and presentation format, drawing on ACR MR OA guidelines and the expertise of group members. Based on ACR recommendations, the method for the following QA tests was planned: central frequency, geometric accuracy, high-contrast spatial resolution, low-contrast detectability, image intensity uniformity and signalto-noise ratio (SNR). Each test was broken down into logical steps which included: MR QA phantom design features, set-up and positioning, pulse sequence and parameters and use of MR images to provide numerical indicators of MR system performance. The performance of these steps by the research team members for each QA test was videoed in sequential order to make it easy for the MR technologists to follow the test method. Editing of the video footage and overlay of audio content was performed by a videographer in consultation with the research team. Educational Tool Evaluation: MR technologists (n=8) in one public (n=4) and one semi-public (n=4) hospital in KSA evaluated the QA training video. Technologists were given supervised access to this resource for two 30-minute sessions per day over one week. A supporting booklet outlining the test methods was also provided. On completion of the educational intervention, each technologist was asked to implement the QA test process in their MRI department for a three-month period by individually conducting weekly QA testing on the MR scanner and documenting the images and numerical results for each test. These findings were compared to images and values independently determined for the same QA tests on each MR scanner as performed by an expert in MR QA following the methodology outlined in the training video. Face-toface semi-structured interviews were conducted with each technologist to ascertain their opinion regarding the effectiveness of the QA training video and their experiences undertaking the QA tests.

PDF UPLOAD

https://abstract.rsna.org/uploads/2017/17016601/17016601_ox5k.pdf

SSK17-09 A Microwave Imaging System and Real-Time Image Reconstruction Algorithm for Intraoperative 3D Monitoring of Thermal Ablation Therapies

Wednesday, Nov. 29 11:50AM - 12:00PM Room: S404AB

Participants

guanbo chen, los angeles, CA (*Presenter*) Nothing to Disclose John Stang, PhD, Los Angeles, CA (*Abstract Co-Author*) Nothing to Disclose Pratik Shah, Los Angeles, CA (*Abstract Co-Author*) Nothing to Disclose Sang Cho, PharmD,MPH, Los Angeles, CA (*Abstract Co-Author*) Nothing to Disclose Eric Leuthardt, Saint Louis, MO (*Abstract Co-Author*) Stockholder, NeuroLutions, Inc Stockholder, General Sensing Ltd Stockholder, OsteoVantage, Inc Stockholder, Pear Therapeutics Inc Stockholder, Face to Face Biometrics Mahta Moghaddam, PhD, Ann Arbor, MI (*Abstract Co-Author*) Nothing to Disclose

For information about this presentation, contact:

guanboch@usc.edu

guanboch@usc.edu

CONCLUSION

We proposed a 3D real-time microwave monitoring method and synthetically validated it for interstitial thermal therapy monitoring. We will further validate on animal models before moving to clinical trials. With this intraoperative temperature monitoring, radiologists will be able to more selectively target tumors, extend the application of thermal ablation to new therapeutic areas, and reduce surgery time.

Background

Thermal ablation is a minimally invasive surgery that is gaining increasing popularity as first-line therapy for soft-tissue tumors. However, its application has been limited by inadequate thermal image guidance. Fiber optic sensors measure temperature only at their tips. B-mode ultrasound is limited to 2D. MRI is not available within the operating room and adds 30-40 minutes to surgery time. To address these challenges, we have developed a microwave monitoring system that can intraoperatively provide a 3D realtime temperature map. The system consists of a multi-antenna imaging cavity, where microwave measurements are collected with a network-analyzer-based measurement system. The data is processed with a differential inverse scattering algorithm, which generates real-time 3D temperature images through a mapping between tissue dielectric change and temperature. In our prior work, the system has been experimentally validated using laboratory phantoms heated with an ablation probe.

Evaluation

To synthetically test the monitoring of the ablation process in the case of brain tumor treated with thermal therapy, we derived a 3D dielectric brain phantom from MRI and simulated the heating of the target region with a multi-physics model of an interstitial ablation probe. In the test, the target region is heated from 37 °C to 70 °C, and 3D temperature maps are generated throughout the procedure.

Discussion

Sample validation results are shown in the figure attached. The 3D temperature maps can be generated as fast as 1 frame/second, provide a resolution of 1 cm, and can track temperature change as small as 1 °C. To further improve temperature accuracy, the mapping model between dielectric and temperature change is currently being refined with empirical studies using *in vitro* tissue samples.



KSNA° 2017

103rd Scientific Assembly and Annual Meeting November 26 to December 1 McCormick Place, Chicago



SSK18

Physics (CT: Radiation Dose II)

Wednesday, Nov. 29 10:30AM - 12:00PM Room: S503AB



AMA PRA Category 1 Credits ™: 1.50 ARRT Category A+ Credit: 1.75

FDA Discussions may include off-label uses.

Participants

Shuai Leng, DPHIL, Rochester, MN (*Moderator*) License agreement, Bayer AG Xinming Liu, PhD, Houston, TX (*Moderator*) Nothing to Disclose

Sub-Events

SSK18-01 Experience with Different Automatic Tube Voltage Selection Software (kV Assist and Care kV) on Four CT Platforms

Participants

Manuel Patino, MD, Boston, MA (*Presenter*) Nothing to Disclose Anushri Parakh, MBBS, MD, Boston, MA (*Abstract Co-Author*) Nothing to Disclose Avinash R. Kambadakone, MD, Boston, MA (*Abstract Co-Author*) Nothing to Disclose Dushyant V. Sahani, MD, Boston, MA (*Abstract Co-Author*) Research support, General Electric Company; Medical Advisory Board, Allena Pharmaceuticals, Inc

For information about this presentation, contact:

mpatino@mgh.harvard.edu

PURPOSE

To assess the effect of ATVS on the applied tube voltage, tube current, image quality and radiation exposure across four scanners from two vendors.

METHOD AND MATERIALS

In this IRB approved study, 341 subjects (age: 58 ± 17 years) underwent abdominopelvic CT exams with ATVS technique set at a reference value of 120kVp on four recently introduced CT platforms. kV assist: Revolution CT, GEHC (Group A, n=90); CarekV: Somatom Definition Flash, Siemens (group B, n=16), Somatom Definition Force, Siemens (group C n=82) and Somatom Definition Edge, Siemens (group D n=153). Subjects were categorized based on body weight (<150lb, 151-200lb, >201lb). Images were reconstructed using ASIR-V 40% for group A, SAFIRE 3 for groups B and D, and ADMIRE A3 for group C. In 86 additional subjects, 100 kVp was selected as reference for ATVS (Group E; Revolution CT). Applied scan parameters (tube voltage and mean tube current) and radiation dose (SSDE) were compared for all body weight categories among the groups; ANOVA was performed.

RESULTS

There was no significant difference in body weight among subjects in groups A-E within each category (p>0.05). Across all groups and weight categories, low tube voltage (<120 kVp) was selected in 48% of exams (165/341). 5% of exams (19/341) were scanned using 90kVp (<200lb). Majority of low kVp scans were performed in subjects <200lb (147/165). Low kVp was selected in 21.6% of subjects (18/83) >201lb. Highest number of low kVp acquisitions were found in Group D (70%) followed by group C (61%) and Group B (31%). Only 3.3% of exams (3/90) in group A (all <200lb) were performed using 100kVp. However, 86% of exams (74/86) were acquired at 100 kVp in group E. SSDE (mGy) was 12.9 \pm 3.3 in group A, 10.9 \pm 2.4 in group B, 11.5 \pm 3 in group C, 11.2 \pm 3.2 in group D, and 7.7 \pm 2.2 in group E (p<0.01).

CONCLUSION

The kVp selection with ATVS not only depends on body composition but on the reference kVp setting and tube current capacity. Using reference of 120kVp, careKV (Siemens) selected low kVp in 31-70% of exams. Using a reference of 100kVp on kV assist (GE), low kVp selection increased to 86% of exams independently of the body weight.

CLINICAL RELEVANCE/APPLICATION

Due to higher image contrast and lower radiation dose, clinical practice is drifting towards low kVp CT acquisitions. Knowledge of ATVS software selection of kV options can facilitate implementation in clinical practice without degrading image quality or CT workflow.

SSK18-02 Automatic Mapping of CT scan Locations on Computational Human Phantoms for Accurate Organ Dose Estimations for a Large Number of Patients

Wednesday, Nov. 29 10:40AM - 10:50AM Room: S503AB

Participants Choonsik Lee, PhD, Rockville, MD (*Abstract Co-Author*) Nothing to Disclose Gleb Kuzmin, MS, Rockville, MD (*Presenter*) Nothing to Disclose

For information about this presentation, contact:

choonsik.lee@nih.gov

PURPOSE

Using Monte Carlo simulations of CT scanners and computational human phantoms, there are several computational solutions available for organ dose estimation from CT. Although most scan parameters can be extracted from DICOM, it is still necessary to manually map the scan locations of patients on phantoms which may cause significant dose difference for organs near the scan boundaries. We developed a method to automate the mapping process and applied it to organ dose estimation for 60 chest CT patients.

METHOD AND MATERIALS

We generated a two-dimensional antero-posterior projection image of the skeleton from given patient CT images. We compared the patient skeleton image with a pre-generated skeleton image from a reference whole body phantom from the top of the head to the bottom of the feet with 1 cm increment to find the best Dice matching score. The mapping algorithm was tested for five partial torso CT sets (22 image sets from the top clavicle with 20 cm scan length with 2 cm increment for each patient) simulated using five full torso CT sets. Illustrative organ doses were calculated for 60 chest CT patients using the algorithm combined with an inhouse CT dose calculator. Automatic mapping algorithm-based organ doses were compared with the data based on the scan location manually mapped by experienced medical physicists.

RESULTS

Comparison of the scan location of simulated partial torso CT with the values of automatically-mapped location in phantoms showed very good agreement (less than 10%) with the Dice score of 57% on average. The automatic detection of the scan location took about a minute per CT. The illustrative organ dose for 60 chest CT patients showed significant difference up to 5-fold for some organs located atnthe scan boundaries across the 60 patients. The organ doses from the automati. Mapping algorithm agreed within 5% with the values calculated from manual mapping of scan locations.

CONCLUSION

Our method will provide faster and more accurate organ dose estimation compared to existing approaches in cases requiring organ dose for a large number of patients such as patient dose monitoring, clinical trials, and epidemiological studies.

CLINICAL RELEVANCE/APPLICATION

The new methods we developed in this study will provide with more accurate patient-specific organ doses, which will help radiologists and patients to better understand the health impact of CT scans.

SSK18-03 A Personal Organ Dose Archive System for Patient Safety in Radiotherapy

Wednesday, Nov. 29 10:50AM - 11:00AM Room: S503AB

Participants

Ying Liang, PhD, New Haven, CT (*Presenter*) Nothing to Disclose Wazir Muhammad, PhD,MS, New Haven, CT (*Abstract Co-Author*) Nothing to Disclose Jun Deng, PhD, New Haven, CT (*Abstract Co-Author*) Nothing to Disclose

For information about this presentation, contact:

ying.liang@yale.edu

PURPOSE

Although state-of-the-art radiotherapy techniques have improved local tumor control over the years, normal tissue complication is still of concern in the clinic. Estimation of normal tissue doses depend primarily on treatment planning system (TPS). However, leakage and scatter doses, imaging doses and doses to non-contoured organs are not well considered by modern TPS. In this work, we aim to develop a personal organ dose archive (PODA) system for individual patients undergoing radiotherapy to track doses of all relevant organs from all radiation events.

METHOD AND MATERIALS

CT images, contours and treatment parameters are exported and extracted from TPS via DICOM format. Deformable image registration and dose mapping are performed with MIM with 3D volumetric imaging. GPU-based Monte Carlo dose engine is used for super-fast 3D dose calculation in patient anatomy. A SQLite database is deployed to manage the data registration and inquiry.

RESULTS

Our PODA system includes four parts: (1) DICOM library; (2) PODA database; (3) GPU-based Monte Carlo dose engine; (4) functional modules. DICOM library hierarchically stores all the raw data for each individual patient. PODA database organizes and manages the general information of all patients. GPU-base dose engine computes organ doses and outputs to PODA database for each event involving ionizing radiation. Major functional modules include Update Organ Dose, Report & Alert and Database Backup & Recovery. The four components work together to track patient organ doses on a daily basis. A proactive early warning is issued if organ dose will exceed pre-set dose criteria by prediction.

CONCLUSION

We have developed a PODA system that can be used to track and accumulate each patient's organ doses associated with the use of sophisticated treatment technologies and image-guidance procedures in modern radiotherapy.

CLINICAL RELEVANCE/APPLICATION

With PODA we can provide an important safety mechanism to help prevent irreversible radiation damage to normal tissues and provide a comprehensive organ dose database to help clinicians make informed decisions for individual patients including pre and

post care management.

SSK18-04 Comparison of Image Quality and Radiation Dose of Female Chest CT Using Organ Dose Modulation with Different Detector Coverage on 16cm Wide-detector CT

Wednesday, Nov. 29 11:00AM - 11:10AM Room: S503AB

Participants Yanan Li, Xian, China (*Presenter*) Nothing to Disclose Niu Gang, MD, Xi'an, China (*Abstract Co-Author*) Nothing to Disclose Fan Ganglian, Xian, China (*Abstract Co-Author*) Nothing to Disclose Jingjing Bai, Xian, China (*Abstract Co-Author*) Nothing to Disclose Xijun Jiao, Xian, China (*Abstract Co-Author*) Nothing to Disclose Jian Yang, MD, PhD, Xian, China (*Abstract Co-Author*) Nothing to Disclose

For information about this presentation, contact:

liyanan976@163.com

PURPOSE

To evaluate the impact of two different detector coverages (80mm and 40mm) on image quality and radiation dose of the female chest CT using organ dose modulation (ODM).

METHOD AND MATERIALS

Forty female patients undergoing chest CT with clinical justifications were prospectively and randomly assigned to two groups: Group A (n=20) with 80mm detector coverage and pitch 0.992:1; Group B (n=20) with40mm detector coverage and pitch 0.984:1. Both groups used the 0.5s rotation speed and the SmartmA and ODM technique for the breasts. The standard deviation (SD) in the aortic arch, carina, and inferior pulmonary vein in both the anterior and posterior lungs were measured. Image quality was evaluated by two experienced radiologists using a 5-point scoring system. The tube current in different directions (A/L/P/R) were recorded from mA Table. The CTDIvol and DLP values were recorded from dose report and effective dose calculated. The above parameters for the two groups were analyzed using SPSS 20.0.

RESULTS

There was no difference in the anatomic coverage between the two groups (258.75 ± 27.85 mm vs. 253.00 ± 24.51 mm). However, Group B with 4mm collimation had lower tube current in all four directions and reduced over-scan range than Group A (29.50 ± 0.60 mm vs. 59.40 ± 7.47 mm, P<0.05), resulting in 25% lower radiation dose in Group B compared with Group A (0.74 ± 0.13 mSv vs. 0.99 ± 0.33 mSv). The ODM feature worked in both groups, and the tube current in the anterior was lower than that in the posterior in both groups (P<0.05), and produced about 30% radiation reduction for the breasts in both groups. There was no significant difference in SD for the aortic arch, carina, and inferior pulmonary vein level between the two groups. The image quality of two group were judged to be clinically acceptable. There was no significant difference in subjective image quality grading (p>0.05) with excellent agreement between the two radiologists (Kappa=0.77, P<0.001).

CONCLUSION

The use of helical scan with 40mm collimation and ODM chest CT ensures good image quality with 25% reduced radiation dose, compared with chest CT that uses helical scan with 80mm collimation and ODM.

CLINICAL RELEVANCE/APPLICATION

The use of helical scan with 40mm collimation and ODM chest CT can dramatically reduce radiation dose while maintaining image quality compared with helical scan with 80mm collimation and ODM.

SSK18-05 Efficacy of Organ Dose Modulation and Metal Artifact Reduction Techniques on Reducing Exposed Radiation Dose on Abdominopelvic Computed Tomography Scans With Metal Hip Prosthesis

Wednesday, Nov. 29 11:10AM - 11:20AM Room: S503AB

Participants

Ok Kyu Song, Seoul, Korea, Republic Of (*Presenter*) Nothing to Disclose Yong Eun Chung, MD, PhD, Seoul, Korea, Republic Of (*Abstract Co-Author*) Nothing to Disclose

For information about this presentation, contact:

songokkyu@yuhs.ac

PURPOSE

To evaluate the effect of metal hip prosthesis on exposed radiation dose and assess the efficacy of organ dose modulatation (ODM) and metal artifact reduction (MAR) protocols on dose reduction.

METHOD AND MATERIALS

Six patients with history of total hip arthroplasty who had both preoperative and postoperative abdominopelvic CT scans using an identical protocol were selected and their preoperative and postoperative CT dose index (CTDI, mGy) were compared. An anthropomorphic phantom was scanned with and without bilateral metal prostheses and exposed surface and deep doses (mGy) at pelvic and extrapelvic cavities were measured using nanoDot dosimetry system. Finally, exposed radiation doses using reference scans, ODM, and two MAR protocols (GSI32 and GSI3; CTDI equivalent to reference scan without and with metal prosthesis respectively) in pelvic and extrapelvic cavities were compared.

RESULTS

Among six patients, the mean CTDI (mGy) increased by 18.1% after metal hip prosthesis implantation (p=0.028, Preoperative CTDI: 8.64 ± 2.47 , Postoperative CTDI 10.20 ± 3.51). On phantom experiment, adding unilateral or bilateral metal prosthesis in pelvis increased CTDI (mGy) by 14.4% and 30.5% respectively. The tube currents were also increased in pelvic cavity but the metal hip

prosthesis had no effect on the tube currents of extrapelvic area. The utilization of MAR and ODM protocols decreased both the surface and the deep organ doses in pelvis. GSI32 showed the most significant dose reduction in the deep pelvic cavity followed by GSI3 and ODM. However, MAR (GSI32, GSI3) protocols increased radiation doses in extrapelvic cavity compared to the reference scan. ODM showed significant reduction of both the surface and deep organ doses in the extrapelvic cavity.

CONCLUSION

Metal hip prosthesis implantation increased exposed radiation doses in abdominopelvic CT scans. MAR protocol can be utilized to reduce the exposed radiation doses in pelvic cavity while improving image quality. When MAR protocol is not applicable, ODM is an alternative protocol that can be utilized to reduce exposed radiation doses of both pelvic and extrapelvic cavities.

CLINICAL RELEVANCE/APPLICATION

Metal artifact reduction and organ dose modulation techniques reduce radiation doses in patients with metal prosthesis implantation.

SSK18-06 Impact of Adjusting the Pulmonary-Embolism CT-protocol on Female Fertility Preservation by Reducing the Radiation Exposure of the Ovaries

Wednesday, Nov. 29 11:20AM - 11:30AM Room: S503AB

Participants

Roland C. Aydin, MD,MS, Garching, Germany (*Presenter*) Nothing to Disclose Karoline S. Barth, Tuebingen, Germany (*Abstract Co-Author*) Nothing to Disclose Dominik Zinsser, MD, Tuebingen, Germany (*Abstract Co-Author*) Nothing to Disclose Klaus Herz, Tubingen, Germany (*Abstract Co-Author*) Nothing to Disclose Christian J. Cyron, PhD, Garching, Germany (*Abstract Co-Author*) Nothing to Disclose Konstantin Nikolaou, MD, Tuebingen, Germany (*Abstract Co-Author*) Nothing to Disclose Konstantin Nikolaou, MD, Tuebingen, Germany (*Abstract Co-Author*) Nothing to Disclose Konstantin Nikolaou, MD, Tuebingen, Germany (*Abstract Co-Author*) Speakers Bureau, Siemens AG; Speakers Bureau, Bracco Group; Speakers Bureau, Bayer AG Mike Notohamiprodjo, Munich, Germany (*Abstract Co-Author*) Nothing to Disclose Roy Marcus, MD, Tubingen, Germany (*Abstract Co-Author*) Nothing to Disclose

For information about this presentation, contact:

roy.marcus@med.uni-tuebingen.de

PURPOSE

To assess in female patients undergoing a clinical pulmonary-embolism CT-protocol the relative and absolute reduction of the radiation exposure on the gonads by using a modified protocol that imposes a caudal imaging limit of the costodiaphragmatic recesses, in lieu of the common imaging window which also captures the supraadrenal glands. Cumulative exposure to radiation remains a concern due to the rising maternal age at primigravida, and the often unavailable exposure during emergencies such as suspected pulmonary embolisms.

METHOD AND MATERIALS

Thirty non-pregnant female patients with suspected pulmonary embolism underwent a contrast enhanced CT of the chest on a 3rd generation dual source CT (SOMATOM Force, Siemens Healthcare) in single-energy mode with automatic tube voltage selection and tube current modulation. Organ dose of the ovaries was automatically calculated using a commercial dose tracking software (Radimetrics, Bayer Schering). Full assessability of the thoracic cavity was assured with the modified imaging window, although incidental findings of e.g. suprarenal growths were precluded.

RESULTS

Median age of the patients analyzed in the retrospective study was 35 years [17 - 42]. The median equivalent dose of the gonads was 0.031 [0.009 - 0.190] mSv for the adapted (shrunk imaging window) and for the non-adapted protocol (typical size imaging window) 0.060 [0.013 - 0.266] mSv. The reduction in radiation dose was statistically significant (p<0.0001). The mean absolute difference in the ovarial radiation dose amounted to 0.041 ± 0.031 mSv, corresponding to a relative reduction in gonadic exposure of 43.8%.

CONCLUSION

For female patients prior to menopause in general, and their subgroup with a history of suspected pulmonary embolisms and thus repeated thoracic CT imaging specifically, an adaption of the CT protocol as outlined conveys a significant cumulative reduction of the radiation exposure on the ovaries.

CLINICAL RELEVANCE/APPLICATION

Shortening the scan range of pulmonary CTA positively affects the ovarian radiation exposure, important in pre-menopausal women undergoing repetitive scans.

SSK18-07 CT-Guided Periradicular Infiltration Therapy: How IR and Protocol Modifications Contribute to Achieving Ultra-Low-Dose

Wednesday, Nov. 29 11:30AM - 11:40AM Room: S503AB

Participants

Fabian Elsholtz, Berlin, Germany (Presenter) Nothing to Disclose

Julia Kamp, MD, Berlin, Germany (Abstract Co-Author) Nothing to Disclose

Janis L. Vahldiek, MD, Berlin, Germany (Abstract Co-Author) Nothing to Disclose

Bernd K. Hamm III, MD, Berlin, Germany (*Abstract Co-Author*) Research Consultant, Toshiba Medical Services Corporation ; Stockholder, Siemens AG; Stockholder, General Electric Company; Research Grant, Toshiba Medical Services Corporation Research Grant, Koninklijke Philips NV; Research Grant, Siemens AG ; Research Grant, General Electric Company; Research Grant, Elbit Imaging Ltd; Research Grant, Bayer AG ; Research Grant, Guerbet SA; Research Grant, Bracco Group; Research Grant, B. Braun Melsungen AG; Research Grant, KRAUTH medical KG ; Research Grant, Boston Scientific Corporation; Equipment support, Elbit Imaging Ltd; Investigator, CMC Contrast AB

For information about this presentation, contact:

fabian.elsholtz@charite.de

PURPOSE

To evaluate robustness and safety of ultra-low-dose protocols for CT-guided periradicular infiltration of the cervical and lumbosacral spine on a CT scanner with iterative reconstruction software.

METHOD AND MATERIALS

This retrospective study included a total of 366 patients who underwent periradicular infiltration therapy of the cervical (n=191) and lumbar (n=175) spine. Respective study group (90 each cervical and lumbosacral) was treated on a new CT scanner with a new intervention protocol using an iterative reconstruction algorithm. Spot scanning was implemented for planning purposes and a basic low setup of 80 kV (cervical) or 100 kV (lumbosacral) and 5 mAs was established during intermittent fluoroscopy. The comparison group comprised 101 (cervical) and 85 (lumbosacral) prior interventions on a scanner without iterative reconstruction software. Dose-length product, number of acquisitions, pain reduction on a numeric analogue scale and protocol changes to achieve a safe intervention were recorded.

RESULTS

Median DLP for the whole intervention was 24.3 mGy*cm in the cervical and 49.3 mGy*cm in the lumbosacral comparison group towards 1.8 mGy*cm in the cervical and 3.2 in the lumbosacral study group. Pain reduction was median -2 in all the cervical and lumbosacral study and comparison group. Raise of the tube current-time product by 5 mAs was needed in 5 patients of the cervical and 3 patients in the lumbosacral study group.

CONCLUSION

Implementation of a new ultra-low-dose intervention protocol resulted in a reduction of dose by 92.6% (cervical) and 64.0% (lumbosacral) without limitation of safety and pain relief.

CLINICAL RELEVANCE/APPLICATION

Dose reduction in CT imaging is of relevant interest from patients and physicians perspective. Changes of the scanner parameters and implementation of IR can significantly reduce overall dose also of interventional procedures. This dose reduction does not impact the procedure itself nor the outcome as seen in periradicular infiltration.

SSK18-08 Prospective Evaluation of Ultra-Low Dose Enhanced Abdominal Computed Tomography (MDCT) Using 100 kV with Tin Filter as Spectral Shaping: Effect on Radiation Dose Reduction and Image Quality with a Third-Generation Dual-Source CT System

Wednesday, Nov. 29 11:40AM - 11:50AM Room: S503AB

Participants

Pierre G. Leyendecker, MD, Strasbourg, France (*Presenter*) Nothing to Disclose Vanina Faucher, MD, Strasbourg, France (*Abstract Co-Author*) Nothing to Disclose Paul R. Magotteaux Sr, MD, Liege, Belgium (*Abstract Co-Author*) Nothing to Disclose Aissam Labani, MD, Strasbourg, France (*Abstract Co-Author*) Nothing to Disclose Mickael Ohana, MD, PhD, Strasbourg, France (*Abstract Co-Author*) Nothing to Disclose Catherine Roy, MD, Strasbourg, France (*Abstract Co-Author*) Nothing to Disclose

For information about this presentation, contact:

pierre.leyendecker@chru-strasbourg.fr

PURPOSE

The purpose of this prospective study was to investigate the radiation dose exposure and image quality of enhanced abdominopelvic single-energy MDCT using a tin filter at 100Kv tube voltage in comparison to the standard enhanced acquisition.

METHOD AND MATERIALS

110 medium size oncologic patients (BMI:25<u>+</u>3.2kg/m2) over 60 years old (mean age:73.2±10.2 years) referred for an enhanced abdominopelvic MDCT examination underwent in addition to our conventional protocol an ultralow dose acquisition with tin filter (TF) in portal venous phase. Our institutional ethical committee reviewed and approved our investigation. The examinations were performed in single energy helical mode with a third-generation dual-source CT (Somatom Force). Both standard acquisition (SP) with an automatic individually-adapted kV (90-110) and tin filter (TP) (100 Sn kV/300mAs) were acquired with automatic milliamperage modulation and identical length of coverage, pitch, reconstructed slice thickness of 2mm, acquisition time and ADMIRE strength : 4. Radiation dose was recorded as dose-length product (DLP), volume CT index (CTDIvol). Effective dose (ED) was calculated. Subjective image quality was evaluated on a 5-grade scale by two blinded independent radiologists and interobserver agreement was calculated. Objective image quality was calculated by signal-to-noise ratio (SNR). The attenuation with standard deviation in liver and psoas muscle were assessed.

RESULTS

Radiation dose was reduced by 82-84% withTF compared to SP (DLP : $290\pm12.0 \text{ vs } 49.6\pm3.2 \text{ mGy.cm}; p<0.0006$, CTDIvol:1.32±0.36 vs 7.25±1.64 mGy; p<0.0001, ED : $4.93\pm0.2 \text{ vs } 0.84\pm0.1 \text{ mSv}$; p<0.0005). The image quality was rated as excellent for both (4.5 for TF, 5 for SP) with an excellent interobserver agreement (Kappa =0.87). All abnormalities discovered on SP were identified on TF. SNR was not significantly different with TF in liver (9.53±0.9 vs 8.10±1.1; p : 0.08) or psoas (6.03±1.5 vs 5.46±0.2 ; p : 0.06), respectively. Attenuation values were slightly lower with TF (91±14HU vs 102±12HU, 52±16HU vs 65±10HU; p= 0.06) for liver and psoas muscle, respectively

CONCLUSION

An ultralow radiation dose (ED<1mSv) for abdominopelvic CT is achieved using a tin filtration as spectral shaping at 100 kV without

degradation of image quality and diagnosis confidence in medium size patients.

CLINICAL RELEVANCE/APPLICATION

The TF acquisition should be proposed for enhanced abdominal CT follow up examinations in oncologic patients.

SSK18-09 Reducing Variability of Radiation Doses in CT

Wednesday, Nov. 29 11:50AM - 12:00PM Room: S503AB

Participants Ryan K. Lee, MD, Philadelphia, PA (*Presenter*) Nothing to Disclose Joel Y. Sun, MD, Philadelphia, PA (*Abstract Co-Author*) Nothing to Disclose Terence A. Matalon, MD, Philadelphia, PA (*Abstract Co-Author*) Speaker, Koninklijke Philips NV Samantha Lockerby, Philadelphia, PA (*Abstract Co-Author*) Nothing to Disclose Eric Soltycki, MS, Philadelphia, PA (*Abstract Co-Author*) Nothing to Disclose

For information about this presentation, contact:

leeryan1@einstein.edu

CONCLUSION

Significant decrease of variance in head, chest, and abd/pelvis CT was achieved using a combination of standardizing protocols across the network and implementing advanced software that effectively managed radiation dose.

Background

While reducing radiation is an important goal, also important in the management of radiation dose is ensuring consistency in the amount of radiation administered for each type of study. Being able to consistently administer the same dose everytime a study is performed is the hallmark of high quality in radiation management. We implemented an approach to reducing variance in CT dose by standardizing protocols and employing software at the scanner to provide consistency across the network.

Evaluation

We measured variance of dose administered to head, chest, and abd/pelvis CT in two periods. The first period is pre-intervention: 1/1/13-7/31/14. We then measured the period after intervention: 1/1/16-12/31/16. Statistical analysis for differences in variability of radiation dose pre- and post-intervention used Bartlett's test. Pre-intervention dose and SD: head CT (n=12,002): 26.4 CTDI with SD of 4.3; chest CT (n=3,149): 8.6 CTDI with SD of 5.2; abd/pelvic CT (n=9833) :12.5 CTDI with SD of 5.2. Post-intervention dose and SD: head CT (n=13,274): 20.1 CTDIvol with SD of 3.4; chest CT (n=3,746): 5.4 CTDI with SD of 2.7; abd/pelvis Ts (n=12,121): 7.7 CTDI with SD 3.3. Post intervention SD was significantly decreased for all studies (p<0.001).

Discussion

Our approach to reducing variability in radiation CT was a multifaceted approach: 1. Establishing the Radiation Dose Optimization Committee, 2. Standardizing Protocols, and 3. Implementing scanner software which reduces variance of dose. We implemented software in scanners that increases tube current to a lesser degree than would be obtained by hold noise constant. The software increases tube current for increasing diameter size at a rate less than would be needed to hold noise constant. Thus for larger patients, allowing for controlled increase in dose to improve signal to noise yet also accepting more noise allowed for better dose management avoiding exponential increase in radiation that occurs with conventional dose modulation.





103rd Scientific Assembly and Annual Meeting November 26 to December 1 McCormick Place, Chicago



SSK19

Radiation Oncology (Outcomes and Quality of Life)

Wednesday, Nov. 29 10:30AM - 12:00PM Room: S104A



AMA PRA Category 1 Credits ™: 1.50 ARRT Category A+ Credit: 1.75

Participants

Jun Deng, PhD, New Haven, CT (*Moderator*) Nothing to Disclose Kathleen Horst, MD, Stanford, CA (*Moderator*) Nothing to Disclose

Sub-Events

SSK19-02 Prospective Investigation of the Association of Pre-Treatment Depression with Quality of Life during Radiotherapy for Prostate Cancer

Wednesday, Nov. 29 10:40AM - 10:50AM Room: S104A

Participants

Sara Walker, Portland, OR (*Abstract Co-Author*) Nothing to Disclose Yiyi Chen, Portland, OR (*Abstract Co-Author*) Nothing to Disclose Amy Leatherwood, RN, Portland, OR (*Abstract Co-Author*) Nothing to Disclose Kyungeen Paik, BS, Portland, OR (*Abstract Co-Author*) Nothing to Disclose Brandy Mirly, RN, Portland, OR (*Abstract Co-Author*) Nothing to Disclose Charles R. Thomas JR, MD, Portland, OR (*Presenter*) Nothing to Disclose Arthur Hung, MD, Portland, OR (*Abstract Co-Author*) Nothing to Disclose

For information about this presentation, contact:

walkesar@ohsu.edu

ABSTRACT

Purpose/Objective(s): Cancer survivors often experience psychological stress, with impact on quality of life (QOL) and mortality. Better understanding the heterogeneity in individuals' psychological adjustment to cancer diagnosis and treatment may help identify valid screening practices for those most in need of psychosocial support. The specific aim of the current study investigates the role of psychological state prior to treatment on the course of QOL during radiotherapy for localized non-metastatic prostate cancer. We hypothesized inverse correlations between depression and QOL. We also categorized participants in three groups based on depressive symptoms (i.e., minimal, mild, moderate+) and hypothesized a significant between group difference in OOL as measured pre-, mid-, and post-treatment.Materials/Methods: The PHQ-9 assessed depression. We grouped participants into Minimal (n=22), Mild (n=8), and Moderate or higher (n=6) depression groups based on PHQ-9 score. The FACT-P assessed QOL, including physical, social, emotional, and functional well-being. Our total sample (N=41) had mean age of 68 (range 54-81) and education of 15.5 years (range 10-20). Most participants (33; 80%) identified as European-American. There were no between-group differences in age, education, or ethnic identity. Repeated measures ANOVA assessed effects of group and time. Associations of variables of interest were also assessed by Pearson's correlation coefficients. Results: Significant inverse correlations were observed between depression and QOL pre-treatment (p p F (1,33)=16.49, ppConclusion: These analyses reflect strong inverse correlations between degree of depressive symptoms and QOL pre-, mid-, and post-treatment. Investigating subgroups based on extent of depressive symptoms was also illuminating in that QOL characteristics of the "moderate or higher" group were distinct from the other two groups, which did not significantly differ from one another. Indeed, a "mild" degree of depression may not be unexpected in inherently distressing circumstances. These findings support the conclusion that there may be a useful clinical cutoff on the PHQ-9 (e.g., mild vs. moderate) for triggering psychosocial support or other intervention. We are of course limited by small samples in our subgroups and these findings can therefore be considered preliminary. Future directions include investigation into other potential contributors to QOL changes, as well as investigation of these factors in other disease or treatment groups.

SSK19-04 Stereotactic Body Radiation Therapy (SBRT): A Strategy to Reduce Disparities in African American Men with Localized Prostate Cancer?

Wednesday, Nov. 29 11:00AM - 11:10AM Room: S104A

Participants

Robert Dess, MD, Ann Arbor, MI (Presenter) Nothing to Disclose

ABSTRACT

Purpose/Objective(s): Prostate cancer (PCa) is the most common cancer in men, and African-Americans (AA) consistently have inferior outcomes compared to Caucasians (C). Technological advances that improve access to care may be one strategy to address this disparity. Stereotactic Body Radiation Therapy (SBRT) is a convenient, non-invasive course, typically involving 5 treatments over a few weeks. In a large cohort with prospectively collected health-related quality of life (HRQOL) data, we sought to explore early efficacy and HRQOL differences between men who self-report as AA compared to C race.Materials/Methods: Between 2008 and 2014, 752 consecutive men were treated with localized, node negative prostate cancer per an institutional protocol. Inclusion criteria for the present study included men with low and intermediate risk PCa treated with SBRT with or without androgen deprivation therapy (ADT). Prospective HRQOL data in the urinary, bowel, sexual and vitality domains were collected via the Expanded Prostate Cancer Index Composite (EPIC)-26 form along with other baseline demographics (Charlson comorbidity,

Anticoagulation use, Partner status, Diabetes (DM), Hypertension, Dyslipidemia, and Coronary artery disease). Cox multivariable analyses (MVA) were utilized to compare 5-year biochemical progression-free survival (bPFS) and 2 year HRQOL between AAs and Cs. Results: The median follow-up was 4.1 years. Of the 510 men who met eligibility criteria, 53% (n=270) were C, 40% (n=202) AA, and 7% (n=38) other. The cohort included 33% low, 38% favorable intermediate (Fav-Int), and 29% unfavorable intermediate (Unfav-Int) risk men, and rates were similar between AAs and Cs (p=0.44). AAs were younger at diagnosis (67 vs 70, p0.05). AA were less likely to report partners (70% vs 82%, p=0.04) or depression (0% vs 10%, pConclusion: In a prospectively followed cohort, tumor control and HRQOL were similar across low and intermediate risk men treated with prostate SBRT, even when adjusting for baseline differences. Long term follow-up is needed to confirm these promising results.

SSK19-05 Patient Safety in Radiation Oncology Departments in Spain: Preliminary Results of the First National Survey

Wednesday, Nov. 29 11:10AM - 11:20AM Room: S104A

Participants

Jose Pardo, Palma De Mallorca, Spain (*Presenter*) Nothing to Disclose Elia del Cerro Penalver, Madrid, Spain (*Abstract Co-Author*) Nothing to Disclose Amalia Palacios, MD, Cordoba, Spain (*Abstract Co-Author*) Nothing to Disclose Agusti Pedro, MD, Barcelona, Spain (*Abstract Co-Author*) Nothing to Disclose Albert Biete, MD, Barcelona, Spain (*Abstract Co-Author*) Nothing to Disclose Gustavo Ossola, , Spain (*Abstract Co-Author*) Nothing to Disclose Daniel Morera, Palma de Mallorca, Spain (*Abstract Co-Author*) Nothing to Disclose Ricardo Esco, MD, Zaragoza, Spain (*Abstract Co-Author*) Nothing to Disclose Esther Jimenez-Jimenez, Palma De Mallorca, Spain (*Abstract Co-Author*) Nothing to Disclose

ABSTRACT

Purpose/Objective(s): To analyze the current status of the patient's safety culture and programs among the radiation oncology departments is Spain through a national survey.Materials/Methods: The survey was targeted to 98 heads of radiation oncology departments, both public and private. Each of them received a questionnaire and the responses were utilized to explore the study aim. Twenty five questions were asked on the following topics: Existence of a patient safety commission in his hospital and participation in the same of someone of the department; If someone in the department has tasks related to patient safety; Existence of maps of processes, risks and a risk probability scale; Check lists employment, Existence of a quality assurance program with indicators to measure the quality of each phase of the radiotherapy process, and when it was last updated; Performance of any external quality control audit; Existence of an anonymous and easy-access system of events notification; Number of adverse events reported in the last 12 months; Organization of regular meetings on issues related to patient safety; Existence of specific actions aimed at improving patient safety; Degree of implementation of the safety culture in its department and, finally, His opinion on the development and implementation by the Spanish Society of Radiation Oncology of an anonymous national system of notification of errors and incidents. Results: At present, 70 questionnaires have been received (participation rate 71.4%). Although 74% of the hospitals have a patient safety commission, only in 59% a radiation oncology staff is a member. In 70.3% of the departments some member has tasks related to patient safety. In the 88.8% there is a map of processes and in 40.7% a map of risks. In 85.1% check lists are used. In 100% of the departments there is a quality assurance program. In 66.6% some adverse effects were reported in the last year. Finally, almost all (96,2%) of the department's heads who responded agreed on the development and implementation by the Spanish Society of Radiation Oncology of an anonymous national system of notification of adverse events. Conclusion: The preliminary results of the survey show that, despite the fact that important work is being done on quality and of patient safety, there is still significant scope for improvement. Collection of questionnaires continues, and the final results will be presented and the final results will be presented when a participation rate of more than 80% has been achieved.

SSK19-07 Cost Effectiveness Analysis of Utilizing 3D Printer Technology to Create Bolus for Radiotherapy: An Institutional Experience

Wednesday, Nov. 29 11:30AM - 11:40AM Room: S104A

Participants Ankur Sharma, MD , Winnipeg, MB (*Presenter*) Nothing to Disclose

For information about this presentation, contact:

asharma5@cancercare.mb.ca

ABSTRACT

Purpose/Objective(s): At our institution, 3D printer technology is utilized in the radiation oncology department for constructing custom bolus. Bolus created using this innovative approach produces a more accurate fit in areas with complex skin contours and reduces air gap when compared to conventional bolus. It is also more convenient for patients and radiation therapists (RTs). As the use of 3D printing technology is expected to increase drastically in radiation oncology, we set out to perform a cost effectiveness analysis and report our findings. Materials/Methods: For the calendar year of 2014, patients who could have potentially had a bolus created using 3D printer technology at our institution were identified. Treatment sites included: sarcoma, anal canal, skin using orthovoltage energy and skin using electrons. Surveys were sent to 5 RTs to estimate the average time required to fabricate and set up a bolus using the conventional technique. Staff time required when using the 3D printer technique was estimated by an experienced physicist. Labour costs were determined for RTs, physicists and machinists, Cost of running and maintaining one linear accelerator and one taking into account staff salary and labour hours. orthovoltage unit was calculated. Cost of material required for 3D printer technique using polylactic acid (PLA) and cost of material using conventional technique was determined. Using the above information, total annual fabrication cost was calculated for both techniques. Total annual set up time was also calculated for both techniques. Potential annual cost savings were determined by subtracting the total annual cost of using the 3D printing method from the total annual cost of using the conventional method. Results: A total of 318 patients received 3204 fractions of radiotherapy. Cost of running the linear accelerator was \$2.64/minute and \$0.73/ minute for the orthovoltage unit. The cost of PLA was .07/cm3 and .11/cm3 for conventional bolus material. Taking into account the cost of our existing 3D printer, total annual accessory fabrication cost was \$18,878.00 using the conventional method and \$12,249.21 using 3D printer technology. Annual set up cost using conventional bolus was \$71, 054.54, compared to \$27,453.00 using 3D printer technology. When the two techniques were compared, potential annual cost saving were \$47,678.53.Conclusion: This analysis, although not perfect, shows that by utilizing a simple consumer

grade 3D printer to create bolus for radiotherapy treatments, there can be substantial cost savings of just under \$50,000.00 annually. When combined with the fact that 3D printed bolus provides a more accurate fit to the skin surface, provides equivalent or superior dosimetrics and adds patient and staff convenience, its usage is bound to become more common in radiation oncology departments. We recommend that utilization of 3D printer technology to create bolus for radiotherapy should become the new standard of care.

SSK19-08 Treatment Time Analysis of Radiotherapy for Breast Cancer Patients Treated with LINAC

Wednesday, Nov. 29 11:40AM - 11:50AM Room: S104A

Participants

Mei Suet Wong, Hong Kong, Hong Kong (Presenter) Nothing to Disclose

For information about this presentation, contact:

Michelle.wong@hksh.com

ABSTRACT

Purpose/Objective(s): To analyze setup time, beam on time and total treatment time of the radiotherapy treatment of breast cancer patients for case scheduling optimization, thus improving the machine throughput and the efficiency of treatment process Materials/Methods: In this study, breast treatment techniques of tangential opposing fields (2F), tangential opposing plus anterior SCF fields (3F) and tangential opposing fields with active breathing control (ABC) were considered. The total numbers of fraction in each case were 15-25. A customized table was used for recording setup time, beam on time and total treatment time for each patient. For 2F, 41 patients with 750 fractions were marked. For 3F, 8 patients with 163 fractions were marked. For ABC, 4 patients with 78 fractions were marked. The mean of setup time (TS), beam on time (TB) and total treatment time (TTx) for all fractions were calculated and compared among 2F, 3F and ABC techniques. To investigate treatment duration variability throughout the course of treatment, the mean of TS, TB and TTx of each fraction were also calculated and analyzed. One-way ANOVA was used in this study. Results: Mean (mins) TSTBTTx2F5.85.010.83F6.66.513.1ABC11.37.618.9The TS, TB and TTx among the three techniques were significantly different (pS between 2F and 3F due to similar setup procedures. In particular, the mean TS (11.3min) and hence TTx (18.9min) were much longer when using ABC technique. ABC device was needed to setup for controlling patient's respiratory motion which increased the total treatment time significantly. For treatment duration variability, the TTx for the first fraction was almost the double of overall fraction average regardless of the technique being used (190%, 208% and 217% for 2F, 3F and ABC respectively). It was due to setup verification performed during first treatment. For 2F and 3F, the TTxs in each fraction starting from second treatment were similar which the means were within 9-11mins. For ABC, the means TTxs of 2nd to 4th fractions were within 23-25mins which were still 30% longer than the average. This suggests 4 fractions were needed for patients to adapt the ABC setting and give stable performance throughout the remaining treatment course. The re-setup rate was low (3%) and only 0.3% patients felt uncomfortable and prolonged the treatment.Conclusion: Our current routine treatment time slot for 2F and 3F is 15mins while 30mins for the first fraction. For ABC, 45mins and 30mins are for first fraction and subsequent fractions respectively. This study suggested that the treatment duration of 2F for each fraction is 10mins and 20mins for first fraction. For 3F, it keeps 15mins as the average and 30mins for the first fraction. As for ABC, 40mins is suggested for the first fraction and 25mins for 2nd to 4th fractions while 20mins for the remaining fractions. The suggested case arrangement is expected to maximize the effective machine occupancy and hence the throughput.

SSK19-09 A Pilot Study to Evaluate a Newly-Developed Needs Assessment Tool for Improving Radiotherapy and General Oncology Management in Nigeria

Wednesday, Nov. 29 11:50AM - 12:00PM Room: S104A

Participants

Chika Nwachukwu, Stanford, CA (Presenter) Nothing to Disclose

ABSTRACT

Purpose/Objective(s): Cancer mortality in low- and middle-income countries are rising at a rapid rate, especially in countries where screening programs are scarce and resources are limited. Fragmented infrastructure, as well as limited human resources hinder access to appropriate cancer care in these regions. The purpose of this study is to develop a tool that assesses the gaps in cancer care, with emphasis on radiotherapy infrastructure, personnel skill level, and barriers to accessing treatment.Materials/Methods: Stanford University has developed a detailed needs assessment tool, in collaboration with the American Cancer Society (ACS) and Clinton Health Access Initiative (CHAI). This tool will be tested in a cross sectional study at two teaching hospitals in Nigeria. Using this newly developed cancer assessment instrument, semi-structured interviews and onsite visits will be conducted to assess gaps in cancer care including radiotherapy infrastructure. Lastly, in collaboration with key hospital personnel, the results of this study will be used to finalize the assessment tool to ensure the local cancer care needs are adequately addressed. Results: The two hospitals sites, Ahmadu Bello University Teaching Hospital (ABUTH) and Lagos University Teaching Hospital (LUTH), were identified by the Nigerian ministry of health as two sites to be developed into comprehensive cancer centers. Both centers currently have chemotherapy delivery capacity, radiotherapy capacity (including linear accelerators, linacs), and are staffed by radiation oncologists, medical oncologists, and a small set of non-specialist clinical staff. Stanford experts have been paired with collaborators at ABUTH and LUTH. The needs assessment tool has two main components, a cancer assessment section and a human capacity section. The cancer assessment section has 6 broad areas ranging from summary and health status of the population to cancer specific needs. The different specialist from LUTH and ABUTH will complete the tool. There are 100 cancer specific needs questions, 20 of which focus directly on radiotherapy. The radiotherapy issues addressed include the demographics of patients receiving treatment (palliative or curative intent), referral patterns for patients, and barriers to care, such as cost of treatment. Furthermore, the tool assesses radiation treatment capacity to include availability of linacs, cobalt machines, brachytherapy machines and their functional capacities. Finally, the human resource section has 20 broad questions, many of which are applicable to radiotherapy staff, ranging from continuing education to the availability of staff, their respective roles, as well as their work flow. Conclusion: The completion of the needs assessment will take place during the site visit at the end of February. The results of the tool will be reported to identify actionable ways to improve cancer care, including the utilization of radiation in this setting.





103rd Scientific Assembly and Annual Meeting November 26 to December 1 McCormick Place, Chicago



SSK20

Vascular Interventional (Embolization)

Wednesday, Nov. 29 10:30AM - 12:00PM Room: E351



AMA PRA Category 1 Credits ™: 1.50 ARRT Category A+ Credit: 1.75

FDA Discussions may include off-label uses.

Participants

Thuong G. Van Ha, MD, Chicago, IL (Moderator) Research Grant, Cook Group Incorporated; Research Consultant, Surefire Medical, Inc

Nikunj R. Chauhan, MD, Cleveland, OH (Moderator) Nothing to Disclose

Sub-Events

SSK20-01 Efficacy of Transarterial Embolization in Managing Non-Variceal Gastrointestinal Bleeding Post-Endoscopy Failure: Systematic Review and Meta-analysis

Participants

Sanjay Bansal, MD, Calgary, AB (*Presenter*) Nothing to Disclose Aman Wadhwani, MD, Calgary, AB (*Abstract Co-Author*) Nothing to Disclose Jonathan J. Dykeman, MD,MSc, Calgary, AB (*Abstract Co-Author*) Nothing to Disclose Eric J. Herget, MD, Calgary, AB (*Abstract Co-Author*) Nothing to Disclose Paul L. Beck, MD,PhD, Calgary, AB (*Abstract Co-Author*) Nothing to Disclose

For information about this presentation, contact:

sanjay.bansal@albertahealthservices.ca

PURPOSE

Non-variceal gastrointestinal bleeding (NVGIB) is a common cause of hospitalization. In patients who have failed endoscopic therapy trans-arterial embolization (TAE) is considered the treatment of choice. The primary objective of this study is to perform a detailed systematic review and meta analysis of the current literature to assess (1) the success of TAE in controlling NVGIB, and (2) evaluate the mortality and morbidity rates post-TAE in patients for whom endoscopy has failed to control NVGIB.

METHOD AND MATERIALS

A search strategy was developed for EMBASE and Medline related to embolization and gastrointestinal bleeding using appropriate exploded medical subheading terms and keywords. Studies included were those examining patients presenting with a NVGIB whose bleeding could not be controlled with endoscopic intervention and subsequently were treated with TAE. The primary outcomes will be all-cause mortality and re-bleeding rates. These will be combined using a random-effects meta-analysis if sufficient data is extracted. Secondary outcomes will include length of hospitalization.

RESULTS

The search yielded 5624 articles from EMBASE and 2874 from Medline. After eliminating duplicates a total of 6421 were identified for further screening. Application of inclusion and exclusion criteria left a final total of 46 articles to be included in the study. Technical success was 97%. 24.65% of patients had bleeding within 30 days of TAE. 12.7% of patients required surgery after TAE. 30 day mortality post embolization was 22.8%. Bowel necrosis occurred in 3% of patients.

CONCLUSION

TAE in the setting of NVGIB, in which endoscopy has failed to control bleeding, is almost always successful acheiving cessation of contrast extravasation. 30 day re-bleed and mortality are high, however this may be confounded by pre-existing comorbidities and clinical instability of patients prior to undergoing embolization. Subgroup analysis will help to delineate this.

CLINICAL RELEVANCE/APPLICATION

In patients with NVGIB that is refractory to endoscopic therapy TAE should be strongly considered as an alternative to surgery as a second option. This is especially true in patients with multiple comorbidities, and/or patients that are clinically unstable, as they are high risk surgical candidates.

SSK20-02 Prostatic Artery Embolization: Identifying the Anatomical Variations in Origin of the Prostatic Artery and Predicting the Best Tube Angle Projection to Visualize its Origin Using Three Dimensional Contrast-enhanced MR Angiography

Wednesday, Nov. 29 10:40AM - 10:50AM Room: E351

Participants

Nagy N. Naguib, MD, MSc, Frankfurt Am Main, Germany (*Presenter*) Nothing to Disclose Nour-Eldin A. Nour-Eldin, MD,PhD, Frankfurt Am Main, Germany (*Abstract Co-Author*) Nothing to Disclose Tatjana Gruber-Rouh, Frankfurt Am Main, Germany (*Abstract Co-Author*) Nothing to Disclose Benjamin Kaltenbach, MD, Frankfurt, Germany (*Abstract Co-Author*) Nothing to Disclose Thomas J. Vogl, MD, PhD, Frankfurt, Germany (*Abstract Co-Author*) Nothing to Disclose

For information about this presentation, contact:

nagynnn@yahoo.com

PURPOSE

To evaluate the ability of Three Dimensional Contrast Enhanced MR Angiography (3D-CE-MRA) in identifying the origin of the prostatic artery (PA) and predicting the best tube angle projection for its visualization before prostatic artery embolization (PAE) in an attempt to find a standard angle for its visualization during intervention

METHOD AND MATERIALS

Pre-embolization CE-MRA studies from 28 males (mean age 66.54 years) were retrospectively evaluated by two radiologists in consensus. Studies were done using a 3 Tesla MRI unit and 3D images were reconstructed using Syngo Vessel View Application. The PA was identified by tracing its course from the prostate back to its origin. Then the 3D figure was rotated in all directions to obtain the best visualization angle of the origin without overlap from other arteries

RESULTS

Of the studied 56 internal iliac arteries (IIA) the PA was detected in 80.1% (n=45); unilaterally in 17.9% (n=5 patients) and bilaterally in 71.4% (n=20 patients). It originated directly from the anterior division of the IIA in 57.78% (n=26), indirectly from the anterior division with a common trunk with other arteries in 13.33% (n=6, 3 with middle rectal, 2 with superior vesical and 1 with internal pudendal) and from different branches in 28.89% (n=13, 8 from internal pudendal, 3 from obturator and 2 from inferior gluteal). For the right PA (detected in 21 patients) the angle projection required for visualizing its origin ranged from 43° left to 45° right (mean 6.33° right +/- 30.4°). Additional cephalocaudal angulation was required in 66.67% (n=14) with angle ranging between 3° and 23° caudal (mean 11.79° caudal +/- 6.69°). For the left PA (detected in 24 patients) the angle projection required for visualizing its origin ranged from 45° left to 37° right (mean 16.04° left +/- 31.49°). Additional cephalocaudal angulation was required in 37.5% (n=9) with an angle ranging between 4° and 23° caudal (mean 13.67° caudal +/- 7.98°)

CONCLUSION

3D-CE-MRA can detect the origin of the PA before PAE and can predict the best tube angle projection to visualize it. There is no standard angle to visualize the origin that can be generally recommended; instead the angle should be individually tailored.

CLINICAL RELEVANCE/APPLICATION

3D-CE-MRA can identify the origin of the PA and predict the best tube angle projection to visualize it before PAE. The preplanning can reduce the need for searching for the origin using radiation during the procedure.

SSK20-03 Prostatic Arterial Embolization with Polyvinyl Alcohol Electrospun Nanofibers in a Canine Model of Benign Prostatic Hyperplasia (BPH): A Preliminary Study

Wednesday, Nov. 29 10:50AM - 11:00AM Room: E351

Participants

Basen Li, Wuhan, China (*Presenter*) Nothing to Disclose Liang Wang, MD, PhD, Wuhan, China (*Abstract Co-Author*) Nothing to Disclose Zhaoyan Feng, MD, Wuhan, China (*Abstract Co-Author*) Nothing to Disclose

For information about this presentation, contact:

libasen@sina.com

PURPOSE

To explore the safety, feasibility and efficacy of embolization with polyvinyl alcohol (PVA) electrospun nanofibers in a canine model of benign prostatic hyperplasia (BPH).

METHOD AND MATERIALS

Five adult male beagle dogs (Beagle A, Beagle B, Beagle C, Beagle D, Beagle E) were included in this study. All beagle dogs were randomly numbered. The beagle dogs were castrated by an urologist. Intramuscular Benzylpenicillin (1,600,000 IU) was injected daily for three days to prevent infection. After one month, 2.5 mg/kg of TP were injected intramuscularly daily for 3 months. All beagle dogs underwent 3T MRI. The prostatic volume (PV) of all dogs was measured on MRI before and at 3 months after initiation of hormone administration. PAE was performed with superselective catheterization of the prostatic artery on each side through a femoral artery puncture after 3 months of TP therapy. Embolization was performed with the use of homemade 150-200 µm polyvinyl alcohol (PVA) electrospun nanofibers. All dogs was sacrificed 1 week, 1 month, 3 months, 6 months and 6 months after PAE, respectively. Histopathologic study was performed by the urologic pathologist.

RESULTS

The canine BPH model was successfully established in all dogs. The mean PV increased significantly after 3 months of hormone administration. DSA clearly depicted of the prostatic arteries after 3 months of hormone administration. PAE was successfully performed in all dogs. No serious PAE-related complication was observed during and after the procedure. In all five dogs, no significant abnormalities were found. Under the microscope, the PVA electrospun nanofibers in blood vessels with no spillover , mild inflammation in the prostate was found in Beagle A 1 week after PAE. The prostate of Beagle B 1 month after PAE showed cystic changes, atrophied gland, decreased inflammatory cells, more fibroblasts, focal hemosiderin deposition, and no evidence of neocapillarization. The parenchyma around the cavity showed atrophy under the microscope. In addition, focal hemosiderin deposition, scattered inflammatory cell infiltration, and fibrosis were found. Remnants of the glandular hyperplasia and embolic particles in blood vessels of the gland were present.

CONCLUSION

PAE with PVA electrospun nanofibers in a canine model of BPH is feasible, effective and safe.

PVA electrospun nanofibers can be used in PAE

SSK20-04 Long-Term Clinical Outcomes and Re-Intervention Rates of Uterine Artery Embolization (UAE) For Symptomatic Fibroids or Adenomyosis: Five-Year Results

Wednesday, Nov. 29 11:00AM - 11:10AM Room: E351

Participants

Ja Kyung Yoon, Seoul, Korea, Republic Of (*Presenter*) Nothing to Disclose Kichang Han, MD, Seoul, Korea, Republic Of (*Abstract Co-Author*) Nothing to Disclose Man Deuk Kim, MD, Seoul, Korea, Republic Of (*Abstract Co-Author*) Nothing to Disclose Yong Seek Kim, MD, Jeonju, Korea, Republic Of (*Abstract Co-Author*) Nothing to Disclose Joon Ho Kwon, Gongju, Korea, Republic Of (*Abstract Co-Author*) Nothing to Disclose Gyoung Min Kim, MD, Seoul, Korea, Republic Of (*Abstract Co-Author*) Nothing to Disclose Jong Yun Won, MD, Seoul, Korea, Republic Of (*Abstract Co-Author*) Nothing to Disclose Jong Yun Won, MD, Seoul, Korea, Republic Of (*Abstract Co-Author*) Nothing to Disclose Do Yun Lee, MD, Seoul, Korea, Republic Of (*Abstract Co-Author*) Nothing to Disclose

For information about this presentation, contact:

jkyoon87@yuhs.ac

PURPOSE

To retrospectively investigate reintervention rates in patients treated with uterine artery embolization (UAE) for symptomatic fibroids or adenomyosis and to elucidate predictive factors for reintervention.

METHOD AND MATERIALS

Between March 2011 and February 2012, 124 patients who underwent UAE were categorized into fibroid group (n=92, 73.6%) or into adenomyosis group with or without fibroids (n=32, 26.4%). Five-year follow-up telephone survey was done to assess reintervention rates. Potential predictive factors for reintervention such as age, body mass index (BMI), as well as three-month follow-up magnetic resonance imaging (MRI) outcomes were analyzed.

RESULTS

Response rate to the telephone survey was 73.4 % (91/124, 67 fibroid and 24 adenomyosis). Technical success was achieved in all patients (100%). Overall reintervention rate was 11.0%, with seven patients in the fibroid group (10.4%) and three patients in the adenomyosis group (12.5%). Subgroup analysis of 15 adenomyosis patients without fibroids (i.e., pure adenomyosis) revealed three reintervention cases (3/15, 20.0%). Reinterventions in the fibroid group were myomectomy (n=5) and hysterectomy (n=2). Among 56 patients with available follow-up MRI, 54 (96.4%) had complete necrosis of the predominant fibroids. One patient with cervical leiomyoma had treatment failure resulting in hysterectomy. Reinterventions in the adenomyosis group were hysterectomy (n=2) and myomectomy (n=1). 13 out of 15 follow-up MRIs of adenomyosis patients with or without adenomyosis (86.6%) demonstrated complete necrosis, resulting in one case of hysterectomy. One of two adenomyosis patients without necrosis (1/15, 13.3%) underwent hysterectomy. In the adenomyosis group, there was a trend towards lower reintervention rate in patients with complete necrosis than in those without necrosis, but without statistical significance.

CONCLUSION

Reintervention rates in fibroid and adenomyosis groups at five years were 10.4% and 12.5%, respectively. Low reintervention and high clinical success rates strengthen the potential of UAE as a viable first line treatment for symptomatic fibroid or adenomyosis.

CLINICAL RELEVANCE/APPLICATION

Uterine artery embolization(UAE) has strong potential as first line treatment for adenomyosis with or without fibroids with low reintervention rate and high clinical success rate.

SSK20-05 Refinements of Preoperative Portal Vein Embolization Using Ethylene-Vinyl Alcohol Copolymer: A Pilot Study

Wednesday, Nov. 29 11:10AM - 11:20AM Room: E351

Participants

Romain Breguet, MD, Geneva, Switzerland (*Abstract Co-Author*) Nothing to Disclose Sana Boudabbous, Geneva, Switzerland (*Abstract Co-Author*) Nothing to Disclose Christoph D. Becker, MD, Thonex, Switzerland (*Abstract Co-Author*) Nothing to Disclose Maxime Ronot, MD, Clichy, France (*Presenter*) Nothing to Disclose Sylvain Terraz, MD, Geneva, Switzerland (*Abstract Co-Author*) Nothing to Disclose

For information about this presentation, contact:

maxime.ronot@aphp.fr

PURPOSE

To evaluate the safety profile and the added value ethylene-vinyl alcohol copolymer (Onyx) injection for selective embolisation of specific portal branches during of preoperative portal vein embolisation (PVE).

METHOD AND MATERIALS

From 2008 to 2011, 110 PVE procedures were performed in our hospital in patients with small future liver remnants (FLR). Under general anaesthesia, PVE was achieved with injection of a mixture of n-butyl-cyanoacrylate (Histoacryl) and iodised oil (Lipiodol) using a 5-F catheter. At the operator's discretion, small portal branches with a great risk of embolic agent migration were embolised with Onyx through a 2.4-F microcatheter. CT volumetry of the FLR was performed before and 4-6 weeks after PVE. Clinical outcome was assessed on medical records.

RESULTS

Twenty-eight patients (median age, 57 ± 17 years) underwent PVE with Histoacryl-Lipiodol and additional Onyx during 29 procedures. The indications for Onyx were embolisation of segment IV (n=21), early bifurcation of portal branches in S6 and S8 (n=5) and PVE in a one-year-old girl with cystic mesenchymal hamartomas. All targeted portal branches were successfully embolised with Onyx and no major complication was observed. Related-procedure adverse events included a self-limited subcapsular haematoma (3%) and two small pieces of glue migration without thrombosis (7%). CT volumetry showed a mean FLR hypertrophy of $64\pm28\%$. Hepatectomy was performed in 25 patients (89%) and cancelled in three patients, due to tumour progression (n=2) or insufficient FLR volume (n=1).

CONCLUSION

PVE with complementary Onyx before liver resection is safe and feasible, and helps to occlude small portal branches that are not accessible with conventional embolic materials.

CLINICAL RELEVANCE/APPLICATION

PVE with complementary Onyx before liver resection is safe and feasible, and helps to occlude small portal branches that are not accessible with conventional embolic materials.

SSK20-06 Emergency Out of Hours Endovascular Hemorrhage Control Procedures: Evolution of Caseload, Casemix and Clinical Outcome between 2009 and 2014

Wednesday, Nov. 29 11:20AM - 11:30AM Room: E351

Awards

Student Travel Stipend Award

Participants

Sook Cheng Chin, MD, Dundee, United Kingdom (*Presenter*) Nothing to Disclose Neil J. Young, MBChB, MRCS, Dundee, United Kingdom (*Abstract Co-Author*) Nothing to Disclose Richard D. White, MBChB, FRCR, Cardiff, United Kingdom (*Abstract Co-Author*) Nothing to Disclose Iain Robertson, FRCR, Glasgow, United Kingdom (*Abstract Co-Author*) Nothing to Disclose Reddi Yadavali, Glasgow, United Kingdom (*Abstract Co-Author*) Nothing to Disclose Ian A. Zealley, MBChB, Dundee, United Kingdom (*Abstract Co-Author*) Nothing to Disclose

For information about this presentation, contact:

s.chin1@nhs.net

PURPOSE

Demand for emergency OOH EVHC procedures is increasing. The most dramatic and urgent cases are those in which IR undertake minimally invasive EHCPs where surgery is physiologically undersirable or technically challenging. We analyzed the changing caseload, casemix and 30-day mortality for emergency OOH EVHC procedures performed in 2009 and 2014 with hopes to inform service design, training and clinical decision making.

METHOD AND MATERIALS

The setting was four centers providing OOH IR services for a population of 3 million. Data related to all OOH EVHC done in 2009 and 2014 were analyzed, including mortality within 30 days of the index procedure. Procedures were categorised by site and etiology of hemorrhage and by whether or not a therapeutic intervention was actually performed.

RESULTS

Between 2009 and 2014: 1. The annual total caseload increased by 40% from 93 to 130 procedures (P<0.05), a per capita increase in caseload from 3.1 to 4.3 per 100,000 population 2. The number of therapeutic procedures increased by 34% from 84 to 113 3. Changes in casemix included significant increases in numbers of lower gastrointestinal (GI), non-surgical iatrogenic etiologies and spontaneous hemorrhage 4. The number of upper GI cases and postoperative bleeding was unchanged 5. The number of post-partum haemorrhage (PPH) cases was significantly reduced 6. 30-day mortality significantly increased from 9% to 18% (P<0.05) 7. Patients in the 2014 cohort were significantly older, mean age (range) 60.6 years (19-94) vs. 52.3 (19-91), (P<0.05)

CONCLUSION

Increasing demand for emergency OOH EHVC procedures was accompanied by increased caseload of lower GI, non-surgical iatrogenic and spontaneous hemorrhage, with fewer PPH cases. Speculation on reasons for changes creates interesting discussion points. The older patients in the 2014 cohort suggests that the observed increase in mortality rate is likely attributable to changing referral thresholds (e.g. more patients with co-morbidities and/or in greater physiological distress). Identifying these trends facilitates service design, effective training and clinical decision-making.

CLINICAL RELEVANCE/APPLICATION

Analysis of changing caseload and casemix of out-of-hours (OOH) endovascular hemorrhage control (EVHC) procedures facilitates efficient service design, effective training and informed clinical decision-making

Honored Educators

Presenters or authors on this event have been recognized as RSNA Honored Educators for participating in multiple qualifying educational activities. Honored Educators are invested in furthering the profession of radiology by delivering high-quality educational content in their field of study. Learn how you can become an honored educator by visiting the website at: https://www.rsna.org/Honored-Educator-Award/ Ian A. Zealley, MBChB - 2016 Honored Educator

SSK20-07 Stent Graft Implantation in Visceral Arteries in Acute Life-Threatening Hemorrhage after Upper Abdominal Surgery: Technical Results and Clinical Outcome

Wednesday, Nov. 29 11:30AM - 11:40AM Room: E351

Participants

Benedikt M. Schaarschmidt, MD, Dusseldorf, Germany (*Presenter*) Nothing to Disclose Johannes Boos, MD, Dusseldorf, Germany (*Abstract Co-Author*) Nothing to Disclose Patric Kroepil, MD, Duesseldorf, Germany (*Abstract Co-Author*) Nothing to Disclose Guenther H. Fuerst, MD, Duesseldorf, Germany (*Abstract Co-Author*) Nothing to Disclose Rotem S. Lanzman, MD, Duesseldorf, Germany (*Abstract Co-Author*) Nothing to Disclose Christoph K. Thomas, MD, Dusseldorf, Germany (*Abstract Co-Author*) Nothing to Disclose

PURPOSE

Vascular erosion of the major visceral arteries (e.g. hepatic artery) due to leaking of pancreatic or jejunal anastomses is a rare but severe complication after upper abdominal surgery, leading to life-threatening delayed intraabdominal bleeding. Due to multiple risk factors and comorbidities, surgery is not always possible, making an interventional approach desireable. However, in major visceral arteries like the hepatic or superior mesenteric artery, vessel patency has to be preserved to prevent organ necrosis; thus a stent graft has to be implanted. The purpose of the present study was to analyze technical and clinical outcome after heparin-bonded stent graft placement to treat acute hemorrhage of the visceral arteries after surgery.

METHOD AND MATERIALS

A retrospective analysis of 22 male and 7 female patients (mean age: 66 years) who underwent heparin-bonded stent graft placement for the treatment of post surgical bleeding between 2009 and 2016 was performed. An explorative data analysis concerning technical success, complications as well as short term survival (<30 days) and long term survival (<90 days) was performed.

RESULTS

Successful stent graft placement and vessel reconstruction could be achieved in 24 of all 29 patients (83%). Surgical conversion was necessary in five patients. Periinterventional complications could be observed in six patients (vasospasms: n=4; pseudoaneurysm perforation: n=1; reversible stent occlusion: n=1). In 13 patients, a total of 14 stent graft related complications could be observed after the intervention (re-bleeding: n=7; stent graft occlusion: n=7), access related complications were observed in three patients. Short term survival was 76% (n=22) and long term survival was 41% (n=12), with most causes of death related to the underlying surgical complication.

CONCLUSION

Endovascular treatment of post-surgical bleeding using heparin-bonded stent grafts is a feasible treatment option with a high technical success rate. However, multiple risk factors and comorbidities in this specific patient cohort lead to a high complication rate and a comparably low long term survival rate.

CLINICAL RELEVANCE/APPLICATION

In patients with delayed intraabdominal bleeding after surgery, endovascular treatment using heparin-bonded stent grafts is a possible treatment option with a high technical success rate.

SSK20-08 Unenhanced MRI of the Pulmonary Vasculature Allows for Detection of Pulmonary AV-Malformations (PAVM) in Patients with Hereditary Hemorrhagic Telangiectasia (HHT / Osler's Disease)

Wednesday, Nov. 29 11:40AM - 11:50AM Room: E351

Participants

Jonas Stroeder, MD, Homburg, Germany (Presenter) Nothing to Disclose

Philippe Jagoda, MD, Homburg/Saar, Germany (Abstract Co-Author) Nothing to Disclose

Alexander Massmann, MD, Homburg/Saar, Germany (Abstract Co-Author) Nothing to Disclose

Arno Buecker, MD, Homburg, Germany (*Abstract Co-Author*) Research Grant, Siemens AG Consultant, Bracco Group Speaker, Bracco Group Consultant, Medtronic plc Speaker, Medtronic plc Research Grant, Novartis AG Research Grant, GlaxoSmithKline plc Research Grant, Biotest AG Research Grant, OncoGenex Pharmaceuticals, Inc Research Grant, Bristol-Myers Squibb Company Research Grant, Eli Lilly & Company Research Grant, Pfizer Inc Research Grant, F. Hoffmann-La Roche Ltd Research Grant, sanofi-aventis Group Research Grant, Merrimack Pharmaceuticals, Inc Research Grant, Sirtex Medical Ltd Research Grant, Concordia Healthcare Corp Research Grant, AbbVie Inc Research Grant, Takeda Pharmaceutical Company Limited Research Grant, Merck & Co, Inc Research Grant, Affimed NV Research Grant, Bayer AG Research Grant, Johnson & Johnson Research Grant, Seattle Genetics, Inc Research Grant, Onyx Pharmaceuticals, Inc Research Grant, Synta Pharmaceuticals Corp Research Grant, Siemens AG Research Grant, Si YMED GmbH Research Grant, St. Jude Medical, Inc Co-founder, Aachen Resonance GmbH

Guenther K. Schneider, MD, PhD, Homburg, Germany (*Abstract Co-Author*) Research Grant, Siemens AG; Speakers Bureau, Siemens AG; Speakers Bureau, Bracco Group; Research Grant, Bracco Group;

PURPOSE

To compare the detection rate of pulmonary AV-Malformations (PAVMs) in Gd-enhanced MR angiography with unenhanced MR imaging techniques in patients with hereditary hemorrhagic telangiectasia (HHT).

METHOD AND MATERIALS

During this retrospective Study 122 patients with HHT underwent a total of 188 MR examinations between 01/2011 and 12/2015. The patients' age varied from 11 to 83 years (mean 48 years). Each examination included a non contrast enhanced SPACE (3D TSE-sequence/ TR 4.733 ms/ TE 101 ms/ FLIP 150°) and a contrast enhanced 3D GRE MRI sequence (TR 2,87ms/ TE 1,07 ms/ FLIP 25°, 0.1 mmol/kg BW MultiHance). Both examinations were read by two experienced radiologists and the number of detected AV-Malformations was reported in agreement for each examination. The contrast enhanced images were always read first and after an blanking interval of 6 weeks, the SPACE was read by the same radiologists; blinded to the results of the first reading. In cases in which therapy was required, catheter angiography was used as a gold standard and in all other cases CE-MRA served as the gold standard. A paired t-test was utilized for statistical evaluation.

RESULTS

4 Examinations had to be excluded due to respiratory artifacts in both sequences. 60 AV-malformations requiring therapy were reported in 35 patients. Using contrast enhanced images, an overall significantly higher number of AV-malformations was detected (166 vs. 96, p<0.001) but none of the AV-malformations requiring therapy (supporting vessel larger than 2 mm) were missed using the unenhanced SPACE sequence.

CONCLUSION

By using a SPACE sequence, the detection of clinical relevant pulmonary AV-malformations in patients with HHT can be safely performed in patients with contraindications for i.v. contrast medium (e.g. pregnancy).

CLINICAL RELEVANCE/APPLICATION

In patients with HHT it is important to find clinically relevant pulmonary AV-malformations, and using the SPACE sequence these can be found even in Patients with contraindications to contrast enhanced MRI.

SSK20-09 High Temporal Resolution Dynamic CE MRA in Detection of Reperfused Pulmonary Arteriovenos Malformations (PAVMs) in HHT-Patients

Wednesday, Nov. 29 11:50AM - 12:00PM Room: E351

Participants

Guenther K. Schneider, MD, PhD, Homburg, Germany (*Presenter*) Research Grant, Siemens AG; Speakers Bureau, Siemens AG; Speakers Bureau, Bracco Group; Research Grant, Bracco Group;

Paul S. Raczeck, MD, Homburg, Germany (Abstract Co-Author) Nothing to Disclose

Melina Mehrmann, Homburg, Germany (Abstract Co-Author) Nothing to Disclose

Alexander Massmann, MD, Homburg/Saar, Germany (Abstract Co-Author) Nothing to Disclose

Arno Buecker, MD, Homburg, Germany (*Abstract Co-Author*) Research Grant, Siemens AG Consultant, Bracco Group Speaker, Bracco Group Consultant, Medtronic plc Speaker, Medtronic plc Research Grant, Novartis AG Research Grant, GlaxoSmithKline plc Research Grant, Biotest AG Research Grant, OncoGenex Pharmaceuticals, Inc Research Grant, Bristol-Myers Squibb Company Research Grant, Eli Lilly & Company Research Grant, Pfizer Inc Research Grant, F. Hoffmann-La Roche Ltd Research Grant, sanofi-aventis Group Research Grant, Merrimack Pharmaceuticals, Inc Research Grant, Sirtex Medical Ltd Research Grant, Concordia Healthcare Corp Research Grant, AbbVie Inc Research Grant, Takeda Pharmaceutical Company Limited Research Grant, Merck & Co, Inc Research Grant, Affimed NV Research Grant, Bayer AG Research Grant, Johnson & Johnson Research Grant, Seattle Genetics, Inc Research Grant, Onyx Pharmaceuticals, Inc Research Grant, Synta Pharmaceuticals Corp Research Grant, Siemens AG Research Grant, Siemens AG Research Grant, iSYMED GmbH Research Grant, St. Jude Medical, Inc Co-founder, Aachen Resonance GmbH

For information about this presentation, contact:

dr.guenther.schneider@uks.eu

PURPOSE

The recommended treatment of PAVMs in HHT patients (Hereditary Hemorrhagic Telangiectasia / Osler disease) is catheter embolization either with coils or by the use of vascular plugs. Although immediate post-interventional imaging may show complete success of embolization therapy, reperfusion may occur due to opening of collateral vessels or reperfusion of the embolized vessel itself. The aim of our study was to evaluate time-resolved contrast-enhanced MR-Angiography for detection of reperfused PAVM.

METHOD AND MATERIALS

65 patients in which treatment of PAVMs by means of platinum coil embolization or implantation of Amplatzer vascular plugs was performed, underwent follow-up studies for detection of reperfused PAVM by contrast enhanced MRA. First, a time-resolved MRA-study was performed with injection of a small contrast medium bolus (0.025 mmol/kg BW (Gd-BOPTA) MultiHance, Bracco). The temporal resolution of the sequence was 3 sec / dataset with a total number of 72 slices. Thereafter a high resolution CE MRA (0.075 mmol/kg BW MultiHance) with a timing based on the findings from the time resolved study was performed. Images were evaluated regarding enhancement of the draining vein. Recanalization was diagnosed when a simultaneous enhancement of feeding artery and draining vein or aneurysm sac was observed on dynamic CE MRA.

RESULTS

Time-resolved MR-Angiography was technically adequate in 61 of 65 cases. In 26 out of the 61 patients diagnosis of 32 reperfused PAVMs was made. In those cases in which diagnosis of reperfused PAVM was unclear on high resolution images, evaluation of the enhancement kinetics of the draining vein on dynamic CE MRA was used for diagnosis and could confirm 14 reperfused PAVM. All reperfused PAVM diagnosed on CE MRA were confirmed by DSA and underwent reembolization.

CONCLUSION

Time resolved contrast-enhanced MR-Angiography is a helpful adjunct to standard high resolution anatomic imaging, allowing for the evaluation of the enhancement kinetics of the draining vein as an indicator of recanalization of PAVM. Compared with CT imaging of embolized PAVM, this is an important advantage of CE MRA.

CLINICAL RELEVANCE/APPLICATION

Reperfusion of PAVM can occur in up to 20 percent of cases and early detection is mandatory to avoid complications. Dynamic CE MRA directly depicts early enhancement of the draining vein as a sign of reperfusion and thus gives important information not gained in conventional acquisitions.







MSRT43

ASRT@RSNA 2017: Rapid Screening Breast MRI - Protocol, Benefits and Financial Impact

Wednesday, Nov. 29 10:40AM - 11:40AM Room: N230B



AMA PRA Category 1 Credit ™: 1.00 ARRT Category A+ Credit: 1.00

Participants

David A. Strahle, MD, Flint, MI (Presenter) Nothing to Disclose

For information about this presentation, contact:

dstrahle@rmipc.net

LEARNING OBJECTIVES

1) Learn the Rapid MRI protocol sequences, the developed reading criteria, and how they give the 'average' MRI radiologist the ability to significantly reduce interpretation time and cut biopsy rates nearly in half. 2) Understand how screening breasts with MRI shifts time of cancer detection up to 6 years earlier than other screening modalities. 3) Identify the three basic steps for evaluating suspicious lesions and six reasons why kinetic evaluation is important to retain in an abbreviated protocol. 4) Discuss the impact a national MRI screening program could have on reducing costs and saving lives. Identify eight financial advantages for insurance carriers who pay for annual screening breast MRIs. 5) Learn how benign lesions as well as malignancy lesions played a critical role in developing the protocol.

ABSTRACT

Several key 'firsts' not published by any other authors... *Recording of all mammographically missed lesions, benign as well as malignant, and the surprising discovery of 452 missed lesions in 234 of 671 women who had a recent negative screening mammogram. *Development of a unique method to correctly identify the proper abbreviated MRI protocol...by letting each acquisition, in and of themselves, define which would work and which would not work in a breast screening environment. *First time initial baseline reading criteria was developed usable by all radiologists, not just 'expert radiologists' allowing biopsy rates to be cut nearly in half compared to any other screening modality. *Requirement to retain important kinetic information in the breast MRI protocol. *The realization of the importance of kinetic activity over morphology in evaluating small lesions - those lesions that would be expected in a MRI breast screening environment. *The time difference between a 3-minute protocol and a 6-minute protocol has no impact on overall patient throughput. *By establishing baseline reading criteria and using our shortened protocol, recall rates are near zero. *Discovering screening with mammograms are viable for women with fatty breasts (half the female population) and, therefore, MRI is not necessarily needed in this subgroup. *The important role benign lesions play in defining the correct acquisitions. *The first time a 4- to 6 year earlier pick up was realized, based on 16.3 new cancers per 1000 women. Breast MRI essentially shifts time of detection up to 6 years earlier than screening the same group of women with mammography. *We identified substantial dollars saved by insurance companies (and patients as well) in 10 major categories. The estimated total dollar savings are high enough (2,000%+ ROI) to absorb the cost of both mammograms and MRI and still yield a significant net savings. *The realization that 715 women in our modest-size county, who have had a negative mammogram within the last 12 months, have breast cancer and their identities are unknown to anyone ... except for the women who have had a Rapid Screening Breast MRI.

Active Handout:David A. Strahle

http://abstract.rsna.org/uploads/2017/17001469/Active MSRT43 11.20.17.pdf







RCA43

Leveraging Machine Learning Techniques and Predictive Analytics for Knowledge Discovery in Radiology (Hands-on)

Wednesday, Nov. 29 12:30PM - 2:00PM Room: S401AB

IN

AMA PRA Category 1 Credits ™: 1.50 ARRT Category A+ Credit: 1.75

Participants

Kevin Mader, DPhil,MSc, Zuerich, Switzerland (*Moderator*) Employee, 4Quant Ltd; Shareholder, 4Quant Ltd Kevin Mader, DPhil,MSc, Zuerich, Switzerland (*Presenter*) Employee, 4Quant Ltd; Shareholder, 4Quant Ltd Joshy Cyriac, Basel, Switzerland (*Presenter*) Nothing to Disclose Bram Stieltjes, MD,PhD, Basel, Switzerland (*Presenter*) Nothing to Disclose Barbaros S. Erdal, PhD, Columbus, OH (*Presenter*) Nothing to Disclose Luciano M. Prevedello, MD, MPH, Columbus, OH (*Presenter*) Nothing to Disclose

For information about this presentation, contact:

bram.stieltjes@usb.ch

LEARNING OBJECTIVES

1) Review the basic principles of predictive analytics. 2) Be exposed to some of the existing validation methodologies to test predictive models. 3) Understand how to incorporate radiology data sources (PACS, RIS, etc) into predictive modeling 4) Learn how to interpret results and make visualizations.

ABSTRACT

During this course, an introduction to machine learning and predictive analytics will be provided through hands on examples on imaging metadata (scan settings, configuration, timestamps, etc). Participants will use open source as well as freely available commercial platforms in order to achieve tasks such as image metadata and feature extraction, statistical analysis, building models, and validating them. Imaging samples will include datasets from a variety of modalities (CT, PET, MR) and scanners. The course will begin with a brief overview of important concepts and links to more detailed references. The concepts will then be directly applied in visual, easily understood workflows where the participants will see how the data are processed, features are selected, and models are built.







RCB43

Intro to Statistics with R (Hands-on)

Wednesday, Nov. 29 12:30PM - 2:00PM Room: S401CD



AMA PRA Category 1 Credits ™: 1.50 ARRT Category A+ Credit: 1.75

Participants

James E. Schmitt, MD, PhD, Philadelphia, PA (*Presenter*) Nothing to Disclose Philip A. Cook, PhD, Philadelphia, PA (*Presenter*) Nothing to Disclose

LEARNING OBJECTIVES

1) Install and launch the R software package. Understand how to search for and download external packages to extend R's functionality. 2) Load data from external files such as txt, csv, and xlsx. 3) Perform basic mathematical operations and utilize data structures to manipulate data. 4) Use loops to perform more complex operations over the data, including true/false logic. 5) Understand the basics of creating plots and histograms. 6) Perform common statistical tests including correlation, Chi-square, and ANOVA.







RCC43

Next Frontier in Imaging: Disease-specific Radiology Reports

Wednesday, Nov. 29 12:30PM - 2:00PM Room: S501ABC

IN

AMA PRA Category 1 Credits ™: 1.50 ARRT Category A+ Credit: 0

Participants

Olga R. Brook, MD, Boston, MA (Moderator) Nothing to Disclose

For information about this presentation, contact:

obrook@bidmc.harvard.edu

LEARNING OBJECTIVES

1) Demonstrate the advantages of disease-specific reporting over organ-system-based reporting. 2) Provide specific examples of the disease-specific templates that have been shown to improve value of imaging in thoracic and abdominal radiology

Sub-Events

RCC43A Disease-specific Report Templates vs. Structured Simple Templates: Next Frontier in Imaging Reports

Participants Olga R. Brook, MD, Boston, MA (*Presenter*) Nothing to Disclose

For information about this presentation, contact:

obrook@bidmc.harvard.edu

LEARNING OBJECTIVES

View learning objectives under main course title.

RCC43B Structured Reporting of Rectal Cancer MRI: A Template for Added Radiologist Value and Enhanced Patient Care

Participants

Marc J. Gollub, MD, New York, NY (Presenter) Nothing to Disclose

LEARNING OBJECTIVES

1) To familiarize the practicing radiologist with concept of targeted oncologic reporting, aimed at addressing key staging information and clinicoradiologic features that must be covered in a templated fashion to properly inform the referring team in a way that adds value and is unambiguous.

RCC43C Value-Driven Disease-Specific Reporting (Renal / Liver)

Participants

Matthew S. Davenport, MD, Cincinnati, OH (Presenter) Royalties, Wolters Kluwer nv; ;

For information about this presentation, contact:

matdaven@med.umich.edu

LEARNING OBJECTIVES

1) Demonstrate the advantages of disease-specific reporting over organ-system-based reporting. 2) Learn the value urologists place on renal mass-specific content that can be used to design a structured template. 3) Review how structured reporting can enable transplant decision making and OPTN compliance.

RCC43D Disease Specific Structured Reporting in Gynecological Oncological Imaging

Participants

Jessica B. Robbins, MD, Madison, WI (Presenter) Nothing to Disclose

LEARNING OBJECTIVES

View learning objectives under main course title.

RCC43E Disease-specific Structured Reporting in Thoracic Imaging: Added Value to the Clinical Team

Participants

Jonathan H. Chung, MD, Chicago, IL (Presenter) Nothing to Disclose

jonherochung@uchicago.edu

LEARNING OBJECTIVES

View learning objectives under main course title.

RCC43F CTE: Structured Reporting and its Potential Beneficiaries: Radiologists, Patients, and Providers

Participants Benjamin Wildman-Tobriner, MD, Durham, NC (*Presenter*) Nothing to Disclose

LEARNING OBJECTIVES

View learning objectives under main course title.







MSRT44

ASRT@RSNA 2017: Male Breast Cancer - What Lies Beneath

Wednesday, Nov. 29 1:00PM - 2:00PM Room: N230B

BR

AMA PRA Category 1 Credit ™: 1.00 ARRT Category A+ Credit: 1.00

Participants

Rita Gidwaney, MD, Novato, CA (Presenter) Nothing to Disclose

LEARNING OBJECTIVES

1) To review the biology and physiology of breast cancer in males. 2) To evaluate the similarities and differences between breast cancer in females and males. 3) To review and analyze the current research of breast cancer in males. 4) To understand the psychological and social implications of breast cancer in men.







MSCU41

Case-based Review of Ultrasound (An Interactive Session)

Wednesday, Nov. 29 1:30PM - 3:00PM Room: S406A

US

AMA PRA Category 1 Credits ™: 1.50 ARRT Category A+ Credit: 1.75

FDA Discussions may include off-label uses.

Participants

Deborah J. Rubens, MD, Rochester, NY (Director) Nothing to Disclose

For information about this presentation, contact:

Deborah_rubens@urmc.rochester.edu

LEARNING OBJECTIVES

1) Recognize the diverse applications of ultrasound throughout the body and identify those situations in which it provides the optimal diagnostic imaging choice. 2) Understand the fundamental interpretive parameters of ultrasound contrast enhancement and its applications. 3) Know the important factors to consider when choosing ultrasound for image guided procedures and how to optimize ultrasound for technical success.

ABSTRACT

Ultrasound is a rapidly evolving imaging modality which has achieved widespread application throughout the body. In this course we will address the major anatomic areas of ultrasound use, including the abdominal and pelvic organs, superficial structures and the vascular system. Challenging imaging and clinical scenarios will be emphasized to include the participant in the decision making process. Advanced cases and evolving technology will be highlighted; including the use of ultrasound contrast media and elastography as diagnostic techniques. The selection of ultrasound for interventional guidance will be addressed, as will the unique applications of ultrasound to emergency imaging including obstetrics and pediatrics.

Sub-Events

MSCU41A Ultrasound Advances: Elastography and Contrast

Participants

Richard G. Barr, MD, PhD, Campbell, OH (*Presenter*) Consultant, Siemens AG; Consultant, Koninklijke Philips NV; Research Grant, Siemens AG; Research Grant, SuperSonic Imagine; Speakers Bureau, Koninklijke Philips NV; Research Grant, Bracco Group; Speakers Bureau, Siemens AG; Consultant, Toshiba Medical Systems Corporation; Research Grant, Esaote SpA; Research Grant, BK Ultrasound; Research Grant, Hitachi, Ltd

LEARNING OBJECTIVES

Review the clinical uses of elastography in routine practice.
 Discuss the advantages and disadvantages of elastography.
 Review the uses of ultrasound contrast - on label and off label.
 Discuss how CEUS can be incorporated into a routine practice.
 Review the materials need to develop a CEUS program.

ABSTRACT

This course will review the clinical uses of ultrasound elastography and contrast enhanced ultrasound. The course will review the uses of ultrasound elastography in routine clinical practice. The advantages and disadvantages of elastography will be discussed on various organ systems. A brief overview of how to develop a CEUS program will be presented. Both on label and off label uses of CEUS will be reviewed. How to incorporate a CEUS program into routine clinical practice will be presented.

Honored Educators

Presenters or authors on this event have been recognized as RSNA Honored Educators for participating in multiple qualifying educational activities. Honored Educators are invested in furthering the profession of radiology by delivering high-quality educational content in their field of study. Learn how you can become an honored educator by visiting the website at: https://www.rsna.org/Honored-Educator-Award/ Richard G. Barr, MD, PhD - 2017 Honored Educator

MSCU41B Vascular Ultrasound

Participants Leslie M. Scoutt, MD, New Haven, CT (*Presenter*) Speaker, Koninklijke Philips NV

For information about this presentation, contact:

leslie.scoutt@yale.edu

LEARNING OBJECTIVES

View Learning Objectives under main course title

ABSTRACT

Case based review of vascular ultrasound

Honored Educators

Presenters or authors on this event have been recognized as RSNA Honored Educators for participating in multiple qualifying educational activities. Honored Educators are invested in furthering the profession of radiology by delivering high-quality educational content in their field of study. Learn how you can become an honored educator by visiting the website at: https://www.rsna.org/Honored-Educator-Award/ Leslie M. Scoutt, MD - 2014 Honored Educator

MSCU41C Obstetric Ultrasound-Urgent and Emergent Cases

Participants

Phyllis Glanc, MD, Toronto, ON (Presenter) Nothing to Disclose

For information about this presentation, contact:

Phyllis.Glanc@sunnybrook.ca

LEARNING OBJECTIVES

View Learning Objectives under main course title

ABSTRACT

This course will present cases related to obstetrics that involve either urgent or emergent care for mother and/or her fetus. This will includes events which may occur in the early post-partum state.

URL

phyllisglanc.com

Active Handout: Phyllis Glanc

http://abstract.rsna.org/uploads/2017/17000491/Active MSCU41C.pdf

MSCU41D Abdominal Ultrasound

Participants Jason M. Wagner, MD, Oklahoma City, OK (*Presenter*) Nothing to Disclose

For information about this presentation, contact:

jason-wagner@ouhsc.edu

LEARNING OBJECTIVES

1) Use Doppler to diagnose hepatic diseases. 2) Recognize common sonographic pitfalls in the diagnosis of gallbladder and kidney conditions. 3) Diagnose abdominal wall abnormalities with ultrasound.

ABSTRACT

Case based review of abdominal ultrasound.









MSES43

Essentials of Neuro Imaging

Wednesday, Nov. 29 1:30PM - 3:00PM Room: S100AB

NR

AMA PRA Category 1 Credits ™: 1.50 ARRT Category A+ Credit: 1.75

Participants

David M. Yousem, MD, Baltimore, MD (*Moderator*) Royalties, Reed Elsevier; Royalties, Oakstone Publishing, LLC; Employee, Medicolegal Consultation; ; ;

Sub-Events

MSES43A Percutaneous Image-guided Spine Interventions

Participants Vikas Agarwal, MD, Pittsburgh, PA (*Presenter*) Nothing to Disclose

For information about this presentation, contact:

agarwalv@upmc.edu

LEARNING OBJECTIVES

1) Analyze relevant imaging and relate clinical information to determine appropriateness for various spinal procedures. 2) Identify the risks and benefits of various spine interventional procedures as well as potential complications. 3) Competently and safely perform various spinal procedures using image guidance.

MSES43B Systematic Approach to Cervical Spine Trauma: Latest Trends in Imaging

Participants

Bhavya Rehani, MD, San Francisco, CA (Presenter) Nothing to Disclose

For information about this presentation, contact:

bhavya.rehani@ucsf.edu

LEARNING OBJECTIVES

1) Develop a systematic approach in evaluation of different forms of traumatic cervical spine injury on CT and MRI. 2) Be aware of the latest trends in imaging which can help in aid in better diagnosis of cervical trauma cases. 3) Identify and report bone and soft-tissue injuries to spine surgeons using a patterned checklist approach.

MSES43C Nomenclature of Degenerative Disc Disease

Participants Kader Karli Oguz, MD, Ankara, Turkey (*Presenter*) Nothing to Disclose

For information about this presentation, contact:

karlioguz@yahoo.com

LEARNING OBJECTIVES

1) Be familiar with the standardized disc nomenclature (version2.0) for reporting of degenerative disc disease. 2) Increase the reproducibility and consistency of radiological reports and use a common terminology with the clinicians.

MSES43D Demyelinating Disorders of the Spinal Cord

Participants

Izlem Izbudak, MD, Baltimore, MD (*Presenter*) Institutional Grant support, Biogen Idec Inc; Consultant, Alexion Pharmaceuticals, Inc; Institutional Grant support, Siemens AG;

For information about this presentation, contact:

iizbuda1@jhmi.edu

LEARNING OBJECTIVES

1) Recognize and differentiate demyelinating lesions of multiple sclerosis from other causes of inflammatory myelitis. 2) Understand etiologic and radiological differences between multiple sclerosis and neuromyelitis optica spectrum disorders. 3) Recognize 5 most common demyelinating diseases of the spinal cord.







MSRO43

BOOST: Lymphoma, Pediatrics, Sarcoma-Science Session with Keynote

Wednesday, Nov. 29 1:30PM - 2:30PM Room: S103CD



AMA PRA Category 1 Credit ™: 1.00 ARRT Category A+ Credit: 1.00

Participants

Hui-Kuo G. Shu, MD, PhD, Atlanta, GA (*Moderator*) Speakers Bureau, Varian Medical Systems, Inc; Stockholder, General Electric Company; Stockholder, Medtronics plc; Stockholder, Mylan NV ; Stockholder, Apple Inc; Stockholder, ICON plc Yolanda D. Tseng, MD, Seattle, WA (*Moderator*) Nothing to Disclose

Sub-Events

MSR043-01 Invited Speaker:

Wednesday, Nov. 29 1:30PM - 1:40PM Room: S103CD

Participants

Yolanda D. Tseng, MD, Seattle, WA (Presenter) Nothing to Disclose

MSR043-02 Identifying Radiation Induced Brain Abnormalities in Adult Survivors of Pediatric Brain Tumor from "Normal-Appearing" MRI Using a Machine Learning Approach

Wednesday, Nov. 29 1:40PM - 1:50PM Room: S103CD

Participants

Leonardo Tang, Atlanta, GA (*Abstract Co-Author*) Nothing to Disclose Silun Wang, MD, PhD, Atlanta, GA (*Presenter*) Nothing to Disclose Liya Wang, MD, Atlanta, GA (*Abstract Co-Author*) Nothing to Disclose Hui Mao, PhD, Atlanta, GA (*Abstract Co-Author*) Nothing to Disclose

PURPOSE

Radiation treatment may cause long-term adverse effects on brain tissue and cognitive function in pediatric brain tumor patients. The aim of this study is to use machine learning methods to search and extract the possible radiation induced abnormalities from the MRI data of a patient cohort, and further to characterize radiation-induced neurodegenerative effects on white and gray matters.

METHOD AND MATERIALS

14 adult survivors of pediatric brain tumors (with median radiation dose of 5400 cGy) who undergone extensive radiation treatment (RT) and demographically matched healthy controls (mean age: 22.7 ± 4.5 vs. 22.9 ± 4.3 , p>0.05) were enrolled in the study. MPRAGE images used in this study were acquired with TR/TE = 2250/4ms, slice thickness = 1 mm, FOV = 256 mm2. All MRI data were preprocessed based the scheme shown in Figure 1 using the Statistical Parametric Mapping (SPM12) software package. Machine learning analysis was conducted using the Pattern Recognition for Neuroimaging Toolbox (PRoNTo) and run on GM and WM separately. The data were mean-centered and a Gaussian Processes Regression (GPR) model was defined using age as the dependent variable and the similarity matrix of imaging data as the independent variables.

RESULTS

The GPR model successfully differentiated the RT and controls with diagnostic accuracy of 100% in both white matter and gray matter analysis. Figure 2 shows the weighted display indicating the specific regions in WM and GM exhibiting the abnormalities in RT subjects comparing to the controls, which contribute to this classification of RT and control. In weighted display in WM, frontal lobe WM (i.e., anterior corpus callosum) contributes to the largest difference between RT and control (deep blue area), which is consistent with our previous results based on the analysis of diffusion tensor images (Wang, et al, 2015, PLOS One). However, in weighted display in GM, there is no specific region that exhibits the difference or contributes to the classification

CONCLUSION

Machine learning based method and model for predicting radiation induced neurodegenerative effect on adult survivor of brain tumor patient led to the successful identification of the abnormal regions in the brain of RT patients using just T1 weighted MPRAGE.

CLINICAL RELEVANCE/APPLICATION

Further development and application of this approach will enable integrated use of machine-learning assisted radiological assessment of treatment effect.

MSR043-03 Profiling Myxofibrosarcoma: Patient and Disease Characteristics as Well as Clinical Outcomes at a Major Tertiary Care Cancer Center

Gaurav Bhattacharya, Ottawa, ON (*Presenter*) Nothing to Disclose Matthew`Tsang, MSc, Ottawa, ON (*Abstract Co-Author*) Nothing to Disclose Horia Marginean, Ottawa, ON (*Abstract Co-Author*) Nothing to Disclose Samy El-Sayed, MD, Ottawa, ON (*Abstract Co-Author*) Nothing to Disclose

For information about this presentation, contact:

gbhattacharya@toh.ca

ABSTRACT

Purpose/Objective(s): Formerly known as a myxoid variant of malignant fibrous histiocytoma (MFH), myxofibrosarcomas occupy their own niche in the World Health Organization classification in the category of fibroblastic and myofibroblastic tumors. With a predisposition for the elderly, they possess a high post treatment local recurrence rate. We take a close look at this soft tissue sarcoma subtype to highlight the incidence as well as outcomes at our large teaching hospital. Materials/Methods: A retrospective chart review was first undertaken to identify myxofibrosarcoma patients over a 10 years span from 1/2005 to 1/2015 with follow up data through to 2/2017 to guarantee at least 2 years of post-treatment data from a pool of aggregated soft tissue sarcoma tumors. Information was gathered via Electronic Medical Records, paper charts and communication with peripheral facilities and family physicians' offices. Sole inclusion criterion was histologic disease confirmation in patients aged = 18. A comprehensive literature review was also undertaken to determine current developments for this histology. Overall survival was analyzed using Kaplan-Meier methodology. Results: Thirty nine patients meeting selection criterion were selected from a total of 968 entries. With a largely male incidence (61.5%), the most common presenting symptom was a painless mass (95%). Median age was 62 years with a median follow up of 45 months. Commonest occurrence was in the extremities and superficial trunk (82%) with a median tumor size of 9.5 cm. Grade 2 disease at 41% was followed by 20.5% for both Grade 1 and 3 diseases according to the FNLCC (Federation Nationale des Centres de Lutte Contre le Cancer) system. Median pre-treatment hemoglobin post diagnosis was 12.8 g/dL. Curative intent treatment was offered in 87% of cases; with surgery in 92% of cases, being the primary modality of treatment. Radiation therapy (median fractionation of 50 Gy in 25 fractions) and chemotherapy were provided in 74% and 18% of cases respectively, primarily in an adjuvant setting for curative intent patients.Post-surgical margins were positive in 22% of patients and lymphovascular invasion identified in only 2 cases. Median time from diagnosis to initiation of primary treatment was 30 days with median time from radiotherapy start to end being 35 days. Sixty percent of curative intent patients receiving radiation had Threedimensional Conformal Radiotherapy (3D-CRT) planning Stage distribution by incidence was: Stage I 18%, Stage II 49%, Stage III 21% and Stage IV 10%. Thirty six percent of patients had a recurrence or disease progression with only 4 having a local component. Of the 11 patients who had a recurrence, 8 were stage II and 3 were stage III. Overall, three and five year overall survival estimates were 70% and 67% respectively. Conclusion: Treatment outcomes for myxofibrosarcoma remain relatively good at our large tertiary cancer centre. More research is required to identify strategies in enhancing both locoregional and systemic control.

MSR043-04 Local Control in Pediatric Adolescent Meningiomas Treated with Proton Radiotherapy

Wednesday, Nov. 29 2:00PM - 2:10PM Room: S103CD

Participants

Anne Sailer, Boston, MA (Presenter) Nothing to Disclose

For information about this presentation, contact:

anne.sailer@my.rfums.org

ABSTRACT

Purpose/Objective(s): Pediatric meningiomas comprise less than 5% of pediatric CNS tumors. Limited pediatric data indicate that extent of surgical resection and tumor grade are strong prognostic factors for relapse free survival, but little data exists on the efficacy of radiotherapy in pediatric meningioma. Here we report the outcomes of pediatric meningioma patients treated with proton radiotherapy (PRT), which was used to minimize late effects of treatment. Materials/Methods: Eighteen patients were treated with PRT from 2005-2015 at our institution. Histologic WHO grade distribution was as follows: seven grade I, (38.8%, one with atypical features); 10 grade II (55.6 %), one grade III (5.6%). Fifteen patients had gross disease at the initiation of PRT. Three patients (with grade II or III tumors) had no visible disease at the time of PRT. The median PRT dose was 54 GyE, delivered in 1.8 GyE fractions (range, 50.4-63.4 GyE). The radiographic response of gross tumor was measured by a change in tumor volume after PRT. Clinical outcome including disease control and toxicities were reviewed and graded according to CTCAE v4.0. Results: The median follow-up time was 4.0 years with an estimated 5-year DFS and Local control rate of 100%. However one patient died from causes unrelated to disease or treatment. Eight of 15 pts with gross disease at PRT (53.3%) had decreased tumor size after PRT treatment; six (33.3%) had stable disease; and one was lost to follow up. Sequelae from treatment were minor and affected 8 of 17 patients and include: Moyamoya disease (5.6%; successfully treated), chronic headaches (18.7%), occasional grade 1-2 headaches (16.7%), radiation retinopathy (5.6%), and central endocrine deficit (11.1%). Patients who experienced hearing loss, vision loss, or seizures after PRT had these conditions at baseline prior to PRT. The mean CTV volume for patients with and without late toxicities was 41.8 cc (6.7-107.7) vs. 46.9 cc (1.7-157.4). Tumor location in the anterior cranial fossa, sphenoid wing, and optic canal were correlated with late side effects compared with other intracranial regions. Tumors near the cavernous sinus, the circle of Willis, or optic nerves were associated with the most co-morbidities at baseline.Conclusion: PRT is both safe and effective in treating pediatric meningioma. Further follow up is needed to determine if gross residual disease at the time of radiation diminishes disease control. Tumor location was more correlated with side effects than target volume.

MSR043-05 Early Experience with Unidirectional Planar Brachytherapy for IORT of Abdominal Malignancies

Wednesday, Nov. 29 2:10PM - 2:20PM Room: S103CD

Participants

Heming Zhen, PhD, Boston, MA (*Presenter*) Nothing to Disclose Julius Turian, PHD, Chicago, IL (*Abstract Co-Author*) Nothing to Disclose Minh B. Luu, Chicago, IL (*Abstract Co-Author*) Nothing to Disclose Neilayan Sen, MD, Chicago, IL (*Abstract Co-Author*) Nothing to Disclose James C. Chu, PhD, Chicago, IL (*Abstract Co-Author*) Nothing to Disclose Ross A. Abrams, MD, Chicago, IL (*Abstract Co-Author*) Nothing to Disclose Dian Wang, MD, PhD, Columbus, OH (*Abstract Co-Author*) Nothing to Disclose

ABSTRACT

Purpose/Objective(s): Recently, an innovative unidirectional Pd-103 low-dose-rate brachytherapy device, CivaSheet (CivaTech Durham, NC) has been developed as a promising IORT tool. The purpose of this study is to report our initial clinical experience using this new IORT technology to boost the tumor bed after preoperative radiotherapy and resection of abdominal malignancies. The positional stability of device following its placement is investigated using sequential post-implant CT scans. Materials/Methods: The CivaTech IORT was utilized to boost the tumor bed after resection of abdominal malignancies in two patients (recurrent retroperitoneal liposarcoma and recurrent gastric adenocarcinoma, respectively). Prior to surgery each patient underwent a CT simulation for IORT boost dosimetry planning. PTV predicted for high risk recurrence after resection were delineated via a joint effort between the radiation oncologist and the surgeon. Eclipse Treatment Planning System (Varian, Palo Alto, CA) was used for dosimetry planning. For patient 1, a 5 x 15 cm2 (108 dots, 0.8 U/dot) sheet was chosen, to prescribe 25 Gy to at least 90% of the PTV. For patient 2, a 5x10 cm2(66 dots, 0.62 U/dot) was chosen to prescribe 26 Gy to at least 90% of the PTV. Each patient underwent a successful resection of intra-abdominal malignancy. Since the Pd-103 radioactive dots are held in a spatial matrix (8 mm spacing) by a bio-absorbable membrane, with a 6 weeks onset to absorption, the positional stability of the device was investigated using post implant sequential CT scans. Dosimetric evaluation was done on CT scans acquired at specific time intervals. Results: The CivaSheet was successfully placed over the tumor bed PTV with its gold face up, which spares any normal tissue structures on top from high dose irradiation. Absorbable stitches were used to secure the device. The CivaSheet placement added 10-12 min of operative time. Postoperative recovery was uneventful for both patients. Patient 1 had CT scans at 2.5 weeks (Pd-103 T1/2 = 17 days) and 3 months post implant. Patient 2 had CT scans at 1 week and 6 weeks post implant. For both patients, all seeds were detected in the tumor bed, without regional or distant migration. A slight trend toward seed clustering was noticed on the 3 months scan for patient 1, but not on the 6 weeks scan for patient 2. PTV dosimetric coverage analysis showed D90 =25.5 Gy (102% Rx) and 29 Gy (116% of Rx) for the two post implant CT scans for patient 1. For patient 2 D90=26 Gy (100% Rx) and 28 Gy (108% Rx) was shown for the two post implant CT scans. No patient experienced complications related to CivsSheet placement or its postoperative presence. Conclusion: We found that the unidirectional CivaTech planar brachytherapy device is safe, suitable and versatile for the treatment of abdominal malignancies. CT dosimetry demonstrated no significant device movement or seed migration, while PTV coverage was well maintained up to 3 months post implant.







MSSR43

RSNA/ESR Hybrid Imaging Symposium: Hybrid Imaging in the Male (An Interactive Session)

Wednesday, Nov. 29 1:30PM - 3:00PM Room: S402AB



AMA PRA Category 1 Credits ™: 1.50 ARRT Category A+ Credit: 1.75

Participants

Alexander Drzezga, MD, Cologne, Germany (*Moderator*) Consultant, Siemens AG; Consultant, Bayer AG; Consultant, General Electric Company; Consultant, Eli Lilly and Company; Consultant, The Piramal Group; Speakers Bureau, Siemens AG; Speakers Bureau, Bayer AG; Speakers Bureau, General Electric Company; Speakers Bureau, Eli Lilly and Company; Speakers Bureau, The Piramal Group Katrine Riklund, MD, PhD, Umea, Sweden (*Moderator*) Nothing to Disclose

Sub-Events

MSSR43A Prostate Cancer: PET, MR or Both?

Participants

Frederik L. Giesel, MD, MBA, Heidelberg, Germany (Presenter) Patent application for F18-PSMA-1007

LEARNING OBJECTIVES

1) Learn about pathophysiology in prostate cancer. 2) Understand how to interpret hybrid imaging of prostate cancer. 3) Learn about the role of hybrid imaging in staging, treatment evaluation and follow-up.

MSSR43B Prostate Cancer: Novel Tracers

Participants

Steven P. Rowe, MD, PhD , Parkville, MD (Presenter) Nothing to Disclose

LEARNING OBJECTIVES

1) Learn about novel tracer and their biochemical properties. 2) Understand the differences of information given by the use of different tracers. 3) Understand how to interpret examinations with different tracers.

MSSR43C Interactive Case Discussion

Participants

Frederik L. Giesel, MD, MBA, Heidelberg, Germany (*Presenter*) Patent application for F18-PSMA-1007 Steven P. Rowe, MD, PhD , Parkville, MD (*Presenter*) Nothing to Disclose

LEARNING OBJECTIVES

1) Learn how to interpret hybrid imaging of prostate cancer. 2) Understand the pathophysiology in relation to imaging.





PS40

Wednesday Plenary Session

Wednesday, Nov. 29 1:30PM - 2:45PM Room: E450A

RO

AMA PRA Category 1 Credits ™: 1.25 ARRT Category A+ Credit: .75

Participants

Richard L. Ehman, MD, Rochester, MN (Presenter) CEO, Resoundant, Inc; Stockholder, Resoundant, Inc;

Honored Educators

Presenters or authors on this event have been recognized as RSNA Honored Educators for participating in multiple qualifying educational activities. Honored Educators are invested in furthering the profession of radiology by delivering high-quality educational content in their field of study. Learn how you can become an honored educator by visiting the website at: https://www.rsna.org/Honored-Educator-Award/ Richard L. Ehman, MD - 2016 Honored Educator

Sub-Events

PS40A Announcement of Education Exhibit Awards

PS40B Announcement of Quality Storyboard Awards

PS40C Annual Oration in Radiation Oncology: Personalized Medicine and Radiation Oncology

Participants

Daphne A. Haas-Kogan, MD, Boston, MA (*Presenter*) Nothing to Disclose Edward Y. Kim, MD, Seattle, WA (*Presenter*) Nothing to Disclose

Precision Medicine provides challenges and opportunities to Radiologists and Radiation Oncologists alike. If harnessed thoughtfully Personalized Medicine offers avenues for renewed significance, relevance, and value of radiation for our cancer patients. For us as Radiation Oncologists, what is the meaning of Personalized Medicine? The first definition is our ability to choose the right therapy for each individual's unique tumor. One example is the promise of using radiomic predictors for radiation planning. Unlike biopsies, that may be difficult to perform, virtually all cancer patients receive imaging scans to track their disease, and the field of radiomics is successfully defining imaging biomarkers based on quantitative descriptions of tumor phenotypes to improve predictions of treatment response and prognosis. Radiomic imaging features will predict overall survival, distant metastasis, treatment response, and somatic mutations, will be a critical tool in identifying patients most likely to benefit from radiation and will help generate radiotherapy plans that will reduce doses to organs at risk and maximize dose to cancerous lesions. The second meaning of Personalized Medicine is our commitment to engineer drugs and design approaches that target the tumor specifically and spare the patient's normal tissues. An example is the opportunity to use focused radiation to not only selectively kill tumor cells but also turn them into immune stimulating centers that work like vaccine, thus targeting the patient's cancer while sparing normal tissues. Immunotherapy and specifically immune checkpoint blockade have demonstrated enormous success in treating solid tumors such as melanoma, lung cancer, and head and neck cancer. However, the majority of patients do not respond to treatment with immune checkpoint blockade alone. This resistance may be the inability of the immune system to adequately recognize tumors as foreign especially as current immune therapies primarily work by releasing the brakes on pre-existing immune responses. Thus, complimentary therapies such as vaccines that catalyze these tumor specific immune responses are needed. However, tumor vaccines are difficult to engineer and generally need to be tumor specific, which dramatically limits their use and effectiveness. Targeted radiation can kill tumor cells in a way that stimulates the immune system to recognize tumors as foreign, resulting in vaccine-like effects. The third meaning of Personalized Medicine in Radiation Oncology includes enhanced precision empowered by a new class of MRI devices that is creating a paradigm shift in radiation therapy delivery. High-precision radiation therapy techniques (e.g. IMRT, SRS, SBRT) can deliver high doses of radiation to tumors with sub-millimeter accuracy while sparing normal tissues, and rely on high resolution imaging as a basis for both treatment planning and intra-treatment setup and monitoring. Currently, the majority of radiation treatment planning is performed via CT-based imaging, and image-guided RT is delivered using X-ray imaging on conventional X-ray-guided linear accelerators with alignment to bone/implanted markers as surrogates of tumor location. Magnetic resonance imaging (MRI) provides several benefits over CT-based imaging including higher soft tissue resolution, functional imaging and continuous imaging without exposing patients to ionizing radiation. For radiation therapy of soft tissue tumors (e.g. Breast, GI, GU, Gyn, Head and Neck, Sarcoma), the higher resolution of MRI can improve target delineation, thereby allowing more precise radiation therapy that can spare surrounding normal tissues, reduce toxicities, and improve outcomes for many of our cancer patients. Last but not least, the fourth meaning of Personalized Medicine is our commitment, as caretakers of patients facing frightening, daunting, overwhelming diagnoses, to attend to each patient's unique needs, as an individual and member of a family and community.







SPHA41

Hospital Administrators Symposium

Wednesday, Nov. 29 1:30PM - 4:50PM Room: N228



ARRT Category A+ Credits: 4.00 AMA PRA Category 1 Credits ™: 3.25

Participants

Gregory N. Nicola, MD, River Edge, NJ (Moderator) Nothing to Disclose

For information about this presentation, contact:

gnnicola@yahoo.oom

Sub-Events

SPHA41A Introduction

Participants Gregory N. Nicola, MD, River Edge, NJ (*Presenter*) Nothing to Disclose

For information about this presentation, contact:

gnnicola@yahoo.com

SPHA41B What's Next in the Quality Payment Program for Year 2

Participants Ezequiel Silva III, MD, San Antonio, TX (*Presenter*) Nothing to Disclose

LEARNING OBJECTIVES

1) Discuss the Year 2 updates to the Medicare Access & CHIP Reauthorization driven Quality Payment Program (QPP). 2) Apply practical solutions to improve scoring under the Merit-Based Incentive Payment System. 3) Postulate radiology's role in the alternative payment models defined by the QPP.

SPHA41C Leveraging Informatics for Improving Department Efficiencies

Participants

William H. Moore, MD, Port Washington, NY (Presenter) Nothing to Disclose

LEARNING OBJECTIVES

1) Understand the layers of data necessary to understand the operational aspects of a department. 2) Be able to Describe the technologist specific metrics. 3) Be able to describe the metric for support staff. 4) Be able to understand and explain the metrics needed for leadership. 5) Understand the importance of monitoring and incentivizing metrics.

SPHA41D A Radiology Alternative Payment Model

Participants Nina E. Kottler, MD, MS, Sydney, Australia (*Presenter*) Nothing to Disclose

For information about this presentation, contact:

nina.kottler@radpartners.com

LEARNING OBJECTIVES

1) Recognize how to motivate a practice to adopt a best practice recommendation using a data-driven methodology. 2) Discuss a data mining infrastructure which provides feedback to ensure high-level adherence to best practice recommendations. 3) Summarize metrics which capture clinical value related to patient care improvement and/or cost reduction. 4) Identify a value proposition to a payor which can be used to enter a performance-based contract.

SPHA41E Question and Answer

Participants Ezequiel Silva III, MD, San Antonio, TX (*Presenter*) Nothing to Disclose William H. Moore, MD, Port Washington, NY (*Presenter*) Nothing to Disclose Nina E. Kottler, MD, MS, Sydney, Australia (*Presenter*) Nothing to Disclose

For information about this presentation, contact:

nina.kottler@radpartners.com

SPHA41G How to Get Your Business Ready for Value

Participants

Andrew R. Menard, JD, Boston, MA (*Presenter*) Board of Directors, Cary Pharmaceuticals Inc; Stockholder, Cary Pharmaceuticals Inc; Board of Directors, Millikelvin Technologies, LLC; Stockholder, Millikelvin Technologies, LLC; Stockholder, Handa Pharmaceuticals, LLC

For information about this presentation, contact:

amenard1@bwh.harvard.edu

LEARNING OBJECTIVES

1) To understand approaches for complying with the Medicare Access and CHIP Reauthorization Act of 2015 (MACRA) including the elements of advanced Alternative Payment Models (APMs) and Merit-based Incentive Payment System (MIPS) under MACRA, how a hospital or health system can demonstrate compliance with the requirements of MIPS, the role of radiologists and radiology departments in demonstrating MIPS and APM compliance, and the benefits and burdens of MIPS and APM approaches.

SPHA41H Certified Electronic Health Records and Radiology

Participants

Andrew B. Rosenkrantz, MD, New York, NY (Presenter) Nothing to Disclose

For information about this presentation, contact:

Andrew.Rosenkrantz@nyumc.org

LEARNING OBJECTIVES

1) To understand how adoption of Certified Electronic Health Records Technology (CEHRT) provides radiologists with an opportunity to further promote their value to patients and referring physicians. 2) To understand how adoption of CEHRT will aid radiologists in satisfying performance requirements for both payment pathways under MACRA. 3) To recognize the historical challenges to radiologists for adopting Certified Electronic Health Records Technology, as well as potential avenues for addressing such challenges moving forward.

SPHA41I Question and Answer

Participants

Mark H. Michalski, MD, Boston, MA (Presenter) Nothing to Disclose

Andrew R. Menard, JD, Boston, MA (*Presenter*) Board of Directors, Cary Pharmaceuticals Inc; Stockholder, Cary Pharmaceuticals Inc; Board of Directors, Millikelvin Technologies, LLC; Stockholder, Millikelvin Technologies, LLC; Stockholder, Handa Pharmaceuticals, LLC

Andrew B. Rosenkrantz, MD, New York, NY (Presenter) Nothing to Disclose







VSIO41

Interventional Oncology Series: Basic Science and Imaging

Wednesday, Nov. 29 1:30PM - 6:00PM Room: S405AB

IR

ARRT Category A+ Credits: 5.00 AMA PRA Category <u>1 Credits ™</u>: <u>4.25</u>

FDA Discussions may include off-label uses.

Participants

S. Nahum Goldberg, MD, Ein Kerem, Israel (*Moderator*) Consultant, AngioDynamics, Inc; Research support, AngioDynamics, Inc; Consultant, Cosman Medical, Inc;

Muneeb Ahmed, MD, Wellesley, MA (*Moderator*) Research Grant, General Electric Company; Stockholder, Agile Devices, Inc; Scientific Advisory Board, Agile Devices, Inc

LEARNING OBJECTIVES

 Characterize the most important cutting-edge advances of interventional oncologic techniques. 2) Gain a better understanding of the intraprocedural and follow-up imaging techniques that facilitate successful state of the art interventional oncologic practice.
 Understand how and why mechanistic studies can have an impact on both daily clinical practice and future therapeutic paradigms. 4) Gain awareness of the extent of potentially beneficial and harmful systemic effects of "focal" interventional oncologic therapy.

ABSTRACT

The first half of the session will has been organized into a thematic unit entitled: "So what's new in" and will provide a series of seven lectures by leaders in the field each dedicated to discussing advances in individual interventional oncologic platforms. For transcatheter therapy, this will include discussion of both novel agents for chemoembolization and new transarterial methods of delivery, as well as the latest techniques for optimizing radioembolization. Advances in four percutaneous ablative techniques: chemical, radiofrequency, microwave, and IRE will each be addressed in turn. A highlight of the session will be two keynote addresses regarding cutting edge imaging that has facilitated the revolution in "image-guided" interventional oncology procedures. Dr. Brad Wood of the NIH, a noted thought leader in the field will present "Intraprocedural imaging - the keystone of IO" whereas Prof. Riccardo Lencioni will lecture on "Cutting edge imaging techniques for follow-up". The second half of the session has been organized into a thematic unit entitled: "Mechanisms Matter: Basic science every IO should know" and will be dedicated to gaining an appreciation of the basic scientific underpinnings of interventional oncology and understand how and why such studies can have an impact on both daily clinical practice and future therapeutic paradigms. This will include lectures that center upon key mechanistic pathways that are being used to improve transcatheter embolization and tumor ablation - particularly in combinationand a lecture on the role of potential mechanistic biomarkers that can be used to predict outcomes. Additionally, two presentations will then outline our current understanding of the potential systemic implications of post-procedure, cytokine-mediated inflammation - the negative effects of leading to tumorigenesis and the potential beneficial immune (abscopic) effects of IO therapies. The session will further include selected complementary abstract presentations that highlight innovative research in these thematic areas.

Sub-Events

VSIO41-01 What's New In...

Participants

S. Nahum Goldberg, MD, Ein Kerem, Israel (*Moderator*) Consultant, AngioDynamics, Inc; Research support, AngioDynamics, Inc; Consultant, Cosman Medical, Inc;

For information about this presentation, contact:

sgoldber@bidmc.harvard.edu

LEARNING OBJECTIVES

View learning objectives under main course title.

VSI041-02 What's New in Embolization Agents

Wednesday, Nov. 29 1:30PM - 1:45PM Room: S405AB

Participants

Stephen J. Hunt, MD, PhD, Philadelphia, PA (Presenter) Nothing to Disclose

LEARNING OBJECTIVES

View learning objectives under main course title.

VSI041-03 Development of a Pumping Device to Form Ideal Lipiodol Emulsion in Transarterial Chemoembolization

Participants Toshihiro Tanaka, MD, Kashihara, Japan (*Presenter*) Nothing to Disclose Kimihiko Kichikawa, MD, Kashihara, Japan (*Abstract Co-Author*) Nothing to Disclose Tetsuya Masada, Kashihara, Japan (*Abstract Co-Author*) Nothing to Disclose Hideyuki Nishiofuku, Kashihara, Japan (*Abstract Co-Author*) Nothing to Disclose Yasushi Fukuoka, Kashihara, Japan (*Abstract Co-Author*) Nothing to Disclose Takeshi Sato, Kashihara, Japan (*Abstract Co-Author*) Nothing to Disclose Shota Tatsumoto, Kashihara, Japan (*Abstract Co-Author*) Nothing to Disclose

For information about this presentation, contact:

toshihir@bf6.so-net.ne.jp

PURPOSE

A pumping device constructed with a membrane made with Sirasu Porous Glass (SPG) was developed to improve the properties of lipiodol emulsion for cTACE. The purpose of this ex vivo study was to examine the physiochemical properties and the stabilities of emulsions formed by using the SPG pumping device were examined and compared with emulsions formed by using a 3-way-cock.

METHOD AND MATERIALS

Epirubicin solutions were mixed with lipiodol with pumping exchanges using the SPG pumping device with the membrane pore size of 50µm in diameter which has hydrophilic surface or a 3-way stopcock. The ratios of epirubicin solution to lipiodol were 1:2 or 1:1. A total of 120 emulsions (SPG 60, 3-way-cock 60) were created to evaluate the percentages of W/O, droplet sizes, viscosities, microscopic findings and these stabilities for 30 minutes.

RESULTS

SPG showed significantly higher %W/O percentages when compared with a 3-way-cock (97.9% vs 68.9% in 1:2 ratio, and 82.1% vs 17.8% in 1:1 ratio, P < .001). The mean droplet sizes in SPG did not show significant change from 40.3µm at 0 minutes to 39.8µm at 30 minutes after the pumping, whereas those in 3-way-cock significantly enlarged from 33.7µm to 56.9µm. The mean values of viscosities in SPG did not show significant change for 30 minutes after the pumping from 123.5cp to 120.6cp, whereas those in 3-way-cock significantly decreased from 157.2cp to 78.5cp.

CONCLUSION

SPG pumping device can form high percentage W/O emulsion with stable droplets size and viscosity. This developed device is promising to increase therapeutic effects in cTACE.

CLINICAL RELEVANCE/APPLICATION

Almost 100% W/O emulsion with stable droplets size and viscosity formed by this developed pumping device could improve therapeutic effect in cTACE for HCC patients.

VSI041-04 What's New in Transarterial Methods of Delivery

Wednesday, Nov. 29 1:55PM - 2:10PM Room: S405AB

Participants

Steven C. Rose, MD, San Diego, CA (*Presenter*) Stockholder, Sirtex Medical Ltd; Proctor, Sirtex Medical Ltd; Scientific Advisory Board, Surefire Medical, Inc; Consultant, Surefire Medical, Inc; Stockholder, Surefire Medical, Inc; Consultant, Embolx, Inc; Consultant, Guerbet SA; Consultant, XLSciTech, Inc

For information about this presentation, contact:

scrose@ucsd.edu

LEARNING OBJECTIVES

1) Understand the effect of deployment of anti-reflux devices (Surefire or occlusion balloons) on the blood pressure within the downstream vascular compartment. 2) Comprehend the effects of anti-reflux devices on blood flow direction and hemodynamics of downstream and surrounding vascular compartments. 3) Understand how anti-reflux devices can be utilized to reduce nontarget embolization (retrograde, antegrade, and within the downstream vascular compartment) to improve safety, and potentially increase the relative delivery of embolics into the targeted tumor(s).

ABSTRACT

Anti-reflux devices (Surefire and occlusion balloons), when properly deployed, prevent retrograde nontarget embolization, as designed. In addition, these devices significantly reduce the blood pressure in the downstream vascular compartment. This causes the direction of blood flow in hepaticoenteric arteries to course hepatopedally, providing a high degree of antegrade protection from nontarget embolization. Due to the compartmental reduction of blood pressure, blood from surrounding hepatic and extrahepatic territories flows into the nontumorous compartmental hepatic arteries, causing embolic agents to be flushed from the nontumorus liver into the arteries supplying the tumors, thus increasing the proportion of intracompartmental embolic delivery into the tumors while minimizing delivery into the nontumorous liver. In summary, the effects of anti-reflux devices on compartmental blood pressures and subsequent changes in blood flow direction are complex, but generally improve both the safety and efficay of tumoral embolization, at least within the liver.

LEARNING OBJECTIVES

View learning objectives under main course title.

VSI041-05 What's New in Radioembolization

Wednesday, Nov. 29 2:10PM - 2:25PM Room: S405AB

Jens Ricke, MD, PhD, Munich, Germany (Presenter) Research Grant, Sirtex Medical Ltd; Research Grant, Bayer AG

LEARNING OBJECTIVES

1) To understand current evidence of radioembolization in HCC and colorectal cancer. 2) To understand prevention of radiation induced liver disease.

VSIO41-06 Using Random Survival Forests as a Decision-Support Tool for Survival Analysis in Metastatic Liver Disease after Radioembolization

Wednesday, Nov. 29 2:25PM - 2:35PM Room: S405AB

Participants

Franziska Schoeppe, MD, Munich, Germany (*Presenter*) Nothing to Disclose Michael Ingrisch, Munich, Germany (*Abstract Co-Author*) Nothing to Disclose Karolin J. Kutter, Munich, Germany (*Abstract Co-Author*) Nothing to Disclose Philipp M. Paprottka, Munich, Germany (*Abstract Co-Author*) Nothing to Disclose

For information about this presentation, contact:

Franziska.Schoeppe@med.lmu.de

PURPOSE

To predict outcome of 90-Yttrium radioembolization (RE) from pre-therapeutic baseline parameters and to identify the relative importance of predictive variables of overall survival (OS) using random survival forests (RSF) as a machine-learning approach.

METHOD AND MATERIALS

In this retrospective study, patients with therapy-refractory metastatic liver disease who underwent RE were analyzed. The RSF was trained on the cohort using previously identified predictive factors of OS after RE derived from a Cox regression model. An individual risk of dying for each patient was determined using RSF. Predictive importance of each variable was determined, and partial dependency of predicted risk on pretherapeutic bilirubin and cholinesterase (CHE) levels was evaluated.

RESULTS

We analyzed 366 patients (mean age 62, range 31 to 91 years) with primary (n=92) and secondary liver cancer (n=274). Median OS was 12 months (interquartile range 5-16) with 228 deaths observed during the observation period. The RSF analysis identified CHE and bilirubin as the most important variables with the RSF-averaged lowest minimal depth of 1.2 and 1.5, followed by the type of primary tumor (1.7), age (2.4), tumor burden (2.8) and presence of extrahepatic disease (3.5). Sex had the highest forest-averaged minimal depth (5.5), indicating little predictive value. Baseline bilirubin levels above 1.5 mg/dl were associated with a steep increase in predicted mortality. Similarly, CHE levels below 7.5 U/ predicted a strong increase in mortality. The trained RSF achieved a concordance index of c=0.657, with a standard error of 0.02, comparable to c=0.652 (0.02) of our previously published Cox model.

CONCLUSION

In conclusion, we have utilized a modern machine learning strategy for prediction of OS after RE. Predictive performance of our model was similar to a previously published Cox regression model and, in addition, our study has confirmed the importance of pre-therapeutic levels of CHE and bilirubin.

CLINICAL RELEVANCE/APPLICATION

In OS analysis RSF may serve an important decision-support tool as it does not only allow for identification of predictive factors but also provides useful estimates on their individual importance.

VSI041-07 What's New in Chemical Ablation

Wednesday, Nov. 29 2:35PM - 2:50PM Room: S405AB

Participants

Erik N. Cressman, MD, Houston, TX (Presenter) Nothing to Disclose

LEARNING OBJECTIVES

1) To understand the history of chemical ablation for solid tumors and the role for chemical ablation. 2) Tol be able to state strengths and weaknesses of chemical ablation in comparison to thermal methods and identify potential opportunities for improvement. 3) To understand basic biophysical principles as they pertain to chemical ablation and how to apply them to study of chemical ablation methods. 4) To understand basic techniques to evaluate the effectiveness of chemical ablation in a basic/translational setting, and will acquire a basic understanding of the molecular biology of the stress response induced in vivo by chemical ablation. 5) To be able to articulate the risks inherent in chemical ablation and identify those risks that are unique to chemical ablation compared to thermal methods.

VSI041-08 What's New in Thermal Ablation (RF)

Wednesday, Nov. 29 2:50PM - 3:05PM Room: S405AB

Participants

Jeong Min Lee, MD, Seoul, Korea, Republic Of (*Presenter*) Grant, Bayer AG; Grant, General Electric Company; Grant, Koninklijke Philips NV; Grant, STARmed Co, Ltd; Grant, RF Medical Co, Ltd; Grant, Samsung Electronics Co, Ltd; Grant, Guerbet SA;

For information about this presentation, contact:

jmsh@snu.ac.kr

LEARNING OBJECTIVES

1) Discuss the clinical role of image-quided radiofrequency ablation in the management of liver malignancies 2) Review unmet

clinical need of radiofrequency ablation for liver malignancies. 3) Review recent technological innovations and advances to enhance therapeutic effectiveness of radiofrequency ablation for liver tumors.

VSIO41-09 Combining Temperature Sensitive Liposomes (TSL) with Radiofrequency Ablation (RFA) for the Treatment of Hepatocellular Carcinoma (HCC)

Wednesday, Nov. 29 3:05PM - 3:15PM Room: S405AB

Participants

Osama A. Omrani, London, United Kingdom (*Presenter*) Nothing to Disclose Ounali Jaffer, MBBS, FRCR, London, United Kingdom (*Abstract Co-Author*) Nothing to Disclose Henry G. Sheppard, London, United Kingdom (*Abstract Co-Author*) Nothing to Disclose Gayathri Delanerolle, MBBCHIR, MSc, London, United Kingdom (*Abstract Co-Author*) Nothing to Disclose

PURPOSE

To assess the literature regarding combining TSL with RFA for the treatment of HCC.

METHOD AND MATERIALS

A literature review was carried out using available online databases, namely PubMed, Cochrane reviews and ClinicalTrials.gov. The results will focus on Thermodox (8), as the most highly investigated form of RFA-TSL.

RESULTS

Phase I: A total of 24 patients were included; 9 (38%) with HCC and 15 (63%) with metastatic tumours to the liver. The safe maximum tolerated dose (MTD) was found to be 50 mg/m2. Combined therapy showed a dose-dependent response (p = 0.04), with >=MTD patients having a median survival of 374 days, versus median survival of 80 days in Phase III, HEAT study: A double-blinded, dummy-controlled, randomised controlled trial included 701 patients with HCC sized 3-7 cm, comparing RFA mono-therapy and RFA-LRLD combined therapy. Total length of RFA procedure was proportional to the size of the lesion, ranging from 12 minutes to 60 minutes. Although the study showed that combination therapy was safe, with reversible neutropenia and no hand-foot syndrome or congestive cardiac failure, intention-to-treat (ITT) group analysis of the primary and secondary end points of Progression-free Survival (PFS) (HR = 0.96, 95% CI: 0.79-1.18) and Overall Survival (OS) (HR = 0.95, 95% CI: 0.76-1.20) were not met. Retrospective analysis of the HEAT study was carried out, dividing the treatment group into two subgroups based on RFA dwell time : <45 minutes versus >= 45 minutes. Multivariate Cox regression analysis showed that RFA dwell time (p = 0.05) and number of lesions (p < 0.001) had a significant impact on survival time. Those with a solitary lesion and RFA dwell time >= 45 minutes (n = 285) had an OS HR of 0.63 (95% CI: 0.41-0.96). OPTIMA study: This RCT is based on this added information, recruiting 550 HCC patients with TSL + RFA >= 45 minutes as the treatment arm, and is scheduled to be completed by December 2019. The study is designed to detect, with 80% power, a HR for OS of 0.67.

CONCLUSION

The combination of TSL with RFA has demonstrated the potential for therapeutic use in cases of hepatocellular carcinoma, with a large randomised clinical trial currently underway to further support this.

CLINICAL RELEVANCE/APPLICATION

RFA is currently indicated for moderately sized HCC lesions (3-7cm), but patients suffer from a high reccurance rate which may be alleviated with doxorubicin-loaded TSL combination therapy.

VSI041-10 What's New in Thermal Ablation (MWA)

Wednesday, Nov. 29 3:15PM - 3:30PM Room: S405AB

Participants

Christopher L. Brace, PhD, Madison, WI (*Presenter*) Consultant, NeuWave Medical, Inc; Shareholder, Symple Surgical, Inc; Consultant, Symple Surgical, Inc; Shareholder, Elucent Medical

For information about this presentation, contact:

clbrace@wisc.edu

LEARNING OBJECTIVES

View learning objectives under main course title.

ABSTRACT

The objective of this presentation is to provide an overview of microwave ablation technologies, with a critical review of current devices, techniques and biophysics considerations. Special emphasis will be given to new or emerging technologies and their clinical utilization.

VSI041-11 A Data-Driven Model for Microwave Ablation

Wednesday, Nov. 29 3:30PM - 3:40PM Room: S405AB

Participants

Krishna Nand Keshava Murthy, MSc, Providence, RI (*Presenter*) Nothing to Disclose Scott Collins, RT, Providence, RI (*Abstract Co-Author*) Nothing to Disclose Benjamin B. Kimia, MENG,PhD, Providence, RI (*Abstract Co-Author*) Nothing to Disclose Damian E. Dupuy, MD, Providence, RI (*Abstract Co-Author*) Research Grant, NeuWave Medical Inc Board of Directors, BSD Medical Corporation Stockholder, BSD Medical Corporation Speaker, Educational Symposia Terrance T. Healey, MD, Providence, RI (*Abstract Co-Author*) Nothing to Disclose Derek Merck, PhD, Providence, RI (*Abstract Co-Author*) Nothing to Disclose

For information about this presentation, contact:

PURPOSE

Image-guided thermal ablation (IGTA) is a minimally invasive alternative cancer treatment to surgery and radiotherapy. Physicians currently use the vendor prescribed expected ablation zone for planning, which is based on ex-vivo bovine liver ablation and is inaccurate for in-vivo settings because of organ perfusion, heat sinks and tissue inhomogeneity. We propose a data driven ablation model computed from real patient data that reduces the risk of untreated tumor or damaging critical structures.

METHOD AND MATERIALS

We did a retrospective study of 5 microwave ablation lung cases (Perseon short tip applicator; 60W, 10 min burn) with CT scans taken pre-, intra-, and post-procedurally. The tumor and ablation zone were segmented from the pre- and post-scan respectively. The applicator tip and tail positions were read from the intra-scan. We used deformable image registration to match the anatomy in the three scans using 3D Slicer software. We then extracted applicator centric angular cross sections of the ablation zone for each case and computed a mean ablation curve by averaging ablation boundary curves. Then we computed the mean of all the mean ablation curves (MoM) as our data driven ablation model.

RESULTS

The real ablation zones and the MoM from our data are closer to a tear drop shape and not ellipsoidal as prescribed by the vendor model (maximum difference ~ 4 mm). We show the implications via 3 commonly encountered scenarios: 1) applicator piercing through a large tumor; 2) applicator to one side of a small tumor; 3) a critical structure (heart wall) adjacent to ablation. In these cases, using just the vendor model could lead to untreated tumor or damage critical structure. This can be avoided knowing the tear drop MoM. This is also illustrated in a real patient case. The average sensitivity of covering the real ablation zone for MoM is 4% better that vendor model.

CONCLUSION

We presented a new data driven ablation model computed from real patient data and showed its implications for ablation planning, treatment and mitigating complications. Future work will involve more data, quantitative analysis, comparing soft tissue (liver) to lung, and other antenna types.

CLINICAL RELEVANCE/APPLICATION

Our ablation model can minimize untreated tumor and damage to critical structures. This may reduce likelihood of post ablation recurrence, mitigate complications and increase physician confidence.

VSI041-12 What's New in Non-Thermal Ablation (IRE)

Wednesday, Nov. 29 3:40PM - 3:55PM Room: S405AB

Participants

Alda L. Tam, MD, Houston, TX (Presenter) Medical Monitor, Galil Medical Ltd; Research Grant, AngioDynamics, Inc;

LEARNING OBJECTIVES

1) Describe the mechanism of action of IRE. 2) Discuss the use of discuss the use of IRE in current clinical applications. 3) Describe the strengths and weakness of IRE in comparison to other ablation modalities. 4) Describe future potential for IRE use in clinical care.

VSI041-13 Imaging and Advances in Basic Research

Participants

Muneeb Ahmed, MD, Wellesley, MA (*Moderator*) Research Grant, General Electric Company; Stockholder, Agile Devices, Inc; Scientific Advisory Board, Agile Devices, Inc

LEARNING OBJECTIVES

View learning objectives under main course title.

VSI041-14 Intraprocedural Imaging: The Keynote of IO

Wednesday, Nov. 29 4:10PM - 4:30PM Room: S405AB

Participants

Bradford J. Wood, MD, Bethesda, MD (*Presenter*) Researcher, Koninklijke Philips NV; Researcher, Celsion Corporation; Researcher, BTG International Ltd; Researcher, W. L. Gore & Associates, Inc ; Researcher, Cook Group Incorporated; Researcher, XAct Robotics; Intellectual property, Koninklijke Philips NV; Intellectual property, BTG International Ltd; Royalties, invivoContrast GmbH; Royalties, Koninklijke Philips NV; ; ;

LEARNING OBJECTIVES

View learning objectives under main course title.

VSI041-15 Cutting Edge Imaging Techniques for Follow-Up

Wednesday, Nov. 29 4:30PM - 4:50PM Room: S405AB

Participants Mark Tann, MD, Indianapolis, IN (*Presenter*) Nothing to Disclose

LEARNING OBJECTIVES

View learning objectives under main course title.

VSI041-16 Role of Biomarkers in IO

Participants

Etay Ziv, MD, PhD, New York, NY (Presenter) Nothing to Disclose

LEARNING OBJECTIVES

View learning objectives under main course title.

VSI041-17 HCC Showing Complete Response According to mRECIST on CT after a First Session of Conventional Chemoembolization: Is Lipiodol Deposition a Good Predictor of Local Progression?

Wednesday, Nov. 29 5:05PM - 5:15PM Room: S405AB

Participants

Marco Dioguardi Burgio, MD, Paris, France (*Abstract Co-Author*) Nothing to Disclose Maxime Ronot, MD, Clichy, France (*Presenter*) Nothing to Disclose Carmen Garcia Alba, MD, Clichy, France (*Abstract Co-Author*) Nothing to Disclose Matthieu Lagadec, MD, Clichy, France (*Abstract Co-Author*) Nothing to Disclose Magaly Zappa, MD, Clichy, France (*Abstract Co-Author*) Nothing to Disclose Annie Sibert, MD, Paris, France (*Abstract Co-Author*) Nothing to Disclose Valerie Vilgrain, MD, Clichy, France (*Abstract Co-Author*) Nothing to Disclose

For information about this presentation, contact:

maxime.ronot@aphp.fr

PURPOSE

To evaluate if the lipiodol deposition pattern can predict local progression in HCC nodules with complete response (CR) according to mRECIST on CT after a first session of conventional chemoembolization (cTACE).

METHOD AND MATERIALS

From January 2012 to May 2014 all consecutive patients undergoing a first cTACE session for HCC were identified. Inclusion criteria were presence of ≤ 3 HCCs and available pre and post-TACE CECT. Each treated tumor response was classified according to mRECIST. The analysis focused on tumors showing CR. For them, the lipiodol deposition pattern was classified as complete (C-Lip, covering the entire tumor volume), or incomplete (I-Lip). Local progression was defined as the reappearance of enhancing areas on arterial-phase showing washout on portal/delayed phase within 2 cm from treated tumors on follow-up CT examinations.

RESULTS

Final population included 50 patients (mean age 62+/-12 yo; 45 male (90%)) with 82 HCCs (mean 26.8+/-14.2 mm). HCCs were solitary in 19 (35%) patients. A total of 46 (52%) HCCs were classified as CR, including 16 (35% - mean 23+/-8 mm) with incomplete, and 30 (65% - mean 23+/-10 mm) with complete lipiodol deposition. After a median follow-up of 14 months (range 3.2-35.9 months), 15/16 (94%) and 10/30 (30%) of I-Lip and C-Lip HCCs showed local progression on CT (p<0.001). No statistical difference regarding delay of recurrence was noted between I-Lip and C-Lip HCCs (mean 334 vs. 401 days p=0.519).

CONCLUSION

Despite showing CR according to mRECIST, HCCs with incomplete lipiodol deposition have a high risk of recurrence and should be considered as incompletely treated.

CLINICAL RELEVANCE/APPLICATION

Nodules showing a complete response according to mRECIST but with incomplete deposition after one session of conventional TACE should be considered as incompletely treated.

VSI041-18 Rationale for Combination Theories

Wednesday, Nov. 29 5:15PM - 5:30PM Room: S405AB

Participants

S. Nahum Goldberg, MD, Ein Kerem, Israel (*Presenter*) Consultant, AngioDynamics, Inc; Research support, AngioDynamics, Inc; Consultant, Cosman Medical, Inc;

LEARNING OBJECTIVES

View learning objectives under main course title.

VSI041-19 Systemic Implications of IO Therapies: Increased Tumorigenesis?

Wednesday, Nov. 29 5:30PM - 5:45PM Room: S405AB

Participants

Muneeb Ahmed, MD, Wellesley, MA (*Presenter*) Research Grant, General Electric Company; Stockholder, Agile Devices, Inc; Scientific Advisory Board, Agile Devices, Inc

LEARNING OBJECTIVES

View learning objectives under main course title.

VSIO41-20 Systemic Implications of IO Therapies: Beneficial Immune Effects?

Wednesday, Nov. 29 5:45PM - 6:00PM Room: S405AB

Participants Joseph P. Erinjeri, MD, PhD, New York, NY (*Presenter*) Nothing to Disclose

LEARNING OBJECTIVES

View learning objectives under main course title.







MSRT45

ASRT@RSNA 2017: Understanding Practice and Ethics Standards in a Changing Health Care Environment

Wednesday, Nov. 29 2:20PM - 3:20PM Room: N230B

PR

AMA PRA Category 1 Credit ™: 1.00 ARRT Category A+ Credit: 1.00

Participants

Ann Obergfell, JD, Fort Wayne, IN (Presenter) Nothing to Disclose

LEARNING OBJECTIVES

1) Know how to access and analyze ASRT Practice Standards for Medical Imaging and Radiation Therapy and the ARRT Standards of Ethics. 2) Assess scenarios to determine if the practice meets acceptable professional performance standards. 3) Apply the ARRT Rules of Ethics to determine if behavior complies with professional expectations and patient safety guidelines.

ABSTRACT

The changing health care environment produces anxiety for imaging professionals as they navigate modifed or new clinical expectations including but not limited to patient safety and patient satisfaction, against institutional and professional performance expectations. The presenter will discuss the ASRT Practice Standards for Medical Imaging and Radiation Therapy, the ARRT Standards of Ethics, and the application and implications of each on daily practice. Specific scenarios related to practice will be analyzed using the Practice Standards to determine appropriateness of practice and the Standards of Ethics to ascertain professional ethical compliance.







RCA44

Learning and Using the Open Source MIRC Teaching File System (Hands-on)

Wednesday, Nov. 29 2:30PM - 4:00PM Room: S401AB

IN

AMA PRA Category 1 Credits ™: 1.50 ARRT Category A+ Credit: 1.75

Participants

Michael R. Cline, MD, Ann Arbor, MI (*Presenter*) Nothing to Disclose Andre M. Pereira, MD, Toronto, ON (*Presenter*) Nothing to Disclose

LEARNING OBJECTIVES

1) Learn the features of MIRC (Medical Imaging Resource Center), RSNA's own software for building teaching files. 2) Learn where to obtain and how to install the software. 3) Become familiar with the RSNA MIRC Wiki, which contains documentation on the software.

ABSTRACT

MIRC (Medical Imaging Resource Center) or TFS (Teaching File System) is a component of RSNA's CTP (Clinical Trials Processor), a suite of tools developed by RSNA to optimize research in radiology mainly with emphasis on workflow and security of patient information. It is offered free of charge by RSNA. Simply put, MIRC can be used to build a radiology teaching file, be it for an individual of for an institution with many simultaneous users. Development started in 2000 and the project has been kept alive along the years, funded by RSNA, also with great support from the community of users. Installation is very streamlined and available for virtually all plataforms and operational systems. All files necessary for installation are available at the download session of RSNA's own MIRC server (http://mirc.rsna.org). This course is aimed to cover basic authoring tools and some advanced functions. After finishing this course the attendee will be proficient in authoring and uploading cases, and also be familiar with the resources for installation and administration of MIRC.

Active Handout: Andre Martins Pereira

http://abstract.rsna.org/uploads/2017/16005101/MIRC_handout_2017.pdf







RCB44

Intro to Statistics with R (Hands-on)

Wednesday, Nov. 29 2:30PM - 4:00PM Room: S401CD



AMA PRA Category 1 Credits ™: 1.50 ARRT Category A+ Credit: 1.75

Participants

James E. Schmitt, MD, PhD, Philadelphia, PA (*Presenter*) Nothing to Disclose Philip A. Cook, PhD, Philadelphia, PA (*Presenter*) Nothing to Disclose

LEARNING OBJECTIVES

1) Install and launch the R software package. Understand how to search for and download external packages to extend R's functionality. 2) Load data from external files such as txt, csv, and xlsx. 3) Perform basic mathematical operations and utilize data structures to manipulate data. 4) Use loops to perform more complex operations over the data, including true/false logic. 5) Understand the basics of creating plots and histograms. 6) Perform common statistical tests including correlation, Chi-square, and ANOVA.







RCC44

Virtual Reality and 3D Printing

Wednesday, Nov. 29 2:30PM - 4:00PM Room: S501ABC

IN

AMA PRA Category 1 Credits ™: 1.50 ARRT Category A+ Credit: 1.75

Participants

Beth A. Ripley, MD, PhD, Seattle, WA (Moderator) Nothing to Disclose

For information about this presentation, contact:

bar23@uw.edubeth.ripley@va.gov

Sub-Events

RCC44A Brief Overview of 3D Printing and Virtual Reality in Medicine

Participants Beth A. Ripley, MD, PhD, Seattle, WA (*Presenter*) Nothing to Disclose

RCC44B Introduction to Augmented Reality

Participants Jesse L. Courtier, MD, San Francisco, CA (*Presenter*) Nothing to Disclose

For information about this presentation, contact:

jesse.courtier@ucsf.edu

LEARNING OBJECTIVES

Following this presentation, participants will: 1. Understand the basic principles of Augmented Reality and how it differs from Virtual Reality 2. Learn how medical images can be displayed as 3D objects in Augmented Reality on various platforms 3. Realize the many potential applications for Augmented Reality in medicine

RCC44C Setting Up a Virtual Reality Lab

Participants

Justin Sutherland, PhD, Ottawa, ON (Presenter) Nothing to Disclose

LEARNING OBJECTIVES

1) Identify and explain the necessary components that work together to make a modern virtual reality system. 2) Describe the currently available and soon to be released virtual reality hardware and software platforms. 3) Explain a number of things to do and avoid when setting up a lab to achieve a high quality virtual reality experience.

RCC44D 3D Printing and Virtual Reality: The NIH Perspective

Participants

Meghan C. McCarthy, PhD, Rockville, MD (Presenter) Nothing to Disclose

RCC44E The Role of Virtual Reality in Medical Education

Participants Matt Bramlet, MD, Peoria, IL (*Presenter*) Nothing to Disclose







MSRO44

BOOST: Lymphoma-Case-based Review (An Interactive Session)

Wednesday, Nov. 29 3:00PM - 4:15PM Room: S103CD



AMA PRA Category 1 Credits ™: 1.25 ARRT Category A+ Credits: 1.50

Participants

Chelsea C. Pinnix, MD, PhD, Houston, TX (*Moderator*) Research Grant, Merck & Co, Inc Leo I. Gordon, MD, Chicago, IL (*Presenter*) Nothing to Disclose Chris R. Kelsey, Durham, NC (*Presenter*) Nothing to Disclose Jurgen Rademaker, MD, New York, NY (*Presenter*) Nothing to Disclose

LEARNING OBJECTIVES

1) Case-based review of staging and treatment response in lymphoma. 2) Discussion of imaging findings in lymphoma and their clinical significance (predominantly CT based but PET and MR will also be reviewed)





SSM01

Breast Imaging (Practice Issues)

Wednesday, Nov. 29 3:00PM - 4:00PM Room: E451A

BR

AMA PRA Category 1 Credit ™: 1.00 ARRT Category A+ Credit: 1.00

FDA Discussions may include off-label uses.

Participants

Jocelyn A. Rapelyea, MD, Washington, DC (*Moderator*) Speakers Bureau, General Electric Company; Jessica W. Leung, MD, Houston, TX (*Moderator*) Nothing to Disclose

Sub-Events

SSM01-01 A Monte Carlo Simulation: Impact of new USPSTF on Breast Cancer Screening on Ages 40-49 across the USA

Wednesday, Nov. 29 3:00PM - 3:10PM Room: E451A

Awards Student Travel Stipend Award

Participants Akshay Goel, MD, New York, NY (*Presenter*) Nothing to Disclose Ralph T. Wynn, MD, New York, NY (*Abstract Co-Author*) Nothing to Disclose Richard S. Ha, MD, New York, NY (*Abstract Co-Author*) Nothing to Disclose

For information about this presentation, contact:

akg9006@nyp.org

PURPOSE

To assess the potential implications of the United States Preventive Services Task Force (USPSTF) for women ages 40-49 in the United States.

METHOD AND MATERIALS

This is an IRB exempt study based on a literature review of multiple factors related to breast cancer screening. Based on the US consensus data, we determined the total number of women between ages 40-49. A Monte Carlo simulation model was tailored to fit our study design, specifically to assess the potential impact of USPSTF guidelines on cost and mortality. We randomized the patients into two groups: A) annual screening starting at age 40 per traditional guidelines vs. B) annual screening starting at age 50 per USPSTF guidelines. Data points from large randomized control trials and the literature were utilized as parameters in our model to predict mortality events, and biopsy events (core biopsy, fine-needle-aspiration). These parameters included: absolute morality A) 0.29% B) 0.36%, medical costs of metastatic breast cancer: \$120,000, cost per mammogram: \$75, and various procedure parameters for fine-needle aspiration and core biopsy. Cost analysis did not include indirect societal and nonmedical costs related to loss of life in a relatively young cohort. Differences in mortality and overall cost were assessed using a two-sided Student's t test.

RESULTS

We determined the cohort size of women ages 40-49 from the US census data to be approximately 20 million. Using our model, we ran our simulation on a cohort of 20 million patients. In the traditional screening group there were 29342 deaths. This was significantly higher compared to the USPSTF non-screening group, which had 36222 deaths (p < .001). In the traditional screened group the average cost per patient was \$622. This was higher compared to the USPSTF non-screening group average cost of \$438 (p < .001).

CONCLUSION

The USPSTF guidelines result in increased mortality for non-screened patients between ages 40-49. The higher average cost per patient in the screened group however may not be clinically significant, when societal and nonmedical mortality costs are taken into account.

CLINICAL RELEVANCE/APPLICATION

Breast cancer screening remains a controversial topic and further work is needed to help patients and clinicians understand new guideline implications on patients between ages 40-49.

SSM01-02 Screening Mammography Audit Metrics Differ Depending on the Reference Standard Used: Systematic Performance Underestimation and a Solution

Wednesday, Nov. 29 3:10PM - 3:20PM Room: E451A

Participants Elizabeth S. Burnside, MD, MPH, Madison, WI (*Presenter*) Nothing to Disclose Christina Shafer, PhD, Madison, WI (*Abstract Co-Author*) Nothing to Disclose Kaitlin Woo, PhD, Madison, WI (*Abstract Co-Author*) Nothing to Disclose Mai A. Elezaby, MD, Madison, WI (*Abstract Co-Author*) Nothing to Disclose Amy M. Fowler, MD, PhD, Madison, WI (*Abstract Co-Author*) Nothing to Disclose Lonie R. Salkowski, MD,PhD, Middleton, WI (*Abstract Co-Author*) Nothing to Disclose Roberta M. Strigel, MD, MS, Madison, WI (*Abstract Co-Author*) Research support, General Electric Company Sijian Wang, Madison, WI (*Abstract Co-Author*) Nothing to Disclose

For information about this presentation, contact:

eburnside@uwhealth.org

PURPOSE

Cancer detection rate (CDR), an important screening mammography audit metric, can be determined using two different reference standards: (1) biopsy results (CDR_B)-widely used by U.S. practices or (2) registry-match (CDR_R)-used in published benchmarks. The purpose of this study was to determine CDR performance based on these two reference standards, which are both available in our practice, and to develop a conversion algorithm for practices using biopsy results when registry data is not available.

METHOD AND MATERIALS

Using consecutive screening mammograms (1/1/2006 to12/31/2013) from a single institution academic breast imaging practice, we calculated CDR_B and CDR_R according to BI-RADS definitions. We compared the outcomes (per year and in aggregate) using McNemar's test. We calculated ascertainment rate (AR)-defined as the fraction of biopsies performed (B_perf) of the number recommended (B_rec)-to reconcile the difference between CDR_B and CDR_R. Finally, we developed an algorithm with 95% confidence intervals to estimate CDR_R (CDR_R-est) using CDR_B.

RESULTS

For 83,895 consecutive screening mammograms, we found the overall CDR_B of 4.79/1000 significantly underestimated the CDR_R of 5.09 (p < 0.001), despite a relatively high AR of 89.0%-Table; a pattern of underestimation that was systematically redemonstrated for each year. We developed a conversion algorithm based on data elements (e.g. positive predictive value of biopsy performed-PPV3) typically available in practices without a registry match: CDR_R-est = CDR_B + (((B_rec-B_perf)*PPV3)/# of screening mammograms), for which the confidence interval contained the observed CDR_R for each year and all years in aggregate.

CONCLUSION

Cancer registry-matching, is onerous, costly, difficult to implement, and therefore not used routinely in practice. The existing guidelines to use CDR_B can significantly underestimate CDR and may lead to erroneous conclusions about performance, thus a conversion algorithm providing an accurate range accounting for practice-level AR, is important to avoid CDR underestimation and promote more accurate comparisons across clinical practices.

CLINICAL RELEVANCE/APPLICATION

Because most practices use biopsy results, not registry-matching as reference standard, systematic underestimation of CDR is likely; a problem addressed by the conversion algorithm that we propose.

SSM01-03 County-level Factors Predicting Low Uptake of Screening Mammography

Wednesday, Nov. 29 3:20PM - 3:30PM Room: E451A

Participants

Samantha L. Heller, MD, PhD, New York, NY (*Presenter*) Nothing to Disclose James S. Babb, PhD, New York, NY (*Abstract Co-Author*) Nothing to Disclose Yiming Gao, MD, New York, NY (*Abstract Co-Author*) Nothing to Disclose Andrew B. Rosenkrantz, MD, New York, NY (*Abstract Co-Author*) Nothing to Disclose Linda Moy, MD, New York, NY (*Abstract Co-Author*) Nothing to Disclose

For information about this presentation, contact:

samantha.heller@nyumc.org

PURPOSE

The purpose of this study is to investigate county-level geographic patterns of mammographic screening uptake throughout the United States and to determine the impact of rural vs. urban settings on breast cancer preventive services.

METHOD AND MATERIALS

This descriptive study used a de-identified aggregate dataset, the County Health Rankings (CHR), to identify the percent of Medicare enrollees age 67-69 per US county having at least one mammogram in 2013. This uptake was matched with U.S. Department of Agriculture Rural Atlas (USDARA) data categorizing counties as metropolitan vs. non-metropolitan and along an urban continuum scale (1-9) based on county population size (large defined as population >= 20,000; small <20,000) and metropolitan proximity. Univariable and multivariable analyses were performed using SAS 9.3 software.

RESULTS

2,243,294 Medicare beneficiaries aged 67-69 were eligible for mammograms. Mean mammographic uptake per county was 60% (range 26%-86%). Uptake was significantly higher for metropolitan vs. non-metropolitan counties in 19 states, significantly lower in 4 states, and not significantly different in the remainder. Uptake was significantly higher for large counties in 25 states and

significantly lower in only 1 state. County-level mammographic uptake was positively correlated with the number of Medicare enrollees (r=+0.27, p<0.001), % white residents (r=+0.16, p<0.001), income level (r=+0.34, p<0.001), and % of residents with some college education (r=+0.40, p<0.001), and negatively correlated with ratio of population to primary-care providers (PCP) ratio (r=-0.31, <0.001), age-adjusted mortality (-0.41, p<0.001), and % Hispanic residents (-0.11, p<0.001). Multivariable analysis demonstrated that the % of white and black residents, income level, PCP ratio, mortality rate, and % of non-English proficient residents were significant independent predictors of mammographic screening uptake.

CONCLUSION

Uptake of mammographic screening services varies widely at the county level and is lower in less metropolitan counties and in counties with smaller populations.

CLINICAL RELEVANCE/APPLICATION

In conjunction with predictive factors such as income, race, and primary care access, county-level geographic categorizations may help identify communities needing breast cancer screening education.

SSM01-04 Attitudes Towards Mobile versus Fixed Facility Preferences for Obtaining a Mammogram Among Latinas

Wednesday, Nov. 29 3:30PM - 3:40PM Room: E451A

Awards

Student Travel Stipend Award

Participants

Allison A. Tillack, MD, PhD, Seattle, WA (*Presenter*) Nothing to Disclose John R. Scheel, MD, PhD, Seattle, WA (*Abstract Co-Author*) Research support, General Electric Company Lauren Mercer, BS, Las Cruces, NM (*Abstract Co-Author*) Nothing to Disclose Gloria D. Coronado, PhD, Portland, OR (*Abstract Co-Author*) Nothing to Disclose Shirley A. Beresford, PhD, Seattle, WA (*Abstract Co-Author*) Nothing to Disclose Yamile Molina, PhD, Chicago, IL (*Abstract Co-Author*) Nothing to Disclose Beti Thompson, PhD, Seattle, WA (*Abstract Co-Author*) Nothing to Disclose

For information about this presentation, contact:

atillack@uw.edu

PURPOSE

Mobile mammography services have been proposed as a way to increase Latinas' screening mammography rates and reduce their disproportionate late-stage presentation compared to White women. However, our recent study suggested that this service may not significantly increase their screening rates. This study evaluates potential reasons why Latinas may not use mobile mammography services and evaluates changes in their preferences after using these services.

METHOD AND MATERIALS

Using a mixed methods approach, we conducted a secondary analysis of survey data (n=538) from a randomized controlled trial to improve screening mammography rates among Latinas in Washington. Descriptive statistics and bivariate regression were used to characterize mammographic location preferences, and to test for associations with demographic factors such as sociodemographics, healthcare access, and perceived breast cancer risk and beliefs. Based on these findings, a qualitative study (n=18) was used to evaluate changes in perceptions after using mobile mammographic services.

RESULTS

More Latinas preferred obtaining a mammogram at a fixed facility (52.3%, n=276) compared to having no preference (46.3%, n=249) and mobile mammography services (1.7%, n=9). Concern about privacy and comfort (15.6%, n=84), having multiple reasons (13.2%, n=71) and concerns about general quality (10.6%, n=57) were common reasons for preferring a fixed facility. Only a history of a prior mammogram was significantly associated with having no mammogram location preference (P<0.05). In the qualitative study, Latinas expressed similar initial concerns about the quality and privacy and comfort of the mobile mammography service, however, became positive towards the mobile mammography services after having a mammogram.

CONCLUSION

While most Latinas preferred obtaining a mammogram at a fixed facility because of concerns about the quality, safety, and privacy of mobile mammography service, positive experiences changed their attitudes towards these services. These findings highlight the need to include community education when using mobile mammography service to increase screening mammography rates in underserved communities.

CLINICAL RELEVANCE/APPLICATION

Mobile mammography services providing screening mammography to underserved communities should study and address concerns and cultural issues related to delivery of these services as part of their program.

SSM01-05 Self-Compression in Mammography: A Randomized, Non-Inferiority Phase 3 Trial

Wednesday, Nov. 29 3:40PM - 3:50PM Room: E451A

Participants

Philippe Henrot, MD, Vandoeuvre-les-Nancy, France (*Presenter*) Nothing to Disclose Guillaume Oldrini, MD, Vandoeuvre-les-Nancy, France (*Abstract Co-Author*) Nothing to Disclose Philippe Troufleau, MD, Vandoeuvre-Les-Nancy, France (*Abstract Co-Author*) Nothing to Disclose Bruno Boyer, MD, Vandoeuvre-les-Nancy, France (*Abstract Co-Author*) Nothing to Disclose Gregory Lesanne, Vandoeuvres les Nancy, France (*Abstract Co-Author*) Nothing to Disclose

p.henrot@nancy.unicancer.fr

PURPOSE

To evaluate the non-inferiority of the self-compression mammography technique on the breast thickness compared to standard compression.

METHOD AND MATERIALS

549 women aged from 50 to 75 years old from 6 institutions were randomly assigned in a 1:1 ratio to the self-compression or standard compression group after checking their capability to run self-compression. The primary outcome was the breast thickness. The predefined non-inferiority margin was a difference of 3 mm for each view: right/left Craniocaudal (CC) and right/left mediolateral oblique (MLO). Compression force in Newton and image quality blindly quoted with a 4-points scale were also recorded for each view. Overall pain (10 points visual analogue scale) was recorded after CC and MLO views. Additional views (lateromedial LM, spot views, ...) were performed after pain evaluation and their number was recorded. 548 women were included in the intention-to-treat analyses (275 in the self-compression group and 273 in the standard compression group).

RESULTS

The reproducibility of the breast thickness measures was excellent for the four views with an intra-class correlation coefficient of 0.917 (95%CI, 0.902 to 0.929). The right CC breast thickness was 50.78 +/- 15.3 mm in self compression and 51.54 +/- 13 in the standard procedure (difference -0.76; 97.5%CI -8 to -1.24, p = 0.001). Compression force was higher in the self-compression arm versus standard compression arm for the 4 views. No difference was reported in the quality score in the two groups. Pain evaluation was 2.86 +/- 2.32 in the self-compression arm and 3.40 +/- 2.42 in the standard arm (p= 0.009). A median of 2 extraviews per woman was performed in both group (p=0.638).

CONCLUSION

Self-compression mammography technique is not inferior to standard compression technique to achieve the minimal breast thickness. Overall pain is inferior in the self-compression technique without compromising image quality.

CLINICAL RELEVANCE/APPLICATION

Self-compression could be proposed in the mammography practice and decrease the discomfort sometimes associated with mammography.

SSM01-06 Breast Radiology: Reduced Diagnostic Efficacy in a Developing South-East Asian Country

Wednesday, Nov. 29 3:50PM - 4:00PM Room: E451A

Participants

Callan R. Double, Sydney, Australia (*Abstract Co-Author*) Nothing to Disclose Hayden J. Munro, Mudgee, Australia (*Abstract Co-Author*) Nothing to Disclose Rhianna Jackson, Mudgee, Australia (*Abstract Co-Author*) Nothing to Disclose Ellen Day, Mudgee, Australia (*Abstract Co-Author*) Nothing to Disclose Kriscia Tapia, Lidcombe, Australia (*Abstract Co-Author*) Nothing to Disclose Patrick C. Brennan, PhD, Lidcombe, Australia (*Presenter*) Nothing to Disclose Maram Alakhras, Sydney, Australia (*Abstract Co-Author*) Nothing to Disclose Phuong Dung Trieu, Sydney, Australia (*Abstract Co-Author*) Nothing to Disclose Thuan Doan Do, Hanoi, Vietnam (*Abstract Co-Author*) Nothing to Disclose Louise Puslednik, Mudgee, Australia (*Abstract Co-Author*) Nothing to Disclose

For information about this presentation, contact:

patrick.brennan@sydney.edu.au

PURPOSE

Breast cancer is the leading cause of death in women worldwide. Prevalence in South-East (SE) Asia has shown a 30% increase in cases in the last ten years. In one developing SE Asian country up to 80% of cancers are being detected at stage 3 or 4, demonstrating the need for improvements in diagnostic efficacy. This study aims to investigate the ability of radiologists from one developing (n=35) and one developed (n=15) SE Asian country, using Australian radiologists (n=53) as a baseline.

METHOD AND MATERIALS

A data set containing 60 mammographic cases were used; 40 being normal and 20 showing malignancies. These were read by radiologists in their own countries. Demographic data were obtained from each reader. Each radiologist placed location markers on the lesions they identified, and provided confidence ratings between 2 and 5 with a higher value indicating higher confidence that a cancer exists. Data were compared between the three country-based radiologist groupings using the nonparametric two-tailed Kruskall Wallis and Mann Whitney U tests with a statistical significance set at P-value of <0.05.

RESULTS

Significant differences in scores were shown between radiologist groupings, with those from the developing SE Asian country demonstrating lower sensitivity, specificity, location sensitivity, ROC and JAFROC values (P<0.05). Demographic data indicated that radiologists from the developing countries were significantly younger (P<0.0001), read fewer mammographic cases each week (P<0.0001), read for fewer hours (P=0.0004) and had read for fewer number of years than their Australian (P<0.0001) radiologists. Similar differences were also shown between the developing and developed SE Asian Country.

CONCLUSION

Important variations in diagnostic efficacy between countries for breast cancer detection have been shown. Cost-effective and versatile educational solutions must be sought to address causal agents, so that the efficacy of cancer detection is not dependent on where women are located.

CLINICAL RELEVANCE/APPLICATION

The ability to detect cancer should be similar for women wherever they are located. This study examines if this is the case in a developing and developed SE Asian country compared with a developed westernised country.







SSM02

Breast Imaging (Tomosynthesis Diagnostic Applications)

Wednesday, Nov. 29 3:00PM - 4:00PM Room: E451B

BR

AMA PRA Category 1 Credit ™: 1.00 ARRT Category A+ Credit: 1.00

Participants

Emily F. Conant, MD, Philadelphia, PA (*Moderator*) Consultant, Hologic, Inc Consultant, Siemens AG Margarita L. Zuley, MD, Pittsburgh, PA (*Moderator*) Research Grant, Hologic, Inc;

Sub-Events

SSM02-01 Digital Breast Tomosynthesis Utilization in the Medicare Population

Wednesday, Nov. 29 3:00PM - 3:10PM Room: E451B

Participants

Gilda Boroumand, MD, Hamden, CT (*Presenter*) Nothing to Disclose Ida Teberian, MD, Philadelphia, PA (*Abstract Co-Author*) Nothing to Disclose Laurence Parker, PhD, Philadelphia, PA (*Abstract Co-Author*) Nothing to Disclose Elizabeth S. Hsu, MD, Ambler, PA (*Abstract Co-Author*) Nothing to Disclose Vijay M. Rao, MD, Philadelphia, PA (*Abstract Co-Author*) Nothing to Disclose David C. Levin, MD, Philadelphia, PA (*Abstract Co-Author*) Nothing to Disclose

For information about this presentation, contact:

gilda.boroumand@yale.edu

PURPOSE

Digital breast tomosynthesis (DBT) has been shown to improve the diagnostic accuracy of breast cancer screening and diagnosis, and was approved by the FDA for clinical use in 2011. However, there is limited literature on the current use of DBT in clinical practice. This study seeks to determine the volume of screening and diagnostic DBT in the Medicare population.

METHOD AND MATERIALS

We evaluated the national Medicare Part B Physician/Supplier Procedure Summary Master Files from 2015, the first (and only) year in which procedural billing codes for DBT are available. Screening and diagnostic full-field digital mammography (FFDM) and DBT volume counts were determined by tabulating global and professional component claims. Medicare specialty codes were used to categorize the specialty of the interpreting physicians as radiologists or non-radiologists.

RESULTS

In 2015, a total of 5,730,635 screening FFDM exams were performed, of which 1,084,256 (18.9%) included DBT as an add-on procedure. Diagnostic FFDM exams totaled 1,402,966, with 226,682 (16.2%) including DBT. The vast majority (over 96%) of mammograms were billed by radiologists. Among radiologists, DBT studies were used in conjunction with 19.1% of the digital screening studies and 16.4% of the digital diagnostic studies. For non-radiologist physicians, DBT studies were used with 16.7% of digital screening studies and 8.7% of digital diagnostic studies.

CONCLUSION

The utilization of DBT was rather limited in the first year of its introduction as a billable Medicare procedure, occurring in conjunction with less than 20% of digital mammography exams. Radiologists appear to be earlier adopters of this technology compared with non-radiologists, possibly related to the fact that the latter have far less involvement in the field.

CLINICAL RELEVANCE/APPLICATION

2015 is the first and only year for which DBT volume data are available and it will be important to follow the adoption of the technology in subsequent years.

SSM02-02 Can Tomosynthesis Reduce the Benign Biopsy Rate within the Assessment Setting of Women Recalled From Breast Screening?

Wednesday, Nov. 29 3:10PM - 3:20PM Room: E451B

Participants

Nisha Sharma, MBChB, Leeds, United Kingdom (*Presenter*) Nothing to Disclose Barbara Dall, MBBCh, Leeds, United Kingdom (*Abstract Co-Author*) Nothing to Disclose Michelle A. McMahon, FRCR, MBBS, Leeds, United Kingdom (*Abstract Co-Author*) Nothing to Disclose Isobel Haigh, Leeds, United Kingdom (*Abstract Co-Author*) Nothing to Disclose

PURPOSE

Digital Breast Tomosynthesis (DBT) within the UK can be used in women recalled for assessment following an abnormal screening mammogram. It is recognised that DBT as a screening tool has improved the cancer detection rate and reduced the false positive rate of women screened. We wanted to assess the impact DBT would have on our assessment clinics regarding biopsy rates and cancers detected. This was an IRB approved prospective study where all women recalled following abnormal screening mammogram were asked to take part in the study. The tomosynthesis study was read within 6 weeks of the assessment clinic which was performed as standard with the DBT images not available for review so was unable to influence the standard assessment.

METHOD AND MATERIALS

The study ran from 01/11/2015 to 29/07/2016. All women recalled following an abnormal screening mammogram were invited to take part in the study. All women had standard assessment performed. The DBT was double read within 6 weeks of attending the assessment clinic. The number of women who had an intervention, which included FNA and core biopsies, was recorded and the outcome of assessment was also recorded

RESULTS

709 women were recruited to the study. 30 women were excluded as they were clinical recalls. 679 women took part in the study. There were a total of 105 breast cancers in this study (36 non invasive and 79 invasive).475/679 women (70%) had a biopsy as part of the standard assessment and 103 cancers were identified in 102 patients (22% PPV).216/694 women (30%) were discharged following further assessment. If DBT had been used in the assessment setting then 199 biopsies would have been performed based on mammographic findings alone and an additional 44 biopsies due to US findings (36%). 103 cancers were identified (42% PPV), 2 cases of non-invasive were only identified by DBT and 2 cases of malignancy missed by DBT.DBT generated 6 additional biopsies, of which 2 were malignant.

CONCLUSION

DBT in the assessment setting is a cost effective imaging tool as it would have reduced the number of benign interventions and improved the positive predictive value of identifying malignancy. 2 cancers were missed on DBT but these were 2 cases of low volume malignancy that may be considered over diagnosis in this current era.

CLINICAL RELEVANCE/APPLICATION

DBT is a vital addition with regards to triple assessment and minimising benign biopsies within the screening assessment setting

SSM02-03 The Radial Scar Dilemma: Incidence and Surgical Upgrade Rates with Tomosynthesis

Wednesday, Nov. 29 3:20PM - 3:30PM Room: E451B

Participants

Reni S. Butler, MD, Madison, CT (*Presenter*) Research Grant, Seno Medical Instruments, Inc. Sarah H. O'Connell, MD, New Haven, CT (*Abstract Co-Author*) Nothing to Disclose Madhavi Raghu, MD, New Haven, CT (*Abstract Co-Author*) Nothing to Disclose Malini Harigopal, MD, New Haven, CT (*Abstract Co-Author*) Nothing to Disclose Liane E. Philpotts, MD, New Haven, CT (*Abstract Co-Author*) Consultant, Hologic, Inc Maryam Etesami, MD, New Haven, CT (*Abstract Co-Author*) Nothing to Disclose Mohammadreza Shervinrad, MD, New Haven, CT (*Abstract Co-Author*) Nothing to Disclose

For information about this presentation, contact:

reni.butler@yale.edu

PURPOSE

To evaluate the incidence and malignant upgrade rates of surgically excised radial scars before and after the implementation of tomosynthesis.

METHOD AND MATERIALS

Institutional review board approval was obtained for this Health Insurance Portability and Accountability Act-compliant protocol. Medical records of patients diagnosed with radial scar at our institution in the last 8 years were retrospectively reviewed. The incidence of radial scar diagnosed as the primary imaging finding in the 3 years prior to tomosynthesis was compared to that in the 5 years after its implementation. For each lesion, type of mammographic finding; patient age and presentation; lesion size; core needle biopsy imaging guidance, needle gauge, and number of samples; core biopsy histology; and final pathology at surgical excision were reviewed, and upgrade to malignancy at surgical excision was calculated. Statistical significance was evaluated using chi square with Yates' correction.

RESULTS

129 surgically excised radial scars were identified, 27 in the 3 years prior to tomosynthesis and 102 in the 5 years since then. The pre-tomosynthesis incidence of radial scar was 0.5/1000 patients, compared to 1.3/1000 patients after tomosynthesis (p<0.0001). Architectural distortion on screening mammography was the most common presentation, representing 58.9% (76/129) of radial scars overall, and 79.4% (81/102) of radial scars after tomosynthesis. 90.7% (117/129) of lesions were evaluated histologically with core needle biopsy prior to surgical excision. Of these, 6.8% (8/117) were upgraded to malignancy on surgical excision. The likelihood of malignant upgrade increased with patient age and lesion size, and decreased with larger volume of tissue sampling. The strongest correlation was seen with presence of atypia on core biopsy pathology. Malignant upgrade for radial scars with atypia was 29.2% (7/24) compared to 1.1% (1/93) for those without atypia on core needle biopsy.

CONCLUSION

The incidence of radial scars has increased significantly since the implementation of tomosynthesis. The low upgrade rate of radial scars without atypia on core needle biopsy suggests that mammographic follow up may be a reasonable alternative to surgical excision for some patients.

CLINICAL RELEVANCE/APPLICATION

 With the increased detection of radial scars with tomosynthesis, it may be possible to identify a subset of patients that can be safely followed.

SSM02-04 Architectural Distortion Outcome: Detection only on Tomosynthesis Versus 2D Mammography

Wednesday, Nov. 29 3:30PM - 3:40PM Room: E451B

Participants

Taghreed I. Alshafeiy, MD, PhD, Port Said, Egypt (*Abstract Co-Author*) Nothing to Disclose Carrie M. Rochman, MD, Charlottesville, VA (*Abstract Co-Author*) Research Consultant, Theraclion Brandi T. Nicholson, MD, Charlottesville, VA (*Abstract Co-Author*) Nothing to Disclose Jonathan Nguyen, MD, Charlottesville, VA (*Abstract Co-Author*) Nothing to Disclose Jennifer A. Harvey, MD, Charlottesville, VA (*Presenter*) Research Grant, Hologic, Inc Stockholder, Hologic, Inc Research Grant, Volpara Health Technologies Limited Stockholder, Volpara Health Technologies Limited

For information about this presentation, contact:

taghreedi.alshafeiy@gmail.com

PURPOSE

To compare the outcome of architectural distortion (AD) detected only on digital breast tomosynthesis (DBT) with AD seen at 2D mammography

METHOD AND MATERIALS

This retrospective study was IRB approved and HIPAA compliant. All consecutive cases with architectural distortion assigned BI-RADS 4 or 5 categories from 2009 to 2016 were included. Three readers with 1 to 10 years of experience reviewed all cases for visibility of AD (2D visible vs. DBT detected). Consensus was achieved when 2 readers agreed. Each reader also assigned level of suspicion using a Likert scale (1 to 5) based on mammographic images only. CNB and surgical excision results were compared between 2D- and DBT-detected AD. Frequencies were compared by way of the McNemar test and the Pearson's Chi-square exact test.

RESULTS

181 AD lesions were included; 122 (67.4%) were 2D-detected while 59 (32.6%) were DBT-detected. The malignancy rate at CNB was significantly higher for 2D-detected AD (38.5%) compared to AD detected only on DBT (6.8%) (p < 0.001). Likewise, the final malignancy rate after excision of high risk and benign discordant lesions was significantly higher for 2D- detected (43.4%) compared to DBT-detected AD (10.2%) (p < 0.001). An US correlate was more likely to be present with AD detected by 2D (n = 103/122, 84.4%) than DBT (n = 33/59, 55.9%) (p < 0.001). When no US correlate was present among DBT-detected AD, the malignancy rate was low (7.7%) but not significantly different than when an US correlate was present (12.1%)(p = 0.65). Regarding the level of suspicion of AD, there was substantial inter-reader agreement (κ Coefficient= 0.61-0.77). When NPV is considered as Likert 1-2, NPV is high (93.8, 81.4, 82.9) but not sufficient to consider follow up over biopsy based on radiologist level of suspicion.

CONCLUSION

DBT-detected AD has significantly lower malignancy outcome compared to 2D-detected AD (10.2% vs. 43.4%), however the malignancy rate is still sufficiently high to warrant biopsy

CLINICAL RELEVANCE/APPLICATION

DBT-detected AD has a lower risk of malignant outcome than AD detected at 2D, but still warrants biopsy even when there is not an US correlate.

SSM02-05 Pure Architectural Distortion on Digital Breast Tomosynthesis: Imaging Characteristics and Histopathologic Outcomes

Wednesday, Nov. 29 3:40PM - 3:50PM Room: E451B

Awards

Student Travel Stipend Award

Participants Akshat C. Pujara, MD, Chicago, IL (*Presenter*) Nothing to Disclose Jamie Hui, MD, Chicago, IL (*Abstract Co-Author*) Nothing to Disclose Lilian Wang, MD, Chicago, IL (*Abstract Co-Author*) Nothing to Disclose

For information about this presentation, contact:

apujara@gmail.com

PURPOSE

To evaluate imaging characteristics of pure architectural distortion on digital breast tomosynthesis (DBT) and assess their association with histopathologic outcomes.

METHOD AND MATERIALS

This retrospective study was approved by the institutional review board and HIPAA-compliant. DBT exams performed between January 2014 and December 2015 were reviewed for architectural distortion without an associated mass. Imaging characteristics evaluated were size, one versus two-view visualization, and conspicuity compared with 2D mammography. Corresponding ultrasound (US) and MRI exams were assessed for correlates to pure architectural distortion on DBT. Biopsy and surgical pathology were reviewed. A two-tailed t test and Fisher's exact tests were performed.

RESULTS

During this two-year period, 101 cases of pure architectural distortion were visualized on DBT in 97 patients (ages 36 - 83 years,

mean 56 years). Core needle biopsy or surgical excision of 95 cases of pure architectural distortion yielded malignant pathology in 43/95 (45%) tissue samples, of which 39/43 (91%) were invasive and 39/43 (91%) were nuclear grades 1 or 2. The most common benign pathologies were radial scar/complex sclerosing lesion and stromal fibrosis, with each present in 19/52 (36%) benign biopsy specimens. Associations between imaging characteristics of pure architectural distortion on DBT and histopathologic outcome were not statistically significant, including size (2.7+1.3 cm malignant vs 2.4+0.9 cm benign; P=0.12), two-view visualization (39/43 malignant vs 44/52 benign; P=0.54), and increased conspicuity on DBT compared with 2D mammography (32/43 malignant vs 36/52 benign; P=0.65). The presence of an US correlate was associated with malignancy (38/43 malignant vs 27/52 benign; P=0.0001). MRI was performed in 31 cases. The presence of an MRI correlate was associated with malignancy (25/25 malignant vs 3/6 benign; P=0.004).

CONCLUSION

Pure architectural distortion on DBT is malignant in nearly half of cases, demonstrating low or intermediate grade invasive cancers in the majority of such cases. The presence of US and MRI correlates is associated with malignancy.

CLINICAL RELEVANCE/APPLICATION

Detection of pure architectural distortion on DBT has a high positive predictive value for malignancy, particularly in the presence of an ultrasound correlate.

SSM02-06 Synthetic 2D Mammography Can Replace Digital Mammography as an Adjunct to Digital Breast Tomosynthesis: Experience with a Wide-angle Tomosynthesis System

Wednesday, Nov. 29 3:50PM - 4:00PM Room: E451B

Participants

Paola Clauser, MD, Vienna, Austria (*Presenter*) Nothing to Disclose Pascal A. Baltzer, MD, Vienna, Austria (*Abstract Co-Author*) Nothing to Disclose Panagiotis Kapetas, Vienna, Austria (*Abstract Co-Author*) Nothing to Disclose Ramona Woitek, MD, Vienna, Austria (*Abstract Co-Author*) Nothing to Disclose Michael Weber, Vienna, Austria (*Abstract Co-Author*) Nothing to Disclose Maria Bernathova, MD, Wien, Austria (*Abstract Co-Author*) Nothing to Disclose Thomas H. Helbich, MD, Vienna, Austria (*Abstract Co-Author*) Research Grant, Medicor, Inc Research Grant, Siemens AG Research Grant, C. R. Bard, Inc

For information about this presentation, contact:

clauser.p@hotmail.it

PURPOSE

To evaluate the lesion detection and diagnostic performance of synthetic 2D mammography (SM) with wide-angle digital breast tomosynthesis (WA-DBT) compared to digital mammography (DM) alone and in combination with WA-DBT.

METHOD AND MATERIALS

Included in this retrospective study were patients who underwent bilateral DM and WA-DBT between March 2015 and June 2015. The standard of reference was histology and/or one-year stability at follow-up. Ultimately, 205 women with 179 lesions were included (89 malignant, 90 benign). Four readers, blinded to results, randomly evaluated images from five different protocols: two view 2v-DM alone; 2v-DM with 2v-WA-DBT; 2v-SM with 2v-WA-DBT; one view (medio-lateral oblique) 1v-DM with 1v-WA-DBT; and 1v-SM with 1v-WA-DBT. Images were evaluated according to the BI-RADS lexicon. Lesion detection, sensitivity, specificity, and accuracy were calculated and compared using multivariate analysis (Generalized Estimating Equations).

RESULTS

Average detection rate was 75.4% for 2v-DM, 80.2% for 2v-DM with WA-DBT, 78.5% for 2v-SM with WA-DBT, 77.4% 1v-DM with WA-DBT, and 75.0% 1v-SM with WA-DBT. Differences in lesion detection were found between reading protocols (P=0.001) and readers (P<0.001). Regardless of inter-reader variations, 2v-DM with 2v-DBT achieved a higher detection compared to 2v-DM (P=0.004). No significant differences in detection were found between 2v-DM with WA-DBT and 2v-SM with WA-DBT (P>0.110). Detection was higher when two views were available, for both SM and DM (P<0.034). Average sensitivity, specificity, and accuracy were: 72.5%, 60.2%, 67.5% for 2v-DM; 82.6%, 64.6%, 75.0% for 2v-DM with WA-DBT; 83.1%, 67.7%, 76.8% for 2v-SM with WA-DBT; 81.7%, 64.0%, 74.7% 1v-DM with WA-DBT; 79.8%, 69.9%, 75.8% 1v-SM with WA-DBT. Sensitivity and accuracy were lower with DM alone compared to the other reading protocols (P<0.001). There were no other significant differences in sensitivity, specificity or accuracy.

CONCLUSION

Compared to 2v-DM alone, 2v-WA-DBT with 2v-DM or 2v-SM improves detection, sensitivity, and accuracy with no significant effect on specificity. 2v-SM with 2v-WA-DBT performed as well as 2v-DM with 2v-WA-DBT. Two-view protocols allow for higher lesion detection.

CLINICAL RELEVANCE/APPLICATION

2v-WA-DBT with 2v-DM and 2v-WA-DBT with 2v-SM allow for a higher detection rate and an improved diagnostic performance than 2v-DM. SM can be safely used to replace DM, in combination with 2v-WA-DBT.





103rd Scientific Assembly and Annual Meeting November 26 to December 1 McCormick Place, Chicago



SSM03

Cardiac (Congenital Cardiovascular Disease)

Wednesday, Nov. 29 3:00PM - 4:00PM Room: S502AB



AMA PRA Category 1 Credit ™: 1.00 ARRT Category A+ Credit: 1.00

FDA Discussions may include off-label uses.

Participants

Randolph K. Otto, MD, Seattle, WA (*Moderator*) Nothing to Disclose Evan J. Zucker, MD, Stanford, CA (*Moderator*) Nothing to Disclose

Sub-Events

SSM03-01 Self-Navigated Free-Breathing Radial Whole-Heart MR Angiography for the Assessment of Coronary Artery Anatomy in Congenital Heart Disease

Wednesday, Nov. 29 3:00PM - 3:10PM Room: S502AB

Awards Student Travel Stipend Award

Participants

Domenico Mastrodicasa, MD, Charleston, SC (Presenter) Nothing to Disclose Moritz H. Albrecht, MD, Charleston, SC (Abstract Co-Author) Nothing to Disclose Georg Apfaltrer, MD, Thal, Austria (Abstract Co-Author) Nothing to Disclose Taylor M. Duguay, Charleston, SC (Abstract Co-Author) Nothing to Disclose Carlo N. De Cecco, MD, PhD, Charleston, SC (Abstract Co-Author) Research Grant, Siemens AG U. Joseph Schoepf, MD, Charleston, SC (Abstract Co-Author) Research Grant, Astellas Group; Research Grant, Bayer AG; Research Grant, General Electric Company; Research Grant, Siemens AG; Research support, Bayer AG; Consultant, Guerbet SA; ; ; Matthias Stuber, PhD, Lausanne, Switzerland (Abstract Co-Author) Founder, Diagnosoft, Inc Stockholder, Diagnosoft, Inc Davide Piccini, Lausanne, Switzerland (Abstract Co-Author) Employee, Siemens AG Arni C. Nutting, MD, Charleston, SC (Abstract Co-Author) Nothing to Disclose Anthony M. Hlavacek, MD, Charleston, SC (Abstract Co-Author) Investigator, Siemens AG Research Grant, Siemens AG Domenico De Santis, MD, Charleston, SC (Abstract Co-Author) Nothing to Disclose Philipp L. von Knebel Doeberitz, Charleston, SC (Abstract Co-Author) Nothing to Disclose Megha Penmetsa, Charleston, SC (Abstract Co-Author) Nothing to Disclose Jiaqian Xu, Charleston, SC (Abstract Co-Author) Nothing to Disclose Antonio R. Cotroneo, MD, Chieti, Italy (Abstract Co-Author) Nothing to Disclose Akos Varga-Szemes, MD, PhD, Charleston, SC (Abstract Co-Author) Research Grant, Siemens AG

For information about this presentation, contact:

schoepf@musc.edu

PURPOSE

To assess a free-breathing self-navigated three-dimensional (SN3D) radial whole-heart MR angiography (MRA) pulse sequence for the evaluation of coronary artery (CA) anatomy in patients with congenital heart disease (CHD).

METHOD AND MATERIALS

SN3D datasets were previously acquired in 109 patients (20.1±11.8 years) as part of a prospective clinical trial for the assessment of CHD anatomy using a 1.5T scanner. SN3D datasets, retrospectively evaluated by three radiologists, were scored based on the appearance of CA segments and reader confidence in determining CA dominance using a two-point scale. A three-point scale was used to rate overall image quality along with the ability to freeze cardiac and respiratory motion. Vessel sharpness of the internal thoracic artery (ITA, representing respiratory motion), the left anterior descending (LAD) and right CA (RCA, representing a combination of respiratory and cardiac motion) were quantitatively measured using a dedicated prototype application (SoapBubble). Wilcoxon statistics, Pearson correlation, and Intra-Class Correlation (ICC) were used to evaluate the data.

RESULTS

The average duration of the SN3D acquisition was 9.1 ± 2.4 minutes. The mean score for overall image quality was 2.35, with excellent agreement (ICC 0.95). A diagnostic study was obtained in 83.7% of scans with excellent image quality in 51.7% of them. The SN3D technique was able to successfully visualize the individual CAs in the following percentage of cases: left main 92.6% (ICC 0.66), LAD 88.3% (ICC 0.59), RCA 87.8% (ICC 0.55), left circumflex 82.8% (ICC 0.74), posterior descending 50.2% (ICC 0.46), and first diagonal 39.8% (ICC 0.64). Diagnostic confidence for the assessment of CA dominance was scored at 1.56. Image quality was affected more by cardiac motion freezing (mean score, 2.18; Pearson's r=0.73, P<0.029) than respiratory motion freezing (mean score, 2.20; r=0.58, P<0.029). The ITA, RCA, and LAD vessel sharpness scores were 53.1, 52.5, and 48.7%, respectively.

CONCLUSION

In the majority of young CHD patients, SN3D MRA allows for the visualization of the proximal CAs with excellent quality. However,

the quality of cardiac motion freezing still has a strong impact on image quality.

CLINICAL RELEVANCE/APPLICATION

SN3D MRA is a promising technique in CHD patients especially when impaired breath-holding capacity limits the visualization of CA anatomy due to motion artifacts.

SSM03-02 Evaluation of 3D Magnetic Resonance Imaging of Autopsied Human Heart Specimens for Computational Modeling of Congenital Heart Diseases

Wednesday, Nov. 29 3:10PM - 3:20PM Room: S502AB

Participants

Wataru Ueki, RT, Suita, Japan (*Presenter*) Nothing to Disclose Yoshiaki Morita, Suita, Japan (*Abstract Co-Author*) Nothing to Disclose Masaru Shiotani, RT, Suita, Japan (*Abstract Co-Author*) Nothing to Disclose Ryo Haraguchi, Suita, Japan (*Abstract Co-Author*) Nothing to Disclose Taka-Aki Matsuyama, Kyoto, Japan (*Abstract Co-Author*) Nothing to Disclose Yukishige Tanida, Suita, Japan (*Abstract Co-Author*) Nothing to Disclose Kazuto Harumoto, Suita, Japan (*Abstract Co-Author*) Nothing to Disclose Atsushi K. Kono, MD, PhD, Suita, Japan (*Abstract Co-Author*) Nothing to Disclose Tetsuya Fukuda, Suita, Japan (*Abstract Co-Author*) Nothing to Disclose

For information about this presentation, contact:

wataru.ueky@gmail.com

PURPOSE

Autopsied human heart specimens of congenital heart disease are valuable for medical education and surgical simulation in understanding complex anatomical structure. Because of the decreasing number of autopsies and the deterioration of human heart specimens over time, digitalization, such as computational modeling using 3D image data, is an effective approach to capture these valuable specimens. This study aimed to compare the visibility of formalin-fixed heart among various 3D MRI sequences and to clarify the optimal sequence for the computational modeling of congenital heart disease.

METHOD AND MATERIALS

Five human hearts with various types of congenital heart diseases obtained during autopsy and preserved with formalin fixation underwent ex vivo MRI with a 3T clinical machine. The different types of 3D MRI sequences were performed in the same spatial resolution (1.0*1.0*1.0mm): T2-SPACE (3D with a constant flip angle to acquire bright blood imaging), True-FISP (SSFP imaging), MPRAGE (inversion-recovery-based T1WI), and FLASH (basic GRE sequence). The autopsied heart was scanned in a plastic container filled with normal saline. Among the four 3D sequences, we compared the contrast ratio between the myocardium and the ventricular lumen and between the vascular wall and the lumen. In addition, we visually assessed the cardiovascular structure using MPR and 3D images.

RESULTS

The average contrast ratios between the myocardium and the ventricular lumen in MPRAGE, T2SPACE, FLASH, and True FISP were 0.80, 0.31, 0.26, and 0.28, respectively. The average contrast ratios between the vascular wall and the lumen were 0.78, 0.43, 0.32, and 0.20, respectively. MPRAGE showed the best contrast for the imaging of both the myocardium and the vascular structure. By visual assessment, MPRAGE also provided more detailed information on morphology and cardiovascular continuity.

CONCLUSION

MPRAGE is the optimal sequence for the computational modeling of human autopsied heart specimens fixed by formalin, which replaces water in cardiac tissue, with congenital heart diseases.

CLINICAL RELEVANCE/APPLICATION

MPRAGE showed the best contrast for imaging a formalin-fixed heart. The computational cardiac modeling of autopsied heart using MPRAGE plays a critical role in surgical simulation and education.

SSM03-03 Right Ventricle Native T1 Mapping and Pulmonary Regurgitation in Patients with Congenital Heart Diseases: Preliminary Data

Wednesday, Nov. 29 3:20PM - 3:30PM Room: S502AB

Participants

Francesco Secchi, MD,PhD, Milano, Italy (*Presenter*) Nothing to Disclose Paola Maria Cannao, MD, Milano, Italy (*Abstract Co-Author*) Nothing to Disclose Marco Ali, Milan, Italy (*Abstract Co-Author*) Nothing to Disclose Francesca Romana Pluchinotta, MD, Boston, MA (*Abstract Co-Author*) Nothing to Disclose Massimo Lombardi, MD, Trondheim, Norway (*Abstract Co-Author*) Nothing to Disclose Francesco Sardanelli, MD, San Donato Milanese, Italy (*Abstract Co-Author*) Speakers Bureau, Bracco Group; Research Grant, Bracco Group; Advisory Board, Bracco Group; Speakers Bureau, Bayer AG; Research Grant, Bayer AG; Advisory Board, General Electric Company Marcello Petrini, Milano, Italy (*Abstract Co-Author*) Nothing to Disclose

For information about this presentation, contact:

francesco.secchi@grupposandonato.it

PURPOSE

To correlate native T1 mapping (nT1) of the right ventricle (RV) with biventricular functional parameters and pulmonary regurgitation.

METHOD AND MATERIALS

We prospectively evaluated 27 patients (24±10y, mean ± standard deviation) who underwent a cardiac magnetic resonance exam at1.5T. Six patients were treated with percutaneous pulmonary valve. For each patient left (LV) and right ventricle (RV) functional evaluation was performed. Pulmonary flow analysis with phase-contrast sequences was performed and regurgitation fraction (RF) was calculated. A native modified look-locker inversion recovery (MOLLI) prototype sequence was acquired at basal, mid and apical-ventricular level in short-axis view in systole, by starting the data acquisition at the individually adopted trigger time. The MOLLI sequence included motion correction and subsequent automatic generation of T1 maps. Spearman and Mann Whitney U test were used for statistical analysis.

RESULTS

LV functional parameters were: end-diastolic volume (EDVi) 77 \pm 20 (mean \pm standard deviation), LV end-systolic volume (ESVi) 29 \pm 16, LV stroke volume (SV) 82 \pm 16 and ejection fraction (EF) 63 \pm 8. RV functional parameters were: RVEDVi 101 \pm 27, RVESVi 47 \pm 17, RVSV 96 \pm 30 and EF 55 \pm 10. Mean RF was 26 \pm 18 % and mean nT1 was 1025 \pm 38 ms. A negative significant correlation between RVEF and nT1 (r=-333, P=.045) and between RF and nT1 (r=-234, P=.047) was found. nT1 was 1006 \pm 95 ms in patients before pulmonary valve treatment and 1087 \pm 87 ms in patients after percutaneous implantation (P = .057).

CONCLUSION

Native RV T1 mapping was negatively correlated with PR and RVEF, reflecting an adaptation of RV muscle to the pulmonary conduit dysfunction. A borderline significant increase of nT1 in patients after pulmonary percutaneous treatment was found.

CLINICAL RELEVANCE/APPLICATION

RV T1 value should be used as an early indicator of RV dysfunction in patients with congenital heart diseases.

SSM03-04 Anatomy of Retroesophageal Major Aortopulmonary Collateral Arteries in Pulmonary Atresia with Ventricular Septal Defect: Results from Preoperative CTA

Wednesday, Nov. 29 3:30PM - 3:40PM Room: S502AB

Participants

Qianjun Jia, MD, Guangzhou, China (*Presenter*) Nothing to Disclose Jinglei Li, MD, Guangzhou, China (*Abstract Co-Author*) Nothing to Disclose Changhong Liang, Guangzhou, China (*Abstract Co-Author*) Nothing to Disclose Meiping Huang, Guangzhou, China (*Abstract Co-Author*) Nothing to Disclose

For information about this presentation, contact:

jiaqianjun@126.com

PURPOSE

There is little information in the literature available on major aortopulmonary collateral arteries (MAPCAs) anatomy, especially about the retroesophageal MAPCAs (REM). This study aimed to assess the anatomy of REM in pulmonary atresia with ventricular septal defect and major aortopulmonary collateral arteries (PA-VSDMAPCAs) patients.

METHOD AND MATERIALS

We retrospectively analysed 130 consecutive PA-VSD-MAPCA patients with preoperative CTA who underwent cardiac surgery. A detailed analysis of the MAPCAs anatomy was made using CT imaging, including the total number, origin and stenosis of MAPCAs, the presence or absence of a retroesophageal course for MAPCAs, relationship between MAPCAs and tracheal at the pulmonary hilum. MAPCAs were divided into two groups on the basis of REM diagnosis by CT: REM group (REM diagnosed by CT, n=94) and Not REM group (no REM diagnosed by CT, n=183).

RESULTS

A REM was identified in 82 of the 130 patients (63%), all of which were located on the side opposite the arch. REM group originate higher level of thoracic vertebrae (level 6), compared with Not REM group (level 5) (P<0.01), and REM group have a higher probability to originate from the lateral side of the aorta median degree of 144, contrast to median degree of 90 for Not REM group (P<0.01). There was a difference in the occurrence of stenosis comparing REM group to Not REM group (89% vs 78%), (χ 2=9.79, P<0.01). A midsegment stenosis was present more often in REM group compared with Not REM group (31% vs 21%), (χ 2=6.27, P=0.01). Relative to trachea, there was a difference in the anterior-posterior position comparing REM to Not REM group at the pulmonary hilum (91% MAPCAs posterior to tracheal vs 51% MAPCAs posterior to tracheal), (χ 2=50.81, P<0.01).

CONCLUSION

Sixty-three percent of patients with PA-VSD-MAPCAs have a retroesophageal MAPCA, and a left aortic arch was associated with a higher prevalence of the retroesophageal MAPCAs. Compared with not retroesophageal MAPCAs, the retroesophageal MAPCAs associated with higher level, more lateral origin, more stenosis, particularly a midsegment stenosis, and were prone to course posterior to tracheal at the pulmonary hilum.

CLINICAL RELEVANCE/APPLICATION

The anatomy of retroesophageal MAPCAs is highly relevant and useful for surgeons in identifying the retroesophageal MAPCAs to perform unifocalization procedures for PA-VSD-MAPCAs patients

SSM03-05 Common Atrium and the Associated Malformations: Evaluation by Low-Dose Dual-Source Computed Tomography

Wednesday, Nov. 29 3:40PM - 3:50PM Room: S502AB

Participants

Yi Zhang, MS, Chengdu, China (*Presenter*) Nothing to Disclose Zhigang Yang, MD, Chengdu, China (*Abstract Co-Author*) Nothing to Disclose Mengxi Yang, MS, Chengdu, China (*Abstract Co-Author*) Nothing to Disclose Ke Shi, Chengdu, China (*Abstract Co-Author*) Nothing to Disclose Rui Li, Nanchong, China (*Abstract Co-Author*) Nothing to Disclose Kaiyue Diao, Chengdu, China (*Abstract Co-Author*) Nothing to Disclose Ying-Kun Guo, MD, Chengdu, China (*Abstract Co-Author*) Nothing to Disclose

For information about this presentation, contact:

loselien@live.cn

PURPOSE

To determine CA characteristics and diagnostic accuracy in assessing associated malformations in these patients with low-dose DSCT.

METHOD AND MATERIALS

This study was approved by the Institutional Review Board, and informed consent was obtained from all patients. Twenty-one pediatric and adolescent CA patients underwent low-dose DSCT. Different ventricular types and associated malformations were assessed. The diagnostic accuracy of DSCT and transthoracic echocardiography (TTE) in evaluating associated malformations were assessed by reference to surgical results. The effective doses of low-dose DSCT were calculated.

RESULTS

Seven CA patients and 14 CA with single ventricle (SV) were finally included. In the CA with SV, three types of SV morphology were distinguished: single left ventricle (n = 4), single right ventricle (n = 5) and undifferentiated ventricle (n = 5). Seventy-eight associated malformations were observed, among which 22 were seen in CA and 56 in CA with SV. DSCT was superior to TTE for detection of intracardiac anomalies (sensitivity: DSCT, 92.31% vs. TTE, 76.92%), anomalies of great vessels (sensitivity: DSCT, 100.00% vs. TTE, 77.50%), and of collateral vessels (sensitivity: DSCT, 100% vs. TTE, 20.00%). The estimated mean effective dose was 0.95 ± 0.44 mSv (<1 mSv).

CONCLUSION

Low-dose DSCT is an excellent alternative for pediatric and adolescent patients with CA, providing morphological details of CA and associated malformations with high accuracy.

CLINICAL RELEVANCE/APPLICATION

Common atrium (CA) is a rare complex congenital heart disease. Those with associated malformations who do not receive surgical treatment usually have a poor prognosis. Low-dose DSCT is an excellent alternative for pediatric and adolescent patients with CA, providing morphological details of CA and associated malformations with the high accuracy needed to conduct treatment effectively.

SSM03-06 Anomalous Right Coronary Artery from the Left (ARCA-L): Dual-Source Computed Tomography Angiography (DSCT) Findings in Southwest China

Wednesday, Nov. 29 3:50PM - 4:00PM Room: S502AB

Participants

Kaiyue Diao, Chengdu, China (*Presenter*) Nothing to Disclose Zhigang Yang, MD, Chengdu, China (*Abstract Co-Author*) Nothing to Disclose Qin Zhao, MD, Chengdu, China (*Abstract Co-Author*) Nothing to Disclose Yue Gao, Chengdu, China (*Abstract Co-Author*) Nothing to Disclose Yingkun Guo, Chengdu, China (*Abstract Co-Author*) Nothing to Disclose

For information about this presentation, contact:

kaiyuediao@qq.com

PURPOSE

We sought to provide the anatomic particularities of anomalous right coronary artery from the opposite (ARCA-L) in Southwest China on a relatively large scale under the postulation that some anatomy features on DSCT could help predict adverse clinical events.

METHOD AND MATERIALS

Over 18000 patients' coronary computed tomography angiography (CCTA) data was screened from Jan 2012 to Aug 2015. The prevalence of ARCA-L was computed and the subtype was decided by the spatial relationship between the right coronary artery with the pulmonic valve. CCTA was used to evaluated the proximal stenosis, observe the high-risk anatomy features including the take-off angle, proximal length as well as the ostium type and analyze the accompany anomalies. Follow-up was done by telephone and the major adverse clinical event (MACE) was recorded. Wilcox test and Chi-square test were used for testing the difference between groups. Cox hazard analysis was performed to identify prognosis predictive factors. P<0.05 was considered significant and Bonferroni correction of P value was used when necessary.

RESULTS

A prevalence of 0.70% (127/18226) was observed in our population and younger people tend to have higher degree of vessel stenosis (the age among the mild vs the middle vs the severe: 64.7 vs 59.6 vs 56.9, p=0.04). RCA origins from below the pulmonary valve was the most common type in our population. The take-off angle and the proximal stenosis length were found to have significant difference between mild (<30%) and severe stenosis (>=60%) group. An average of 15.3 \pm 9.2 months' follow-up was conducted on 65 non-CAD patients. Stenosis severity was the most predictive factor among the anatomy features with a RR of 5.23 (95% CI: 2.34 to 8.47, P<0.001).

CONCLUSION

ARCA-L found on CCTA in the Southwest China has a comparable prevalence with other regions with certain variations in high-risk anatomy features. Stenosis severity was the most reliable prognosis predictive factor for patients with conservative therapy.

CLINICAL RELEVANCE/APPLICATION

Our study proved some potentially malignant anatomic features on CCTA for evaluating patients with ARCA-L. Avoiding overloading exercise might be necessary for such patients.





103rd Scientific Assembly and Annual Meeting November 26 to December 1 McCormick Place, Chicago



SSM04

Cardiac (Acute Chest Pain/Cardiopulmonary Disease)

Wednesday, Nov. 29 3:00PM - 4:00PM Room: S504AB



AMA PRA Category 1 Credit ™: 1.00 ARRT Category A+ Credit: 1.00

FDA Discussions may include off-label uses.

Participants

Matthew D. Cham, MD, New York, NY (*Moderator*) Nothing to Disclose Jacobo Kirsch, MD, Weston, FL (*Moderator*) Nothing to Disclose

Sub-Events

SSM04-01 High-Risk Plaque Features Predict Ischemia in Acute Chest Pain: A Direct Comparison to On-Site Calculation of CT Derived FFR

Wednesday, Nov. 29 3:00PM - 3:10PM Room: S504AB

Participants

Yahang Tan, Philadelphia, PA (*Abstract Co-Author*) Nothing to Disclose Harold I. Litt, MD, PhD, Philadelphia, PA (*Presenter*) Research Grant, Siemens AG; Research Grant, Heartflow, LLC; ;

For information about this presentation, contact:

tanyahang@163.com

PURPOSE

The discordance between stenosis and ischemia may affect triage efficiency in acute chest pain patients after coronary CT, therefore methods to predict ischemia based on CT data are relevant to this population. CT derived FFR (cFFR) calculated on-site can evaluate the hemodynamic significance of a lesion quickly. High-risk plaque features (HRF) are also predictive of events in acute chest pain patients. We evaluated the correlation between HRF and cFFR in patients with suspected acute coronary syndrome (ACS).

METHOD AND MATERIALS

Patients with suspected ACS from the ACRIN PA 4005 and CT-COMPARE trials who had undergone both CT and either stress testing or catheter angiography were included. cFFR was calculated on-site using experimental software (Siemens cFFR). Degree of stenosis and presence of HRF (positive remodeling (PR), low attenuation plaque, spotty calcification) were assessed by two readers. Ischemia was defined as cFFR<=0.80. Logistic regression analysis was used to evaluate whether HRFs were independently associated with ischemia on a per-vessel level.

RESULTS

Degree of stenosis, HRF and cFFR were assessed in 320 vessels in 148 patients. Average total processing time for cFFR was approximately 40 minutes per patient. By cFFR, ischemia was present in 94 vessels (29%). In multivariate analyses, risk of ischemia was observed for PR (OR=2.64; 95%CI: 1.13-6.17; p=0.025), presence of 1 (OR=3.48; 95%CI: 1.50-8.14; p=0.004) and >1 (OR=4.43; 95%CI: 1.29-15.20; p=0.018) HRFs independent of stenosis. In 148 vessels with 30-90% stenosis, ischemia was present in 78 vessels (53%). In multivariate analyses, 70-90% stenosis (OR=20.22; 95%CI: 5.12-79.79; p<0.001), presence of 1 and >1 HRFs (OR=2.39; 95%CI: 1.05-5.45, p=0.038; OR=4.73, 95% CI:1.09-12.77, p=0.036, respectively) remained predictors of ischemia, while 50-70% stenosis and PR did not.

CONCLUSION

In patients presenting acute chest pain, presence of any HRF, stenosis>50% and PR are associated with cFFR<=0.80, while in vessels with 30-90% stenosis, presence of any HRF and 70-90% stenosis remained. Therefore, assessment of HRF may determine the need for further testing in acute chest pain patients.

CLINICAL RELEVANCE/APPLICATION

CT derived FFR calculated on-site allows rapid evaluation of the significance of a stenosis. Assessment of high-risk plaque may determine the need for further testing in acute chest pain patients.

SSM04-02 Coronary CT Angiography-Derived Fractional Flow Reserve Based on Machine Learning for Risk-Stratification of Non-Culprit Lesions in Patients with Acute Coronary Syndrome

Wednesday, Nov. 29 3:10PM - 3:20PM Room: S504AB

Participants Christian Tesche, MD, Charleston, SC (*Presenter*) Nothing to Disclose Taylor M. Duguay, Charleston, SC (*Abstract Co-Author*) Nothing to Disclose Rozemarijn Vliegenthart, MD, PhD, Groningen, Netherlands (*Abstract Co-Author*) Instutional Research Grant, Siemens Healthineers Carlo N. De Cecco, MD, PhD, Charleston, SC (*Abstract Co-Author*) Research Grant, Siemens AG Moritz H. Albrecht, MD, Charleston, SC (*Abstract Co-Author*) Nothing to Disclose U. Joseph Schoepf, MD, Charleston, SC (*Abstract Co-Author*) Research Grant, Astellas Group; Research Grant, Bayer AG; Research Grant, General Electric Company; Research Grant, Siemens AG; Research support, Bayer AG; Consultant, Guerbet SA; ; ; Akos Varga-Szemes, MD, PhD, Charleston, SC (*Abstract Co-Author*) Research Grant, Siemens AG Domenico De Santis, MD, Charleston, SC (*Abstract Co-Author*) Nothing to Disclose Ullrich Ebersberger, MD, Charleston, SC (*Abstract Co-Author*) Nothing to Disclose Richard Bayer, Charleston, SC (*Abstract Co-Author*) Nothing to Disclose Sheldon Litwin, Charleston, SC (*Abstract Co-Author*) Nothing to Disclose Ellen Hoffmann, Munich, Germany (*Abstract Co-Author*) Nothing to Disclose Daniel H. Steinberg, MD, Charleston, SC (*Abstract Co-Author*) Nothing to Disclose

For information about this presentation, contact:

schoepf@musc.edu

PURPOSE

This study sought to investigate the prognostic value of coronary CT angiography (CCTA)-derived fractional flow reserve (CT-FFR) in patients with acute coronary syndrome (ACS) and multivessel disease to gauge significance and guide management of non-culprit lesions.

METHOD AND MATERIALS

We analyzed data of 48 patients (55.8±9.6 years, 60% male) who were admitted for symptoms suggestive of ACS and underwent dual-source CCTA followed by invasive coronary angiography (ICA) with culprit lesion intervention. Culprit lesions were retrospectively identified on CCTA utilizing images obtained during ICA. Non-culprit lesions with >=30% luminal stenosis and deferred intervention were evaluated using a machine learning CT-FFR algorithm (Frontier, Siemens) to determine lesion-specific ischemia, defined as CT-FFR <=0.80. Follow-up was performed to record major adverse cardiac events (MACE).

RESULTS

CT-FFR identified lesion-specific ischemia in 23/81 non-culprit lesions. After a median follow-up of 19.5 months, MACE occurred in 14 patients (29%). Univariate Cox regression analysis revealed that CT-FFR <=0.80 (hazard-ratio (HR) 3.77 [95%CI 1.16-12.29], p=0.027), Framingham risk score (FRS) (HR 2.96 [1.01-7.63], p=0.038), and a CAD-RADSTM classification >=3 (HR 3.12 [1.03-10.17], p=0.051) were predictors of MACE. In a risk-adjusted model controlling for FRS and CAD-RADSTM >=3, CT-FFR <=0.80 remained a predictor of MACE (1.56 [1.01-2.83], p=0.048). Receiver operating characteristics analysis including FRS, CAD-RADSTM classification >=3, and CT-FFR <=0.80 (Area under the curve [AUC] 0.78) showed incremental discriminatory power over FRS alone (AUC 0.66, p=0.032).

CONCLUSION

CT-FFR <=0.80 of non-culprit lesions in patients with ACS and multivessel disease adds prognostic value to identify risk for future MACE.

CLINICAL RELEVANCE/APPLICATION

CT-FFR may have utility to risk-stratify the vulnerability of non-culprit lesions for the prediction of future major adverse cardiac events in patients with acute coronary syndrome (ACS) and multivessel disease.

SSM04-03 Fully Automated Volumetry of Peripheral Lung Vasculature based on Pulmonary CT Angiography for Non-Invasive Diagnosis of Pulmonary Hypertension

Wednesday, Nov. 29 3:20PM - 3:30PM Room: S504AB

Participants

Claudius Melzig, MD, Heidelberg, Germany (Presenter) Nothing to Disclose

Oliver Weinheimer, Heidelberg, Germany (Abstract Co-Author) Nothing to Disclose

Benjamin Egenlauf, Heidelberg, Germany (Abstract Co-Author) Nothing to Disclose

Michael Messerli, MD, St. Gallen, Switzerland (Abstract Co-Author) Nothing to Disclose

Ekkehard Gruenig, MD, Heidelberg, Germany (Abstract Co-Author) Nothing to Disclose

Hans-Ulrich Kauczor, MD, Heidelberg, Germany (*Abstract Co-Author*) Research Grant, Siemens AG; Research Grant, Bayer AG; Speakers Bureau, Boehringer Ingelheim GmbH; Speakers Bureau, Siemens AG; Speakers Bureau, Koninklijke Philips NV; Speakers Bureau, Bracco Group; Speakers Bureau, AstraZeneca PLC;

Claus P. Heussel, MD, Heidelberg, Germany (*Abstract Co-Author*) Stockholder, STADA Arzneimittel AG; Stockholder, GlaxoSmithKline plc; Consultant, Boehringer Ingelheim GmbH; Research funded, Boehringer Ingelheim GmbH; Speaker, Novartis AG; Speaker, Basilea Pharmaceutica Ltd; Speaker, Bayer AG

Fabian Rengier, MD, Heidelberg, Germany (Abstract Co-Author) Nothing to Disclose

PURPOSE

To evaluate fully automated volumetry of peripheral lung vasculature based on pulmonary CT angiography (CTPA) for non-invasive diagnosis of pulmonary hypertension (PH).

METHOD AND MATERIALS

93 consecutive patients who underwent right heart catheterisation (RHC) and CTPA within two weeks for suspected PH at our institution were retrospectively reviewed. 19 patients with chronic thromboembolic PH were secondarily excluded resulting in the final study population of 74 patients (mean age 66.2 years, 50 female). In-house developed software was used for fully automated segmentation of the pulmonary vasculature and peripheral vascular volume within 10 mm, 15 mm and 20 mm from the lung borders was caculated for each patient. Vascular volumes were compared between patients with PH (mean pulmonary arterial pressure (mPAP) >= 25 mm Hg) and patients without PH using Stundent's T-test. ROC analyses were done, AUC-values of the vascular volume within 10 mm, 15 mm and 20 mm of the lung periphery were compared and diagnostic accuracy for the detection of PH assessed.

42 out of 74 patients had PH (mPAP 37 \pm 11 mm Hg, 57%), 32 had nomal mPAP-values (17 \pm 4 mm Hg). Peripheral vascular volumes were significantly enlarged in patients with PH: 86 \pm 29 vs. 66 \pm 23 cmCubed within 20 mm, 59 \pm 24 vs. 42 \pm 19 cmCubed within 15 mm and 31 \pm 17 vs. 19 \pm 14 cmCubed within 10 mm of the lung periphery (p-values < 0.002). AUC-values for the detection of PH were 0.73 for 20 mm, 0.74 for 15 mm and 0.75 for 10 mm of the peripheral vascular volume. Highest diagnostic accuracy was achieved at a cut-off value of 19.4 cm for the 10 mm peripheral vascular volume which identified RHC-confirmed PH with 74% sensitivity, 72% specificity, 78% positive and 67% negative predictive value.

CONCLUSION

Fully automated volumetry of peripheral lung vasculature based on CTPA revealed significantly enlarged peripheral vascular volumes in patients with RHC-confirmed PH compared with patients without PH. Vascular volume within 10 mm of the lung periphery demonstrated the best diagnostic performance and identified PH with high diagnostic accuracy.

CLINICAL RELEVANCE/APPLICATION

Fully automated volumetry of peripheral lung vasculature based on CTPA is a promising, non-invasive tool to identify patients who require further workup for suspected PH.

SSM04-04 Quantitative Assessment of Pulmonary Hypertension Severity Using Late Gadolinium Enhancement and T1 Mapping Techniques of 3T Cardiac Magnetic Resonance

Wednesday, Nov. 29 3:30PM - 3:40PM Room: S504AB

Participants

Ming-xi Liu, Beijing, China (*Presenter*) Nothing to Disclose Zhan-Hong Ma, Beijing, China (*Abstract Co-Author*) Nothing to Disclose Tao Jiang, MD, Beijing, China (*Abstract Co-Author*) Nothing to Disclose Juan-Ni Gong, Beijing, China (*Abstract Co-Author*) Nothing to Disclose Jing An, Beijing, China (*Abstract Co-Author*) Nothing to Disclose Xiaojuan Guo, PhD, Beijing, China (*Abstract Co-Author*) Nothing to Disclose Lu Liang, Beijing, China (*Abstract Co-Author*) Nothing to Disclose Yuan-Hua Yang, Beijing, China (*Abstract Co-Author*) Nothing to Disclose

PURPOSE

To quantitatively assess the severity of pulmonary hypertension (PH) using late gadolinium enhancement (LGE) and T1 mapping techniques.

METHOD AND MATERIALS

We retrospectively analyzed the data of ten control subjects and 21 patients with clinically diagnosed PH caused by chronic thrombotic PH, Takayasu arteritis, idiopathic PH, atrial septal defect, and Ebstein anomaly. CMR examinations were performed with a 3T scanner including LGE, Cine, and T1 mapping sequences. Based on the New York Heart Association (NYHA) functional class and right heart catheterization, the patients were divided into mild and moderate PH patients and severe cases. Myocardial fibrosis volume (FV), percentage of myocardial fibrosis (pFV), and the parameters reflecting right ventricle function were calculated. Native T1, post-contrast T1, and ECV values in the regions of interest (ROI) at the mid-ventricular short-axis section were measured for the anterior and posterior interventricular insertion points (AIP and PIP), septum (S) (Figure 1), lateral wall and blood pool. Student's t-test, Pearson correlation coefficient and the receiver operating characteristic (ROC) were used for data statistics.

RESULTS

Myocardial fibrosis was present in 19/21 (90.48%) PH patients. FV in PH patients was (5.81 ± 4.76) ml, and the median of pFV was 8.33%. Significant differences between the PH patients and control subjects were present for ECV - AIP (t = -2.878, P = 0.011), ECV - PIP (t = -3.816, P = 0.002), and ECV - S (t = -3.749, P = 0.002). ECV - AIP and ECV - PIP were significantly different from the lateral wall (t = 2.406 and 3.970, P = 0.024 and 0.001). Table 1 illustrates those correlations between the parameters above and values of right heart catheterization in PH patients. Based on ROC curves (Figure 2), it was observed pFV > 7.25% is capable of identifying severe from mild and moderate PH patients.

CONCLUSION

The pFV and ECV values in the IP and septum could be other markers associated with PH cardiomyopathy. With the increase in PAP and PVR, the areas of myocardial fibrosis were inclined to expand, whereas the extent of myocardial fibrosis did not increase significantly.

CLINICAL RELEVANCE/APPLICATION

CMR quantitative assessment of myocardial fibrosis in the IP and septum may provide more information on the myocardial state, right heart function, treatment and prognosis in PH in the future.

SSM04-05 Incidental Solid Pulmonary Nodules in Emergent Coronary CT Angiography for Suspected Acute Coronary Syndrome: Impact of Revised 2017 Fleischner Society Guidelines

Wednesday, Nov. 29 3:40PM - 3:50PM Room: S504AB

Participants

Jan-Erik Scholtz, MD, Boston, MA (*Presenter*) Nothing to Disclose Michael T. Lu, MD, Boston, MA (*Abstract Co-Author*) Nothing to Disclose Sandeep S. Hedgire, MD, Boston, MA (*Abstract Co-Author*) Nothing to Disclose Nandini M. Meyersohn, MD, Boston, MA (*Abstract Co-Author*) Nothing to Disclose Mannudeep K. Kalra, MD, Boston, MA (*Abstract Co-Author*) Nothing to Disclose Jo-Anne O. Shepard, MD, Boston, MA (*Abstract Co-Author*) Nothing to Disclose Udo Hoffmann, MD, Boston, MA (*Abstract Co-Author*) Nothing to Disclose Brian B. Ghoshhajra, MD, Waban, MA (*Abstract Co-Author*) Consultant, Siemens AG; Consultant, Medtronic plc

janerikscholtz@gmail.com

PURPOSE

A major criticism of coronary computed tomography angiography (CTA) for suspected acute coronary syndrome (ACS) is that it leads to more downstream testing, mostly follow-up chest CT for lung nodules, than alternative diagnostic tests. In 2017 the Fleischner Society released guidelines with the potential to substantially reduce follow-up testing for incidental lung nodules. Our aim was to evaluate the effect of the revised 2017 Fleischner Society Guidelines on recommendations for follow-up chest CT of incidental lung nodules versus 2005 guidelines in Emergency Department (ED) patients undergoing coronary CTA for ACS assessment.

METHOD AND MATERIALS

Our IRB approved retrospective study included 2,066 ED patients with suspected ACS who underwent coronary CTA between 2012 and 2016. All patients with incidental lung nodules were abstracted from the Radiology Information System (RIS). Recommendations for follow-up chest CT for incidental solid pulmonary nodules according to the 2005 and 2017 Fleischner Guidelines were compared. Patients with a history of smoking were classified as "high risk". Data were analyzed with Student's t test.

RESULTS

413 patients (20%) aged >= 35 years had indeterminate solid pulmonary nodules. 301 patients (73%) were considered low risk and most patients (347/413; 84%) had < 6mm nodules. Per 2017 Fleischner Society Guidelines, follow-up CT of solid lung nodules would only be recommended in 66 (3.2%) of all patients compared to 191 patients (9.2%) based on the 2005 guidelines which resulted in a net reduction of 65% (p<0.001).

CONCLUSION

Application of the 2017 Fleischner Society Guidelines resulted in significantly fewer recommended downstream follow-up CT recommendations for solid nodules compared to 2005 guidelines in patients who underwent emergent coronary CTA for suspected ACS.

CLINICAL RELEVANCE/APPLICATION

Incidental lung nodules are common on coronary CTA; adoption of the 2017 Fleischner Society Guidelines will substantially reduce the number of follow-up chest CT recommendations.

SSM04-06 Lung Cancer Detected on Calcium Scoring CT: Factors Affecting Delayed Diagnosis and Predictors for Survival

Wednesday, Nov. 29 3:50PM - 4:00PM Room: S504AB

Participants

Jin Young Kim, MD, Seoul, Korea, Republic Of (*Abstract Co-Author*) Nothing to Disclose Young Joo Suh, MD, Seoul, Korea, Republic Of (*Presenter*) Nothing to Disclose Byoung Wook Choi, MD, Seoul, Korea, Republic Of (*Abstract Co-Author*) Nothing to Disclose

For information about this presentation, contact:

rongzusuh@gmail.com

PURPOSE

To investigate the factors affecting delay in diagnosis among patients who had lung cancer which was detected on coronary artery calcium (CAC) scoring CT and to determine prognostic factors which can predict mortality.

METHOD AND MATERIALS

A total of 156 patients (94 men, mean age 68.5±8.95 years) who underwent CAC scoring CT between January 2010 and December 2014 and were subsequently diagnosed as lung cancer, were retrospectively enrolled. Delayed diagnosis was defined as time interval between CAC scoring CT and the diagnosis of lung cancer more than 1 year. For cases with delayed diagnosis, the reason of delay was assessed. Follow-up clinical outcome data regarding clinicopathologic stage of lung cancer at the time of diagnosis and all-cause mortality were obtained. Logistic regression analysis was performed to identify predictors for advanced stage (stage IV), and Cox proportional hazard regression analysis was performed to determine predictors for mortality.

RESULTS

Among 156 lung cancers, 59 lesions (37.8%) had been delayed in diagnosis. The most common reason was missed lesion on CAC scoring CT (49.2%), and the followings were follow-up strategy with imaging than tissue confirmation in subsolid lesion (22.0%), and interpretation error (malignant lesion being considered as inflammatory lesion, 16.9%). In multivariate logistic regression analysis, age (Odds ratio[OR) 1.047, 95% confidence interval[CI] 0.997-1.099) and lesion size (OR 1.023, 95% CI 0.998-1.049) were significant positive predictors for the advanced stage (P<0.2), and subsolid lesion characteristics (OR 0.186, 95% CI 0.0724-0.478) was a negative predictor (P=0.0005). In multivariate Cox proportional hazard regression analysis, age (hazard ratio[HR] 1.062, 95% CI 1.013-1.114) and lesion size (HR 1.023, 95% CI 1.008-1.038) showed increased hazard ratio for mortality (P<0.2), and subsolid lesion characteristics had decreased hazard ratio (HR 0.34, 95% CI 0.15-0.77;P=0.01).

CONCLUSION

On CAC scoring CT, concerns for detection and interpretation errors for lung cancer may prevent delayed diagnosis. Older age and larger lesion size may have poor survival, in contrast, subsolid lesion characteristics may have better survival.

CLINICAL RELEVANCE/APPLICATION

Concerns for detection and interpretation of lung nodule on CAC scoring CT is required to reduce diagnostic delay of lung cancer, especially in patients with older age and larger lesion size.







SSM05

Chest (Thoracic Malignancy/Thymic and Esophageal)

Wednesday, Nov. 29 3:00PM - 4:00PM Room: S404AB



AMA PRA Category 1 Credit ™: 1.00 ARRT Category A+ Credit: 1.00

Participants

Jin Mo Goo, MD, PhD, Seoul, Korea, Republic Of (*Moderator*) Research Grant, Samsung Electronics Co, Ltd; Research Grant, DRTECH Co, Ltd

Carol C. Wu, MD, Houston, TX (Moderator) Author, Reed Elsevier

Sub-Events

SSM05-01 Whole-Tumor Histogram Analysis of Apparent Diffusion Coefficient Maps for the Differentiation of Thymic Carcinoma from Lymphoma

Wednesday, Nov. 29 3:00PM - 3:10PM Room: S404AB

Participants wei zhang, nan jing, China (*Presenter*) Nothing to Disclose

For information about this presentation, contact:

fskzhangwei@126.com

PURPOSE

To assess the performance of whole-tumor histogram analysis of apparent diffusion coefficient (ADC) maps in differentiating thymic carcinoma from lymphoma, and compare with that of commonly used hot-spot region of interest (ROI) based ADC measurement.

METHOD AND MATERIALS

Diffusion weighed imaging (DWI) data of 15 patients with thymic carcinoma and 13 patients with lymphoma were retrospectively collected and processed with mono-exponential model. The measurement of ADCs were performed by using histogram-based and hot-spot ROI based approach. In histogram-based approach, following parameters were generated, including mean ADC (ADCmean), median ADC (ADCmedian), 10 and 90 percentile of ADC (ADC10 and ADC90), kurtosis and skewness. The difference of ADCs between thymic carcinoma and lymphoma was compared using t test. Receiver operating characteristic analyses were conducted to determine and compare the differentiating performance of ADCs.

RESULTS

Lymphoma demonstrated significantly lower ADCmean, ADCmedian, ADC10, ADC90 and hot-spot ROI based (mean) ADCs than thymic carcinoma (all p values < 0.001), while no differences were found on kurtosis (P=0.412) and skewness (P=0.273). ADC10 demonstrated optimal differentiating performance [cut-off value, 0.403×10^{-3} mm2/s; area under curve (AUC), 0.977; sensitivity, 92.31%; specificity, 93.33%], followed by ADCmean, ADCmedian, ADC90 and hot-spot ROI based ADC. The AUC of the ROC curve of ADC10 was significantly higher than that of hot-spot ROI based ADC (0.977 vs 0.797, P=0.036).

CONCLUSION

Compared with commonly used hot-spot ROI based ADC measurement, histogram analysis of ADC maps holds the promise in improving the differentiating performance between thymic carcinoma and lymphoma.

CLINICAL RELEVANCE/APPLICATION

our preliminary study results indicated that histogram analysis of ADC maps could be a promising approach to improve the differentiating performance between thymic carcinoma and lymphoma.

SSM05-02 Can CT Textural Analysis Predict the World Health Organization (WHO) Classification of Thymic Epithelial Neoplasms?

Wednesday, Nov. 29 3:10PM - 3:20PM Room: S404AB

Participants

Shaunagh McDermott, FFR(RCSI), Boston, MA (*Presenter*) Nothing to Disclose Florian J. Fintelmann, MD, Boston, MA (*Abstract Co-Author*) Consultant, McKesson Corporation; Royalties, Reed Elsevier Valentina Nardi, Boston, MA (*Abstract Co-Author*) Nothing to Disclose Michael Lanuti, MD, Boston, MA (*Abstract Co-Author*) Nothing to Disclose Azadeh Tabari, Boston, MA (*Abstract Co-Author*) Nothing to Disclose

PURPOSE

To evaluate if CT textural analysis (CTTA) can differentiate between low-risk and high-risk thymic epithelial neoplasms (TENs) on routine CT images.

METHOD AND MATERIALS

The preoperative CT scans of 48 patients diagnosed with a TEN over a 10-year period were reviewed with respect to contour, enhancement pattern, degree of enhancement (relative to skeletal muscle), calcification, pleural effusion, pleural seeding, pericardial effusion, and invasion of local structures. CTTA was performed with commercially available software (TexRAD) that applies a filtration-histogram technique for characterizing tumor heterogeneity. TENs were divided into two groups based on the WHO classification (low-risk = types A, AB and B1; high-risk = types B2, B3 and C). Student t-test was used to compare the mean value of each texture parameter between the two groups. Receiver operating characteristics (ROC) analysis was performed and area under the curve (AUC) was calculated for texture parameters that differed significantly. Sensitivity and specificity were calculated using the cut-off value with the highest AUC.

RESULTS

28 low-risk TENs (3 type A, 18 type AB, 7 type B1) and 20 high-risk TENs (11 type B2, 6 type B3, 3 type C) were included. The degree of enhancement differed significantly between the two groups (p=0.021). No significant difference was identified with respect to contour, enhancement pattern, calcification, pleural effusion or seeding, pericardial effusion, or invasion of local structures. Histogram analysis of CT values showed statistically significant differences in average Mean (SSF0, p=0.03) standard deviation (SD)(SSF0,p=0.006), entrophy (SSF0, p=0.04), mean positive pixels (MPP)(SFF6, p=0.008) and kurtosis (SSF3, p=0.02) values between the low-risk group (Mean 67.1 +/- 20.2/SD 21.2 +/- 6.5/entropy 4.3 +/- 0.3/MPP 32.8 +/- 21.1/kurtosis 0.23 + 0.75) and high-risk group (Mean 55.4 +/- 12.6/SD 16.6 +/- 3.6 /entrophy 4.1 +/- 0.2/MPP 21.1 +/- 6.4/kurtosis 1.14 +/- 1.83). Using an MPP threshold of 26.5, the sensitivity and specificity for differentiating low-risk from high-risk lesions was 90% and 54%, respectively (AUC 0.72).

CONCLUSION

CTTA may be able to separate TENs into low- and high-grade WHO histologic subtypes.

CLINICAL RELEVANCE/APPLICATION

The ability to preoperatively predict the WHO subtype of thymic epithelial neoplasms may help determine the need for preoperative adjuvant treatment.

SSM05-03 A Comparison between 3T MR and Endoscopic Ultrasound for Preoperative T Staging of Potentially Resectable Esophageal Cancer with Histopathological Correlation

Wednesday, Nov. 29 3:20PM - 3:30PM Room: S404AB

Participants Jia Guo, Zhengzhou, China (*Presenter*) Nothing to Disclose Hongkai Zhang, Zhengzhou, China (*Abstract Co-Author*) Nothing to Disclose Zhaoqi Wang, Zhengzhou, China (*Abstract Co-Author*) Nothing to Disclose Hui Liu, Shanghai, China (*Abstract Co-Author*) Nothing to Disclose Xu Yan, Shanghai, China (*Abstract Co-Author*) Nothing to Disclose Dominik Nickel, Erlangen, Germany (*Abstract Co-Author*) Employee, Siemens AG Hailiang Li, Zhengzhou, China (*Abstract Co-Author*) Nothing to Disclose Jinrong Qu, Zhengzhou, China (*Abstract Co-Author*) Nothing to Disclose

For information about this presentation, contact:

qjryq@126.com

PURPOSE

To compare the value of 3T magnetic resonance imaging (MRI) and endoscopic ultrasonography (EUS) in the preoperative T staging of potentially resectable esophageal cancer.

METHOD AND MATERIALS

Patients with resectable EC diagnosed by clinical and pathological biopsy were prospectively collected. All patients underwent MRI (including T2-TSE-BLADE, DWI and a radial-VIBE sequence prototype) and EUS within one week before surgery. T staging was assigned on MR and EUS by two independent radiologists and one endoscopist in accordance with the 7th edition of AJCC TNM Classification for EC. Two readers separately determined the EC segment and evaluated the MR image quality using a 5-point score. The consistency of image quality score between two MRI readers and the correlation coefficient between image quality and EC segment were calculated using SPSS 20.0. Considering postoperative pathological T staging results as the gold standard, the performance of MRI (T2-TSE-BLADE + DWI + radial-VIBE) and EUS was evaluated based on the calculation of sensitivity, specificity, positive predictive value and negative predictive value.

RESULTS

A total of 70 patients were enrolled in the study, 16 cases were stage T1, 18 cases were stage T2, 30 cases were stage T3, and 6 cases were stage T4a. The evaluation of the image quality by two readers was almost identical (Kappa=0.825, P <0.001). The correlation coefficients between image quality score and EC segment by two readers were (r = -0.665, P <0.01)and (r = -0.619, P <0.01). The sensitivity values obtained by the two MRI readers for T1-T4a staging were 93.75%, 100%, 90%, 100% and 81.25%, 94.44%, 93.33%, 100%, and the specificity values were 100%, 94.23%, 100%, 98.44% and 100%, 90.38%, 97.50%, 100%; using EUS, the sensitivity and specificity values for T1-T4a staging were 81.25%, 83.33%, 53.33%, 50% and 96.3%, 67.31%, 92.50%, 98.44%.

CONCLUSION

MRI was comparable to EUS in the staging of T1 and T2, and showed advantage over EUS for T3 and T4a staging. MRI can accurately assess the depth of invasion of EC, which can be used as a routine examination for preoperative staging of EC and provide the basis for the formulation of a clinical treatment plan.

CLINICAL RELEVANCE/APPLICATION

(dealing with preoperative T staging of esophageal cancer)"MRI was comparable to EUS in the staging of T1 and T2, and showed

SSM05-04 Accuracy of a Machine Learning Algorithm for Anterior Mediastinal Mass Diagnosis

Wednesday, Nov. 29 3:30PM - 3:40PM Room: S404AB

Awards Student Travel Stipend Award

Participants Nityanand Miskin, MD, Boston, MA (*Presenter*) Nothing to Disclose Rachna Madan, MD, Boston, MA (*Abstract Co-Author*) Nothing to Disclose Andetta R. Hunsaker, MD, Boston, MA (*Abstract Co-Author*) Nothing to Disclose Mark M. Hammer, MD, Boston, MA (*Abstract Co-Author*) Nothing to Disclose

For information about this presentation, contact:

nmiskin@partners.org

PURPOSE

The purpose of this study is to evaluate the accuracy of a machine learning algorithm as a diagnostic aid for anterior mediastinal masses (AMM), and to compare the accuracy to expert clinical assessment.

METHOD AND MATERIALS

Cases were identified by searching our medical record for patients with an AMM evaluated with CTs, from 2012-2015. 223 cases were found: 103 thymomas, 40 lymphomas, 12 germ cell tumors, 65 benign lesions (cyst, thymic hyperplasia), and 3 fibrosing mediastinitis. The latter group was excluded as there were too few for reliable diagnosis. We divided the remaining 220 cases into 122 training and 98 test cases. One thoracic radiologist reviewed the training cases for the following: size, attenuation in Hounsfield Units, attenuation homogeneity, shape, midline location, intralesional fat, calcification, vascularity, cystic spaces, preservation of fatty septum, supraclavicular, mediastinal, or internal mammary lymphadenopathy (LAD), chest wall invasion, lung invasion, pulmonary metastases, pleural metastases, and pleural effusion. We evaluated the predictive efficacy of each parameter, as well as age and sex, using the Weka machine learning software. Parameters most predictive of diagnosis were then used to generate a ruleset-based classifier using the JRip algorithm. A thoracic radiologist then blindly reviewed the 98 test cases for the presence of each parameter, to be fed into the classifier, and provided a best-guess diagnosis. A related-samples McNemar test was performed to assess differences in accuracy.

RESULTS

Using the machine learning software, the most predictive parameters for the diagnosis of an AMM were: age, sex, size, attenuation, shape, midline location, internal mammary LAD, mediastinal invasion, and pleural effusion. For the training set, the ruleset classifier correctly diagnosed 103/122 cases (84%). For the test set, the radiologist's best-guess diagnosis achieved an accuracy of 72/98 (74%). The ruleset classifier achieved an accuracy of 79/98 (81%). No significant difference in accuracy was seen (p=0.23). A ruleset-based classifier was constructed from the data.

CONCLUSION

A ruleset-based classifier can achieve accuracy comparable to a thoracic radiologist when evaluating the diagnosis of an anterior mediastinal mass.

CLINICAL RELEVANCE/APPLICATION

This algorithm is a potential semi-automated tool for accurate anterior mediastinal mass diagnosis in resource poor areas.

SSM05-05 Combination of DCE-MRI and DWI in Predicting the Treatment Effect of Concurrent Chemoradiotherapy in Esophageal Carcinoma

Wednesday, Nov. 29 3:40PM - 3:50PM Room: S404AB

Participants

Changmin Liu, RT,RT, BinZhou, China (*Presenter*) Nothing to Disclose Shaoshui Chen, RT,RT, BinZhou, China (*Abstract Co-Author*) Nothing to Disclose Fangling Ning, Binzhou, China (*Abstract Co-Author*) Nothing to Disclose Shuanghu Yuan, PhD, Jinan, China (*Abstract Co-Author*) Nothing to Disclose Qing Lei Shi, Beijing, China (*Abstract Co-Author*) Nothing to Disclose Judong Luo, Jinan, China (*Abstract Co-Author*) Nothing to Disclose Yanzhang Hao, Binzhou, China (*Abstract Co-Author*) Nothing to Disclose Zhenbo Wang, Binzhou, China (*Abstract Co-Author*) Nothing to Disclose Dianzhong Geng, Jinan, China (*Abstract Co-Author*) Nothing to Disclose

PURPOSE

To study the value of dynamic contrast-enhanced magnetic resonance imaging (DCE-MRI) combined with diffusion-weighted imaging (DWI) in evaluating the effect of concurrent chemoradiotherapy (CCRT) in patients with esophageal carcinoma.

METHOD AND MATERIALS

A total of 76 patients with newly diagnosed esophageal carcinoma were enrolled in this study. All the participants were examined with DCE-MRI and DWI at baseline (pre-treatment) and during the third week after the start of CCRT (post-treatment). The volume transfer constant (Krans), rate contrast (Kep), the contrast agent percentage in the extracel–lular fluid space (Ve), and the apparent diffusion coefficient (ADC) were measured by two radiologists with greater than 10 years' individual experience. The changes in lesion volume on CT were measured at the completion of radiotherapy and was used as an endpoint to evaluate the predictive ability of DCE-MRI and DWI. All the quantitative parameters were analyzed with the paired t-test and a p-value of less than 0.05 indicated statistical significance.

RESULTS

A total of 76 and 56 DCE-MRI and DWI scans were available for analysis at baseline and at the third week, respectively. Pretreatment Krans, pre-treatment Kep, pre-treatment ADC (P < 0.05), and post-treatment Krans (P < 0.05) and Δ Krans, Δ ADC (P < 0.05) were significantly different after CCRT. Based on the binary logistic model, the ROC analysis demonstrated that the combined predictors demonstrated a high diagnostic performance with a threshold of 0.211 and an AUC of 0.939. The sensitivity and specificity were 98.6% and 73.8%, respectively.

CONCLUSION

The combination of DCE-MRI and DWI, as a noninvasive method, allows for the visualization of esophageal carcinoma lesions and can be used as an early biomarker in the prediction of the effect of CCRT three weeks after treatment initiation.

CLINICAL RELEVANCE/APPLICATION

DCE-MR can detect the effects of radio- and chemotherapy at early time points and is recommended as part of a MR study prior to esophageal carcinoma.

SSM05-06 CT Features of Thymic Epithelial Tumors: Correlation with the Clinical Stage Classification Using the Recently Proposed TNM Staging System

Wednesday, Nov. 29 3:50PM - 4:00PM Room: S404AB

Participants

Akiko Sumi, MD, Kurume, Japan (*Presenter*) Nothing to Disclose Kiminori Fujimoto, MD, PhD, Kurume, Japan (*Abstract Co-Author*) Nothing to Disclose Asako Kuhara, Kurume, Japan (*Abstract Co-Author*) Nothing to Disclose Atsushi Kawaguchi, Kurume, Japan (*Abstract Co-Author*) Nothing to Disclose Naoko Ikehara, MD, Kurume, Japan (*Abstract Co-Author*) Nothing to Disclose Shuji Nagata, MD, Kurume, Japan (*Abstract Co-Author*) Nothing to Disclose Toshi Abe, MD, Kurume, Japan (*Abstract Co-Author*) Nothing to Disclose

For information about this presentation, contact:

sumi_akiko@kurume-u.ac.jp

PURPOSE

To evaluate the CT features of thymic epithelial tumors with recently proposed TNM staging system and to determine the CT features helpful in predicting patient outcome.

METHOD AND MATERIALS

This retrospective study included 116 patients with thymic epithelial tumor surgically treated. Two radiologists interpreted independently the 21 categories of CT findings and finally classified each category into two groups. Correlation of these categories with new TNM staging system and with prognosis were assessed.

RESULTS

The patients were 68 women and 48 men (median age, 59 years; range, 27-82 years). WHO histologic classification included Type A in 10, Type AB in 22, Type B1 in 28, Type B2 in 24, Type B3 in 10, and Carcinoma in 22 patients. The clinical stage using by TNM staging system were stage I in 92, stage II in 3, stage IIIa in 10, stage IIIb in 2, stage IVa in 3, and stage IVb in 6 patients. In the present study, stage II and greater (stage II-IV) tumors were considered an invasive tumor. There was statistically significant relationship between WHO histologic classification and tumor invasiveness (Fisher, P < .001). In multivariable analysis, there were statistically significant differences in tumor contour, adjacent chest wall change, pericardial thickness, and vascular invasion between stage I and stage II-IV (all, P < .05). Multivariate analysis using a stepwise forward Cox proportional hazards regression model showed that tumors with lobulated and irregular contour, lobulated and irregular contour with mediastinal fat, presence of hemorrhage/cyst/necrosis, and presence of band-like opacity in the lung were significantly associated with disease progression (all, P < .05). Patients with three or four of these factors had a significantly shorter cause-specific survival than the other patients (P < .001).

CONCLUSION

CT characteristics of thymic epithelial tumors may be helpful in the classification of the new TNM staging system and the prediction of the worse prognosis.

CLINICAL RELEVANCE/APPLICATION

CT features suggestive of invasiveness in thymic epithelial tumor were irregular contour, absence of chest wall's fat layer, presence of pericardial thickness or vascular invasion. Patients with these factors had the worse prognosis.





103rd Scientific Assembly and Annual Meeting November 26 to December 1 McCormick Place, Chicago



SSM06

Chest (Vascular)

Wednesday, Nov. 29 3:00PM - 4:00PM Room: S406B



AMA PRA Category 1 Credit ™: 1.00 ARRT Category A+ Credit: 1.00

Participants

Jonathan H. Chung, MD, Chicago, IL (*Moderator*) Nothing to Disclose Archana T. Laroia, MD, Fargo, ND (*Moderator*) Nothing to Disclose

Sub-Events

SSM06-01 Diagnostic Accuracy of Non-ECG-Gated Chest CT in the Assessment of Cardiac Chamber Enlargement and Hypertrophy Compared to Cardiac MRI

Wednesday, Nov. 29 3:00PM - 3:10PM Room: S406B

Awards Student Travel Stipend Award

Participants

Diego A. Eifer, MD,MSc, Toronto, ON (*Presenter*) Nothing to Disclose Elsie Nguyen, MD, Toronto, ON (*Abstract Co-Author*) Nothing to Disclose Paaladinesh Thavendiranathan, MD, Toronto, ON (*Abstract Co-Author*) Nothing to Disclose Kate Hanneman, MD, FRCPC, Toronto, ON (*Abstract Co-Author*) Nothing to Disclose

For information about this presentation, contact:

kate.hanneman@uhn.ca

PURPOSE

To establish gender specific cut-off values for cardiac chamber enlargement and left ventricular hypertrophy (LVH) on non-ECGgated chest CT using cardiac MRI as the reference standard.

METHOD AND MATERIALS

218 patients who had contrast enhanced non-ECG-gated chest CT (64-320 detector) and cardiac MRI (1.5-3T) performed within 7 days were identified retrospectively (53% male, 52.9 \pm 15.8 years, mean interval between CT and MRI 3.4 \pm 2.2 days). The presence of cardiac chamber enlargement and left ventricular hypertrophy (LVH) was established by cardiac MRI as the reference standard, according to current guidelines. Multiple measurements were obtained on axial CT images to evaluate left atrial (LA), left ventricular (LV), right atrial (RA) and right ventricular (RV) chamber size, and LV wall thickness, blinded to the reference standard. ROC analysis was performed to determine optimal gender-specific CT measurement cut-off values for the diagnosis of chamber enlargement (LAE, LVE, RAE, and RVE, respectively) and LVH, with specificity (Sp) >=90%. Inter-observer agreement was evaluated with intra-class correlation (ICC) in a random subset (n=40).

RESULTS

LAE was present in 69 (34%), LVE in 47 (23%), RAE in 45 (21%), RVE in 32 (15%) and LVH in 38 (19%). The following CT measurements were the best discriminators. For LAE, LA anterior-posterior (AP) diameter >=50 mm for males (sensitivity (Sn)=47%, Sp=92%, AUC=0.795) and >=44 mm for females (Sn=54%, Sp=92%, AUC=0.839). For LVE, LV transverse diameter >=58 mm for males (Sn=55%, Sp=92%, AUC=0.842) and >=53 mm for females (Sn=29%, Sp=93%, AUC=0.771). For RAE, RA transverse diameter >=67 mm for males (Sn=59%, Sp=91%, AUC=0.825) and >=63 mm for females (Sn=75%, Sp=92%, AUC=0.925). For RVE, RV transverse diameter >=58 mm for males (Sn=56%, Sp=90%, AUC=0.805) and >=57 mm for females (Sn=57%, Sp=91%, AUC=0.850). For LVH, LV maximal wall thickness >=17 mm for males (Sn=55%, Sp=91%, AUC=0.881) and >=15 mm for females (Sn=78%, Sp=92%, AUC=0.910). Inter-observer agreement was excellent (ICC range 0.887-0.973).

CONCLUSION

Cardiac chamber enlargement and LVH can be reliably identified on contrast enhanced non-ECG-gated chest CT with moderate sensitivity and high specificity.

CLINICAL RELEVANCE/APPLICATION

This study provides gender-specific cut-off values for measurements that can easily be obtained on axial non-ECG-gated CT images to identify cardiac chamber enlargement and LVH with high specificity.

SSM06-02 Correlating Computed Tomography Test Bolus Imaging Dynamics with Pulmonary Vascular Resistance in Pulmonary Hypertension

Wednesday, Nov. 29 3:10PM - 3:20PM Room: S406B

For information about this presentation, contact:

dbaruah@mcw.edu

PURPOSE

Pulmonary vascular resistance (PVR) is an important parameter in the management of pulmonary hypertension and serves as a primary endpoint to assess the treatment efficacy in several newer targeted therapies. Currently, invasive cardiac catheterization is the gold standard to accurately assess the severity of pulmonary hypertension by providing hemodynamic measures such as PVR and mean pulmonary artery pressure (mPAP). Currently there are no established CT parameters to correlate with PVR. We propose an innovative method using test bolus imaging parameters performed for routine CTPA to correlate with PVR.

METHOD AND MATERIALS

This is an IRB approved retrospective study performed in two separate institutions. Patients included are with known pulmonary hypertension who had a CTPA study within one month of right heart catheterization. CTPA were performed on a 64 slice multidetector CT. Bolus dynamics with 15 mL of intravenous nonionic contrast (Omnipaque 350) and repeated axial images with breath hold at the level of the main pulmonary artery. Full width at half maximum (FWHM) of the test bolus is the width of the main pulmonary artery enhancement curve at half its maximum density.

RESULTS

Out of 221 patients who had undergone CTPA study between January 2010 to December 2013 for evaluation of pulmonary hypertension, 52 of them also had a right heart catheterization within one month of CTPA. Of these 52 patients, 37 fulfilled the selection criteria. A correlation of established size parameters and also FWHM was obtained with catheter angiographic data. There was a strong correlation between FWHM and mPAP (r=0.65, p value<0.00001), PVR (r=0.8, p value<0.00001) and PVR (r=0.75, p value<0.00001) (Fig. 3a, 3b and 3c). There was a poor correlation between MPA, RPA, LPA, MPA/Aorta ratio, A/B and RV/LV and mPAP, PVR and PVRI.

CONCLUSION

This innovative study shows routine CT test bolus dynamic information (FWHM) from CTPA is a simple, reliable and easily available noninvasive method that has a very strong correlation with mPAP and PVR/PVRI as compared with conventional CTPA parameters.

CLINICAL RELEVANCE/APPLICATION

Being noninvasive, these CTPA test bolus parameters are potentially helpful for follow up of patients with pulmonary hypertension, mainly to assess treatment response and progression. Among all the parameters we evaluated the FWHM of test bolus correlates strongly with catheter angiographic parameters.

SSM06-03 Correlation between the Degree of Systemic Collateral Supply and the Severity of Chronic Thromboembolic Pulmonary Hypertension: A CT Angiography Study Using Intra-Arterial Injection

Wednesday, Nov. 29 3:20PM - 3:30PM Room: S406B

Awards

Student Travel Stipend Award

Participants Wenyu Sun, MD, Sendai, Japan (*Presenter*) Nothing to Disclose Hideki Ota, MD, PhD, Sendai, Japan (*Abstract Co-Author*) Nothing to Disclose Haruka Sato, Sendai, Japan (*Abstract Co-Author*) Nothing to Disclose Koichiro Sugimura, MD, PhD, Sendai, Japan (*Abstract Co-Author*) Nothing to Disclose Kei Takase, MD, PhD, Sendai, Japan (*Abstract Co-Author*) Nothing to Disclose

For information about this presentation, contact:

sunwenyu910920@gmail.com

PURPOSE

It is known that systemic collateral supply develops in chronic thromboembolic hypertension (CTEPH). The aim of this study was to assess whether the degree of shunts from systemic artery to the pulmonary vascular system identified by CT angiography using intra-arterial injection was associated with clinical severity in patients with CTEPH.

METHOD AND MATERIALS

A total of 23 patients with inoperable CTEPH were referred to our cardiology department. During diagnostic right and left heart cardiac catheterization, CT angiography using intra-arterial injection from a catheter in the ascending aorta was performed. One-hundred-and-five ml of 1/3 diluted iodine contrast media (35 ml of 350mgI/ml contrast media and 70 ml of saline) was injected at a speed of 9 ml/sec. CT was imaged at scan delay of 9 sec with a 80-kVp tube voltage setting. Two radiologists evaluated CT images by consensus reading. We measured CT values of the pulmonary trunk (HUpt), sub-segmental pulmonary arteries (HUpa) and segmental pulmonary veins (HUpv).HUdiff was calculated as HUpa (or HUpv) - HUpt. The shunt level was zero of HUdiff < 50. For each additional 50 increase of HUdiff, the shunt level was increased by 1. Two shunt scores in each patient were defined separately as the sum of shunt levels in 42 sub-segmental arteries and 18 segmental veins. Mean pulmonary artery pressure (mPAP) and pulmonary vascular resistance (PVR) were measured by right heart catheterization. Correlations between the shunt scores and hemodynamics were evaluated by Pearson's correlation. A p value < 0.05 was considered to reflect statistical significance.

RESULTS

The mean ± standard deviation of mPAP in the 23 patients was 41.4 ± 8.9 mmHg [range, 25-58]. The mean arterial shunt score was 15.3 ± 16.4 [range, 0-60]; the venous shunt score was 11.7 ± 10.2 [range,1-41]. The shunt score of pulmonary vein was significantly correlated with the mean PAP (r = 0.56, p < 0.01), whereas the shunt score of pulmonary artery was not (r = 0.13, p = 0.56)

CONCLUSION

Localization of shunts from systemic artery to pulmonary vessels was possible. The degree systemic collateral supply as indicated by the shunt score may attribute to the clinical severity of inoperable CTEPH.

CLINICAL RELEVANCE/APPLICATION

Systemic collateral supply localized by CT angiography was correlated with the severity of inoperable CTEPH and may give information for stratifying balloon pulmonary angioplasty.

SSM06-04 Treatment Effect of Balloon Pulmonary Angioplasty in CTEPH Quantified by Automatic Comparative Imaging in CTPA

Wednesday, Nov. 29 3:30PM - 3:40PM Room: S406B

Participants

Zhiwei Zhai, Leiden, Netherlands (*Presenter*) Nothing to Disclose Hideki Ota, MD, PhD, Sendai, Japan (*Abstract Co-Author*) Nothing to Disclose Marius Staring, PhD, Leiden, Netherlands (*Abstract Co-Author*) Nothing to Disclose Jan Stolk, Leiden, Netherlands (*Abstract Co-Author*) Nothing to Disclose Koichiro Sugimura, MD, PhD, Sendai, Japan (*Abstract Co-Author*) Nothing to Disclose Kei Takase, MD, PhD, Sendai, Japan (*Abstract Co-Author*) Nothing to Disclose Berend C. Stoel, PhD, Leiden, Netherlands (*Abstract Co-Author*) Nothing to Disclose

For information about this presentation, contact:

z.zhai@lumc.nl

PURPOSE

Balloon pulmonary angioplasty (BPA) in patients with inoperable chronic thromboembolic pulmonary hypertension (CTEPH) can have variable outcomes. To gain more insight into this variation, we aimed to visualize and quantify changes in lung perfusion using CT pulmonary angiography (CTPA). We validated these measurements of perfusional changes against hemodynamic changes measured during right-heart catheterization.

METHOD AND MATERIALS

We studied 14 consecutive CTEPH patients (12 female; age: 65 ± 17), who underwent CTPA and right-heart catheterization, before and after BPA. Post-treatment images were registered to pre-treatment CT scans (using the Elastix toolbox) to obtain corresponding locations. Pulmonary vascular trees and their centerlines were detected using a graph-cuts method and distance transform. Areas distal from vessels were defined for measuring perfusional changes in the parenchyma. Subsequently, the density changes within the vascular and parenchymal areas were calculated and corrected for inspiration level differences, and displayed in color-coded overlays. For quantification, the median and inter-quartile range (IQR) of the density changes were calculated in the vascular and parenchymal areas (Δ VD and Δ PD, respectively). The recorded changes in hemodynamic parameters included changes in systolic, diastolic and mean pulmonary artery pressure (Δ SPAP, Δ dPAP and Δ mPAP, respectively) and in vascular resistance (Δ PVR). The Spearman's correlation coefficients between perfusional changes and hemodynamic changes were tested.

RESULTS

PAP and PVR were significantly improved after BPA. Comparative imaging maps showed distinct patterns in perfusional changes between patients. Within vessels, the IQR of Δ VD correlated with Δ sPAP (R=-0.58, p=0.03), Δ dPAP (R=-0.71, p=0.005), Δ mPAP (R=-0.71, p=0.005) and Δ PVR (R=-0.77, p=0.001, see Figure). In the parenchyma, the median of Δ PD correlated with Δ dPAP (R=-0.71, p=0.005) and Δ mPAP (R=-0.68, p =0.008).

CONCLUSION

Comparative imaging in CTEPH patients offers insight into differences in BPA treatment effect. Quantification of these perfusional changes provides non-invasive measures that reflect hemodynamic changes.

CLINICAL RELEVANCE/APPLICATION

CTPA studies before and after balloon pulmonary angioplasty in CTEPH can demonstrate density changes in the vascular and parenchymal areas and is recommended to monitor treatment effects.

SSM06-05 Radiologist Performance in the Detection of Pulmonary Embolism: Features That Favor Correct Interpretation and Risk Factors for Errors

Wednesday, Nov. 29 3:40PM - 3:50PM Room: S406B

Participants

Seth J. Kligerman, MD, Denver, CO (*Presenter*) Nothing to Disclose Jason W. Mitchell, MD, Ellicott City, MD (*Abstract Co-Author*) Nothing to Disclose Jacob W. Sechrist III, MD, Pittsburgh, PA (*Abstract Co-Author*) Nothing to Disclose Adam K. Meeks, MD, Baltimore, MD (*Abstract Co-Author*) Nothing to Disclose Jeffrey R. Galvin, MD, Baltimore, MD (*Abstract Co-Author*) Nothing to Disclose Charles S. White, MD, Baltimore, MD (*Abstract Co-Author*) Consultant, Koninklijke Philips NV

For information about this presentation, contact:

skligerman@umm.edu

PURPOSE

To assess factors contributing to accurate detection and erroneous interpretation of PE

METHOD AND MATERIALS

over 15 months, all CTPA studies were recrospectively re-read by a chest radiologist (rad) with 9 yrs experience. Any disagreement with the initial read was independently assessed by 2 additional chest rads. Studies with uniform disagreement from initial read were labeled false - (FN, miss) or false + (FP overcall). Studies concordant between initial and re-read were true + (TP) or true - (TN). Number (single vs. multiple), most proximal extent (central [C], lobar [L], segmental [S], and subsegmental [SS]), and specific location of PE were recorded. Also assessed were specialty training, experience, time of study, kV used, resident preliminary read, use of iterative recon (IR), signal to noise ratio (SNR), and reports describing study as 'limited'. Parametric and non-parametric statistical testing was performed (significance p<0.05)

RESULTS

Of 2555 CTPA cases assessed, there were 230 TP (170 multiple, 60 single PE), 2271 TN, 35 FN (15 multiple and 20 single PE), and 19 FP studies. Overall sensitivity, specificity, PPV, NPV and accuracy of rads was 86.8%, 99.2%, 92.4%, 98.5%, and 97.9%. Sensitivity for detection of multiple PE (92.4%) was significantly higher than single PE (74.1%, p<0.01). Sensitivity for C (100%) and L (97.8%) PE was significantly higher than S (85.9%) and SS (74%, p<0.01 for both). Sensitivity of thoracic rads (91.7%) was higher than non-thoracic (82.8%) but only reached significance for isolated PE (89.2% vs 61.4%, P<0.02). SNR of both TP (13.4) and TN (13.8) studies was significantly higher than FN (11) and FP(11.6). Other factors were not significant. Compared to other S and SS, there were significantly more FNs in the upper lobe posterior and lower lobe lateral S or SS. There were significantly more FP in the inferior lingula. FP studies were more likely to be described as 'limited' in the report.

CONCLUSION

Accuracy for PE detection is high but errors occur, especially in isolated S or SS PE in posterior S or SS of upper and lateral S or SS in lower lobes. Sensitivity was higher in studies with high SNR and if read by thoracic rads

CLINICAL RELEVANCE/APPLICATION

This study demonstrates that although radiologists are accurate in the detection of PE, errors occur most commonly due to location or PE in specific ' blind spots', especially in studies with poor SNR and when interpreted by a non-thoracic radiologist.

SSM06-06 The Power of Axial Scans with 16cm Wide-Detector Scanner: Dose Reduction in Triple-Rule-Out CT Angiography

Wednesday, Nov. 29 3:50PM - 4:00PM Room: S406B

Awards Trainee Research Prize - Medical Student

Participants Yuhuan Chen, MD, Xianyang, China (*Presenter*) Nothing to Disclose Qi Yang, Xianyang, China (*Abstract Co-Author*) Nothing to Disclose Taiping He, Xianyang, China (*Abstract Co-Author*) Nothing to Disclose Yongjun Jia, MMed, Xianyang City, China (*Abstract Co-Author*) Nothing to Disclose Xiujuan Zuo, Xianyang, China (*Abstract Co-Author*) Nothing to Disclose Tang Hui, Xianyang, China (*Abstract Co-Author*) Nothing to Disclose Chuangbo Yang, MMed, Xianyang City, China (*Abstract Co-Author*) Nothing to Disclose Chuangbo Yang, MMed, Xianyang City, China (*Abstract Co-Author*) Nothing to Disclose Dong Han, MD, Xianyang, China (*Abstract Co-Author*) Nothing to Disclose Xinyang Zhu, MD,MD, Xianyang, China (*Abstract Co-Author*) Nothing to Disclose Zhen Tang Liu, xi`an, China (*Abstract Co-Author*) Nothing to Disclose Shan Dang, Xianyang, China (*Abstract Co-Author*) Nothing to Disclose

For information about this presentation, contact:

754955678@qq.com

PURPOSE

To explore the value of using three consecutive axial scans in the triple-rule-out (TRO) examination for chest pain on a 16cm widedetector CT system.

METHOD AND MATERIALS

Forty patients with acute chest pain underwent TRO scan and were assigned to study group (group A, n=20) and control group (group B, n=20). In both groups, 120kV tube voltage and automatic current modulation to obtain noise index of 21HU and contrast agent iopamidol (370 mg / ml) were used. For Group A, the time-density curves for pulmonary artery and aorta were monitored to calculate the scan delay time. Two-phasic contrast injection was used: 25mgI/kg/s for 12s in 1st phase and at 3.0ml/s injection rate for 20ml in 2nd phase. The pulmonary artery, coronary artery and aorta were scanned in succession in axial mode to cover the thoracic entrance to the top of the diaphragm. For Group B, scan was triggered by the threshold (100HU) for pulmonary artery to include the thoracic portal to the top of the diaphragm; the coronary artery was scanned after 7 seconds delay, followed immediately by scanning aorta in an helical mode. Contrast agent injection (SD) of the thoracic aorta, pulmonary artery, coronary artery, fat and erector spinae muscle were measured to calculate SNR and CNR. Image quality was also assessed using a 5-point system (5: best, 1: worst). Measurements were statistically compared.

RESULTS

There was no difference in age, heart rate and body mass index between the two groups (P> 0.05); The CT number, SNR, CNR and subjective score of the two groups were statistically the same (p>0.05). However, There was a significant difference in total effective radiation dose between group A ($3.3\pm1.2 \text{ mSv}$) and group B ($5.56\pm0.67\text{mSv}$) (P<0.05), resulting in40.3% effective dose reduction using the 3 consecutive axial scan mode.

CONCLUSION

Using 3 consecutive axial scans in in triple-rule-out (TRO) CTA on a 16cm wide-detector CT reduces both radiation dose and exposure times while maintaining image quality compared with the conventional TRO scanning protocol.

CLINICAL RELEVANCE/APPLICATION

 Axial scans may be used on a 16cm wide-detector CT in triple-rule-out CTA to reduce radiation dose and maintain image quality.







SSM07

Emergency Radiology (Musculoskeletal and Spine)

Wednesday, Nov. 29 3:00PM - 4:00PM Room: S403B



AMA PRA Category 1 Credit ™: 1.00 ARRT Category A+ Credit: 1.00

Participants

Mariano Scaglione, MD, Castel Volturno, Italy (*Moderator*) Nothing to Disclose Ferco H. Berger, MD, Toronto, ON (*Moderator*) Nothing to Disclose

Sub-Events

SSM07-01 Dual Energy CT for Opportunistic Bone Mineral Density Screening: Identifying Patients at Risk for Fragility Fractures

Wednesday, Nov. 29 3:00PM - 3:10PM Room: S403B

Participants

Tony W. Trinh, MD, Boston, MA (*Presenter*) Nothing to Disclose Bharti Khurana, MD, Boston, MA (*Abstract Co-Author*) Nothing to Disclose Andrew Primak, PhD, Malvern, PA (*Abstract Co-Author*) Employee, Siemens AG Aaron D. Sodickson, MD, PhD, Boston, MA (*Abstract Co-Author*) Institutional Research Agreement, Siemens AG; Consultant, Bayer AG

For information about this presentation, contact:

TWTRINH@BWH.HARVARD.EDU

PURPOSE

To test the hypothesis that Dual Energy CT derived surrogates for bone mineral density can differentiate between elderly patients with a demonstrated fragility fracture and control patients without fractures.

METHOD AND MATERIALS

12,595 consecutive abdominal/pelvic dual energy CT (DECT) scans (Siemens FLASH scanner, Syngo Via software version VB10) from 4/2013 to 6/2016 were retrospectively reviewed. 585 met inclusion criteria for non-contrast scan in a female aged >=65 with exclusion criteria of osseous metastases, spinal hardware, or motion. The cohort included 101 patients with fragility fractures defined as spinal compression, femoral neck, or pelvic insufficiency fractures visible on the study CT scan. The control group included 97 patients without fragility fractures. Recorded metrics included L1 (or the nearest adjacent non-fractured) vertebral body HU values, calcium concentration (converted from iodine to calcium concentration using a scaling factor derived from calcium phantom calibration scans), and calcium HU values (determined from a virtual non-calcium subtraction algorithm).

RESULTS

Mean average vertebral body ROI values for the fracture and control groups, respectively, were: 86 and 132 HU, 60 and 88 mg/ml Ca, and 119 and 162 calcium HU (t-test p<0.00001 for all). ROC analysis showed areas under the curve of 0.75, 0.72 and 0.72 for HU values, Ca concentration, and Ca HU values, respectively. Selecting a high sensitivity value of 90% for use as a meaningful screening test yields threshold values of 138 HU, 172 mg/ml Ca, and 94 Ca HU, with resultant specificities of 42%, 36%, and 38% for HU values, Ca concentration, and Ca HU values, respectively.

CONCLUSION

Patients with fragility fractures have significantly decreased vertebral body HU values, as well as DECT derived Ca concentration and Ca HU values. Ability of these measures to predict patients at risk for fragility fractures is comparable at high sensitivity values considered acceptable for screening. Further work is needed to optimize DECT techniques in order to determine optimal cutoff values, and to potentially improve performance compared to traditional HU values.

CLINICAL RELEVANCE/APPLICATION

Dual Energy CT derived surrogates for bone mineral density may allow for opportunistic bone mineral density screening in patients undergoing abdominal and pelvic CT for other reasons.

SSM07-02 A Focused MRI Protocol for Efficient Detection of Pathology Associated with Thoracolumbar Spine Fractures

Wednesday, Nov. 29 3:10PM - 3:20PM Room: S403B

Participants

Syed M. Karim, MD, Boston, MA (*Presenter*) Nothing to Disclose Christopher M. Bono, MD, Boston, MA (*Abstract Co-Author*) Advisory Panel, UnitedHealth Group Royalties, Wolters Kluwer nv Mitchell A. Harris, PhD, Boston, MA (*Abstract Co-Author*) Nothing to Disclose Aaron D. Sodickson, MD, PhD, Boston, MA (*Abstract Co-Author*) Institutional Research Agreement, Siemens AG; Consultant, Bayer

For information about this presentation, contact:

smkarim@post.harvard.edu

METHOD AND MATERIALS

Retrospective study of adult patients from 2 affiliated Level I trauma centers. Eligible patients presented to the emergency department between 2008 & 2015 with >= 1 fracture of the thoracic or lumbar spine on CT and MRI of the entire thoracic & lumbar spine within 10 days of CT. Exclusion criteria: > 4 levels fractured, pathologic fractures, isolated transverse/spinous process fractures, osteoporotic fractures, prior vertebral augmentation, prior TL spine instrumentation. Patients with neurologic deficits were not excluded. MRIs were reviewed independently by an orthopaedic spine surgeon and an emergency radiologist. MRIs were reviewed for posterior ligamentous complex (PLC) integrity, marrow edema, epidural hematoma, and cord contusion. Pathology identified outside of 3 levels above & below the fractured level(s) ('focused zone') were reviewed by the spine surgeon to determine if treatment would be altered.

RESULTS

126 patients with 216 fractures on CT identified. Demographics: 81 males (64%); median age 49; 62 (49%) TL junction injuries; 47 (37%) managed operatively. PLC injury identified by at least one reader in 41 (33%) patients with percent agreement for PLC injury between two readers of 96%; κ =0.91. Both readers independently agreed there was no pathology on the complete MRIs outside the focused zone in 101 (80%) patients. None of the outside pathology altered patient management. Percent agreement for the absence of outside pathology was 87%; κ =0.47.

CONCLUSION

A focused MRI protocol of 3 levels above & below a known thoracolumbar spine fracture(s) may miss radiographic pathology, but this pathology does not alter patient care.

SSM07-03 Radiological Predictors for Medial Collateral Ligament (MCL) Injury of the Elbow in the Emergency Department (ED)

Wednesday, Nov. 29 3:20PM - 3:30PM Room: S403B

Awards

Trainee Research Prize - Medical Student

Participants Jordan Lebovic, BA, Boston, MA (*Presenter*) Nothing to Disclose George Dyer, MD, Boston, MA (*Abstract Co-Author*) Nothing to Disclose Bharti Khurana, MD, Boston, MA (*Abstract Co-Author*) Nothing to Disclose

For information about this presentation, contact:

jordan_lebovic@hms.harvard.edu

PURPOSE

The Medial Collateral Ligament (MCL) is a primary stabilizer of the elbow and is well visualized on MRI. Specific radiological findings indicating MCL injury on radiographs and CT are under recognized by radiologists. Unrecognized MCL injury can cause post-operative instability and recurrent dislocations. The purpose of this study is to determine whether radiological findings can predict MCL injury in patients with elbow fracture-dislocations.

METHOD AND MATERIALS

Operative reports of 287 patients with elbow fracture-dislocations were reviewed to identify patients with injured and intact MCL. Radiology reports were also reviewed for MCL injury. Both Xrays and CTs were analyzed specifically for MCL injury by radiologist and elbow surgeon.

RESULTS

Only 4.5% (13/287) of the radiology reports for patients with elbow-fracture dislocations mentioned the status of the MCL attachment sites. 46 MCL injuries were evaluated and 19 were found to have either a fracture of the medial epicondyle or the sublime tubercle (5 sublime tubercle fractures and 14 medial epicondyle fractures). 16 intact MCLs were confirmed by operative visualization. 0 of the 16 intact MCLs had either a medial epicondyle fracture or a sublime tubercle fracture. 43% of patients with known MCL injury were found to have fracture (s) at the MCL attachment sites. Using fractures of either the medial epicondyle or sublime tubercle as predictor of MCL status had a sensitivity of 63% (CI 51%-74%), a specificity of 100% (CI 79%-100%) and a negative predictive value of .37 (CI .27-.50).

CONCLUSION

While MRI remains the optimal modality to assess for MCL injury, it is rarely used in ED for elbow fracture-dislocations. Presence of fractures involving medial epicondyle and sublime tubercle on radiographs and CT are critical and must be reported by radiologists to help guide the management.

CLINICAL RELEVANCE/APPLICATION

Using radioglogical predictors for MCL injury could identify patients requiring MCL repair, and thereby prevent post-operative instability and recurrent dislocations.

SSM07-04 Imaging of Necrotizing Fasciitis of the Upper Extremity: Distinguishing Cellulitis from Necrotizing Fasciitis

Participants Mohammad Mansouri, MD, MPH, Boston, MA (*Presenter*) Nothing to Disclose Michael H. Lev, MD, Boston, MA (*Abstract Co-Author*) Consultant, General Electric Company; Institutional Research Support, General Electric Company; Stockholder, General Electric Company; Consultant, MedyMatch Technology, Ltd ; Consultant, Takeda Pharmaceutical Company Limited; Consultant, D-Pharm Ltd Ajay K. Singh, MD, Boston, MA (*Abstract Co-Author*) Nothing to Disclose

PURPOSE

Cellulitis is a relatively common infection of the skin and subcutaneous tissues which may comprise up to 14% of emergency visits.Necrotizing fasciitis (NF) is a potentially fatal, uncommon infection of the soft tissues which can be difficult to diagnose and distinguish from cellulitis.We aim to analyze and compare imaging findings of cellulitis and NF of upper extremity in our large academic medical center.

METHOD AND MATERIALS

This is a HIPAA compliant, IRB approved, retrospective study of cases imaged between 2003 and 2017. Imaging database of our institution was searched for all cases of upper extremity cellulitis and NF. The reference standard for diagnosis was surgery, and/or clinical follow-up. Medical records were reviewed for patient clinical and imaging variables.

RESULTS

A total of 50 cases were included (mean age:44.5, 25 male 25 female). 15 cases had proven NF by surgery and 35 cases had cellulitis proven surgically and/or clinical follow-up. CT was acquired in 60.0% of NF cases (9/15) and 74.3% of cellulitis cases (26/35). Other imaging modalities used were MRI, plain radiograph, and US. Air was significantly more common present in NF compared with cellulitis (53.3%,8/15 and 20.0%,7/35 respectively) (p=0.04). Other common associated imaging findings with NF were subfascial fluid (n=6) and fascial thickening (n=8). NF was significantly more likely to be fatal compared with cellulitis (20.0%,3/15 and 0%,0/35 respectively) (p=0.02). All cases of cellulitis with soft tissue air, had history of recent incision and drainage, penetrating trauma, IV drug use, injection of steroid or immunization. Skin thickening and superficial subcutaneous tissue involvement was seen in all cases of cellulitis who had CT or MR. Soft tissue abscess was seen more commonly in cellulitis (31.4%,11/35) compared with NF (26.7%,4/15). Cellulitis cases who had soft tissue abscess, had significantly more intramuscular edema (66.7%, 6/9), compared with the cases without abscess (13.6%,3/22)(p=0.007).

CONCLUSION

Soft tissue air, fascial thickening and subfascial fluid collection are significantly more common in the NF than cellulitis.Majority of soft tissue air in cellulitis cases can be explained by history of recent trauma, IV drug use, immunization, incision and drainage, and injection.

CLINICAL RELEVANCE/APPLICATION

Soft tissue air, fascial thickening and subfascial fluid collection are significantly more commonly seen in the NF than cellulitis.

SSM07-05 One-Shot Volume Wrist CT as a Screening Tool: Impact on Detection and Treatment of Fractures

Wednesday, Nov. 29 3:40PM - 3:50PM Room: S403B

Participants

Monique Brink, MD, PhD, Nijmegen, Netherlands (*Presenter*) Research Grant, Toshiba Medical Systems Corporation Arjan Steenbakkers, MD, Nijmegen, Netherlands (*Abstract Co-Author*) Nothing to Disclose Micha Holla, Nijmegen, Netherlands (*Abstract Co-Author*) Nothing to Disclose Jacky W. De Rooy, MD, Nijmegen, Netherlands (*Abstract Co-Author*) Nothing to Disclose Jan Paul Frolke, Nijmegen, Netherlands (*Abstract Co-Author*) Nothing to Disclose Simon Cornelisse, MD, Nijmegen, Netherlands (*Abstract Co-Author*) Nothing to Disclose Peter Brink, Maastricht, Netherlands (*Abstract Co-Author*) Nothing to Disclose Michael Edwards, Nijmegen, Netherlands (*Abstract Co-Author*) Nothing to Disclose Mathias Prokop, PhD, Nijmegen, Netherlands (*Abstract Co-Author*) Nothing to Disclose Simeau, Toshiba Medical Systems Corporation; Research Grant, Toshiba Medical Systems Corporation;

For information about this presentation, contact:

Monique.Brink@radboudumc.nl

PURPOSE

Although conventional radiography (CR) is standard, computed tomography (CT) improves fracture detection in patients with wrist fractures. We implemented a fast set-up volume CT protocol in our clinic. Our objective was to evaluate fracture detection and therapeutic impact of this one-shot volume CT protocol in clinical practice.

METHOD AND MATERIALS

Between June 2013 and April 2014, we performed a prospective study on all adult patients with suspicion of acute fractures of the wrist or carpus. After informed consent, all patients first underwent CR, thereafter volume CT of the wrist, and then one year follow-up. Likelihood of fracture presence on a five-point scale was prospectively collected before and after CT. Three surgeons blinded to actual patient treatment independently proposed a treatment regimen (functional, cast, or operation), both based on anonymous clinical and radiological data, first with knowledge of CR, and thereafter with knowledge of CT. A radiologist and a surgeon served as reference standard for presence of fractures based on all data. Observer variability was evaluated with Fleiss kappa statistics. We performed receiver operating curve analyses for fracture detection and calculated proportion of wrists with treatment changes based on CT as compared to CR.

RESULTS

Ninety-eight patients participated (37 % male, mean age 53, range 18-87 years old), with 100 wrist CTs (mean DLP: 36 mGycm). CT detected true-positive fractures in 61 (41 radial, 14 ulnar, 26 carpal fractures), and CR in 45 patients (39 radial, 13 ulnar, 6 carpal fractures). AUC for fracture detection was 0.85 (95% CI:0.77-0.93) for CR and 0.97 (95% CI: 0.93-1.00) for CT. Agreement

on treatment was moderate after CR (Fleiss kappa 0.61 (95% CI 0.51-0.70)) and good after CT (0.75 (95% 0.66-0.84). Treatment changed in 24 (24%, 95% CI 16-33%) - 31 (31%, 95% CI 23-41%) wrists, mostly including refraining from cast immobilization (14-16 patients).

CONCLUSION

Volume CT increases accuracy of fracture detection, mainly of carpal injuries. This has a significant impact on cast immobilization changes in this patient population.

CLINICAL RELEVANCE/APPLICATION

Implementation of low threshold, fast-set up volume CT in patients with suspicion of wrist fractures improves carpal fracture detection and has a high potential to avoid unnecessary cast treatment.

SSM07-06 Emergency Department Overcrowding Delays Time to Radiography and Adversely Affects Outcomes for Hip Fracture Patients

Wednesday, Nov. 29 3:50PM - 4:00PM Room: S403B

Awards

Student Travel Stipend Award

Participants

Brendan Kelly, BMBCh, Dublin, Ireland (*Presenter*) Nothing to Disclose Eric J. Heffernan, MBBCh, FRCR, Elm Park, Ireland (*Abstract Co-Author*) Nothing to Disclose Cormac E. O Brien, MRCPI, MRCP, Dublin 4, Ireland (*Abstract Co-Author*) Nothing to Disclose John Ryan, Dublin, Ireland (*Abstract Co-Author*) Nothing to Disclose Isabelle M. Godson-Tracy, Dublin, Ireland (*Abstract Co-Author*) Nothing to Disclose John Cronin, MBBCh, Dublin, Ireland (*Abstract Co-Author*) Nothing to Disclose Daniel P. Ahern, MBBCh, Dublin, Ireland (*Abstract Co-Author*) Nothing to Disclose Conor Hurson, Dublin, Ireland (*Abstract Co-Author*) Nothing to Disclose

For information about this presentation, contact:

brendan.kelly@ucdconnect.ie

PURPOSE

The purpose of this study was to identify if ED overcrowding caused a delayed TTR in our institution and if so what effect it has on patient outcome.

METHOD AND MATERIALS

Patients were identified using the hip fracture database at a tertiary referral urban hospital with an annual ED census of over 53,000 patients. 154 consecutive cases were analysed. ED electronic records (Maxims[™]) and Radiology (PACS) records were then used to assess the Time to Radiography (TTR). Results were analysed using logistic regression in SPSS[™].

RESULTS

154 patients were included (115 female). Mean age was 81.04 (SD; range) (10.28; 44-102). Mean TTR was 110 minutes (73.1; 4-431). The mean total number of patients in the ED at presentation was 59.8 (16.67; range 27-99). Using ANOVA increasing numbers of patients was significantly associated with increasing time to radiography (p=0.003). Furthermore the TTR was significantly less (61 minutes vs. 113 minutes) when the ED was not above capacity of 33 patients (p<0.001). A regression model built to predict radiography in less than 60 minutes showed that only the total number of patients in the ED was independently associated with TTR (p=0.03). Analysing the hip fracture database for outcomes, delay to imaging was not associated with a delay in time to surgery (p=0.174), but was significantly associated with Time To Ward (TTW) (p=0.03) and length of stay (p=0.024).

CONCLUSION

TTR and overall outcomes for patients with a hip fracture are negatively impacted by the number of patients in the ED when they arrive.

CLINICAL RELEVANCE/APPLICATION

The authors hope these data will highlight the need for adequate resourcing of the ED and the healthcare system to deal with overcrowding and, in doing so, help avoid poorer outcomes for patients with time-dependent pathology.









SSM08

Gastrointestinal (CT Technique)

Wednesday, Nov. 29 3:00PM - 4:00PM Room: E353A



AMA PRA Category 1 Credit ™: 1.00 ARRT Category A+ Credit: 1.00

Participants

Myeong-Jin Kim, MD, PhD, Seoul, Korea, Republic Of (*Moderator*) Nothing to Disclose Naveen Kulkarni, MD, Milwaukee, WI (*Moderator*) Nothing to Disclose

Sub-Events

SSM08-01 Impact of Iterative Reconstruction Algorithms on CT Texture Features of the Liver Parenchyma

Wednesday, Nov. 29 3:00PM - 3:10PM Room: E353A

Participants

Pamela K. Sung, MD, Seoul, Korea, Republic Of (*Presenter*) Nothing to Disclose Jeong Min Lee, MD, Seoul, Korea, Republic Of (*Abstract Co-Author*) Grant, Bayer AG; Grant, General Electric Company; Grant, Koninklijke Philips NV; Grant, STARmed Co, Ltd; Grant, RF Medical Co, Ltd; Grant, Samsung Electronics Co, Ltd; Grant, Guerbet SA; Ijin Joo, MD, Seoul, Korea, Republic Of (*Abstract Co-Author*) Nothing to Disclose Tae-Hyung Kim, MD, Seoul, Korea, Republic Of (*Abstract Co-Author*) Nothing to Disclose Sanghyup Lee, MD, Seoul, Korea, Republic Of (*Abstract Co-Author*) Nothing to Disclose

PURPOSE

To evaluate whether CT reconstruction algorithms affect CT texture features of the liver parenchyma.

METHOD AND MATERIALS

This retrospective study included 72 patients (normal liver, n=36; chronic liver disease (CLD), n=36) who underwent 4-phase liver CT scan on a Brilliance iCT scanner (Philips Healthcare). All CT images were reconstructed with filtered back projection (FBP), hybrid iterative reconstruction (iDose4TM), and iterative model-based reconstruction (IMR, L1). On the arterial phase (AP) and portal venous phase (PVP) CT imaging, quantitative texture analysis of the liver parenchyma with single-slice ROI measurement was performed at the level of hepatic hilum using a filtration-histogram statistic-based method (TexRAD) with different filter values (fine, medium, coarse). Texture features including mean attenuation (M), standard deviation (SD), entropy (E), mean of positive pixels (MPP), skewness (S), and kurtosis (K) were compared among three reconstruction methods and between normal liver and CLD.

RESULTS

Iterative reconstruction techniques affected various CT texture features of the liver parenchyma in the same individuals, across the different filters. Among the CT texture features, SD and E were significantly different regardless of filter values, both on the AP and PVP imaging between iDose/IMR vs. FBP, and iDose vs. IMR(P<.05). When comparing patients with CLD with patients with normal liver, E from the AP images of fine filter was significantly different regardless of reconstruction algorithms(P<.05).

CONCLUSION

CT texture features of the liver parenchyma on a filtration-histogram method were significantly affected by CT reconstruction algorithms.

CLINICAL RELEVANCE/APPLICATION

Texture analysis using a uniform reconstruction algorithm would be important for a more reliable inter-subject comparison as well as intra-subject longitudinal monitoring.

SSM08-02 Diagnostic Accuracy of Anatomic CT Angiography-based Virtual Hepatic Venous Pressure Gradient in Patients with Portal Hypertension

Wednesday, Nov. 29 3:10PM - 3:20PM Room: E353A

Participants

Xiaolong Qi, Guangzhou, China (*Presenter*) Nothing to Disclose Jinlin Hou, Guangzhou, China (*Abstract Co-Author*) Nothing to Disclose Weimin An, Guangzhou, China (*Abstract Co-Author*) Nothing to Disclose Ruizhao Qi, Beijing, China (*Abstract Co-Author*) Nothing to Disclose Lei Wang, Beijing, China (*Abstract Co-Author*) Nothing to Disclose Yanna Liu, Guangzhou, China (*Abstract Co-Author*) Nothing to Disclose Changchun Liu, Beijing, China (*Abstract Co-Author*) Nothing to Disclose Chuan Liu, Guangzhou, China (*Abstract Co-Author*) Nothing to Disclose Yi Xiang, Guangzhou, China (*Abstract Co-Author*) Nothing to Disclose Jialiang Hui, Guangzhou, China (*Abstract Co-Author*) Nothing to Disclose Zhao Liu, Guangzhou, China (*Abstract Co-Author*) Nothing to Disclose

Yongzhao Zhao, Shanghai, China (Abstract Co-Author) Nothing to Disclose Yanjie Zhu, Shanghai, China (Abstract Co-Author) Nothing to Disclose Jiale Huang, Shanghai, China (Abstract Co-Author) Nothing to Disclose Jinjun Chen, Guangzhou, China (Abstract Co-Author) Nothing to Disclose Jianbo Zhao, Guangzhou, China (Abstract Co-Author) Nothing to Disclose Wei Xiong, Guangzhou, China (Abstract Co-Author) Nothing to Disclose Jinghui Dong, Beijing, China (Abstract Co-Author) Nothing to Disclose Xingshun Qi, Shenyang, China (Abstract Co-Author) Nothing to Disclose Guangyan Si, Luzhou, China (Abstract Co-Author) Nothing to Disclose Bo Liu, Guangzhou, China (Abstract Co-Author) Nothing to Disclose Jie Tian, Beijing, China (Abstract Co-Author) Nothing to Disclose Guoxin Li, Guangzhou, China (Abstract Co-Author) Nothing to Disclose Xiaoshun He, Guangzhou, China (Abstract Co-Author) Nothing to Disclose Yongping Yang, Beijing, China (Abstract Co-Author) Nothing to Disclose Fuquan Liu, Beijing, China (Abstract Co-Author) Nothing to Disclose Zhiwei Li, Beijing, China (Abstract Co-Author) Nothing to Disclose Group Chess, Guangzhou, China (Abstract Co-Author) Nothing to Disclose

For information about this presentation, contact:

qixiaolong@vip.163.com

PURPOSE

To access the performance of virtual hepatic venous pressure gradient (vHVPG) in diagnosing clinically significant portal hypertension (CSPH) and predicting risk of variceal hemorrhage (VH).

METHOD AND MATERIALS

102 patients were prospectively recruited in 3 high-volume liver centers in China between August 2016 and March 2017 [NCT02842697]. All participants were scheduled to undergo clinically-indicated hepatic venous pressure gradient (HVPG) measurement, CT angiography (CTA), and Doppler ultrasound. vHVPG values were calculated from the reconstructed threedimensional model of hepatic vein-portal vein system and computational fluid dynamics analysis. The performance of vHVPG in diagnosing CSPH (HVPG >= 10 mmHg) and predicting risk of VH (HVPG >= 12 mmHg) were assessed and compared with that of the imaging-based models (HVPGCT score, Portal diameter) and serum-based models (aspartate aminotransferase [AST] to alanine aminotransferase ratio [AAR], AST to platelet count ratio index [APRI], fibrosis index based on 4 factors [FIB-4]).

RESULTS

As expected, vHVPG was successfully interpreted in patients both with and without CSPH [Figure 1A, 1B]. For diagnosing CSPH, area under receiver operating characteristics curve (AUC), sensitivity, specificity, positive predictive value (PPV), and negative predictive value (NPV) of vHVPG were 0.875 (0.796-0.953), 0.759 (0.639-0.928), 0.895 (0.737-0.100), 0.969 (0.925-0.100), and 0.459 (0.365-0.581), respectively. Also, for predicting risk of VH, AUC, sensitivity, specificity, PPV, and NPV were 0.865 (0.777-0.953), 0.822 (0.726-0.904), 0.828 (0.690-0.966), 0.923 (0.861-0.983), and 0.649 (0.538-0.781), respectively. Overall, vHVPG showed a better diagnostic performance than that of imaging-based models (HVPGCT score, Portal diameter) and serum-based models (AAR, APRI, FIB-4) [Figure 1C, 1D].

CONCLUSION

The proposed vHVPG provides a novel approach for predicting degree of portal hypertension noninvasively and might facilitate patient counseling, decision-making regarding individualized diagnosis and monitoring. Moreover, it is promising to serve as a surrogate measurement of HVPG when invasive procedure is not available.

CLINICAL RELEVANCE/APPLICATION

(Dealing with portal hypertension) The vHVPG could be used in non-invasive diagnosis of clinically significant portal hypertension and predicting risk of complications like variceal hemorrhage in patients with portal hypertension.

SSM08-03 Dual-Energy CT in Patients with Small HCC: Utility of Noise Reduced Monoenergetic Images on Detection of Wash Out and Image Quality in Delayed Phase

Wednesday, Nov. 29 3:20PM - 3:30PM Room: E353A

Participants

Megumi Matsuda, MD, Toon, Japan (*Presenter*) Nothing to Disclose Takaharu Tsuda, MD, PhD, Toon, Japan (*Abstract Co-Author*) Nothing to Disclose Hiroaki Tanaka, MD, Onsen-Gun, Japan (*Abstract Co-Author*) Nothing to Disclose Teruhito Mochizuki, MD, Toon, Japan (*Abstract Co-Author*) Nothing to Disclose

METHOD AND MATERIALS

From April 2016 to March 2017, 20 patients with 33 small HCCs who underwent liver dynamic CT using dual-source dual-energy CT were enrolled. Delayed phase images were generated by 120-kVp-equivalent linear-blended and monoenergetic reconstructions at 40, 55 and 70 keV by standard monoenergetic reconstruction algorithm (sMERA: 40, 55, 70) and nMERA: 40+, 55+, 70+. As the objective analysis of image quality, liver-to-lesion contrast (CR), signal-to-noise ratio of the liver parenchyma and tumor (SNR liver, and SNR tumor), and contrast-to-noise ratio of the tumor (CNR) were calculated and compared. We selected 40+, 55+ and M120 images based on the results of earlier objective analysis, and two independent readers scored conspicuity of wash out in small HCC (tumor conspicuity) on 4-point scales and image quality on 5-point scales as the subjective analysis.

RESULTS

There was no significant difference between CR in nMERA and that in sMERA. At 40keV and 55keV, SNR liver, SNR tumor and CNR in the nMERA were significantly higher than those in the sMERA. The CR, SNR liver, SNR tumor, and CNR at 40+ image were significantly higher than those at other images except for 55+ image. There was no significant difference in these evaluation items between at 40+ image and at 55+ image. According to two observers, the scores of tumor conspicuity and image quality were greatest at 55+ image. The agreements of tumor conspicuity and image quality at 40+, 55+, and M120 images were good or

excellent between the two observers.

CONCLUSION

The 40+ and 55+ images can improve image quality and conspicuity of wash out in small HCC in the delayed phase, especially 55+ image may be most appropriate to detect the wash out of small HCC in delayed phase from the results of both objective and subjective analysis.

CLINICAL RELEVANCE/APPLICATION

The virtual monoenergetic images reconstructed with nMERA, especially 55+ image is useful to detect wash out of HCC in delayed phase.

SSM08-04 Assessment of Patient Size Cutoffs for Acceptable 80 kV And Mixed-kV Image Quality at Abdominal Volume-Mode 2-Rotation kV-mA Switching Dual Energy CT

Wednesday, Nov. 29 3:30PM - 3:40PM Room: E353A

Participants

Luis S. Guimaraes, MD, Toronto, ON (*Presenter*) Nothing to Disclose Dipanjali Mondal, MBBS, FRCR, Oxford, United Kingdom (*Abstract Co-Author*) Nothing to Disclose Dinesh Gooneratne, MBChB, FRANZCR, Toronto, ON (*Abstract Co-Author*) Nothing to Disclose Maria Twomey, MBChB, FFR(RCSI), Toronto, ON (*Abstract Co-Author*) Nothing to Disclose Ravi Menezes, PhD, Toronto, ON (*Abstract Co-Author*) Nothing to Disclose Kartik S. Jhaveri, MD, Toronto, ON (*Abstract Co-Author*) Nothing to Disclose Patrik Rogalla, MD, Toronto, ON (*Abstract Co-Author*) Institutional Research Grant, Toshiba Medical Systems Corporation

For information about this presentation, contact:

luis.guimaraes@uhn.ca

PURPOSE

Volume-mode 2-rotation kV-mA Switching (V2S) Dual Energy CT (DECT) is a unique DECT technical solution available in 320-row scanners that utilizes 80 kV data. Our purpose was to determine patient size limits that result in unacceptable 80 kV and mixed-kV image quality with this technology (not yet investigated), so that the benefits of V2S DECT can be appropriately utilized.

METHOD AND MATERIALS

We retrospectively reviewed 4-phase V2S DECT abdominal scans reconstructed with 3mm slice thickness, noting patients' weight, body mass index (BMI), anteroposterior diameter (AP) and lateral width (LW). Three GI radiologists examined images in the middle of the liver, pancreas and kidneys, grading overall image quality (IQ) of 80 kV and mixed-kV datases (1=excellent to 5=severe degradation) and image artifacts/reader confidence (1=no artifacts/high confidence to 5= severe artifacts, nondiagnostic). Quantitative assessment of noise and enhancement-to-noise-ratio (ENR) in each organ and abdominal fat was completed. Patient sizes that resulted in unacceptable IQ rankings (i.e., >=4 by any of the 3 readers) were determined.

RESULTS

Forty patients were included. Mean IQ scores were not significantly different for different organs (p > 0.054). Difference of mean weight, LW and AP+LW between patients with acceptable and unacceptable IQ was statistically significant (p values of 0.227, 0.0018 and 0.0008), in contradistinction to the difference between BMIs (p=0.0749). There was no statistically significant difference between noise/ENR levels of patients with acceptable and unacceptable quality. Median patient sizes (weight, BMI, LW and AP+LW) that resulted in unacceptable image quality and artifacts were 86 kg, 28.1 kg/m2, 38.3 cm and 73.3 cm. Weight, LW and AP+LW cutoffs that resulted in unacceptable image quality were 74.9 kg, 35.9 cm and 65.9 cm. IQ of mixed-kV datasets was acceptable in all patients with unacceptable 80 kV IQ. Readers agreement was moderate (k=0.522).

CONCLUSION

In very large patients image noise and artifacts can render low kV images unacceptable. Knowledge of the cutoffs for each technology allows better patient selection for low kV and DECT.

CLINICAL RELEVANCE/APPLICATION

Knowledge of size cutoffs for acceptable IQ at 80 kV with V2S DECT allows for appropriate implementation of the low kV and DECT imaging performed with the tested technique.

SSM08-05 K-Edge Spectral Photon-Counting CT Using Dual Contrast Protocol for Peritoneal Cavity Imaging

Wednesday, Nov. 29 3:40PM - 3:50PM Room: E353A

Participants

Salim Si-Mohamed, Lyon, France (*Presenter*) Nothing to Disclose Arnaud Thivolet, Lyon, France (*Abstract Co-Author*) Nothing to Disclose Pierre-Emmanuel Bonnot, Lyon, France (*Abstract Co-Author*) Nothing to Disclose Daniel Bar-Ness, Bron, France (*Abstract Co-Author*) Nothing to Disclose Monica Sigovan, PhD, Lyon, France (*Abstract Co-Author*) Nothing to Disclose Philippe Coulon, PhD, Suresnes, France (*Abstract Co-Author*) Nothing to Disclose Philippe Coulon, PhD, Suresnes, France (*Abstract Co-Author*) Employee, Koninklijke Philips NV Caroline Bouillot, Bron, France (*Abstract Co-Author*) Nothing to Disclose Vahan Kepenekian, Lyon, France (*Abstract Co-Author*) Nothing to Disclose Loic Boussel, MD, Lyon, France (*Abstract Co-Author*) Nothing to Disclose Philippe C. Douek, MD, PhD, Lyon, France (*Abstract Co-Author*) Nothing to Disclose Pascal Rousset, Pierre Benite Cedex, France (*Abstract Co-Author*) Nothing to Disclose

For information about this presentation, contact:

salim.si-mohamed@chu-lyon.fr

PURPOSE

To assess the feasibility of using a prototype spectral photon-counting computed tomography (SPCCT) to explore the peritoneal cavity in rats using simultaneously two contrast agents within blood and peritoneal compartments.

METHOD AND MATERIALS

Approval from the animal ethics committee was obtained. SPCCT with multiple energy bins was performed in two sets of two adult rats using gadolinium intraperitoneal (IP) and iodine intravenous (IV) injections (Protocol A), and conversely (Protocol B). After the 10 minutes needed to perform IP injection, helical scans were performed to explore the abdomen and pelvis without and 30 and 60 seconds after injection. Delayed 3 minutes helical scans were then performed only on organs of interest (OOI), e.g. liver (standard parenchyma enhancement reference), kidney and bladder (contrast agents urinary clearance). Two radiologists performed in consensus a qualitative analysis on conventional CT and K-edge images using a peritoneal opacification index (POI) in 13 regions, as defined in the peritoneal cancer index (score=0 to 3 per region depending on the degree of opacification). Regions of interest were manually drawn on material decomposition iodine and gadolinium K-edge images in OOI for measuring the concentrations of contrast agents.

RESULTS

IP diffusion of both contrast agents was excellent with similar POI on conventional and peritoneal k-edge images of 36/39, 36/39 in protocol A, and 34/39, 37/39 in protocol B. K-edge images showed clear visual separation of the contrast agents with a good IV enhancement (POI of IV agents=0/39 in the 4 rats) and IP opacification. Quantitative analysis in OOI showed IV contrast agent enhancement in the liver (e.g 1.6 ± 0.3 mg/mL for iodine, 1.3 ± 0.2 mg/mL for gadolinium at 30 seconds), and excretion in the renal pelvis (e.g 27.8 ± 0.2 mg/mL for iodine, 7.8 ± 0.5 mg/mL for gadolinium at 60 seconds). Progressive IP excretion of the contrast agents within the bladder was present, consistent with blood diffusion and renal excretion.

CONCLUSION

SPCCT can be used to perform a complete peritoneal dual contrast protocol using K-edge imaging which has potential to evaluate detection and tumoral response of peritoneal metastases.

CLINICAL RELEVANCE/APPLICATION

SPCCT with K-edge imaging is feasible using dual contrast agents within peritoneal and blood compartments allowing a good assessment of the peritoneal cavity in rats.

SSM08-06 Material Density Iodine Images in Dual-Energy CT: Detection and Characterization of Hypervascular Liver Lesions Compared to Magnetic Resonance Imaging

Wednesday, Nov. 29 3:50PM - 4:00PM Room: E353A

Participants

Daniela Muenzel, MD, Munich, Germany (*Presenter*) Nothing to Disclose Anushri Parakh, MBBS, MD, Boston, MA (*Abstract Co-Author*) Nothing to Disclose Manuel Patino, MD, Boston, MA (*Abstract Co-Author*) Nothing to Disclose HeiShun Yu, MD, Boston, MA (*Abstract Co-Author*) Nothing to Disclose Grace C. Lo, MD, Boston, MA (*Abstract Co-Author*) Nothing to Disclose Dushyant V. Sahani, MD, Boston, MA (*Abstract Co-Author*) Research support, General Electric Company; Medical Advisory Board, Allena Pharmaceuticals, Inc Avinash R. Kambadakone, MD, Boston, MA (*Abstract Co-Author*) Nothing to Disclose Ernst J. Rummeny, MD, Munich, Germany (*Abstract Co-Author*) Nothing to Disclose

PURPOSE

To determine the diagnostic potential of Material Density (MD) iodine images in dual-energy CT (DECT) for the detection and characterization of hypervascular liver lesions, using MRI as reference standard.

METHOD AND MATERIALS

Fifty-two patients with 236 hypervascular liver lesions (benign, n=31; malignant, n=205; mean diameter, 29.4mm) were included. All of them underwent both contrast-enhanced DECT and contrast-enhanced abdominal MRI within three months. Late arterial phase CT imaging was performed with dual energies of 140 and 80 kVp. Protocol A showed monoenergetic 65 keV images, and protocol B presented MD-iodine images. Three radiologists independently evaluated randomized images, and lesion detection, characterization, and reader confidence were recorded. Liver to lesion contrast ratio (LLR) and contrast-to-noise ratio (CNR) were assessed. Paired t tests were used to compare LLR, CNR, and the number of detected lesions.

RESULTS

All three observers correctly identified more liver lesions using protocol B vs protocol A: 83.13% vs 63.64%, 84.57% vs 68.09%, and 79.37% vs 65.52%. There was no significant difference between the three observers in classification of a lesion as benign or malignant. LLR was significantly increased in protocol B (2.8 ± 2.33) compared to protocol A (0.77 ± 0.55) and MRI (0.61 ± 0.66). CNR was significantly higher in protocol B (0.08 ± 0.04) compared to protocol A (0.01 ± 0.01) and MRI (0.01 ± 0.01). However, higher diagnostic confidence was reported more frequently by the experienced radiologist when using protocol B vs protocol A (84.6% vs 75%).

CONCLUSION

MD iodine images obtained from dual-energy CT increase the conspicuity in the detection of hypervascular liver lesions with comparable diagnostic performance to MRI.

CLINICAL RELEVANCE/APPLICATION

MD iodine images in DECT improve detectability of hypervascular benign and malignant liver lesions. Improved diagnostic confidence with dual-energy CT can potentially help to reduce the number of additional diagnostic procedures.

Honored Educators

 Presenters or authors on this event have been recognized as RSNA Honored Educators for participating in multiple qualifying educational activities. Honored Educators are invested in furthering the profession of radiology by delivering high-quality educational content in their field of study. Learn how you can become an honored educator by visiting the website at: https://www.rsna.org/Honored-Educator-Award/ Dushyant V. Sahani, MD - 2012 Honored EducatorDushyant V. Sahani, MD - 2015 Honored EducatorDushyant V. Sahani, MD - 2016 Honored EducatorDushyant V. Sahani, MD - 2017 Honored Educator





103rd Scientific Assembly and Annual Meeting November 26 to December 1 McCormick Place, Chicago



SSM09

Gastrointestinal (Esophagus and Stomach)

Wednesday, Nov. 29 3:00PM - 4:00PM Room: E353B



AMA PRA Category 1 Credit ™: 1.00 ARRT Category A+ Credit: 1.00

Participants

Douglas S. Katz, MD, Mineola, NY (*Moderator*) Nothing to Disclose Bhavin Jankharia, MD, Mumbai, India (*Moderator*) Nothing to Disclose

Sub-Events

SSM09-01 The Application Value of Spectral CT Low Dose Scanning Protocol Preoperatively Optimized for T Stage on Esophageal Cancer

Wednesday, Nov. 29 3:00PM - 3:10PM Room: E353B

Participants

Yue Zhou, Zhengzhou, China (*Presenter*) Nothing to Disclose Jianbo Gao, MD, Zhengzhou, China (*Abstract Co-Author*) Nothing to Disclose

PURPOSE

To evaluate the T stage for esophageal cancer using low dose spectral CT technique, and to discuss the diagnosed accuracy of T stage based on low dose scanning.

METHOD AND MATERIALS

Fifty-two patients with esophageal cancer confirmed by surgery or esophagoscopy randomly divided into two groups were enrolled in our study. Dual-phase chest CT enhancement was performed by using GE HD750 CT. Spectral CT were performed in study group with 350mgI/kg contrast medium injection, while control group underwent conventional 120KVp CT with 450mgI/kg contrast medium injection. Patients were divided into two sub-groups with A/C (FBP reconstruction) and B/D (ASIR). The SNRs, CNRs and subjective image quality score were calculated in four groups. Radiation dose were measured automatically in study group and control group. T stages were evaluated by a radiologist with 10 years experience of CT diagnosis.

RESULTS

The CNR and SNR in four groups showed significant difference (P<0.05). The SNR in group B was the highest, followed by group A, group C was the lowest. The overall image quality score and anatomy detailed score among four groups exhibited significant difference (P<0.05). Group B was the highest while group C was the lowest. The sensitivity and accuracy in study group (A and B) in terms of T1/2 stage were higher than control group (C and D). With regard to T3, the sensitivity and specificity in study group (A and B) were higher than control group (C and D). The accuracy in diagnosis of T4 between study group and control group were similar.

CONCLUSION

Low dose spectral CT scanning optimized the image quality for chest CT enhancement and reduced the radiation and contrast medium dose. Compared to conventional CT, low dose spectral scanning promoted the differential diagnosis between T1/2 and T3, and improved the sensitivity and specificity in differential diagnosis between T1/2 and T3.

CLINICAL RELEVANCE/APPLICATION

Low dose spectral CT scanning reduced the contrast medium and radiation dose, and improved the sensitivity and specificity in differential diagnosis between T1/2 and T3 for esophageal cancer.

SSM09-03 Fractal Dimension Analysis of Glucose Metabolism in Esophageal Cancer by FDG-PET: Correlation between the Quantitative Evaluation of Tumor Heterogeneity and Malignancy

Wednesday, Nov. 29 3:20PM - 3:30PM Room: E353B

Participants

Toru Tochigi, MD, Chiba, Japan (*Presenter*) Nothing to Disclose Kiyohiko Shuto, MD, PhD, Chiba, Japan (*Abstract Co-Author*) Nothing to Disclose Koichi Hayano, MD, Chiba, Japan (*Abstract Co-Author*) Nothing to Disclose Shinichi Okazumi, MD, PhD, Chiba, Japan (*Abstract Co-Author*) Nothing to Disclose Hisahiro Matsubara, MD, PhD, Chiba, Japan (*Abstract Co-Author*) Nothing to Disclose

For information about this presentation, contact:

tochigi819@gmail.com

PURPOSE

Intratumoral heterogeneity is a well-recognized characteristics of cancer. The purpose of this study is to assess the heterogeneity

of the intratumoral glucose metabolism using fractal analysis, and evaluate its prognostic value in patients with esophageal squamous cell carcinoma (ESCC).

METHOD AND MATERIALS

18F-fluorodeoxyglucose positron emission tomography (FDG-PET) was performed in 125 consecutive patients with ESCC. FDG-PET images were analyzed using a fractal analysis software, where differential box-counting method was employed to calculate the fractal dimension (FD) of the tumor lesion. Maximum standardized uptake value (SUVmax) and FD were compared with overall survival (OS).

RESULTS

The median FD was 1.97 (range, 1.7941 - 2.0359). The survival curve was analyzed using the median FD as the cutoff value. The survival rate in the high-FD group was significantly better than that in the low-FD group as determined by the Kaplan-Meier method (P = 0.0029). In the multivariate survival analysis, the FD was identified as an independent prognostic factor for the overall survival (<0.0001). Furthermore, we analyzed the overall survival rate in the patients who were treated with surgery alone and with neoadjuvant chemotherapy. The Kaplan-Meier analysis of this data also showed that the high-FD group had a significantly better survival than did the low-FD group (P = 0.0011, P = 0.0177)

CONCLUSION

Metabolic heterogeneity measured by fractal analysis can be a novel imaging biomarker for survival in patients with ESCC.

CLINICAL RELEVANCE/APPLICATION

The preoperative tumor metabolic heterogeneity was a useful biomarker for OS of patients with ESCC, and was independent of clinical markers such as TNM-staging.

SSM09-05 MRI of the Gastric Antrum for the Quantification of Gastric Motility: Comparison between Obese and Normal Weight Patients

Wednesday, Nov. 29 3:40PM - 3:50PM Room: E353B

Participants

Simona Picchia, MD, Rome, Italy (*Presenter*) Nothing to Disclose Marco Rengo, MD, Rome, Italy (*Abstract Co-Author*) Nothing to Disclose Damiano Caruso, MD, Rome, Italy (*Abstract Co-Author*) Nothing to Disclose Davide Bellini, MD, Latina, Italy (*Abstract Co-Author*) Nothing to Disclose Carola Severi, MD,PhD, Rome, Italy (*Abstract Co-Author*) Nothing to Disclose Andrea Laghi, MD, Rome, Italy (*Abstract Co-Author*) Nothing to Disclose

For information about this presentation, contact:

simona.picchia@gmail.com

PURPOSE

To compare differences in gastric motility between obese and normal weight patients with MRI.

METHOD AND MATERIALS

Motility antral scans were obtained by Magnetic Resonance Imaging (MRI) after a liquid meal: patients drunk 650-ml standardized liquid meal over 10 min (Nutridrink) plus two egg yolks and one albumen and 150 ml of water. This 525-kcal meal was composed of 25% fat, 25% protein, and 50% carbohydrate. Imaging was performed on a 1.5-Tesla system. CineMRI for motility analysis was performed using a coronal and axial 2DtrueFISP. Images have been acquired before (T0), immediately after the end of the meal assumption (T1) and every 20 minutes (T2-T5), for a total exam time of 100 minutes. Each gastric motility scan lasted 60 seconds, with 100 images acquired in free breathing. Images have been evaluated on a dedicated software. Two measurements were evaluated. The distal antral contraction waves (ACWs) and the antral diameter. The ACWs were measured as the distance between the proximal and distal border of a segmental contraction of the distal antrum. The antral diameter was measured at the level of the measured ACWs. The measurement lines have been propagated into the next image of the MRI sequence, and the newly detected distance registered. This process has been repeated for every single image of the cine sequence. The temporal changes of the antrum diameter and ACWs over time have been plotted on a graph thus displaying gastric motility frequencies and magnitude. Results obtained in obese and normal weight patints were compared.

RESULTS

Twenty patients were included in the study (10 obese and 10 normal weight). Motility antral scans in obese antrum showed that, during fasting and in the late-postprandial period of a liquid meal, the length of the antrum was significantly shorter with lower maximal contraction amplitude and frequency.

CONCLUSION

MRI is able to identify differences in antral motility between obese and normal weight patients.

CLINICAL RELEVANCE/APPLICATION

This study confirmed the presence of antral motility disfunction in obese patients. These results can be correlated with the previously published in vitro evidence that in antral smooth muscle of obese patients the alteration in VIP pathway occurs, suggesting that smooth muscle might represent a new therapeutical targets in gastrointestinal motility disorders.

SSM09-06 Imaging Assessment of Lauren Classification for Gastric Cancer Using a Non-Gaussian Fractional Order Calculus Diffusion Model

Wednesday, Nov. 29 3:50PM - 4:00PM Room: E353B

Lei Tang, MD, Beijing, China (*Abstract Co-Author*) Nothing to Disclose Yi Sui, PhD, Chicago, IL (*Abstract Co-Author*) Nothing to Disclose Kejia Cai, PhD, Chicago, IL (*Abstract Co-Author*) Nothing to Disclose Xiaohong J. Zhou, PhD, Chicago, IL (*Abstract Co-Author*) Nothing to Disclose

For information about this presentation, contact:

mkaraman@uic.edu

PURPOSE

To evaluate the performance of a new set of parameters (D, β , and μ) from a fractional order calculus (FROC) diffusion model for imaging assessment of Lauren classification in gastric cancer.

METHOD AND MATERIALS

With IRB approval, 41 patients (12 females and 29 males) with gastric cancer underwent MRI scans at 1.5T. Surgical specimens were obtained for pathology analysis to determine the cancer type according to Lauren classification, resulting in 10 patients with diffuse type, 23 with intestinal type, and 8 with mix type. For the statistical analysis, the diffuse and mix types were combined as mixed-and-diffuse type (MDT) to be differentiated from the intestinal type (IT). The MRI protocol included T1-weighted (VIBE), T2-weighted (turbo spin echo with respiratory-trigger), and diffusion-weighted imaging with 11 *b*-values (0 to 2000 s/mm2). Three parameters of the FROC model, diffusion coefficient *D*, fractional order parameter β (which correlates with intra-voxel tissue heterogeneity), and a microstructural quantity μ were estimated from the diffusion data. The mean values of FROC parameters over the tumor regions of interest were computed. Receiver operating characteristic (ROC) analysis was then performed to assess the performance of FROC model for gastric cancer type differentiation. The combination of FROC parameters (*D*, β , μ) were compared to using only *D*, which is equivalent to apparent diffusion coefficient.

RESULTS

A significant difference between MDT and IT were observed in the combination of *D*, β , and μ with a *p*-value < 0.05. The combination of FROC parameters also produced a better accuracy (74.3% vs. 69%), specificity (73.9% vs. 56%), and area under the curve (78.5% vs. 65.2%) than using *D* alone, while providing a comparable sensitivity (75% vs. 78.2%).

CONCLUSION

The combined FROC parameters (D, β , μ) outperformed D in non-invasive imaging assessment of Lauren classification for gastric cancer.

CLINICAL RELEVANCE/APPLICATION

The combined FROC parameters (D, β , μ) perform better than using diffusion coefficient alone for imaging assessment of Lauren classification in patients with gastric cancer.





103rd Scientific Assembly and Annual Meeting November 26 to December 1 McCormick Place, Chicago



SSM10

Genitourinary (Gynecology and Genitourinary Ultrasound)

Wednesday, Nov. 29 3:00PM - 4:00PM Room: E351

GU US

AMA PRA Category 1 Credit ™: 1.00 ARRT Category A+ Credit: 1.00

FDA Discussions may include off-label uses.

Participants

Harris L. Cohen, MD, Memphis, TN (*Moderator*) Nothing to Disclose Mary C. Frates, MD, Sharon, MA (*Moderator*) Nothing to Disclose

Sub-Events

SSM10-01 Impact of Contrast-Enhanced Ultrasound in the Secondary Prevention of Testicular Tumors

Wednesday, Nov. 29 3:00PM - 3:10PM Room: E351

Participants

DARIO DE ROSA, MD, NAPOLI, Italy (*Abstract Co-Author*) Nothing to Disclose Pietro Gisonni, Napoli, Italy (*Abstract Co-Author*) Nothing to Disclose Giuseppina Dell'Aversano Orabona, MD, NAPOLI, Italy (*Presenter*) Nothing to Disclose Maria Chiara Imperato, Napoli, Italy (*Abstract Co-Author*) Nothing to Disclose Martina Caruso, Napoli, Italy (*Abstract Co-Author*) Nothing to Disclose Dolores Ferrara, Napoli, Italy (*Abstract Co-Author*) Nothing to Disclose Arturo Brunetti, MD, Naples, Italy (*Abstract Co-Author*) Nothing to Disclose

For information about this presentation, contact:

darioderosa18@gmail.com

PURPOSE

This study evaluated the role of contrast-enhanced ultrasound CEUS in the secondary prevention of testicular tumours.

METHOD AND MATERIALS

Forty patients (median age 25 years, range 18-36 yrs) with a focal testicular lesion underwent B-mode ultrasound (US), Doppler and CEUS. Then all patients underwent orchiectomy and the histological exam of the mass was performed. Histological features and ultrasound images were recorded and compared for each patient.

RESULTS

The medium diameter of the lesions was 12 mm (range 3- 29 mm). 30 of 50 patients had malignant tumours (75%), 5 had benign tumours (12,5%) and 5 non-neoplastic lesions (12,5%).B-mode US detected neoplastic characteristics only in 9 of the 35 tumoural lesions; with color-Doppler techniques in 10 of 35 tumours was found intralesional hypervascularization (B-mode and color-Doppler US findings suggestive of neoplastic disease were irregular margins and internal hypervascularization).On qualitative CEUS evaluation 34 of the 35 neoplastic lesions showed intense enhancement; on quantitative CEUS all tumours showed different kinetics from the surrounding parenchyma, according to a rapid wash in and wash out for malignant tumours and rapid wash-in but delayed wash-out for benign tumours (CEUS findings suggestive of neoplastic disease were intense enhancement of contrast, rapidity of wash-in and wash-out and peak characteristics).

CONCLUSION

In this study, we confirmed the CEUS high accuracy in the differentiation between malignant and benign small lesions and its utility in the early diagnosis of testicular cancer.Conventional US revealed in all patients the presence of a solid testicular mass and color-Doppler revealed presence of increased blood flow signal, but in small testicular tumours it did not show vascularization and only CEUS was able to do a differential dignosis.Using CEUS, the temporal perfusion dynamics of the contrast enhancement help in the differentiation between malignant and benign tumours; the intensity of contrast enhancement helps in the differentiation between neoplastic and non-neoplastic lesions.Therefore, CEUS is useful in the secondary prevention of small testicular masses with an ambiguous color-Doppler pattern and permits, rapidly and without damage, to predict the lesion nature.

CLINICAL RELEVANCE/APPLICATION

CEUS can add relevant information for surgical decision making in small testicular lesions.

SSM10-02 Utility of Ultrasound Elastography (Acoustic Radiation Force Impulse Imaging) in Differentiating Ovarian Endometriomas from Hemorrhagic Ovarian Cysts; In Correlation with Histopathology

Wednesday, Nov. 29 3:10PM - 3:20PM Room: E351

Meera Krishnakumar, MD, Chennai, India (*Abstract Co-Author*) Nothing to Disclose Natesan Chidambaranathan, MD, PhD, Chennai, India (*Abstract Co-Author*) Nothing to Disclose Sudhakar H. K., DMRD, MD, Chennai, India (*Abstract Co-Author*) Nothing to Disclose Kapali Sunder, MD, DMRD, Chennai, India (*Abstract Co-Author*) Nothing to Disclose Sooraj Prasannakumar, MBBS, Chennai, India (*Abstract Co-Author*) Nothing to Disclose Sandhya Gh JR, MBBS, Chennai, India (*Abstract Co-Author*) Nothing to Disclose

For information about this presentation, contact:

jayasudha.sambedu@gmail.com

PURPOSE

To study the usefulness of ARFI in the differentiation of ovarian endometriomas and hemorrhagic ovarian cysts.

METHOD AND MATERIALS

It is a prospective observational study conducted in the department of radiodiagnosis of our institution from january to december 2016. The study population consisted of 35 women(n=40, 5 women with bilateral lesions) of reproductive age group (20-45 y) presenting to the department of radiodiagnosis with unilateral or bilateral adnexal cystic lesions with homogenous internal echoes, diagnosed by grey scale ultrasound.Cystic lesions with mural nodules/solid components/ internal vascularity were excluded from the study. Measurements were performed with SIEMENS ACUSON S 2000 ultrasound system enabled with virtual touch quantification software.Grayscale ultrasound with full bladder was performed on all the patients to clearly define the pelvic anatomy and the lesion position. The lesion was identified and a region of interest (1x0.5cm box within the lesion) within the lesion was selected. The stiffness was measured well within the capsule of the lesion. Five succesful measurements were taken for ARFI shear wave velocity, measured in meters per second and the median value was calculated.Histopathology results, post surgery were obtained for all the 40 lesions and correlated with the SWV values.

RESULTS

Ultrasound elastography (ARFI)was performed on all the 40 lesions and the median shear wave velocities(SWV) were calculated. The definitive diagnosis was made by post operative histopathological examination results and the SWV values were correlated. Out of the 40 cystic lesions, 23 lesions were endometriomas and 17 lesions were hemorrhagic cysts. All the lesions histopathologically proven as endometriomas had higher SWV values compared to those proven as hemorrhagic ovarian cysts. A cut-off value of 2.85m/s was established, concluding the lesions with SWV values above 2.85m/s were more likely to be endometriomas and those below 2.85m/s were more likely to be hemorrhagic cysts with a sensitivity and specificity of 94% and 100% respectively.

CONCLUSION

ARFI imaging is a feasible technique for pre-operative discrimination of ovarian endometriomas and hemorrhagic ovarian cysts.

CLINICAL RELEVANCE/APPLICATION

With the use of this modality clear preoperative diagnosis of the two lesions can be established and the existing diagnostic dilemma leading to unnecessary surgeries can be avoided.

SSM10-03 Quantitative Shear-Wave Elastography of the Testicle: Normal Values and Assessment of the Common Pathological Conditions on a Large Cohort

Wednesday, Nov. 29 3:20PM - 3:30PM Room: E351

Participants

Pierre De Marini, Strasbourg, France (*Presenter*) Nothing to Disclose Aissam Labani, MD, Strasbourg, France (*Abstract Co-Author*) Nothing to Disclose Quentin Minault, Strasbourg, France (*Abstract Co-Author*) Nothing to Disclose Mickael Ohana, MD, PhD, Strasbourg, France (*Abstract Co-Author*) Nothing to Disclose Herve Lang Sr, MD, Strasbourg, France (*Abstract Co-Author*) Nothing to Disclose Catherine Roy, MD, Strasbourg, France (*Abstract Co-Author*) Nothing to Disclose

For information about this presentation, contact:

catherine.roy@chru-strasbourg.fr

PURPOSE

Shear wave elastography (SWE) is the last development in ultrasonic assessment of the tissue elasticity. Our aim was to evaluate the values of the stiffness in normal parenchyma and in common pathologies in order to determine a threshold value for diagnosis.

METHOD AND MATERIALS

This prospective study recorded 235 patients (mean age 43.2±17.2 years, range 17-90) using a Toshiba AplioTM 500 (Toshiba Medical Systems, Japan).Young modulus(YM) values were recorded by mean of a circular ROI over the color map. The cohort was divided into two groups according the grey scale aspect : a normal group of 110 patients with 902 values (67 bilateral, 43 unilateral+125controlateral -3 localizations (superior, mid , inferior) - including microlithiasis and hydrocele) and a pathological group of 125 patients with 375 values (87 lesions up to 5mm, 38 diffuse abnormalities). Final diagnosis was done by clinical findings, follow up or histological analysis. For statistical analysis a Mann-Whitney test was used and the optimal cut off value was calculated from the ROC curves analysis. A P value below 0.05 was considered as significant.

RESULTS

The YM values of free lesion testicle was 4.56 ± 1.53 kPa, median = 3.85kPa.There was no significant difference concerning the side, the localization, the presence of hydrocele or stage I or II microlithiasis. There was a significant higher mean value stiffness with age (>60 years: 4.97kPa; p<0.001), stage III microlithiasis (6.27kPa; p<0.001) and in case of contralateral tumor (5.60kPa; p<0.001). The stiffness values and cut off thresholds were for tumors (n= 48, mean = 21.31 ± 7.01 kPa, median =19.60kPa , p<0.001) and 16.1kPa(Se= 0.82 - CI95[0.48-0.98], Sp= 0.81 kPaCI95[0.74-0.86], AUC= 0.881), orchitis (n=43, mean = 9.48 ± 3.91 kPa, median =6.65kPa, p<0.001) and 5.7kPa (Se= 0.63 - CI95[0.49-0.76], Sp= 0.77 - CI95[0.70-0.83], AUC=0.764) and fibrosis (n=34, mean = 31.55 ± 9.08 kPa, median =25.20kPa, p<0.001) and 26.3kPa (Se= 0.82 - CI95[0.63-0.94], Sp= 0.85 -

CI95[0.79-0.90], AUC= 0.872), respectively. By analyzing the distributions between the different pathologies, the difference was statistically significant between orchitis and fibrosis (p= 0.002) and tumors and fibrosis (p<0.001).

CONCLUSION

SWE is a complementary tool to differentiate fibrosis from a tumoral process.

CLINICAL RELEVANCE/APPLICATION

Quantitative SWE is an efficient mean to differentiate a fibrous tissue from a tumoral process on a localized gray scale lesion.

SSM10-04 Clinical Significance of the Slope of the Increasing Pressure Curve When Injecting Ultrasound Contrast Agent during the Evaluation of the Fallopian Tubal Patency

Wednesday, Nov. 29 3:30PM - 3:40PM Room: E351

Participants

Ye Qiang, Nanjing, China (*Presenter*) Nothing to Disclose Yiyun Wu, Nanjing, China (*Abstract Co-Author*) Nothing to Disclose Meimei Zhang, Nanjing, China (*Abstract Co-Author*) Nothing to Disclose

For information about this presentation, contact:

13913306601@139.com

PURPOSE

To explore the association between Fallopian tubal patency and the slope of the increasing pressure curve for ultrasound contrast agent.

METHOD AND MATERIALS

A total of 145 patients underwent hysterosalpingo contrast sonography (HyCoSy) between August 2015 and January 2016. HyCoSy was performed with the Voluson E8 ultrasound system (GE Healthcare, Zipf, Austria) equipped with an RIC5-9-D probe. The ultrasound contrast agent was injected and the pressure curve was recorded with a liquid-injecting machine (YLD YZ-800, Yi Lida Corp., Zhu Hai, China) that records the injection pressure in real time and automatically traces it as a pressure curve. We used SonoVue (Bracco International BV, Amsterdam, The Netherlands) as the ultrasound contrast medium. The statistical analysis was performed with SPSS Statistics, version 19 (IBM, Chicago, USA), and P < 0.05 was deemed statistically significant.

RESULTS

We divided the patients into three groups according to their different Fallopian tubal patency status: 71 patients (48.97%) in bilateral tubal patency group, 45 (31.03%) in unilateral tubal patency group (one side patent, and the other either passable or occluded), and 20 in bilateral tubal lesion group (both sides passable or occluded). The slopes of the increasing pressure curves for the three groups were 1.242 ± 0.572 , 1.472 ± 0.638 and 2.068 ± 1.236 kpa/s, respectively. There was some correlation between the slope of the increasing pressure curve and tubal patency (R = 0.287, P < 0.05). The slopes differed significantly between the bilateral tubal patency group and the bilateral tubal lesion group (P < 0.05) and between the unilateral tubal patency group and the unilateral tubal patency group and the unilateral tubal patency group was not significant (P > 0.05).

CONCLUSION

The slope of the curve tracing the increase in the pressure of the injected contrast agent during HyCoSy is associated with the tubal patency.

CLINICAL RELEVANCE/APPLICATION

Therefore, it can be used as an objective index of tubal patency, and should have utility in both diagnosis and treatment.

SSM10-05 Vasectomy Related Changes in the Scrotum on Ultrasound

Wednesday, Nov. 29 3:40PM - 3:50PM Room: E351

Participants Pramod K. Gupta, MD, Plano, TX (*Presenter*) Nothing to Disclose Ann M. Mottershaw, MD, Dallas, TX (*Abstract Co-Author*) Nothing to Disclose Vidisha V. Ghole, MD, Irving, TX (*Abstract Co-Author*) Nothing to Disclose

For information about this presentation, contact:

pramod.gupta@va.gov

PURPOSE

-Vasectomy is a popular method of male contraception, so that a signification proportion of men referred for scrotal sonography will have had a vasectomy. -The purpose of our study is to evaluate the sonographic changes in the scrotum after vasectomy and compare them with the sonographic appearance of non vasectomy patients.

METHOD AND MATERIALS

We performed a comparative study of 75 patients with a history of vasectomy and 75 patients without this history who were referred for scrotal sonography for various indications. Ultrasound findings in these two groups were tabulated and compared.

RESULTS

Certain ultrasonographic findings were more commonly observed in the patients with vasectomy than in non-vasectomy patients. These findings were: Thickened epididymides (41% versus 2%), Tubular ectasia of epididymis(57% versus 4%), both thickened epididymides and epididymal tubular ectasia together (36% versus 2%), sperm granulomas (21% versus 2%), tubular ectasia of rete

testis (29% versus 7%), mediastinal cysts (15% versus 4%), medial rotation of the testis in the scrotal sac which is determined by location of testis-epididymis complex (33% versus 3%). No significant difference was found in the incidence of epididymal cysts, varicoceles and hydroceles in the vasectomy and non vasectomy groups.

CONCLUSION

There was significantly higher incidence of thickened epididymides, epididymal tubular ectasia, sperm granulomas, tubular ectasia of rete testis and mediastinal cysts in the post vasectomy patients as compared to non vasectomy patients. These changes most likely occur due to postvasectomy obstruction, sperm statis and increased intraluminal pressure in the efferent ducts, epididymis and vas deferens. Medial rotation of the testis in the scrotal sac was also more common in the vasectomy group, which is likely due to iatrogenic changes in the structural support mechanism of the testis with resultant increased mobility of the testis within the scrotum.

CLINICAL RELEVANCE/APPLICATION

Familiarity with common ultrasound findings in vasectomy patients may help suggest post vasectomy status when history is not provided and in some cases may help avoid unnecessary intervention.

SSM10-06 Transvaginal Ultrasound (TVUS) Shear Wave Elastography (SWE) for the Evaluation of Benign Uterine Pathologies

Wednesday, Nov. 29 3:50PM - 4:00PM Room: E351

Awards

Student Travel Stipend Award

Participants Man Zhang MD I

Man Zhang, MD,PhD, Ann Arbor, MI (*Presenter*) Nothing to Disclose Ashish P. Wasnik, MD, Ann Arbor, MI (*Abstract Co-Author*) Nothing to Disclose William Masch, MD, Boston, MA (*Abstract Co-Author*) Nothing to Disclose Jonathan M. Rubin, MD, PhD, Ann Arbor, MI (*Abstract Co-Author*) Equipment support, General Electric Company; Equipment support, Siemens AG; Equipment support, Koninklijke Philips NV; Ruth C. Carlos, MD, MS, Ann Arbor, MI (*Abstract Co-Author*) Nothing to Disclose Katherine E. Maturen, MD, Ann Arbor, MI (*Abstract Co-Author*) Nothing to Disclose

For information about this presentation, contact:

zhangman@gmail.com

PURPOSE

To evaluate myometrial stiffness using TVUS SWE in women with benign myometrial pathologies including adenomyosis and leiomyoma vs. normal myometrium, using pelvic MR as the reference standard.

METHOD AND MATERIALS

Between January 2015 to June 2016, premenopausal women without a history of gynecologic malignancy presenting with pelvic pain and/or bleeding were enrolled in this IRB-approved prospective study. TVUS was performed in SWE mode with multiple regions of interest (ROIs) (>=1 cm2) in the uterus. Multiple shear wave velocities (SWVs) were recorded in each location and averaged. Reference pelvic MR exams were performed with multiplanar T2WI, and T1WI pre and post IV gadolinium administration . MR exams were reviewed in consensus by two radiologists blinded to the US findings, and the presence or absence of adenomyosis and/or leiomyomata was assessed using published criteria. US images were reviewed in consensus by two different radiologists and SWV for each ROI tabulated by anatomic area. Continuous variables were analyzed using means, t-tests and ANOVA, assuming p <0.05 for statistical significance.

RESULTS

34 premenopausal women (mean age 36.8 years, range 22-52) were enrolled with mean time between US and MR 11 days (\pm 27, range 0-118). MR diagnosed adenomyosis in 6 women involving 12 uterine locations, and leiomyomata in 12 women involving 28 uterine locations. Mean SWV in 16 women with normal myometrium was 4.3 m/s (\pm 1.7, range 1.8-9.4), compared with 5.7 m/s (\pm 2.3, range 1.7-9.9) in 18 women with adenomyosis or leiomyomata (p <0.0002, 95% CI of difference -2.2, -0.6).

CONCLUSION

Our pilot study demonstrated that myometrial SWVs were higher in women with adenomyosis or leiomyomata than in women with normal myometrium (p < 0.0002), indicating increased tissue stiffness associated with common benign myometrial diseases.

CLINICAL RELEVANCE/APPLICATION

Because women with benign myometrial conditions have increased myometrial stiffness, quantitative ultrasound SWE may be helpful in diagnosis and treatment response assessment for these disorders.

Honored Educators

Presenters or authors on this event have been recognized as RSNA Honored Educators for participating in multiple qualifying educational activities. Honored Educators are invested in furthering the profession of radiology by delivering high-quality educational content in their field of study. Learn how you can become an honored educator by visiting the website at: https://www.rsna.org/Honored-Educator-Award/ Ruth C. Carlos, MD, MS - 2015 Honored EducatorKatherine E. Maturen, MD - 2014 Honored Educator







SSM11

Health Service, Policy and Research (Medical Practice Management)

Wednesday, Nov. 29 3:00PM - 4:00PM Room: S104B

ΗР

AMA PRA Category 1 Credit ™: 1.00 ARRT Category A+ Credit: 1.00

Participants

Stephen Hobbs, MD, Lexington, KY (*Moderator*) Author with royalties, Wolters Kluwer nv Melissa M. Chen, MD, San Antonio, TX (*Moderator*) Nothing to Disclose

Sub-Events

SSM11-01 Clinical Utility Inpatient Abdomen MRI Following an Abdominal CT

Wednesday, Nov. 29 3:00PM - 3:10PM Room: S104B

Awards

Student Travel Stipend Award

Participants

HeiShun Yu, MD, Boston, MA (*Presenter*) Nothing to Disclose

Gauruv S. Likhari, MD, Houston, TX (*Abstract Co-Author*) Nothing to Disclose Peter F. Hahn, MD, PhD, Belmont, MA (*Abstract Co-Author*) Stockholder, Abbott Laboratories; Stockholder, Medtronic plc; Stockholder, CVS Caremark Corporation; Stockholder, Kimberly-Clark Corporation; Stockholder, LANDAUER, Inc; Spouse, Stockholder, Medtronic plc; Spouse, Stockholder, Gilead Sciences, Inc; Spouse, Bondholder, Bristol-Myers Squibb Company; Spouse, Bondholder, Johnson & Johnson

Debra A. Gervais, MD, Boston, MA (Abstract Co-Author) Nothing to Disclose

Dushyant V. Sahani, MD, Boston, MA (*Abstract Co-Author*) Research support, General Electric Company; Medical Advisory Board, Allena Pharmaceuticals, Inc

PURPOSE

The purpose of this study was to assess the diagnostic yield of abdomen magnetic resonance imaging (MRI) in the inpatient setting following computed tomography (CT).

METHOD AND MATERIALS

All inpatient abdominopelvic MRIs performed on patients from October 1, 2014 to September 30, 2015 were identified and medical records were retrospectively reviewed for the following information: clinical impact of MRI on patient care and length of stay (LOS). Only MRIs with a preceding CT were included in the study.

RESULTS

A total of 221 MRIs were included. Forty exams were deemed technically inadequate due to motion while 9 more patients did not tolerate a full examination. The most common indications were focal liver lesion (n=101), pancreaticobiliary ductal dilatation (n=39), abnormal liver function tests (n=26), acute pancreatitis (n=14), abdominal pain (n=10) and fever/sepsis (n=9). Eighty-three (38%) MRI exams were recommended on CT and 138 (62%) were requests from the care team. In 63 (29%) cases, MRI offered new information over CT. Thirty-two MRIs recommended by radiologists affected patient management whereas only 31 MRIs (23%; p = .010) recommended by the care team affected management. Twenty-nine of these cases changed immediate inpatient management, requiring further intervention (IR drainage, ERCP or surgery) or changing medical therapy. MRI identified abscesses (n=17), choledocholithiasis (n=8) or confirmed cholecystitis (n=2), which were not confidently diagnosed on CT. Patient LOS increased in 24 patients in order to receive an MRI. The average scan time for inpatient MRI was 57 minutes compared to 35 minutes for an outpatient MRI.

CONCLUSION

Inpatient abdomen MRIs have limited impact on patient care following a CECT while they entail higher scan time, utilize more resources and increase patient LOS. Therefore, it is prudent to reserve MRI exams for select clinical indications in consultation with a subspecialty radiologist, allowing other exams to be performed on an outpatient basis, to maximize its value.

CLINICAL RELEVANCE/APPLICATION

In a climate of rising healthcare costs, we must be mindful when utilizing scarce resources, particularly abdominopelvic MRI, which may only be necessary in select indications.

SSM11-02 Diagnostic Performance of MRI for Differentiation of Papillary Renal Cell Carcinoma versus Non-Papillary Renal Tumors: A Systematic Review and Meta-analysis

Wednesday, Nov. 29 3:10PM - 3:20PM Room: S104B

For information about this presentation, contact:

stella.kang@nyumc.org

PURPOSE

To perform a systematic review and meta-analysis of the performance of MRI in differentiation of papillary-type renal cell carcinoma (RCC) from non-papillary renal tumors.

METHOD AND MATERIALS

We performed searches of three electronic databases from January 2000 through March 2017 for studies that utilized MRI techniques to differentiate papillary RCC from other renal lesions. Methodologic quality was assessed to identify potential sources of bias using QUADAS-2. Diagnostic performance was summarized quantitatively using bivariate random-effects modeling.

RESULTS

12 studies involving 1,382 patients and 343 papillary RCC lesions met inclusion criteria. The overall quality of studies was moderate. Six studies using relative tumor enhancement for papillary RCC prediction were pooled quantitatively, with overall sensitivity of 79.3% (95% CI, 62-90%) and specificity of 91.3% (95% CI,76.4-97.1%). All six studies used comparator groups of clear cell RCC and oncocytic tumors. These studies' performance characteristics demonstrated a threshold effect (rho = -0.5), supporting a tradeoff in sensitivity for specificity among the chosen quantitative enhancement thresholds, and therefore representation along a summary receiver operator characteristic (ROC) curve. The area under the summary ROC curve was 0.85. Inclusion of tumor T2 characteristics increased specificity from 84% to 95.6%. Three studies used signal loss on in-phase imaging to predict papillary RCC but marked statistical heterogeneity precluded pooling. There were less than 3 studies focused solely on use of tumor T2 signal characteristics compared with renal cortex or diffusion weighted imaging for papillary RCC prediction.

CONCLUSION

Meta-analysis supports moderate sensitivity and excellent specificity of tumor enhancement for differentiation of papillary RCC versus non-papillary renal tumors and further, prospective study of test accuracy may be warranted. The apparent heterogeneity in test performance among studies is accounted for in part by a tradeoff in sensitivity for specificity among the different enhancement thresholds selected for test positivity. Though requiring further study, inclusion of T2 signal characteristics of the renal tumor may further improve specificity.

CLINICAL RELEVANCE/APPLICATION

The high specificity of contrast-enhanced MRI for detection of papillary RCC among renal tumors may be useful in candidate selection for watchful waiting, given the general indolence of this tumor subtype.

SSM11-03 Piradsv2: Correlation with Clinical Risk Scores and Implications for Risk Stratification

Wednesday, Nov. 29 3:20PM - 3:30PM Room: S104B

Participants

Florian Richter, MS, Dresden, Germany (*Abstract Co-Author*) Nothing to Disclose Angelika Borkowetz, MD, Dresden, Germany (*Abstract Co-Author*) Nothing to Disclose Verena Plodeck, MD, Dresden, Germany (*Abstract Co-Author*) Nothing to Disclose Thomas Brauer, MD, Dresden, Germany (*Abstract Co-Author*) Nothing to Disclose Manfred Wirth, Dresden, Germany (*Abstract Co-Author*) Nothing to Disclose Michael Laniado, MD, Dresden, Germany (*Abstract Co-Author*) Nothing to Disclose Ivan Platzek, MD, Dresden, Germany (*Presenter*) Nothing to Disclose

For information about this presentation, contact:

florian-tobias.richter@charite.de

PURPOSE

The aim of this study was to assess the relationship between PIRADSv2 scores and clinical risk scores in patients with prostate cancer and thus evaluate the potential role of the PIRADS score in risk stratification.

METHOD AND MATERIALS

Two hundred patients with suspected prostate cancer were included in this retrospective study. Patient age varied between 41 and 82y (66y on average). The mean prostate-specific antigen level (± SD) at the time of the biopsy was 10.52 ± 9.0 ng/ml. All patients underwent multiparametric prostate MRI (mpMRI) at 3T. The PIRADSv2 scoring system was used for MRI lesion classification. All patients underwent MRI/ultrasound fusion-guided biopsy. Based on the biopsy results and additional parameters (PSA value, clinical stage, count of positive biopsy punches etc.) the following clinical risk scores were calculated for each patient: D'Amico score, UCSF-CAPRA score and Epstein Criteria. The relationship between the maximum PIRADS score and the clinical risk scores was analyzed using a logistic regression model and Tukey's range test as a post-hoc test.

RESULTS

The highest PIRADS score was 5 in 35/200 patients, 4 in 62/200 patients, 3 in 66/200 patients and 2 in 27/200 cases. In 10/200 patients no lesions could be identified based on MRI. PIRADS scores of 5 (p < 0.001) and 4 (p < 0.01) were shown to be significant predictors for all three clinical risk scores, while maximum PIRADS scores of 1, 2 or 3 were not significant predictors. Patients with a PIRADS score of 5 had significantly higher clinical risk scores than patients with a maximum PIRADS of 1, 2 or 3 (D`Amico: p < 0.001; UCSF-CAPRA: p < 0.001; Epstein: p < 0.001), while there was no significant difference between PIRADS 4 and lower maximum PIRADS scores. Among patients with PIRADS 5, the percentage of high-risk cases was 86.3% according to the D'Amico score, 90.2% according to UCSF-CAPRA and 94.1% according to the Epstein Criteria.

A PIRADS score of 5 is a significant predictor for the three evaluated clinical risk scores. A PIRADS score of 5 is associated with significantly higher clinical risk scores than maximum PIRADS 1, 2 or 3. Patients with a PIRADS score of 5 include a large precentage of high-risk prostate cancer cases.

CLINICAL RELEVANCE/APPLICATION

The results imply that a PIRADS score of 5 can help identify high-risk prostate cancer cases even before the tumor is confirmed by biopsy.

SSM11-04 MRI Orders Prioritization and Associated Effects on Appropriate Utilization of MRI at a Large Public Hospital

Wednesday, Nov. 29 3:30PM - 3:40PM Room: S104B

Awards

Student Travel Stipend Award

Participants

Anna Trofimova, MD, PhD, Atlanta, GA (*Presenter*) Nothing to Disclose Pinar Keskinocak, Atlanta, GA (*Abstract Co-Author*) Nothing to Disclose Bethany M. Cavazuti, MD, Atlanta, GA (*Abstract Co-Author*) Nothing to Disclose Elizabeth A. Krupinski, PhD, Atlanta, GA (*Abstract Co-Author*) Nothing to Disclose Amanda S. Corey, MD, Atlanta, GA (*Abstract Co-Author*) Nothing to Disclose

For information about this presentation, contact:

atrofim@emory.edu

PURPOSE

To determine changes in MRI order prioritization and downstream effects on appropriate utilization of MRI at a large public hospital from 2012 to 2015.

METHOD AND MATERIALS

Retrospective IRB approved study of MRI exams (MRIs) performed at a large public hospital from 2012 to 2015. The following parameters were analyzed: total number of MRIs; number of STAT and routine MRIs; type of MRI exams; ordering hospital services; mean total turnaround time (MTAT) for different MRIs per month; for MRIs performed in 2015 - per the day of the week and time of the day when the order was placed. The analyzed data were used to develop an on-line survey distributed to ordering providers to assess their knowledge of the order priority policy and evaluate factors which contribute to decision making in prioritization of MRI orders.

RESULTS

From 2012 to 2015 the total number of MRIs have increased by 35% reaching 10921 in 2015. STAT MRIs increased by 76%, routine MRIs increased by 12%. STAT MRIs increased by 72% for outpatients, 132% for inpatients and decreased by 35% for ER patients. MRI of the brain, lumbar spine and head/neck MRA represented 58% of all MRIs scans. The total number of brain MRIs increased by 82%, routine brain MRIs increased by 2%. 5 out of 89 hospital services ordered 70% of brain MRIs and 70% of those were ordered STAT. In 2015 MTAT for STAT brain MRI was 52% higher than for routine orders. MTAT is significantly affected by month of the year for STAT brain MRI, for routine brain MRIs MTAT is significantly higher for orders placed on Sunday and from 7 pm till 8 am. 97 providers (36% faculty; 64% trainees) completed the survey. Only 4% of responders were familiar with the timing of the STAT MRI order per hospital policy with significant difference as a function of specialty and level of training. Prevalent expectations for time to complete STAT MRI was "same day" for ER and inpatient and "2-3 days" for outpatient MRI orders.

CONCLUSION

Misuse of order priority system leads to disproportionate increase in STAT MRI orders with STAT brain MRI total turnaround time being 52% higher than routine brain MRI.

CLINICAL RELEVANCE/APPLICATION

Inappropriate MRI order prioritization significantly affects diagnostic imaging resources utilization and decreases quality of patient care by increasing turnaround time when STAT MRI is indicated.

Honored Educators

Presenters or authors on this event have been recognized as RSNA Honored Educators for participating in multiple qualifying educational activities. Honored Educators are invested in furthering the profession of radiology by delivering high-quality educational content in their field of study. Learn how you can become an honored educator by visiting the website at: https://www.rsna.org/Honored-Educator-Award/ Elizabeth A. Krupinski, PhD - 2017 Honored Educator

SSM11-05 Improvement of Provider and Patient Satisfaction in a Large Outpatient Imaging Practice Following Practice-Wide Implementation of a Structured Service-Excellence Training Program

Wednesday, Nov. 29 3:40PM - 3:50PM Room: S104B

Participants

Monica Salama, Houston, TX (*Abstract Co-Author*) Nothing to Disclose Joseph R. Steele Jr, MD, Houston, TX (*Abstract Co-Author*) Consultant, Adient Medical Inc; Stockholder, Adient Medical Inc; Habib Tannir, MS, Houston, TX (*Presenter*) Nothing to Disclose

PURPOSE

Low patient satisfaction scores and the need to improve upon referrals prompted us to address the experience we were providing. The implementation of our Service Excellence Academy (SEA) has already led to measurable improvement in our scores, increased

collaboration and positively charged our work environment.

METHOD AND MATERIALS

Informal interviews with providers showed they believed they were providing excellent service, but Press-Ganey scores showed patients did not always perceive the service as excellent. To improve providers' understanding of what patients and family members consider excellent service and thereby improve patient satisfaction, we created the SEA by evaluating best practices of service leaders across industries, and applying the strategies to our culture and healthcare setting. This ten-hour, three-module program was designed as an interactive discussion, leveraging clinical examples and role-playing. Sessions were led by one content expert and a member of leadership. The involvement of the leadership connected real examples and demonstrated their commitment to the culture shift.

RESULTS

Since launching the SEA in 2015, we have seen our outpatient survey scores stabilize, rise and recover from outside influences. All metrics show percentile improvement ranging from 9% to 34%. We are also using our employee survey as a benchmark to establish if we have affected the environment we create for ourselves. Finally, we collected feedback before, during and after the sessions to validate the engagement and buy-in of the participants. Participants felt a greater connection with the institutional culture, were more comfortable making decisions, felt more empowered and had developed greater empathy and skills to meet the needs of others.

CONCLUSION

Large scale training of providers and staff is possible and effective. Implementation of the SEA demonstrated both objective and subjective improvement of the patient and employee satisfaction. We have implemented strategies to build upon relationships and empowered our team members to make this a living part of our culture that continues to adapt, grow and improve our outcomes. This program is now being adapted for institutional implementation.

CLINICAL RELEVANCE/APPLICATION

Open lines of communication create an environment where colleagues are more inclined to consult on challenging cases, or proactively discuss options before ordering, resulting in better outcomes.

SSM11-06 Implementing a Comprehensive System to Optimize Performance on the Quality Payment Program of MACRA Across a Multi-Site Practice

Wednesday, Nov. 29 3:50PM - 4:00PM Room: S104B

Participants Richard E. Heller III, MD, Chicago, IL (*Presenter*) Nothing to Disclose Basak Ertan, El Segundo, CA (*Abstract Co-Author*) Nothing to Disclose Nina E. Kottler, MD, MS, Sydney, Australia (*Abstract Co-Author*) Nothing to Disclose Abraham J. Bronner, MD, Harvey, IL (*Abstract Co-Author*) Nothing to Disclose

For information about this presentation, contact:

richard.heller@radpartners.com

PURPOSE

The Medicare Access and CHIP Reauthorization Act (MACRA) of 2015 revised the system used by the Centers for Medicare and Medicaid Services (CMS) to pay physicians for care provided to Medicare patients [1]. The Quality Payment Program (QPP), created by MACRA, is intended to incentivize providers to deliver care that increases value and improves quality and/or lowers cost [2]. The QPP specifies four performance categories, each containing various numbers of required measures. Performance above a threshold will result in a bonus payment. Poor performance, or non-participation, will result in payment deductions, with these payment changes beginning in 2019. The program is intended to be budget neutral, meaning that the penalties fund the bonuses. Our radiology group, consisting of locally-led practices with over 350 radiologists serving more than 260 sites in nine states, developed a comprehensive, robust, and adaptable program to manage performance on these measures. The size of our practice provided both challenges and opportunities. The practice has the scale to invest in resources to optimize our performance, but simultaneously the large and multi-centric nature of our practice makes coordination more challenging. The primary goal of our program is to support our broader practice mission of enhancing value for healthcare systems and improving patient care. This is done alongside the financial incentives created by MACRA and the QPP. This presentation describes our approach and the development of our MACRA program.

RESULTS

For each practice, the above questions were answered and a spreadsheet was created (Figure). The figure lists several of our sites, as well as the pace they are reporting at, their patient-facing status, and which measures in the four performance categories they are reporting. Note that we are only reporting on Quality and Improvement Activity measures. Since no practice (radiology or otherwise) has to manually report Cost data, no requirements for this performance category were included. Additionally, since all of our practices are considered non-patient-facing, which has a reduced reporting burden including exclusion from the fourth performance category, Advancing Care Information, no measures here are reported.

CONCLUSION

We have described a comprehensive program for management of the Quality Payment Program created by MACRA, and the various measures required of physicians who provide services to Medicare patients. As the financial implications of the QPP are substantial, starting with a +/- swing of four percent in 2019 and quickly escalating, medical practices serving Medicare patients must have a robust program to manage the complex system with its numerous and still evolving variables. In addition, the intuition behind MACRA, that is payment for better and more value-based care, supports our broader practice goals of enhancing value and improving patient care.

METHODS

Our process has three main components. First, we created a diversified team to develop and manage our MACRA program. Second, we reviewed the necessary decisions and then determined how to best match the reporting requirements with the goals of our

program and our practice strengths. Finally, we established an education program along with performance tracking to ensure optimal and consistent achievement of the desired measures. We initially created a multi-disciplinary team to develop and manage our MACRA program. The team is led by the chief revenue officer, someone with extensive experience in healthcare revenue cycle management. The other members of the team include physicians, support analysts, billing and coding specialists, and information technology (IT) personnel. Another skillset, which was provided by the physician liaisons, was societal and policy affairs expertise. This was felt to be crucial as our practice recognizes the importance of working in conjunction with the American College of Radiology. The team then set about determining the key questions and answering them. This includes: 1) Will each practice report as patient-facing or non-patient-facing? 2) Should the local sites report as a group or as individuals? 3) Which measures should each site report on? 4) How will the measures be reported (claims or registry)? 5) What pace should each local practice choose to report at? Each of these five questions had to be answered for every local practice. We then developed an educational program for our radiologists. This was composed of three live web-based seminars, group emails, and posts on our internal practice website. Radiologists were given opportunities to ask questions, raise concerns, and make suggestions. After education, we began tracking performance through use of analysts and IT solutions. We provide monthly feedback to the practices on their performance in the form of a scorecard.

PDF UPLOAD

https://abstract.rsna.org/uploads/2017/17013906/17013906_mdyx.pdf





103rd Scientific Assembly and Annual Meeting November 26 to December 1 McCormick Place, Chicago



SSM12

Informatics (Machine Learning in Radiology)

Wednesday, Nov. 29 3:00PM - 4:00PM Room: S404CD



AMA PRA Category 1 Credit ™: 1.00 ARRT Category A+ Credit: 1.00

FDA Discussions may include off-label uses.

Participants

Norio Nakata, MD, Tokyo, Japan (*Moderator*) Nothing to Disclose Nabile M. Safdar, MD, Milton, GA (*Moderator*) Nothing to Disclose Luciano M. Prevedello, MD, MPH, Columbus, OH (*Moderator*) Nothing to Disclose

Sub-Events

SSM12-01 An Artificial Intelligence Method for Auto-Contouring in Abdominal Magnetic Resonance Imaging-Guided Adaptive Radiation Therapy

Wednesday, Nov. 29 3:00PM - 3:10PM Room: S404CD

Participants

Fan Liang, Cleveland, OH (*Abstract Co-Author*) Nothing to Disclose Pengjiang W. Qian, PhD, Wuxi, China (*Abstract Co-Author*) Nothing to Disclose Kuan-Hao Su, Cleveland, OH (*Abstract Co-Author*) Research Grant, Koninklijke Philips NV Atallah Baydoun, MD, Cleveland, OH (*Presenter*) Nothing to Disclose Asha Leisser, Cleveland, OH (*Abstract Co-Author*) Fellow, Koninklijke Philips NV Steven Van Hedent, MD, Cleveland, OH (*Abstract Co-Author*) Nothing to Disclose Jung-Wen Kuo, Cleveland, OH (*Abstract Co-Author*) Nothing to Disclose Parag Parikh, MD, Saint Louis, MO (*Abstract Co-Author*) Nothing to Disclose Yonggang Lu, St. Louis, MO (*Abstract Co-Author*) Nothing to Disclose Raymond F. Muzic Jr, PhD, Cleveland, OH (*Abstract Co-Author*) Research Grant, Koninklijke Philips NV Bryan J. Traughber, MD, Cleveland Heights, OH (*Abstract Co-Author*) Spouse, Employee, Koninklijke Philips NV

For information about this presentation, contact:

fxl84@case.edu

PURPOSE

Manual contouring remains the most laborious task in radiation therapy planning and is a major barrier in implementing routine Magnetic Resonance Imaging (MRI) guided-guided Adaptive Radiation Therapy (MR-ART). To address this, we propose a new artificial intelligence-based auto-contouring method for abdominal MR-ART modeled after human brain cognition for manual contouring.

METHOD AND MATERIALS

Our algorithm is based on two types of information flow: top-down and bottom-up. Top-down information is derived from simulation MR images. It grossly delineates the object based on its high-level information class by transferring the initial planning contours onto daily images. Bottom-up information is derived from pixel data by a supervised, self-adaptive, active learning based support vector machine. It uses low and middle level pixel features such as intensity and location to distinguish each target boundary from the background. The final result is obtained by fusing top-down and bottom-up outputs in a unified framework through fuzzy logic. For evaluation, we used a dataset of four patients with locally-advanced pancreatic cancer treated with MR-ART using a clinical system (MRIdian, Viewray, Oakwood Village, OH). Each set included the simulation MRI and on-board T1 MRI corresponding to a randomly selected treatment session. Each MRI had 144 axial slices of 266×266 pixels. Using Dice Similarity Index (DSI) and Hausdorff Distance Index (HDI), we compared manual and automated contours for liver, left and right kidney and spinal cord.

RESULTS

Average auto-segmentation time was 2 minutes per set. Visually, the automatic and manual contours were similar. Fused results achieved better accuracy than either the bottom up or top down method alone. DSI values were above 0.82±0.03, except for the spinal canal. The spinal canal contours yielded a low HDI value at the expense of a relatively low DSI value.

CONCLUSION

With a DSI significantly higher than the usually reported 0.7, our novel algorithm yields a high segmentation accuracy. To our knowledge, this is the first fully automated contouring approach using T1 MRI images for adaptive radiotherapy.

CLINICAL RELEVANCE/APPLICATION

Minimal computational time coupled with high accuracy make our algorithm ideal for the MR-ART implementation thus minimizing the time gap between image acquisition and radiation delivery.

SSM12-02 Personalized Survival Prediction Using Random Forest Survival Model on MR Radiomic Features in

Gliomas

Wednesday, Nov. 29 3:10PM - 3:20PM Room: S404CD

Participants

Cheng-Yu Chen, MD, Taipei, Taiwan (*Presenter*) Nothing to Disclose Chia-Feng Lu, PhD, Taipei, Taiwan (*Abstract Co-Author*) Nothing to Disclose Fei-Ting Hsu, PhD, Taipei, Taiwan (*Abstract Co-Author*) Nothing to Disclose Paul Blakeley, Taipei, Taiwan (*Abstract Co-Author*) Nothing to Disclose Li-Chun Hsieh, Taipei, Taiwan (*Abstract Co-Author*) Nothing to Disclose Yu-Chieh J. Kao, Taipei, Taiwan (*Abstract Co-Author*) Nothing to Disclose Ping-Huei Tsai, MD, PhD, Taipei, Taiwan (*Abstract Co-Author*) Nothing to Disclose Yung-Hsiao Chiang, Taipei, Taiwan (*Abstract Co-Author*) Nothing to Disclose Wan-Yuo Guo, MD, PhD, Taipei, Taiwan (*Abstract Co-Author*) Nothing to Disclose Ming-Hsong Chen, MD, PhD, Taipei, Taiwan (*Abstract Co-Author*) Nothing to Disclose Chih-Chun Wu, MD, New York, NY (*Abstract Co-Author*) Nothing to Disclose Liang-Wei Chen, Taipei, Taiwan (*Abstract Co-Author*) Nothing to Disclose Hung Wen Kao, MD, Taipei, Taiwan (*Abstract Co-Author*) Nothing to Disclose Yuan-Hao Chen, Taipei, Taiwan (*Abstract Co-Author*) Nothing to Disclose Husn Jiang Wen, Taipei, Taiwan (*Abstract Co-Author*) Nothing to Disclose Husn Jiang Wen, Taipei, Taiwan (*Abstract Co-Author*) Nothing to Disclose Husn Jiang Chen, Taipei, Taiwan (*Abstract Co-Author*) Nothing to Disclose Husn Jiang Chen, Taipei, Taiwan (*Abstract Co-Author*) Nothing to Disclose Husn Jiang Chen, Taipei, Taiwan (*Abstract Co-Author*) Nothing to Disclose Husn Jiang Chen, Taipei, Taiwan (*Abstract Co-Author*) Nothing to Disclose

For information about this presentation, contact:

sandy0932@gmail.com

PURPOSE

To determine the feasibility of personalized survival prediction using MR radiomic features for patients with glioma.

METHOD AND MATERIALS

The MRI and survival data of 178 subjects with primary glioma were obtained from the Cancer Imaging Archive, including 100 glioblastoma data from the TCGA-GBM collection and 78 lower-grade glioma (grade II or III) data from the TCGA-LGG collection. This dataset was randomly partitioned into two subsets, 80% for model training (142 subjects) and 20% for validation (36 subjects). MRI, pathology, and DNA data (IDH and 1p/19q status) of 8 patients with primary glioma were recruited from local hospitals to further test the constructed prediction model. MR radiomic features were calculated from the postcontrast T1 weighted images and apparent diffusion coefficients based on the previously proposed approach. A Random Forest Survival model was constructed using the MR radiomics as predictors. The most informative predictors (260 of 868 features) was selected based on their hierarchy in the decision trees, i.e. the importance scores among all the predictors.

RESULTS

The receiver operating characteristic curves on the validation data (36 subjects) showed a promising prediction performance of the proposed survival model with the area under the curve between 0.826 and 0.971 at different time points after diagnosis. The personalized survival prediction on the 8 testing patients also provided plausible predictions in concordance with the current understanding of the prognosis in different grading, IDH, and 1p/19q status. The only exception is a grade III glioma (subject #2) who had a poorer survival prediction than glioblastoma. The real survival of recruited patients will be recorded by continuous monitoring to verify the proposed model.

CONCLUSION

The established survival prediction model based on MR radiomics is feasible and can be used to promote the personalized medicine of prognosis and treatment strategy in glioma.

CLINICAL RELEVANCE/APPLICATION

Predicting individual survival by efficient MR radiomics and machine learning can benefit the healthcare in patients with glioma from providing a reliable prognosis without high-cost gene assays.

SSM12-03 Automatic Cancer Staging from PET/CT Reports for Large Cohort Studies Using Natural Language Processing and Machine Learning

Wednesday, Nov. 29 3:20PM - 3:30PM Room: S404CD

Participants

Christian A. Bluethgen, MD,MSc, Zurich, Switzerland (*Presenter*) Nothing to Disclose Caroline Zellweger, Zurich, Switzerland (*Abstract Co-Author*) Nothing to Disclose Sara Bacanovic, MD, Zurich, Switzerland (*Abstract Co-Author*) Nothing to Disclose Andreas Boss, MD, Zurich, Switzerland (*Abstract Co-Author*) Nothing to Disclose Irene A. Burger, New York, NY (*Abstract Co-Author*) Nothing to Disclose Anton S. Becker, MD, Zurich, Switzerland (*Abstract Co-Author*) Nothing to Disclose

For information about this presentation, contact:

christian.bluethgen@usz.ch

PURPOSE

To evaluate supervised machine learning (ML) algorithms for automatic cancer stage classification of >12'000 patients based on the radiology report.

METHOD AND MATERIALS

The radiology reports of >12'000 FDG-PET/CT exams between 2007 and 2014 were extracted from the hospital database. A randomly selected set (n = 1254) was manually read and split into subsets for training (80%) and testing (20%). Each report was assigned to one of five distinct cancer stages: 0 = No cancer, 1 = minimal/inactive residual, 2 = single tumor, 3 = locally advanced

disease, 4 = distant metastasis. The reports were preprocessed using basic natural language processing (NLP) techniques. Five common ML classifiers were evaluated: Naive Bayes Classifier (NBC), Support Vector Machines (SVM), Decision Trees (DTC), Random Forest (RFC), and K-nearest neighbors (KNN). Performance was expressed as area under the receiver operating curve (Az) obtained by stratified 10-fold cross-validation of the training set as well as the classification accuracy of the test set.

RESULTS

The number of reports assigned to each stage showed the following distribution: n0=324, n1=336, n2=161, n3 = 142, n4=291. SVM exhibited the best performance in the training set (Az = 0.90 / 0.87 / 0.81 / 0.87 / 0.91 for class 0/1/2/3/4, respectively), followed by NBC (0.88 / 0.86 / 0.79 / 0.85 / 0.90), RFC (0.85 / 0.73 / 0.75 / 0.81 / 0.88), KNN (0.85 / 0.79 / 0.74 / 0.80 / 0.82) and DTC (0.70 / 0.59 / 0.55 / 0.64 / 0.70). Mean classification accuracy of the test set was highest for NBC (0.57), followed by SVC (0.55), RFC (0.5), KNN (0.48) and DTC (0.45). Classification for the whole cohort was feasible with all classifiers.

CONCLUSION

Automatic detection of cancer stages was feasible with all tested ML methods. SVM and NBC performed best among the tested classifiers.

CLINICAL RELEVANCE/APPLICATION

Automatic cancer staging from radiology reports using natural language processing and supervised machine learning is a useful tool for the creation of large cohort studies.

SSM12-04 Semantic Image Segmentation in Breast MR Image with Deep Convolutional Neural Network

Wednesday, Nov. 29 3:30PM - 3:40PM Room: S404CD

Participants

Beomhee Park, Seoul, Korea, Republic Of (*Presenter*) Nothing to Disclose Namkug Kim, PhD, Seoul, Korea, Republic Of (*Abstract Co-Author*) Stockholder, Coreline Soft, Inc Joon Beom Seo, MD, PhD, Seoul, Korea, Republic Of (*Abstract Co-Author*) Nothing to Disclose Ilsang Woo, MS, Seoul, Korea, Republic Of (*Abstract Co-Author*) Nothing to Disclose Jaeyoung Kwon, Seoul, Korea, Republic Of (*Abstract Co-Author*) Nothing to Disclose Sang-Wook Lee, BS, Seoul, Korea, Republic Of (*Abstract Co-Author*) Nothing to Disclose Seunghyun Choi, MSc, Seoul, Korea, Republic Of (*Abstract Co-Author*) Nothing to Disclose Guk Bae Kim, Seoul, Korea, Republic Of (*Abstract Co-Author*) Nothing to Disclose Beom Seok Ko, Seoul, Korea, Republic Of (*Abstract Co-Author*) Nothing to Disclose

For information about this presentation, contact:

beomheep@gmail.com

PURPOSE

To propose and validate the semantic segmentaion method with deep-learning in breast MR images to differentiation of various kinds of tissues for deformation modeling of breast parenchyma with tumor and 3D printing.

METHOD AND MATERIALS

This research is an advanced task for 3D printing and prediction of deformation model of breast parenchyma with tumor between prone and supine position. At first, it is necessary to segment the image on the regions of interest accurately. For the segmentation model of CNN, 10 volumetric breast MR images with prone and supine position of a patient were collected and drawn with five areas (background, lung_heart, muscle_bone, parenchyma_cancer, fat_skin) manually by an expert. The data were split into 8 subjects for training and 2 subjects for validation. Because of no significant change in the axial direction, each subject was considered as 2D images with axial direction so that it was trained with 1732 images and validated with 410 images. And we constructed segmentation model based on U-net. However, U-net showed low performance in this task so that the structures were overall modified and the batch normalization was added. Because it is somewhat similar between prone and supine position images, we compared network trained each position image with sum of them. To calculate accuracy and loss, we used the dice coefficient. Although it trained with axial 2D images, we evaluated the performance with 3D volume results to measure accurately. In addition, the accuracies were measured on each class, because each class has different quantity in the 3D volume.

RESULTS

Building the ground truth took 4-5 hours per subject, while it took about 20 seconds per subject with NVIDIA TITAN X. The result which is predicted with network trained each position image was higher than sum of them. The total accuracy is about 98% on whole cases. In addition, it shows the lowest accuracy on the parenchyma_cancer class as supine-86 % and prone-90 % on average) because it has large variation.

CONCLUSION

We applied semantic segmentation method for breast MR image, and it showed high performances to segment on our regions of interest and greatly reduced time as compared with manual process.

CLINICAL RELEVANCE/APPLICATION

This segmentation method can be used to differentiation of various kinds of tissues for deformation modeling of breast parenchyma with tumor in breast MR images between prone and supine position.

SSM12-05 A Clinically-Actionable Fully Convolutional Network for Brain Tumor Segmentation

Wednesday, Nov. 29 3:40PM - 3:50PM Room: S404CD

Participants Raghav Subramania

Raghav Subramaniam, Stanford, CA (*Abstract Co-Author*) Nothing to Disclose Mu Zhou, PhD, Mountain View, CA (*Presenter*) Nothing to Disclose Olivier Gevaert, PhD, Stanford, CA (*Abstract Co-Author*) Nothing to Disclose

For information about this presentation, contact:

rsub@stanford.edu

PURPOSE

We propose a fully convolutional network (FCN) for glioblastoma (GBM) segmentation using MRI data that has very few tunable parameters, making easy to drop in to clinical applications.

METHOD AND MATERIALS

We tackle the task of using an algorithm to automatically segment three-dimensional MRI images of GBM patients' brains-classifying each voxel of the image as cancerous--regions of edema, necrosis, and active tumor-or not. Our network uses six convolutional layers with true three-dimensional filters, followed by a voxel-wise softmax classifier. Our pre-processing pipeline is parameter-free and only depends on the voxel values of the input MRI image. We forgo post-processing and use the raw outputs of the network as our output segmentations. We trained and validated our network using MRI and ground-truth expert segmentation data from the BRATS 2015 dataset. This dataset contains 220 examples, and we used 75% of these for training and the remaining 25% for validation.

RESULTS

For the cancerous vs. non-cancerous task, with a 75%/25% training/validation split and no post-processing, we achieve the following validation results. We achieve an average Dice score of 0.865, an average Jaccard score of 0.771, and an average overlap score of 0.927. In the attached figure, we provide a histogram of validation Dice scores for the cancerous vs. non-cancerous task with four-fold cross-validation. For comparison, the average pairwise Dice score between the eleven experts who put together the ground truth data is 88%.

CONCLUSION

The proposed FCN algorithm performs almost as well as human experts and represents a segmentation solution that is clinically actionable. It can be used seamlessly in a clinical diagnostic environment with very little manual tuning.

CLINICAL RELEVANCE/APPLICATION

Accurate, automatic medical image algorithms like the proposed segmentation technique can assist radiologists in their interpretation of medical images.

SSM12-06 Automatic Classification of Acute Ischemic Stroke Patient within 4.5 Hours Symptom Onset: Comparison between Deep and Shallow Learning Approaches

Wednesday, Nov. 29 3:50PM - 4:00PM Room: S404CD

Participants

Younggon Kim, Seoul, Korea, Republic Of (*Presenter*) Nothing to Disclose Hyunna Lee, PhD, Seoul, Korea, Republic Of (*Abstract Co-Author*) Nothing to Disclose Eunjae Lee, Seoul, Korea, Republic Of (*Abstract Co-Author*) Nothing to Disclose Dongwha Kang, Seoul, Korea, Republic Of (*Abstract Co-Author*) Nothing to Disclose Namkug Kim, PhD, Seoul, Korea, Republic Of (*Abstract Co-Author*) Stockholder, Coreline Soft, Inc

For information about this presentation, contact:

younggon2.kim@gmail.com

PURPOSE

Determination of symptom onset time for acute ischemic stroke is crucial because the treatment options highly depend on time window. Here, we propose automatic methods based on deep learning (DL) which is the state of art of machine learning and support vector machine (SVM) to classify acute ischemic stroke patients within 4.5 hours symptom onset and compare their performances.

METHOD AND MATERIALS

We retrospectively evaluated 214 patients within 24 hours of symptom detection and underwent 1.5T magnetic resonance imaging (MRI). Some patients were excluded due to missing MRI sequences (22), low image quality (3), false infarct segmentation (7), or small infarct size (33 and 42 for SVM and DL). Finally, 140 and 149 patients were analyzed for the DL and SVM, respectively. Infarct legions were automatically segmented on apparent diffusion coefficient (ADC) maps by applying adaptive thresholding based on histogram normalization. Fluid attenuated inversion recovery (FLAIR) images were registered into the corresponding ADC map. For DL, only axial slices containing infarct regions were used as inputs of Inception V3 network. For SVM, image features including intensity, gradient, and texture information were extracted from infarct regions. The classifier parameters were tuned based on F0.5 and class weights to obtain good specificity.

RESULTS

A 5-fold cross-validation was conducted for training and testing of DL and SVM. For using single modality, accuracy and sensitivity of DLs are significantly higher than those of SVMs (p<0.05, t-test), with a similar level of specificity. The DL using all of three modalities tended to show significantly better performance in terms of accuracy (0.88 ± 0.02), sensitivity (0.95 ± 0.04), and specificity (0.78 ± 0.04), except sensitivity of ADC (0.96 ± 0.05).

CONCLUSION

We proposed the automatic classification systems for acute ischemic stroke patients within 4.5 hours of symptom onset using deep and shallow learning methods. In results, the DL showed good identification of acute ischemic stroke patients within 4.5 hours of symptom onset.

CLINICAL RELEVANCE/APPLICATION

The proposed classification systems might be useful for identifying unknown-onset stroke patients who could be candidates for

reperfusion therapy.







SSM13

Molecular Imaging (Analysis and Quantification)

Wednesday, Nov. 29 3:00PM - 4:00PM Room: S504CD



AMA PRA Category 1 Credit ™: 1.00 ARRT Category A+ Credit: 1.00

FDA Discussions may include off-label uses.

Participants

Benjamin Larimer, PhD, Charlestown, MA (*Moderator*) Nothing to Disclose Pedram Heidari, MD, Boston, MA (*Moderator*) Nothing to Disclose

Sub-Events

SSM13-02 Quantification of Adipose Tissue and Organ Fat Content Using Whole-Body Dixon Fat-Water Separation Technique

Wednesday, Nov. 29 3:10PM - 3:20PM Room: S504CD

Participants

Ling Yuan, Beijing, China (*Presenter*) Nothing to Disclose Huadan Xue, MD, Beijing, China (*Abstract Co-Author*) Nothing to Disclose Zheng Yu Jin, MD, Beijing, China (*Abstract Co-Author*) Nothing to Disclose

For information about this presentation, contact:

lindayuan1991@126.com

PURPOSE

The purpose of this study is to utilize whole-body Dixon fat-water separation technique to quantify adipose tissue (AT) distribution and fat content of different organs, to investigate characteristics of fat distribution, and to determine whether these quantitative parameters are risk factors of metabolic syndrome (MS).

METHOD AND MATERIALS

We recruited 39 male volunteers and 71 female volunteers, with an average age of 58.7±9.1 years and an average BMI of 26.1kg/m2, among which 19 female and 11 male volunteers were diagnosed with metabolic syndrome. Whole-body fat and water images were acquired using a Dixon-VIBE sequence on MAGNETOM Skyra 3T MR scanner. Scan parameters were as follows: TR 5.26ms, TE 1.24ms, Flip angle 9°, FOV 500mm x 500mm, 44-60 slices, slice thickness 5.0mm, total acquisition time 60s. ImageJ software was applied to measure the volume of intra-thoracic AT (ITAT), intra-abdominal AT (IAAT), truncal subcutaneous AT (TSAT), and lower limb AT (LLAT). Osirix software was utilized to measure fat fraction(FF) of liver, pancreas, L2-L4 vertebral bodies, and skeletal muscle of lower limbs.

RESULTS

Compared with female group, male volunteers possessed more ITAT and IAAT, less TSAT, LLAT and total adipose tissue (TAT), and a higher ratio of IAAT (IAAT%). The senior group (>=60 years old) contained more ITAT, IAAT, and IAAT% than the junior group (<60 years old). Compared with premenopausal females, post-menopausal females had less TAT, more ITAT, and higher IAAT%. FF of skeletal muscle in lower limbs was higher in senior, female, and postmenopausal groups. FF of the vertebral body was higher in post-menopausal groups. Multiple binary logistic regression analysis demonstrated that volume of IAAT was a risk factor for MS.

CONCLUSION

The Dixon fat-water separation technique can be used to quantify whole-body adipose tissue and fat fraction of different organs. Distribution of adipose tissue and organ fat fraction varied in different sex and age groups. Accumulation of intra-abdominal adipose tissue may increase the risk of developing metabolic syndrome.

CLINICAL RELEVANCE/APPLICATION

This technique allows precise quantification of whole-body fat, which may enable the individualized diagnosis and evaluation of diseases with mal-distribution of adipose tissue or fat content.

SSM13-03 CEST MRI of Surgically-Removed Prostate Correlates with Histological Stratification

Wednesday, Nov. 29 3:20PM - 3:30PM Room: S504CD

Participants

Kejia Cai, PhD, Chicago, IL (*Presenter*) Nothing to Disclose Rongwen Tain, PhD, Chicago, IL (*Abstract Co-Author*) Nothing to Disclose Brandon Caldwell, Chicago, IL (*Abstract Co-Author*) Nothing to Disclose Jiaxuan Zhang, Chicago, IL (*Abstract Co-Author*) Nothing to Disclose Weiguo Li, Chicago, IL (*Abstract Co-Author*) Nothing to Disclose Virgilia Macias, MD, Chicago, IL (*Abstract Co-Author*) Nothing to Disclose Andre Balla, MD, Chicago, IL (*Abstract Co-Author*) Nothing to Disclose Alessandro Scotti, Chicago, IL (*Abstract Co-Author*) Nothing to Disclose Xiaohong J. Zhou, PhD, Chicago, IL (*Abstract Co-Author*) Nothing to Disclose Karen Xie, DO, Chicago, IL (*Abstract Co-Author*) Nothing to Disclose Winnie A. Mar, MD, Chicago, IL (*Abstract Co-Author*) Nothing to Disclose Michael Abern, Chicago, IL (*Abstract Co-Author*) Nothing to Disclose

PURPOSE

While multiparametric MRI combining T2-weighted (T2-w) imaging with functional imaging techniques can provide moderate sensitivity and specificity for diagnosis of prostate tumor, there is still a great need in developing novel MRI methods for reliable risk stratification of prostate lesions. Chemical exchange saturation transfer (CEST) MRI as an emerging metabolic and molecular MRI method based on endogenous tissue contrasts has been demonstrated to assess aggressiveness of brain tumor. The aim of this study was to investigate the value of CEST MRI in the risk stratification of prostate pathologies. To pave the path for in vivo clinical studies, this study was initiated by scanning whole surgically-removed prostates with high resolution and correlating with the corresponding pathological images.

METHOD AND MATERIALS

Under an approved IRB protocol, whole prostate specimens from patients (n=5, 62 ± 3 yrs) were studied immediately after surgery. MRI was performed on a horizontal 9.4-T animal MRI scanner with a commercial volume coil (72 mm in diameter). T2-w fast spin echo and diffusion-weighted images (DWI) were acquired. In addition, ADC was constructed from DWI images. CEST Z-spectra were then collected using a customized sequence with a frequency-selective saturation pulse (B1 = 100 Hz, 2 s). CEST data was corrected for static field B0 inhomogeneity. CEST asymmetry contrast was computed and normalized by signal at +100 ppm. Immediately after MRI, the specimens were processed for histopathological studies. Prostate lesions and Gleason patterns were prescribed by a clinical pathologist on histological images (H&E stained) from the slices close to the MR imaging planes.

RESULTS

By comparing the CEST contrast maps with the corresponding histological images, we found CEST contrast in tumor was significantly lower than that of normal tissue ($4.8\pm0.1 \text{ vs. } 6.5\pm0.3 \text{ \%}$, p<0.05). On the other hand, CEST contrast in benign prostatic hyperplasia (BPH) (12.7%) was much higher than that of both normal tissue and tumor. In general, CEST contrast maps demonstrated a close correlation with regional Gleason patterns in histological images.

CONCLUSION

CEST MRI contrast, once further confirmed with a large sample size and in vivo clinical studies, may have great potential for risk stratification of prostate pathologies.

CLINICAL RELEVANCE/APPLICATION

CEST MRI has the clinical potential for characterization of prostate diseases.

SSM13-04 Utilizing Radiomics to Differentiate Hot and Cold Tumor Immune-Microenvironment in Biopsy-Proven Malignant Melanoma: A Pilot Study

Wednesday, Nov. 29 3:30PM - 3:40PM Room: S504CD

Participants

Laurent Dercle, MD, New York, NY (*Presenter*) Nothing to Disclose Amelie Bigorgne, Paris, France (*Abstract Co-Author*) Nothing to Disclose Qiao Huang, PhD, New York, NY (*Abstract Co-Author*) Nothing to Disclose Philip Lichtenstein, MD, New York, NY (*Abstract Co-Author*) Nothing to Disclose Hao Yang, New York, NY (*Abstract Co-Author*) Nothing to Disclose Lin Lu, New York, NY (*Abstract Co-Author*) Nothing to Disclose Yajun Li, Changsha, China (*Abstract Co-Author*) Nothing to Disclose Lawrence H. Schwartz, MD, New York, NY (*Abstract Co-Author*) Nothing to Disclose Lawrence H. Schwartz, MD, New York, NY (*Abstract Co-Author*) Nothing to Disclose Sovertis AG Committee member, ICON plc Committee member, BioClinica, Inc Binsheng Zhao, DSc, New York, NY (*Abstract Co-Author*) License Agreement, Varian Medical Systems, Inc; Royalties, Varian Medical Systems, Inc; License Agreement, Keosys SAS; License Agreement, Hinacom Software and Technology, Ltd; License Agreement, ImBio, LLC; License Agreement, AG Mednet, Inc; Research Grant, ImBio, LLC; Aurelien Marabelle, Villejuif, France (*Abstract Co-Author*) Nothing to Disclose

For information about this presentation, contact:

laurent.dercle@gmail.com

PURPOSE

An immunogenic tumor microenvironment (hot) is a strong and independent predictor of improved patient outcome. Additionally, new immune checkpoint inhibitor therapies can activate anti-tumor immune response and trigger an immune-infiltration which is responsible for the pseudoprogression phenomenon. Pseudo-progression masks effective therapy efficacy since a transitory increase in tumor volume is observed. We aimed to explore if radiomics can predict the immune-infiltration profile in malignant metastatic melanoma patients treated with immune checkpoint blockade by anti-PD-1.

METHOD AND MATERIALS

We retrospectively recruited metastatic melanoma patients treated with anti-PD1. All patients had a contrast-enhanced CT-scan as well as a tumor biopsy with a 360 gene panel RNA-expression profile. We divided patients in two categories: hot and cold tumor immune microenvironment. "Hot" was defined by a quantitative expression of RNA above the median in at least two out of four key immune pathways: cytotoxic lymphocytes (CD8A and CD8B), human inducible T-cell co-stimulator (ICOS); and interleukin 2 (IL2). We contoured the tumor lesions in 3D and extracted 89 radiomic imaging features. Area under the curve (AUC) calculated the accuracy of imaging features for the detection of hot immune infiltration. 61 lesions in total were contoured: 33 hot and 28 cold. The two best imaging features for the detection of a hot immune infiltration were Entropy of Grey Level Concurrence Matrix and Skewness. Their respective AUCs (95CI; p-value) were: 0.75 (0.62-0.88; P=0.001) and 0.74 (0.60-0.88; P=0.001). Combining these two features, a correct classification of hot vs. cold (95CI) was achieved in 77% (65-87%) of lesions.

CONCLUSION

This pilot study provides proof of concept regarding an association between tumor imaging phenotype assessed by radiomics on CT-scan and the presence of a hot tumor immune infiltration according to biopsy RNA-sequencing. Prospective validation in larger cohorts is warranted.

CLINICAL RELEVANCE/APPLICATION

The classification of tumor immune microenvironment by imaging biomarkers could provide prognostic information and improve response assessment accuracy, especially in immuno-oncology.

SSM13-05 Using the Least Solid State Detectors to Achieve the Most: Pushing the Envelope of Digital Photon Counting TOF PET by Simulating Sparse-Ring Configuration

Wednesday, Nov. 29 3:40PM - 3:50PM Room: S504CD

Participants

Jun Zhang, PhD, Columbus, OH (*Presenter*) Nothing to Disclose Bin Zhang, PhD, Cleveland, OH (*Abstract Co-Author*) Employee, Koninklijke Philips NV Michelle I. Knopp, Columbus, OH (*Abstract Co-Author*) Nothing to Disclose Michael V. Knopp, MD, PhD, Columbus, OH (*Abstract Co-Author*) Nothing to Disclose

For information about this presentation, contact:

zhang.538@osu.edu

PURPOSE

To leverage and go beyond accepted conventions in PET detector designs by investigating the new generation solid state digital photon counting (DPC) PET detectors in simulated sparse-ring PET configuration for oncologic FDG PET/CT

METHOD AND MATERIALS

A solid state DPC PET/CT system (Vereos) with 23,040 individual crystal-to-SiPM detector couplings (18 fiat modules, 4 tangential by 5 axial array tiles on each, 8x8 matrix pixels on each tile) was used. Investigational wholebody FDG PET/CT of 10 oncology patients were performed (13.1±0.4mCi FDG; 75±5min p.i). PET was reconstructed using 3D TOF OSEM in 4x4x4mm3 using A) full ring data, and sparse-ring PET simulation by disabling B) 1 pixel of every 2 pixels in tangential (50% crystal-detector reduction), C) 1 of every 3 pixels in tangential (33% reduction), D) 1 of every 4 pixels in tangential (25% reduction) and E) the 2nd and 4th entire rings in axial (40% reduction). NEMA phantom with hot spheres was performed using the same approaches. All results were compared and analyzed to assess image quality (IQ) and PET quantification

RESULTS

All lesions on the full-ring PET were visible on sparse-ring PET simulation (C)-(E). though most lesions were identifiable on sparse-ring PET in (B), artifacts appeared. Reducing the number of crystal-detector couplings to 25% (D) maintained PET IQ without giving significant SUV variances compared to full-ring PET (p<0.01). Keeping detector rings intact in tangential with 40% detector reduction in axial using (E) surprisingly demonstrated good results without compromising much of IQ. Applying counts-adaptive reconstructions by optimizing recon parameters further improved PET IQ. Radically either up to 40% cost can be saved or up to 40% axial FOV can be extended without adding new detectors. Comprehensive data assessment will be presented

CONCLUSION

1:1 coupling of crystal:detector DPC PET is a technology leap however with trade-off of high cost limited axial FOV. The study challenged its current designs and pushed the envelope to go beyond its boundaries in improving axial FOV and system sensitivity without adding additional cost by sparse-ring PET simulation.

CLINICAL RELEVANCE/APPLICATION

Solid state digital PET is a technology leap with great potentials of using least solid state detectors to achive the most without adding cost while retaining reliable image quality for oncology PET and the study investigated this using sparse-ring PET simulation.

SSM13-06 Texture Analysis of 68Ga-DOTATATE Positron Emission Tomography and Computed Tomography Images as a Prognostic Biomarker in Adults with Neuro-Endocrine Cancers Treated with 177Lu-DOTATATE

Wednesday, Nov. 29 3:50PM - 4:00PM Room: S504CD

Participants

Charlotte Atkinson, MBChB,FRCR, Bondi Beach, Australia (*Abstract Co-Author*) Nothing to Disclose Balaji Ganeshan, PhD, London, United Kingdom (*Presenter*) CEO, TexRAD Ltd; Director, Feedback plc; Director, Stone Checker Software Ltd; Director, Prostate Checker Ltd Raymond Endonzo, London, United Kingdom (*Abstract Co-Author*) Nothing to Disclose Simon Wan, London, United Kingdom (*Abstract Co-Author*) Nothing to Disclose Matthew Aldridge, London, United Kingdom (*Abstract Co-Author*) Nothing to Disclose Ashley M. Groves, MBBS, Hitchin, United Kingdom (*Abstract Co-Author*) Investigator, GlaxoSmithKline plc Investigator, General Electric Company Investigator, Siemens AG Jamshed Bomanji, London, United Kingdom (*Abstract Co-Author*) Nothing to Disclose Kenneth A. Miles, MD, MSc, London, United Kingdom (*Abstract Co-Author*) Nothing to Disclose Mark Gaze, London, United Kingdom (*Abstract Co-Author*) Nothing to Disclose

For information about this presentation, contact:

PURPOSE

Neuroendocrine tumors (NETs) are a rare, heterogeneous group of cancers whose behavior can be hard to predict. A better understanding of prognosis would aid individualized management decisions. We aim to demonstrate the prognostic potential of tumor heterogeneity and avidity in NETs using PET and CT textural analysis (PTA & CTTA) and standardized uptake values (SUV).

METHOD AND MATERIALS

The baseline 68Gallium-DOTATATE PET/CT scans of 49 prospectively recruited patients with NETs (carcinoid, pancreatic, thyroid, head and neck, catecholamine-secreting and unknown primary tumors) treated with 177Lutetium-DOTATATE at a tertiary center were retrospectively analyzed. Non-contrast CT and PET heterogeneity was assessed using a commercially available TexRAD texture analysis software (TexRAD Ltd www.texrad.com, part of Feedback Plc, Cambridge, UK) which employed a filtration-histogram technique. Regions of interest encircled the most prominent metastases of each patient (up to 5 tumour foci) as seen on the 68Ga-DOTATATE PET scan. Gallium uptake on PET was quantified as SUVmax and SUVmean. Association between imaging and clinical markers with progression-free (PFS) and overall survival (OS) were assessed using univariate Kaplan-Meier and multivariate Cox regression analysis.

RESULTS

Clinical factors did not generally predict survival. Measures of texture heterogeneity (quantified as skewness and kurtosis) on unfiltered and filtered (fine-medium texture scale) CT and unfiltered PET images predicted PFS (CT: p=0.0126, PET: p=0.0047) and OS (CT: p=0.0061, PET: p=0.0028). Furthermore patients with SUVmax >8.73 and SUVmean >5.19 showed significantly superior PFS (p=0.0164) and OS (p=0.0061). Multivariate analysis identified that CTTA (fine texture scale - skewness: HR=6.98, 95%CI=2.281-21.372, p=0.001) and SUVmax (HR=4.439, 95% CI=1.679-11.739, p=0.003) were independent predictors of PFS. PTA (without filtration skewness : HR=20.68, 95%CI=3.24-131.99, p=0.001) was an independent predictor of OS.

CONCLUSION

68Ga-DOTATATE PET/CT texture heterogeneity and SUV measurements could act as prognostic biomarkers in NETs and potentially play a key role in risk stratifying these patients.

CLINICAL RELEVANCE/APPLICATION

68Ga-DOTATATE PET/CT texture heterogeneity analysis and SUV measurements independently predict survival in NETs. Their role as prognostic biomarkers could significantly improve stratification of NET patients.



KSNA° 2017

103rd Scientific Assembly and Annual Meeting November 26 to December 1 McCormick Place, Chicago



SSM14

Musculoskeletal (Ultrasound)

Wednesday, Nov. 29 3:00PM - 4:00PM Room: E353C



AMA PRA Category 1 Credit ™: 1.00 ARRT Category A+ Credit: 1.00

FDA Discussions may include off-label uses.

Participants

Mary M. Chiavaras, MD, PhD, Ancaster, ON (Moderator) Nothing to Disclose

Kenneth S. Lee, MD, Madison, WI (*Moderator*) Grant, General Electric Company; Research support, SuperSonic Imagine; Research support, Johnson & Johnson; Consultant, Echometrix, LLC; Royalties, Reed Elsevier

Sub-Events

SSM14-01 Ultrasound-Guided Treatment of Calcific Tendinitis of the Rotator Cuff: Efficacy of Percutaneous Lavage Using Sodium Hexametaphosphate (SHMP) in Comparison with Simple Saline

Wednesday, Nov. 29 3:00PM - 3:10PM Room: E353C

Participants

Federico Bruno, MD, L'Aquila, Italy (*Presenter*) Nothing to Disclose Simone Quarchioni, Laquila, Italy (*Abstract Co-Author*) Nothing to Disclose Ester Cannizzaro, MD, L'Aquila, Italy (*Abstract Co-Author*) Nothing to Disclose Silvia Mariani, MD, L'Aquila, Italy (*Abstract Co-Author*) Nothing to Disclose Francesco Arrigoni, Coppito, Italy (*Abstract Co-Author*) Nothing to Disclose Luigi Zugaro, L'Aquila, Italy (*Abstract Co-Author*) Nothing to Disclose Antonio Barile, MD, L'Aquila, Italy (*Abstract Co-Author*) Nothing to Disclose Carlo Masciocchi, MD, L'Aquila, Italy (*Abstract Co-Author*) Nothing to Disclose

For information about this presentation, contact:

federico.bruno.1988@gmail.com

PURPOSE

To determine the efficacy of percutaneous US-guided needle lavage of symptomatic rotator cuff calcifications using a sodium hexametaphosphate (SHMP) solution (0.5%), in comparison with the same technique using simple saline

METHOD AND MATERIALS

We evaluated 24 calcifications (4 type A, 11 type B, 9 type C according to Gartner classification, mean size 24.7mm, range 9-31mm) in 24 patients (13 males, 11 females, mean age 34.8 years). Patients were divided into 2 groups and treated by percutaneous fragmentation and lavage using SHMP (Group 1, 12 patients) or simple saline (Group 2, 12 patients). Pre- and postprocedure (at 2 and 4 weeks follow-up) imaging evaluation was performed in all patients, including conventional radiography (RX) and ultrasound (US) examination to assess location, size and type of calcifications. Imaging findings after treatment were evaluated by two independent raters and defined as "partial" or "subtotal" dissolution. Pre- and post-procedure clinical evaluation (at 2 and 4 weeks follow-up) was assessed using the Constant Shoulder Score for functionality and the VAS Score for pain

RESULTS

The two study groups were homogeneous in terms of patient demographics, size and type of calcifications. 2 weeks after treatment in Group 1 we found subtotal dissolution of calcifications in 8 patients (66.7%) and partial dissolution in 4 (33.3%); of these, 2 (50%) showed subtotal dissolution at the 4 weeks follow-up. In Group 2 we found subtotal dissolution in 58.3% and partial in 41.7% (p<=0.05). 1 patient (20%) showed subtotal dissolution at the 4 weeks follow-up. Clinical evaluation showed significant improvement in VAS and Constant scores in 91.7% of patients of Group 1 and in 83.3% of Group 2 (p<=0.05). No major complications were reported in both groups.

CONCLUSION

The use of SHMP showed superior results in terms of imagingfindings and clinical improvement compared to the treatment with simple saline

CLINICAL RELEVANCE/APPLICATION

With its chemical action of calcium chelation and dissolution, besides the mechanical action, percutaneous lavage with SHMP is an effective procedure, suitable for different types of calcifications, providing a safe, valid and cost-effective alternative treatment management for calcific tendinitis

SSM14-02 Effect of Compression Stockings on the Development of Delayed-Onset Muscle Soreness: A Quantitative Assessment with 3T MRI, Contrast-Enhanced Ultrasound (CEUS) and Acoustic Radiation Force Impulse (ARFI) Elastography

Participants

Rafael Heiss, Erlangen, Germany (*Abstract Co-Author*) Nothing to Disclose Marion Kellermann, Erlangen, Germany (*Abstract Co-Author*) Nothing to Disclose Wolfgang Wust, MD, Erlangen, Germany (*Presenter*) Speakers Bureau, Siemens AG Casper Grim, Osnabruck, Germany (*Abstract Co-Author*) Nothing to Disclose Bernd Swoboda, Erlangen, Germany (*Abstract Co-Author*) Nothing to Disclose Michael Uder, MD, Erlangen, Germany (*Abstract Co-Author*) Speakers Bureau, Bracco Group; Speakers Bureau, Siemens AG; Speakers Bureau, Bayer AG; Research Grant, Siemens AG; Thilo Hotfiel, Erlangen, Germany (*Abstract Co-Author*) Nothing to Disclose

PURPOSE

To investigate the influence of commercially available sport compression garments on changes in muscle perfusion, muscle stiffness and the development of exercise induced intramuscular edema in the context of DOMS.

METHOD AND MATERIALS

DOMS was induced in fifteen healthy participants. They had to perform a standardized eccentric exercise of the calf muscles. After exercise a conventional sports compression sock (class I, 18-21 mmHg) was placed accordingly manufacturer's instructions at one randomized calf for 60h. MRI (normalized T2 signal intensity and T2-time), CEUS (Peak enhancement (PE) and Wash-in Area Under Curve (WIAUC)) and ARFI (shear wave velocities (SWV)) of the gastrocnemius muscle (GM), as well as creatine kinase activity, extension range of the ankle joint, calf circumference and muscle soreness were assessed at baseline and 60 h after exercise at both calves.

RESULTS

After exercise the normalized T2 signal intensity $(1.0\pm0.30 \text{ vs. } 1.94\pm1.05, p=0.008)$, the T2-time $(37.52\pm9.67 \text{ vs. } 55.64\pm12.72 \text{ ms}, p=0.015)$ was significantly higher in the GM in the compressed calf; but no change for WIAUC $(4322\pm521 \text{ vs. } 11730\pm3536, p=0.88)$, PE $(474\pm54 \text{ vs. } 1185\pm345, p=0.51)$ and ARFI SWV $(2.16\pm0.31 \text{ vs. } 2.13\pm0.32, p=0.60)$ were observed. In the non-compressed calf all assessed parameters changed significantly: T2: $1.0\pm0.16 \text{ vs. } 2.20\pm1.16, p=0.001$; T2-time: $37.75\pm9.28 \text{ vs. } 55.67\pm14.78 \text{ ms}, p=0.005$, WIAUC: $2461\pm660 \text{ vs. } 5297\pm743, p=0.01$, PE: $328\pm45 \text{ vs. } 753\pm31, p=0.005$, ARFI SWV: $2.2\pm0.26 \text{ vs. } 1.78\pm0.24\text{m/s}, p=0.008$. No significant difference was observed in normalized T2 signal intensity (p=0.397), T2-time value (p=0.953), WIAUC (p=0.93) and PE (p=0.730) in the GM comparing the compressed and non-compressed lower leg after exercise. Only ARFI SWV values in the same comparison revealed a statistically significant difference (p=0.001).

CONCLUSION

Our results indicate that wearing conventional sports compression socks after inducing DOMS may shorten the normalization of muscle stiffness, but have no significant effect on the degree of intramuscular edema or perfusion of the MGM. Furthermore, no effects on occurring muscle soreness or reduced range of motion were noticed.

CLINICAL RELEVANCE/APPLICATION

Muscle injuries are common sports injuries. Delayed onset muscle soreness (DOMS), an entity of ultrastructural muscle injury is one of the most common reasons for impaired muscle performance in professional and recreational athletes.

SSM14-03 Repeated Ultrasound-Guided Core Needle Biopsy of Musculoskeletal Lesions: Clinical Utility According to the Types of the Lesions

Wednesday, Nov. 29 3:20PM - 3:30PM Room: E353C

Participants

Kyungjun Min, Seoul, Korea, Republic Of (*Presenter*) Nothing to Disclose Hye Won Chung, MD, Seoul, Korea, Republic Of (*Abstract Co-Author*) Nothing to Disclose Sang Hoon Lee, Seoul, Korea, Republic Of (*Abstract Co-Author*) Nothing to Disclose Min Hee Lee, MD, Seoul, Korea, Republic Of (*Abstract Co-Author*) Nothing to Disclose Myung Jin Shin, MD, Seoul, Korea, Republic Of (*Abstract Co-Author*) Nothing to Disclose

PURPOSE

To evaluate the clinical utility of repeated ultrasound-guided core needle biopsy(US-CNB) of musculoskeletal lesions according to the types of the lesions.

METHOD AND MATERIALS

We retrospectively reviewed 1996 consecutive US-CNBs performed for bone or soft-tissue lesions in 1914 patients during 10 years at a single institution. Repeated biopsy cases for the same lesion were enrolled in this study. The reasons for repeat biopsies were nondiagnostic results, different from clinical expectations, or negative culture results. The reference standard was culture result for infection and pathological diagnosis at excisional biopsy for others. Concordance rate of initial and repeat biopsies were compared according to the types of the lesions by tumors, infection, or others. McNemar's test were used for their statistical significance (p <.05).

RESULTS

Of the 30 cases of repeat biopsy, final pathologies were bone and soft tissue tumor, 18(60%); infection, 8(27%); and others, 4(13%). Among the 18 tumors, 16(89%) cases were soft tissue tumors and 14(78%) were malignancy. The overall concordance rate of initial biopsy was 23%(7/30) and that for repeat biopsy was 60%(18/30), which revealed significantly higher concordance for repeated biopsy (p=0.001). The initial and repeated concordance rates of bone and soft tissue tumor were 22%(4/18) and 72% (13/18), respectively. Repeated US-CNB for bone and soft tissue tumor increased diagnostic rate significantly compared to the initial biopsy (p=0.008). The pathogen concordance rates between the initial and repeated US-CNB for infectious cases were 0% (0/8) and 13%(1/8), which showed no significant difference (p=1.000).

CONCLUSION

Reneated LIS-CNR of musculoskeletal hone and soft tissue tumors can be useful for accurate diagnoses. However, in cases of

infection, repeated US-CNB may have limited clinical utility for pathogen determination.

CLINICAL RELEVANCE/APPLICATION

Repeated US-CNB can be useful for accurate diagnoses of musculoskeletal bone and soft tissue lesions. However, we should consider the types of the lesions. Although repeated CNB increased diagnostic rate for bone and soft tissue tumors, but did not increase the pathogen determination for infection.

SSM14-04 Adhesive Capsulitis of the Shoulder: Evaluation with US-Arthrography Using a Sonographic Contrast Agent

Wednesday, Nov. 29 3:30PM - 3:40PM Room: E353C

Participants

Man Lu, PhD, Chengdu, China (*Presenter*) Nothing to Disclose Xueqing Chen, Chengdu, China (*Abstract Co-Author*) Nothing to Disclose

For information about this presentation, contact:

graceof@163.com

CONCLUSION

Consequently, US-arthrography was more effective method than US for assessment of AC. Filling defects of joint cavity and synovitis-like abnormality in the joint are characteristic US-arthrography findings for diagnosing AC.

Background

Adhesive capsulitis (AC) is a painful and disabling disorder, which caused restricted motion and chronic pain of shoulder. Intracavitary contrast-enhanced ultrasound has recently applied to assess obstructive bile duct diseases, tubal patency, vesicoureteric reflux and so on.

Evaluation

The aim of this study was to detect the value of US-arthrography by injecting the contrast agent SonoVue into glenohumeral joint compared with US in diagnosing AC.

Discussion

US and US-arthrography images of 45 patients with AC were compared with that of 45 control subjects without AC with MRI as a gold standard.Patients with AC had a significantly thickened CHL (3.1 mm) and inferior capsule (3.5 mm) on US, and a decreased volume of axillary recess (1.14 ml) on US-arthrography compared with the control subjects. Filling defect (91.1%) and synovitis-like abnormality (75.6%) in the joint on US-arthrography were more sensitive than that of rotator interval abnormality (71.1%), thickened CHL more than 3 mm (64.4%), thickened inferior capsule more than 3.5 mm (66.7%) on US respectively for diagnosis of AC.

SSM14-05 Contrast-Enhanced Ultrasound (CEUS) as a New Method in Diagnostic Imaging of Muscle Injuries: Systematic Comparison of Conventional Ultrasound, CEUS and Findings in MRI

Wednesday, Nov. 29 3:40PM - 3:50PM Room: E353C

Participants

Rafael Heiss, Erlangen, Germany (*Presenter*) Nothing to Disclose Dane Wildner, Erlangen, Germany (*Abstract Co-Author*) Speaker, Bracco Group Deike H. Strobel, MD, Erlangen, Germany (*Abstract Co-Author*) Nothing to Disclose Kolja Gelse, MD, Erlangen, Germany (*Abstract Co-Author*) Nothing to Disclose Casper Grim, Osnabruck, Germany (*Abstract Co-Author*) Nothing to Disclose Bernd Swoboda, Erlangen, Germany (*Abstract Co-Author*) Nothing to Disclose Michael Uder, MD, Erlangen, Germany (*Abstract Co-Author*) Nothing to Disclose Speakers Bureau, Bayer AG; Research Grant, Siemens AG; Thilo Hotfiel, Erlangen, Germany (*Abstract Co-Author*) Nothing to Disclose

PURPOSE

To emphasize the diagnostic value of contrast-enhanced ultrasound (CEUS) in imaging of muscle injuries with different degrees of severity by comparing findings to the established imaging modalities as conventional ultrasound and magnet resonance imaging (MRI).

METHOD AND MATERIALS

A total of 15 patients were examined after indirect muscular injuries on the lower extremity. Within 24 - 48 hours after injury, a conventional sonography and a CEUS were performed. Direct after the sonography, an MRI was performed as a 'gold standard' in order to graduate the lesion and to determine the spatial extent of the lesion as a reference variable. The classification was carried out according to the modified, four-stage Peetron classification described by Ekstrand et al..

RESULTS

All 15 injuries were identified on MRI and CEUS, whereas 10 injuries showed abnormalities in conventional ultrasound. The determination and measurement revealed significant differences between conventional ultrasound and CEUS depending on the injuries' severity. CEUS revealed an impairment of microcirculation in grade I lesions (corresponding to intramuscular edema observed in MRI), which were not detectable in conventional ultrasound.

CONCLUSION

Our results indicate that performing CEUS seems to be a sensitive additional diagnostic modality in the assessment of muscle injuries in the acute phase after injury. Our results provide advantages of CEUS in imaging of low grade lesions compared to

conventional ultrasound, as they show its superiority in the identifiability of intramuscular edema.

CLINICAL RELEVANCE/APPLICATION

Muscle injuries are frequently observed during recreational and professional sports and have been reported as one of the most common sports injuries. Diagnostic imaging is essential to provide a correct assessment of the injury's severity. So far MRI has shown its superiority over ultrasound examination and has been reported as the preferred modality providing detailed image analysis and characterization of an intramuscular lesion. In clinical practice, however, MRI is often reserved for high-level athletes or serious injuries in which a pronounced structural damage is expected. In conventional ultrasound diagnostic of low grade lesions (ultrastructural lesions and muscle strains), the concerned muscle tissue often appears normal. In this context CEUS may be a new investigative tool in the diagnostic imaging of low grade muscle lesions.

SSM14-06 Quantitative Assessment of Skin Stiffness in Localized Scleroderma Using Ultrasound Shear-Wave Elastography

Wednesday, Nov. 29 3:50PM - 4:00PM Room: E353C

Participants

Liyun Wang, Chengdu, China (*Presenter*) Nothing to Disclose Li Qiu, Chengdu, China (*Abstract Co-Author*) Nothing to Disclose Feng Yan, Chengdu, China (*Abstract Co-Author*) Nothing to Disclose Yujia Yang, Chengdu, China (*Abstract Co-Author*) Nothing to Disclose Xi Xiang, Chengdu, China (*Abstract Co-Author*) Nothing to Disclose

For information about this presentation, contact:

liyunwang1992@qq.com

PURPOSE

The purpose of this study was to evaluate the usefulness of ultrasound shear-wave elastography (US-SWE) in characterization of localized scleroderma (LS), as well as in the disease staging.

METHOD AND MATERIALS

21 patients with 37 LS lesions were enrolled in this study. The pathological stage (edema, sclerosis or atrophy) of the lesions was characterized by pathological examination. The skin elastic modulus (E-values, including Emean, Emin, Emax and Esd) and thickness (h) was evaluated both in LS lesions and site-matched unaffected skins (normal controls) using US-SWE. The relative difference (ERD) of E-values was calculated between each pair of lesion and its normal control for comparison among different pathological stages.

RESULTS

Of the 37 LS lesions, 2 were in edema, 22 in sclerosis and 13 in atrophy. US-SWE results showed a significant increase of skin elastic modulus and thickness in all lesions (p<0.001 in sclerosis and p<0.05 in atrophy) compared to the normal controls. The measured skin elastic modulus and thickness were greater in sclerosis than in atrophy. However, once normalized by skin thickness, the atrophic lesions, which were on average thinner, appeared significantly stiffer than those of the sclerosis (normalized ERD: an increase of 316.3% in atrophy vs. 50.6% in sclerosis compared to the controls, p = 0.007).

CONCLUSION

These findings suggest that US-SWE allows to quantitatively evaluate the skin stiffness of LS lesions in different stages; however, the E-values directly provided by US-SWE system alone do not distinguish between the stages, and the normalization by skin thickness is necessary. This non- invasive, real-time imaging technique is an ideal tool for assessing and monitoring LS disease severity and progression.

CLINICAL RELEVANCE/APPLICATION

Ultrasound shear-wave elastography can measure skin stiffness in LS patients which can be used to assesse and monitor LS disease severity and progression.





SSM15

Nuclear Medicine (Head and Neck Imaging)

Wednesday, Nov. 29 3:00PM - 4:00PM Room: S505AB



AMA PRA Category 1 Credit ™: 1.00 ARRT Category A+ Credit: 1.00

Participants

Don C. Yoo, MD, E Greenwich, RI (*Moderator*) Consultant, Endocyte, Inc Akash Sharma, MD, Saint Louis, MO (*Moderator*) Nothing to Disclose

Sub-Events

SSM15-01 Integrated 11C-MET PET/MRI for Detection of Recurrent Glioma

Wednesday, Nov. 29 3:00PM - 3:10PM Room: S505AB

Participants

Cornelius Deuschl, Essen, Germany (*Presenter*) Nothing to Disclose Julian Kirchner, Dusseldorf, Germany (*Abstract Co-Author*) Nothing to Disclose Thorsten D. Poeppel, Essen, Germany (*Abstract Co-Author*) Nothing to Disclose Benedikt M. Schaarschmidt, MD, Dusseldorf, Germany (*Abstract Co-Author*) Nothing to Disclose Harald H. Quick, PhD, Essen, Germany (*Abstract Co-Author*) Nothing to Disclose Ken Herrmann, Essen, Germany (*Abstract Co-Author*) Nothing to Disclose Ken Herrmann, Essen, Germany (*Abstract Co-Author*) Co-founder, SurgicEye GmbH Stockholder, SurgicEye GmbH Consultant, Sofie Biosciences Consultant, Ipsen SA Consultant, Siemens AG Research Grant, Advanced Accelerator Applications SA Research Grant, Ipsen SA Christoph Moenninghoff, MD, Essen, Germany (*Abstract Co-Author*) Nothing to Disclose

Lale Umutlu, MD, Essen, Germany (*Abstract Co-Author*) Nothing to Disclose Michael Forsting, MD, Essen, Germany (*Abstract Co-Author*) Nothing to Disclose Marc U. Schlamann, Essen, Germany (*Abstract Co-Author*) Nothing to Disclose

For information about this presentation, contact:

Cornelius.deuschl@uk-essen.de

PURPOSE

The objective of this study was to evaluate hybrid 11C-MET PET/MRI for detection of recurrent glioma.

METHOD AND MATERIALS

Fifty consecutive patients with histopathological proven glioma (9 Low Grade Glioma (LGG), 33 High Grade Glioma (HGG), 8 Oligodendroglioma (OGG)) were prospectively enrolled for a hybrid 11C-MET PET/MRI to differentiate recurrent glioma from treatment induced changes. Sole MRI data were analyzed based on RANO. Sole PET data and in a second session hybrid 11C-PET/MRI data were assessed for metabolic respectively metabolic and morphologic glioma recurrence. Reference standard was either histopathological report (n = 22) or follow-up imaging (n=28), whereas only patients of at least 6 months with follow up imaging were included. Based on the reference standard 35 patients were classified with recurrent glioma, whereas 15 patients with treatment induced changes.

RESULTS

Hybrid 11C-MET PET/MRI was performed in 50 patients for differentiation between recurrent glioma and treatment induced changes. Sensitivity, specificity, positive predictive value and negative predictive was calculated 86,11%, 71,43%, 88,57%, 66,67 for 11C-MET PET alone; 96,77%, 73,68%, 85,71%, 93,33% for MRI alone and 97,14%, 93,33%, 97,14%, 93,33% for hybrid 11C-PET/MRI, respectively. In all 50 patients diagnoses based on the reference standard were correct in 82% for 11C-MET PET, 88% for MRI alone and 96% for hybrid 11C-PET/MRI. A significant difference was found among hybrid 11C-MET PET/MRI and 11C-MET PET (p=0,016), whereas no significant difference was found among hybrid 11C-PET/MRI alone and 11C-MET PET alone. Furthermore, significant (P < 0.05) higher scores were found for diagnostic confidence when comparing 11C-MET PET/MRI (4,26 \pm 0,777) to 11C-MET PET alone (3,44 \pm 0.705) or to MRI alone (3,56 \pm 0.733).

CONCLUSION

Hybrid 11C-MET PET/MRI offers metabolic and morphological information for the assessment of glioma recurrence. The hybrid imaging concept increases accuracy and showed significant higher scores for diagnostic confidence when compared to MRI or PET.

CLINICAL RELEVANCE/APPLICATION

Hybrid 11C-MET PET/MRI might have the potential to strengthen RANO classification by adding the metabolic information. This should be evaluated in larger study cohorts.

SSM15-02 Does 18F-FDG PET/MR Increase the Diagnostic Performance for Recurrence Diagnostics in Comparison to MRI in Patients Suffering From Adenoid Cystic Carcinoma of the Head and Neck?

Participants Benedikt M. Schaarschmidt, MD, Dusseldorf, Germany (*Abstract Co-Author*) Nothing to Disclose Julian Kirchner, Dusseldorf, Germany (*Presenter*) Nothing to Disclose Cornelius Deuschl, Essen, Germany (*Abstract Co-Author*) Nothing to Disclose Christian Buchbender, Duesseldorf, Germany (*Abstract Co-Author*) Nothing to Disclose Philipp Heusch, MD, Duesseldorf, Germany (*Abstract Co-Author*) Nothing to Disclose Verena Ruhlmann, Essen, Germany (*Abstract Co-Author*) Nothing to Disclose

PURPOSE

To compare the diagnostic performance between 18F-fluorodeoxyglucose positron emission tomography / magnetic resonance (18F-FDG PET/MR) and MR imaging for the detection of recurrent adenoid cystic carcinoma (ACC) of the head and neck and locoregional metastases.

METHOD AND MATERIALS

In this retrospective analysis, a total of 31 dedicated 18F-FDG PET/MR examinations of the head and neck performed for recurrence diagnostics and locoregional metastases detection in patients after primary therapy of ACC were included (12 patients, mean age 59 years). In separate sessions, MRI and 18F-FDG PET/MR images were analyzed by two individual readers. Tumor recurrence or metastatic disease was confirmed by clinical and radiological follow-up examinations. Sensitivity, specificity, positive predictive value (PPV) and negative predictive value (NPV) were calculated on a per lesion basis and diagnostic accuracy between both modalities was compared using McNemar's test. p<0.05 was considered as statistically significant.

RESULTS

Tumor recurrence and / or locoregional metastases were detected in 20 examinations. 18F-FDG PET/MR correctly identified all 20 suspicious examinations, while MRI detected 19 of 20 examinations. On a per lesion basis, sensitivity, specificity, PPV and NPV were 77%, 94%, 95% and 73% for MRI and 96%, 84%, 90% and 93% for 18F-FDG PET/MR, respectively. On a per lesion basis, the diagnostic accuracy of 18F-FDG PET/MR (91%) was significantly higher in comparison to MRI (84%, p<0.05).

CONCLUSION

In patients suffering from ACC of the head and neck, 18F-FDG PET/MR is superior to MRI in detection tumor recurrence and locoregional metastases. Especially the superior NPV of 18F-FDG PET/MR is advantageous in regular follow-up examinations after primary tumor treatment in patients suffering from ACC.

CLINICAL RELEVANCE/APPLICATION

In comparison to MRI, 18F-FDG PET/MR provides a superior diagnostic performance in follow-up examinations after primary treatment of adenoid cystic carcinoma of the head and neck.

SSM15-03 4'-[Methyl-11C]-Thiothymidine PET/CT for Early Assessment of Disease Control Of Chemoradiotherapy for Head and Neck Squamous Cell Carcinoma: Comparison with FDG PET/CT

Wednesday, Nov. 29 3:20PM - 3:30PM Room: S505AB

Participants

Katsuya Mitamura, Kita-gun, Japan (*Presenter*) Nothing to Disclose Yuka Yamamoto, MD, PhD, Kagawa, Japan (*Abstract Co-Author*) Nothing to Disclose Takashi Norikane, Kita-gun, Japan (*Abstract Co-Author*) Nothing to Disclose Hiroshi Hoshikawa, MD, Kita-gun, Japan (*Abstract Co-Author*) Nothing to Disclose Jun Toyohara, Tokyo, Japan (*Abstract Co-Author*) Nothing to Disclose Yoshihiro Nishiyama, MD, Kagawa, Japan (*Abstract Co-Author*) Nothing to Disclose

PURPOSE

A new radiopharmaceutical, 4'-[methyl-11C]-thiothymidine (4DST), has been developed as an in vivo cell proliferation marker based on the DNA incorporation method. The purpose of this study was to evaluate the usefulness of 4DST PET/CT for early assessment of disease control of chemoradiotherapy for head and neck squamous cell carcinoma (HNSCC), in comparison with 2-deoxy-2-18Ffluoro-D-glucose (FDG) PET/CT.

METHOD AND MATERIALS

A total of 28 patients with HNSCC underwent 4DST and FDG PET/CT studies before, during, and after therapy. Uptake of 4DST and FDG was examined visually and semiquantitatively using standardized uptake value (SUV) for before, during and after therapy (SUVbefore, SUVduring and SUVafter, respectively). Percent change (during) was calculated from SUVbefore and SUVduring and percent change (after) was calculated from SUVbefore and SUVafter. Based on histopathological verification or radiologic follow-up, patients were divided into relapse-free and relapse groups. Relapse-free group was defined as those having no local recurrence or distant metastasis.

RESULTS

In all 28 patients, focally increased 4DST and FDG uptake in primary lesion was visible. On both 4DST PET/CT scans during and after therapy, 23 patients showed no increased uptake in primary lesion. On FDG PET/CT scans during and after therapy, 16 and 18 patients showed no increased uptake in primary lesion, respectively. Twenty-two patients were found to be relapse-free group and 6 to be relapse group. SUVduring and SUVafter values from 4DST PET/CT in relapse-free group were significantly lower than those in relapse group (p<0.001, respectively). The percent change (during) and percent change (after) values from 4DST PET/CT in relapse-free group were significantly higher than those in relapse group (p<0.001, respectively). Using FDG PET/CT, SUVduring, SUVafter, percent change (during) and percent change (after) were not significant differences between relapse-free and relapse groups.

CONCLUSION

The results of this preliminary study suggest that, compared with FDG PET/CT, 4DST PET/CT may be useful for early assessment of disease control of chemoradiotherapy in patients with HNSCC.

CLINICAL RELEVANCE/APPLICATION

4DST PET/CT may be useful for early assessment of disease control of chemoradiotherapy in patients with HNSCC.

SSM15-04 The Value 18F-FDG PET/CT in Early Stage Squamous Cell Carcinoma of the Oral Cavity

Wednesday, Nov. 29 3:30PM - 3:40PM Room: S505AB

Participants

Jennifer Murphy, MBBCh, MRCPI, Dublin, Ireland (*Presenter*) Nothing to Disclose David McGoldrick, Dublin, Ireland (*Abstract Co-Author*) Nothing to Disclose Caoilfhionn Ni Leidhin, MBBCh, Dublin, Ireland (*Abstract Co-Author*) Nothing to Disclose Afshin Nasoodi, MD, FRCR, Belfast, United Kingdom (*Abstract Co-Author*) Nothing to Disclose Grainne Govender, Ballsbridge, Ireland (*Abstract Co-Author*) Nothing to Disclose Ronan A. Mcdermott, MBBCh, Dublin, Ireland (*Abstract Co-Author*) Nothing to Disclose Niall Sheehy, MBBS, Dublin, Ireland (*Abstract Co-Author*) Nothing to Disclose Ciaran J. Johnston, MD, Dublin, Ireland (*Abstract Co-Author*) Nothing to Disclose

For information about this presentation, contact:

murphyjennifern@gmail.com

PURPOSE

The purpose of this study is to evaluate the value of 18-F fluorodeoxyglucose (FDG) positron emission tomography/computed tomography (PET/CT) for staging of early stage squamous cell carcinoma (SCC) of the oral cavity. Nodal staging on 18F-FDG PET/CT was compared with magnetic resonance imaging (MRI) of the neck and correlated with pathological staging on neck dissections.

METHOD AND MATERIALS

A retrospective review of all patients with clinically T1 and T2, biopsy-proven, squamous cell carcinoma of the oral cavity, and a clinically node-negative neck, between 2012 and 2017 was carried out. All patients that underwent both 18F-FDG PET/CT and MRI neck prior to surgical resection were included. The N and M stages on PET/CT were recorded, according to the AJCC/UICC TNM staging system, along with any incidental findings requiring further investigation. N stage on MRI was also recorded. Pathology reports were reviewed for pathological staging of the primary tumour and nodal status.

RESULTS

Sixty-four patients have been reviewed to date. Fifty-seven (89%) patients proceeded to neck dissection. Of these patients, 47 (82.5%) were histologically-proven node negative and 10 (17.5%) had histologically-proven nodal metastases. Of those patients with nodal metastases, 4 patients were staged N1 on PET/CT and 6 were staged N0. There were 2 patients with nodal metastases staged N1 on PET/CT but N0 on MRI. Of the node negative patients, 44 were staged N0 on PET/CT and 3 were staged N1. This yields a sensitivity of 40%, specificity of 93.6%, positive predictive value of 57.1% and negative predictive value of 88%. All patients were staged as M0 on PET/CT. Incidental findings requiring further clinical and radiological investigation were detected on PET/CT in 23 (35.9%).

CONCLUSION

Occult cervical nodal metastases are relatively infrequent in early stage SCC of the oral cavity with a clinically node negative neck. The relatively high specificity and negative predictive value of PET/CT in this study is due to the low prevalence of nodal metastases in this patient cohort. This study demonstrates that PET/CT is of limited value in conjunction with MRI for the detection of nodal metastases in these patients.

CLINICAL RELEVANCE/APPLICATION

The clinically node negative neck in early stage SCC of the oral cavity poses a potential treatment dilemma. PET/CT is of limited value in the detection of nodal metastases in these patients.

SSM15-05 Clinical Value of Three-Dimensional SPECT/CT Imaging For Assessment of Jaw Bone Invasion in Oral Cancers

Wednesday, Nov. 29 3:40PM - 3:50PM Room: S505AB

Participants

Tadaki Nakahara, MD, Tokyo, Japan (*Presenter*) Nothing to Disclose Hidetaka Miyashita, Tokyo, Japan (*Abstract Co-Author*) Nothing to Disclose Kenichi Ode, Tokyo, Japan (*Abstract Co-Author*) Nothing to Disclose Yu Iwabuchi, Tokyo, Japan (*Abstract Co-Author*) Nothing to Disclose Yohji Matsusaka, Tokyo, Japan (*Abstract Co-Author*) Nothing to Disclose Seiji Asoda, Tokyo, Japan (*Abstract Co-Author*) Nothing to Disclose Hideyuki Shiba, Tokyo, Japan (*Abstract Co-Author*) Nothing to Disclose Hiromasa Kawana, Tokyo, Japan (*Abstract Co-Author*) Nothing to Disclose Yuji Ogata, Tokyo, Japan (*Abstract Co-Author*) Nothing to Disclose Taneaki Nakagawa, Tokyo, Japan (*Abstract Co-Author*) Nothing to Disclose Masahiro Jinzaki, MD, Tokyo, Japan (*Abstract Co-Author*) Nothing to Disclose Masahiro Jinzaki, MD, Tokyo, Japan (*Abstract Co-Author*) Support, Toshiba Medical Systems Corporation; Support, General Electric Company

For information about this presentation, contact:

nakahara@rad.med.keio.ac.jp

PURPOSE

Imaging diagnosis of jaw bone invasion in oral cancers is still challenging due to dental artifacts as well as difficulty in detecting morphological change of early invasion. We have recently developed three-dimensional (3D) single-photon emission computed

tomography-computed tomography (SPECT/CT) imaging. We aimed to investigate the diagnostic performance of 3D SPECT/CT imaging for jaw bone invasion in comparison with other imaging modalities.

METHOD AND MATERIALS

Preoperative 3D SPECT/CT, contrast-enhanced CT (ceCT), and MRI images in 14 oral cancer patients were retrospectively evaluated by an oral surgeon. Each of the 3 image sets was independently reviewed with the knowledge of the tumor locations as to the likelihood of jaw bone invasion. When reviewing 3D SPECT/CT images, 3D volume-rendered SPECT/CT images with and without clip-plane editing were generated in order to grasp 2D and 3D bone anatomy and metabolism. The likelihood was classified using a 5-point diagnostic confidence scale. A jaw bone without cancer invasion that was scored as 1, 2 or 3 was considered true negative. A jaw bone with cancer invasion that was scored as 4 or 5 was considered true positive. Imaging results were compared with postsurgical results.

RESULTS

Seven of the 14 patients had jaw bone invasion of cancer cells and the other 7 did not. The sensitivity, specificity, positive and negative predictive values in the diagnosis of jaw bone invasion were 100% (7/7), 71% (5/7), 78% (7/9) and 100% (5/5) in 3D SPECT/CT, 43% (3/7), 86% (6/7), 75% (3/4), 60% (6/10) in ceCT, and 57% (4/7), 86% (6/7), 80% (4/5) and 67% (6/9) in MRI, respectively. Receiver operating characteristic analysis showed that 3D SPECT, ceCT and MRI had an area under the curve of 0.837, 0.786 and 0.704, respectively (not statistically different). Two cases with false-positive findings in 3D SPECT/CT had destruction of both periosteal and alveolar bones with severe inflammatory cell infiltration around the tumor sites.

CONCLUSION

3D SPECT/CT may be more sensitive than ceCT or MRI in the detection of jaw bone invasion.

CLINICAL RELEVANCE/APPLICATION

3D SPECT/CT appears more sensitive than ceCT or MRI in detecting jaw bone invasion in oral cancers and may be useful when jaw bone invasion is unclear with ceCT or MRI.

SSM15-06 The Usefulness of Initial Treatment Effects Based On PERSIST Criteria in Predicting the Three Years Disease Free Survival of Head and Neck Cancer

Wednesday, Nov. 29 3:50PM - 4:00PM Room: S505AB

Participants

Shigeki Nagamachi, MD, PhD, Fukuoka, Japan (*Presenter*) Nothing to Disclose Masanari Nonokuma, Fukuoka, Japan (*Abstract Co-Author*) Nothing to Disclose Youichi Mizutani, Miyazaki, Japan (*Abstract Co-Author*) Nothing to Disclose Tamasa Terada, Miyazaki, Japan (*Abstract Co-Author*) Nothing to Disclose Takayuki Kawabata, Miyazaki, Japan (*Abstract Co-Author*) Nothing to Disclose Tetsuya Tono, Miyazaki, Japan (*Abstract Co-Author*) Nothing to Disclose Kengo Yoshimitsu, MD, Fukuoka, Japan (*Abstract Co-Author*) Nothing to Disclose Toshinori Hirai, MD, PhD, Miyazaki, Japan (*Abstract Co-Author*) Nothing to Disclose

PURPOSE

The study was done to evaluate the usefulness of the initial treatment effects based on PERSIST criteria in predicting the disease free survival (DFS) 3 years after the initial therapy of head and neck cancer (HNC).

METHOD AND MATERIALS

We analyzed retrospectively fifty-one cases of HNC, 35 male and 16 female, 18 hypo-pharynx cancer, 9 gingival cancer, 9 tongue cancer, 7 laryngeal cancer, 4 maximal cancer and 4 oropharynx cancer. All cases were performed FDG-PET/CT on both before and after the initial therapy. Chemo-radiotherapies were done in 35 patients and radiotherapies were done in 16 patients. We divided all patients into 2 groups, the responders (CMR+PMR) and the non-responders (SMD+PMD), based on the result of RECIST criteria. Then we compared the diagnostic ability of predicting DFS 3 years after the initial therapy among the result of initial therapeutic effect by PERCIST criteria and three kinds of FDG uptake parameters. The FDG uptake parameters were SUL max (< 16.0) ,SUL peak (< 12.0) and TLG(< 180g) obtained before the initial therapy respectively.

RESULTS

Among 36 responders, 25 cases (69.0%) reached 3 years DFS. In contrast, only 5 of 15 cases non-responders (33.0%) could reach 3 years DFS. The diagnostic accuracy of initial treatment effects based on PERSIST criteria for predicting 3 years DFS was 68.6%. Regarding FDG uptake indices before the initial therapy, TLG (<180g) was the most powerful predictor among three kinds of indexes (TLG 68.6%, SUL max 51.0%, SUL peak 52.9 %, in accuracy).

CONCLUSION

We could predict 3 years DFS with high probability based on the result of PERCIST criteria after the initial therapy in patients of HNC. Similarly, TLG (<180g) before the initial therapy was also good predictor of 3 years DFS.

CLINICAL RELEVANCE/APPLICATION

The result of the initial therapy based on PERCIST is useful not only for diagnosing therapeutic effect but also for predicting DFS 3 years after the initial therapy in HNC patients.





103rd Scientific Assembly and Annual Meeting November 26 to December 1 McCormick Place, Chicago



SSM16

Neuroradiology (Gadolinium Deposition)

Wednesday, Nov. 29 3:00PM - 4:00PM Room: N226



AMA PRA Category 1 Credit ™: 1.00 ARRT Category A+ Credit: 1.00

Participants

Srinivasan Mukundan, MD, PhD, Durham, NC (*Moderator*) Institutional research support, Siemens AG; Institutional research support, Toshiba Medical Systems Corporation; Consultant, Toshiba Medical Systems Corporation; Yvonne W. Lui, MD, New York, NY (*Moderator*) Nothing to Disclose

Sub-Events

SSM16-01 Assessment of the Neurologic Effects of Intracranial Gadolinium Deposition Using a Large Population Based Cohort

Wednesday, Nov. 29 3:00PM - 3:10PM Room: N226

Participants

Robert J. McDonald, MD, PhD, Rochester, MN (*Presenter*) Consultant, General Electric Company; Investigator, General Electric Company

Jennifer S. McDonald, PhD, Rochester, MN (Abstract Co-Author) Research Grant, General Electric Company

Terry Therneau, PhD, Rochester, MN (Abstract Co-Author) Nothing to Disclose

Laurence J. Eckel, MD, Rochester, MN (Abstract Co-Author) Nothing to Disclose

David F. Kallmes, MD, Rochester, MN (*Abstract Co-Author*) Research support, Terumo Corporation Research support, Medtronic plc Research support, Sequent Medical, Inc Research support, Benvenue Medical, Inc Research support, General Electric Company Consultant, General Electric Company Consultant, Medtronic plcConsultant, Johnson & Johnson

Rickey Carter, PhD, Rochester, MN (Abstract Co-Author) Nothing to Disclose

Clifford R. Jack JR, MD, Rochester, MN (Abstract Co-Author) Stockholder, Johnson & Johnson Research Consultant, Eli Lilly and Company

Ronald C. Petersen, MD, PhD, Rochester, MN (Abstract Co-Author) Nothing to Disclose

For information about this presentation, contact:

mcdonald.robert@mayo.edu

PURPOSE

The neurotoxic potential of intracranial gadolinium (Gd) deposition following intravenous administration of gadolinium based contrast agents (GBCAs) is undefined. In the current study, we used the world's largest prospective population-based cohort on aging to study the effects of Gd exposure on neurologic and neurocognitive function.

METHOD AND MATERIALS

The Mayo Clinic Study of Aging (MCSA) cohort was enumerated from the Rochester Epidemiology Project in 2004 to study the incidence and natural history of cognitive impairment and dementia. All participants underwent extensive longitudinal clinical (neurologic evaluation, neuropsychological testing) assessment at baseline and 15-month follow-up intervals. Neurologic and neurocognitive scores were compared using standard multivariate methods between MCSA patients with no history of prior Gd exposure and those who underwent prior Gd-enhanced MRI. Progression from normal cognitive status to mild-cognitive impairment and dementia was assessed using multistate Markov model analysis.

RESULTS

Among 4261 cognitively normal study participants aged 50-90 (mean age (SD): 71.9 yrs (10.7), mean study participation (SD): 3.7 yrs (3.0)), 1092 (25.6%) received one or more GBCA doses (median: 2 doses, range: 1-28 doses) unrelated to their participation in the MCSA. Median time since first Gd exposure was 5.6 years (IQR=2.2-9.3 years). After adjusting for age, sex, education level, baseline neurocognitive performance, Charlson comorbidity index, and ApoE4 status, GBCA exposure was not a significant predictor of cognitive decline (changes in clinical dementia rating (p=.48), Blessed dementia scale (p=.68), or mental status exam score (p=.55)), diminished neuropsychological performance (p=.13), or diminished motor performance (Unified Parkinson's Disease Rating Scale (p=.43)). No dose-related effects were observed among these metrics (p=.89-.20). Finally, Gd exposure was not an independent risk factor in the rate of cognitive decline from normal cognitive status to dementia in this cohort (p=.91).

CONCLUSION

GBCA administration was not associated with worse overall neurologic or neurocognitive performance nor does it significantly affect the natural progression of cognitive decline in a large population-based cohort.

CLINICAL RELEVANCE/APPLICATION

Despite evidence of Gd accumulation following intravenous GBCA administration, Gd exposure is not associated with adverse neurologic outcomes.

Rats

Wednesday, Nov. 29 3:10PM - 3:20PM Room: N226

Participants

Federico Maisano, Colleretto Giacosa, Italy (*Presenter*) Employee, Bracco Group Simona Bussi, BMedSc, Colleretto Giacosa, Italy (*Abstract Co-Author*) Bracco Group employee Alessandra Coppo, BMedSc, Colleretto Giacosa, Italy (*Abstract Co-Author*) Bracco Group employee Catherine Botteron, Plan-les-Ouates, Switzerland (*Abstract Co-Author*) Bracco Group Employee Valerie Fraimbault, Plan-les-Ouates, Switzerland (*Abstract Co-Author*) Bracco Group Employee Antonello Fanizzi, MD, Colleretto Giacosa, Italy (*Abstract Co-Author*) Employee, Bracco Group Elisa De Laurentiis, PhD, Colleretto Giacosa, Italy (*Abstract Co-Author*) Employee, Bracco Group Sonia Colombo Serra, Colleretto Giacosa, Italy (*Abstract Co-Author*) I'm a Bracco Group employee. Fabio Tedoldi, Collereto Giacosa, Italy (*Abstract Co-Author*) Employee, Bracco Group

For information about this presentation, contact:

federico.maisano@bracco.com

PURPOSE

To investigate whether significant differences exist among macrocyclic MR contrast agents with respect to their retention in cerebellum, brain, kidneys and other organs.

METHOD AND MATERIALS

Gadobutrol (Gadovist®; Bayer), gadoterate meglumine (Gd-DOTA, Dotarem®; Guerbet), gadoteridol (ProHance®; Bracco) or Saline solution (0.9% w/v NaCl) were administered at 0.6 mmol/kg (1.2 mL/kg for saline) four times a week for five weeks to healthy male Wistar Han rats, randomly assigned to each of the four groups (n=15/group). After the end of the treatment, a recovery period of 4 weeks (28 d) was allowed before sacrifice. Organs (blood, cerebrum, cerebellum, liver, femur, kidneys and skin) were then collected for ICP-MS determination of gadolinium. Based on available amounts of samples, the LOQ (Limit of Quantitation) for Gd was 0.1 nmol/mL for blood, 0.1 nmol/g for cerebrum/cerebellum, 0.5 nmol/g for femur, 1 nmol/g for liver and skin. 1.7 nmol/g for kidneys. Statistical analysis was carried out by an independent expert.

RESULTS

Both in cerebellum and in cerebrum ProHance resulted in significantly (p < 0.001) lower levels of gadolinium compared both to Dotarem and to Gadovist. Also in the kidneys ProHance showed a residue that was significantly lower than both Dotarem (6 times higher; p < 0.01) and Gadovist (8 times higher; p < 0.001). In the femur, the differences were less pronounced, with only gadoterate meglumine showing a lower accumulation than gadobutrol (p < 0.001) and gadoteridol (p < 0.05). Gd concentration in blood, liver and skin samples was < LOQ.

CONCLUSION

After repeated injections of the 3 macrocyclic GBCAs and a 4-week off-dose period, ProHance resulted in significantly lower gadolinium concentrations than either Dotarem or Gadovist in cerebellum, cerebrum and kidneys. The observed differences, in the absence of dechelation, point to differences in wash-out rates, with gadoteridol being the GBCA that is most efficiently removed from both CNS and renal tissues.

CLINICAL RELEVANCE/APPLICATION

This non-clinical study shows that also macrocyclic MR contrast agents differ in the extent of retention in CNS and renal tissues, with ProHance giving less retention than Gadovist or Dotarem.

SSM16-03 Absence of Toxicity in Extended Duration Study of Gadolinium in Rodent Brains after Repeat Dosing of Gadodiamide: Investigation of Concentration, Location and Cell Ultrastructure

Wednesday, Nov. 29 3:20PM - 3:30PM Room: N226

Participants

Paul M. Evans, BSC,PhD, Amersham, United Kingdom (*Presenter*) Employee, General Electric Company Michael Marino, Niskayuna, NY (*Abstract Co-Author*) Employee, General Electric Company Adrian Smith, Amersham, United Kingdom (*Abstract Co-Author*) Employee, General Electric Company Janell M. Crowder, Niskayuna, NY (*Abstract Co-Author*) Employee, General Electric Company Lisa Lowery, Niskayuna, NY (*Abstract Co-Author*) Employee, General Electric Company Christine Morton, Niskayuna, NY (*Abstract Co-Author*) Employee, General Electric Company Jason Castle, Niskayuna, NY (*Abstract Co-Author*) Employee, General Electric Company Victoria Cotero, Niskayuna, NY (*Abstract Co-Author*) Employee, General Electric Company Mark Hibberd, Marlborough, MA (*Abstract Co-Author*) Employee, General Electric Company

For information about this presentation, contact:

paul.m.evans@ge.com

PURPOSE

Recent studies report low levels of gadolinium based contrast agents in the brain following repeat exposure. The purpose of this study was to evaluate the levels of Omniscan in the rat brain up to one year post-dosing, to evaluate the location of retained gadolinium, and to determine if there were any neurohistopathological sequelae.

METHOD AND MATERIALS

This study reports on a 50-week experimental endpoint from a previously published study (Smith et al. Radiology, 282:3, March 2017) together with additional analyses at the 1, 20 and 50 week timepoints. Gadolinium concentrations were quantified in blood and brains of rats 50 weeks after the cessation of dosing (cumulative dose 12 mmol/kg over 5 weeks) using inductively coupled plasma mass spectrometry (ICP-MS). Brain sections at standard toxicological levels were evaluated by standard toxicological

assessment. A portion of the Deep Cerebellar Nucleus (DCN) was reserved and processed for transmission electron microscopic (TEM) cell ultrastructure analysis and TEM with electron dispersive spectroscopy (TEM-EDS).

RESULTS

Gadolinium levels at 50 weeks were comparable to those observed at 20 weeks. Toxicologic histopathology analysis revealed no findings, and cell ultrastructural TEM analysis similarly revealed no findings, indicating that this extended period of gadolinium exposure for up to 1 year did not result in any tissue injury. A TEM-EDS analysis of gadolinium localization in the DCN showed approximately 100 nanometer foci located in the basal lamina, abluminal to the endothelium.

CONCLUSION

We conclude that whilst a small portion of gadolinium in the brain after repeat doses of GBCA is subject to long term retention (approximately 1/1,000,000 of the injected dose), this does not result in any observable tissue injury. We further propose that this gadolinium is in perivascular foci, and we have not found foci in the brain parenchyma.

CLINICAL RELEVANCE/APPLICATION

These observations are consistent with clinical observations of brain Gd in the human brain but without histopathological changes or a corresponding clinical syndrome.

SSM16-04 Long Term Deposition with Slow Clearance of Gadolinium in Cerebellum After Repeated Injections of Gadodiamide as compared to Gadoterate Meglumine in Rats

Wednesday, Nov. 29 3:30PM - 3:40PM Room: N226

Participants

Philippe Robert, Roissy Charles De Gaulle, France (*Presenter*) Employee, Guerbet SA Veronique Vives, Roissy Charles De Gaulle, France (*Abstract Co-Author*) Employee, Guerbet SA Justine Letien, MSc, ROISSY CDG Cedex, France (*Abstract Co-Author*) Employee, Guerbet SA Marlene Rasschaert, ROISSY CDG Cedex, France (*Abstract Co-Author*) Employee, Guerbet SA Cecile Factor, Roissy CDG Cedex, France (*Abstract Co-Author*) Employee, Guerbet SA Gaelle Jestin-Mayer, Roissy CDG Cedex, France (*Abstract Co-Author*) Employee, Guerbet SA Mounia Hasnaoui, ROISSY CDG Cedex, France (*Abstract Co-Author*) Employee, Guerbet SA Jean-Marc Idee, PharmD, Paris, France (*Abstract Co-Author*) Employee, Guerbet SA Sebastien Ballet, PhD, Roissy-Cdg, France (*Abstract Co-Author*) Employee, Guerbet SA Claire Corot, PhD, Roissy, France (*Abstract Co-Author*) Employee, Guerbet SA

For information about this presentation, contact:

philippe.robert@guerbet-group.com

PURPOSE

The objective of this study is to compare the long-term kinetics of Gd deposition in the cerebellum for gadodiamide (Omniscan®, linear contrast agent) and gadoterate meglumine (Dotarem®, macrocyclic contrast agent).

METHOD AND MATERIALS

Injection protocol: N=120 healthy rats received 5 intravenous injections of 2.4 mmol/kg of gadodiamide or gadoterate meglumine (N=60/agent) over a period of 5 weeks (1 injection per week) according to a published protocol (Robert 2016). Rats were divided in 6 groups with 0, 1, 2, 3, 4 and 5 months of washout period (N=10/agent, groups M0, M1, M2, M3, M4 and M5 respectively). Gd dosing: At each delay, animals were sacrificed. Blood and cerebellum were sampled and total Gd concentrations were dosed by the ICP-MS technic. Pharmaco-kinetics analysis: tissue Gd elimination kinetics in the cerebellum were fitted to estimate the tissue elimination half-lives in days along the 5 months of washout.

RESULTS

At all time-points, a significantly higher concentration of total Gd was found in cerebellum for gadodiamide groups as compared to gadoterate groups. Five months after the last injection, 30-fold more Gd was measured in the cerebellum in the gadodiamide group $(2.29\pm0.30 \text{ nmol/g})$ versus gadoterate $(0.075\pm0.037 \text{ nmol/g})$, p<0.0001). At this time-point, no remaining Gd was detected in the blood for both products. For gadodiamide, mean half-life of elimination (T1/2) of Gd accumulated in the cerebellum was 410 days. For comparison, more than 87% of Gd was cleared from the cerebellum with a T1/2 of 15 days for gadoterate meglumine.

CONCLUSION

A 30-fold higher total Gd concentration in the cerebellum was found 5 months after gadodiamide treatment as compared to gadoterate. Elimination of Gd from the cerebellum was 28-fold slower after injection of gadodiamide as compared to gadoterate meglumine. Recent studies have shown that a large amount of Gd is present under dechelated form one month after repeated injections of linear Gd contrast agents (Frenzel 2017) in contrary to macrocyclic Gd contrast agents which are excreted in chelated form. Such speciation analysis are ongoing on these long term data.

CLINICAL RELEVANCE/APPLICATION

After injection of linear Gd-based contrast agent gadodiamide, long term total Gd concentration in the cerebellum is 30-fold higher and elimination rate is 28-fold slower as compared to the macrocyclic gadoterate meglumine.

SSM16-05 Penetration and Distribution of Gadolinium-Based Contrast Agents into Cerebrospinal Fluid in Humans

Wednesday, Nov. 29 3:40PM - 3:50PM Room: N226

Participants

Florian Berger, MD,BSC, Baden, Switzerland (*Presenter*) Nothing to Disclose Rahel A. Kubik-Huch, MD, Baden, Switzerland (*Abstract Co-Author*) Nothing to Disclose Tilo Niemann, MD, Baden, Switzerland (*Abstract Co-Author*) Nothing to Disclose Hans-Ruedi Schmid, MD, Baden, Switzerland (*Abstract Co-Author*) Nothing to Disclose Johannes M. Froehlich, PhD, Bern, Switzerland (*Abstract Co-Author*) Consultant, Guerbet SA Hans Juerg Beer, PhD, Zurich, Switzerland (*Abstract Co-Author*) Nothing to Disclose Michael J. Thali, MD, Zurich, Switzerland (*Abstract Co-Author*) Nothing to Disclose Thomas Kraemer, PhD, Zurich, Switzerland (*Abstract Co-Author*) Nothing to Disclose

For information about this presentation, contact:

Florian.Berger@irm.uzh.ch

PURPOSE

Signal hyperintensity on unenhanced T1-weighted magnetic resonance (MR) images correlating with gadolinium deposition has been reported after multiple administrations of gadolinium-based contrast agents (GBCAs). This increase seems to be primarily associated with the repeated use of linear GBCAs. Recent studies on healthy rats have furthermore demonstrated that the blood-cerebrospinal fluid (CSF) barrier is permeable to not only linear but also macrocylcic GBCAs. The aim of our clinical study was to evaluate whether gadolinium (Gd) can be detected in CSF, to the best of our knowledge, for the first time in humans.

METHOD AND MATERIALS

This study was approved by the local Ethics committee with patient's consent authorizing use of tissue samples in research studies. For inclusion, all patients with a lumbar puncture between January and August 2016 were screened for at least one previous MR examination with GBCA administration (gadoterate meglumine at a dose of 0.1 mmol/kg bodyweight) within a time frame of 60 days prior to CSF extraction. A total of 39 consecutive samples fullfilling these criteria were identified. These patients were enrolled and their CSF was analyzed for the presence of Gd. The control group consisted of 10 patients without any prior intravenous GBCA administration according to medical files. Gd measurements in the CSF were performed using inductively coupled plasma mass spectrometry by monitoring the response of the 158Gd isotope.

RESULTS

In all cases with prior GBCA administration, Gd could be detected in the CSF. Gd concentration in the CSF showed a steady increase over 6 hours following the intravenous injection of the contrast agent. A significant decrease of Gd concentration compared to the peak values could be detected 24 hours after injection. Less amounts but still measurable concentrations of Gd could be detected several days/weeks after contrast enhanced MR examination. Control groups were all negative for Gd presence as expected.

CONCLUSION

Gadoterate meglumine, a macrocyclic GBCA, crosses the blood-brain barrier in humans and penetrates the CSF, in accordance with previous preclinical studies on healthy rats. Traces of GBCA can be detected in the CSF days/weeks after iv administration.

CLINICAL RELEVANCE/APPLICATION

It seems that the glio-vascular pathway via the CSF is a potential entrance way for GBCA into the brain.

SSM16-06 Cerebrospinal Fluid (CSF) Gadolinium Accumulation after Intravenous Gadobutrol-Enhanced MRI

Wednesday, Nov. 29 3:50PM - 4:00PM Room: N226

Awards

Student Travel Stipend Award

Participants

Avinash Nehra, MD, Rochester, MN (Presenter) Nothing to Disclose

Robert J. McDonald, MD, PhD, Rochester, MN (Abstract Co-Author) Consultant, General Electric Company; Investigator, General Electric Company

Amy Bluhm, Rochester, MN (Abstract Co-Author) Nothing to Disclose

Tina Gunderson, Rochester, MN (Abstract Co-Author) Nothing to Disclose

David L. Murray, MD, PhD, Rochester, MN (Abstract Co-Author) Nothing to Disclose

Paul Jannetto, Rochester, MN (Abstract Co-Author) Nothing to Disclose

David F. Kallmes, MD, Rochester, MN (*Abstract Co-Author*) Research support, Terumo Corporation Research support, Medtronic plc Research support, Sequent Medical, Inc Research support, Benvenue Medical, Inc Research support, General Electric Company Consultant, General Electric Company Consultant, Medtronic plcConsultant, Johnson & Johnson

Laurence J. Eckel, MD, Rochester, MN (Abstract Co-Author) Nothing to Disclose

Jennifer S. McDonald, PhD, Rochester, MN (Abstract Co-Author) Research Grant, General Electric Company

For information about this presentation, contact:

nehra.avinash@mayo.edu

PURPOSE

Recent studies in the setting of an intact blood brain barrier (BBB) have demonstrated intracranial gadolinium deposition following MRI with gadolinium-based contrast agents (GBCAs). While the mechanism of gadolinium distribution from bloodstream to neuronal tissue remains unclear, a proposed mechanism is through the blood-cerebrospinal fluid (CSF) barrier. This study evaluates gadolinium accumulation in the CSF after intravenous Gadobutrol administration.

METHOD AND MATERIALS

Patients who underwent a Gadobutrol-enhanced MRI and subsequent lumbar puncture (LP) within a period of 30 days (Gadobutrol group) were included versus a control group who had an LP without prior history of receiving gadolinium-enhanced MRI. Serum samples were also obtained following MRI exam. Gadolinium in CSF and serum samples was quantified using inductively coupled plasma mass spectrometry. Intact BBB was defined as total CSF protein less than or equal to 35 mg/dL. The relationship between gadolinium clearance and patient characteristics (ie. age, gender, CSF protein), and between serum and CSF gadolinium concentration were examined using regression models.

RESULTS

Eighty two (n=82) pediatric and adult patients (68 Gadobutrol, 14 control) were included. Time between Gadobutrol exposure and CSF collection ranged from 1.1 and 594 hours. Gadolinium was detected in the CSF of all Gadobutrol group patients (range 0.2 to 1494 ng/mL); alternatively the median gadolinium concentration in the control group patients was 0 ng/mL (IQR 0 - 0 ng/mL). Pediatric patients (<18 years) and those with an intact BBB had significantly faster clearance of gadolinium compared to adult patients and those with compromised BBB (CSF protein >35 mg/dL) (p=0.046 and <0.001, respectively). Furthermore there was significant correlation between gadolinium concentrations in the serum (range 2.2 - 277.8 ng/mL) and CSF samples (p<.0001).

CONCLUSION

Intravenous administration of Gadobutrol results in gadolinium accumulation within the CSF, even in the setting of normal renal function and no BBB dysfunction. Further research is required to determine the mechanism and clinical significance of gadolinium accumulation in CSF.

CLINICAL RELEVANCE/APPLICATION

Gadolinium accumulates in the CSF following intravenous administration of Gadobutrol in the absence of neurologic pathology and normal renal function, suggesting a route for intracranial deposition.





103rd Scientific Assembly and Annual Meeting November 26 to December 1 McCormick Place, Chicago



SSM17

Neuroradiology (Intracranial Vascular Imaging: Pipe Dream or Reality?)

Wednesday, Nov. 29 3:00PM - 4:00PM Room: N227B



AMA PRA Category 1 Credit ™: 1.00 ARRT Category A+ Credit: 1.00

Participants

Salman Qureshi, MBChB, BSc, Sale, United Kingdom (*Moderator*) Nothing to Disclose James R. Fink, MD, Seattle, WA (*Moderator*) Institutional Grant support, Guerbet SA

Sub-Events

SSM17-01 Reduced Intravoxel Incoherent Motion Microvascular Perfusion Predicts Delayed Cerebral Ischemia and Vasospasm After Cerebral Aneurysm Rupture

Wednesday, Nov. 29 3:00PM - 3:10PM Room: N227B

Participants

Jeremy J. Heit, MD, PhD, Stanford, CA (Presenter) Consultant, Terumo Corporation

Max Wintermark, MD, Lausanne, Switzerland (Abstract Co-Author) Advisory Board, General Electric Company;

Michael A. Marks, MD, Stanford, CA (Abstract Co-Author) Consultant, Medtronics plc Stockholder, Likemark Medical, Inc Research Grant, Siemens AG

Greg Zaharchuk, MD, PhD, Stanford, CA (*Abstract Co-Author*) Research Grant, General Electric Company; Consultant, General Electric Company;

Gary K. Steinberg, MD, PhD, Stanford, CA (Abstract Co-Author) Nothing to Disclose

Adrienne M. Moraff, MD, Stanford, CA (Abstract Co-Author) Nothing to Disclose

Christian Federau, Basel, Switzerland (Abstract Co-Author) Nothing to Disclose

PURPOSE

Cerebral arterial vasospasm and clinical delayed cerebral ischemia (DCI) following aneurysmal subarachnoid hemorrhage (aSAH) accounts for up to 30% of the morbidity and mortality in these patients. Neurologic examinations, daily transcranial Doppler ultrasound (TCD), and screening CT/CT Angiography/CT Perfusion studies have limited sensitivity and specificity in identifying DCI. Intravoxel incoherent motion (IVIM) MRI extracts microvascular perfusion information from a multi-b value diffusion-weighted sequence. We determined whether decreased IVIM perfusion on brain MRI may identify patients with DCI and cerebral vasospasm.

METHOD AND MATERIALS

We performed a retrospective cohort study of patients with aneurysmal SAH rupture at our neurovascular center. Consecutive patients who underwent a brain MRI after ruptured aneurysm treatment with neurologic deterioration and possible DCI were included. Intravoxel incoherent motion was included in all MRI examinations during the study period. Patient demographic, DCI development, aneurysm and vasospasm treatment, and outcome data were determined by electronic medical record review. Statistical analysis was performed using Excel and SPSS.

RESULTS

16 patients (11 female; 5 male; p=0.9) were included. 10 patients (63%) developed DCI and vasospasm requiring endovascular treatment (DCI+ group) and 6 (37%) did not (DCI- group). DCI+ patients were younger (mean 59 years versus 70 years in the DCI-group; p=0.03); there were no differences in medical co-morbidities between these groups. Presentation Glasgow Coma Scale, Hunt and Hess Scale, and Fisher Grade were also similar between these groups. 20 MRI studies (14 in DCI+ and 6 in DCI-) were performed. All MRIs were performed prior to endovascular vasospasm treatment in DCI+ patients. Whole brain microvascular blood volume on IVIM was significantly reduced in DCI+ patients (mean±sd 0.13±0.02 mm2/s) compared to DCI- patients (0.9±0.03 mm2/s; p=0.03). There was no significant difference in arterial spin labeling or perfusion weighted imaging measures of cerebral perfusion between DCI+ and DCI- patients.

CONCLUSION

Decreased microvascular blood volume on IVIM correlates with DCI development following cerebral aneurysm rupture.

CLINICAL RELEVANCE/APPLICATION

IVIM perfusion may be a useful biomarker for DCI and a triage tool for endovascular vasospasm treatment. Prospective studies should validate this hypothesis.

SSM17-02 Assessment of Steal Phenomenon in MMD Patients with Combination of T-ASL and MRA

Wednesday, Nov. 29 3:10PM - 3:20PM Room: N227B

Participants XINYI GAO, MSc, Shanghai, China (*Presenter*) Nothing to Disclose

For information about this presentation, contact:

PURPOSE

Steal phenomenon is an independent risk factor for future stroke. We aimed to generalize the steal phenomenon conducted by the first and the second collaterals separately using t-ASL combining with MRA in MMD patients, and to explore the relationship between pre-operation hemorrhage and the steal phenomenon.

METHOD AND MATERIALS

Forty-three patients with bilateral moyamoya disease underwent t-ASL, MRA and DSA. Clinical factors including sex, age, hypertension, diabetes metabolic, hyperlipidemia, current smoking, history of taking Aspirin were gathered. Correlation analysis was used to compare the relationship between the amount of steal phenomenon and Suzuki staging. Univariate logistic regression analyses were performed to examine the relationship between pre-operation hemorrhage and each of the factors separately. Forward stepwise multivariate logistic regression analyses were performed to determine the crucial risk factor.

RESULTS

In every MMD patient steal phenomenon was positive (total amount 136). SP could be divided into five types on t-ASL images (ICA-contralateral ACA, ICA-contralateral MCA, anterior circulation-ipsilateral posterior circulation, posterior circulation-ipsilateral anterior circulation, external carotid circulation) and three groups according to MRA and t-ASL. The amount of SP was not associated with SUZUKI stage (P=0.122, 0.689). Out of all the clinical and imaging factors, high SUZUKI stage (P=0.038) and the existence of the steal phenomenon completely conducted by the second collateral (P=0.002) showed great power for predicting pre-operation hemorrhage. Forward stepwise multivariate logistic regression analyses revealed steal phenomenon completely conducted by the second collateral (OR: 29.499, 95% CI: 3.629-239.780; P =0.002) was more powerful than high SUZUKI stage (OR: 0.265, 95% CI: 0.098-0.718; P =0.009).

CONCLUSION

Steal phenomenon in MMD can be divided into five types by t-ASL and three groups according to MRA and t-ASL. Comparing with high SUZUKI stage, the existence of the steal phenomenon completely conducted by the second collateral is a stronger risk factor for pre-operation hemorrhage in MMD patients.

CLINICAL RELEVANCE/APPLICATION

Comparing with high SUZUKI stage, the existence of the steal phenomenon completely conducted by the second collateral is a stronger risk factor for pre-operation hemorrhage in MMD patients.

SSM17-03 High Resolution Time-of-Flight Magnetic Resonance Angiography with Volume Rendering Algorithm for Detection of Cerebral Aneurysms: Correlation with Standard Digital Subtraction Angiography (DSA)

Wednesday, Nov. 29 3:20PM - 3:30PM Room: N227B

Participants

A Leum Lee, MD, Bucheon-Si, Korea, Republic Of (*Presenter*) Nothing to Disclose Chul-Ho Sohn, MD, Seoul, Korea, Republic Of (*Abstract Co-Author*) Nothing to Disclose Yeunjeong Kim, Bucheon, Korea, Republic Of (*Abstract Co-Author*) Nothing to Disclose Jungbin Lee, MD, Bucheon, Korea, Republic Of (*Abstract Co-Author*) Nothing to Disclose Kee-Hyun Chang, Bucheon, Korea, Republic Of (*Abstract Co-Author*) Nothing to Disclose

For information about this presentation, contact:

aleerad@schmc.ac.kr

PURPOSE

We investigated the diagnostic performance and increased discriminative value of the biomarkers of high-resolution MRA(HR-MRA) with volume rendering(VR) post-processing techniques for the detection of cerebral aneurysms compared with conventional MRA(C-MRA), using digital subtraction angiography(DSA) as the gold standard.

METHOD AND MATERIALS

HR-MRA was performed for 38 patients with 51 possible aneurysms on C-MRA. For each possible aneurysm, two readers recorded their level of confidence on a 5-point scale. All patients were performed DSA, which was used as the standard of reference. ROC analysis was conducted to determine the effectiveness of C-MRA and HR-MRA in detecting aneurysm with and without VR. The sensitivity, specificity, PPV, and NPV for each category was calculated. AUC and the 95% CI of the area were computed to evaluate the detective ability. The increased discriminative value of the biomarkers was examined by calculation of NRI and IDI indices.

RESULTS

DSA revealed 37 aneurysms in 26 patients. Both in aneurysm-based and patient-based analyses, HR-MRA showed higher diagnostic accuracy than C-MRA, and when a VR algorithm was added, increased diagnostic accuracy was revealed(C-MRA vs. HR-MRA p<0.01; in addition of VR, p<0.01, respectively). Although the addition of VR to the HR-MRA did not improve the AUC(0.8031 vs. 0.8658, p=0.16), the IDI(19.38%, Z=3.18, p<0.01) and NRI(46.3%, Z=6.32, p<0.01) were statistically significant. When using the 5-point scale of MRA finding, C-MRA showed better performance than that of categorized MRA finding, without statistically significant difference of AUC (p=0.27). And the addition of VR to the HR-MRA did not improve the AUC(0.9228 vs. 0.9188, p=0.14), but the IDI(29.5%, Z=4.3, p<0.01) and NRI(73%, Z=15.39, p<0.01) were statistically significant. For aneurysms less than 3 mm, when HR-MRA with VR was applied, the detection rate was further increased than that of aneurysms greater than or equal to 3 mm.

CONCLUSION

The application of HR-MRA with a VR algorithm improved diagnostic performance for the detection of intracranial aneurysms, especially when the aneurysm was less than 3 mm.

CLINICAL RELEVANCE/APPLICATION

The application of HR-MRA with a VR algorithm has high accuracy, sensitivity and specificity for the detection of intracranial aneurysms, which is recommended to improve diagnostic performance for the detection of intracranial aneurysms.

SSM17-04 Comparative Study of 4D CTA and DSA for Vascular Assessment in Moyamoya Disease

Wednesday, Nov. 29 3:30PM - 3:40PM Room: N227B

Participants

Bing Tian, MD, Shanghai, China (*Presenter*) Nothing to Disclose Bing Xu, Shanghai, China (*Abstract Co-Author*) Nothing to Disclose Qi Liu, MD, PhD, Shanghai, China (*Abstract Co-Author*) Nothing to Disclose Jianping Lu, MD, Shanghai, China (*Abstract Co-Author*) Nothing to Disclose

PURPOSE

We use 4D CTA to evaluate the vascular changes in moyamoya disease, including the vascular stenosis (modified Suzuki score, Houkin score) and collateral circulation (basicranial moyamoya vessels, posterior circulation collaterals and ECA collaterals). DSA was used as the gold standard to determine the value of noninvasive angiography in moyamoya disease.

METHOD AND MATERIALS

101 patients with confirmed moyamoya disease were underwent 4D CTA and DSA with an interval of <1 week. Two neuroradiologists evaluated the 4D CTA (VR and MIP) and DSA images independently or jointly in the case of disagreement. The performance of 4D CTA relative to DSA was determined using consistency checks (kappa values, 95% CI) and correlation analysis.

RESULTS

We obtained the following kappa values for consistency between 4D CTA and DSA: modified Suzuki score, 0.714 (0.649-0.778); Houkin score, 0.846 (0.780-0.911); the basicranial moyamoya vessels, 0.594 (0.525-0.663); posterior circulation collaterals, 0.435 (0.325-0.544); and ECA collaterals, 0.591 (0.483-0.699). The corresponding correlation coefficients (P values) were 0.843 (<0.001), 0.872 (<0.001), 0.792 (<0.001), 0.635 (<0.001) and 0.797 (<0.001).

CONCLUSION

In the evaluation of the vascular changes of moyamoya disease, 4D CTA (VR and MIP) showed strong consistency and correlation with DSA in terms of the vascular stenosis score, but was insufficient in collateral circulation evaluation.

CLINICAL RELEVANCE/APPLICATION

We adopted the modified Suzuki score and Houkin score to evaluate intracranial vascular stenosis in MMD, and also evaluated collateral circulation (the basicranial moyamoya vessels, and collaterals from the posterior circulation and ECA). Here, we discuss the value of 4D CTA for vascular assessments in adult MMD patients as compared with the gold standard, DSA. Upon analyzing the 4D CTA and DSA images of 101 adult patients with confirmed MMD, we concluded the following: (1) 4D CTA has high consistency and correlation with DSA in terms of the Suzuki and Houkin scores; and (2) 4D CTA has fair correlation and moderate consistency with DSA for the assessment of collateral circulation, specifically, the basicranial moyamoya vessels, and collaterals from the posterior circulation and ECA.

SSM17-05 4D Flow MRI Analysis of Cerebral Blood Flow Before and After High-Flow EC-IC Bypass Surgery

Wednesday, Nov. 29 3:40PM - 3:50PM Room: N227B

Awards

Trainee Research Prize - Fellow

Participants

Erika Orita, Bunkyo-ku, Japan (*Presenter*) Nothing to Disclose Tetsuro Sekine, MD, PhD, Tokyo, Japan (*Abstract Co-Author*) Nothing to Disclose Yasuo Murai, MD, Tokyo, Japan (*Abstract Co-Author*) Nothing to Disclose Ryo Takagi, MD, Tokyo, Japan (*Abstract Co-Author*) Nothing to Disclose Yasuo Amano, MD, Tokyo, Japan (*Abstract Co-Author*) Nothing to Disclose Takahiro Andoh, Tokyo, Japan (*Abstract Co-Author*) Nothing to Disclose Kotomi Iwata, Tokyo, Japan (*Abstract Co-Author*) Nothing to Disclose Makoto Obara, Minato-Ku, Japan (*Abstract Co-Author*) Nothing to Disclose Shinichiro Kumita, MD, Tokyo, Japan (*Abstract Co-Author*) Nothing to Disclose Shinichiro Kumita, MD, Tokyo, Japan (*Abstract Co-Author*) Nothing to Disclose

For information about this presentation, contact:

erika-orita@nms.ac.jp

PURPOSE

One of the treatment options for complex ICA aneurysm is the ligation of the ICA with the high-flow extracranial-intracranial (EC-IC) bypass surgery. Though the cerebral hemodynamics is thought to be changed drastically after the surgery, there has been no published papers performing quantitative evaluation. The purpose of this study was to clarify the change of the hemodynamics after the high-flow EC-IC bypass surgery by using time-resolved 3D-phase contrast (4D Flow) MRI.

METHOD AND MATERIALS

We enrolled 11 patients (2 men; mean age 62.8) who underwent ICA ligation and high-flow EC-IC bypass surgery with radial artery graft for treatment of a complex ICA aneurysm. They underwent 4D Flow MRI preoperatively and 3 weeks after the bypass surgery. The imaging parameters; 3.0-T MRI (Aheiva, Philips), TR/TE=8.4/5.4, VENC=100cm/sec, voxel size=0.82X0.82X1.4mm, heart phase= 15, scan time= approx. 6 min. We measured blood flow volume (BFV) of bilateral ICAs, BA, and bypass artery by using GT Flow (Gyro Tools). The BFV of each vessel and total brain BFV (t-BFV = bilateral ICAs + BA + bypass) were compared between before

and after surgery by using paired t-test. We evaluated post-operative hyperperfusion based on CT perfusion and clinical symptoms within 3 weeks after the surgery.

RESULTS

In all patients, the patency of the bypass artery was confirmed by 4D Flow MRI. The BFV of contralateral ICA and BA were statistically increased after the surgery (ICA: $5.89\pm2.08 \text{ vs.}$ $7.22\pm1.88 \text{ m/sec}$ (p=.0018), BA: $3.06\pm0.17 \text{ vs.}$ $4.12\pm0.14 \text{ m/sec}$ (p<.001)). T-BFV was statistically increased after surgery (12.99 $\pm8.65 \text{ vs.}$ $15.18\pm3.14 \text{ m/sec}$ (p=.0067)). While, there was no evidence of hyperperfusion in any cases based on CT perfusion or clinical symtoms.

CONCLUSION

In the current study, we could prove that the drop of BFV from sacrificed ICA is compensated by both native arteries (contralateral ICA and BA) and the bypass. Though the CT perfusion and clinical symtoms confirmed there is no hyperperfusion, the t-BFV increased 16.8%. It may indicate 4D Flow MRI could reveal the subtle hyperperfusion. In conclusion, 4D Flow MRI could quantify the change of hemodynamics after the high-flow bypass surgery. It provides insight to the autoregulation system in the cerebral blood flow.

CLINICAL RELEVANCE/APPLICATION

4D Flow MRI is one of the optimized imaging modalities for the quantitative assessment of the cerebral hemodynamic change after high-flow EC-IC bypass surgery.

SSM17-06 Angiogram-negative Non-perimesencephalic Subarachnoid Hemorrhage: A Meta-Analysis of Follow up Strategies

Wednesday, Nov. 29 3:50PM - 4:00PM Room: N227B

Participants

Long Tu, MD, New Haven, CT (*Presenter*) Nothing to Disclose Yiyuan Fang, New Haven, CT (*Abstract Co-Author*) Nothing to Disclose Xiao Wu, New Haven, CT (*Abstract Co-Author*) Nothing to Disclose Ajay Malhotra, MD, Stamford, CT (*Abstract Co-Author*) Nothing to Disclose

PURPOSE

The purpose of this study is to synthesize the current literature into recommendations regarding the follow up of nonperimesencephalic subarachnoid hemorrhage. Specifically, we will investigate the utility of various imaging modalities (CTA, DSA, MRA) of repeat imaging after an initially negative angiographic study (usually CTA or DSA).

METHOD AND MATERIALS

PUBMED, EMBASE, SCOPUS and research meeting abstracts were searched up to March 2017 for studies of patients with spontaneous subarachnoid hemorrhage (SAH) and an initially negative angiographic study (DSA, CTA, or MRA). Title/abstract and then full text screening was performed by two independent reviewers. Study quality was assessed via the Cochrane Risk of Bias Tool (CRBT). Where appropriate, meta-analysis was conducted using random effects models.

RESULTS

A total of 1917 studies were identified, of which 178 underwent full text review; 95 studies were included. Diagnostic methods for initial angiographic as well as follow up studies were variable. Preliminary assessment of study quality by CRBT also showed variability; however, most studies had a low risk of bias. Preliminary data suggest superiority of DSA and CTA to MRA for follow up of angiogram-negative NPSAH.

CONCLUSION

Spontaneous SAH may be categorized as perimesencephalic, diffuse aneurysmal, peripheral (convexity, sulcal), or CT-negative (detected only on lumbar puncture) based on the distribution of acute hemorrhage. Follow up imaging for patients with perimesencephalic patterns of hemorrhage has been shown to be unlikely to find an underlying structural lesion or to change outcome for this relatively benign entity. The optimal management strategies for non-perimesencephalic SAH however are not clear. Preliminary data from our meta-analysis suggest superiority of DSA (including rotational 3D angiogram) and CTA over MRA for NPSAH with an initially negative angiographic study.

CLINICAL RELEVANCE/APPLICATION

Our study will make recommendations on the optimal management of the more concerning (non-perimesencephalic) subtypes of spontaneous SAH based on existing literature.





103rd Scientific Assembly and Annual Meeting November 26 to December 1 McCormick Place, Chicago



SSM18

Neuroradiology (Radiation and Image Quality)

Wednesday, Nov. 29 3:00PM - 4:00PM Room: N229



AMA PRA Category 1 Credit ™: 1.00 ARRT Category A+ Credit: 1.00

Participants

Margaret N. Chapman, MD, Boston , MA (*Moderator*) Nothing to Disclose Amy F. Juliano, MD, Boston, MA (*Moderator*) Nothing to Disclose

Sub-Events

SSM18-01 The Feasibility of One-stop Axial Scanning Coronary CTA Combined with Spiral Scanning of Head-Neck CTA: Image Quality and Radiation Dose

Wednesday, Nov. 29 3:00PM - 3:10PM Room: N229

Participants

Li Wei, PhD,MD, Liaocheng, China (*Presenter*) Nothing to Disclose Daliang Liu, PhD,MD, Liaocheng, China (*Abstract Co-Author*) Nothing to Disclose Peiji Song, Liaocheng, China (*Abstract Co-Author*) Nothing to Disclose Hui Cui, MD,MD, Liao Cheng, China (*Abstract Co-Author*) Nothing to Disclose Xianghui Wan, Liaocheng, China (*Abstract Co-Author*) Nothing to Disclose Lingling Wang, Shanghai, China (*Abstract Co-Author*) Nothing to Disclose Jie X. Duan, MD, Liaocheng, China (*Abstract Co-Author*) Nothing to Disclose

For information about this presentation, contact:

Weili286@163.com

PURPOSE

To investigate the feasibility and advantages of 'one-stop' axial scanning of coronary and spiral scanning of head-neck CTA.

METHOD AND MATERIALS

78 patients were randomly divided into three groups: Group A (n=26) performed helical scanning of head and neck CTA and axial scanning of CCTA altogether with one-time injection of contrast medium. The switching delay between the two scanning modes was as short as 1.1 s. Group B (n=26) performed conventional head-neck CTA exams with a scanning range from aortic arch to calvarium. Group C (n=26) performed conventional CCTA scanning. The effective radiation dose (ED) and usage of contrast medium volume were recorded for each patient. Double-blinded evaluation of the image quality of the three groups were completed by two physicians.

RESULTS

The image quality of coronary and head and neck in Group A was not different from that in Group B and Group C $(4.63\pm0.42,4.34\pm0.73,p>0.05)$. The volume of contrast medium used in Group A was significantly less that the total volume in Group B and C $(53.1\pm3.9m]:115.2\pm10.6m]$, t=15.9 p<0.001). The ED in Group A was not different from the combined ED in Group B and C $(2.1\pm0.4mSv vs. 1.9\pm0.5mSv)$.

CONCLUSION

The "one-stop" scanning protocol enabled CTA of coronary and head-neck with one-time injection of contrast medium, resulting a reduction of 50% contrast medium dose, while the image quality and radiation dose were comparable with separate scanning protocols.

CLINICAL RELEVANCE/APPLICATION

The combination of axial and spiral CT angiography is the first choice for evaluation of cardiovascular and cerebrovascular diseases.

SSM18-02 Achieving Good Images in Head CT with Optimized Iterative Reconstruction Algorithm (ASIR-V) in Combination with EC2 to Further Reduce Radiation Dose

Wednesday, Nov. 29 3:10PM - 3:20PM Room: N229

Participants

Yanan Zhu, Ankang, China (*Presenter*) Nothing to Disclose Faqing Lei, Ankang, China (*Abstract Co-Author*) Nothing to Disclose Zhian Pi, Ankang, China (*Abstract Co-Author*) Nothing to Disclose Jun Yao, Ankang, China (*Abstract Co-Author*) Nothing to Disclose Zhengjun Li, Ankang, China (*Abstract Co-Author*) Nothing to Disclose Heping Zhou, MD, Ankang, China (*Abstract Co-Author*) Nothing to Disclose Jianying Li, Beijing, China (*Abstract Co-Author*) Employee, General Electric Company

Xianfeng Qu, Ankang, China (Abstract Co-Author) Nothing to Disclose

For information about this presentation, contact:

zhuyanan1977@163.com

PURPOSE

To evaluate the head CT image quality and radiation dose reduction potential with optimized third generation adaptive statistical iterative reconstruction (ASIR-V).

METHOD AND MATERIALS

Prospectively enrolled 80 adults for non-enhanced head CT on a 16cm wide-detector 256-row Revolution CT scanner. Participants were randomly divided into two groups: Group 1 (n=40) with the standard low dose scan and reconstruction protocol of 120kVp / 200mAs and 60%ASIR-V algorithm; Group 2 with the reduced radiation dose of 120kVp / 120mAs scan protocol. Images in Group 2 were reconstructed using ASIR-V at 0%-100% to select the optimal strength for getting the highest subjective image quality. The subjective image quality was evaluated by 2 board-certificated radiologists using a 5-point scoring system with 3 and above being acceptable for diagnosis. Enhanced Contrast Level 2(EC2) reconstruction was done at the optimal ASIR-V (in Group 2). The CT numbers and their standard deviation (SD) of cerebellum and centrum ovale were measured to calculate signal to noise ratio (SNR) and contrast to noise ratio (CNR) for cerebellum. Radiation dose was recorded. Measurements from the two groups were compared between the optimal ASIR-V (in Group 2) in combination with EC2 and the conventional Group (Group 1).

RESULTS

With the increase of ASIR-V strength from 0% to 100%, noise decreased while CNR and SNR increased monotonically. The highest subjective image quality was achieved at 70% ASIR-V. There was no statistical difference in the noise in centrum ovale and the overall subjective image quality scores between Group 1 and the group of 70% ASIR-V in combination with EC2. However, compared with the conventional group (Group 1), the group of 70% ASIR-V in combination with EC2 significantly raised the CNR of the cerebellum by 21.4% (3.74 ± 0.84 vs. 4.59 ± 0.73) (P<0.05). On the other hand, compared with the standard low dose group, the reduced dose group with 70% ASIR-V significantly reduced effective radiation dose by 56% (0.44 vs. 1.01 mSv) (P<0.05).

CONCLUSION

The CT image quality of the head was acceptable on a 256-row, 16cm wide-detector CT with 70% ASIR-V algorithm in combination with EC2 at 44% dose, compared with standard low dose head CT scan and reconstruction protocol.

CLINICAL RELEVANCE/APPLICATION

Good images of the 120mAs head can be achieved on a wide-detector CT with 70% Asir-V in combination with EC2 reconstruction to reduce the radiation dose.

SSM18-03 Multiphase CT Angiography in Acute Stroke: Radiation Dose and Patterns of Use

Wednesday, Nov. 29 3:20PM - 3:30PM Room: N229

Participants Lorenzo M. Piergallini, MD, Milan, Italy (*Presenter*) Nothing to Disclose Cristina De Mattia, Milan, Italy (*Abstract Co-Author*) Nothing to Disclose Marina Sutto, Milan, Italy (*Abstract Co-Author*) Nothing to Disclose Guglielmo Carlo Pero, MD, Milan, Italy (*Abstract Co-Author*) Nothing to Disclose Paola Enrica Colombo, MD, MPH, Milano, Italy (*Abstract Co-Author*) Nothing to Disclose Alberto Torresin, PhD, Milano, Italy (*Abstract Co-Author*) Nothing to Disclose

For information about this presentation, contact:

lorenzo.piergallini@gmail.com

PURPOSE

In the rapidly evolving field of acute stroke diagnosis and management, multiphase CTA (mCTA) has been recently developed, allowing better evaluation of collateral filling with temporal resolution and permitting a semi-quantitative collaterals score. To assess radiation dose and patterns of use of mCTA in a stroke referral center, we reviewed all patients who underwent mCTA. We also illustrate how the imaging protocol was modified to reduce the effective dose.

METHOD AND MATERIALS

All patients presenting with acute stroke symptoms who underwent our stroke imaging protocol were retrospectively evaluated. The protocol consists of non-contrast CT (NCCT) and mCTA. After intracranial hemorrhage was excluded on NCCT, mCTA was performed. Most patients were imaged on a Siemens Somatom Definition scanner. In case the former was unavailable a Philips Brilliance 16 was used. Scan parameters are shown in Tables 1 and 2. Iodine-based contrast medium (60mL,370mg/mL) was injected at 5mL/s followed by 40mL of saline solution at 5mL/s. From April 2017 the 3 mCTA phases on Definition were lowered from 120kVp to 100kVp, keeping the other parameters constant. The assessment of organ doses (brain and lens) was performed on stylized human phantoms implemented in CT-Expo v2.3 software.

RESULTS

From 1st June 2015 to April 10th 2017 we analyzed 274 consecutive patients who underwent NCCT and mCTA (median age 68, range 14-92, males percentage 56%). Radiation doses are reported in Tables 1 and 2. Effective dose (according to ICRP 103) ranges from 9.4 to 10.4mSv for the old protocols, aligned with previous reports for mCTA, and lower than the protocols including CT perfusion, in particular for eye lens. The new 100kVp protocol allows a reduction of the effective dose of 30%, from 10.4 to 7.3 mSv.

CONCLUSION

The NCCT+mCTA protocol was designed to be fast to perform and interpret, in order to provide critical information on brain parenchyma and vasculature while minimizing door-to-groin time in patients who are candidates for mechanical thrombectomy. By

lowering voltage of mCTA to 100kVp the effective dose reduction was substantial, without perceived loss of diagnostic accuracy from multiple viewers and even enhancing arterial contrast.

CLINICAL RELEVANCE/APPLICATION

Multiphase CT angiography as part of an acute stroke imaging protocol is associated with low radiation dose and provides critical information on brain parenchyma and vasculature.

SSM18-04 Carotid-CTA at 70 Kilovolt (kV) in Comparison to Automated Tube Voltage Adaption in Respect to Radiation Exposure and Image Quality

Wednesday, Nov. 29 3:30PM - 3:40PM Room: N229

Participants

Matthias S. May, MD, Erlangen, Germany (*Presenter*) Speakers Bureau, Siemens AG Achim Eller, MD, Erlangen, Germany (*Abstract Co-Author*) Nothing to Disclose Marco Wiesmueller, MD, Erlangen, Germany (*Abstract Co-Author*) Speakers Bureau, Siemens Healthcare GmbH Michael M. Lell, MD, Erlangen, Germany (*Abstract Co-Author*) Nothing to Disclose Michael Uder, MD, Erlangen, Germany (*Abstract Co-Author*) Speakers Bureau, Bracco Group; Speakers Bureau, Siemens AG; Speakers Bureau, Bayer AG; Research Grant, Siemens AG; Wolfgang Wust, MD, Erlangen, Germany (*Abstract Co-Author*) Speakers Bureau, Siemens AG

For information about this presentation, contact:

matthias.may@uk-erlangen.de

PURPOSE

To evaluate a 70 kV protocol in computed tomography angiography (CTA) of the carotid arteries in respect to image quality and radiation exposure compared to automated tube voltage adaption.

METHOD AND MATERIALS

Ninety consecutive patients were included in this prospective study. Fourty-five (64, 35 - 84 years) were randomized to the study group (70 kV, 167 ref.mAs) and 45 (65, 24 - 87 years) were randomized to the control group (automated kV adaption, 70 - 150 kV). CT dose index (CTDIvol) and dose length product (DLP) were recorded from the examination protocol. Image quality was assessed by region of interest (ROI) measurements and calculations of signal to noise (SNR) and contrast to noise ratio (CNR). Subjective image quality and image artifacts were evaluated by two observers with a 4-point scale (3-excellent; 0-not diagnostic).

RESULTS

Radiation exposure was significantly lower in the study group (CTDIvol reduction of 22%, DLP reduction 20%; each p<0.001). Contrast (p=0.15), SNR (p=0.4), and CNR (p=0.5) did not show significant differences between the groups. Subjective image quality was without significant differences between the two groups (p=0.56). Also artifacts due to contrast medium influx were without significant difference (p=0.17). Artifacts due to beam hardening in the height of the shoulder girdle were significantly more affecting in the scans from the study group (p=0.04) while there was also no significant difference on the height of the skull base (p=0.65).

CONCLUSION

Carotid-CTA using fixed 70 kV is feasible at very low radiation dose levels while overall image quality is constant to protocols using automated tube voltage selection.

CLINICAL RELEVANCE/APPLICATION

Lowest available tube voltages (70 kV) can increase the radiation dose efficiency in CT angiographies of the carotids compared to individual tube voltage adaptation.

SSM18-05 Dual Energy CT Angiography of the Carotid Arteries: Quality, Bone Subtraction and Radiation Dosage Using Second- and Third-Generation Dual-Source CT

Wednesday, Nov. 29 3:40PM - 3:50PM Room: N229

Participants

Yu Chen, MD, Beijing, China (*Presenter*) Nothing to Disclose Yuanli Zhu, Beijing, China (*Abstract Co-Author*) Nothing to Disclose Huadan Xue, MD, Beijing, China (*Abstract Co-Author*) Nothing to Disclose Zhengyu Jin, Beijing, China (*Abstract Co-Author*) Nothing to Disclose

PURPOSE

To study the differences in vascular image quality, bone substraction, and dose of radiation of dual energy CT angiography (CTA) of the supraaotic trunks using second- and third-generation dual-source CT (DSCT). Comparing the diagnostic performance of arterial stenosis between the third-generation dual-source CT and digital subtracted angiography (DSA).

METHOD AND MATERIALS

CTA of the supraaortic trunks in 40 patients were retrospectively reviewed. 20 patients used second-generation dual-energy CT (DECT) system (100/Sn140 kp tube voltage) and 40-mL contrast material. Another 20 patients used third-generationDECT system (90/Sn150 kV tube voltage) and 30-mL contrast material. The attenuation was measured in common carotid artery (CCA), C7 segment of internal carotid arteries, and cervical muscle (CM). The noise of CCA and CM was recorded. The signal-to-noise ratio (SNR) of CCA and contrast-to-noise ratio (CNR) were calculated. 5-scoring system was used for bone removal of C1-C7 segments of internal carotid arteries (1=poor, 5=excellent). DSA was performed if necessary. Accuracy, sensibility, specificity were calculated.

RESULTS

The attenuation of third-generation group was significant higher on C7 (P=0.001), and not different on CCA (all P = 0.317) compared with that of second-generation group. Both SNR and CNR of CCA were significantly higher in second-generation group than third-generation group (both p < 0.05). The dose-length product in second-generation group was lower than that of third-generation group (299.7 ± 16.7 vs. 218.3 ± 27.8 mGy×cm, P<0.001). Scores of the bone removal of C2, C3, C4 and C7 were were evaluated as 5 score in the third-generation group, which were higher than that of second-generation group were lower (all P < 0.05). 6 patients in the third-generation group received DSA examination, the accuracy, sensibility, specificity for detecting >50% arterial stenosis were 98.8%, 100% and 98.8%.

CONCLUSION

Third-generation dual-energy scan mode is is able to decrease the volume of contrast material, reduce the radiation dose and improve the image quality of bone removal compared with second-generation grouu. the accuracy, sensibility, specificity are high compared with DSA.

CLINICAL RELEVANCE/APPLICATION

Dual-energy scan mode of third-generation CT provides better bone-subtraction quality of carotid arteries and is equal to DSA in detecting arterial stenosis.

SSM18-06 Using a Low Tube Voltage Protocol with Adaptive Statistical Iterative Reconstruction in Craniocervical Computed Tomographic Angiography Provides Better Image Quality with a Reduced Radiation Dose

Wednesday, Nov. 29 3:50PM - 4:00PM Room: N229

Participants

Chih-Wei Chen, MD, Kaohsiung City, Taiwan (*Presenter*) Nothing to Disclose Po-An Chen, MD, Kaohsiung, Taiwan (*Abstract Co-Author*) Nothing to Disclose Yun-Pei Lin, Kaohsiung City, Taiwan (*Abstract Co-Author*) Nothing to Disclose Yu Yen, MD, Kaohsiung City, Taiwan (*Abstract Co-Author*) Nothing to Disclose Chiung Chen Chuo, Kaohsiung City, Taiwan (*Abstract Co-Author*) Nothing to Disclose Rita S. Wu, Kaohsiung City, Taiwan (*Abstract Co-Author*) Nothing to Disclose Ping-Hong Lai, Kaohsiung, Taiwan (*Abstract Co-Author*) Nothing to Disclose

PURPOSE

To evaluate image quality and radiation dose by using a lower kVp protocol (100 kVp) and 50% ASiR-V for Craniocervical Computed Tomographic Angiography (CCCTA) in comparison with the conventional protocol (120 kVp).

METHOD AND MATERIALS

A total of 121 volunteers (47 men, 74 women; age range, 15-78 years) were enrolled and randomly divided into 3 groups: group A (conventional protocol): 120 kVp and filtered back-projection reconstruction; group B: 120 kVp and 50% ASiR-V; group C: 100 kVp and 50% ASiR-V. All patients were scanned by a 256-slice CT machine with the slice thickness of 0.625 mm. Objective values(arterial attenuation value, signal-to-noise ratio [SNR], contrast-to-noise ratio [CNR]) of arteries was obtained at head, neck and shoulder levels and compared among three groups. Subjective image quality and radiation dose (volume CT dose index [CTDIvol], dose-length product [DLP]) were also compared. The quantitative parameters and radiation dose were analysis by ANOVA. Subjective image quality was evaluated by two experienced radiologists independently and inter-rater reliability was calculated using kappa (k) analysis.

RESULTS

For the radiation dose, the CTDIvol and DLP of group C were the lowest among three groups. For the objective values, the arterial attenuation in head, neck and shoulder were significant higher in group C than those in group A and B (each P <0.05). The SNR and CNR of group B and C were significant higher than the conventional group A (each P <0.05), and there were no significant difference for the SNR and CNR between group B and C. In subjective image quality analysis, group C revealed significant better image quality than group A and B (P <0.05). The inter-rater reliability was good (k=0.73).

CONCLUSION

In CCCTA, using 100 kVp and 50% ASiR-V protocol showed better arterial attenuation, SNR, CNR and subjective imaging quality with a reduced radiation dose compared to the conventional protocol.

CLINICAL RELEVANCE/APPLICATION

Using ASiR-V with a lower kVp protocol in CCCTA, better objective and subjective imaging quality can be obtained with a reduced radiation dose compared to the conventional protocol.





103rd Scientific Assembly and Annual Meeting November 26 to December 1 McCormick Place, Chicago



SSM19

Pediatrics (Interventional Radiology)

Wednesday, Nov. 29 3:00PM - 4:00PM Room: S102CD



AMA PRA Category 1 Credit ™: 1.00 ARRT Category A+ Credit: 1.00

FDA Discussions may include off-label uses.

Participants

Kamlesh U. Kukreja, MD, Bellaire, TX (*Moderator*) Nothing to Disclose Anne Marie Cahill, MBBCh, Philadelphia, PA (*Moderator*) Nothing to Disclose

Sub-Events

SSM19-01 Pediatric Percutaneous Renal Biopsies: Comparison of Complications between Real-Time Ultrasound Guidance and Ultrasound Marking Techniques

Wednesday, Nov. 29 3:00PM - 3:10PM Room: S102CD

Participants

Shireen Hayatghaibi, MA, MPH, Houston, TX (*Presenter*) Nothing to Disclose Daniel J. Ashton, MD, Houston, TX (*Abstract Co-Author*) Nothing to Disclose Robert Orth, MD,PhD, Houston, TX (*Abstract Co-Author*) Nothing to Disclose

For information about this presentation, contact:

sehayatg@texaschildrens.org

PURPOSE

To compare the complications from percutaneous renal biopsies performed using real time ultrasound-guidance versus preprocedure ultrasound-aided skin marking in children.

METHOD AND MATERIALS

An a priori analysis yielded a sample size of 850 procedures required to detect a difference in complications between the two groups (power: 0.8). Consecutive patients who underwent a percutaneous renal biopsy at our tertiary care academic medical center were retrospectively identified. Demographic information, biopsy technique, and post-biopsy complications were recorded. Complications were categorized according to Society of Interventional Radiology (SIR) criteria. Complication rates were compared using Fisher's exact test.

RESULTS

The study population consisted of 850 renal biopsy procedures in 626 patients. Real-time ultrasound guidance was performed in 375 biopsies (age range: 0-29, mean: 12.1 yrs); 475 biopsies used pre-procedure ultrasound-aided skin marking (age range: 2-27, mean: 13.6 yrs). Diagnostic yield was obtained in all biopsies with real-time ultrasound (mean cores: 2.63+/-1.52) and in 471/475 (99.2%) of those using pre-procedure skin marking (mean cores: 2.64+/-0.72; p=0.91). Overall, 283 (33.3% of biopsies) complications were detected in the study cohort; 60 (16% of biopsies) in the real-time ultrasound guidance group and 223 (47% of biopsies) in the conventional skin marking group (p<0.001). In the real-time ultrasound group, 43 complications (11.5% of biopsies) were SIR A and 8 (2.1% of biopsies) SIR B. In the skin marking group, 156 (32.8%) biopsies resulted in SIR A complications and 54 (11.4%) SIR B. The groups were statistically different for both SIR A (p<0.001) and SIR B (p<0.001) complications. There was no detectable difference in major complications between the groups [p=0.83; real-time ultrasound guided: 6 (1.6%) SIR C and 3 (0.8%) SIR D; skin marking: 12 (2.5%) SIR C and 1 (0.2%) SIR D].

CONCLUSION

Patients who underwent real-time ultrasound-guided renal biopsies had significantly fewer minor complications, including those that required follow-up medical care (SIR B), compared to those who underwent pre-procedure ultrasound-aided skin marking.

CLINICAL RELEVANCE/APPLICATION

Patients with an ultrasound-guided renal biopsy required less additional medical care for complications. This is important in value based healthcare that pursues quality outcomes at controlled costs.

SSM19-02 Onyx Embolization in Pediatric Neuro-interventional Procedures

Wednesday, Nov. 29 3:10PM - 3:20PM Room: S102CD

Participants

Tahaamin Shokuhfar, MD, Chicago, IL (*Presenter*) Nothing to Disclose Anas Al-Smadi, MD, Chicago, IL (*Abstract Co-Author*) Nothing to Disclose Sameer A. Ansari, MD,PhD, Chicago, IL (*Abstract Co-Author*) Nothing to Disclose Michael C. Hurley, MBBCh, Dublin, Ireland (*Abstract Co-Author*) Nothing to Disclose

For information about this presentation, contact:

tahaamin.shokuhfar@northwestern.edu

PURPOSE

Although AVMs are rare among pediatric population, nearly half of spontaneous intracranial hemorrhages in children are due to these malformations. Onyx, as an FDA approved embolizant for adults, has limited studies regarding its safety and efficacy among children. Here, we evaluate the safety and efficacy of Onyx embolization in pediatric neurointerventional procedures.

METHOD AND MATERIALS

In this study, all pediatric Onyx embolization of intracranial AVM cases are evaluated over a period of 10 years. Medical record and radiology imaging were reviewed for each patient regarding demographic data, clinical presentations, embolization procedure and related complications.

RESULTS

Seventy-two patients (female = 26 (36%)) with intracranial AVMs underwent total of 122 embolization procedures. Age of patients ranged between 1 month to 17 years with the mean of 10.2 years. Forty-four patients underwent a single embolization procedure and staged embolization was required for the remaining 28 patients prior to definitive treatment. Onyx embolization resulted in complete occlusion of the AVM in 10 patients (14%). A total of 66 patients underwent subsequent surgical treatment. Overall 13 complications occurred in total of 122 Onyx embolizations (10.6%) which resulted in 7 transient neurological deficits and 6 clinically silent complications (Table 1). None of the complications resulted in mortality or permanent morbidity. No significant demographic characteristic differences observed in patients with or without complications.

CONCLUSION

In this study we propose the safe and effective utilization of Onyx for embolization of pediatric cerebral AVMs. The relative low rate of complications (10.6%) along with no mortality or permanent morbidity, suggests the safe utilization of Onyx as a preoperative or primary embolization treatment of pediatric intracranial AVMs. However, specific attention should be considered for its indications and technical limitations according to the broad spectrum of complications.

CLINICAL RELEVANCE/APPLICATION

Onyx utilization can be feasible for preoperative or primary embolization in the treatment of pediatric AVMs. We report here the largest series of Onyx embolizations of brain AVMs in the pediatric population. The results, in terms of clinical and angiographic improvement, with a low rate of transient morbidity and no permanent morbidity or mortality, are encouraging.

SSM19-03 Magnetic Resonance-Guided Focused Ultrasound Surgery for Treatment of Osteoid Osteoma in Pediatric Patients Only: A Multicenter Experience

Wednesday, Nov. 29 3:20PM - 3:30PM Room: S102CD

Participants

Francesco Arrigoni, Coppito, Italy (*Presenter*) Nothing to Disclose Alessandro Napoli, MD, Rome, Italy (*Abstract Co-Author*) Nothing to Disclose Alberto Bazzocchi, MD, Bologna, Italy (*Abstract Co-Author*) Nothing to Disclose Simone Quarchioni, Laquila, Italy (*Abstract Co-Author*) Nothing to Disclose Roberto Scipione, MD, Rome, Italy (*Abstract Co-Author*) Nothing to Disclose Luigi Zugaro, L'Aquila, Italy (*Abstract Co-Author*) Nothing to Disclose Antonio Barile, MD, L'Aquila, Italy (*Abstract Co-Author*) Nothing to Disclose Carlo Catalano, MD, Rome, Italy (*Abstract Co-Author*) Nothing to Disclose Carlo Masciocchi, MD, L'Aquila, Italy (*Abstract Co-Author*) Nothing to Disclose

For information about this presentation, contact:

arrigoni.francesco@gmail.com

PURPOSE

To retrospectively evaluate the effectiveness and safety of MRgFUS of Osteoid Osteoma in paediatric patients (age <18 years) based on the experience of three university hospitals. Since OOs mostly affect patients in paediatric age, it is of paramount importance that the employed techniques be as minimally invasive as possible. MRgFUS aims to become the standard care, producing no skin lesion or damage to the soft tissues.

METHOD AND MATERIALS

Over a period of 4 years, we used MRgFUS on 33 patients (age <18 years, mean 13.8) affected by symptomatic non-spinal Osteoid Osteoma. Inclusion criteria were: (i) clinical diagnosis of osteoid osteoma (pain, more typically nocturnal, relieved by NSAIDs: mean pre-treatment VAS value: 7.5 (CI: 4-10)); (ii) positive imaging for OO with typical features; (iii) subperiosteal or cortical lesions only: a periosteal reaction or a cortical thickening (more than 6 mm) surrounding the lesion was considered as a technical contraindication for MRgFUS treatment. The outcomes were evaluated with clinical and imaging follow-up studies up to 5 and 3 years, respectively.

RESULTS

After treatment, absence of pain was observed in 31 patients (94% of complete success; VAS: 0), confirming the effectiveness of the procedure. One patient reported VAS: 1 during follow-up, but because the condition was considered satisfactory by the patient, an additional treatment was not deemed necessary. Only one patient was treated twice to obtain complete pain relief. Nor relapse or complications were observed. The long term imaging control showed a progressive restoration to the original condition of the bone segments without signs of treatment or residual inflammatory findings.

CONCLUSION

MDRELIC is cafe and effective for treatment of celected localizations of esteemid esteemay for superficial locions it could be

considered the first and definitive choice for patients in paediatric age. The possibility of treating only subperiosteal or cortical lesions is a limit but non too notable, because the greater part of the osteoid osteomas belong to these two categories. This touch-less approach does not leave any sign of the procedure nor interference with the normal growth of the bone.

CLINICAL RELEVANCE/APPLICATION

This treatment could represent the less invasive step for the treatment of Osteoid Osteoma.

SSM19-04 Mynxgrip Vascular Closure Device Use in Pediatric Neurointerventional Procedures

Wednesday, Nov. 29 3:30PM - 3:40PM Room: S102CD

Participants

Tahaamin Shokuhfar, MD, Chicago, IL (*Presenter*) Nothing to Disclose Anas Al-Smadi, MD, Chicago, IL (*Abstract Co-Author*) Nothing to Disclose Sameer A. Ansari, MD,PhD, Chicago, IL (*Abstract Co-Author*) Nothing to Disclose Michael C. Hurley, MBBCh, Dublin, Ireland (*Abstract Co-Author*) Nothing to Disclose Ali Shaibani, MD, Chicago, IL (*Abstract Co-Author*) Nothing to Disclose

PURPOSE

The application of arterial closure devices has been broadly investigated and previously approved in adults but their feasibility and safety have not been approved in pediatric patients and any application of such devices in children is considered off-label. The decision to use the Mynxgrip in our practice has been made based on the low reported rate of complications in adults and the fact of no intra-luminal component regarding the usage of Mynxgrip.

METHOD AND MATERIALS

A Retrospective review of all pediatric patients undergoing diagnostic or interventional neurovascular procedures was conducted. Mynxgrip was applied to any pediatric patient with adequate depth of subcutaneous tissue and common femoral artery (CFA) diameter. Patients' demographic and procedural data was recorded. Hemostasis status and complication reassessment for outpatients and pre-operational inpatients were documented.

RESULTS

During the period of 36 months, a total of 83 Mynxgrip was deployed on 53 children (23 male and 30 female, mean age = 14.5 years) undergoing diagnostic/interventional neuro-endovascular procedures through common femoral artery access site. About 46% procedures were diagnostic angiography and the remaining were angiography with embolization. CFAs' diameter were ranged between 4mm to 8.5mm with the average diameter of 6.24 (SD± 1.16). Deployment of Mynxgrip was successful in 82 procedures (98.8%). There was a single (1.2%) device failure and no other immediate or delayed major complications were recorded.

CONCLUSION

Comparing with the manual compression as the current standard of care, the application of Mynxgrip in our practice brought immediate hemostasis at common femoral artery access site, along with earlier ambulation and shorter duration of hospitalization.

CLINICAL RELEVANCE/APPLICATION

To the best of our knowledge, current study is the first report of the application of Mynxgrip arterial closure device among pediatric population. We reported the feasibility of Mynxgrip as a safe and efficient way of hemostasis achievement at CFA arteriotomy site in children undergoing diagnostic or neuro-interventional procedures.

SSM19-05 Percutaneous Ablation of Malignant and Locally Aggressive Solid Tumor in Pediatric Patients

Wednesday, Nov. 29 3:40PM - 3:50PM Room: S102CD

Participants

Adrian J. Gonzalez, MD, New York, NY (*Presenter*) Nothing to Disclose Majid Maybody, MD, New York, NY (*Abstract Co-Author*) Nothing to Disclose Elena N. Petre, MD, New York, NY (*Abstract Co-Author*) Nothing to Disclose Joseph P. Erinjeri, MD, PhD, New York, NY (*Abstract Co-Author*) Nothing to Disclose Hooman Yarmohammadi, MD, New York, NY (*Abstract Co-Author*) Nothing to Disclose Franz E. Boas, MD,PhD, New York, NY (*Abstract Co-Author*) Co-founder, Claripacs, LLC; In-kind support, Bayer AG; Investor, Labdoor; Investor, Qventus; Investor, CloudMedx; Investor, Notable Labs Stephen B. Solomon, MD, New York, NY (*Abstract Co-Author*) Research Grant, General Electric Company

For information about this presentation, contact:

gonzala2@mskcc.org

PURPOSE

Present the oncologic outcomes of our series of pediatric patients treated with ablation for primary and metastatic cancers.

METHOD AND MATERIALS

Retrospective review of a HIPAA compliant prospectively maintained percutaneous ablation database. All ablations performed in patients younger than 18 years since 2002 were reviewed. RFA was performed using the the Cool-tip system (Covidien, Boulder, CO). Cryoablation was performed using the Endocare system (HealthTronics, Inc. Austin TX).Patients were watched for 4 hours after ablation and discharged home in the absence of complications. Patients were admitted for pain or other complications. CT and/or PET/CT scan was obtained 1 month after ablation. Subsequent imaging studies were obtained as indicated by the pediatric oncologist to assess for findings of local tumor progression (LTP). Patient and tumor characteristics were described and summarized. Survival end points of interest include overall survival (OS) and local tumor progression free survival (LTPFS). Survival end points were method.

8 pediatric patients were identified in our database that includes 1471 patients treated with ablation since 2002. There were 4 males and 4 females. Mean age was 12.8 years (range 3 - 17). Mean weight was 49.5 kilos (15 - 60 kilos). These 8 patients underwent 12 ablations to treat 9 lesions. Mean lesion size was 3.4 cm (Range 0.8 -7.8 cm). Mean hospital stay was 2.1 days (median 2.3 days, range 0-4). There was one major complication (SIR classification D) in a patient with lung metastases from chondrosarcoma. He developed parenchymal bleeding that required intubation for less than 24 hrs. Mean follow up was 79 months. OS at 5 years was 75%. Median LTPFS was not reached. At the end of follow up 2 lesions developed LTP. LTPFS rates were 88% at 1 year and 77% at five years .

CONCLUSION

Ablation can be performed safely and effectively in a carefully selected group of pediatric patients with cancer. We consider that the use of these technologies should be used more often and in conjunction with other cancer treatments, always in the setting of multidisciplinary consensus.

CLINICAL RELEVANCE/APPLICATION

Ablation can be performed safely and with good results in pediatric patients.

SSM19-06 Transjugular Intrahepatic Portosystemic Shunts (TIPS): Safety and Efficacy in the Pediatric Population

Wednesday, Nov. 29 3:50PM - 4:00PM Room: S102CD

Awards

Student Travel Stipend Award

Participants

Zachary S. Jeng, MD, Houston, TX (*Presenter*) Nothing to Disclose Raphael J. Yoo, MD,MS, Houston, TX (*Abstract Co-Author*) Nothing to Disclose Daniel J. Ashton, MD, Houston, TX (*Abstract Co-Author*) Nothing to Disclose

For information about this presentation, contact:

jeng@bcm.edu

PURPOSE

To report the experience of a tertiary pediatric referral center with creation and revision of transjugular intrahepatic portosystemic shunts (TIPS) in children and adolescents.

METHOD AND MATERIALS

10 consecutive patients over a 10 year period with 9 undergoing TIPS creation and 1 undergoing TIPS revision (initially placed at an outside institution). 8 patients were under the age of 18: 2 infants (ages 9 and 10 mos), 5 children (ages ranging from 5 y, 11 mo to 12 y, 1 mo), and 1 adolescent (age 16 y, 6 mo). All had gastroesophageal variceal bleeding as the reason for TIPS creation/revision. Causes of liver dysfunction were biliary atresia in 5 patients, cystic fibrosis in 1, veno-occlusive disease secondary to chemotherapy in 1, and Ellis-van Creveld Syndrome in 1.

RESULTS

The technical success rate was 100%. 6 patients received Viatorr endografts while 1 patient received a Luminex endograft and a Wallstent. 4 TIPS were created using a 10 mm endograft, 2 using an 8 mm endograft, and 1 using a 2 cm endograft. The mean portosystemic pressure gradient was reduced from 19 mmHg to 8 mmHg. Flow was successfully restored in the patient undergoing TIPS revision. Primary patency during initial ultrasound follow-up performed 1 to 2 days post procedure was 100%. Follow-up imaging performed up to 23 months post procedure demonstrated 100% stent patency. There were no major complications or mortalities associated with TIPS creation. One patient continued to experience intermittent hemoptysis, though likely related to underlying cystic fibrosis, while one developed a single episode of transient hyperammonemia. One patient underwent balloon angioplasty 3 days post TIPS creation for decreased hemoglobin and concern for GI bleeding with no stenosis or thrombosis discovered on portal venogram. There were no other repeat interventions, shunt dysfunctions, or recurrent episodes of GI bleeding. 6 children have since received hepatic transplants with 3 children receiving transplants 23, 20, and 8 days post TIPS creation.

CONCLUSION

TIPS placement can be successfully performed in young pediatric patients with low complications rates and excellent initial and intermediate patency.

CLINICAL RELEVANCE/APPLICATION

TIPS is a well-documented method for treating portal HTN and its sequela in adults. With increasing use in the pediatric population, we wanted to determine its effectiveness and safety in children.





103rd Scientific Assembly and Annual Meeting November 26 to December 1 McCormick Place, Chicago



SSM20

Physics (MR: New Techniques)

Wednesday, Nov. 29 3:00PM - 4:00PM Room: S403A



AMA PRA Category 1 Credit ™: 1.00 ARRT Category A+ Credi<u>t: 1.00</u>

FDA Discussions may include off-label uses.

Participants

Timothy J. Carroll, PhD, Chicago, IL (*Moderator*) Nothing to Disclose Geoffrey D. Clarke, PhD, San Antonio, TX (*Moderator*) Nothing to Disclose

Sub-Events

SSM20-01 Hyperpolarized Water as an Alternative MRI Contrast Agent

Wednesday, Nov. 29 3:00PM - 3:10PM Room: S403A

Participants

Sebastian Fischer, MD, Frankfurt, Germany (*Presenter*) Nothing to Disclose Richard D. Maeder, Frankfurt, Germany (*Abstract Co-Author*) Nothing to Disclose Maxim Terekhov, Mainz, Germany (*Abstract Co-Author*) Nothing to Disclose Stefan Zangos, MD, Frankfurt Am Main, Germany (*Abstract Co-Author*) Nothing to Disclose Thomas Prisner, Frankfurt, Germany (*Abstract Co-Author*) Nothing to Disclose Thomas J. Vogl, MD, PhD, Frankfurt, Germany (*Abstract Co-Author*) Nothing to Disclose Vasyl Denysenkov, Frankfurt, Germany (*Abstract Co-Author*) Nothing to Disclose

For information about this presentation, contact:

sebastian.fischer@kgu.de

CONCLUSION

Hyperpolarized water might be a promising future alternative to Gadolinium based contrast agents in MR angiography or even further diagnostics without risking the potential adverse effects or intracorporal remnants of Gadolinium based contrast agents.

Background

The administration of Gadolinium based contrast agents is associated with the risk of allergic reactions and the development of a systemic nephrogenic fibrosis (NSF). Current research showed remnants of some types of Gadolinium based MR contrast agents in the brain - with unknown long-term effects. Purpose of our work is the development of an alternative method to create MRI contrast by using dynamic nuclear polarization (DNP). The tested liquid-state Overhauser DNP is a technique to achieve hyperpolarization by microwave irradiation of electron spins in TEMPOL radicals, which are coupled with the nuclear spins of water molecules.

Evaluation

Our setup comprises a 42 GHz microwave source and an in-bore DNP polarizer, equipped with a multimode resonator inside a standard clinical 1.5 T scanner, which allows a continuous hyperpolarization of water molecules with a flow rate about 1.2 ml/min. In this work we characterized the performance of the DNP setup for MR imaging in various vascular models by comparing it to standard Gadolinium-based contrast media. We used 2D and 3D scan protocols with GRE- and VIBE-sequences for measurements, which feature up to a 30-fold signal enhancement of the hyperpolarized aqueous solution. A comparison to Gadolinium enhanced signals of physiologic intravascular conditions shows 12-fold enhancement rates and an increased absolute sensitivity.

Discussion

The used liquid state in-bore DNP setup creates hyperpolarized water, which features high T1 MR signal enhancements and a short relaxation time. SNR and CNR values were substantially improved by DNP and capillary diameters down to 75µm could be visualized. In our comparing experiments the hyperpolarized water showed an enhancement higher than gadolinium, which allows imaging down to small vascular structures in a standard clinical 1.5 T scanner.

SSM20-02 Intravoxel Incoherent Motion Diffusion-weighted Imaging of Bone Marrow Microstructure in Patients with Acute Leukemia

Wednesday, Nov. 29 3:10PM - 3:20PM Room: S403A

Participants

Jinliang Niu, MD, PhD, Taiyuan, China (*Presenter*) Nothing to Disclose Hong Zhu, Taiyuan, China (*Abstract Co-Author*) Nothing to Disclose Wenqi Wu, Taiyuan, China (*Abstract Co-Author*) Nothing to Disclose Yang Wang, Taiyuan, China (*Abstract Co-Author*) Nothing to Disclose

PURPOSE

Intravoxel Incoherent Motion Diffusion-weighted Imaging of Bone Marrow Microstructure in Patients with Acute Leukemia

METHOD AND MATERIALS

28 patients with AL underwent MRI scans at 1.5T using conventional diffusion weighted imaging (DWI) and IVIM (b=0, 10, 25, 50, 100, 200, 400, 600, 800, 1000, 1200s/mm2) in the sagittal plane covering the lumbar bone marrow before standard chemotherapy. The IVIM parameters (perfusion fraction [f], molecular diffusion coefficient [D], and perfusion-related D [D*] and apparent diffusion coefficient (ADC) were extracted from the bone marrow images. The microvessel density (MVD) and vascular endothelial growth factor(VEGF) was confirmed by bone marrow biopsy of the iliac crests, whichwere used to evaluate bone marrow microstructure. All patients were divided into complete remission (CR) and non-remission (NR) group according to the treatment response.

RESULTS

All patients underwent the first remission induction chemotherapy, with 19 patients achieved CR and 9 patients achieved NR.The ADC and D* values were not significant different between the two groups. However, D value of CR group was significantly higher (p=0.003), and f value of CR group was significantly lower (p=0.039) than those of NR group. Using receiver operator characteristic (ROC) analysis, the area under the curve (AUC) of D and f were 0.848 and 0.746 respectively in evaluating prognosis of AL before treatment. The fshowed significantly statistical correlations with MVD (r= 0.384) and VEGF (r= 0.439).

CONCLUSION

The D, f value ofbone marrow could play a potential role in prognosticating patients with AL. The f value could be used as noninvasive biomarkers to evaluate the microstructure bone marrow.

CLINICAL RELEVANCE/APPLICATION

Evaluation of bone marrow microstructure and prognosis of leukemia patients

SSM20-03 Auto-Calibrated Correlation Time Diffusion Brain qMRI and the Principle of Diffusional Homeostasis

Wednesday, Nov. 29 3:20PM - 3:30PM Room: S403A

Participants

Hernan Jara, PhD, Boston, MA (*Presenter*) Patent holder, qMRI algorithms; Royalties, World Scientific Publishing Co; ; ; Stephan W. Anderson, MD, Cambridge, MA (*Abstract Co-Author*) Nothing to Disclose Osamu Sakai, MD, PhD, Boston, MA (*Abstract Co-Author*) Nothing to Disclose

For information about this presentation, contact:

hiara@bu.edu

CONCLUSION

A fully automated and auto-calibrating DCT mapping algorithm has been developed and could be useful for aiding in the diagnosis of pathologic entities that disrupt diffusional homeostasis such as acute ischemic stroke.

Background

Standard diffusion MRI is based on the pulsed field gradient (PFG) experiment and probes molecular water motions at the 10-100millisecond time scale depending on experimental conditions. Despite the very different water micro-environment in gray matter (GM) and white matter (WM), one of the most remarkable findings of DPFG MRI is the near equality of the mean diffusivities of water in both tissues at diffusion times reported in the literature. Correlation time diffusion (DCT) MRI is based on T1 relaxometry and therefore probes water diffusion at the very short time scale of the correlation time: approximately 20ps for brain tissue. We hypothesize that the herein termed "*principle of diffusional homeostasis*" is valid at such short time scales and apply it to develop a self-calibrating DCT mapping algorithm whereby the one external model parameter -specifically, the magnetization transfer coupling constant (kappa in Fig. 1)-- is auto-determined by minimizing the WM-to-GM diffusional differences to within one half the standard deviation.

Evaluation

This is a HIPAA compliant prospective study approved by the local IRB that included ten patients without major abnormalities ranging in age from 2 to 87years. MR images acquired with the mixed turbo spin echo pulse (mixed-TSE) sequence were qMRI processed generating maps of T1, T2, and PD. These maps were used to generate DCT maps using an algorithm which calculates the pure correlation time without magnetization transfer effects. In all ten cases, the DCT maps were in quantitative agreement (<5%) with the DPFG maps for GM, WM, and cerebrospinal fluid.

Discussion

The developed fully auto-calibrating DCT mapping algorithm is based on the assumption of diffusional homeostasis, which is supported by a wealth of DPFG evidence in the healthy brain. Differences between DCT and DPFG may arise in pathologic conditions whereby the long time scale diffusion tissue properties may be abnormal via restricted diffusion.

SSM20-04 Metal Artifact Reduction for Myocardial Scar Assessment in Patients with Cardiac Implanted Electronic Devices Using Cardiac Magnetic Resonance

Wednesday, Nov. 29 3:30PM - 3:40PM Room: S403A

Participants

Jadranka Stojanovska, MD, MS, Ann Arbor, MI (*Presenter*) Consultant, Guerbet SA El-Sayed H. Ibrahim, PhD, MSc, Ann Arbor, MI (*Abstract Co-Author*) Employee, General Electric Company Yuxi Pang, PhD, Ann Arbor, MI (*Abstract Co-Author*) Nothing to Disclose Maryam Ghadimi Mahani, MD, Ann Arbor, MI (*Abstract Co-Author*) Nothing to Disclose

For information about this presentation, contact:

jstoanov@umich.edu

CONCLUSION

The developed wideband IR technique minimizes the CIED-generated hyperintensity artifacts without increasing scan time, and allows for accurate identification of arrhythmogenic substrate in VT patients.

Background

An important application of late gadolinium enhancement (LGE) cardiac magnetic resoncance (CMR) is assessment of myocardial scar in patients with ventricular tachycardia (VT) before ablation. LGE imaging in patients with cardiac implanted electronic devices (CIEDs) is challenging because of device-generated metal artifacts that compromise the effect of the inversion recovery (IR) pulse and obscure the region of interest. In 2016 we have performed 180 CMRs in patients with CIED at our institution. In this abstract we will discuss the use of modified IR technique to alleviate metal artifacts and improve diagnostic image quality.

Evaluation

The modified sequence includes a wideband IR pulse with adjustable frequency offset and bandwidth, which allows for optimal myocardial signal nulling in the presence of off-resonance effects. A phantom experiment was conducted on a 1.5T scanner using conventional and wideband IR sequences with different frequency offset and bandwidth (BW) values. Then, 20 patients (18 males, age=62±17) with CIEDs (8 Boston Scientific, 10 Medtronic, and 2 St Jude) were imaged on the same scanner using the conventional and optimized wideband LGE techniques prior to ablation. The imaging parameters were optimized for each patient. Conventional IR sequence resulted in severe artifacts that obscured ventricular segments in 15 out of 20 patients. The wideband IR sequence significantly minimized the artifacts. Optimal BW was in the range of 2000-3000Hz with optimal frequency shift up to 1000Hz.

Discussion

Increasing the IR frequency BW results in better artifact reduction, although this comes at the cost of incomplete myocardial nulling. So, BW should be set to the minimum value that eliminates the artifact, which is affected by the device type and location. Similarly, the frequency offset of the IR pulse affects the artifact appearance, so proper setting of the frequency offset could allow for removing the artifact without the need to increase the frequency BW.

SSM20-05 TSE-Based DWI of the Prostate as an Alternative to SS-SE-EPI DWI

Wednesday, Nov. 29 3:40PM - 3:50PM Room: S403A

Participants

Antonio Luna, MD, Jaen, Spain (*Presenter*) Consultant, Bracco Group; Speaker, General Electric Company; Speaker, Toshiba Medical Systems Corporation

Paula Montesinos de la Vega, Madrid, Spain (Abstract Co-Author) Employee, Koninklijke Philips NV

Lidia Alcala Mata, MD, Jaen, Spain (Abstract Co-Author) Nothing to Disclose

Teodoro Martin, MD, Jaen, Spain (Abstract Co-Author) Nothing to Disclose

Jordi Broncano, MD, Cordoba, Spain (Abstract Co-Author) Nothing to Disclose

Javier Sanchez, MD, PhD, Madrid, Spain (Abstract Co-Author) Nothing to Disclose

CONCLUSION

DWI TSE has a potential role as an alternative to SS-SE-EPI DWI in MR protocols for prostate cancer detection.

Background

DWI is a key MR imaging contrast for prostate cancer detection. In clinical practice, a SS-SE-EPI sequence is used. EPI readout is prone to geometrical distortion and susceptibility artifact due to the presence of air content within the rectum or metallic implants. These limitations make more difficult the proper spatial localization of the lesions. Also, the use of DWI to localize suspicious areas in targeted MR/ultrasound fusion guided biopsy is limited. Turbo Spin Echo-based DWI is proposed as a potential alternative to eliminate geometric distortion and local susceptibility artefacts. In this presentation, its geometric validation is performed to demonstrate spatial accuracy of DWI-TSE images compared with conventional DWI-SE-EPI sequence.

Evaluation

All images were acquired in a 3.0 T Achieva scanner (Philips Healthcare, The Netherlands) with a 16ch body coil on 15 patients with prostate cancer in targeted MR/ultrasound guided biopsy. On these patient, two DWI sequence were performed with equal b values (0, 1000 and 1500 s/mm2) wit DWI-SE-EPI (TR/TE=4500/90ms) and DWI-TSE (TR/TE=11173/131ms) sequences. DWI images were acquired in the same orientation of conventional TSE T2-weighted sequence. Both acquisitions shared equivalent spatial resolution (2.6x2.8x4.5 mm3) with no gap between slices. Total scan time was 118s and 290s for SS-SE-EPI and TSE respectively. ADC maps were calculated using b0 and b 1000 s/mm2 for both sequences. SNR and CNR were compared for all b values and ADC maps. Also, the presence of geometric distortion and susceptibility artifacts was recorded. Both sequences were also compared to target prostate biopsy using an specific MR/ultrasound fusion device.

Discussion

TSE-based DWI presented free geometric distorted images in all cases with similar CNR, although with a moderate increase in acquisition time. Also, this approach permits to delineate lesions for targeted biopsy with advantage over SS-SE-EPI DW-sequence due to good geometrical performance.

SSM20-06 Measuring Frequency Drift in MR Spectroscopy on a 3 T MRI

Wednesday, Nov. 29 3:50PM - 4:00PM Room: S403A

Gregory A. Book, MS, Hartford, CT (*Presenter*) Nothing to Disclose Alecia D. Dager, PhD, Hartford, CT (*Abstract Co-Author*) Nothing to Disclose Malgorzata Marjanska, PhD, Minneapolis, MN (*Abstract Co-Author*) Nothing to Disclose Godfrey Pearlson, MD, Hartford, CT (*Abstract Co-Author*) Consultant, Astellas Group

For information about this presentation, contact:

gregory.book@hhchealth.org

gregory.book@hhchealth.org

CONCLUSION

Change in gradient temperature from heavy usage negatively impacts scanning quality for MRS sequences. Methods exist to compensate for frequency drift, but significant drift can still negatively impact quantification of the metabolite concentrations due to the poor water suppression. Quantifying the time required for gradients to stabilize after intense use, in this example of a Siemens Skyra 3 T, can inform scheduling of MRS studies to maximize their stability, and reduce the need for drift correction tools.

Background

MR spectroscopy (MRS) is susceptible to frequency drift caused by gradient warming, more so than other MR imaging modalities. Frequent switching of gradients in fMRI and DTI causes heating and the frequency of the magnet to change in an unpredictable way. Frequency drift in functional brain imaging can cause spatial drift over time, especially in the z direction, but is easily corrected by realignment. Frequency drift in MRS degrades the water suppression and quality of the spectrum through increased linewidth. We examine the effects of gradient heating on frequency drift and map the time required for gradients to stabilize on a specific magnet.

Evaluation

Drift was tested on a Siemens 3 T Skyra MRI, with a 32-channel receive-only head-coil, standard gradients, and an MRS phantom. Using a PRESS sequence, transmitter voltage and water suppression flip angle were adjusted to produce optimal water suppression. At 10 minute intervals over a period of 3 hours, magnet frequency was adjusted to convergence and the new frequency recorded. Two 9 min fMRI sequences (TR = 700ms) were run starting 20 minutes after initial frequency measurement.

Discussion

Frequency drift was negligible prior to perturbation of gradients from fMRI, but increased 5.6Hz/min to a peak of 70 Hz above baseline after the second fMRI sequence. Frequency returned to baseline 120 minutes after completion fMRI at a rate of 0.83 Hz/min for the first 60 minutes. Spectra collected using LASER sequence after perturbation showed significant drift, and spectra collected before perturbation showed no drift.





103rd Scientific Assembly and Annual Meeting November 26 to December 1 McCormick Place, Chicago



SSM21

Radiation Oncology (Breast Cancer)

Wednesday, Nov. 29 3:00PM - 4:00PM Room: S105AB



AMA PRA Category 1 Credit ™: 1.00 ARRT Category A+ Credit: 1.00

Participants

Tracy M. Sherertz, MD, San Francisco, CA (*Moderator*) Nothing to Disclose Kathleen Horst, MD, Stanford, CA (*Moderator*) Nothing to Disclose

Sub-Events

SSM21-01 Outcomes of Early Stage Breast Cancer with Nodal Micrometastases

Wednesday, Nov. 29 3:00PM - 3:10PM Room: S105AB

Participants

Yazan A. Abuodeh, MBBS, Tampa, FL (Presenter) Nothing to Disclose

ABSTRACT

Purpose/Objective(s): Nodal micrometastases (N1mi) in breast cancer patients carry a slightly worse prognosis compared to node negative disease. This study aims to assess factors predictive of N1mi outcome and the effect of treatment modality for this cohort.Materials/Methods: Retrospective analysis of T0-T2 N1mi breast cancer patients were obtained by chart review and the Total Cancer Care Database from 2000-2014. Patient, tumor, and treatment characteristics were analyzed in regards to outcome, which include: locoregional failure (LRF), distant metastasis (DM), disease free survival (DFS), and overall survival (OS). Coxregression univariate (UVA) and multivariate (MVA) analyses were used to determine association between variables and outcome. Variables predictive of outcome on UVA (pResults: We identified 129 female breast cancer patients with stage IB/IIB, with a median age of 58 (30-58) years. Patients were most commonly Caucasian (85%) with left breast involvement (54%). Patients were either treated with breast conserving therapy (BCT) (n=48,37%), mastectomy only (n=52, 40%), or mastectomy with postmastectomy radiation (PMRT) (n=29, 23%)." Axillary evaluation was either by sentinel biopsy alone (n=85, 66%) or by axillary dissection (n=44, 34%). Invasive ductal carcinoma was found in 106 (82%) patients. Tumor stage was primarily T1 (46.5%) and T2 (51.9%), with 2 (1.6%) T0. Median tumor size was 2(0-5) cm. Grades were 1,2,3, and unknown in 24(18.6%),66 (51.2%),38(29.5%) and 1(0.8%), respectively. Multifocal disease (MF) and lymphovascular space invasion (LVSI) were present in 29(22.5%) and 32(24.8%) patients, respectively. Number of involved lymph nodes were 1, 2, 3 in 115(89%), 11(9%), and 3(2%) patients, with extracapsular extension present in 6(5%) cases. Estrogen receptor, and HER2neu were positive in 116(90%) and 13(10%) patients, respectively. Oncotype Dx scores were low, intermediate, high or was not done in 34(26%), 21(16%), 6(5%), and 68(53%), respectively. Systemic treatment was delivered as chemotherapy, hormonal, and targeted therapy in 71(55%), 111(86%), and 9(7%), respectively. With a median follow up of 39 months, there were 2 (2%) LRF, 5 (4%) DM, and 4 (3%) deaths. On univariate analysis, no factors predicted for LRF, but MF and size predicted for DM and DFS (pConclusion: Locoregional control of N1mi disease was not affected by treatment modality. Larger tumors or MF have worse DM and DFS, and may benefit from systemic treatment intensification.

SSM21-02 Her-2 Positive is Associated with Increased Risk of Locoregional Recurrence of Breast Cancer Patients Treated with Neoadjuvant Chemotherapy and Breast Conserving Surgery

Wednesday, Nov. 29 3:10PM - 3:20PM Room: S105AB

Participants

Qing-Lin Rong, Oak Brook, IL (Presenter) Nothing to Disclose

ABSTRACT

Purpose/Objective(s): Neoadjuvant chemotherapy (NAC) decreases tumor size and increase the chance of breast conserving surgery (BSC) for patients with large primary tumors. This study is to evaluate the outcomes of this group of patients and identify risk factors of locoregional recurrence (LRR) for further individualized treatment.Materials/Methods: A total of 108 breast cancer patients treated with NAC and BSC between 1999 and 2013 were retrospectively reviewed. There were 4 clinical stage I, 66 stage II and 38 stage III patients. After surgery, 103 (95.4%) had negative margins. 99 (91.7%) patients received adjuvant radiotherapy (RT) to the whole breast, with 41 patients received supraclavicular nodal RT simultaneously. Of patients with positive hormone receptor disease, 76 (88.4%) received endocrine therapy. Of patients with positive Her-2 disease, 16 (61.5%) received targeted therapy with trasuzumab. The rates of locoregional recurrence (LRR), distant metastasis (DM), disease-free survival (DFS) and overall survival (OS) were calculated using the Kaplan-Meier method, and differences were compared using the log-rank test.Results: The overall clinical response to NAC was achieved in 92 (85.2%) patients, with a complete response rate of 6.5% and a partial response rate of 78.7%. 32 (100%) patients with cT3-4 disease and 56 (84.8%) with cT2 achieved T-stage degradation. For 38 patients with clinical stage III, 30 (78.9%) was downstaged, and 8 (21.1%) achieved pathologic complete response (pCR). For 66 patients with clinical stage II, 30 (45.5%) was downstaged, and 8 (12.1%) achieved pCR. With a median follow-up time of 64 months, 12 patients had LRR, including 6 breast recurrence and 6 regional recurrences. Eighteen patients had DM. The 5-year rates of LRR, DM, DFS and OS for all patients were 11.0%, 15.1%, 77.9% and 97.0%, respectively. In univariate analysis, patients with Her-2 positive disease had higher LRR rate as compared with Her-2 negative (27.0% vs. 6.3%, P = 0.020), whereas there were no significant differences in LRR between clinical III and stage I-II (15.4% vs. 10.0%, P = 0.448) or between pathologic stage III and stage 0-II (10.8% vs. 11.1%, P = 0.518). Conclusion: BCS performed selectively after NAC for breast cancer patients is safe, and the LRR is acceptably low. Her-2 positive is associated with increased risk of LRR, although 61% Her-2 positive patients

received anti HER-2 targeted therapy. Further study is warranted to verify this finding.

SSM21-03 Interplay between AlignRT Tracking Accuracy and Breast Surface Topography

Wednesday, Nov. 29 3:20PM - 3:30PM Room: S105AB

Participants Yulin Song, PhD, West Harrison, NY (*Abstract Co-Author*) Nothing to Disclose He Zhu, BS, New York, NY (*Abstract Co-Author*) Nothing to Disclose Ceferino H. Obcemea, PhD, Washington, DC (*Abstract Co-Author*) Nothing to Disclose Boris Mueller, MD,MPH, West Harrison, NY (*Abstract Co-Author*) Nothing to Disclose Jeho Jeong, PhD, New York, NY (*Abstract Co-Author*) Nothing to Disclose Ziad Saleh, PhD, West Harrison, NY (*Presenter*) Nothing to Disclose Xiaoli Tang, PhD, Chapel Hill, NC (*Abstract Co-Author*) Nothing to Disclose Melissa Zinovoy, MD, West Harrison, NY (*Abstract Co-Author*) Nothing to Disclose Daphna Y. Gelblum, MD, MS, Commack, NY (*Abstract Co-Author*) Nothing to Disclose Borys R. Mychalczak, MD, New York, NY (*Abstract Co-Author*) Nothing to Disclose

For information about this presentation, contact:

songy@mskcc.org

PURPOSE

AlignRT is a commercial 3D-optical surface imaging system specifically designed for radiation oncology applications. It is often used for chest surface motion tracking for the breast cancer patients treated with deep-inspiration breath-hold (DIBH) protocol. Since AlignRT tracking accuracy and reliability are highly ROI-dependant, a variation in breast topography could result in incorrect patient shifts. So far, no study has examined how AlignRT tracking accuracy is affected by changes in breast surface topography. The goal was to understand hidden interconnections and establish corresponding clinical guidelines.

METHOD AND MATERIALS

An anthropomorphic phantom and 8 breast phantoms of different shapes were used in this study. The diameters of the breast phantoms were 12.9, 15.0, 15.8, 16.0, 17.7, 21.5, and 28.0 cm with central elevations of 1.7, 5.4, 3.0, 3.8, 1.4, 0.9, and 1.5 cm. For each set of measurements, a breast phantom was attached to the anthropomorphic phantom. A reference surface image was acquired. To eliminate ROI-dependency effect, an identical ROI was used throughout the study. The couch was then manually shifted by -1.0, -2.0, 1.0, and 2.0 cm in VRT, LAT, and LNG directions sequentially. The AlignRT-measured shifts were obtained by acquiring a static treatment surface image and registering with the reference surface image.

RESULTS

We found that AlignRT tracking accuracy was not significantly affected by variations in breast topography as long as an ROI much larger than the breast was used. Breast tissue with higher elevations tended to yield better tracking results. A couch shift further away from isocenter tended to produce less accurate tracking results. The tracking uncertainties were found to be ~ 1.0 mm in translations and $\sim 1.0^{\circ}$ in rotations. These often occurred in LAT shift and yaw rotation.

CONCLUSION

For breast and chest wall applications, AlignRT tracking accuracy is independent of breast surface topography as long as a large ROI (covering the entire breast, SCV, axilla, sternum, and some lateral aspects of the chest) is used.

CLINICAL RELEVANCE/APPLICATION

AlignRT uses structured light to measure 3D surface of a cancer patient for pre-treatment setup and intra-fractional motion tracking.

SSM21-04 Analysis of Treatment Effectiveness and Complications Associated with Accelerated Partial Breast Brachytherapy in Patients Treated at a Single Institution

Wednesday, Nov. 29 3:30PM - 3:40PM Room: S105AB

Participants

Daniel H. Miller, MD, Jacksonville, FL (*Abstract Co-Author*) Nothing to Disclose Nicholas Pflederer, Omaha, NE (*Presenter*) Nothing to Disclose Timothy D. Malouff, MD, Jacksonville, FL (*Abstract Co-Author*) Nothing to Disclose Don Nguyen, Omaha, NE (*Abstract Co-Author*) Nothing to Disclose Elizabeth A. Edney, MD, Omaha, NE (*Abstract Co-Author*) Nothing to Disclose Edibaldo Silva, MD,PhD, Omaha, NE (*Abstract Co-Author*) Nothing to Disclose William Hunter, MD, Omaha, NE (*Abstract Co-Author*) Nothing to Disclose Cam Nguyen, MD, Omaha, NE (*Abstract Co-Author*) Nothing to Disclose

For information about this presentation, contact:

NicholasPflederer@Creighton.edu

ABSTRACT

Purpose/Objective(s): MammoSite[™] is a form of Accelerated Partial Breast Irradiation (APBI) designed to deliver targeted doses of radiation from within breast tumors. This method of radiation delivery allows higher doses of radiation, reduces treatment fractions, and aims to reduce toxicities from external beam radiation therapy. While the use of MammoSite[™] has been well studied, the results from the only randomized control trial, RTOG 0413/NSABP B-39, are pending. We aim to present efficacy and toxicity data for follow-up of over five-years for patients receiving MammoSite[™] at our institution. Materials/Methods: We performed a retrospective analysis of patients at a single institution who presented with early stage breast cancer and received breast conserving surgery. These patients elected to receive accelerated partial breast irradiation (APBI) using the MammoSite[™] catheter device. Patients were treated with 30.6 - 34.0 Gy in 3.4 Gy fractions given twice daily with fractions at least six hours apart utilizing either a spherical or ellipsoidal catheter device. Patient data was collected regarding the specific treatment and planning

volumes, complications and toxicities occurring during and after treatment, and the overall outcome of each patient relating to tumor-free survival.Results: From October 2005 through November 2010, 78 patients with 79 lesions were treated with APBI using the MammoSite[™] catheter device and were eligible for our retrospective analysis. Patients with less than 24 months follow up were excluded from the study. 79.5% of patients were ER positive, 55% were PR positive, and 17.9% were HER2/neu positive. Seven patients (9.0%) had N1 disease. The median follow-up time was 80 months. Of the patients in our study, there were a total of 10 recurrences (12.8%), with 5 local recurrences (6.4%), 2 local recurrences that developed into distant metastases (2.6%), and 3 distant metastases (3.8%). Two recurrences were considered new primary lesions due to receptor status change in the new tumor. Specific toxicities include 12 patients with skin erythema (15.4%), 7 patients with seroma (9%), 8 patients with localized edema (10.3%), and 6 patients with infection (7.7%).Conclusion: This case series of 78 patients with a median follow-up of 80 months, from a single institution, provides important data regarding failure analysis with MammoSite[™] accelerated partial breast irradiation. Our results show a higher rate of metastatic recurrence in the group of patients with positive nodal disease as expected. Further prospective analysis, such as the B-39 trial, is required to fully assess the efficacy and safety of MammoSite[™] in the treatment of cancer with APBI.

SSM21-05 Prospective Study of Accelerated Partial Breast Irradiation Using Three Dimensional-Conformal Radiotherapy for Early Stage Breast Cancer

Wednesday, Nov. 29 3:40PM - 3:50PM Room: S105AB

Participants

Michio Yoshimura, Kyoto, Japan (*Presenter*) Nothing to Disclose Kimiko Hirata, MD,PhD, Kyoto, Japan (*Abstract Co-Author*) Nothing to Disclose Yuka Ono, MD, Kyoto, Japan (*Abstract Co-Author*) Nothing to Disclose Minoru Inoue, MD,PhD, Kyoto, Japan (*Abstract Co-Author*) Nothing to Disclose Masahiro Hiraoka, MD, PhD, Kyoto, Japan (*Abstract Co-Author*) Nothing to Disclose Takashi Mizowaki, MD, Kyoto, Japan (*Abstract Co-Author*) Nothing to Disclose

ABSTRACT

Purpose/Objective(s): In Japan, only a few trials of accelerated partial breast irradiation (APBI) using three dimensional-conformal radiotherapy (3D-CRT) have been reported so far. The aim of this study is to evaluate the efficacy and safety of APBI using 3D-CRT for Japanese women. Materials/Methods: Eligibility criteria for this protocol included age=40 years old, no preoperative systemic treatment, stage Tis-2N0-1M0, negative surgical margins (>5 mm) following breast conserving surgery, and surgical clips intraoperatively placed at the cranial, caudal, medial, and lateral edge of the seroma cavity. For image-registration, the positions of the clips in daily kV x-ray images were matched to those in the planning digitally reconstructed radiographs. We adopted beam arrangements of four- or five- 6 MV X-ray noncoplanar fields with 5-mm multi-leaf collimator. The prescribed dose was 38.5 Gy in 10 fractions over 2 weeks. The toxicity grading was based on Common Toxicity Criteria for Adverse Events (CTCAE) v4.0.Results: Between January 2012 and June 2016, 50 patients with early stage breast cancer were enrolled for the trial of APBI using 3D-CRT following breast conserving surgery at Kyoto University Hospital. Since two of them were excluded because of the dose constraint of contralateral breast, we analyzed 48 patients who underwent APBI. All patients completed the radiation treatment. The median age was 57.5 years old (range, 42-81 years old). The disease was Stage 0 in 6 (13%), Stage IA in 34 (70%), Stage IIA in 8 (17%) patients. Seven patients received adjuvant chemotherapy, followed by APBI within 6 weeks after the end of chemotherapy. At the median follow-up of 31 months (range, 5.4-55 months), no locoregional recurrence or distant metastases of breast cancer were observed. Two-year overall survival was 100 %. Grade 2 adverse events were breast atrophy (4%), breast pain (2%), fibrosis (2%), dermatitis (2%), fever (2%), and pigmentation (2%). Grade 3 soft tissue cellulitis of the breast was observed in one patient. There was no grade 4-5 toxicity. Cosmesis outcomes by four point scale were excellent/good for 77% of patients at pretreatment state and for 63% at 1 year after APBI. The cosmesis scales were improved in 3 patients (6%), worsened in 7 patients (15%), and unchanged in the rest of the patients (79%) at 1 year after APBI. Conclusion: Two-year disease control treated with this APBI protocol using 3D-CRT for Japanese early-stage breast cancer patients was good, and the adverse events and cosmesis outcomes were feasible and satisfactory.

SSM21-06 Risk of Early Onset Breast Cancer among Women Exposed to Thoracic CT in Pregnancy or Early Postpartum

Wednesday, Nov. 29 3:50PM - 4:00PM Room: S105AB

Participants Kirsteen R. Burton, MD, MBA, Toronto, ON (*Presenter*) Nothing to Disclose Alison Park, Toronto, ON (*Abstract Co-Author*) Nothing to Disclose Michael Fralick, Toronto, ON (*Abstract Co-Author*) Nothing to Disclose Joel Ray, Toronto, ON (*Abstract Co-Author*) Nothing to Disclose

For information about this presentation, contact:

kirsteen.burton@utoronto.ca

PURPOSE

The risk of breast cancer may be higher with direct exposure to ionizing radiation from thoracic computed tomography (CT) during pregnancy or postpartum, when breast tissue undergoes proliferation and differentiation.

METHOD AND MATERIALS

We completed a retrospective population-based cohort study. Universal health care databases in Ontario, Canada were used to identify deliveries between 1995-2014. The main exposure was thoracic CT in pregnancy or <= 42 days postpartum. Exposure to VQ scan was used as an active comparator, as there is no direct-beam radiation to the breast. Each was compared to pregnancies unexposed to thoracic CT or VQ scan. The primary study outcome was newly diagnosed breast cancer starting 366 days after the index delivery date.

RESULTS

5,859 pregnancies were exposed to thoracic CT, 97% of which had intravenous contrast; 4075 to VQ scan; and 1,292,059 to neither. After a mean (SD) duration of follow-up of 11.1 (5.7) years, a total of 10,129 women were diagnosed with breast cancer, of which 9,039 (89.2%) were aged <= 50 years. There were 27 new cases of breast cancer (7.1 per 10,000 person-years) following

thoracic CT vs. 10,080 (7.0 per 10,000 person-years) among the unexposed - an adjusted HR of 1.17 (95% CI 0.80-1.70). Following VQ scan exposure, the incidence rate of breast cancer was also 7.0 per 10,000 person-years - an adjusted HR of 1.23 (95% CI 0.81-1.87) compared to the unexposed cohort.

CONCLUSION

Exposure to thoracic CT during pregnancy or postpartum was not associated with an increased short-term risk of maternal breast cancer.

CLINICAL RELEVANCE/APPLICATION

Published recommendations about the safety of ionizing radiation in pregnancy and postpartum have typically focused on the potential teratogenic effects to the fetus, while mentioning the possibility of a higher risk of breast cancer. Although an increased risk of breast cancer following radiological ionizing radiation exposure during pregnancy or lactation has been postulated, this has never been quantified. The current findings help inform those guidelines.





103rd Scientific Assembly and Annual Meeting November 26 to December 1 McCormick Place, Chicago



SSM22

Vascular Interventional (Biopsy)

Wednesday, Nov. 29 3:00PM - 4:00PM Room: E352



AMA PRA Category 1 Credit ™: 1.00 ARRT Category A+ Credit: 1.00

FDA Discussions may include off-label uses.

Participants

Hyeon Yu, MD, Seoul, Korea, Republic Of (*Moderator*) Nothing to Disclose Charles Martin III, MD, Pepper Pike, OH (*Moderator*) Scientific Advisory Board, Boston Scientific Corporation

Sub-Events

SSM22-01 Incidence of Bleeding Complications after Percutaneous Core Needle Biopsy and the Association with Aspirin Usage and Length of Aspirin Discontinuation

Wednesday, Nov. 29 3:00PM - 3:10PM Room: E352

Participants

Jamison A. Harvey, Rochester, MN (*Presenter*) Nothing to Disclose Theodora A. Potretzke, MD, Madison, WI (*Abstract Co-Author*) Nothing to Disclose Tina Gunderson, Rochester, MN (*Abstract Co-Author*) Nothing to Disclose Grant D. Schmit, MD, Rochester, MN (*Abstract Co-Author*) Nothing to Disclose Robert McBane, MD, Rochester, MN (*Abstract Co-Author*) Nothing to Disclose Anil N. Kurup, MD, Rochester, MN (*Abstract Co-Author*) Research Grant, Galil Medical Ltd Royalties, UpToDate, Inc Paul Wennberg, MD, Rochester, MN (*Abstract Co-Author*) Nothing to Disclose Thomas D. Atwell, MD, Rochester, MN (*Abstract Co-Author*) Nothing to Disclose

For information about this presentation, contact:

harvey.jamison@mayo.edu

PURPOSE

To report rate of major bleeding complications after percutaneous image-guided core biopsy and to determine risk related to aspirin use and length of aspirin discontinuation prior to biopsy.

METHOD AND MATERIALS

Following IRB approval, we retrospectively reviewed a prospectively-maintained database for all percutaneous image-guided core biopsies performed at our institution between 9/1/2005 and 9/1/2016 (n=30,966). Patients were excluded if aspirin usage data was missing (n=633). Bleeding complications were defined using the Common Terminology Criteria for Adverse Events (CTCEA, version 3) established by the National Cancer Institute and were considered significant if grade 3 or higher. Multivariate models were adjusted for age, gender, platelet count, international normalized ratio (INR), and biopsy target. Three categorizations of aspirin use were examined: any use within 10 days prior, length of discontinuation (>10 days/no aspirin, 8-10, 4-7, and 0-3 days prior), and use on day of biopsy. Associations with bleeding complications were modeled using generalized estimating equations logistic regression models. P-values <=.05 were considered significant.

RESULTS

30,333 biopsies in 21,938 unique subjects were included (mean (SD) age 58 years (16), 57% male). 7,921 (26.1%) biopsies were performed in patients who received aspirin within 10 days of biopsy, 47.5% of which (3,761) took it within 3 days prior to biopsy. 98 significant bleeding complications (grade 3 or higher) occurred across all included cases (0.32%), 34 in those with aspirin use during the prior 10 days (0.43%), 22 within 0-3 days (0.58%), and 17 with aspirin use on same day as biopsy (1.9%). Aspirin use within 10 days of biopsy increased the bleeding risk, but not significantly (OR 1.5 [.96-2.3], p=.08). Days since discontinuation showed significant increase in bleeding only between 0-3 days versus >10 days/no aspirin groups (OR 2.1 [1.3-3.6], p=.004). Aspirin use on day of biopsy showed the greatest increase in risk (OR 6.6 [3.8-11.5], p<.001).

CONCLUSION

Major bleeding complications after percutaneous core biopsy are rare. Aspirin use within 3 days of biopsy is associated with increased risk of bleeding.

CLINICAL RELEVANCE/APPLICATION

A short period of aspirin cessation prior to biopsy may be sufficient to decrease risk of bleeding although risk remains low even in those with recent aspirin use.

SSM22-02 A Team-Science Approach to Support Personalized Cancer Care: Role and Value of Interventional Radiology in Clinical Trials

Participants

Alda L. Tam, MD, Houston, TX (*Presenter*) Medical Monitor, Galil Medical Ltd; Research Grant, AngioDynamics, Inc; Vassiliki Papadimitrakopoulou, MD, Houston, TX (*Abstract Co-Author*) Nothing to Disclose
Ignacio Wistuba, MD, Houston, TX (*Abstract Co-Author*) Nothing to Disclose
J. Lee, PhD,DDS, Houston, TX (*Abstract Co-Author*) Nothing to Disclose
Joe E. Ensor, PhD, Houston, TX (*Abstract Co-Author*) Nothing to Disclose
Neda Kalhor, Houston, TX (*Abstract Co-Author*) Nothing to Disclose
Edward S. Kim, MD, Houston, TX (*Abstract Co-Author*) Nothing to Disclose
George R. Blumenschein JR, MD, Houston, TX (*Abstract Co-Author*) Nothing to Disclose
John V. Heymach, MD,PhD, Houston, TX (*Abstract Co-Author*) Nothing to Disclose
Roy S. Herbst, MD, Houston, TX (*Abstract Co-Author*) Nothing to Disclose
Marshall E. Hicks, MD, Houston, TX (*Abstract Co-Author*) Nothing to Disclose
Waun K. Hong, MD, Houston, TX (*Abstract Co-Author*) Nothing to Disclose
Sanjay Gupta, MD, Houston, TX (*Abstract Co-Author*) Nothing to Disclose

For information about this presentation, contact:

alda.tam@mdanderson.org

PURPOSE

Biopsy yield is critical for determining a patient's trial eligibility and treatment. We report our experience with supporting the BATTLE and BATTLE-2 lung cancer trials, focusing on the role of interventional radiologists (IRs).

METHOD AND MATERIALS

The medical records of patients who underwent percutaneous image-guided biopsy for the BATTLE and BATTLE-2 trials were reviewed. A radiology-based, 3-point, lesion scoring system was developed. Lesions were scored a 3 (most likely to yield sufficient material for biomarker analysis) if they met the following criteria: size \geq 2 cm, solid mass, demonstrate imaging evidence of viability, and technically easy to sample. Lesions that did not meet all four criteria, were scored a 2 with the missing criteria noted as negative factors. The lesions biopsied were retrospectively scored by two IRs and univariate and multivariate analyses were performed to evaluate the score's ability to predict successful yield for biomarker adequacy.

RESULTS

A total of 555 biopsies were performed for BATTLE and BATTLE-2. Overall yield for analysis of the required biomarkers was 86.1% (478/555) and 84% (268/319) and 88.9% (210/236) for BATTLE and BATTLE-2, respectively (p=0.09). Lesions receiving a score of 3 were adequate for biomarker analysis in 89% of cases. Lesions receiving a score of 2 with more than one negative factor were adequate for biomarker analysis in 69.2% (p=0.03) and 74% (p=0.04) of cases when scored by IR1 and IR2, respectively. The kappa statistic between the two IRs scoring was 0.55 [95% CI: (0.48, 0.61)] indicating moderate agreement as lesions were scored the same by both IRs in 78.4% of cases.

CONCLUSION

A team-science approach can facilitate consistent yields for biomarker analysis in clinical trials. IRs play a critical role for lesion selection.

CLINICAL RELEVANCE/APPLICATION

By leveraging the expertise of the individual specialties (medical oncology, pathology, IR), achieving consistently high adequacy rates from image-guided biopsies for biomarker analysis is feasible.

SSM22-03 Causes of Inadequate Sampling in IR Biopsies: Review of 3256 Biopsies

Wednesday, Nov. 29 3:20PM - 3:30PM Room: E352

Participants

Peter T. Hoang, MD, Phoenix, AZ (*Presenter*) Nothing to Disclose Andrew R. Fleck, MD, Phoenix, AZ (*Abstract Co-Author*) Nothing to Disclose Alex L. Wallace, MD, Phoenix, AZ (*Abstract Co-Author*) Nothing to Disclose Jeffry S. Kriegshauser, MD, Phoenix, AZ (*Abstract Co-Author*) Research support, General Electric Company Sailen G. Naidu, MD, Phoenix, AZ (*Abstract Co-Author*) Nothing to Disclose Grace Knuttinen, MD, PhD, Phoenix, AZ (*Abstract Co-Author*) Nothing to Disclose Rahmi Oklu, MD, PhD, Scottsdale, AZ (*Abstract Co-Author*) Nothing to Disclose

PURPOSE

The role of the interventional radiologist in the Precision Medicine Initiative has become increasingly important in providing the necessary tissue for genetic analysis. However, inadequate sampling rate for DNA testing exceed 20% resulting in repeat biopsies and delays in treatment. The aim of this study was to evaluate variables that associate with inadequate biopsy sampling in a large tertiary medical center.

METHOD AND MATERIALS

This IRB approved, HIPAA compliant study involved a search of our radiology department database for biopsies performed from January 2015 to December 2015. 3256 biopsies were included in the study in which 104 biopsies were ordered for genetic testing. Electronic medical records including radiology and pathology reports were reviewed for lesion size, tissue type, biopsy equipment, aggregate core length, number of samples obtained and the operator experience. Statistical analysis was performed using univariate analysis and logistic regression.

RESULTS

Inadequate tissue sampling rate was 20.1% (21/104). Univariate analysis showed an association between inadequate samples and smaller needle gauge (p=0.02) and smaller core length (p=0.01). There was no association with lesion size (p=0.39) and operator

experience (p=0.8). In logistic regression, the inadequate sampling rate was not different when obtaining 2 or more samples or an aggregate core length of 1-2 cm (P=0.95 and p=0.73). Temno (BD) devices resulted in 31% inadequate sampling rate, Bard (CR Bard) in 8% and BioPince (Argon Medical) in 8%. Genetic testing led to appropriate selection of therapy in 80% of the patients with adequate sampling.

CONCLUSION

Smaller needle gauge and smaller core lengths were associated with higher inadequate sampling rates. There was no added benefit to obtaining more than 2 to 3 biopsy samples or more than 1 to 2 centimeters of aggregate core tissue length. Adequate tissue for DNA testing is critical; results show that they can guide selection of therapy.

CLINICAL RELEVANCE/APPLICATION

Adequate tissue for DNA testing is critical; it can guide selection of therapy.

SSM22-04 Freehand Ultrasound-Guided Targeted Transperineal Prostatic Biopsy Technique (FUGTTPB) for Suspicious Lesions Identified By Magnetic Resonance Imaging (MRI)

Wednesday, Nov. 29 3:30PM - 3:40PM Room: E352

Participants Joel Lim, MBBS, Perth, Australia (*Presenter*) Nothing to Disclose Tonya Halliday, MBChB, Glasgow, United Kingdom (*Abstract Co-Author*) Nothing to Disclose Sally Burrows, Perth, Australia (*Abstract Co-Author*) Nothing to Disclose Victoria Toal, Perth, Australia (*Abstract Co-Author*) Nothing to Disclose Yuranga Weerakkody, MBBCh, Auckland, New Zealand (*Abstract Co-Author*) Nothing to Disclose James E. Anderson, MBBCh, Perth, Australia (*Abstract Co-Author*) Nothing to Disclose

For information about this presentation, contact:

jushi1989@hotmail.com

PURPOSE

FUGTTPB has many advantages over the traditional transrectal ultrasound-guided technique including lower infection rates. This study aims to investigate the cancer detection rates of this novel technique by comparing Prostate Imaging Reporting and Data System Version 2 (PI-RADS) and Gleason scores.

METHOD AND MATERIALS

A retrospective cohort study was conducted of all men who underwent an MRI Prostate between January 2015 and December 2016 with a lesion graded as PI-RADS 3 or greater followed by FUGTTBP in our institution. These were performed in the outpatient setting with the index lesion targeted free hand without the use of a grid or image fusion, guided by transrectal ultrasound.

RESULTS

99 men (mean age 65 years) referred by 20 Urologists underwent MRI at 6 centres with 129 lesions identified. 75% were imaged based on clinical suspicion whilst 25% were followed for a previous prostatic malignancy. Cancer detection rates for PI-RADS 3, 4 and 5 lesions were 42% (95% CI 27.9 - 57.3), 63% (95% CI 46.9 - 75.9) and 97% (95% CI 77.5 - 99.6) respectively. The PI-RADS 3 and 5 rates are comparable to the only published study comparing PI-RADS Version 2 and Gleason scores. The PI-RADS 4 rate was slightly lower but this may be attributed to the varying experience of the 13 MRI reporters and 4 patients having PI-RADS 4 lesions which were non-index lesions as they also had PI-RADS 5 lesions. 3 patients had positive cores beyond the target area but these were not identified as suspicious on MRI. Only 1 core from each patient was positive and all were graded as Gleason 6 with tumour lengths of 1 mm or less.

CONCLUSION

This pilot study demonstrates promising cancer detection rates of the FUGTTPB technique especially for higher grade PI-RADS lesions. However, it is limited by MRI sensitivity as 3 patients had tiny positive cores outside of the target area. Given the numerous benefits, further evaluation of this technique may result in evolution of prostatic biopsy techniques.

CLINICAL RELEVANCE/APPLICATION

MRI has shown promise in identifying clinically significant prostatic tumours. Targeting these via the FUGTTPB technique has numerous benefits.

SSM22-05 Preliminary Study to Compare the Effectiveness of Four Hemostatic Methods: Locally Injected FFP, Systemic FFP, Local Gelfoam Insertion, or Local Coil Insertion for Preventing Bleeding Complications

Wednesday, Nov. 29 3:40PM - 3:50PM Room: E352

Participants

John R. Haaga, MD, Cleveland, OH (*Presenter*) Nothing to Disclose Jon Davidson, MD, Cleveland, OH (*Abstract Co-Author*) Nothing to Disclose Shiraz Rahim, MD, Cleveland, OH (*Abstract Co-Author*) Nothing to Disclose Indravadan J. Patel, MD, Cleveland, OH (*Abstract Co-Author*) Nothing to Disclose Dean A. Nakamoto, MD, Beachwood, OH (*Abstract Co-Author*) Research agreement, Toshiba Medical Systems Corporation Nami R. Azar, MD, Highland Heights, OH (*Abstract Co-Author*) Nothing to Disclose

For information about this presentation, contact:

John.Haaga@uhhospitals.org

PURPOSE

To assess the efficacy of local hemostatic techniques in coagulopathic patients with abnormal INR. These techniques included: 1) local injection of fresh frozen plasma 2)systemic administration of fresh frozen plasma 3)local insertion of gelfom 4)local insertion of

METHOD AND MATERIALS

Data was collected from 4 IRB approved studies totaling 182 patients. Procedures and biopsies included 80 liver biopsies, 35 abscess drainages, 21 soft tissue masses, 18 kidney biopsies, 7 cholecystostomies, and 13 chest tubes. Causes of the coagulopathy included anticoagulation treatment, liver failure, hematologic malignancy, chemotherapy, and idiopathic.The most common causes were coumadin and liver failure in 118 patients. INR ranges for each group were: 91 patients treated with local injection of FFP (INR1.4-3.0, avg 2.1), 40 patients treated with gelfoam (INR 2.1-2.9, avg 2.32), 35 patients with systemic FFP (INR 1.4-3.4, avg 2.1), and 16 patients treated with angiographic coils (INR avg1.3).. Average amount of FFP used was 20 cc injected locally and 5.2 units intravenously. Average of 2 coils were used per patient.

RESULTS

Bleeding complications were: drop in hemoglobin, visible hematoma, required transfusion, or intervention.Total//significant bleeding complications were 0//0% for locally injection of FFP, 17.1//2.8% for systemic FFP, 12.5//0% for gelfoam, and 37//12.5% for coils. 6 nonbleeding complications occurred in systemic FFP group and included shortness of breath, shortness of breath requring intubation (systemic group), 1 infection and death in 3 (2 volume overload, 1 idiosyncratic).

CONCLUSION

Of these methods used for hemostasis, local injection of FFP was the most effective, followed by gelfoam, systemic FFP, and local coils. These data provide a basis for organizing a larger prospective, randomized multiinstitutional study to confirm these findings and to study the cost benefit of the FFP groups.

CLINICAL RELEVANCE/APPLICATION

Percutaneous techniques play a major role for diagnoses and treatments. While normal patients have a low complication risk, coagulopathic patients are at greater risk of bleeding. Our comparison of different hemostatic methods provides preliminary data that the new 'local injection of blood products' technique is superior to other methods studied. Before this new method can be used widely, more data needs to be collected from large randomized, prospective studies.

SSM22-06 Percutaneous Hepatic Fiducial Gold Marker Implantation for Real-time Tumor-tracking Radiotherapy

Wednesday, Nov. 29 3:50PM - 4:00PM Room: E352

Participants

Ryo Morita, MD, Sapporo, Japan (*Presenter*) Nothing to Disclose Yusuke Sakuhara, MD, Sapporo, Japan (*Abstract Co-Author*) Nothing to Disclose Takeshi Soyama, Sapporo, Japan (*Abstract Co-Author*) Nothing to Disclose Daisuke Abo, MD, Sapporo, Japan (*Abstract Co-Author*) Nothing to Disclose Kohsuke Kudo, MD, Sapporo, Japan (*Abstract Co-Author*) Nothing to Disclose Norio Katoh, MD, Sapporo, Japan (*Abstract Co-Author*) Nothing to Disclose Hiroki Shirato, MD, PhD, Sapporo, Japan (*Abstract Co-Author*) Nothing to Disclose

For information about this presentation, contact:

ryo561201@me.com

PURPOSE

The purpose of this study was to evaluate the safety and complications associated with percutaneous fiducial global gold marker implantation into the liver parenchyma for real-time tumor-tracking radiotherapy (RTRT).

METHOD AND MATERIALS

This retrospective study was approved by our institutional review board. Using a medical record and database review, we evaluated data from 100 patients with hepatobiliary malignancies who underwent 116 percutaneous fiducial gold marker implantations in the liver as preparation for RTRT from 1999 to 2016. We used global markers that were 2 mm in diameter. All marker implantations were performed using Seldinger's method. Technical success was defined as completion of gold marker placement at the intended liver parenchyma. Clinical success was defined as successful tracking of the gold marker and completion of planned RTRT. In addition, we assessed complications related to the marker placement.

RESULTS

The technical success rate for fiducial gold marker implantation was 90% (104/116). Twelve of 116 markers could not be used for RTRT because of marker migration after implantation (n=9) or inappropriate location of the implanted marker (n=3). In 9 patients, markers migrated out of the liver; however, no complications occurred from not retrieving them. The clinical success rate was 99% (114/115), and we used another marker and completed RTRT for 1 tumor. Pain occurred in 16 patients, fever in 7, hemorrhage in 7, pneumothorax in 1, and nausea in 1. No major complications occurred.

CONCLUSION

Percutaneous fiducial gold marker implantation into the liver for RTRT is a safe and feasible procedure.

CLINICAL RELEVANCE/APPLICATION

Percutaneous fiducial global gold marker implantation into the liver for image-guided radiotherapy is safe and feasible. Physicians should monitor patients for migration of the implanted marker.







SSM23

Vascular Interventional (Bone/ST Intervention)

Wednesday, Nov. 29 3:00PM - 4:00PM Room: E450B



AMA PRA Category 1 Credit ™: 1.00 ARRT Category A+ Credit: .50

Participants

Gordon McLennan, MD, Chagrin Falls, OH (*Moderator*) Research Grant, Siemens AG; Research Consultant, Medtronic plc; Advisory Board, Siemens AG; Advisory Board, Surefire Medical, Inc; Advisory Board, Stealth Medical; Advisory Board, Rene Medical; Data Safety Monitoring Board, B. Braun Melsungen AG

Charles Martin III, MD, Pepper Pike, OH (*Moderator*) Scientific Advisory Board, Boston Scientific Corporation

Sub-Events

SSM23-01 Has Gender Diversity Improved Among Interventional Radiology Fellows From 1991 to 2015? A Comparative Study With Other Related Fields

Wednesday, Nov. 29 3:00PM - 3:10PM Room: E450B

Participants

Paul H. Yi, MD, Baltimore, MD (*Presenter*) Nothing to Disclose
William Barge, Peoria, IL (*Abstract Co-Author*) Nothing to Disclose
Douglas B. Yim, MD, San Diego, CA (*Abstract Co-Author*) Nothing to Disclose
Kelvin K. Hong, MD, Baltimore, MD (*Abstract Co-Author*) Scientific Advisory Board, Boston Scientific Corporation; Scientific Advisory
Board, BTG International Ltd; Research support, Merit Medical Systems, Inc;

For information about this presentation, contact:

paulyi88@gmail.com

PURPOSE

Although prior studies have shown a significant increase in women in most medical specialties over the past several decades, Interventional Radiology (IR) has traditionally been a male-predominate field and it remains unknown if gender diversity in IR has improved over time. The purpose of this study was to analyze trends in gender diversity in IR in comparison with other related fields over the past 25 years.

METHOD AND MATERIALS

We reviewed data from the American Association of Medical Colleges reported in annual issues on medical education in the Journal of the American Medical Association for the years 1991-2015. We assessed the percentages of women resident and/or fellows in IR fellowships and other related training programs, including Diagnostic Radiology residency, Endovascular Neuroradiology fellowship, Radiation Oncology residency, as well of Medical Students and Residents from all specialties. Changes in the percentages of females from 1991 to 2015 were calculated for each group using Chi-Square tests and Pearson's Correlation Coefficient, as appropriate; statistical significance was set at p<0.05.

RESULTS

From 1991 to 2015, the percentage of females in IR fellowship increased from 0% to 23% (r=0.72; p<0.0001). Similarly, from 1991 and 2015, the percentage of females in medical school and in residency (all specialties) improved from 38% to 47% (p<0.001) and 30% to 46% (p<0.001), respectively. In 2015, IR had the lowest percentage of females at 9.3% compared to 47% of medical students, 46% of all residents, 29% of radiation oncology, and 27% of diagnostic radiology (p<0.001 for all).

CONCLUSION

Although the percentage of women trainees in IR fellowship has significantly increased over the past 25 years, IR is lagging behind other related fields and the general medical student and trainee population in terms of gender diversity. We recommend increased recruitment efforts towards women at different levels of training both during and after medical school to recruit more women into the field of IR.

CLINICAL RELEVANCE/APPLICATION

IR has the lowest representation of women among related specialties. We recommend increased recruitment efforts towards women at different levels of training to help improve gender diversity in IR.

SSM23-02 Percutaneous Vertebroplasty in Aged Patients with Osteoporotic Vertebral Compression Fractures: A Bicentric Retrospective Cohort Study

Wednesday, Nov. 29 3:10PM - 3:20PM Room: E450B

For information about this presentation, contact:

byzhongir@sina.com

PURPOSE

We aim to evaluate the effectiveness and safety of Percutaneous Vertebroplasty (PVP) in patients aged 80 and over with osteoporotic vertebral compression fractures (OVCFs) in two hospitals.

METHOD AND MATERIALS

Patients underwent their first PVP due to OVCFs between January 2006 and December 2014 in two large academic centers were selected to this bicentric retrospective cohort study. Patients were divided into two groups by age (aged 80 or older and no older than 80). The primary outcome of this study was pain relief at 1month and 1 year measured by visual analogue scale (VAS) score. Complications, including new vertebral compression fractures (VCFs) were recorded during the follow-up.

RESULTS

A total of 699 patients (382 in Hospital A and 317 in Hospital B) were included in this study and 139 (19.9%) of them were aged 80 or older. Chi-square test or one-way ANOVA showed that there was no statistical difference of the parameters about the patients between the two hospitals. For the aged patients, mean VAS score decreased from 6.9(95% CI 6.8-7.1) at baseline to 2.3(2.2-2.5) at 1 month (P<0.0001) and 1.8(1.7-1.9) at 1 year (P<0.0001). Compared to the patients no older than 80, there was no statistical difference of the VAS score. During the median follow-up of 1136 (range 5-2924) days, 40 (28.8%) patients had new VCFs with a median time of 80 (range 5-1022) days. No major complication occurred.

CONCLUSION

PVP is an effective and safe approach for the patients aged 80 or older with OVCFs.

CLINICAL RELEVANCE/APPLICATION

PVP should be regarded as a safe and effective treatment approach for patients aged 80 or older with OVCFs.

SSM23-03 Human Observer Detection Performance of Moving Objects in Fluoroscopic Image Series

Wednesday, Nov. 29 3:20PM - 3:30PM Room: E450B

Participants

Taylor Richards, Durham, NC (Presenter) Nothing to Disclose

Steve D. Mann, PhD, Durham, NC (*Abstract Co-Author*) Nothing to Disclose Ehsan Samei, PhD, Durham, NC (*Abstract Co-Author*) Research Grant, General Electric Company; ; Research Grant, Siemens AG; ; Advisory Board, medInt Holdings, LLC

For information about this presentation, contact:

taylor.richards@duke.edu

PURPOSE

Evaluate human observer detection performance of moving objects in fluoroscopic image series as a function of object velocity and x-ray pulse-width.

METHOD AND MATERIALS

Simulated fluoroscopic image series of a translating wire (1 mm diameter, 30 mm length) in white Gaussian noise were presented to seven trained readers using a 4-alternative forced choice study paradigm. Image series were simulated at eight frames-per-second (8 fps), two wire velocities (10 mm/s, 25 mm/s) and two x-ray pulse-widths (4 ms, 120 ms). Object contrast and image spatiotemporal noise power were held constant for all image series.Each reader was trained to maintain a constant viewing position (50 cm) and to utilize a template image sequence to inform eye-tracking. A total of 200 image series, 50 series for each pulse-width velocity combination, were reviewed by every reader. Their task was to select the image sequence which contained the translating wire.Binary response data from all readers was analyzed using a generalized linear mixed effects model with a probit link function. The model included pulse-width and velocity as fixed effects, and an intercept reader random effect.

RESULTS

Average observer detection performance ranged from 48% correct at the longest pulse-width and fastest velocity (120 ms, 25 mm/s) to 89% at the shortest pulse-width and slowest velocity (4 ms, 10 mm/s). X-ray pulse-width and object velocity were significant predictors of human detection performance (p-value << 0.0001) with an estimated effect size of -0.96 (95% CI: -1.12, -0.79) and -0.90 (95% CI: -1.17, -0.65) respectively. The standard deviation of the reader random effect was estimated at 0.57. The reader random effect can be largely attributed to the fact that one reader group observed each case for double the amount of time (17.7 seconds) as the other reader group (8.7 seconds) and thereby increased average detection performance by 28% correct.

CONCLUSION

Human detection performance of moving objects in fluoroscopic image series decreased significantly and independently with increased velocity and increased pulse-width. Average observation time also effected detection performance.

CLINICAL RELEVANCE/APPLICATION

The use of fluoroscopic imaging for diagnostic and interventional tasks involving substantial anatomic motion may be optimized for detection performance by appropriate x-ray pulse-width selection.

General Payments Correlate with Academic Productivity?

Wednesday, Nov. 29 3:30PM - 3:40PM Room: E450B

Awards

Student Travel Stipend Award

Participants Derek T. Kim, Port Jefferson, NY (*Presenter*) Nothing to Disclose Amanjit S. Baadh, MD, New York, NY (*Abstract Co-Author*) Nothing to Disclose Abieyuwa Eweka, MD, Mineola, NY (*Abstract Co-Author*) Nothing to Disclose Rose Calixte, PhD, Mineola, NY (*Abstract Co-Author*) Nothing to Disclose Jason C. Hoffmann, MD, Mineola, NY (*Abstract Co-Author*) Consultant, Merit Medical Systems, Inc; Speakers Bureau, Merit Medical Systems, Inc

For information about this presentation, contact:

jhoffmann@winthrop.org

PURPOSE

While the intent of the Physician Open Payments Program (OPP) reportedly is to increase transparency, the public receives minimal information about what these payments may entail, and patients may assume these are inappropriate or signify bias. To our knowledge, no analysis of payments in relation to academic productivity exists in the literature. Therefore, our goal was to study this relationship among interventional radiology (IR) chiefs at U.S. academic institutions.

METHOD AND MATERIALS

Per institution guidelines, IRB approval was not needed as the project used only publicly available information. A list of IR section chiefs at academic institutions with IR fellowships was created. All non-royalty general payments (NRGP) made to IRs in 2015 was downloaded from the OPP website. Pubmed search was used to correlate this with the academic productivity of each IR chief. Spearman correlation was used to measure the association between productivity and payment. Fisher's Z transformation was used to compute the 95% confidence interval for the correlation as a measurement of the strength of the association. In addition, 2015 payments to IR division chiefs were compared to 2015 payments to IR non-chiefs.

RESULTS

Out of 95 U.S. hospitals with an IR fellowship, 89 chiefs were identified. In 2015, 77 IR chiefs received at least one NRGP, averaging \$9,911.88±23,183.91 (median \$1628.97). In 2015, 1723 non-chief IRs received at least one NRGP, averaging \$3,112.10±16,244.24 (median \$243.79). A test of normality of the IR chiefs' NRGP and Pubmed publications revealed that both variables significantly deviate from normal distribution. Thus, the Spearman correlation coefficient is the appropriate measure of their association. Correlation between IR chiefs' productivity and payment is 0.44 with a 95% confidence interval of 0.24-0.59, representing a weak to moderate positive association.

CONCLUSION

A positive association exists between payment amount reported in the OPP system and academic productivity amongst IR section chiefs at academic U.S. institutions in 2015. The median IR chief 2015 NRGP was 668% higher than for non-chief IRs.

CLINICAL RELEVANCE/APPLICATION

The general public should be informed that IR chief payments and relationships with industry may have a link to academic productivity. The greater NRGP for academic IR chiefs may reflect a greater responsibility to interact with industry.

SSM23-05 How Comprehensive are Interventional Radiology Residency Websites?

Wednesday, Nov. 29 3:40PM - 3:50PM Room: E450B

Awards

Student Travel Stipend Award

Participants

Paul H. Yi, MD, Baltimore, MD (*Presenter*) Nothing to Disclose
Sherwin Novin, Madison, WI (*Abstract Co-Author*) Nothing to Disclose
Taylor L. Vanderplas, Madison, WI (*Abstract Co-Author*) Nothing to Disclose
Douglas B. Yim, MD, San Diego, CA (*Abstract Co-Author*) Nothing to Disclose
Kelvin K. Hong, MD, Baltimore, MD (*Abstract Co-Author*) Scientific Advisory Board, Boston Scientific Corporation; Scientific Advisory
Board, BTG International Ltd; Research support, Merit Medical Systems, Inc;

For information about this presentation, contact:

paulyi88@gmail.com

PURPOSE

Interventional Radiology (IR) residency began its first application cycle this past year. As the majority of residency applicants turn to the Internet to evaluate potential residency programs, maintaining a comprehensive website is crucial for attracting the best and brightest medical students. The purpose of this study was to evaluate the comprehensiveness of IR residency websites during the first application cycle.

METHOD AND MATERIALS

We searched all integrated IR residency programs listed on the Society for Interventional Radiology website for the presence of a dedicated residency website. For programs with a dedicated website, we searched for the presence of 38 criteria previously identified as important considerations for medical students applying to Radiology residency (Image 1). We compared prevalence of these criteria between different regions of the country and size of residency program using T-tests and ANOVA.

RESULTS

Of 61 IR residency programs identified, 44 (72%) had dedicated websites. Of these 44, only 1 program had at least 2/3 of criteria assessed and only 10 programs (23%) had half or more. On average, the websites reported 37% of items evaluated. The most frequently included information was contact e-mail (93%), mailing address (89%), resident social life (64%) and the area surrounding each residency (61%). The least commonly included information was about procedure simulation experience (5%) and description of teaching didactics (5%). There was no significant difference in website comprehensiveness between regions (p = 0.49), or between "large" programs (3+ residents/year) and "small" programs (>3 residents/year) [P = 0.36].

CONCLUSION

Nearly one-third of integrated IR residency programs do not have a dedicated website, and those that do exist are inadequately comprehensive, with less than 40% of assessed criteria present. Contact information and information about life outside of work were the most commonly included information with comparatively less frequent description of the clinical training opportunities. Addressing these gaps in website content will help IR residencies better inform prospective applicants and, in turn, help recruit the best and brightest into the field.

CLINICAL RELEVANCE/APPLICATION

Ensuring comprehensive interventional radiology residency program websites will help recruit the best and brightest medical students into the field.

SSM23-06 Comparative Utilization of Carotid Stenting and Carotid Endarterectomy in the Medicare Population in Recent Years

Wednesday, Nov. 29 3:50PM - 4:00PM Room: E450B

Participants Sarah I. Kamel, MD, Philadelphia, PA (*Presenter*) Nothing to Disclose David C. Levin, MD, Philadelphia, PA (*Abstract Co-Author*) Nothing to Disclose Laurence Parker, PhD, Philadelphia, PA (*Abstract Co-Author*) Nothing to Disclose Vijay M. Rao, MD, Philadelphia, PA (*Abstract Co-Author*) Nothing to Disclose

For information about this presentation, contact:

sarah.kamel@jefferson.edu

PURPOSE

In the late 1990s, multiple controlled trials demonstrated that carotid endarterectomy (CEA) is superior to optimal medical therapy for stroke prevention, particularly in patients with high grade symptomatic stenosis. CEA is preferred to carotid artery stenting (CAS) given that the perioperative risk of stroke or death can be up to two fold higher with CAS. Our purpose was to study the recent trends of CEA and CAS in the Medicare population in response to the literature.

METHOD AND MATERIALS

The nationwide Medicare Part B fee-for-service databases for 2003-2015 were used. We selected CPT codes 35301 (thromboendarterectomy, carotid) and 37215 (intravascular stent placement, cervical carotid). The databases indicate procedure volume for each code, which were used to calculate utilization rates per 100,000 Medicare beneficiaries. Medicare specialty codes indicated the specialty of the performing physician.

RESULTS

Utilization rate of carotid endarterectomy was at its highest in 2003 at 355 per 100,000 and has declined steadily to 156 in 2015 (-56%). A CPT code for CAS first became available in 2005. CAS utilization peaked in 2006 at 28, ranged between 25-26 studies from 2007 to 2011 and then declined to 16 by 2015 (-43% compared with peak) In 2015, the percent share of carotid stenting by specialty was: cardiology 45%, vascular surgery 20%, radiology 14%, neurosurgery 8%, neurology 6%, other 6%.

CONCLUSION

Since CEA has been demonstrated to have lower perioperative mortality compared to CAS, it is not surprising that CEA was performed nearly ten times as often in 2015. Considering the proven efficacy of CEA, it is surprising that its utilization rate has dropped 56% since 2003 and that in recent years, CAS use has also declined. Perhaps this decrease in intervention is due to improved efficacy of medical management of atherosclerosis in addition to stricter guidelines defining patients who would most benefit from carotid intervention.

CLINICAL RELEVANCE/APPLICATION

The utilization of both CEA and CAS is declining.





103rd Scientific Assembly and Annual Meeting November 26 to December 1 McCormick Place, Chicago



MSCU42

Case-based Review of Ultrasound (An Interactive Session)

Wednesday, Nov. 29 3:30PM - 5:00PM Room: S406A

US

AMA PRA Category 1 Credits ™: 1.50 ARRT Category A+ Credit: 1.75

FDA Discussions may include off-label uses.

Participants

Deborah J. Rubens, MD, Rochester, NY (Director) Nothing to Disclose

For information about this presentation, contact:

deborah_rubens@urmc.rochester.edu

LEARNING OBJECTIVES

1) Recognize the diverse applications of ultrasound throughout the body and identify those situations in which it provides the optimal diagnostic imaging choice. 2) Understand the fundamental interpretive parameters of ultrasound contrast enhancement and its applications. 3) Know the important factors to consider when choosing ultrasound for image guided procedures and how to optimize ultrasound for technical success.

ABSTRACT

Ultrasound is a rapidly evolving imaging modality which has achieved widespread application throughout the body. In this course we will address the major anatomic areas of ultrasound use, including the abdominal and pelvic organs, superficial structures and the vascular system. Challenging imaging and clinical scenarios will be emphasized to include the participant in the decision making process. Advanced cases and evolving technology will be highlighted; including the use of ultrasound contrast media and elastography as diagnostic techniques. The selection of ultrasound for interventional guidance will be addressed, as will the unique applications of ultrasound to emergency imaging including obstetrics and pediatrics.

Sub-Events

MSCU42A Gynecologic and Transvaginal Ultrasound

Participants

Mindy M. Horrow, MD, Philadelphia, PA (Presenter) Spouse, Employee, Merck & Co, Inc

For information about this presentation, contact:

horrowm@einstein.edu

LEARNING OBJECTIVES

1) Describe sonographic techniques and findings that are most useful in the diagnosis of tubal ectopic pregnancy. 2) Review the findings of retained products of conception. 3) Categorize the various non-gynecologic causes of acute pelvic pain that may be diagnosed with transvaginal imaging. 4) Describe the sonographic findings of acute ovarian torsion.

Honored Educators

Presenters or authors on this event have been recognized as RSNA Honored Educators for participating in multiple qualifying educational activities. Honored Educators are invested in furthering the profession of radiology by delivering high-quality educational content in their field of study. Learn how you can become an honored educator by visiting the website at: https://www.rsna.org/Honored-Educator-Award/ Mindy M. Horrow, MD - 2013 Honored EducatorMindy M. Horrow, MD - 2016 Honored Educator

MSCU42B Ultrasound in Interventional Radiology

Participants Devang Butani, MD, Rochester, NY (*Presenter*) Nothing to Disclose

For information about this presentation, contact:

devang_butani@urmc.rochester.edu

LEARNING OBJECTIVES

1) Understand the role of Ultrasound in Interventional Radiology (IR). 2) Learn how to avoid complications by using ultrasound. 3) Be aware about the limitations of ultrasound in IR.

ABSTRACT

Ultrasound is vital in the practice of Interventional Radiology, where it is used for screening, planning, targeting/guidance and evaluating effectiveness of interventions. A case based format is used to demonstrate the various roles.

MSCU42C Ultrasound of Pediatric Abdominal Emergencies

Participants

Harriet J. Paltiel, MD, Boston, MA (Presenter) Nothing to Disclose

LEARNING OBJECTIVES

1) List the most common gastrointestinal tract causes of an acute abdomen in children. 2) Discuss the appropriate imaging evaluation of patients based on age and clinical presentation. 3) Describe the sonographic features of these entities.

ABSTRACT

This case-based review will include a discussion of the sonographic imaging features of some of the most important pediatric gastrointestinal causes of an acute abdomen, including bowel atresia, necrotizing enterocolits, pyloric stenosis, midgut malrotation and volvulus, acute appendicitis, and intussusception.

MSCU42D Small Parts Ultrasound

Participants Deborah J. Rubens, MD, Rochester, NY (*Presenter*) Nothing to Disclose

For information about this presentation, contact:

Deborah_rubens@urmc.rochester.edu

LEARNING OBJECTIVES

1) Review some of the common pathologic entities involving superficial glands and structures. 2) Emphasize the unique technical parameters which are critical to optimize the imaging of small parts. 3) Test the attendant's knowledge of some critical decision pathways in superficial pathology.

ABSTRACT

High frequency ultrasound is a powerful tool to assess superficial structures including the neck (thyroid, parathyroid, other neck masses) chest and abdominal wall, extremities and the scrotum. Accurate performance requires optimizing scanning frequency for adequate tissue penetration and Doppler sensitivity to differentiate fluid collections from tumors, to assess organs for blood flow and to diagnose inflammatory conditions. Cases will be selected to emphasize thyroid, neck, testicular and scrotal pathology; particularly those cases requiring urgent intervention. Additional cases will include symptomatic lumps and bumps and the incidental lesions one commonly encounters in superficial scanning.







MSES44

Essentials of Musculoskeletal Imaging

Wednesday, Nov. 29 3:30PM - 5:00PM Room: S100AB

мк

AMA PRA Category 1 Credits ™: 1.50 ARRT Category A+ Credit: 1.75

Sub-Events

MSES44A MRI of the Brachial Plexus

Participants

Christopher F. Beaulieu, MD, PhD, Stanford, CA (Presenter) Nothing to Disclose

LEARNING OBJECTIVES

1) Update the learner's knowledge of brachial plexus anatomy. 2) Understand key technical factors affecting MRI of the brachial plexus. 3) Be able to recognize common intrinsic and extrinsic lesions of the brachial plexus.

Active Handout:Christopher Frederick Beaulieu

http://abstract.rsna.org/uploads/2017/17000048/Active MSES44A.pdf

MSES44B Radiographic Assessment of Arthritis

Participants

Andrew J. Grainger, MRCP, FRCR, Leeds, United Kingdom (Presenter) Nothing to Disclose

LEARNING OBJECTIVES

1) To understand how radiographic imaging contributes to the diagnosis and management of arthritis. 2) To recognize features of arthritis on conventional radiographs which help in the differential diagnosis of arthritis. 3) To be able to identify common pitfalls and normal variants which may simulate arthritic change.

Active Handout: Andrew J. Grainger

http://abstract.rsna.org/uploads/2017/17000051/Active MSES44B.pdf

MSES44C Avoiding Pitfalls in Lower Extremity Trauma

Participants Thomas L. Pope, MD, Denver, CO (*Presenter*) Nothing to Disclose

For information about this presentation, contact:

thomas.pope@shcr.com

LEARNING OBJECTIVES

1) Describe the pathology most likely to be missed in lower extremity trauma. 2) Outline a survey of the most common lesions missed in quality assurance program. 3) Suggest major ways to avoid missing lesions with very subtle pathology.

ABSTRACT

Lower extremity (LE) trauma is one of the most frequently encountered clinical situations in the ED setting. Imaging of the LE, therefore, makes up a significant portion of the studies interpreted by ED and general radiologists. Much of the pathology is straightforward and not extremely challenging. However, there are many lesions which may be missed without meticulous attention to technique and imaging. This presentation will outline the most common potential pitfalls and problem areas in the interpretation of LE trauma imaging, particularly in regard to radiographs and CT imaging. Suggestions for the interpreting radiologist to possibly avoid these errors will be outlined.

MSES44D Chondroid Lesions in Bone as Incidental Finding: What to Do?

Participants

Milko C. de Jonge, MD, Woerden, Netherlands (Presenter) Nothing to Disclose

For information about this presentation, contact:

milkodejonge@gmail.com

LEARNING OBJECTIVES

1) To discuss the incidence and prevalence of chondroid lesions in bone. 2) Describing the typical imaging findings of chondroid lesions on conventional imaging and MRI. 3) To discuss the difference in imaging findings between benign and malignant chondroid lesions. 4) What to do with equivocal cases i.e. what to do with an indeterminate lesion if found incidentally. 5) When and how to biopsy.

Active Handout: Milko Charles de Jonge

http://abstract.rsna.org/uploads/2017/17000054/Active MSES44D.pdf







MSSR44

RSNA/ESR Hybrid Imaging Symposium: Hybrid Imaging of the Brain (An Interactive Session)

Wednesday, Nov. 29 3:30PM - 5:00PM Room: S402AB



AMA PRA Category 1 Credits ™: 1.50 ARRT Category A+ Credit: 1.75

Participants

Alexander Drzezga, MD, Cologne, Germany (*Moderator*) Consultant, Siemens AG; Consultant, Bayer AG; Consultant, General Electric Company; Consultant, Eli Lilly and Company; Consultant, The Piramal Group; Speakers Bureau, Siemens AG; Speakers Bureau, Bayer AG; Speakers Bureau, General Electric Company; Speakers Bureau, Eli Lilly and Company; Speakers Bureau, The Piramal Group Katrine Riklund, MD, PhD, Umea, Sweden (*Moderator*) Nothing to Disclose

Sub-Events

MSSR44A Neurodegenerative Disorders

Participants

Henryk Barthel, Leipzig, Germany (*Presenter*) Research support, The Piramal Group; Consultant, The Piramal Group; Travel support, The Piramal Group

LEARNING OBJECTIVES

1) To learn about pathophysiology in neurodegenerative disorders. 2) To learn about different tracers and how to interpret the findings. 3) To understand the role of hybrid imaging in neurodegenerative disorders.

MSSR44B Brain Tumors

Participants

Gagandeep Choudhary, MD, MBBS, Birmingham, AL (Presenter) Nothing to Disclose

LEARNING OBJECTIVES

1) To get an overview of brain tumours and tracers used. 2) To learn how to interpret the examinations. 3) To understand the role of hybrid imaging of brain tumours.

Active Handout:Gagandeep Choudhary

http://abstract.rsna.org/uploads/2017/16003680/Active MSSR44B.pdf

MSSR44C Interactive Case Discussion

Participants

Henryk Barthel, Leipzig, Germany (*Presenter*) Research support, The Piramal Group; Consultant, The Piramal Group; Travel support, The Piramal Group

Gagandeep Choudhary, MD, MBBS, Birmingham, AL (Presenter) Nothing to Disclose

LEARNING OBJECTIVES

1) To learn about evaluation of hybrid imaging in neurodegenerative disorders. 2) To learn about evaluation of hybrid imaging of brain tumours.







MSRT46

ASRT@RSNA 2017: The Radiographer's Role in Computed Tomography Colonography (CTC)

Wednesday, Nov. 29 3:40PM - 4:40PM Room: N230B



AMA PRA Category 1 Credit ™: 1.00 ARRT Category A+ Credit: 1.00

Participants

Rachel Baldwin-Cleland, MSc, London, United Kingdom (Presenter) Nothing to Disclose

LEARNING OBJECTIVES

1) Provide an account, based upon national survey data, of the current roles and scope of practice of CTC radiographers in England. 2) Improve participant's knowledge of the range of skills of CTC Radiographers practicing in England. 3) Introduce the ongoing work of the Bowel Cancer Screening CTC radiographer educational development group in England, and explain how this will influence working practice within CTC in the future.

Active Handout:Rachel Baldwin-Cleland

http://abstract.rsna.org/uploads/2017/17001472/Active MSRT46.pdf





103rd Scientific Assembly and Annual Meeting November 26 to December 1 McCormick Place, Chicago



RCA45

Rectal MRI (Hands-on)

Wednesday, Nov. 29 4:30PM - 6:00PM Room: S401AB



AMA PRA Category 1 Credits ™: 1.50 ARRT Category A+ Credit: 1.75

Participants

David H. Kim, MD, Middleton, WI (*Presenter*) Co-founder, VirtuoCTC, LLC; Shareholder, Cellectar Biosciences, Inc; Shareholder, Elucent Medical;

Mukesh G. Harisinghani, MD, Boston, MA (*Presenter*) Nothing to Disclose Marc J. Gollub, MD, New York, NY (*Presenter*) Nothing to Disclose Courtney C. Moreno, MD, Suwanee, GA (*Presenter*) Nothing to Disclose Raj M. Paspulati, MD, Cleveland, OH (*Presenter*) Nothing to Disclose Gaiane M. Rauch, MD, PhD, Houston, TX (*Presenter*) Nothing to Disclose Zahra Kassam, MD, London, ON (*Presenter*) Nothing to Disclose

LEARNING OBJECTIVES

1) Critically evaluate the primary tumor to accurately place in the appropriate T category. 2) 2. Apply specific criteria to determine regional lymph node status. 3) Recognize relevant anatomic landmarks used in Rectal MRI cancer staging to help determine management.

ABSTRACT

This workshop will be led by members of the Society of Abdominal Radiology Rectal Cancer Disease Focused Panel. This group helps set the interpretation standards for rectal cancer MRI in the United States. In this 1.5 hour Hands-on Workshop, the participants will have the opportunity to review a number of rectal staging MRI cases on stand-alone computers or on a personal mobile device. The selected cases are intended to give a broad overview of the common issues encountered in rectal cancer staging, including appropriately categorizing the correct T category of the tumor as well as determining regional lymph node status. The relevant anatomic relationships of the tumor with adjacent structures for surgical and potential neoadjuvant options will be emphasized. An interactive platform will allow participants to see overall class performance for questions posed by the expert reviewer. Each case will be reviewed after a short interval to allow a participant to form an opinion prior to the expert review. This workshop is intended to give a practical, hands-on approach to rectal cancer staging by MRI.





103rd Scientific Assembly and Annual Meeting November 26 to December 1 McCormick Place, Chicago



RCC45

Deep Learning—An Imaging Roadmap

Wednesday, Nov. 29 4:30PM - 6:00PM Room: S501ABC

IN

AMA PRA Category 1 Credits ™: 1.50 ARRT Category A+ Credit: 1.75

FDA Discussions may include off-label uses.

Participants

Paula M. Jacobs, PhD, Bethesda, MD (Moderator) Nothing to Disclose

For information about this presentation, contact:

Paula.Jacobs@nih.gov

LEARNING OBJECTIVES

1) Understand the framework of 'Deep Learning', Machine Learning, and Neural Net computer algorithms. 2) Comprehend what aspects of radiology practice are most amenable to machine learning deployment. 3) Understand the academic, commercial and clinical perspectives on how the field will likely develop and how NCI's Cancer Imaging Archive (TCIA) can accelerate development of this new technology.

ABSTRACT

Deep Learning, an independent self-learning computational environment that uses multilayered computational neural nets, has generated considerable excitement (as well as concerns and misperceptions) in medical imaging. Deep learning computational techniques, such as convolutional neural networks (CNNs) generate multiple layer feature classifiers that extract disease relevant features from entire regions of medical images without the need for localization or pre-segmentation of lesions. Although CNNs require training on very large image datasets that encompass particular disease expressions, they can be diagnostically effective since no human input of segmentation features such as size, shape, margin sharpness, texture, and kinetics are required. But their immediate and future applicability as tools for unsupervised medical decision-making are, as yet, not well understood by most clinical radiologists. This overview session of Deep Learning will provide a clearer picture by presenters who are active in that field and who can clarify how the unique characteristics of Deep Learning could impact clinical radiology. It will address how radiologists can contribute to, and benefit from, this new technology. Topics of this multi-speaker session will cover: 1) the general principles of deep learning computational schemas and their mechanisms of handling image inputs and outputs. 2) new technology including hardware shifts in microprocessors from CPU's to GPU devices that offer significant computational advantages 3) how to ensure that Deep Learning results are consistently clinically relevant and meaningful including nodal element tuning and provability so as to assure medical care consistency and reproducibility. 4) how to develop and leverage datasets for deep learning on archives such as the NIH The Cancer Imaging Archive (TCIA) including requirements for input image dataset magnitude and completeness of disease spectrum representation. 5) how to embed essential non-imaging data needed as inputs, (e.g. EHR, outcome, cross-disciplinary metadata, and the data pre-processing required to make DICOM ready for Deep Learning. The presentations will be at a level understandable and relevant to the RSNA radiologist audience.

Sub-Events

RCC45A Computer Science 'Deep Learning' Research by the Academic Community

Participants

Fred W. Prior, PhD, Little Rock, AR (Presenter) Nothing to Disclose

LEARNING OBJECTIVES

1) Understand the basic concepts of Machine Learning and Deep Learning and how they differ. 2) Gain insights into how these techniques are being used in quantitative imaging (Radiomic) research.

RCC45B Commercial Development and Deployment of 'Deep Learning' Technology

Participants Abdul Hamid Halabi, Santa Clara, CA (*Presenter*) Employee, NVIDIA Corporation

For information about this presentation, contact:

ahalabi@nvidia.com

RCC45C Radiology Clinician Perspectives

Participants

Bradley J. Erickson, MD, PhD, Rochester, MN (*Presenter*) Stockholder, OneMedNet Corporation; Stockholder, VoiceIt Technologies, LLC; Stockholder, FlowSigma; Researcher, nVIDIA Corporation

For information about this presentation, contact:

bje@mayo.edu

LEARNING OBJECTIVES

1) Understand the differences between an algorithm that works in the lab and one that works in clinical practice. 2) Identify common weaknesses in study design that can lead to better apparent performance than might be realized in practice. 3) Recognize challenges in practical workflow that might impede clinical adoption of some tools.





103rd Scientific Assembly and Annual Meeting November 26 to December 1 McCormick Place, Chicago



SPCB41

Cybersecurity

Wednesday, Nov. 29 4:30PM - 6:00PM Room: E450B

IN

AMA PRA Category 1 Credits ™: 1.50 ARRT Category A+ Credit: 1.75

Participants

Patrick Hope, Arlington, VA (*Presenter*) Nothing to Disclose James Jacobson, Flanders, NJ (*Presenter*) Employee, Siemens AG Seth D. Carmody, PhD, Silver Spring, MD (*Presenter*) Nothing to Disclose

LEARNING OBJECTIVES

1) Better understand how to make your facility cybersecure. 2) Understand ways to avoid cyber attacks. 3) Learn what the medical device industry is doing to inform medical imaging companies about preventing cyber attacks. 4) Learn what a leading manufacturer is doing to make devices more cyber secure.

ABSTRACT

Cybersecurity is a high priority for physicians, hospitals, and manufacturers of all internet-connected devices, and even more so when patient safety and health information is at stake. MITA has led efforts to strengthen cybersecurity for imaging systems which reach far beyond the radiology suite. MITA published a 2015 whitepaper http://www.nema.org/Standards/Pages/Cybersecurity-for-Medical-Imaging.aspx that explained how well-structured and governed collaboration is required to safeguard the patients' protected health information and their physical safety.





103rd Scientific Assembly and Annual Meeting November 26 to December 1 McCormick Place, Chicago



SPDL41

Neuro and MSK (Case-based Competition)

Wednesday, Nov. 29 4:30PM - 6:00PM Room: E451B



AMA PRA Category 1 Credits ™: 1.50 ARRT Category A+ Credit: 1.75

Participants

Paul J. Chang, MD, Chicago, IL (*Presenter*) Co-founder, Stentor/Koninklijke Philips NV; Researcher, Koninklijke Philips NV; Advisory Board, Bayer AG; Advisory Board, Aidoc Ltd; Advisory Board, McCoy Neety Panu, MD, FRCPC, Thunder Bay, ON (*Presenter*) Nothing to Disclose Gregory L. Katzman, MD, Chicago, IL (*Presenter*) Nothing to Disclose Omer A. Awan, MD, Philadelphia, PA (*Presenter*) Nothing to Disclose

For information about this presentation, contact:

pchang@radiology.bsd.uchicago.edu

omer.awan@tuhs.temple.edu

LEARNING OBJECTIVES

1) Be introduced to a series of neuradiology and musculoskeletal radiology case studies via an interactive team game approach designed to encourage 'active' consumption of educational content. 2) Use their mobile wireless device (tablet, phone, laptop) to electronically respond to various imaging case challenges; participants will be able to monitor their individual and team performance in real time. 3) Receive a personalized self-assessment report via email that will review the case material presented during the session, along with individual and team performance. *This interactive session will use RSNA Diagnosis Live™*. *Please bring your charged mobile wireless device (phone, tablet or laptop) to participate*.

ABSTRACT

The extremely popular audience participation educational experience, Diagnosis Live!, is an expert-moderated session featuring a series of interactive case studies that will challenge radiologists' diagnostic skills and knowledge. The session features a lively, fast-paced game format: participants will be automatically assigned to teams who will then use their personal mobile devices to test their knowledge in a fast-paced session that will be both educational and entertaining. After the session, attendees will receive a personalized self-assessment report via email that will review the case material presented during the session, along with individual and team performance.





103rd Scientific Assembly and Annual Meeting November 26 to December 1 McCormick Place, Chicago



SPSC41

Controversy Session: Early Stage Prostate Cancer - To Treat or Not to Treat?

Wednesday, Nov. 29 4:30PM - 6:00PM Room: E451A



AMA PRA Category 1 Credits ™: 1.50 ARRT Category A+ Credit: 1.75

Participants

Abhishek A. Solanki, MD, Maywood, IL (*Moderator*) Consultant, Blue Earth Diagnostics Ltd; Advisory Board, Blue Earth Diagnostics Ltd

For information about this presentation, contact:

abhishek.solanki@lumc.edu

LEARNING OBJECTIVES

1) Review the management options for localized prostate cancer. 2) Describe the advantages of immediate treatment of localized prostate cancer. 3) Describe the disadvantages and harms of immediate treatment of localized prostate cancer.

ABSTRACT

Prostate cancer is the most commonly diagnosed malignancy in men in the United States. However, the relatively indolent natural history of localized prostate cancer has raised concern regarding potential overdiagnosis and overtreatment. Many men elect immediate curative treatment with radical prostatectomy, external beam radiotherapy, or brachytherapy, but active surveillance remains a reasonable option for many men. The results of multiple recent studies have shed light into the advantages and disadvantages of immediate treatment over active surveillance, helping clinicians and patients with shared decision making to identify the optimal approach.

Sub-Events

SPSC41A General Overview of Treatment Options of Early Stage Prostate Cancer

Participants Stanley L. Liauw, MD, Chicago, IL (*Presenter*) Nothing to Disclose

For information about this presentation, contact:

sliauw@radonc.uchicago.edu

LEARNING OBJECTIVES

View learning objectives under main course title.

ABSTRACT

The management of localized prostate cancer could be considered controversial. While local therapy is often successful in limiting the progression of disease, treatment also carries morbidity that can adversely affect quality of life. This overview highlights some of the difficulties in managing localized prostate cancer, and reviews considerations for the clinician to individualize decision making.

SPSC41B Why Should We Treat Early Stage Prostate Cancer?

Participants

Jason Efstathiou, Boston, MA (*Presenter*) Consultant, Blue Earth Diagnostics Ltd; Consultant, TARIS BioMedical, Inc; Consultant, Bayer AG; Advisory Board, Merck KGaA

LEARNING OBJECTIVES

View learning objectives under main course title.

SPSC41C Why Should We Not Treat All Patients with Early Stage Prostate Cancer?

Participants

Ronald Chen, MD, Chapel Hill, NC (Presenter) Consultant, Accuray Incorporated

LEARNING OBJECTIVES

1) To understand the potential benefits and harms of treatment vs no treatment in patients with localized prostate cancer. 2) To understand the difference between active surveillance vs watchful waiting. 3) To understand the most appropriate patients for consideration of active surveillance and watchful waiting.

ABSTRACT

Not all patients with localized prostate cancer require immediate treatment. Many patients with an early diagnosis of slow-growing prostate cancer will die with, rather than from the prostate cancer. The over-treatment of many of these patients is a well-recognized issue, which leads to treatment-related side effects that harm the patient rather than benefit them. On the other hand,

patients with more aggressive prostate cancer do benefit from aggressive treatment. This session will describe active surveillance and watchful waiting as two options for select patients with early prostate cancers, and appropriate selection of patients to offer these options.





SPSC42

Controversy Session: Evidence-based Interventional Radiology: How Long Can We Wait for the Evidence?

Wednesday, Nov. 29 4:30PM - 6:00PM Room: E351

IR

AMA PRA Category 1 Credits ™: 1.50 ARRT Category A+ Credit: 1.75

FDA Discussions may include off-label uses.

Participants

Brian S. Funaki, MD, Chicago, IL (Moderator) Data Safety Monitoring Board, Novate Medical Ltd

LEARNING OBJECTIVES

1) To understand the role of randomized controlled trials in establishment of practice patterns. 2) To understand the importance of registrirs and other forms of big data. 3) To recognize the benefits and limitations of case series data. 4) To determine the contributions to practice by different types of data.

Sub-Events

SPSC42A Randomized Controlled Trials-The Importance of Level One Evidence

Participants

Suresh Vedantham, MD, Saint Louis, MO (Presenter) Research support, Cook Group Incorporated

For information about this presentation, contact:

vedanthams@mir.wustl.edu

LEARNING OBJECTIVES

1) State the advantages of randomized controlled trials in minimizing bias. 2) Explain the drawbacks of randomized controlled trial design.

SPSC42B Registry Data-The Importance Moving Forward

Participants

Jeremy C. Durack, MD, New York, NY (Presenter) Scientific Advisory Board, Adient Medical Inc; Investor, Adient Medical Inc;

LEARNING OBJECTIVES

1) Understand where registries fit in the evidence hierarchy. 2) Learn strategies for registry development and deployment to reduce burden on PIs and participants. 3) Understand why registry participation is particularly important during this period of transition in healthcare.

SPSC42C Retrospective Series-Undervalued Data!

Participants

Charles E. Ray JR, MD, PhD, Chicago, IL (*Presenter*) Editor, Thieme Medical Publishers, Inc; Consultant, W. L. Gore & Associates, Inc; ; ; ;

For information about this presentation, contact:

chray@uic.edu

LEARNING OBJECTIVES

1) Discuss the role of all types of publications, including randomized controlled trials, registry data, and retrospective case series, in determining best practice patterns. 2) Understand the differences in the types of data presented in the literature, and the role each should play in determining best practice patterns. 3) Understand the benefits and limitations of types of study designs commonly used in IR publications. 4) Formulate an opinion on what type of data are necessary before implementing changes to daily IR practice.







SPSC43

Controversy Session: MR Imaging Enhancers (Muscle Relaxants, Rectal Gel, Vaginal Gel): Are They Really Necessary?

Wednesday, Nov. 29 4:30PM - 6:00PM Room: E353B



AMA PRA Category 1 Credits ™: 1.50 ARRT Category A+ Credit: 1.75

FDA Discussions may include off-label uses.

Participants

Hero K. Hussain, MD, Ann Arbor, MI (Moderator) Nothing to Disclose

LEARNING OBJECTIVES

1) To determine the advantages and disadvantages of imaging enhancers on image quality and diagnostic capability. 2) To assess the effect of imaging enhancers on MRI workflow. 3) To examine the financial effects of imaging enhancers on the patient and the imaging department. 4) To evaluate the impact of potential side effects of imaging enhancers on the patient and the imaging department.

Sub-Events

SPSC43A The Case FOR the Use of Imaging Enhancers for MRI of Prostate and Rectal Cancer

Participants

Caroline Reinhold, MD, MSc, Montreal, QC (Presenter) Consultant, GlaxoSmithKline plc

LEARNING OBJECTIVES

View learning objectives under main course title.

ABSTRACT

The Case FOR the Use of Imaging Enhancers for MRI of Prostate and Rectal Cancer will be made.1) To determine the advantages of antispasmodic agents and rectal contrast on the image quality and diagnosis for MR examinations of the prostate and rectum. 2) To propose an efficient work flow for administering imaging enhancers. 3) To propose screening guidelines to minimize potential side effects of imaging enhancers on the patient and the imaging department.

Honored Educators

Presenters or authors on this event have been recognized as RSNA Honored Educators for participating in multiple qualifying educational activities. Honored Educators are invested in furthering the profession of radiology by delivering high-quality educational content in their field of study. Learn how you can become an honored educator by visiting the website at: https://www.rsna.org/Honored-Educator-Award/ Caroline Reinhold, MD, MSc - 2013 Honored EducatorCaroline Reinhold, MD, MSc - 2014 Honored EducatorCaroline Reinhold, MD, MSc - 2017 Honored Educator

SPSC43B The Case AGAINST the Use of Imaging Enhancers for MRI of Prostate and Rectal Cancer

Participants

Donald G. Mitchell, MD, Philadelphia, PA (Presenter) Consultant, CMC Contrast AB

For information about this presentation, contact:

dgm101@jefferson.edu

LEARNING OBJECTIVES

View learning objectives under main course title.

SPSC43C The Case FOR the Use of Imaging Enhancers for MRI of the Female Pelvis

Participants

Andrea G. Rockall, MRCP, FRCR, London, United Kingdom (Presenter) Nothing to Disclose

LEARNING OBJECTIVES

View learning objectives under main course title.

ABSTRACT

The case to support the use of image enhancers in female pelvic MRI will be made.

Honored Educators

Presenters or authors on this event have been recognized as RSNA Honored Educators for participating in multiple qualifying educational activities. Honored Educators are invested in furthering the profession of radiology by delivering high-quality

educational content in their field of study. Learn how you can become an honored educator by visiting the website at: https://www.rsna.org/Honored-Educator-Award/ Andrea G. Rockall, MRCP, FRCR - 2017 Honored Educator

SPSC43D The Case AGAINST the Use of Imaging Enhancers for MRI of the Female Pelvis

Participants

Evan S. Siegelman, MD, Philadelphia, PA (Presenter) Consultant, BioClinica, Inc; Consultant, ICON plc;

For information about this presentation, contact:

Evan.Siegelman@uphs.upenn.edu

LEARNING OBJECTIVES

View learning objectives under main course title.

ABSTRACT

Upon completion of this presentation, participants should be able to: 1. Apply principles of MR imaging to optimize female pelvic imaging protocols without the use of imaging enhancers and perform MR studies that are not inferior to MR studies performed with MR enhancers. 2. Assess the cost savings and improvement in workflow when muscle relaxants, vaginal gel and rectal gel are not administered.

Honored Educators

Presenters or authors on this event have been recognized as RSNA Honored Educators for participating in multiple qualifying educational activities. Honored Educators are invested in furthering the profession of radiology by delivering high-quality educational content in their field of study. Learn how you can become an honored educator by visiting the website at: https://www.rsna.org/Honored-Educator-Award/ Evan S. Siegelman, MD - 2013 Honored Educator







SPSC44

Controversy Session: The Doctor's Doctor or the Patient's Physician: Can Radiologists Simultaneously Be Both?

Wednesday, Nov. 29 4:30PM - 6:00PM Room: N226

PR

AMA PRA Category 1 Credits ™: 1.50 ARRT Category A+ Credit: 1.75

Participants

Tessa S. Cook, MD, PhD, Philadelphia, PA (*Moderator*) Nothing to Disclose Geraldine B. McGinty, MD, MBA, New York, NY (*Presenter*) Nothing to Disclose Saurabh Jha, MD, Philadelphia, PA (*Presenter*) Speakers Bureau, Toshiba Medical Systems Corporation C. Matthew Hawkins, MD, Atlanta, GA (*Presenter*) Nothing to Disclose

For information about this presentation, contact:

hawkcm@gmail.com

tessa.cook@uphs.upenn.edu

LEARNING OBJECTIVES

1) Discuss the challenges associated with creating two separate reports, one for the referring physician and one for the patient. 2) Understand the barriers to effectively connecting radiologists with patients and caregivers. 3) Identify opportunities to improve the interface between patients, caregivers, and radiologists.



KSNA[®] 2017

103rd Scientific Assembly and Annual Meeting November 26 to December 1 McCormick Place, Chicago



SPSC45

Controversy Session: LUNG-RADS[™] or Not: Which Nodule Management Protocol Should Be Used for Reporting Lung Cancer Screening CT?

Wednesday, Nov. 29 4:30PM - 6:00PM Room: N227B



AMA PRA Category 1 Credits ™: 1.50 ARRT Category A+ Credit: 1.75

Participants

William C. Black, MD, Lebanon, NH (*Moderator*) Nothing to Disclose Ella A. Kazerooni, MD, Ann Arbor, MI (*Presenter*) Nothing to Disclose Marjolein A. Heuvelmans, MD,PhD, Groningen, Netherlands (*Presenter*) Nothing to Disclose

For information about this presentation, contact:

william.c.black@hitchcock.org

ellakaz@umich.edu

LEARNING OBJECTIVES

1) Understand the rationale for using the ACR Lung CT Screening Reporting and Data System (Lung-RADSTM). 2) Understand the advantages and limitations of using Lung-RADSTM. 3) Be Aware of alternative nodule management protocols that can be used for reporting lung cancer screening CT.

ABSTRACT

The ACR Lung CT Screening Reporting and Data System (Lung-RADS[™]) was developed as a tool for the interpretation of lung cancer CT screening examinations as a way to standardizing reporting using a common nomenclature and structure, and track screening outcomes. Abnormalities are placed into categories 1-4 based on their risk of lung cancer as primarily defined by nodule size and stucture (solid, part solid and non solid) and their risk of lung cancer, each with a management recommendation. Lung-RADS[™] is the reporting schema used in the American College of Radiology's Lung Cancer Screening Registry (ACR LSCR). As lung cancer CT screening is rolled out nationally in the United States, this reporting schema creates a mechanism by which to evaluate the performanc eof lung cancer screening in practice. The over 2200 facilities enrolled in the ACR LCSR receive reports with both facility and radiologist level data, which includes the use of Lung-RADS[™] categories in their practice and comparative data for purpose of quality assurance and quality improvement. With nearly two years of screening data reported into the ACR LCSR, data on Lung-RADS[™] category use and subsequent diagnostic testing/intervention and cancer detection rates can be used to refine Lung-RADS[™] in the future. As technology progresses and volumetric tools become more available in practice, moving from nodule diameter measurements to nodule volume for measurement and growth rates is a future goal.

URL

www.acr.org/Quality-Safety/Resources/LungRADS www.acr.org/Quality-Safety/National-Radiology-Data-Registry/Lung-Cancer-Screening-Registry

Active Handout:William C. Black

http://abstract.rsna.org/uploads/2017/17001860/Active SPSC45.pdf

Honored Educators

Presenters or authors on this event have been recognized as RSNA Honored Educators for participating in multiple qualifying educational activities. Honored Educators are invested in furthering the profession of radiology by delivering high-quality educational content in their field of study. Learn how you can become an honored educator by visiting the website at: https://www.rsna.org/Honored-Educator-Award/ Ella A. Kazerooni, MD - 2014 Honored Educator





103rd Scientific Assembly and Annual Meeting November 26 to December 1 McCormick Place, Chicago



MSRO49

BOOST: Lymphoma-eContouring

Wednesday, Nov. 29 4:45PM - 6:00PM Room: S104B



AMA PRA Category 1 Credits ™: 1.25 ARRT Category A+ Credits: 1.50

Participants

Chris R. Kelsey, Durham, NC (*Presenter*) Nothing to Disclose Bradford Hoppe, MD, Jacksonville, FL (*Presenter*) Nothing to Disclose Maria A. Thomas, MD, PhD, Saint Louis, MO (*Presenter*) Nothing to Disclose Sarah A. Johnson, MD, Toronto, ON (*Presenter*) Nothing to Disclose

For information about this presentation, contact:

mthomas@radonc.wustl.edu

LEARNING OBJECTIVES

1) Improve knowledge of involved site radiation therapy contouring for Hodgkin lymphoma and practice the technique. 2) Improve knowledge of involved site radiation therapy contouring for non-hodgkin lymphoma and practice the technique.